

Distribution Agreement

In presenting this thesis or dissertation as a partial fulfillment of the requirements for an advanced degree from Emory University, I hereby grant to Emory University and its agents the non-exclusive license to archive, make accessible, and display my thesis or dissertation in whole or in part in all forms of media, now or hereafter known, including display on the world wide web. I understand that I may select some access restrictions as part of the online submission of this thesis or dissertation. I retain all ownership rights to the copyright of the thesis or dissertation. I also retain the right to use in future works (such as articles or books) all or part of this thesis or dissertation.

Signature:

Amaan M. Kazerouni

Date

Studies Towards the Synthesis of Malagasy Alkaloids, and
Development and Applications of Regio- and Enantioselective Group IX Metal-Catalysed
Reactions

By

Amaan M. Kazerouni
Doctor of Philosophy

Chemistry

Simon B. Blakey, Ph.D.
Advisor

Dennis C. Liotta, Ph.D.
Committee Member

Frank E. McDonald, Ph.D.
Committee Member

Accepted:

Lisa A. Tedesco, Ph.D.
Dean of the James T. Laney School of Graduate Studies

Date

Studies Towards the Synthesis of Malagasy Alkaloids, and
Development and Applications of Regio- and Enantioselective Group IX Metal-Catalysed
Reactions

By

Amaan M. Kazerouni
B.S., University of West Georgia, 2015

Advisor: Simon B. Blakey, Ph.D.

An abstract of
A dissertation submitted to the Faculty of the
James T. Laney School of Graduate Studies of Emory University
in partial fulfillment of the requirements for the degree of
Doctor of Philosophy
in Chemistry
2020

Abstract

Studies Towards the Synthesis of Malagasy Alkaloids, and Development and Applications of Regio- and Enantioselective Group IX Metal-Catalysed Reactions

By Amaan M. Kazerouni

Part I of this dissertation describes efforts towards the synthesis of two monoterpenoid indole alkaloids – 11-demethoxymyrtoidine and myrtoidine. These alkaloids were isolated from *Strychnos myrtoides* and *Strychnos mostuoides* in the western regions of Africa and have been found to potentiate chloroquine activity against resistant strains of *Plasmodium falciparum* malaria. The core of these alkaloids was constructed using a previously developed iminium ion cascade annulation. A convergent strategy to install the EF dihydropyran/butyrolactone fragment of these alkaloids is discussed, as well as an alternate strategy involving a Semmelhack alkoxypalladation/carbonylation cascade reaction. Finally, studies towards the development of an enantioselective iminium ion cascade reaction using asymmetric ion-pairing catalysis are described.

Part II of this dissertation describes the development of regio- and enantioselective Rh- and Ir-catalysed allylic C–H functionalisation reactions and their application towards the synthesis of natural products containing non-canonical amino acid residues. Allylic C–H sulfamidation of allylbenzene derivatives is discussed, as well as the development of a new class of planar chiral rhodium indenyl catalysts for enantioselective allylic C–H amidation. DFT calculations indicate that allylic C–H activation of the olefin substrate is both rate- and enantiodetermining in this reaction, while C–N reductive elimination is regiodetermining, resulting from the electronic asymmetry imposed by the planar chiral indenyl ligand. Finally, the evolution of a synthetic route to darobactin A, a ribosomally-synthesised and post-translationally modified peptide with preliminary biological activity against Gram-negative bacteria, is described.

Studies Towards the Synthesis of Malagasy Alkaloids, and
Development and Applications of Regio- and Enantioselective Group IX Metal-Catalysed
Reactions

By

Amaan M. Kazerouni
B.S., University of West Georgia, 2015

Advisor: Simon B. Blakey, Ph.D.

A dissertation submitted to the Faculty of the
James T. Laney School of Graduate Studies of Emory University
in partial fulfillment of the requirements for the degree of
Doctor of Philosophy
in Chemistry
2020

Acknowledgements

First, I want to thank my mentor and doctoral advisor, Simon Blakey. Your door was always open to me, and during the many bleak periods that inevitably accompany a Ph.D., I always left your office feeling more hopeful and energised than when I entered. I cannot say this enough, but thanks, also, for being such an incredibly supportive mentor during perhaps the most difficult year of my life: coming back to lab after my three month hiatus was one of the hardest things I've had to do, and your understanding and encouragement played a big part in that.

I would like to thank the members of my Ph.D. Committee, Frank McDonald and Dennis Liotta. You have been integral parts of my development as a scientist and provided invaluable advice and perspectives during my annual milestone meetings. I also want to thank Megumi Fujita, my undergraduate advisor, for giving me my first research experience at the University of West Georgia and starting me on the path I find myself on today.

I want to thank Shaoxiong Wu and Bing Wang from the NMR center, not only for providing help whenever I asked for it, but also for trusting me as an NMR service instructor for two years. Additionally, I want to thank Steve and Claire from the stockroom for ensuring that we were never short on supplies, including coffee every morning and doughnuts every Friday. I would like to thank Ana Velez and Kira Walsh for keeping the graduate program running smoothly.

The graduate experience is only as good as the people you share it with, and five years' worth of Blakey lab members have made mine an experience to remember. Eric, I cannot thank you enough for being an awesome mentor for my first couple of years. I did not realise how important your presence was to me until you left, and Team Alkaloids was suddenly whittled down to one. Robert, you are such an awesome dude, and I'm so glad all your plans got messed up and your original postdoctoral advisor moved to Switzerland and you ended up in the Blakey lab. Honestly, we really lucked out there.

Caitlin, my oldest friend at Emory! I'm glad we were able to work on a project together before we were done, and also that I was able to see Abel's first few months. I have no doubt that

you are as conscientious and caring a mother as you have been a friend. Taylor, I have enjoyed watching you develop as a chemist during your time here, especially your ability to take on unfamiliar projects and familiarise yourself with brand new concepts and techniques. I'm so excited for us to go through this defence and graduation process together. Jacob (Burman), we didn't always agree with one another, but I valued our friendship, nonetheless. I will always be grateful to you for staying put and getting me out of the building when the fire nation attacked.

David and Quincy. My boys! You made the last three years so incredibly fun, it's actually ridiculous. Working in a lab without you guys will definitely take some getting used to, but I guess I'll just have to find other co-workers to bully. I hope that my latest gift of unused TLC plates is enough to make up for all the *borrowing* of lab resources you guys routinely (and baselessly) accuse me of. Finally, I want to thank all past and present Blakey lab members who have made my time at Emory an amazing experience. Alas, five and a half years is far too short a time to work among such excellent and admirable hobbits.

Other friends without whom this Ph.D. would have been a bleak affair are listed here, and in no particular order. Shahzad and Kanisha, for being my family in Atlanta for so long. Jacob (Hewell) and Phong, for being steadfast friends and always being there when I've needed them. Quinton, for helping me put together my postdoctoral applications. Tarak, Josh, and Echo, for always being ready to get B-dubs and play video games on any given weekend. Ana, for ensuring that I actually did some of the stuff on my Atlanta bucket list before leaving. Aakash and Prithvi, two of my oldest friends in the world, without whom the recent lockdown would have been impossible to endure. Rohan, just for being a bro.

Lastly, and certainly most importantly, I want to thank my family, beginning with my parents Sharmeela and Mehdi Kazerouni. I cannot even begin to articulate how lucky I am, and we are, to have two people like you in our corner. Your love and implacable support have been the bedrock of everything I have achieved or will achieve. I cannot fathom how difficult it has been for you to live on the other side of the world from us, but you made sure that we never felt the

distance. I hereby promise in writing on this super official looking document that I will call home more, because apparently texting doesn't count.

I want to thank my aunt and uncle, Madhavi and Beheruz Sethna, for giving new meaning to the phrase "home away from home". You have been a second set of parents to us here in the U.S. and having you guys just an hour away for the last few years has been more important to me than I can say. I will always be grateful for your love, advice, care, and cookies.

I owe huge thanks to my brothers, Ameen and Ayaan, my best friends in the world for as long as I've been a functioning human person. Everything I have done, or will do, is down to you. This journey was also made so much easier by my virtual Ph.D. support group, consisting of Ayaan and my sister-in-law Anum. Soon, I'll have my Ph.D. too, and we can all pick on Dadash together.

Table of Contents

Part I: Studies Towards the Synthesis of Malagasy Alkaloids

Chapter 1. Introduction to the Malagasy Alkaloids

1.1 The <i>Strychnos</i> alkaloids	1
1.2 The Malagasy alkaloids	3
1.2.1 Structure	3
1.2.2 Biological activity	4
1.2.2.1 Chloroquine resistance to <i>Plasmodium falciparum</i>	4
1.2.2.2 Antimalarial activity of the Malagasy alkaloids	6
1.2.3 Prior synthetic studies	6
1.2.3.1 Synthesis of the malagashanol core (Canesi, 2020)	6
1.2.3.2 Synthesis of 11-demethoxy-16- <i>epi</i> -myrtoidine (Tang, 2016)	8
1.3 Conclusion	9
1.4 References	10

Chapter 2. Early Synthetic Studies Towards the Malagasy Alkaloids in the Blakey Lab

2.1 Pictet-Spengler cyclisations in indole alkaloid synthesis	13
2.2 Total synthesis of aspidophytine (Corey, 1999)	15
2.3 Iminium ion cascades to access the Malagasy alkaloids	16
2.3.1 Development of the cascade annulation to assemble the Malagasy core	16
2.3.2 Expanding the scope of the cascade reaction and total synthesis of malagashanine	17
2.3.3 Electronic tuning of the hemiaminal substrates controls the regioisomeric outcome of the cascade reaction	18
2.4 Prior studies towards the synthesis of 11-demethoxymyrtoidine	20
2.5 Conclusion	22

2.6	References	23
Chapter 3. Synthetic Studies Towards 11-Demethoxymyrtoidine and Myrtoidine		
3.1	A convergent strategy towards 11-demethoxymyrtoidine and myrtoidine: installation of a pre-formed butyrolactone ring	26
3.1.1	Retrosynthetic plan	26
3.1.2	Synthesis of substrates for model systems	28
3.1.3	Synthesis of ketone 3.7 and kinetic enol triflate 3.6	29
3.1.3.1	Synthesis of Malagasy core 3.11	29
3.1.3.2	Oxidative cleavage of core structure 3.11	30
3.1.3.3	Synthesis of kinetic enol triflate 3.6	32
3.1.4	Forging the C15–C20 bond	33
3.1.4.1	Plan A – Stille coupling	33
3.1.4.2	Plan B – 1,2-addition to ketone 3.7	37
3.2	An alternate strategy to assemble the dihydropyran/furanone EF ring system – alkoxy-palladation/carbonylation cascade reaction	41
3.3	Studies towards an enantioselective cascade annulation using asymmetric ion-pairing catalysis	44
3.3.1	Chiral anion-binding catalysis	45
3.3.2	Anion-binding catalysis	47
3.3.2.1	Prior work	47
3.3.2.2	Squaramides as anion-binding asymmetric ion-pairing catalysts	48
3.4	Conclusion	52
3.5	Experimental	53
3.6	Spectral data	75
3.7	References	94

Part II: Development and Applications of Regio- and Enantioselective Group IX

Metal-Catalysed Reactions

Chapter 4. Introduction to Rh- and Ir-Catalysed Allylic C–H Functionalisation

4.1 Allylic C–H functionalisation <i>via</i> π -allyl complexes	99
4.2 Early contributions to RhCp*-catalysed allylic C–H amination	100
4.3 RhCp*-catalysed intermolecular allylic C–H functionalisation using external oxidants	101
4.3.1 Allylic C–N bond formation	101
4.3.2 Allylic C–O bond formation	103
4.3.3 Allylic C–C bond formation	103
4.3.4 Mechanistic investigations	106
4.4 Allylic C–H amidation <i>via</i> direct C–N reductive elimination from M(V) nitrenoid intermediates	107
4.4.1 RhCp*- and IrCp*-catalysed allylic C–H amidation	107
4.4.2 Mechanistic investigation	110
4.5 Conclusion	111
4.6 References	113

Chapter 5. Development of 2nd-Generation Regio- and Enantioselective Allylic C–H Functionalisation

5.1 Introduction	119
5.2 Development of alternate nitrenoid precursors for 2 nd -generation allylic C–N bond formation	121
5.2.1 Survey of alternative electrophilic amines for allylic C–H amination	121
5.2.2 Development of allylic C–H sulfamidation using tosyl azide as a nitrenoid precursor	122
5.2.3 Scope and limitations of allylic C–H sulfamidation	123

5.3 A new planar chiral catalyst for regio- and enantioselective allylic C–H amidation	125
5.3.1 Overview of known chiral piano-stool cyclopentadienyl (Cp) complexes	125
5.3.2 Introduction to the indenyl ligand	127
5.3.3 Catalyst preparation and development of enantioselective allylic C–H amidation (Dr. Caitlin Farr and Christopher Poff)	128
5.3.4 Scope and limitations of enantioselective allylic C–H amidation	130
5.3.5 Computational studies (Bohyun Park, Joongee Won, Kimberly Sharp)	133
5.4 Conclusion	135
5.5 Experimental	137
5.6 Spectral data	173
 Chapter 6. Studies Towards the Total Synthesis of Darobactin A	
6.1 Introduction	255
6.2 Darobactin A – structure and biology	257
6.3 Synthetic strategies towards related cyclophane macrocycle natural products	258
6.3.1 Synthesis of celogentin C	259
6.3.2 Synthesis of streptide	262
6.4 Evolution of synthetic strategy towards darobactin A	263
6.4.1 Initial approach – enantioselective allylic amidation/oxidative cleavage sequence	263
6.4.2 Revised approach – olefin carboamination	269
6.4.3 Current approach – iterative aminoquinoline-directed β C–H functionalisation of alanine	273
6.4.3.1 Aminoquinoline-directed β C–H alkylation of amino acids	274
6.4.3.2 Model studies with phenylalanine	276
6.4.3.3 β C–H arylation with aryl iodide	277

6.5 Conclusion and future work	279
6.6 Experimental	280
6.7 Spectral data	289
6.8 References	300

List of Figures

Chapter 1

Figure 1.1: Alkaloids isolated from *strychnos myrtoides* and *strychnos mostuoides* **3**

Chapter 2

Figure 2.1: Aspidophytine and haplophytine **15**

Chapter 3

Figure 3.1: The Malagasy alkaloids **26**

Figure 3.2: 3D depiction of ketone **3.7** **40**

Figure 3.3: Squaramide catalysts provided by the Jacobsen lab for an initial catalyst screen **50**

Chapter 5

Figure 5.1: Unnatural amino acid residues are present in diverse classes of biologically relevant small molecules **119**

Figure 5.2: Unsuccessful substrates for allylic C–H sulfamidation **124**

Figure 5.3: Known chiral “piano-stool” cyclopentadienyl (Cp) ligands **126**

Figure 5.4: The indenyl effect – transition metal indenyl complexes are known to slip between η^5 and η^3 coordination modes **127**

Figure 5.5: Assignment of absolute stereochemistry of the Rh-indenyl complex (Christopher Poff) **129**

Figure 5.6: Unsuccessful nitrenoid precursors for enantioselective allylic C–H amidation **131**

Figure 5.7: Energy coordinate diagram for the **(R,R)**-**5.44**-catalysed allylic C–H amidation of allylbenzene with *tert*-butyl dioxazolone (Bohyun Park, Joonghee Won, Kimberly Sharp) **134**

Chapter 6

Figure 6.1: General representation of RiPP biosynthesis	255
Figure 6.2: RiPPs containing cyclophane macrocycles	256
Figure 6.3: Darobactins A–E	257
Figure 6.4: Celogentin C	259
Figure 6.5: Streptide	262

List of Schemes

Chapter 1

- Scheme 1.1:** Biosynthesis of strychnine **2**
- Scheme 1.2:** Proposed biogenetic scheme of N_b,C(21)-secocuran alkaloids from strychnobrasiline **4**
- Scheme 1.3:** Synthesis of the main core of malagashanol (**1.13**) by Canesi and co-workers **7**
- Scheme 1.4:** Synthesis of 11-demethoxy-16-*epi*-myrtoidine (**16-*epi*-1.11**) by Tang and co-workers **8**

Chapter 2

- Scheme 2.1:** Pictet-Spengler cyclisations in indole alkaloid synthesis **13**
- Scheme 2.2:** Synthesis of the curan skeleton *via* an interrupted Pictet-Spengler cyclisation by Van Tamelen and co-workers **14**
- Scheme 2.3:** Synthesis of aspidophytine (**2.12**) *via* an interrupted Pictet-Spengler cascade reaction by Corey and co-workers **15**
- Scheme 2.4:** An iminium ion cascade reaction to access the tetracyclic core of the Malagasy alkaloids **16**
- Scheme 2.5:** Olefin geometry in trisubstituted allylsilanes is directly translated to the relative stereochemistry at C16 **17**
- Scheme 2.6:** Cascade annulation of oxocarbenium ion intermediates to provide the tetracyclic core of mattogrossine **18**
- Scheme 2.7:** Cascade cyclisation of substrate containing a methoxy substituent **18**
- Scheme 2.8:** Electronic tuning of the hemiaminal substrate results in a regiodivergent cascade **19**
- Scheme 2.9:** Regiodivergent cascade to access the akuammiline alkaloids **19**

Scheme 2.10 Proposed approach to 11-demethoxymyrtoidine from carboxylic acid 2.48 or methyl ester 2.49	20
Scheme 2.11: Attempts to functionalise the allylic C18 position	21
Scheme 2.12: Attempted C20 acylation of 2.57 with pre-oxidised allylic C18	21
Chapter 3	
Scheme 3.1: Convergent strategies to install a pre-formed furanone F ring	27
Scheme 3.2: Synthesis of substrates for model systems	28
Scheme 3.3: Synthesis of the tetracyclic core of the Malagasy alkaloids	29
Scheme 3.4: Attempts at direct oxidative cleavage of exocyclic olefin 3.11	30
Scheme 3.5: Attempts at oxidative cleavage of exocyclic olefin 3.11 under μW conditions	30
Scheme 3.6: Oxidative cleavage of diol 3.28 and structural assignment of ketone 3.7	32
Scheme 3.7: Previous synthesis of kinetic enol triflate 3.6 (Dr. Ricardo Delgado)	32
Scheme 3.8: TBDPS deprotection of vinyl triflate 3.6	36
Scheme 3.9: Grignard reaction with bromofuranone 3.17 predominantly forms aldol addition and condensation products	37
Scheme 3.10: Addition of silyloxyfuran 3.36 to model ketone 3.13 using Paintner's conditions for the selective C3 functionalisation of 4-alkoxy-2-furanones	37
Scheme 3.11: Some common alcohol-derived alkyl radical precursors	38
Scheme 3.12: Tertiary alcohol 3.38 is very sterically encumbered and especially prone to elimination under mildly acidic conditions	39
Scheme 3.13: Nucleophilic attack of ketone 3.7 with the lithium anion of silyloxyfuran 3.36 results in enone 3.43 as the major product	39
Scheme 3.14: The Semmelhack reaction in total synthesis	42
Scheme 3.15: Proposed Semmelhack reaction to synthesise the hexacyclic core of the myrtoidines	42

Scheme 3.16: Synthesis of alkynediol 3.54	43
Scheme 3.17: Attempted Semmelhack reaction. Trace amounts of 3.57 (tentatively assigned) were observed by LCMS	43
Scheme 3.18: Chiral anion-directed ion-pairing catalysed Pictet-Spengler reaction (Hiemstra, 2008)	45
Scheme 3.19: Prior work in the Blakey lab towards employing chiral anion-directed ion-pairing catalysis in the Malagasy cascade annulation	46
Scheme 3.20: Anion-binding ion-pairing catalysed Povarov cyclisation with a hydrogen bond-donating chiral urea catalyst (Jacobsen, 2010)	47
Scheme 3.21: Anion-binding ion-pairing catalysis with a chiral thiourea dual hydrogen bond-donor for intermolecular condensation of <i>N</i> -benzylindole (3.77) with <i>O</i> -TMS-hemiaminal (3.78) (Dr. Danny Mancheno)	47
Scheme 3.22: Enantioselective Mukaiyama aldol reaction. Squaramide catalyst enhances the Lewis acidity of TBSOTf and induces enantioselectivity by forming an anion-binding ion-pair	48
Scheme 3.23: TMSOTf mediated cascade annulation provides diene 3.86 as the major product	49
Scheme 3.24: Proposed mechanism for the formation of diene 3.86 from <i>O</i> -TMS-hemiaminal 3.26	50
 Chapter 4	
Scheme 4.1: Pd-catalysed allylic C–H functionalisation	99
Scheme 4.2: Early advances in RhCp [*] -catalysed allylic C–H functionalisation	101
Scheme 4.3: RhCp [*] -catalysed intermolecular allylic C–H amination (Dr. Jacob Burman)	102
Scheme 4.4: RhCp [*] -catalysed allylic C–H etherification using alcohols as nucleophiles (Taylor Nelson)	103

Scheme 4.5: RhCp*-catalysed allylic C–H arylation using <i>N</i> -substituted indoles as nucleophiles (Dr. Caitlin Farr)	104
Scheme 4.6: RhCp*-catalysed allylic C–H arylation using electron-rich (hetero)aromatics as nucleophiles (Glorius, 2018)	104
Scheme 4.7: RhCp*-catalysed allylic C–H arylation using triarylboroxines as nucleophiles (Glorius, 2019)	105
Scheme 4.8: Proposed catalytic cycle for RhCp*-catalysed allylic C–H amination, supported by stoichiometric, kinetic, electrochemical, and computational studies (Dr. Robert Harris, Taylor Nelson, Daniel Salgueiro, et al.)	106
Scheme 4.9: RhCp*- and IrCp*-catalysed allylic C–H amidation using dioxazolones as oxidative amidating reagents (Dr. Jacob Burman)	108
Scheme 4.10: Regioselectivity of IrCp TM -catalysed allylic C–H activation is correlated with ¹ J _{CH} coupling constants (Rovis, 2020)	109
Scheme 4.11: Development of a new Ir-catalyst for allylic C–H functionalisation (Rovis, 2020)	109
Scheme 4.12: Proposed catalytic cycle for the 2 nd -generation allylic C–H amidation	111
 Chapter 5	
Scheme 5.1: Allylic amidation/oxidative cleavage sequence to synthesise dipeptides containing non-canonical amino acid residues	119
Scheme 5.2: Initial investigations of alternate nitrenoid precursors for allylic C–N bond formation	121
Scheme 5.3: Diversification of sulfonamide products	125
Scheme 5.4: Group IX metal planar chiral complexes	128
Scheme 5.5: Synthesis and chiral resolution of planar chiral Rh(III)-indenyl complex (Dr. Caitlin Farr and Christopher Poff)	128

Scheme 5.6: Optimised reaction conditions for enantioselective allylic C–H amidation (Dr. Caitlin Farr) **129**

Chapter 6

Scheme 6.1: Total synthesis of celogentin C *via* a Knoevenagel condensation/radical Michael addition sequence (Castle, 2009) **259**

Scheme 6.2: Total synthesis of celogentinc C *via* 8-aminoquinoline-directed β C–H arylation of Leu² (Chen, 2010) **260**

Scheme 6.3: Formal synthesis of celogentin C *via* addition to a Michael acceptor equipped with a chiral auxiliary (Jia, 2010) **261**

Scheme 6.4: Total synthesis and stereochemical re-assignment of streptide (Boger, Seyedsayamdost, 2019) **263**

Scheme 6.5: Initial retrosynthetic plan to access darobactin A *via* an allylic amidation/oxidative cleavage sequence to assemble the Trp³-Lys⁵ cross-link **264**

Scheme 6.6: Preparation and racemic allylic C–H amidation of racemic homoallylic stereogenic olefin **265**

Scheme 6.7: Preparation and enantioselective allylic C–H amidation of (*R*)-**6.38** **265**

Scheme 6.8: Enantioselective amidation of 4-phenylbutene with Phth-alanine dioxazolone (Dr. Caitlin Farr) **266**

Scheme 6.9: Amino acid stereocenters racemise during dioxazolone synthesis (Quincy McKoy) **267**

Scheme 6.10: Synthesis of stereogenic amino acid-derived dioxazolones **267**

Scheme 6.11: Revised plan to establish the Trp³-Lys⁵ cross-link – stereoselective carboamination of acrylate **6.57** **269**

Scheme 6.12: CoCp*-catalysed intermolecular carboamination of acrylates *via* C(sp²)–H activation of phenoxyacetamide (Glorius, 2016) **270**

Scheme 6.13: Preliminary experiment – enantioselective carboamination of <i>N</i> -methoxyacrylamide with phenoxyacetamide	271
Scheme 6.14: Co-catalysed enantioselective intermolecular carboamination of monosubstituted acrylates and strained bicyclic olefins with aryloxyamides (Cramer, 2020)	272
Scheme 6.15: Proposed Co-catalysed enantioselective three-component carboamination with an internal acrylate, an aryl boronic acid, and a dioxazolone (Christopher Poff)	272
Scheme 6.16: Current plan to establish the Trp ³ -Lys ⁵ cross-link – iterative β C–H arylation/alkylation sequence of alanine 6.78 equipped with an 8-aminoquinoline directing auxiliary	273
Scheme 6.17: 8-Aminoquinoline-directed β C–H functionalisation of amino acids	274
Scheme 6.18: β C–H alkylation of phenylalanine with alkyl iodides lacking β hydrogen atoms (Shi, Chen, 2013)	275
Scheme 6.19: Modified conditions for β C–H alkylation of phenylalanine with alkyl iodides containing β hydrogen-atoms (Shi, 2014)	275
Scheme 6.20: Model β C–H alkylation of phenylalanine 6.81 with protected iodopropylamines	276
Scheme 6.21: β C–H alkylation of phenylalanine 6.81 with alkyl iodide 6.94	277
Scheme 6.22: Synthesis of C ₃ -alkenylated indoles 6.98 and 6.99	278
Scheme 6.23: Aminoquinoline-directed β C–H arylation with aryl bromides	278

List of Tables

Chapter 3

Table 3.1: Dihydroxylation of exocyclic olefin 3.11	31
Table 3.2: Optimising the synthesis of kinetic enol triflate 3.6	33
Table 3.3: Evaluation of reaction conditions for the Stille coupling model triflate 3.15 with vinyl stannane 3.31	34
Table 3.4: Key Stille coupling to forge the C15–C20 bond and structural assignment of coupling product 3.4	35
Table 3.5: Anion-binding ion-pairing catalysis using chiral squaramides to enhance the Lewis acidity of silyl triflates	51

Chapter 5

Table 5.1: Optimisation of allylic C–H sulfamidation of allylbenzene with tosyl azide	122
Table 5.2: Scope of olefin coupling partners	123
Table 5.3: Scope of dioxazolone coupling partners	130
Table 5.4: Scope of olefin substrates	132

Part I: Studies Towards the Synthesis of Malagasy Alkaloids

Chapter 1. Introduction to the Malagasy Alkaloids

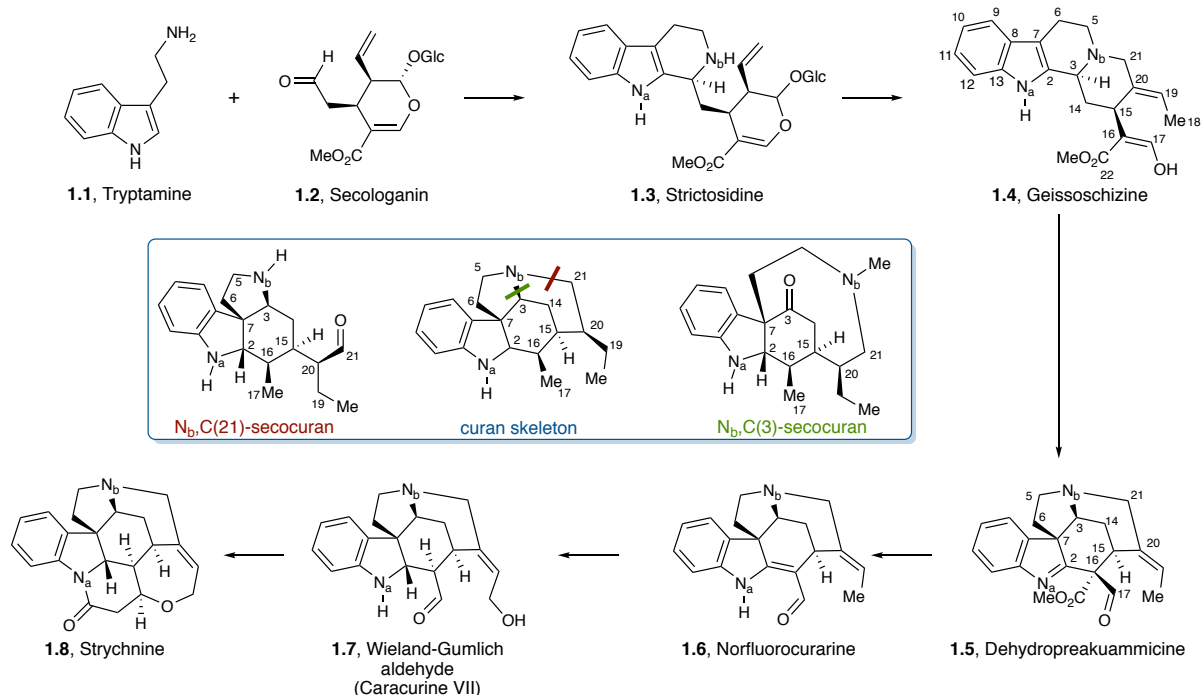
In this chapter, we will discuss the historical significance of the *Strychnos* alkaloids and their importance to the synthetic chemistry community. Following this, we will narrow our focus to the Malagasy alkaloids, a class of alkaloids belonging to the broader *strychnos* family, and consider their structure, biological activity, and prior efforts to synthesise them. Part I of this dissertation will focus on strategies for the synthesis of N_b,C(21)-secocuran Malagasy alkaloids.

1.1 The *Strychnos* alkaloids

The *Strychnos* alkaloids are an important class of indole monoterpeneoids that have been the subject of intense study due to their diverse pharmacological activities and complex polycyclic architectures.^{1,2} In the decades since Woodward's landmark synthesis of strychnine,³ arguably the most infamous member of this class of alkaloids, several *Strychnos* alkaloids have been synthesised in the laboratory, and they continue to intrigue and challenge the synthetic chemistry community.^{2,4-6} Indeed, these alkaloids continue to provide an ideal platform for the development of creative synthetic strategies and methodologies of increasing efficiency, with strychnine itself being synthesised no less than 18 times.⁷⁻¹⁰

Biogenetically (Scheme 1.1), the *Strychnos* alkaloids are thought to originate from Pictet-Spengler condensation of tryptamine (**1.1**) and secoiridoid monoterpene secologanin (**1.2**) to generate strictosidine (**1.3**).^{6,9,10} Deglycosylation further converts this to geissoschizine (**1.4**), the common intermediate and major divergence point in the biosynthesis of several different families of monoterpeneoid indole alkaloids.¹ Oxidative cyclisation and skeletal rearrangement of geissoschizine leads to dehydropreakuammicine (**1.5**), which possesses the curan skeleton

¹ The numbering system from the biogenetic precursor geissoschizine (**1.4**) and subsequent curan-type alkaloids is used throughout Part I of this dissertation.



Scheme 1.1: Biosynthesis of strychnine

(Scheme 1.1, blue inset, center) present in the majority of *Strychnos* alkaloids, characterised by a bridged pentacyclic framework with a two-carbon unit at C20 and an oxidised one-carbon unit at C16.¹¹ Dehydropreakuammicine (**1.5**) then decarboxylates to form norfluorocurarine (**1.6**). Hydroxylation and reduction of this intermediate gives rise to the Wieland-Gumlich aldehyde (caracurine VII, **1.7**), independently postulated by Woodward¹² and Robinson,¹³ and confirmed by Heimberger and Scott¹⁴ to be a biogenetic precursor to strychnine (**1.8**).²

Minor subsets of curan type alkaloids – the *N_b,C(3)-* and *N_b,C(21)-*secocuran Malagasy alkaloids (Scheme 1.1, blue inset, left and right)³ – have been isolated from western African shrubs *Strychnos myrtoides*, *Strychnos mostuoides*, and *Strychnos diplotricha*.^{15–17}

² Strychnine's final two carbons are derived from acetic acid.³⁴

³ *N_b,C(3)-* and *N_b,C(21)-*secocurans derive their name from the cleavage (“seco-”) of the *N_b-C3* and *N_b-C21* bonds, respectively.

1.2 The Malagasy alkaloids

1.2.1 Structure

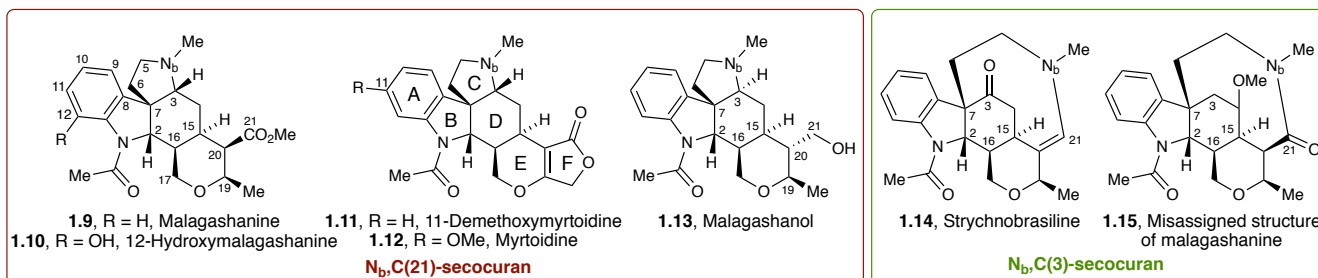
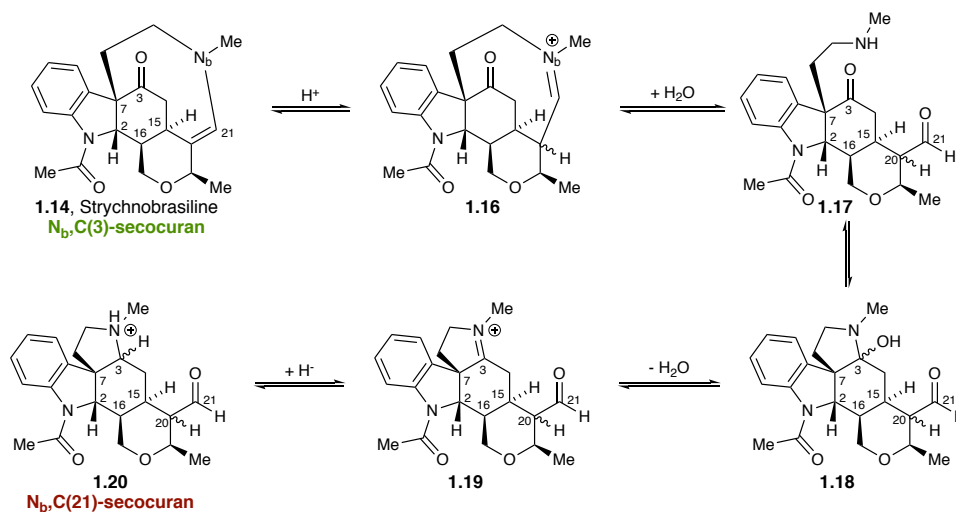


Figure 1.1: Alkaloids isolated from *Strychnos myrtoides* and *Strychnos mostuoides*

Ethnobotanical studies conducted in the western regions of Madagascar in the early 1990s have shown that local populations self-treat malaria by using low doses of chloroquine in combination with adjuvants from local shrubs *Strychnos myrtoides* and *Strychnos mostuoides*.^{18,19} Several alkaloids have been isolated and characterised from these plants, including malagashanine (**1.9**), 12-hydroxymalagashanine (**1.10**), 11-demethoxymyrtoidine (**1.11**), myrtoidine (**1.12**), malagashanol (**1.13**), and strychnobrasiline (**1.14**). Minor C3 epimers of 11-demethoxymyrtoidine (**1.11**) and myrtoidine (**1.12**), as well as C19 epimers of 12-hydroxymalagashanine (**1.10**) were also isolated (Figure 1.1).^{15–17}

The structure of malagashanine was initially assigned to be N_b,C(3)-secocuran **1.15**, which was structurally similar to the major previously isolated alkaloid strychnobrasiline (**1.14**).¹⁸ In a follow up study, the correct structure of malagashanine (**1.9**) was unambiguously established by X-ray crystallography.²⁰ Thus, malagashanine (**1.9**) was the first in a new series of N_b,C(21)-secocuran alkaloids. However, unlike the broader class of *Strychnos* and *Aspidosperma* alkaloids, which possess a *syn*-stereochemical relationship between the C2–H, C7–C6, and C3–H bonds, alkaloids **1.9–1.12** display inverted stereochemistry at C3, resulting in a synthetically challenging *trans* fusion between the C and D rings. This stereochemical peculiarity is absent in malagashanol (**1.13**), which additionally contains a *trans* relative stereochemical relationship between C19 and C20, another structural divergence from the malagashanines (**1.9** and **1.10**). Additionally,

myrtoindines **1.11** and **1.12** contain a butyrolactone moiety (F ring) that is absent in all other Malagasy alkaloids.^{16,17}



Scheme 1.2: Proposed biogenetic scheme of $N_b,C(21)$ -secocuran alkaloids from strychnobrasiline (**1.14**)

A biogenetic pathway for the formation of $N_b,C(21)$ -secocuran alkaloids from strychnobrasiline (**1.14**) was proposed by Martin et. al. (Scheme 1.2).¹⁶ Protonation of the enamine and subsequent hydrolysis of the resulting iminium ion **1.16** provides an aldehyde with a pendant secondary amine **1.17**. Condensation with the C3 ketone provides iminium ion **1.19** which can be reduced to form the $N_b,C(21)$ -secocuran core **1.20** of the Malagasy alkaloids. In addition to explaining the formation of the $N_b,C(21)$ -secocuran series of alkaloids, this proposed scheme also accounts for the co-occurrence of minor C3 and C20 epimers of these alkaloids. In a biomimetic synthetic approach to malagashanine (**1.9**) from strychnobrasiline (**1.14**),²¹ it was found that reduction of the C3 iminium ion occurred primarily from the bottom face, providing the C3 epimer of malagashanine. The parent alkaloid itself was never observed.

1.2.2 Biological activity

1.2.2.1 Chloroquine resistance in *Plasmodium falciparum*

Despite global efforts to control and eliminate malaria, it remains a major health concern resulting in an estimated 405,000 deaths from 218 million cases in 2018, with the World Health Organisation (WHO) African region carrying a disproportionately high number of cases (~93%).

The WHO recommends artemisinin-based combination therapies (ACTs) as the first-line treatment for *Plasmodium falciparum* malaria. However, chloroquine remains the treatment of choice in some countries, particularly against *P. vivax* malaria in areas where resistant strains have not yet developed.²² Despite the initial effectiveness of chloroquine in treating *P. falciparum* malaria, chloroquine-resistant (CQR) strains of the parasite are responsible for 80% of infections and 90% of malaria-related deaths,²³ highlighting the importance of understanding the mechanism by which resistance to antimalarial drugs like chloroquine is developed.

P. falciparum grows in the red blood cell by ingesting haemoglobin from the cytosol of the host and degrading it in the digestive vacuole (DV) to its component peptides – essential nutrients required for the parasite to grow – and heme, which is incorporated into an inert crystalline polymer, hemozoin. Without this biocrystallisation, heme can be toxic in large concentrations.²⁴ Chloroquine activity against chloroquine-sensitive (CQS) parasites is a result of the diffusion and accumulation of chloroquine in the DV. While unprotonated chloroquine can diffuse freely through the plasmodium membrane, it gets protonated in the acidic DV producing charged species which cannot permeate through the membrane.²⁵ Once accumulated inside the DV, chloroquine is believed to interfere with the parasite detoxification process by binding to heme and preventing its incorporation into hemozoin, leading to increased concentrations and damage to the plasmodium membranes.²⁶

CQR *Plasmodium falciparum* has been shown to accumulate significantly less chloroquine than CQS parasites, leading to the observed drug resistance.^{27,28} This decreased accumulation has been correlated with point mutations in the *P. falciparum* chloroquine resistance transporter (PfCRT) protein, though the cause for this is the subject of debate. One hypothesis is that the mutations cause alterations in the pH of the DV resulting in reduced diffusion of chloroquine as well as lower binding affinity to heme. Another possibility is increased efflux of chloroquine from CQR strains of the parasite.²⁹

1.2.2.2 Antimalarial activity of the Malagasy alkaloids

While the crude alkaloid extract of *S. myrtoides* alone displayed no antimalarial activity, significant enhancement of chloroquine action was observed against CQR strains of *P. falciparum*. In particular, malagashanine (**1.9**) and strychnobrasiline (**1.14**), the major alkaloid extracts from *S. myrtoides* and *S. mostuoides*, were shown to potentiate chloroquine activity. The crude alkaloid extract also displayed *in vivo* chloroquine potentiating activity against CQR strains of *P. yoelii*.¹⁸ Similarly, alkaloids **1.2-1.5** also potentiated *in vitro* chloroquine activity against CQR strains of *P. falciparum*, albeit to a lesser extent.¹⁶

As alluded to earlier, possible factors contributing to chloroquine resistance include decreased influx of chloroquine into the digestive vacuoles (DV) of CQR parasites, or increased chloroquine efflux from CQR parasites, or both. Rasoanaivo and co-workers demonstrated that chloroquine efflux from CQR strains of *P. falciparum* that were pre-loaded with isotopically labelled chloroquine was inhibited by malagashanine (**1.9**). In the same report, the authors showed that malagashanine (**1.9**) also likely activates chloroquine influx into resistant parasites.³⁰

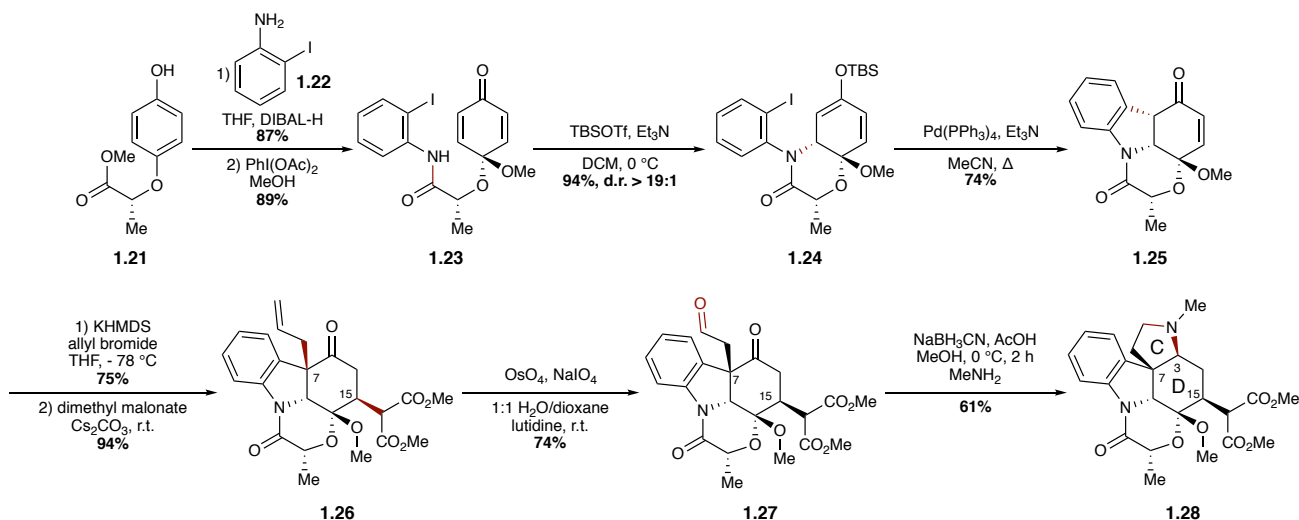
1.2.3 Prior synthetic studies

While the broader family of *strychnos* alkaloids have received considerable attention from the synthetic community, culminating in some truly elegant total syntheses, remarkably little progress has been made towards the synthesis of the N_b,C(21)-secocuran Malagasy alkaloids. The only completed total synthesis from this sub-family of alkaloids was published by the Blakey Lab in 2017 and will be discussed in greater detail in Chapter 2 of this dissertation. The rest of this chapter will focus on prior external synthetic efforts towards these alkaloids. These reports were published while the studies presented in Part 1 of this dissertation were ongoing.

1.2.3.1 Synthesis of the malagashanol core (Canesi, 2020)

Malagashanol (**1.13**) is one of the minor alkaloids isolated from the stem bark of *Strychnos myrtoides* in 1999.¹⁶ There have been no total syntheses of this natural product to date, although Canesi and co-workers reported the synthesis of the main core of this alkaloid in 2020.³¹ Their

strategy centred around the synthesis of a densely functionalised common advanced intermediate which could ostensibly serve as a divergence point for the synthesis of several *strychnos* alkaloids.



Scheme 1.3: Synthesis of the main core of malagashanol (**1.13**) by Canesi and coworkers

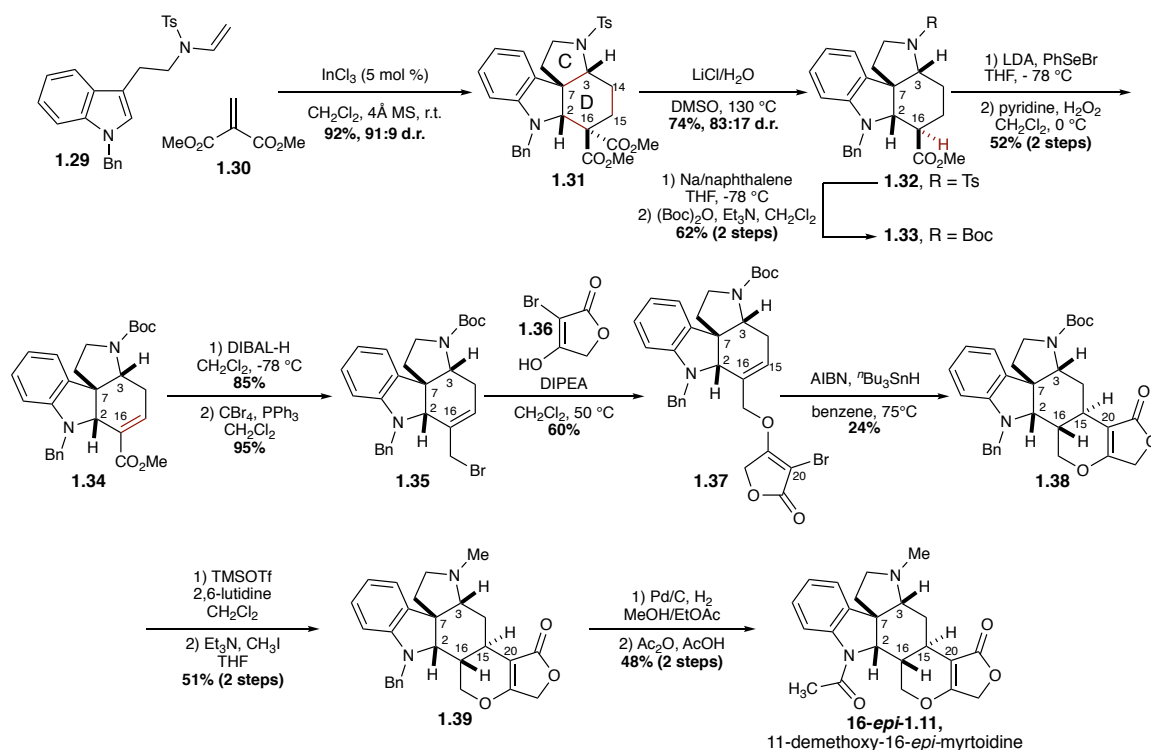
To this end, phenol **1.21** was condensed with the aluminate salt of 2-iodoaniline (**1.22**) to form the corresponding amide in 87% yield. Oxidative dearomatization with $\text{PhI}(\text{OAc})_2$ provided dienone **1.23** (89% yield) which was set up for an aza-Michael addition with the pendant amide, and the resulting enolate was trapped with TBSOTf to provide **1.24** in 94% yield. The excellent diastereoselectivity of this process could be attributed to the presence of the lactate derivative on the amide. Intramolecular cross-coupling with the pendant enolate then closed the indoline ring to provide the key tetracyclic intermediate **1.25** in 74% yield in a 95:5 mixture of diastereomers.⁴ Allylation of intermediate **1.25** (78% yield) to set the C7 quaternary center, followed by another Michael addition at C15 with dimethyl malonate provided intermediate **1.26** (94% yield). Lemieux-Johnson oxidative cleavage of the terminal olefin provided aldehyde **1.27** in 74% yield. Finally, a double reductive amination with methylamine furnished the pyrrolidine moiety present in the secocuran core of the Malagasy alkaloids in 61% yield (**1.28**). Unfortunately, this method

⁴In addition to the malagashanol core, intermediate **1.25** was advanced to the core structures of isosplendine and strychnosplendine, and was used to complete the synthesis of strychnopivotine.³⁵

of installing the C3 stereocenter is limited to the Malagasy alkaloids containing the *cis* fusion between the C and D rings.

1.2.3.2 Synthesis of 11-demethoxy-16-*epi*-myrtoidine (Tang, 2016)

11-Demethoxymyrtoidine (**1.11**) is one of the N_b,C(21)-secocuran Malagasy alkaloids isolated from *strychnos myrtoides*, containing the synthetically challenging *trans* fusion between the C and D rings. Despite almost three intervening decades since its isolation, no total synthesis of this alkaloid has been reported. In 2016, Tang and coworkers reported the development of a formal [2+2+2] cascade reaction to assemble the tetracyclic core of the Malagasy alkaloids, and the subsequent synthesis of the C16 epimer of 11-demethoxymyrtoidine (**16-*epi*-1.11**).³²



Scheme 1.4: Synthesis of 11-demethoxy-16-*epi*-myrtoidine (**16-*epi*-1.11**) by Tang and coworkers

Thus, vinyltryptamine **1.29** was treated with methyl acrylate (**1.30**) and a Lewis acid catalyst to provide tetracyclic core **1.31** in 92% yield and 91:9 d.r. This reaction sets the relative stereochemistry at C2, C7, and C3, and notably results in a *trans* fusion between the C and D rings in the major diastereomer, due to the inverted stereochemistry at C3. Krapcho decarboxylation then set the relative stereochemistry at C16 (**1.32**, 74% yield, 83:17 d.r.). However, following

protecting group manipulations (**1.32** → **1.33**), the C16 stereochemistry was ablated by selenoxide elimination to provide **1.34**. Reduction and Appel bromination provided **1.35**, which could be substituted with bromotetronic acid **1.36** to provide **1.37**. Radical cyclisation of **1.37** furnished the hexacyclic skeleton of the myrtoïdines **1.38**; however, the relative stereochemistry at C16 was inverted. Protecting group manipulations of intermediate **1.38** then completed the synthesis of 11-demethoxy-16-*epi*-myrtoïdine (**16-epi-1.11**).

1.3 Conclusion

The *Strychnos* alkaloids are class of monoterpenoid indole alkaloids which have been popular targets for synthetic chemists for a long time due to their challenging polycyclic architectures and compelling pharmacological activities. In particular, the Malagasy alkaloids, secocurans isolated from shrubs in western Madagascar, exhibit chloroquine potentiating activity in CQR strains of *P. falciparum* malaria. Although ACTs are the first-line treatment for malaria, they are not readily available to most households in developing countries due to their prohibitive costs. On the other hand, the effectiveness, low cost, and ease of manufacture of chloroquine makes it a more preferred drug.³³ Therefore, a clearer understanding of how chemosensitisers like the Malagasy alkaloids can potentiate chloroquine activity in CQR parasites is of paramount importance. However, the Malagasy alkaloids have received very little attention from the synthetic chemistry community. Chapter 2 of this dissertation will focus on prior work in the Blakey lab on the development of a cascade strategy to diastereoselectively access the tetracyclic core of these alkaloids.

1.4 References

- (1) Brown, R. T. *INDOLES -The Monoterpenoid Indole*; Wiley, **1983**, 25.
- (2) Bosch, J.; Bonjoch, J.; Amat, M. Chapter 2 The Strychnos Alkaloids. In *Alkaloids: Chemistry and Pharmacology*; Academic Press Inc., **1996**, 48, 75–189.
- (3) Woodward, R. B.; Cava, M. P.; Ollis, W. D.; Hunger, A.; Daeniker, H. U.; Schenker, K. The Total Synthesis of Strychnine. *J. Am. Chem. Soc.* **1954**, 4749–4751.
- (4) Boonsombat, J.; Zhang, H.; Chughtai, M. J.; Hartung, J.; Padwa, A. A General Synthetic Entry to the Pentacyclic Strychnos Alkaloid Family, Using a [4 + 2]-Cycloaddition/Rearrangement Cascade Sequence. *J. Org. Chem.* **2008**, 73, 3539–3550.
- (5) He, W.; Wang, P.; Chen, J.; Xie, W. Recent Progress in the Total Synthesis of: Strychnos Alkaloids. *Org. and Biomol. Chem.* **2020**, 1046–1056.
- (6) Saya, J. M.; Ruijter, E.; Orru, R. V. A. Total Synthesis of Aspidosperma and Strychnos Alkaloids through Indole Dearomatisation. *Chem. Eur. J* **2019**, 8916–8935.
- (7) Mori, M. Total Synthesis of Strychnine. *Heterocycles* **2010**, 81, 259–292.
- (8) Ohshima, T.; Xu, Y.; Takita, R.; Shibasaki, M. Enantioselective Total Synthesis of (-)-Strychnine: Development of a Highly Practical Catalytic Asymmetric Carbon-Carbon Bond Formation and Domino Cyclisation. In *Tetrahedron* **2004**, 60, 9569–9588.
- (9) Bonjoch, J.; Solé, D. Synthesis of Strychnine. *Chem. Rev.* **2000**, 100, 3455–3482.
- (10) Cannon, J. S.; Overman, L. E. Is There No End to the Total Syntheses of Strychnine? Lessons Learned in Strategy and Tactics in Total Synthesis. *Angew. Chem. Int. Ed.* **2012**, 51, 4288–4311.
- (11) Le Men, J.; Taylor, W. I. A Uniform Numbering System for Indole Alkaloids. *Experientia* **1965**, 21, 508–510.
- (12) Woodward, R. B. Biogenesis of the Strychnos Alkaloids. *Nature* **1948**, 162, 155–156.
- (13) Robinson, R. The Structural Relations of Natural Products. In *Oxford University Press*; **1955**, 112
- (14) Heimberger, S. I.; Scott, A. I. Biosynthesis of Strychnine. *J. Chem. Soc. Chem. Commun.* **1973**, 6, 217–218.
- (15) Rasoanaivo C.; Galeffi, G.; De Vincente, Y.; Nicoletti, M. Malagashanine and Malagashine, Two Alkaloids of Strychnos Mostueoides. *Rev. Latinoam. Quim.* **1991**, 22, 32–34.

- (16) Martin, M.-T.; Rasoanaivo, P. R.; Palazzino, G.; Galeffi, C.; Nicoletti, M.; Trigalo, F.; Frappier, F. Minor Nb,C(21)-Secocuran Alkaloids of *Strychnos Myrtoides*. *Phytochemistry* **1999**, *51*, 479–486.
- (17) Rasoanaivo, P.; Palazzino, G.; Nicoletti, M.; Galeffi, C. The Co-Occurrence of C(3) Epimer Nb,C(21)-Secocuran Alkaloids in *Strychnos Diplotricha* and *Strychnos Myrtoides*. *Phytochemistry* **2001**, *56*, 863–867.
- (18) Rasoanaivo, P.; Ratsimamanga-Urverg, S.; Milijaona, R.; Rafatro, H.; Rakoto-Ratsimamanga, A.; Galeffi, C.; Nicoletti, M. In Vitro and in Vivo Chloroquine-Potentiating Action of *Strychnos Myrtoides* Alkaloids against Chloroquine-Resistant Strains of *Plasmodium Malaria*. *Planta Med.* **1994**, *60*, 13–16.
- (19) Rasoanaivo, P.; Petitjean, A.; Ratsimamanga-Urverg, S.; Rakoto-Ratsimamanga, A. Medicinal Plants Used to Treat Malaria in Madagascar. *J. Ethnopharmacol.* **1992**, *37*, 117–127.
- (20) Cairra, M. R.; Rasoanaivo, P. Structure of Malagashanine, a New Alkaloid with Chloroquine-Potentiating Action. *J. Chem. Crystallogr.* **1995**, *25*, 725–729.
- (21) Trigalo, F.; Joyeau, R.; Pham, V. C.; Youté, J. J.; Rasoanaivo, P.; Frappier, F. Synthesis of Modulators of Chloroquine Resistance in *Plasmodium Falciparum*, Analogues of Malagashanine from *Strychnobrasiline*. *Tetrahedron* **2004**, *60*, 5471–5474.
- (22) World malaria report 2019 <https://www.who.int/news-room/feature-stories/detail/world-malaria-report-2019> (accessed May 5, 2020).
- (23) Mangoyi, R.; Hayeshi, R.; Ngadjui, B.; Ngandeu, F.; Bezabih, M.; Abegaz, B.; Razafimahefa, S.; Rasoanaivo, P.; Mukanganyama, S. Glutathione Transferase from *Plasmodium Falciparum* - Interaction with Malagashanine and Selected Plant Natural Products. *J. Enzyme Inhib. Med. Chem.* **2010**, *25*, 854–862.
- (24) Chinappi, M.; Via, A.; Marcatili, P.; Tramontano, A. On the Mechanism of Chloroquine Resistance in *Plasmodium Falciparum*. *PLoS One* **2010**, *5*, 14064.
- (25) Homewood, C. A.; Warhurst, D. C.; Peters, W.; Baggaley, V. C. Lysosomes, PH and the Anti-Malarial Action of Chloroquine [9]. *Nature*. Nature Publishing Group 1972, *235*, 50–52.
- (26) Sugioka, K.; Shimosegawa, Y.; Nakano, M. Estrogens as Natural Antioxidants of Membrane Phospholipid Peroxidation. *FEBS Lett.* **1987**, *210*, 37–39.
- (27) Fitch, C. D. *Plasmodium Falciparum* in Owl Monkeys: Drug Resistance and Chloroquine Binding

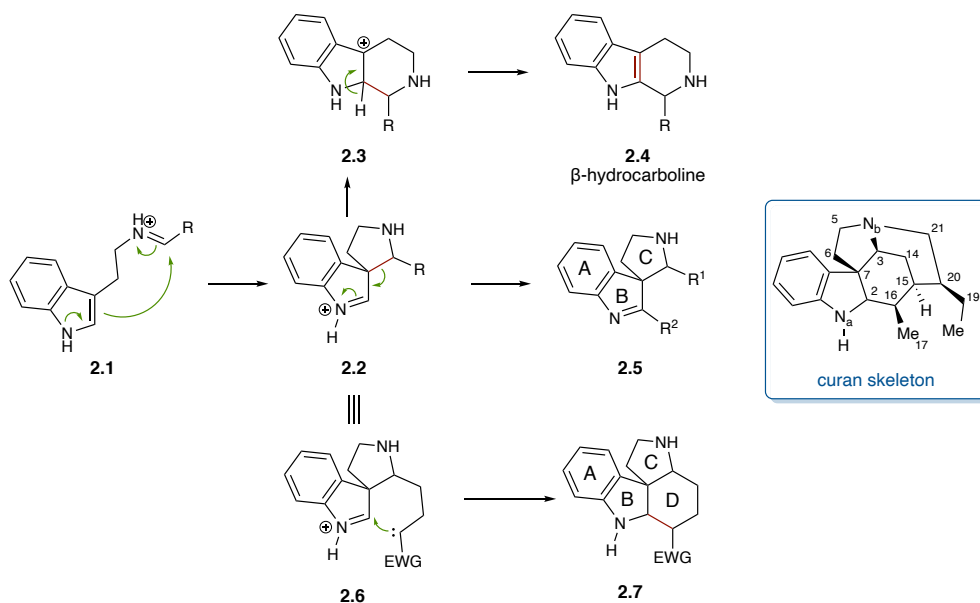
- Capacity. *Science* **1970**, *169*, 289–290.
- (28) Saliba, K. J.; Allen, R. J. W.; Zisis, S.; Bray, P. G.; Ward, S. A.; Kirk, K. Acidification of the Malaria Parasite's Digestive Vacuole by a H⁺-ATPase and a H⁺-Pyrophosphatase. *J. Biol. Chem.* **2003**, *278*, 5605–5612.
- (29) Bray, P. G.; Martin, R. E.; Tilley, L.; Ward, S. A.; Kirk, K.; Fidock, D. A. Defining the Role of PfCRT in Plasmodium Falciparum Chloroquine Resistance. *Mol. Microbiol.* **2005**, *56*, 323–333.
- (30) Ramanitrahasimbola, D.; Rasoanaivo, P.; Ratsimamanga, S.; Vial, H. Malagashanine Potentiates Chloroquine Antimalarial Activity in Drug Resistant Plasmodium Malaria by Modifying Both Its Efflux and Influx. *Mol. Biochem. Parasitol.* **2006**, *146*, 58–67.
- (31) Maertens, G.; Deruer, E.; Denis, M.; Canesi, S. Common Strategy for the Synthesis of Some Strychnos Indole Alkaloids. *J. Org. Chem.* **2020**, *85*, 6098–6108.
- (32) Zhu, J.; Cheng, Y.-J.; Kuang, X.-K.; Wang, L.; Zheng, Z.-B.; Tang, Y. Highly Efficient Formal [2+2+2] Strategy for the Rapid Construction of Polycyclic Spiroindolines: A Concise Synthesis of 11-Demethoxy-16-Epi-Myrtoidine. *Angew. Chemie Int. Ed.* **2016**, *55*, 9224–9228.
- (33) Slater, A. F. G. Chloroquine: Mechanism of Drug Action and Resistance in Plasmodium Falciparum. *Pharmacol. Ther.* **1993**, *57*, 203–235.
- (34) Schlatter, C.; Waldner, E. E.; Schmid, H.; Maier, W.; Gröger, D. Zur Biosynthese Des Strychnins. 135. Mitteilung Über Alkaloide. *Helv. Chim. Acta* **1969**, *5*, 776–789.
- (35) Maertens, G.; Canesi, S. Synthesis of the Strychnos Alkaloid (-)-Strychnopivotine and Confirmation of Its Absolute Configuration. *Chem. Eur. J.* **2016**, *22*, 7090–7093.

Chapter 2. Early Synthetic Studies Towards the Malagasy Alkaloids in the Blakey Lab

In this chapter, we will discuss the inspiration behind, and the development of, an iminium ion cascade annulation to diastereoselectively assemble the tetracyclic core of the Malagasy alkaloids by Dr. Ricardo Delgado. Following that we will discuss prior synthetic studies towards 11-demethoxymyrtoidine conducted by Dr. Danny Mancheno.

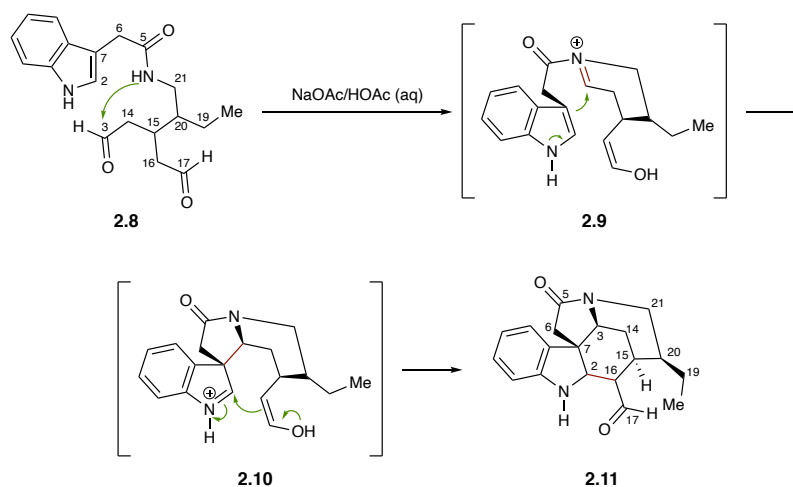
2.1 Pictet-Spengler cyclisations in indole alkaloid synthesis

Cascade reactions have been a major driving force in the total synthesis of many monoterpenoid indole alkaloids.¹⁻³ In particular, strategies involving indole dearomatisation have been widely employed to assemble the diverse polycyclic cores present in the *Strychnos* and *Aspidosperma* families.⁴ Many of these biomimetic cascade reactions have been inspired by the Pictet-Spengler cyclisation of tryptamine and secologanin to form strictosidine, the first step in the biogenetic pathway of monoterpenoid indole alkaloids (see Scheme 1.1).^{5,6}



Scheme 2.1: Pictet-Spengler cyclisations in indole alkaloid synthesis

In a typical Pictet-Spengler reaction (Scheme 2.1), tryptamine (or any electron-rich aromatic ring with a pendant amine) condenses with an aldehyde to form tryptiminium ion **2.1**, which can be nucleophilically attacked by indole C3 to form pyrrolidine-containing indolium ion **2.2**. At this stage, C2-C3 migration and subsequent rearomatisation completes the reaction to furnish β -hydrocarboline **2.4** as the final product. In the case of C2-substituted indoles (**2.5**), the intermediate cannot rearomatise and can terminate after the formation of the pyrrolidine ring, with R¹ and R² functioning as chemical handles to complete the assembly of the curan skeleton (blue inset, Scheme 2.1). In the context of indole alkaloid synthesis, this approach can efficiently furnish the ABC ring system and has been strategically implemented in the total synthesis of several monoterpenoid indole alkaloids (including strychnine). Alternatively, the Pictet-Spengler reaction can be interrupted by trapping of the indolium ion **2.6** with a pendant carbon nucleophile to complete the tetracyclic core of the curan family (**2.7**).⁴



Scheme 2.2: Synthesis of the curan skeleton *via* an interrupted Pictet-Spengler cyclisation by Van Tamelen and co-workers

A seminal example of this latter approach was reported by Van Tamelen and co-workers as early as 1960 (Scheme 2.2).⁷ Treatment of dialdehyde **2.8** with sodium acetate in acetic acid formed iminium ion **2.9** which resulted in Pictet-Spengler cyclisation to form **2.10**. The resulting indolium ion could undergo a Mannich-type cyclisation to furnish the curan core (**2.11**). This early example laid an important foundation for several subsequent syntheses of monoterpenoid indole

alkaloids using creative strategies to trap the transient indolium ion by nucleophilic attack at C2. A relevant example is Corey's 1999 synthesis of aspidophytine (**2.12**, Figure 2.1).⁸

2.2 Total synthesis of aspidophytine (Corey, 1999)

Aspidophytine (**2.12**, Figure 2.1) is a complex hexacyclic indole alkaloid characterised by a C3–C14 fused lactone. It was originally isolated by acid-mediated degradation of dimeric indole alkaloid haplophytine (**2.13**)⁹ and is considered to be its biosynthetic and potential synthetic precursor. As such, these alkaloids have been popular targets for synthetic chemists, and a number of total syntheses of both aspidophytine (**2.12**)^{8,10–15} and haplophytine (**2.13**)^{16–20} have been reported to date, beginning with Corey's pioneering construction of aspidophytine in 1999.⁸

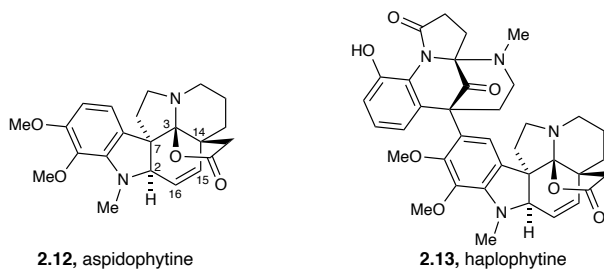
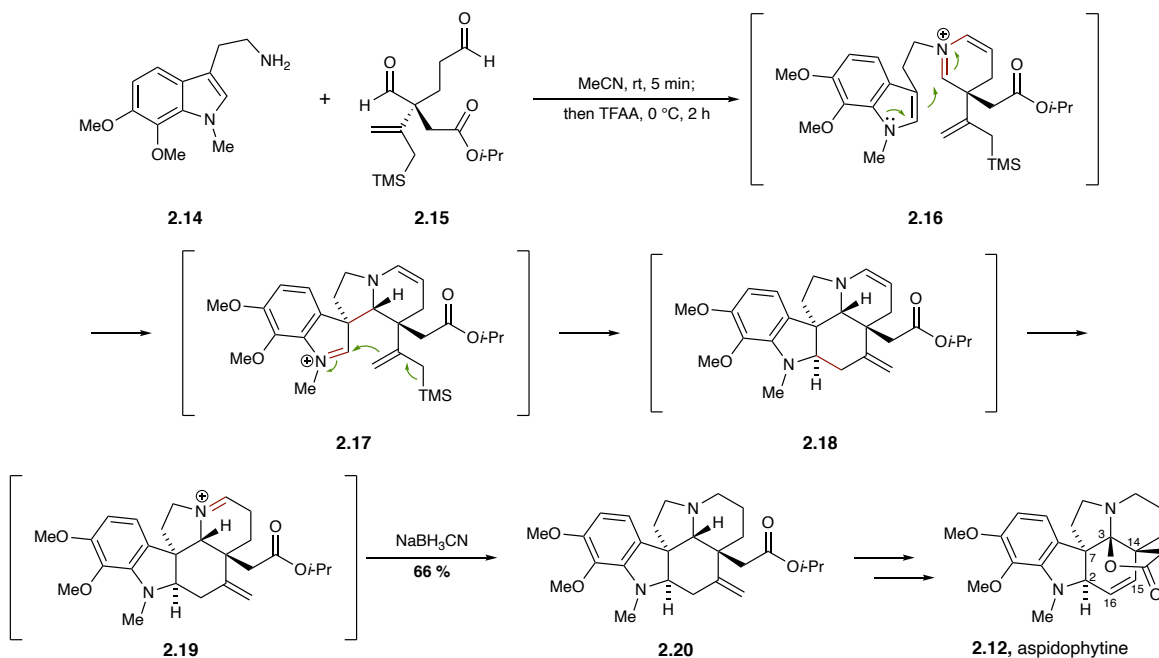


Figure 2.1: Aspidophytine and haplophytine



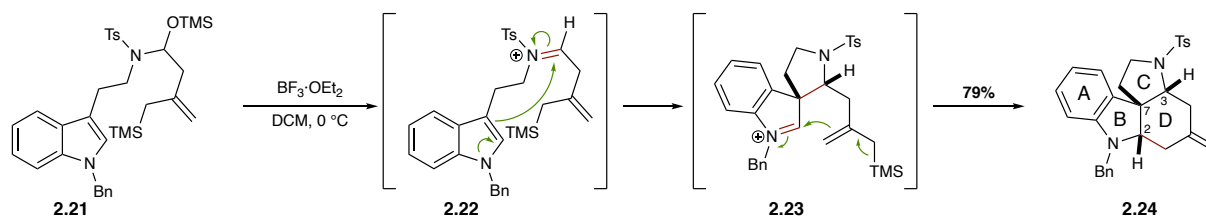
Scheme 2.3: Synthesis of aspidophytine (**2.12**) via an interrupted Pictet-Spengler cascade reaction by Corey and co-workers

The Corey group developed an elegant cascade strategy to access the *Aspidosperma* skeleton, reminiscent of Van Tamelen's interrupted Pictet-Spengler cyclisation (see Scheme 2.2). In this approach (Scheme 2.3), tryptamine **2.14** was condensed with enantioenriched dialdehyde **2.15** to form cyclic iminium ion **2.16**, which could undergo Pictet-Spengler cyclisation to form intermediate **2.17**. At this stage, intramolecular aza-Sakurai cyclisation between the pendant allylsilane and the indolium ion completed the construction of the pentacyclic core **2.18**. Finally, ionic hydrogenation of enamine **2.18** with NaBH_3CN provided **2.20** in 66% yield. Through this cascade reaction, Corey and co-workers were able to construct 3 rings and 3 contiguous stereocenters (C2, C7, and C3) present in the alkaloid, and subsequently completed the first total synthesis of aspidophytine (**2.12**).

2.3 Iminium ion cascades to access the Malagasy alkaloids

2.3.1 Development of the cascade annulation to assemble the Malagasy core

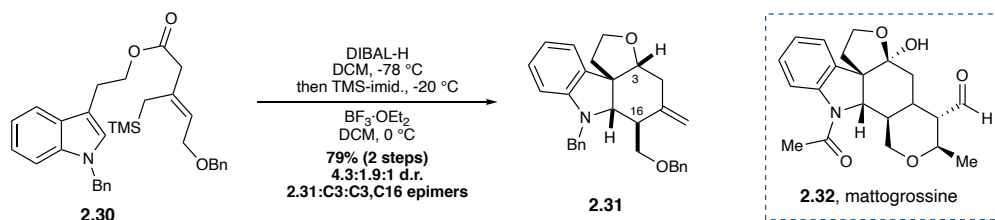
Inspired by Corey's approach to aspidophytine, Dr. Ricardo Delgado, a former graduate student in the Blakey lab, developed an iminium ion cascade reaction to access the tetracyclic skeleton of the Malagasy alkaloids (Scheme 2.4).²¹ In this sequence, Lewis acid mediated decomposition of hemiaminal **2.21** was employed to generate the required tryptiminium ion **2.22**, rather than the condensation of tryptamine with the corresponding aldehyde, as is more prevalent in Pictet-Spengler chemistry, due to the propensity of the required β,γ -unsaturated allylsilane to isomerise into conjugation with the aldehyde.⁵



Scheme 2.4: An iminium ion cascade reaction to access the tetracyclic core of the Malagasy alkaloids

⁵ The α,α -disubstitution in Corey's dialdehyde **2.15** (see Scheme 2.3) obviates the need for such a strategy to access the required iminium ion.

at C16. This intermediate was successfully carried forward to complete the first total synthesis of malagashanine (**2.29**).²²

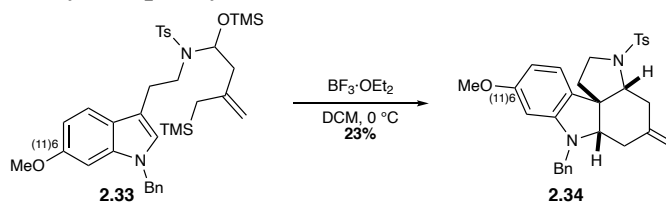


Scheme 2.6: Cascade annulation of oxocarbenium ion intermediates to provide the tetracyclic core of mattogrossine

This cascade annulation could also be extended to the cyclisation of analogous oxocarbenium ions, generated by Lewis acid-mediated decomposition of the corresponding mixed acetal intermediates (Scheme 2.6).²³ Starting from ester **2.30**, the cascade reaction provided the tetracyclic core **2.31** of mattogrossine (**2.32**), an indole alkaloid isolated from *Strychnos mattogrossensis*,²⁴ with a structurally similar pentacyclic framework as the Malagasy alkaloids.

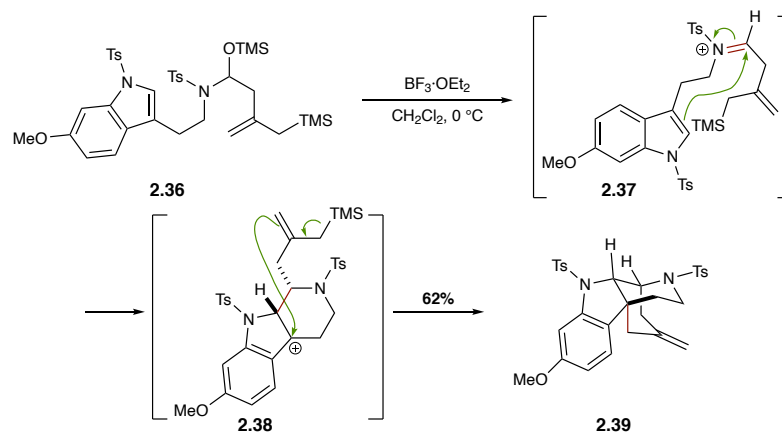
2.3.3 Electronic tuning of the hemiaminal substrates controls the regioisomeric outcome of the cascade reaction

The electronics of the nitrogen protecting groups in the hemiaminal substrates were shown to be critical to the success of the cascade cyclisation to access the Malagasy core (see Scheme 2.4).²¹ The electron-donating benzyl group on the indole nitrogen serves to enhance the C3 nucleophilicity, leading to C3 attack of the iminium ion. The strongly withdrawing tosyl group on the hemiaminal nitrogen serves to hinder Pictet-Spengler migration from C3–C2, allowing attack of the pendant allylsilane to occur competitively. Notably, an electronically similar protecting group strategy was employed in the formal [2+2+2] cascade employed by Tang and co-workers in the synthesis of 11-demethoxy-16-*epi*-myrtoidine (see Scheme 1.4).²⁵

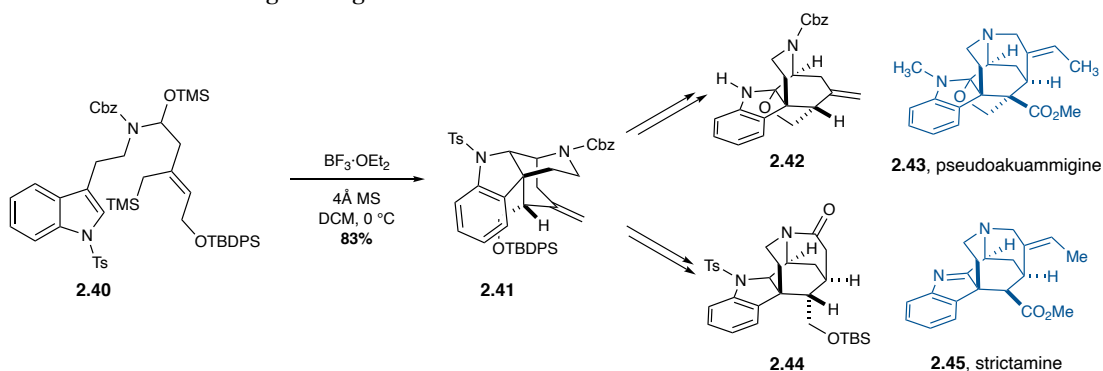


Scheme 2.7: Cascade cyclisation of substrate containing a methoxy substituent

The importance of electronic tuning of the hemiaminal substrate is underscored in the cascade reaction of hemiaminal **2.33** containing a methoxy substituent at the 6-position (Scheme 2.7).²¹ Under the standard reaction conditions, this substrate was converted to the Malagasy core in a diminished yield of 23%, instead providing the Pictet-Spengler β -hydrocarboline as the major product. It was hypothesised that the electron-donating nature of the methoxy substituent promotes C2–C3 migration, leading to the Pictet-Spengler product. This result has important implications for the synthesis of myrtoidine (see Figure 1.1), which contains a methoxy substituent at the 11-position (6-position by indole numbering), as it indicated that an iminium ion cascade strategy to access myrtoidine would likely have to involve late-stage introduction of the methoxy substituent.



Scheme 2.8: Electronic tuning of the hemiaminal substrate results in a regiodivergent cascade

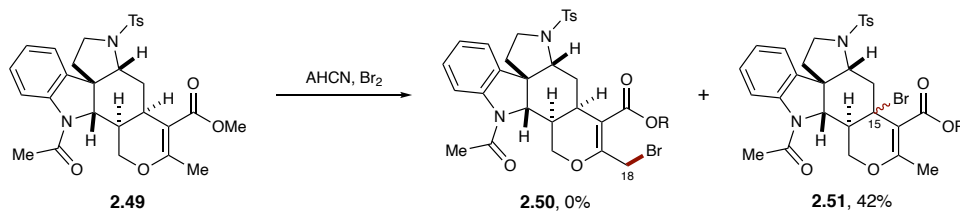


Scheme 2.9: Regiodivergent cascade to access the akuammiline alkaloids

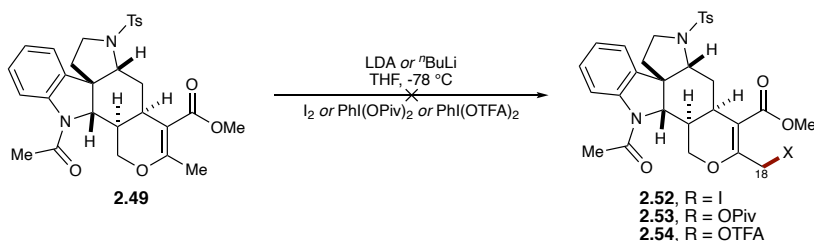
The introduction of a tosyl protecting group at the indole nitrogen (Scheme 2.8) resulted in C2 nucleophilic attack of the iminium ion **2.37** to provide C3 carbocation **2.38**, which could be

the butyrolactone product **2.55**,³¹ and instead resulted in C20 decarboxylation to provide **2.56** (Scheme 2.11 C).

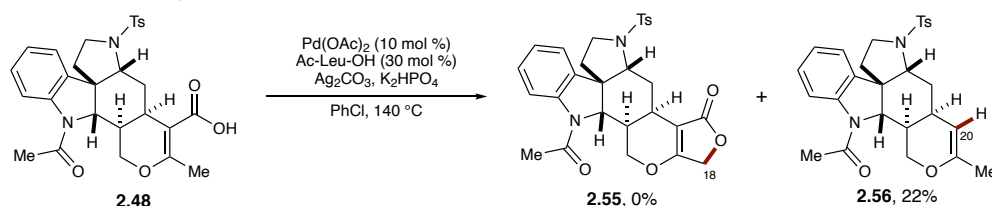
A. Radical bromination of allylic C18



B. Oxidation of C18 via an extended enolate

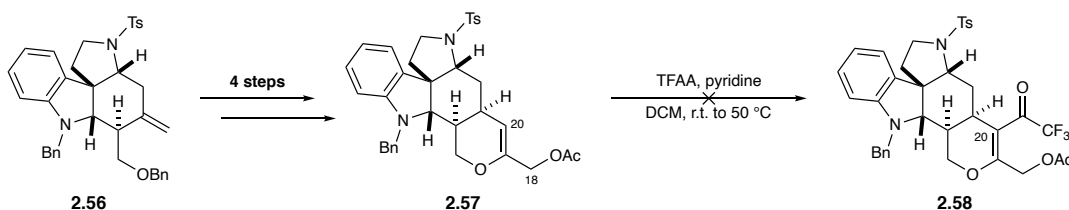


C. Direct C18-H carboxylation



Scheme 2.11: Attempts to functionalise the allylic C18 position

In a revised strategy, it was determined that the route to malagashanine could be intercepted at an earlier stage to install a pre-oxidised C18 methylene group. To this end, tetracyclic core **2.56** was converted in 4 steps to acetoxymethyl dihydropyran **2.57** (Scheme 2.12). Unfortunately, treatment with (OTFA)₂O did not yield the desired trifluoroacetate **2.58**. It was hypothesised that, under the reaction conditions, the C18 substituent is oriented to block the convex face of substrate, rendering the olefin unreactive.⁷



Scheme 2.12: Attempted C20 acylation of **2.57** with pre-oxidised allylic C18

⁷ The hydroacylation-hydrogenation-cycloetherification-dehydration sequence to build the dihydropyran moiety in **3.13** was adapted from the route to malagashanine. A C20 acylation was successful in the synthesis of malagashanine which lacks any C18 substitution.²²

2.5 Conclusion

Interrupted Pictet-Spengler cyclisations of tryptiminium ions have been creatively employed in the syntheses of several monoterpenoid indole alkaloids. Inspired by Corey's synthesis of aspidophytine, and the elegant Pictet-Spengler/aza-Sakurai cyclisation cascade developed to construct the *Aspidosperma* core, the Blakey lab developed a powerful cascade annulation to diastereoselectively assemble the tetracyclic core of the Malagasy alkaloids. This technique was subsequently used in the total synthesis of malagashanine. Additionally, a regiodivergent cascade was developed to access the isomeric core of the akuammiline alkaloids. Due to the efficiency of the Malagasy cascade reaction, a similar strategy was pursued in the total syntheses of 11-demethoxymyrtoidine and myrtoidine, two related alkaloids in the Malagasy family, and various strategies to install the additional butyrolactone moiety were developed. Chapter 3 of this dissertation will focus on new strategies to complete the synthesis of 11-demethoxymyrtoidine and myrtoidine.

2.6 References

- (1) Nicolaou, K. C.; Edmonds, D. J.; Bulger, P. G. Cascade Reactions in Total Synthesis. *Angew. Chem. Int. Ed.* **2006**, *45*, 7134–7186.
- (2) Smith, J. M.; Moreno, J.; Boal, B. W.; Garg, N. K. Cascade Reactions: A Driving Force in Akuammiline Alkaloid Total Synthesis. *Angew. Chem. Int. Ed.* **2015**, *54*, 400–412.
- (3) Nicolaou, K. C.; Chen, J. S. The Art of Total Synthesis through Cascade Reactions. *Chem. Soc. Rev.* **2009**, *38*, 2993–3009.
- (4) Saya, J. M.; Ruijter, E.; Orru, R. V. A. Total Synthesis of Aspidosperma and Strychnos Alkaloids through Indole Dearomatisation. *Chem. Eur. J.* **2019**, *25*, 8916–8935..
- (5) Bonjoch, J.; Solé, D. Synthesis of Strychnine. *Chem. Rev.* **2000**, *100*, 3455–3482.
- (6) Cannon, J. S.; Overman, L. E. Is There No End to the Total Syntheses of Strychnine? Lessons Learned in Strategy and Tactics in Total Synthesis. *Angew. Chem. Int. Ed.* **2012**, *51*, 4288–4311.
- (7) van Tamelen, E. E.; Dolby, L. J.; Lawton, R. G. A Biogenetically-Patterned Laboratory Synthesis in the Strychnine - Curare Alkaloid Series. *Tetrahedron Lett.* **1960**, *1*, 30–35.
- (8) He, F.; Bo, Y.; Altom, J. D.; Corey, E. J. Enantioselective Total Synthesis of Aspidophytine. *J. Am. Chem. Soc.* **1999**, *121*, 6771–6772.
- (9) Rae, I. D.; Rosenberger, M.; Szabo, A. G.; Willis, C. R.; Yates, P.; Zacharias, D. E.; Jeffrey, G. A.; Douglas, B.; Kirkpatrick, J. L.; Weisbach, J. A. Haplophytine. *J. Am. Chem. Soc.* **1967**, *89*, 3061–3062.
- (10) Nicolaou, K. C.; Dalby, S. M.; Majumder, U. A Concise Asymmetric Total Synthesis of Aspidophytine. *J. Am. Chem. Soc.* **2008**, *130*, 14942–14943.
- (11) Sumi, S.; Matsumoto, K.; Tokuyama, H.; Fukuyama, T. Stereocontrolled Total Synthesis of (-)-Aspidophytine. *Tetrahedron* **2003**, *59*, 8571–8587.
- (12) Mejía-Oneto, J. M.; Padwa, A. Application of the Rh(II) Cyclisation/Cycloaddition Cascade for the Total Synthesis of (±)-Aspidophytine. *Org. Lett.* **2006**, *8*, 3275–3278.

- (13) Mejía-Oneto, J. M.; Padwa, A. Total Synthesis of the Alkaloid (±)-Aspidophytine Based on Carbonyl Ylide Cycloaddition Chemistry. *Helv. Chim. Acta* **2008**, *91*, 285–302.
- (14) Satoh, H.; Ueda, H.; Tokuyama, H. Divergent Total Synthesis of (-)-Aspidophytine and Its Congeners via Fischer Indole Synthesis. *Tetrahedron* **2013**, *69*, 89–95.
- (15) Yang, R.; Qiu, F. G. General Entry to Aspidosperma Alkaloids: Enantioselective Total Synthesis of (-)-Aspidophytine. *Angew. Chemie Int. Ed.* **2013**, *52*, 6015–6018.
- (16) Satoh, H.; Ojima, K.-I.; Ueda, H.; Tokuyama, H. Bioinspired Total Synthesis of the Dimeric Indole Alkaloid (+)-Haplophytine by Direct Coupling and Late-Stage Oxidative Rearrangement. *Angew. Chem. Int. Ed.* **2016**, *55*, 15157–15161.
- (17) Doris, E. Total Syntheses of (+)-Haplophytine. *Angew. Chem. Int. Ed.* **2009**, *48*, 7480–7483.
- (18) Tian, W.; Chennamaneni, L. R.; Suzuki, T.; Chen, D. Y.-K. A Second-Generation Formal Synthesis of (+)-Haplophytine. *Eur. J. Org. Chem.* **2011**, *2011*, 1027–1031.
- (19) Nicolaou, K. C.; Dalby, S. M.; Li, S.; Suzuki, T.; Chen, D. Y.-K. Total Synthesis of (+)-Haplophytine. *Angew. Chem. Int. Ed.* **2009**, *48*, 7616–7620.
- (20) Ueda, H.; Satoh, H.; Matsumoto, K.; Sugimoto, K.; Fukuyama, T.; Tokuyama, H. Total Synthesis of (+)-Haplophytine. *Angew. Chem. Int. Ed.* **2009**, *48*, 7600–7603.
- (21) Delgado, R.; Blakey, S. B. Cascade Annulation Reactions To Access the Structural Cores of Stereochemically Unusual Strychnos Alkaloids. *Eur. J. Org. Chem.* **2009**, *2009*, 1506–1510.
- (22) Kong, A.; Mancheno, D. E.; Boudet, N.; Delgado, R.; Andreansky, E. S.; Blakey, S. B. Total Synthesis of Malagashanine: A Chloroquine Potentiating Indole Alkaloid with Unusual Stereochemistry. *Chem. Sci.* **2017**, *8*, 697–700.
- (23) Kong, A.; Andreansky, E. S.; Blakey, S. B. Stereochemical Complexity in Oxocarbenium-Ion-Initiated Cascade Annulations for the Synthesis of the ABCD Core of Mattogrossine. *J. Org. Chem.* **2017**, *82*, 4477–4483.

- (24) Angeno, L.; Belem-Pinheiro, M. L.; Imbiriba Da Rocha, A. F.; Poukens-Renwart, P.; Quetin-Leclercq, J.; Warin, R. An Indolinic Cryptoalkaloid from *Strychnos Mattogrossensis*. *Phytochemistry* **1990**, *29* (8), 2746–2749.
- (25) Zhu, J.; Cheng, Y.-J.; Kuang, X.-K.; Wang, L.; Zheng, Z.-B.; Tang, Y. Highly Efficient Formal [2+2+2] Strategy for the Rapid Construction of Polycyclic Spiroindolines: A Concise Synthesis of 11-Demethoxy-16-Epi-Myrtoidine. *Angew. Chemie Int. Ed.* **2016**, *55*, 9224–9228.
- (26) Andreansky, E. S.; Blakey, S. B. An Iminium Ion Cascade Annulation Strategy for the Synthesis of Akuammiline Alkaloid Pentacyclic Core Structures. *Org. Lett.* **2016**, *18*, 6492–6495.
- (27) Kazerouni, A. M.; Mancheno, D. E.; Blakey, S. B. Model Studies for the Total Synthesis of 11-Demethoxymyrtoidine and Myrtoidine. *Heterocycles* **2019**, *99*, 389.
- (28) Mancheno, D. E. Development of a Copper Catalyzed Aminoacetoxylation Reaction of Olefins, Development of an Intermolecular and Diastereoselective Iminium Cascade Reaction and Studies Towards the Synthesis of a Malagasy Alkaloid. Emory University, **2013**.
- (29) Ehrenstein, W.; Korte, F. Zur Darstellung von 1-Oxo-1,3,6,7-tetrahydro-5H-furo[3.4-b]-pyranen Und -thiopyranen. *Chem. Ber.* **1971**, *104*, 734–738.
- (30) Andrews, I. P.; Lewis, N. J.; McKillop, A.; Wells, A. S. Oxidation of Substituted Pyridines PyrCHRSiMe₃ (R=H, Me, Ph) and Substituted Quinolines QnCH₂SiMe₃ with Hypervalent Iodine Reagents. *Heterocycles* **1996**, *43*, 1151–1158.
- (31) Novák, P.; Correa, A.; Gallardo-Donaire, J.; Martin, R. Synergistic Palladium-Catalyzed C(sp³)-H Activation/C(sp³)-O Bond Formation: A Direct, Step-Economical Route to Benzolactones. *Angew. Chem. Int. Ed.* **2011**, *50*, 12236–12239.

Chapter 3. Synthetic Studies Towards 11-Demethoxymyrtoidine and Myrtoidine

In this chapter, we will focus on new strategies to complete the synthesis of 11-demethoxymyrtoidine and myrtoidine. We will begin with a retrosynthetic discussion of convergent strategies to install a pre-formed butyrolactone fragment while forging the C15–C20 bond of the alkaloids. We will then discuss the development of model systems to explore the feasibility of these approaches, and their subsequent application towards the synthesis of these alkaloids. Following this, we will move on to an alternate approach relying on a Semmelhack alkoxy/carbonylation/alkoxylation cascade sequence, before discussing our studies towards the development of an asymmetric iminium ion cascade annulation.

3.1 A convergent strategy towards 11-demethoxymyrtoidine and myrtoidine: installation of a pre-formed butyrolactone ring

3.1.1 Retrosynthetic plan

Previous attempts to intercept and divert the synthetic route to malagashanine (**3.3**, Figure 3.1) towards 11-demethoxymyrtoidine (**3.1**) and myrtoidine (**3.2**) had proved to be unsuccessful (see Chapter 2).^{1,2} Therefore, we chose to develop a more convergent approach to the myrtoidines and introduce a pre-formed furanone F-ring, which we anticipated would significantly streamline the syntheses of these alkaloids.

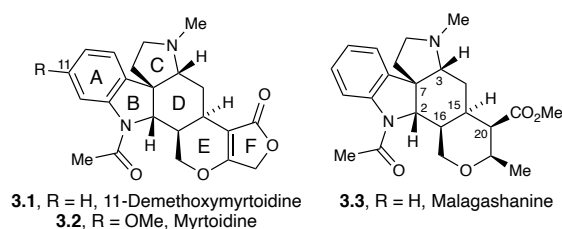
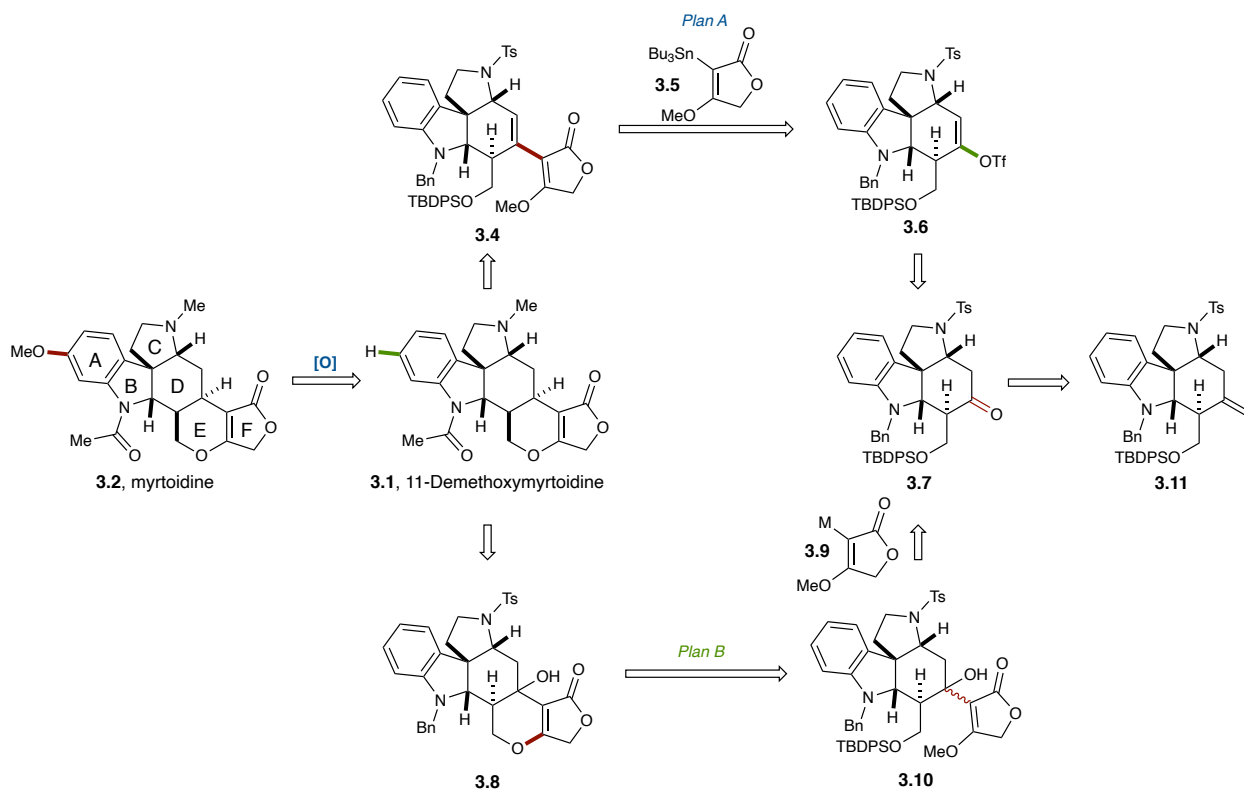


Figure 3.1: The Malagasy alkaloids

The retrosynthetic plan for this convergent approach is depicted in Scheme 3.1. Myrtoidine (**3.2**) could be accessed *via* a late-stage C11–H oxidation of 11-demethoxymyrtoidine (**3.1**). This

alkaloid could be formed by olefin reduction and cycloetherification of silyl ether **3.4** to close the E ring dihydropyran (*Plan A*). The key step in this synthesis would be the Stille cross-coupling of enol triflate **3.6** and vinylstannane **3.5** to forge the C15–C20 bond. Triflate **3.6** would be generated from the kinetic enolate of ketone **3.7**.



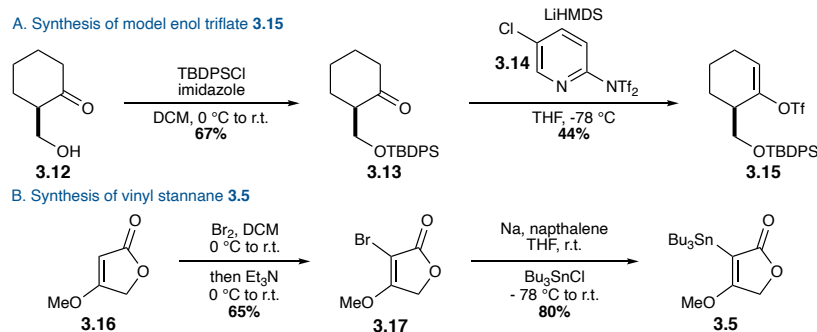
Scheme 3.1: Convergent strategies to install a pre-formed furanone F-ring

Alternatively, 11-demethoxymyrtoidine (**3.1**) could be accessed by radical deoxygenation of tertiary alcohol **3.8**, following cycloetherification of silyl ether **3.10** (*Plan B*). This tertiary alcohol would be generated by 1,2-addition of a suitable organometallic nucleophile **3.9** to ketone **3.7**, which would derive from oxidative cleavage of exocyclic olefin **3.11**. This tetracyclic core would be assembled using the previously developed iminium ion cascade annulation³ that was instrumental in the successful total synthesis of malagashanine (**3.3**),⁴ and which would stereospecifically set 4 of the 5 stereocenters present in the myrtoidines. As discussed in Chapter 2, this cascade annulation is incompatible with electron-donating substitution at the 11-position,

which results in a regiodivergent cascade reaction.^{3,5} Therefore, a late-stage C11–H oxidation of 11-demethoxymyrtoidine (**3.1**) was chosen as the optimum route to myrtoidine (**3.2**).

3.1.2 Synthesis of substrates for model systems

Before committing any advanced intermediates to the synthesis of ketone **3.7** and triflate **3.6**, we chose to conduct exploratory studies on a model system. To this end, primary alcohol **3.12**⁶ was protected with TBDPSCI to provide ketone **3.13** (Scheme 3.2 A). Deprotonation of **3.13** with excess LiHMDS at -78 °C, followed by treatment with Comins' reagent (**3.14**)⁷ selectively delivered the kinetic enol triflate **3.15** in 44% yield. The low reaction temperature was critical for selectivity for the kinetic enolate, necessitating the use of **3.14** as the triflating reagent; the cheaper alternative, phenyl triflimide (PhNTf₂), was not sufficiently reactive at -78 °C, and delivered a mixture of the kinetic and thermodynamic enol triflates at 0 °C.

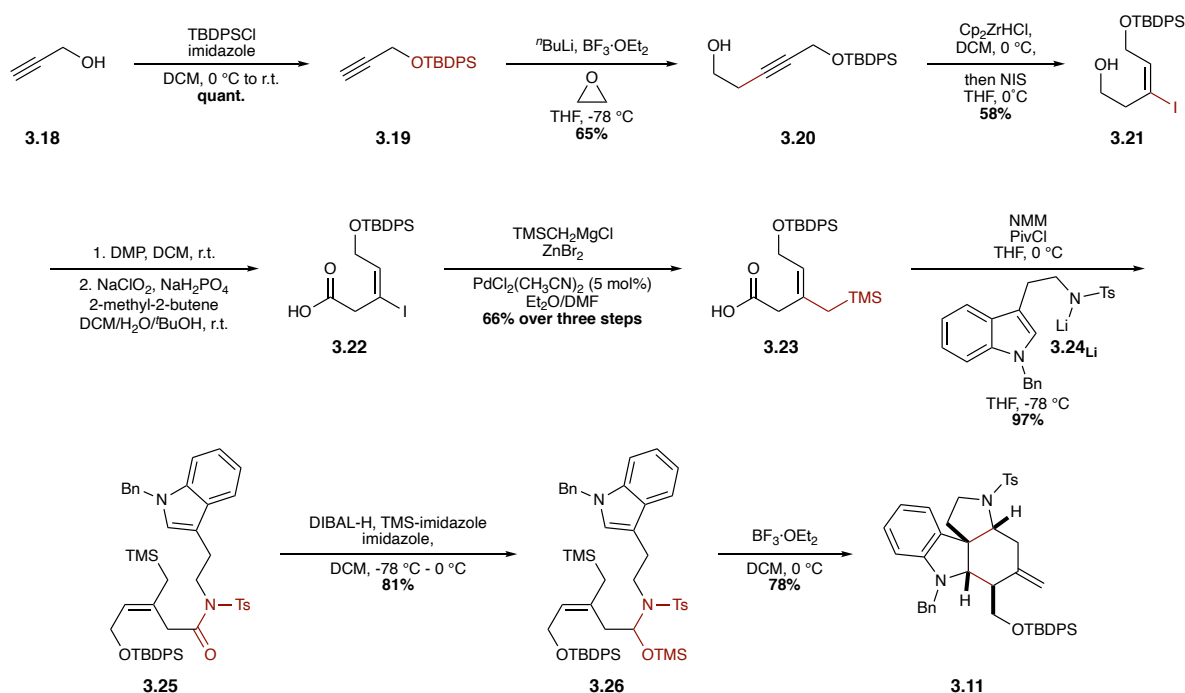


Scheme 3.2: Synthesis of substrates for model systems

Known vinylstannane **3.5** was synthesised in two steps from commercially available 4-methoxy-2(5*H*)-furanone **3.16** (Scheme 3.2 B). Dibromination and elimination of **3.16** provided vinyl bromide **3.17** in 65% yield.⁸ Reduction with freshly prepared sodium naphthalenide and treatment with tributyltin chloride provide the desired vinyl stannane **3.5** in 80% yield.⁹

3.1.3 Synthesis of ketone **3.7** and kinetic enol triflate **3.6**

3.1.3.1 Synthesis of Malagasy core **3.11**



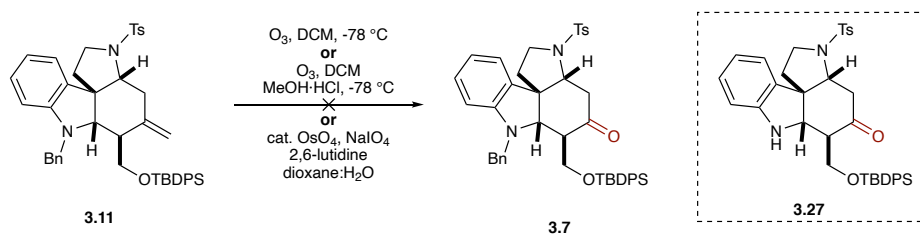
Scheme 3.3: Synthesis of the tetracyclic core of the Malagasy alkaloids

Having established a strategy to complete the synthesis of 11-demethoxymyrtoidine (**3.1**), we turned our attention to the synthesis of the tetracyclic core of the Malagasy alkaloids (**3.11**) from commercially available propargyl alcohol (**3.18**, Scheme 3.3).^{4,5} Following alcohol protection with TBDPSCl to provide **3.19**, alkyne alkylation with condensed oxirane provide homo-propargyl alcohol **3.20** in 65% yield. Alkoxide-directed hydrozirconation of the resulting internal alkyne with Schwartz's reagent according to Ready's procedure,¹⁰ followed by quenching with *N*-iodosuccinimide (NIS) regioselectively afforded alkenyl iodide **3.21** in 55% yield. As discussed in Chapter 2, the olefin geometry set at this stage is directly translated to the relative stereochemistry at C16 of the Malagasy core.⁴ Dess-Martin oxidation to the aldehyde, followed by Pinnick-Lindgren oxidation generated the carboxylic acid **3.22**, which was subjected crude to a Negishi cross-coupling with TMSCH₂MgCl and ZnBr₂ to provide the (*E*)-allylsilane **3.23** in 66% yield over three steps. Conversion of **3.23** to its mixed pivaloyl anhydride and subsequent condensation with the lithium anion of tryptamine **3.24** furnished the linear amide **3.25** in 97% yield. DIBAL-

H reduction and trapping with TMS-imidazole then generated the *O*-TMS hemiaminal **3.26**, which could be treated with $\text{BF}_3 \cdot \text{OEt}_2$ to provide the tetracyclic core **3.11** in 78% yield. Alternatively, amide **3.25** could be converted in one-pot to **3.11** by adding $\text{BF}_3 \cdot \text{OEt}_2$ to the *O*-TMS hemiaminal **3.26** reaction mixture at 0 °C.

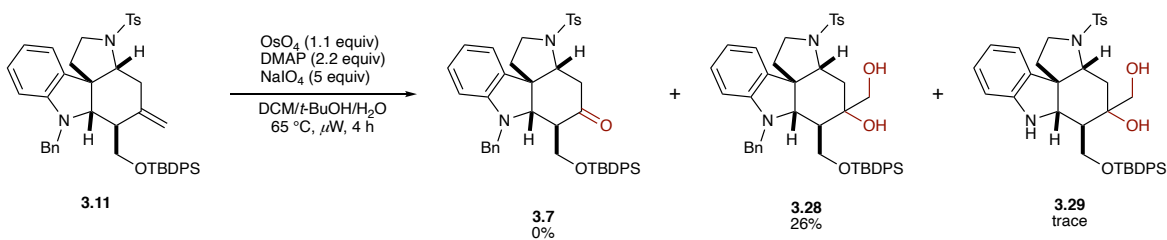
3.1.3.2 Oxidative cleavage of core structure **3.11**

With a robust and scalable route to **3.11** in hand, we examined the oxidative cleavage of the exocyclic olefin to form the corresponding ketone **3.7** (Scheme 3.4). Ozonolysis of the tetracyclic core resulted in decomposition of the starting material, presumably due to the Lewis basicity of the benzylated indoline nitrogen. We hypothesised that protonating the indoline nitrogen would protect the substrate from decomposition under the oxidative conditions. Unfortunately, ozonolysis in the presence of methanolic HCl was similarly unsuccessful, resulting in a mixture of unidentified compounds and small quantities of debenzylated ketone **3.27**. Previous work in the Blakey lab had also shown that catalytic Lemieux-Johnson oxidation was unsuccessful, leaving behind substantial amounts of unreacted starting material.¹¹



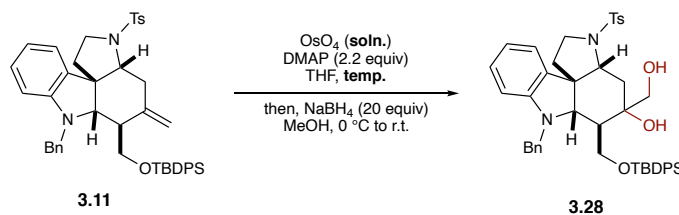
Scheme 3.4: Attempts at direct oxidative cleavage of exocyclic olefin **3.11**

We attempted to drive the reaction forward using OsO_4 (1.1 equiv) and NaIO_4 (5 equiv) in a μW reactor at 65 °C in a solvent mixture of DCM, *t*BuOH, and water (Scheme 3.5). However, after 4 hours, no trace of the desired ketone **3.7** was observed. Instead, the dihydroxylated product **3.28** was isolated in 26% yield, along with trace amounts of the debenzylated diol **3.29** (identified



Scheme 3.5: Attempts at oxidative cleavage of exocyclic olefin **3.11** under μW conditions

by HRMS). Subjecting olefin **3.11** to these conditions for 24 hours resulted in complete decomposition of the starting material and a mixture of unidentified side products.

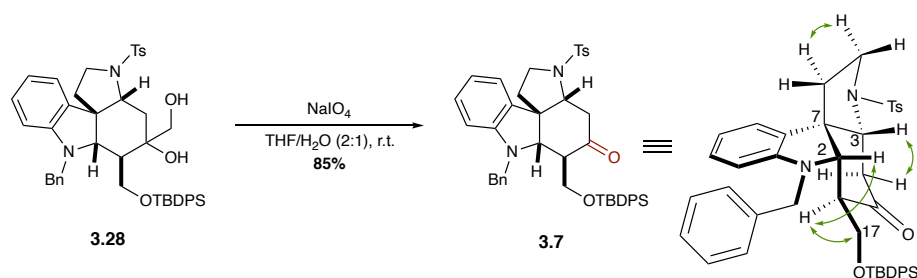


Entry	OsO_4 soln.	temp.	3.28 ^a	3.11 ^a
1	25 wt% in ^t BuOH	r.t.	33%	61%
2	25 wt% in ^t BuOH	40 °C	18%	58%
3	0.7 M in THF	r.t.	76%	—

Table 3.1: Dihydroxylation of exocyclic olefin **3.11**. ^aYields of **3.28** and recovered **3.11** are of isolated products

Given the difficulties encountered in developing a one-step oxidative cleavage reaction, we turned our attention towards developing the dihydroxylation of exocyclic olefin **3.11**. Prior work done by Dr. Ricardo Delgado has established that the osmate ester produced by the reaction of OsO_4 with **3.11** is not easily reduced with commonly used reagents like aqueous Na_2SO_3 , instead requiring a stronger reducing agent like NaBH_4 to convert to the diol product **3.28**.¹¹ With this in mind, we began optimising the dihydroxylation reaction using a NaBH_4 quench (Table 3.1). When a 25 wt% solution of OsO_4 in ^tBuOH was used, the diol product was isolated in 33% yield along with 61% of unreacted **3.11** (entry 1). In an attempt to drive the reaction to completion, the dihydroxylation was performed at a slightly elevated temperature. However, under these conditions the yield of **3.28** dropped to 18% and 58% of the olefin starting material was recovered (entry 2). We hypothesised that ^tBuOH from the OsO_4 solution could be reducing the solubility of the olefin substrate, resulting in the observed lower yields. When OsO_4 (0.7 M in THF) was used in the reaction, we observed complete consumption of the starting material and isolated diol **3.28** in 76% yield after reduction of the osmate ester with NaBH_4 (entry 3). Diol **3.28** was isolated as an inconsequential 1:1 mixture of diastereomers. The oxidative cleavage of diol **3.28** with NaIO_4 in THF/ H_2O (2:1) proceeded uneventfully to provide ketone **3.7** in 85% yield (Scheme 3.6). The structure of ketone **3.7** was assigned by COSY experiments, as well as by comparison to the

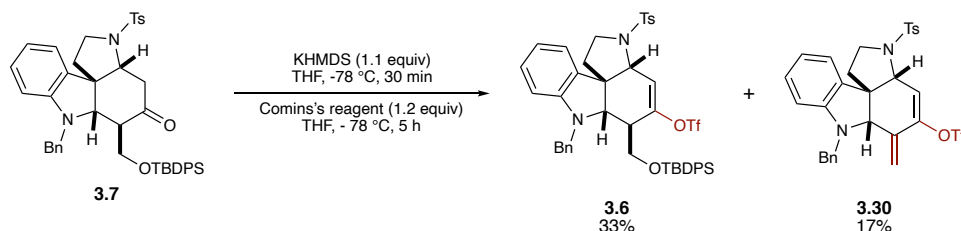
structure of the olefin precursor **3.11**. Key COSY correlations are depicted with green arrows in Scheme 3.6.



Scheme 3.6: Oxidative cleavage of diol **3.28** and structural assignment of ketone **3.7**.

3.1.3.3 Synthesis of kinetic enol triflate **3.6**

Kinetic enol triflate **3.6** has previously been synthesised in the Blakey lab by Dr. Ricardo Delgado¹¹ by treating ketone **3.7** with KHMDS (1.1 equiv) at -78 °C for 30 minutes, followed by addition of Comins' reagent (1.2 equiv)⁷ and stirring for 5 hours (Scheme 3.7). This reaction was fairly low yielding, providing the desired triflate **3.6** in 33% yield as well as unsaturated kinetic enol triflate **3.30** in 17% yield. We set out to improve the yield of the kinetic enol triflate **3.6** and suppress the formation of unsaturated triflate **3.30**, which presumably arises from deprotonation at the thermodynamic position and elimination of the silanol prior to triflate formation.



Scheme 3.7: Previous synthesis of kinetic enol triflate **3.6** (Dr. Ricardo Delgado)

We hypothesised that slow addition of the ketone **3.7** to a cold solution of excess base would improve selectivity for the formation of the kinetic enolate by suppressing equilibration to the thermodynamic product and subsequent elimination of the silanol. Thus, we subjected ketone **3.7** to the conditions developed for the synthesis of model triflate **3.15** [LiHMDS (3 equiv), Comins' reagent (3 equiv), THF, -78 °C (see Scheme 3.2 A)]. However, under these conditions, we still observed a 1.4:1 (by crude ¹H NMR) mixture of triflate **3.6** and unsaturated triflate **3.30**.

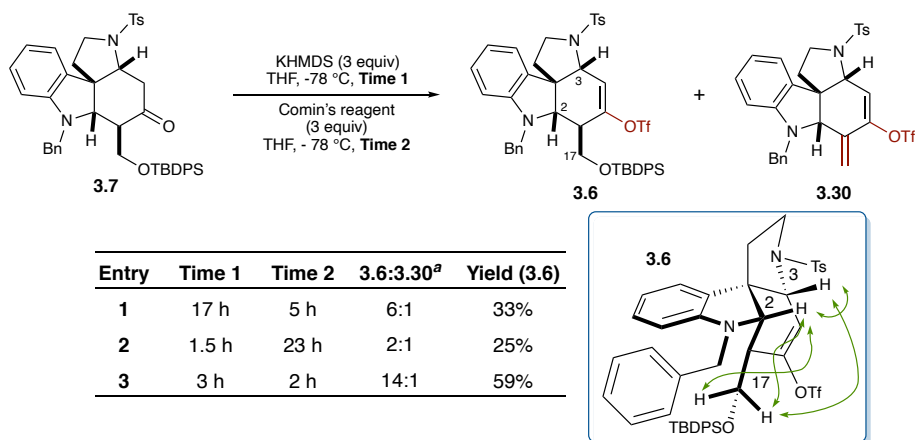


Table 3.2: Optimising the synthesis of kinetic enol triflate **3.6**. ^aRatios determined by crude ¹H NMR. Blue inset: NOESY correlations among C17-, C2-, and C3-protons

We reverted back to using KHMDS as the strong base for this reaction. With 3 equiv KHMDS and 3 equiv Comins' reagent, we evaluated the effect of varying the reaction time for each stage of the reaction (Table 3.2). We observed that allowing the reaction to stir for extended periods with KHMDS (entry 1) or with Comins' reagent (entry 2) resulted in diminished yields of the kinetic enol triflate **3.6**, and increased quantities of the unsaturated triflate **3.30**. Ultimately, we discovered that slow addition of the ketone to a solution of KHMDS (3 equiv) in THF at -78 °C was necessary. Allowing this reaction to stir at -78 °C for 2 hours, followed by addition of Comins' reagent (3 equiv) at -78 °C and stirring for 2 additional hours afforded the kinetic enol triflate **3.6** in 59% yield (entry 3). NOESY correlations among the C17-, C2-, and C3-protons indicated that no epimerisation of the C2- and C3-stereocenters was occurring (Table 3.2, blue inset) under the basic reaction conditions. We hypothesise that this difference in reactivity between Li⁺ and K⁺ bases is a result of slower conversion of the lithium enolate to the triflate as compared to the potassium enolate, allowing competitive equilibration to the thermodynamic enolate and subsequent silanol elimination.

3.1.4 Forging the C15–C20 bond

3.1.4.1 Plan A – Stille coupling

In order to test the efficacy of the Stille coupling between kinetic enol triflate **3.6** and vinyl stannane **3.5** in Plan A (see Scheme 3.1), we evaluated different reaction conditions using model

triflate **3.15** (Table 3.3). We began our investigation using Corey's conditions for the Stille cross-coupling of sterically congested systems.¹² Thus, triflate **3.15** was reacted with stannane **3.5** in the presence of Pd(PPh₃)₄ (10 mol %), LiCl (6 equiv), and CuCl (5 equiv) in dry DMSO at 60 °C for 24 hours under rigorously anaerobic conditions. LiCl is known to accelerate the oxidative addition of vinyl triflates to Pd(o) complexes.¹³ Furthermore, under these conditions, the vinyl stannane is presumed to transmetallate with CuCl to produce a vinyl Cu(I) species which accelerates the subsequent transmetallation step with the Pd(II) catalytic intermediate.

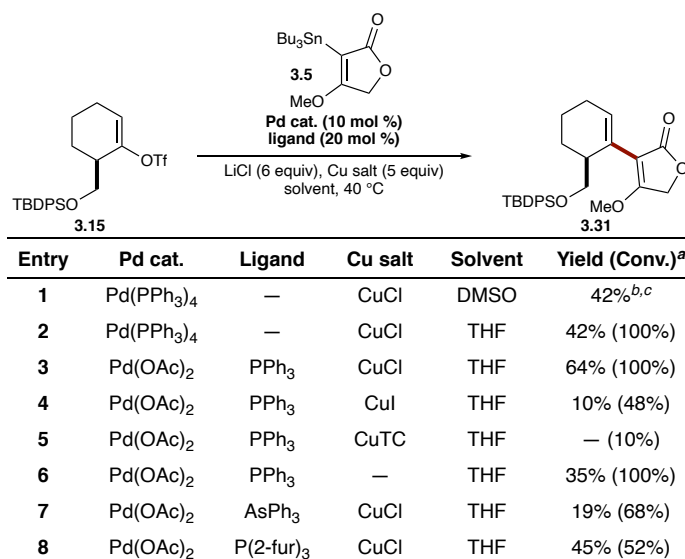


Table 3.3: Evaluation of reaction conditions for the Stille coupling of model triflate **3.15** with vinyl stannane **3.31**.

^aDetermined by integration against 1,4-dinitrobenzene as an internal ¹H NMR standard. ^bIsolated yield. ^cReaction was run at 60 °C

Under Corey's conditions, coupling product **3.31** was isolated in 42% yield. Protodemetalation of the stannane was the major side reaction. To suppress this the reaction was performed at a lower temperature (40 °C) in THF (entry 2). While there was no change in yield of **3.31**, complete consumption of triflate **3.15** was observed. The use of Pd(OAc)₂ (10 mol %) and PPh₃ (20 mol %) to generate a coordinatively unsaturated Pd(o) catalyst improved the yield of **3.31** to 64% (entry 3). A brief survey of Cu(I) salts revealed that CuCl was the most superior additive (entries 4 and 5), while a control experiment established that a copper(I) salt was necessary for useful yields of the product (entry 6). Alternative ligands like AsPh₃ and P(2-fur)₃

were also employed, due to their well-documented ability to further accelerate the transmetalation step.¹³ However, the use of AsPh_3 dramatically reduced the yield of **3.31** to 19% (entry 7), while $\text{P}(2\text{-fur})_3$ reduced the yield of **3.31** to 45% (entry 8). Intriguingly, minimal side reactions of the vinyl triflate were observed when $\text{P}(2\text{-fur})_3$ was used as the ligand and 48% of unreacted starting material was observed by crude ^1H NMR.

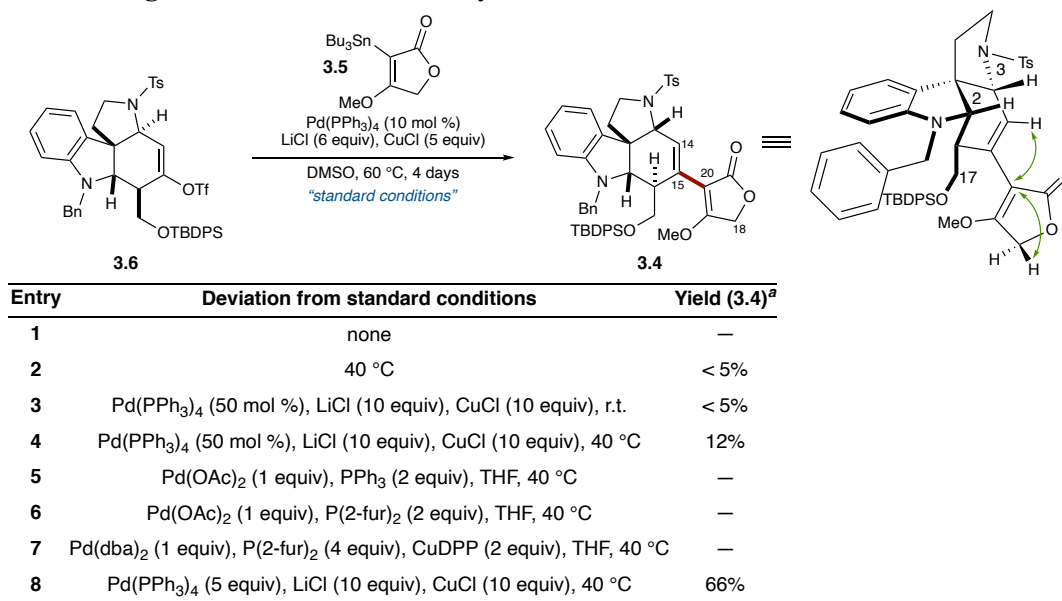
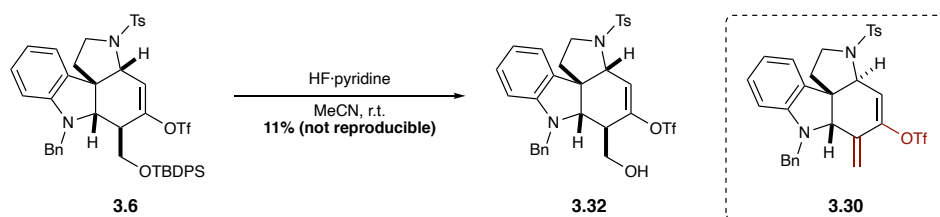


Table 3.4: Key Stille coupling to forge the C15–C20 bond and structural assignment of coupling product **3.4**. ^aYields are of isolated products

We next set our sights on the cross-coupling between enol triflate **3.6** and vinyl stannane **3.5** (Table 3.4). No coupling product **3.4** was observed under the standard conditions laid out by Corey and co-workers (entry 1). Extensive protodemetalation of stannane **3.5** was observed, and no unreacted **3.5** was observed by crude ^1H NMR. A lower reaction temperature of 40 °C allowed us to isolate and characterise coupling product **3.4** for the first time, but in very low yields (entry 2). In Baran's synthesis of Cortistatin A,¹⁴ some success was seen in a similarly congested system by increasing the catalyst loading to 50 mol % and the stoichiometries of LiCl and CuCl to 10 equiv each at room temperature. However, under these conditions, the yield of **3.4** remained low (entry 3). Increasing the temperature back to 40 °C with higher catalyst loading improved the yield somewhat to 12% (entry 4). Under these conditions, significant consumption of vinyl triflate **3.6** was observed, as well as protodemetalation of stannane **3.5**. This indicates that slightly elevated

temperatures were necessary for the triflate to engage the Pd(o) catalyst, despite the occurrence of competing protodemetalation of stannane **3.5**. Based on our survey of reaction conditions with model triflate **3.15** (see Table 3.3), we performed the reaction with Pd(OAc)₃ (1 equiv) as the precatalyst and PPh₃ (2 equiv) as the ligand. However, under these conditions no coupling product **3.4** was observed, and the starting triflate **3.6** was recovered nearly quantitatively. The use of P(2-fur)₃ as the ligand resulted in complete decomposition of the starting materials, and no triflate **3.6** or coupling product **3.4** was isolated (entries 6 and 7). We reverted back to using Pd(PPh₃)₄ as the catalyst, as it was the only catalyst with which we were able to isolate coupling product **3.4**. The use of super-stoichiometric Pd(PPh₃)₄ (5 equiv) afforded coupling product **3.4** in 66% yield. Characterisation and structural assignment of coupling product **3.4** was achieved by COSY, HMQC, and HMBC experiments. Key HMBC correlations are depicted with green arrows in Table 3.4.



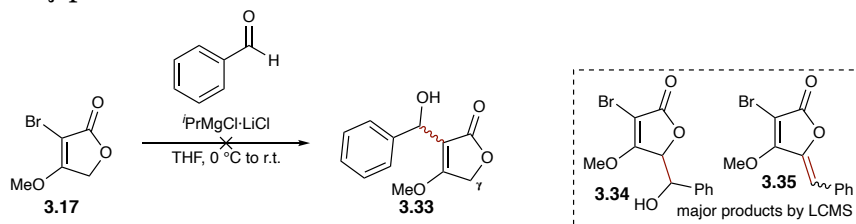
Scheme 3.8: TBDS deprotection of vinyl triflate **3.6**

We hypothesised that removing the deprotection of the primary alcohol in triflate **3.6** would reduce the steric congestion around the triflate and allow the Stille coupling to compete with protodemetalation of the vinyl stannane **3.5**. Treatment of triflate **3.6** with HF-pyridine in MeCN at room temperature delivered the primary alcohol **3.32** in 11% yield (Scheme 3.8). However, we were unable to reliably reproduce the results of this reaction, and consistently observed the formation of unsaturated triflate **3.30**.

Based on the difficulties encountered in the optimisation of this reaction, and the rather forcing conditions required to isolate any meaningful quantities of **3.4**, at this stage we decided to turn to Plan B outlined in Scheme 3.1 above.

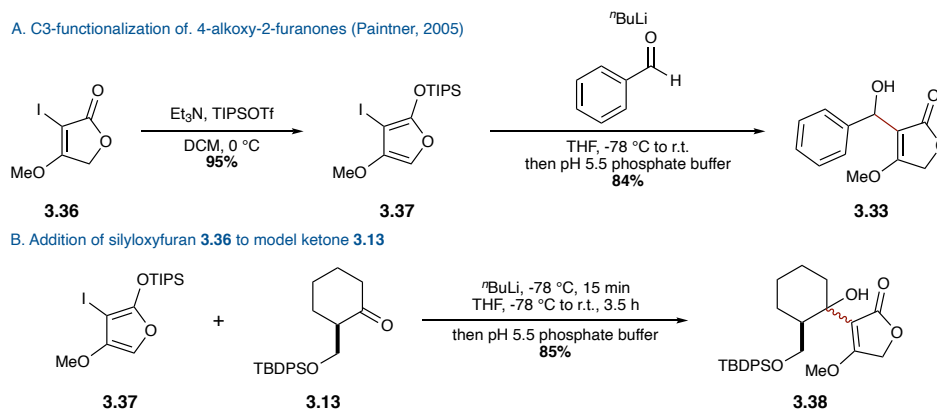
3.1.4.2 Plan B – 1,2-addition to ketone 3.7

In this revised strategy, we envisioned that an organometallic nucleophile derived from bromofuranone **3.17** could attack ketone **3.7** to form the elusive C15–C20 bond. To test this hypothesis, bromofuranone **3.17** was treated with a solution of $i\text{PrMgCl}\cdot\text{LiCl}$ (1.3 M in THF) at 0 °C to generate the Grignard reagent, followed by addition of benzaldehyde as a model electrophile (Scheme 3.9). Under these conditions, no trace of the desired benzyl alcohol **3.33** was seen. The major side products observed by LCMS were C5 aldol addition and condensation products **3.34** and **3.35**, respectively. 4-Alkoxy-2-furanones such as **3.17** have been reported to be reactive at the C5-position under strongly basic conditions due to their tendency to aromatise upon deprotonation at the γ -position.



Scheme 3.9: Grignard reaction with bromofuranone **3.17** predominantly forms aldol addition and condensation products

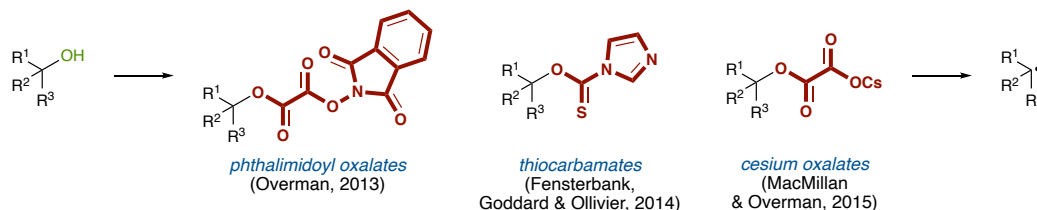
In 2005, Paintner and co-workers reported the regioselective C3 functionalisation of 4-alkoxy-2-furanones *via* 2-silyloxyfuran intermediates.¹⁵ In this methodology, iodofuranone **3.36** was treated with Et_3N and TIPSOTf to provide silyloxyfuran **3.37** in excellent yield (Scheme 3.10 A). These products could then smoothly undergo lithium-halogen exchange without deleterious



Scheme 3.10: Addition of silyloxyfuran **3.36** to model ketone **3.13** using Paintner's conditions for the selective C3 functionalisation of 4-alkoxy-2-furanones

side reaction occurring through γ -deprotonation, and the resulting organolithiates could be treated with a wide range of electrophiles. Mildly acidic work-up ensured complete hydrolysis of the silyloxyfuran moiety back to the furanone. Excited by these results, we treated silyloxyfuran **3.37** with $n\text{BuLi}$ at $-78\text{ }^\circ\text{C}$ for 15 min, before adding a solution of cyclohexanone **3.13** to the reaction and allowing it to warm up to room temperature (Scheme 3.10 B). After quenching the reaction with a pH 5.5 phosphate buffer, we isolated tertiary alcohol **3.38** in 85% yield.

After establishing a method to install the furanone fragment, we next turned our attention to the radical deoxygenation of model tertiary alcohol **3.38**. We conducted a brief literature survey of visible light induced radical deoxygenations,¹⁶ as these reactions can be performed catalytically and do not use toxic and hazardous reagents that are common to the Barton-McCombie deoxygenation.^{17–19} Alkyl radical species have been generated from various redox-active esters derived from alcohol starting materials, some of which are depicted in Scheme 3.11.^{20–22} In particular, we were drawn to oxalates²² and phthalimidoyl oxalates,²⁰ reported by MacMillan and Overman, due to the abundance of tertiary alkyl radicals that have been generated from these precursors.

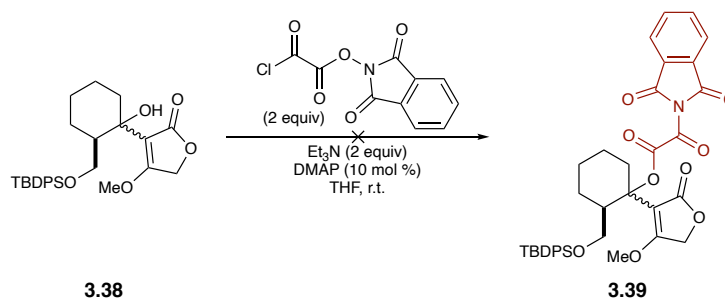


Scheme 3.11: Some common alcohol-derived alkyl radical precursors

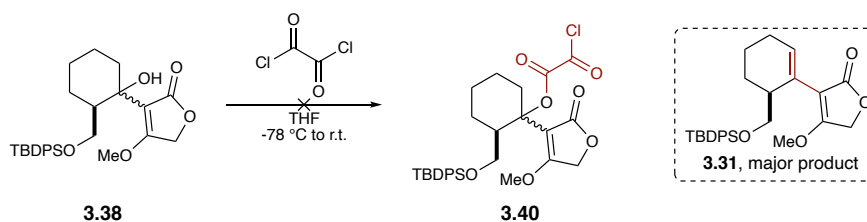
To this end, we subjected alcohol **3.38** to the standard conditions for the synthesis of tertiary phthalimidoyl oxalates as laid out by Overman and co-workers (Scheme 3.12 A).²⁰ Unfortunately, no phthalimidoyl oxalate **3.39** was observed and the starting tertiary alcohol was isolated in quantitative yield. We hypothesised that steric encumbrance around the alcohol was hindering its reaction with the bulky phthalimidoyl oxalyl chloride. Likewise, no acyl chloride product **3.39** was observed when **3.38** was treated with oxalyl chloride (Scheme 3.12 B). Surprisingly, the major

product observed under these conditions was elimination product **3.31**, which matched the product isolated from the model Stille coupling reaction (see Table 3.3).

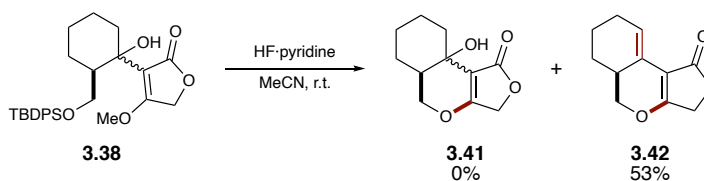
A. Attempted synthesis of phthalimidoyl oxalate **3.38**



B. Attempted synthesis acyl chloride **3.39**

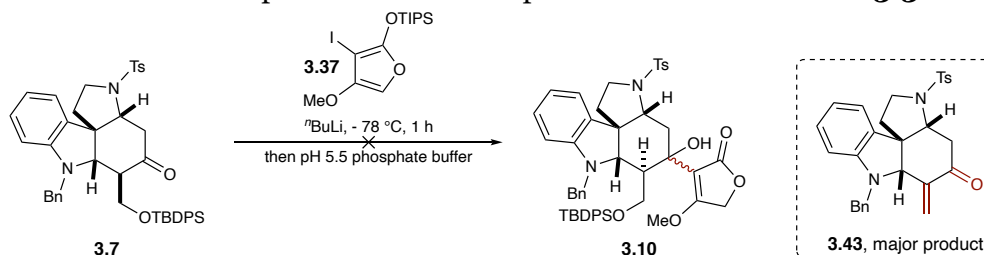


C. Unexpected formation of diene **3.41**



Scheme 3.12: Tertiary alcohol **3.38** is very sterically encumbered and especially prone to elimination under mildly acidic conditions

We attempted to facilitate the synthesis of phthalimidoyl oxalate **3.39** by deprotecting the primary alcohol to trigger the cycloetherification, thereby releasing the steric hindrance caused by the bulky TBDPS group. To our surprise, when alcohol **3.38** was treated with HF·pyridine in MeCN at room temperature, elimination of the tertiary alcohol had occurred in addition to cycloetherification, and diene **3.42** was isolated in 53% yield (Scheme 3.12 C). This result, together with the elimination product observed upon treatment of alcohol **3.38** with oxalyl



Scheme 3.13: Nucleophilic attack of ketone **3.7** with the lithium anion of silyloxyfuran **3.36** results in enone **3.43** as the major product

chloride, suggests that this tertiary alcohol is particularly susceptible to elimination under mildly acidic conditions. While this was not the anticipated outcome of this reaction, we had nevertheless established a reliable method to assemble the tricyclic dihydropyran/furanone ring system.

With this in mind, we attempted to form the C15–C20 bond by addition of the lithium anion of silyloxyfuran **3.37** to ketone **3.7** (Scheme 3.13). Unfortunately, the tertiary alcohol product **3.10** was not observed under these conditions. Instead, the major product observed was enone **3.42**, arising from elimination of the silanol.⁸ We hypothesise that nucleophilic attack of ketone **3.7** is not competitive with α -deprotonation with the generated organolithium compound to form the kinetic enolate at -78 °C, which subsequently equilibrates to form the thermodynamic enolate. This enolate can then eliminate silanol to form product enone **3.43**.

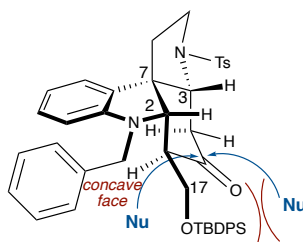


Figure 3.2: 3D depiction of ketone **3.7**

Presumably, this is a function of the increased steric hindrance around ketone **3.7** as compared to ketone **3.13**, which underwent nucleophilic attack smoothly with silyloxyfuran **3.37**. Examination of a molecular model indicates that attack of the ketone from the convex face of the cyclohexane ring is extremely sterically hindered by the presence of the bulky TBDPS group (Figure 3.2). These factors might prevent the approach of a bulky nucleophile like **3.37**_{Li} from the required Bürgi-Dunitz angle.²³

The use of CeCl_3 as an additive to generate the less basic organocerium nucleophile did not effectively suppress α -deprotonation, and a mixture of ketone **3.7** and enone **3.43** were obtained. Furthermore, all attempts to form the Grignard reagent from silyloxyfuran **3.37** were

⁸ Enone **3.43** was identified and characterised by matching its ¹H NMR spectrum to the major product observed by Dr. Ricardo Delgado during his attempts to synthesise the corresponding enol triflate with lithium bases.¹¹

unsuccessful, and the iodide was recovered quantitatively. 3-halofurans are known to undergo magnesium-halogen exchange a considerably slower rate than 2-halofurans,²⁴ and we hypothesise that the electron-donating 2-silyloxy and 4-methoxy substituents further contributed to this observed lack of reactivity.

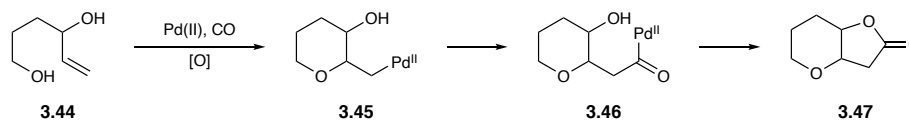
3.2 An alternate strategy to assemble the dihydropyran/furanone EF ring system – alkyoxypalladation/carbonylation cascade reaction

Thus far, we had been unsuccessful at establishing an efficient method to forge the C15–C20 bond and introduce the butyrolactone F ring present in 11-demethoxymyrtoidine (**3.1**) and myrtoidine (**3.2**). The Stille coupling strategy (Section 3.1.4.1, *Plan A*) had suffered from low yields due to competing protodemetalation of the vinyl stannane coupling partner at elevated reaction temperatures. Alternatively, the carbonyl attack strategy (Section 3.1.4.2, *Plan B*), provided no product whatsoever, which we hypothesise was due to steric congestion around the ketone. Given that the only method with which we had observed any significant C15–C20 bond formation was the Stille cross-coupling, we anticipated that we could forge the C15–C20 bond by reacting enol triflate **3.6** with a coupling partner that was less sterically demanding than vinyl stannane **3.5** and less prone to competing protodemetalation.

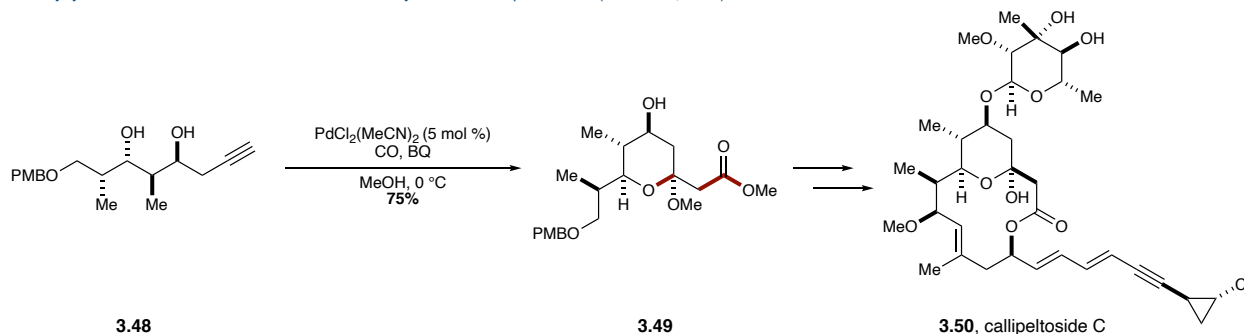
The Semmelhack reaction is an extremely efficient Pd(II)-catalysed cascade reaction for the generation of at least two C–O and one C–C bond (Scheme 3.12 A).^{25,26} The reaction is initiated by oxypalladation across an unsaturated C–C bond to form an alkyl-Pd(II) species **3.45** which can undergo a migratory insertion with carbon monoxide to form the highly reactive acyl-Pd(II) species **3.46**. Trapping with an inter- or intramolecular (shown) alcohol nucleophile and subsequent reductive elimination provides the fused lactone product **3.47**. An external oxidant can then re-oxidise the Pd(0) back to the active Pd(II) catalyst. The broad functional group compatibility and mild reaction conditions of this transformation have allowed this reaction to

act as a key complexity building step in the synthesis of many structurally diverse natural products, two examples of which are described below.

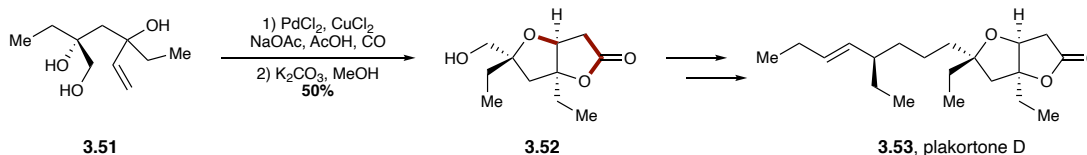
A. General reaction scheme for the Semmelhack reaction



B. Alkynyl intermolecular Semmelhack reaction in the synthesis of callipeltoside C (MacMillan, 2008)

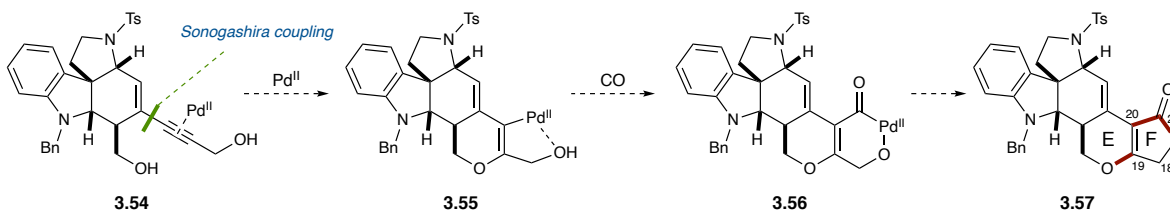


C. Alkenyl intramolecular Semmelhack reaction in the synthesis of plakortone D (Kitching, 2002)



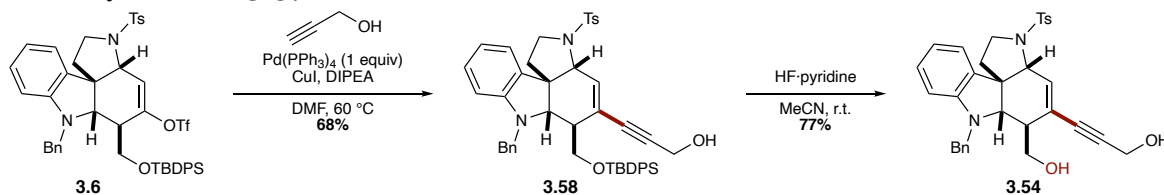
Scheme 3.14: The Semmelhack reaction in total synthesis

In MacMillan's synthesis of callipeltoside C (Scheme 3.14 B),²⁷ an alkynyl Semmelhack reaction was employed to assemble the central tetrahydropyran ring and install the ester present in the natural product. The unsaturation left behind by the alkyne was leveraged to form ketal **3.49** and this intermediate was advanced to the natural product (**3.50**). The Semmelhack reaction was key to establishing the relative stereochemistry of the central THP ring. In Kitching's synthesis of plakortone D (Scheme 3.14 C),²⁸ alkenyl triol **3.51**, containing a pendant alcohol rather than an intermolecular alcohol, was subjected to Semmelhack conditions to diastereoselectively produce tetrahydrofuran-fused lactone **3.52** in 63% yield. This intermediate could then be advanced to the natural product (**3.53**).



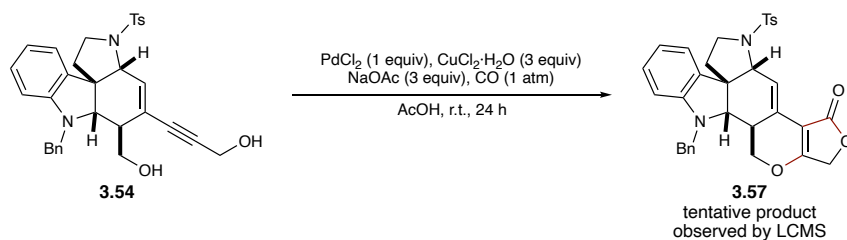
Scheme 3.15: Proposed Semmelhack reaction to synthesise the hexacyclic core of the myrtoïdines

We proposed that alkynediol **3.54** could be synthesised by Sonogashira coupling with propargyl alcohol (Scheme 3.15). Treatment of **3.54** with a Pd(II) catalyst would result in a 6-*endo*-dig oxypalladation across the alkyne to form alkenyl-Pd(II) species **3.55**. We hypothesised that the presence of the pendant propargyl alcohol would direct the reaction to favour 6-*endo*-dig cyclisation over 5-*exo*-dig. Migratory insertion with carbon monoxide would then form acyl-Pd(II) species **3.56**, which could be trapped by the propargyl alcohol to provide the hexacyclic core of the myrtoïdines **3.57**.



Scheme 3.16: Synthesis of alkynediol **3.54**

The Sonogashira coupling of triflate **3.6** with propargyl alcohol proceeded smoothly to provide enyne **3.58** in 68% yield (unoptimised, Scheme 3.16).²⁹ We hypothesise that the reactive nature of the *in situ* generated copper acetylide, as well as the linear (and therefore less sterically demanding) nature of the alkyne rendered this reaction much more feasible than the previously attempted Stille coupling with vinyl stannane **3.5**. Treatment of **3.58** with HF·pyridine in MeCN provided the desired alkynediol **3.54** in 77% yield.



Scheme 3.17: Attempted Semmelhack reaction. Trace amounts of **3.57** (tentatively assigned) were observed by LCMS

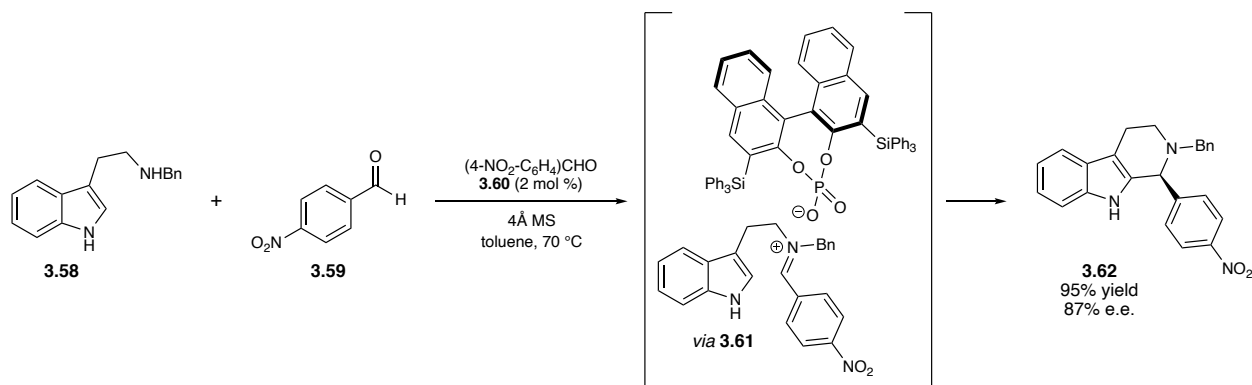
When alkynediol **3.54** was treated with PdCl₂ (1 equiv), CuCl₂·H₂O (3 equiv) and NaOAc (3 equiv), in AcOH under a balloon of carbon monoxide (Scheme 3.17), complete consumption of the starting diol was observed. Furthermore, when the crude reaction mixture was assayed by LCMS, a peak matching the mass of the desired hexacyclic lactone **3.57** was observed. Unfortunately, since this reaction was performed on <1 mg of the starting diol, complete isolation and

characterisation of the major product was very difficult. However, this initial test reaction establishes that the Semmelhack reaction indeed shows promise as a viable path towards completing the synthesis of 11-demethoxymyrtoidine (**3.1**) and myrtoidine (**3.2**).

3.3 Studies towards an enantioselective cascade annulation using asymmetric ion-pairing catalysis

As described above, the iminium ion cascade reaction previously developed by the Blakey lab remains an extremely efficient method to assemble the tetracyclic core of the Malagasy alkaloids (Scheme 4.1).^{1,3,4,30} Proceeding through the generation of a prochiral iminium ion intermediate, followed by stereospecific Pictet-Spengler and aza-Sakurai cyclisations, this reaction represents the stereodetermining step in the racemic synthesis of malagashanine,⁴ as well as in our proposed route to 11-demethoxymyrtoidine and myrtoidine. Methods of enantioinduction that largely rely on covalent interactions, such as chiral Lewis acid- or transition metal-catalysis, are ineffective due to the lack of Lewis basicity in the putative iminium ion. In contrast, asymmetric ion-pairing catalysis has been demonstrated as an ideal platform for enantioselective reactions involving charged reactive intermediates, in which the charged intermediates are held in a chiral environment by electrostatic interactions with a counterion.³¹ As elegantly delineated by Brak and Jacobsen,³¹ there are two common manifolds for ion-pairing catalysis of reactions involving cationic intermediates like iminium ions: 1) chiral anion-directed ion-pairing catalysis, and 2) anion-binding catalysis. The Blakey lab has studied both modes of catalysis in the context of the Malagasy cascade reaction.

3.3.1 Chiral anion-directed catalysis

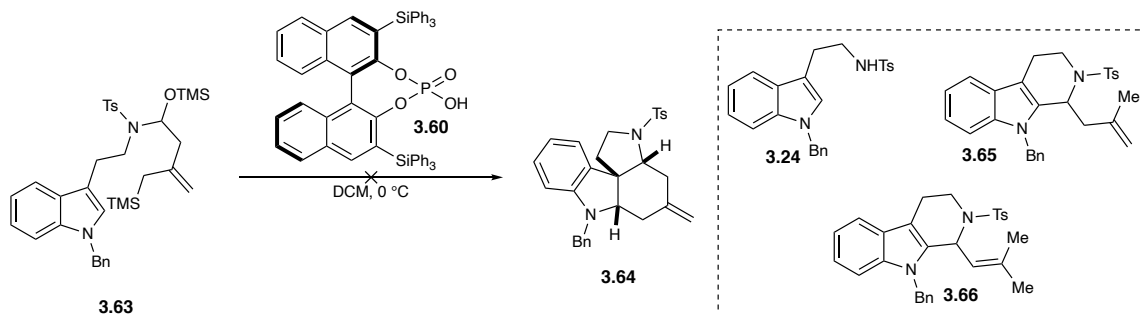


Scheme 3.18: Chiral anion-directed ion-pairing catalysed Pictet-Spengler reaction (Hiemstra, 2008).

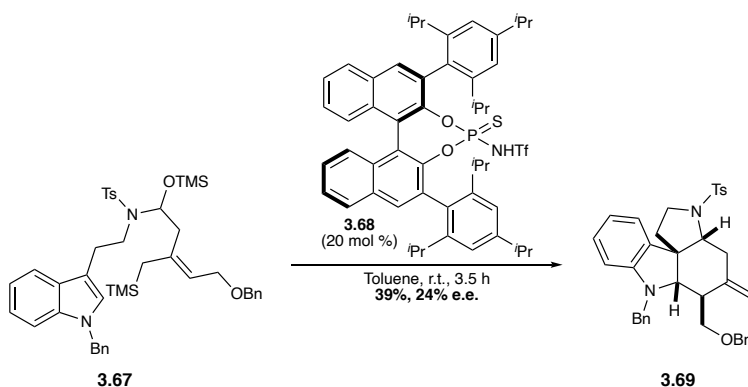
In this mode of ion-pairing catalysis, cationic reaction intermediates like iminium ions are electrostatically paired with chiral anions, usually phosphates and borates, for asymmetric reactions. A particularly relevant example of this type of catalysis was demonstrated by Hiemstra and co-workers in the context of enantioselective Pictet-Spengler reactions of *N*-benzyltryptamine (**3.58**, Scheme 4.2).³² The iminium ion formed by condensation with aldehyde **3.59** could form a chiral ion pair **3.61** with the conjugate base of a chiral phosphoric acid catalyst (**3.60**) to provide tetrahydro- β -carboline **3.62** in 95% yield and 87% e.e.

Similar strategies were pursued by previous members of the Blakey lab to enantioselectively assemble the Malagasy core (Scheme 3.19). With a stoichiometric quantity of the same chiral phosphoric acid **3.60**, Dr. Ricardo Delgado observed minimal formation of the desired tetracyclic core **3.64** from hemiaminal **3.63** (Scheme 3.19 A).¹¹ Instead, tryptamine **3.24**, and tetrahydro- β -carbolines **3.65** and **3.66** were observed as the major products. Dr. Aidi Kong³³ was able to improve upon this result and demonstrated that 20 mol % of the more acidic chiral phosphoramidate **3.68**³⁴ could catalyse the cascade annulation of *O*-TMS-hemiaminal **3.67** to provide the tetracyclic core **3.69** in 39% yield and 24% e.e. (Scheme 3.19 B), along with multiple other side products (analogous to those observed by Dr. Delgado). Building upon these results, and based upon the observation that the hemiaminal cascade substrate was prone to protodesilylation under Brønsted acidic conditions, Dr. Eric Andreansky showed that the use of

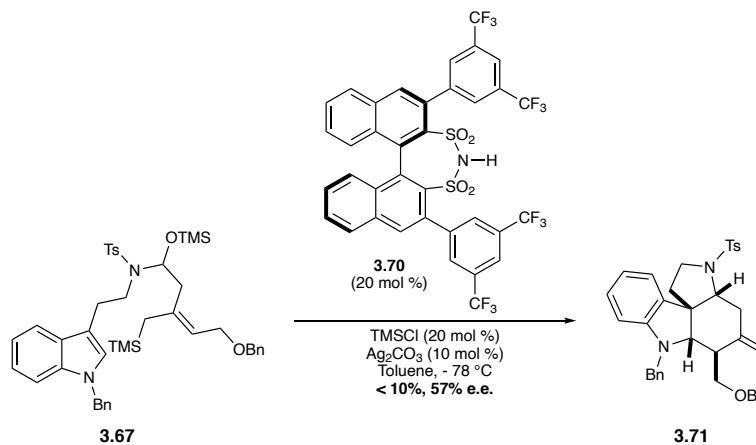
A. Chiral phosphoric acid catalyst for enantioselective iminium ion cascade annulation (Dr. Ricardo Delgado)



B. Chiral phosphoramidate catalyst for enantioselective iminium ion cascade annulation (Dr. Aidi Kong)



C. Chiral disulfonimide catalyst for enantioselective iminium ion cascade annulation (Dr. Eric Andreansky)

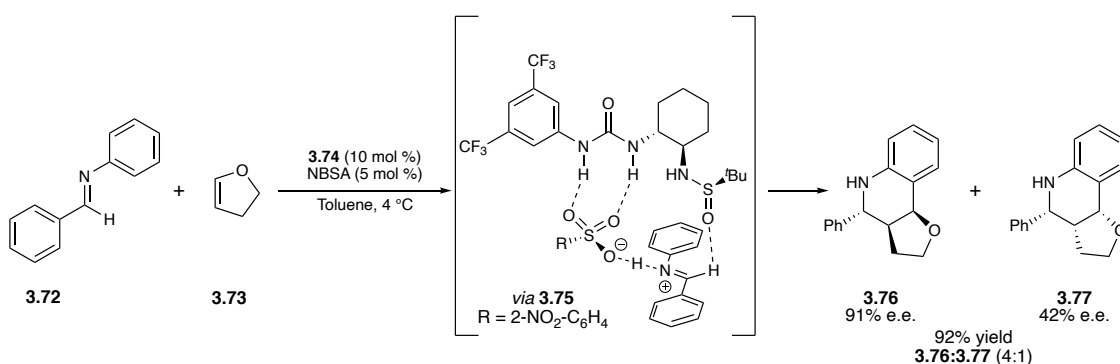


Scheme 3.19: Prior work in the Blakey lab towards employing chiral anion-directed ion-pairing catalysis in the Malagasy cascade annulation

chiral disulfonimide **3.70** (20 mol %)³⁵ could provide tetracyclic core **3.71** in < 10% yield and 57% e.e. The hypothesis was that the disulfonimide catalyst was converted *in situ* to the *N*-TMS-disulfonimide before being desilylated to form the active chiral anion.³⁶ Unfortunately, despite the promising results obtained by Dr. Delgado, Dr. Kong, and Dr. Andreansky, this mode of ion-pairing catalysis was not shown to be competent in the context of Malagasy alkaloid synthesis.

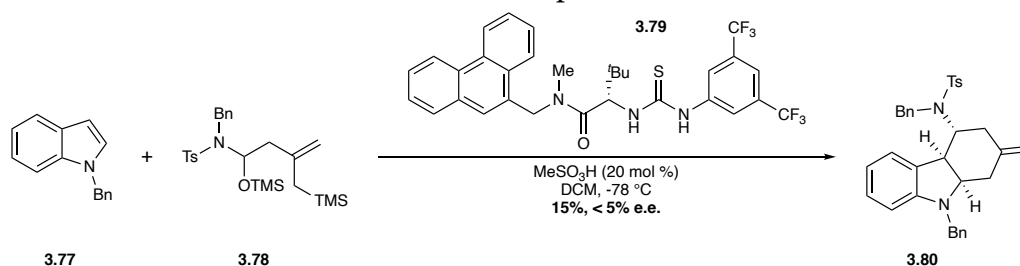
3.3.2 Anion-binding catalysis

3.3.2.1 Prior work



Scheme 3.20: Anion-binding ion-pairing catalysed Povarov cyclisation with a hydrogen bond-donating chiral urea catalyst (Jacobsen, 2010)

In this second mode of ion-pairing catalysis, chiral dual hydrogen bond-donors like ureas or thioureas can bind an anion that electrostatically interacts with a cationic intermediate, thus forming a chiral ion-pair.³¹ This method of catalysis has largely been driven by Jacobsen and co-workers. An example of this type of catalysis is the combination of an achiral sulfonic acid (NBSA) and a chiral urea **3.75** to catalyse a Povarov cyclisation of imine **3.72** with dihydrofuran (**3.73**, Scheme 3.20).³⁷ Enantioinduction in this reaction was determined to be a result of the association of the protonated imine with a urea-sulfonate complex.

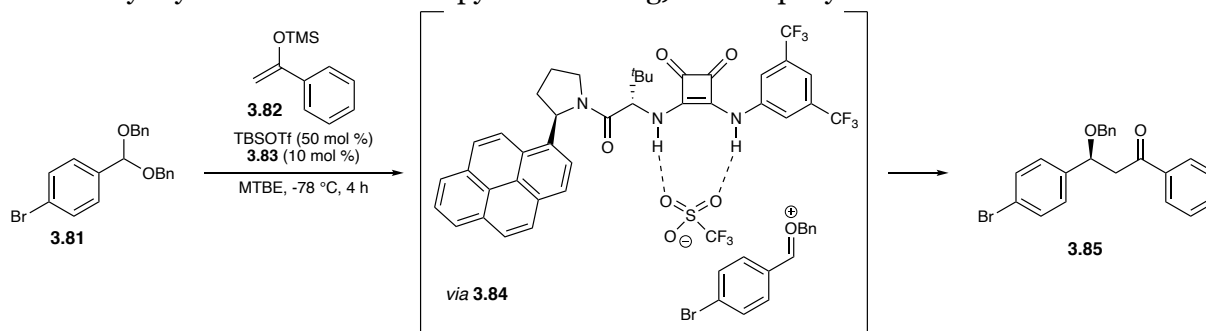


Scheme 3.21: Anion-binding ion-pairing catalysis with a chiral thiourea dual hydrogen bond-donor for intermolecular condensation of *N*-benzylindole (**3.77**) with *O*-TMS-hemiaminal (**3.78**) (Dr. Danny Mancheno)

Dr. Danny Mancheno² attempted to apply these principles to the intermolecular cyclisation of *N*-benzylindole (**3.77**) with *O*-TMS-hemiaminal **3.78** by using methylsulfonic acid in conjunction with chiral thiourea **3.79** (Scheme 3.21).³⁸ However, under these conditions, the desired tricyclic product **3.80** was obtained in 15% with < 5% e.e.

3.3.2.2 Squaramides as anion-binding asymmetric ion-pairing catalysts

In the example shown above, association of the sulfonic acid with the chiral thiourea catalyst **3.79** enhanced its Brønsted acidity, and consequently the hydrogen bond-donating ability. In contrast, Jacobsen and co-workers have reported squaramides as catalytic dual hydrogen bond-donors capable of enhancing the Lewis acidity of commonly employed Lewis acids.³⁹ In one relevant example, squaramide **3.83** (50 mol %) was employed alongside TBSOTf (10 mol %) in MTBE at -78 °C to catalyse the enantioselective Mukaiyama aldol reaction between dibenzyl acetal **3.81** and silyl enol ether **3.82** (Scheme 3.22). Experimental studies indicate that association of TBSOTf with the squaramide enhances its Lewis acidity, which promotes formation of the oxocarbenium ion from dibenzyl acetal **3.81**. Enantioinduction in this reaction is a result of the chiral ion pair **3.84** that is formed between the oxocarbenium ion and the squaramide-bound triflate anion. Ketone product **3.85** was obtained in quantitative yield and 88% e.e. Importantly, control experiments showed that previous reported analogous urea and thiourea catalysts were ineffective at promoting this reaction, indicating that squaramide catalysts (particularly those with bulky aryl substituents on the pyrrolidine ring) are uniquely suited to bind the triflate anion.



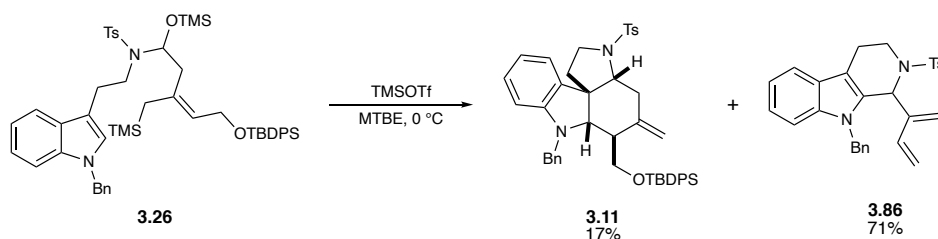
Scheme 3.22: Enantioselective Mukaiyama aldol reaction. Squaramide catalyst enhances the Lewis acidity of TBSOTf and induces enantioselectivity by forming an anion-binding ion-pair

These results appeared promising in our quest to develop an asymmetric variant of the cascade annulation to access the Malagasy core. Earlier efforts had established that strong Brønsted acids led to competing side reactions, predominantly protodesilylation, whereas weaker Brønsted acids suffered from poor catalyst turnover. Following a seminar at Emory University from Zach Wickens, at the time a postdoctoral researcher in the Jacobsen lab, we undertook a

collaboration with Jacobsen and co-workers to explore the use of chiral squaramides in our cascade annulation.⁹

The first major challenge with this endeavour was the reaction solvent. Whereas our cascade annulation is performed in DCM under our standard conditions, Jacobsen and co-workers report that ethereal solvents were best for obtaining high enantioselectivity. Under these reaction manifolds, strong ion-pairing interactions are required for greater selectivity,³¹ i.e. contact ion pairs containing no solvent molecules between them are favoured. Contact ion pairs are energetically favoured in solvents of low dielectric constant, such as MTBE ($\epsilon = 4.50$), which is consistent with the greater enantioselectivity observed in ethereal solvents than in DCM ($\epsilon = 8.93$).

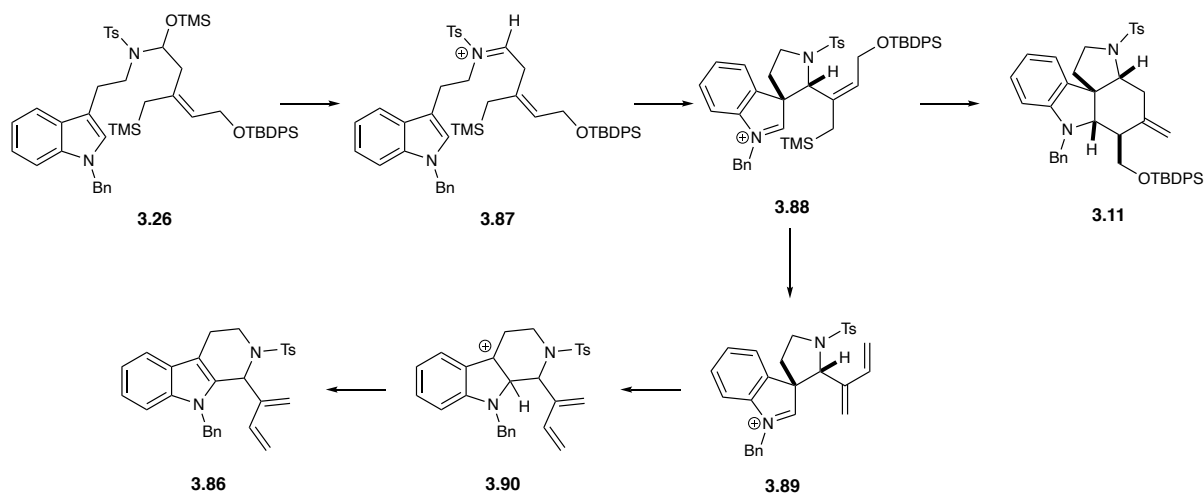
Secondly, while the cascade reaction is typically performed using $\text{BF}_3 \cdot \text{OEt}_2$, the triflate counterion is essential for strong interaction with the squaramide catalyst to hold the putative iminium ion intermediate in an appropriately stereodefined environment. Therefore, we conducted initial test reactions to determine whether silyl triflates could promote the racemic cascade reaction in ethereal solvents.



Scheme 3.23: TMSOTf mediated cascade annulation provides diene **3.86** as the major product

Treatment of *O*-TMS-hemiaminal **3.26** with TMSOTf (3 equiv) in MTBE at 0 °C provided the desired tetracyclic core **3.11** in 17% yield (Scheme 3.23). However, the major product isolated after consumption of the hemiaminal starting material was identified to be diene **3.86**, characterised by ^1H NMR, HRMS, and COSY experiments. This product distribution remained unchanged in the presence of 1 equiv TMSOTf, as well as in other ethereal solvents like Et_2O .

⁹ This work was done prior to the publication of the enantioselective Mukaiyama aldol reaction discussed above (see Scheme 3.22).



Scheme 3.24: Proposed mechanism for the formation of diene **3.86** from *O*-TMS-hemiaminal **3.26**

Our proposed mechanistic hypothesis for the formation of **3.86** is depicted in Scheme 3.24. Iminium ion **3.87** can undergo initial Pictet-Spengler cyclisation to form the pyrrolidine ring **3.88**. Aza-Sakurai cyclisation with the pendant allylsilane can then furnish the tetracyclic Malagasy core **3.11**. Alternatively, competing Lewis acid-mediated elimination of the silanol provides diene **3.89** (along with additional TMS⁺). Due to the absence of a pendant nucleophile, **3.89** can undergo a C3–C2 alkyl migration to form carbocation **3.90** which subsequently aromatises to provide the observed tetrahydro- β -carboline product **3.86**.

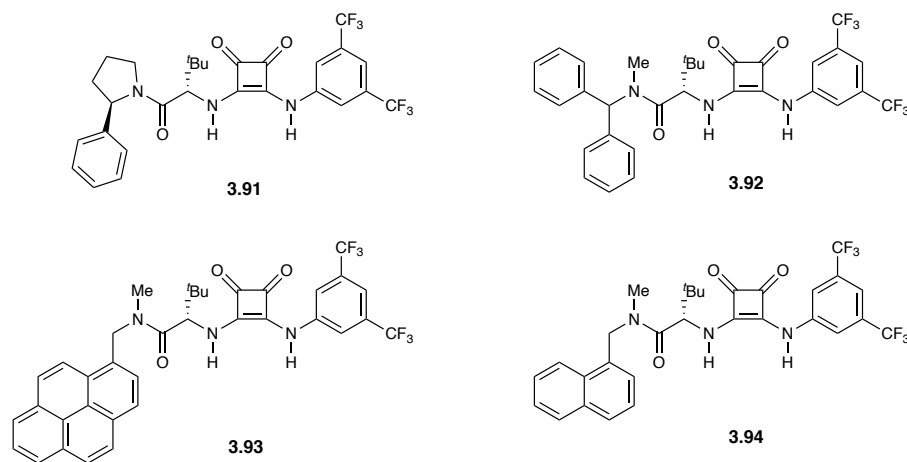
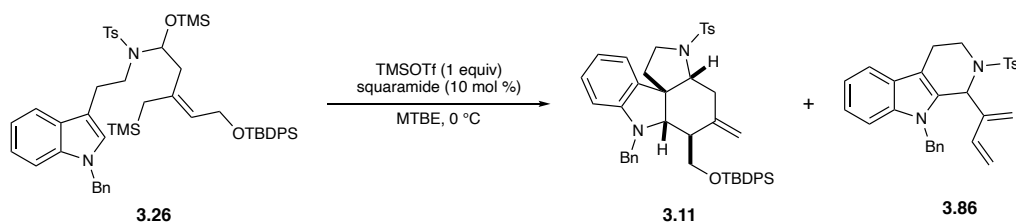


Figure 3.3: Squaramide catalysts provided by the Jacobsen lab for an initial catalyst screen

While the racemic reactions with TMSOTf produced the desired product in low yields, they nevertheless established that TMSOTf was capable of producing tetracyclic core **3.11**. Therefore, we turned our attention towards the synthesis of enantioenriched **3.11** using chiral squaramides that were kindly provided by the Jacobsen lab (Figure 3.3). With TMSOTf (1 equiv) and squaramide catalysts **3.91**, **3.92**, and **3.94** (10 mol %), no significant change in yield of **3.11** was observed compared to the racemic results (entries 1–3, Table 3.5). Additionally, consistent formation of diene **3.86** was observed. We hypothesised that if Lewis acid-mediated elimination of silanol was indeed responsible for the formation of diene **3.86**, a slightly bulkier silyl triflate might inhibit or slow down this process. Unfortunately, this change did not affect the ratio of **3.11**:**3.86** significantly (entries 4 and 5). The highest observed enantioselectivity was observed with catalyst **3.92** and TMSOTf (22% yield, 15% e.e.). Presumably, this low enantioselectivity is due to the occurrence of competing “background” cyclisation without the squaramide catalyst, leading to racemic **3.11**. While the low enantioselectivities observed were nevertheless promising and established the feasibility of this strategy of enantioinduction in the Malagasy cascade, we were unable to suppress the silanol elimination to form diene **3.86**. Based on these results, our efforts to develop an enantioselective cascade reaction were halted.



Entry	Lewis acid	Catalysts	Yield ^a	e.e.	3.11:3.86 ^a
1	TMSOTf	3.91	17%	5%	1:2.3
2	TMSOTf	3.92	22%	15%	1:2.1
3	TMSOTf	3.94	18%	13%	1:2.2
4	TESOTf	3.92	23%	13%	1:2.4
5	TESOTf	3.93	17%	9%	1:2.2

Table 3.5: Anion-binding ion-pairing catalysis using chiral squaramides to enhance the Lewis acidity of silyl triflates

3.4 Conclusion

We developed and studied new strategies to assemble the EF dihydropyran/furanone ring system present in 11-demethoxymyrtoidine (**3.1**) and myrtoidine (**3.2**). Our initial approaches involved a convergent reaction in which a pre-formed butyrolactone was introduced to the system, either by Pd-catalysed cross coupling or by nucleophilic attack of a C15-situated ketone. While model systems for both these reactions were promising, both reactions suffered from low reactivity and competing side reactions. In particular we hypothesised that the sterically congested environment around C15 was hindering its reactivity with a bulky furanone reaction partner. We then turned to an alternate strategy in which we could assemble the EF ring system *via* a Semmelhack alkoxy-palladation/carbonylation sequence. The synthesis of the required substrate and the forging of the C15–C20 bond by Sonogashira coupling proceeded smoothly and initial results of the Semmelhack reaction were promising. Additionally, in collaboration with the Jacobsen lab, we applied their newly developed squaramides as dual hydrogen bond-donors to enhance the Lewis acidity of silyl triflates while forming a chiral ion pair with the putative iminium ion intermediate of the cascade annulation. Unfortunately, we observed extensive formation of elimination product **3.86** under these conditions, as well as low enantioselectivity, presumably resulting from the occurrence of uncatalysed cascade cyclisations. Consequently, this investigation into asymmetric cascade annulations was abandoned. This chapter concludes Part I of this dissertation.

3.5 Experimental

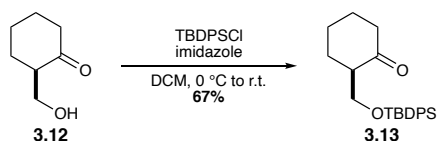
General Information

All reactions were carried out under nitrogen atmospheres with anhydrous solvents in oven- or flame-dried glassware using standard Schlenk technique, unless otherwise stated. Anhydrous dimethyl sulfoxide (DMSO), obtained from EMD Millipore, was distilled over anhydrous CaH_2 and stored over activated 4Å molecular sieves. Anhydrous *N,N*-dimethylformamide (DMF), acetonitrile (CH_3CN), and methanol (MeOH) were obtained from EMD Millipore and were stored over activated 4Å molecular sieves. Anhydrous tetrahydrofuran (THF), diethyl ether (Et_2O), and dichloromethane (CH_2Cl_2) were obtained by passage through activated alumina using a *Glass Contours* solvent purification system. Solvents for workup, extraction, and column chromatography were used as received from commercial suppliers without further purification. All other reagents were purchased from Sigma Aldrich, Strem Chemicals, Alfa Aesar, or Oakwood Chemicals and used as received without further purification, unless otherwise stated. ^1H and ^{13}C nuclear magnetic resonance (NMR) spectra were recorded on a Varian Inova 600 spectrometer (600 MHz ^1H , 150 MHz ^{13}C), a Bruker 600 spectrometer (600 MHz ^1H , 150 MHz ^{13}C), a Varian Inova 500 spectrometer (500 MHz ^1H , 125 MHz ^{13}C), and a Varian Inova 400 spectrometer (400 MHz ^1H , 100 MHz ^{13}C) at room temperature in CDCl_3 (neutralised and dried over anhydrous K_2CO_3) with internal CHCl_3 as the reference (7.26 ppm for ^1H , 77.16 ppm for ^{13}C), unless otherwise stated. Chemical shifts (δ values) were reported in parts per million (ppm) and coupling constants (J values) in Hz. Multiplicity was indicated using the following abbreviations: s = singlet, d = doublet, t = triplet, q = quartet, qn = quintet, m = multiplet, br = broad. Infrared (IR) spectra were recorded using a Thermo Electron Corporation Nicolet 380 FT-IR spectrometer. High resolution mass spectra (HRMS) were obtained using a Thermo Electron Corporation Finigan LTQFTMS (at the Mass Spectrometry Facility, Emory University). Analytical thin layer chromatography (TLC) was performed on precoated glass backed Silicycle SiliaPure® 0.25 mm silica gel 60 plates and visualised with UV light, ethanolic *p*-anisaldehyde, or aqueous potassium permanganate

(KMnO₄). Flash column chromatography was performed using Silicycle SiliaFlash® F60 silica gel (40–63 μm) on a Biotage Isolera One system. Preparatory TLC was performed on precoated glass backed Silicycle SiliaPure® 1.0 mm silica gel 60 plates. We acknowledge the use of shared instrumentation provided by grants from the NIH and the NSF.

Procedures and Characterisation

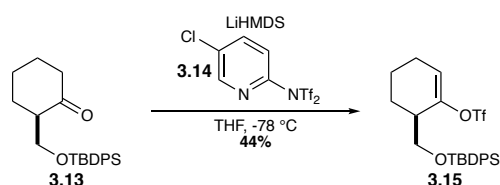
Silyl ether **3.13**



A solution of hydroxymethyl cyclohexanone **3.12** (1.24 g, 9.67 mmol) in DCM (50 mL) was cooled to 0 °C. Imidazole (1.32 g, 19.35 mmol) was added, followed by TBDPSCl (2.75 mL, 10.64 mmol). The resulting mixture was allowed to stir at room temperature for 16 hours. The reaction was quenched with water (50 mL). The layers were separated, and the aqueous layer was extracted with DCM (3 x 50 mL). The combined organic extracts were washed with brine (100 mL), dried over anhydrous Na₂SO₄, filtered, and concentrated under reduced pressure. Purification by flash chromatography on silica gel (99:1 to 95:5 to 90:10 Hex/EtOAc) provided silyl ether **3.13** (2.4 g, 67%). ¹H NMR spectrum matches previously reported data.⁴⁰

¹H NMR (CDCl₃, 400 MHz) δ 7.70 – 7.55 (m, 4H), 7.44 – 7.33 (m, 6H), 4.00 (dd, *J* = 10.4, 4.8 Hz, 1H), 3.67 (dd, *J* = 10.4, 7.7 Hz, 1H), 2.67 – 2.48 (m, 1H), 2.41 – 2.19 (m, 3H), 2.09 – 1.99 (m, 1H), 1.95 – 1.83 (m, 1H), 1.72 – 1.59 (m, 2H), 1.52 – 1.40 (m, 1H), 1.04 (s, 9H).

Vinyl triflate **3.15**

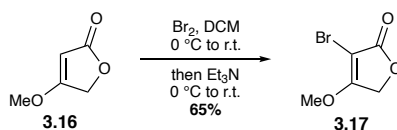


A solution of LiHMDS (3.69 mL, 1.0 M in THF, 3.69 mmol) in THF (16.0 mL) was cooled to -78 °C. A solution of ketone **3.13** (0.450 g, 1.23 mmol) in THF (6.0 mL) was added slowly over 1 hour

and the resulting mixture was allowed to stir at $-78\text{ }^{\circ}\text{C}$ for 1 hour. A solution of Comins' reagent (**3.14**, 1.45 g, 3.69 mmol) in THF (7.0 mL) was added. The resulting mixture was allowed to stir at $-78\text{ }^{\circ}\text{C}$ for 2 hours. The reaction was quenched with saturated aqueous NH_4Cl (20.0 mL) and allowed to warm up to room temperature. The layers were separated, and the aqueous layer was extracted with Et_2O (3 x 25 mL). The combined organic extracts were washed with 5% aqueous NaOH (2 x 15.0 mL) and brine (20.0 mL), dried over anhydrous Na_2SO_4 , filtered, and concentrated under reduced pressure. Purification by flash column chromatography (95:5 pentane/ Et_2O) provided vinyl triflate **3.15** (0.272 g, 44%).

$^1\text{H NMR}$ (CDCl_3 , 600 MHz) δ 7.68 – 7.62 (m, 4H), 7.47 – 7.36 (m, 6H), 5.86 (td, $J = 4.0, 1.4$ Hz, 1H), 3.76 – 3.72 (m, 2H), 2.63 (dq, $J = 6.0, 1.9$ Hz, 1H), 2.18 (td, $J = 4.3, 2.3$ Hz, 2H), 2.00 (dddd, $J = 13.3, 9.2, 6.1, 3.3$ Hz, 1H), 1.86 (dddd, $J = 13.3, 9.1, 6.0, 3.3$ Hz, 1H), 1.66 (ddp, $J = 18.2, 9.2, 3.0$ Hz, 1H), 1.59 – 1.52 (m, 1H), 1.05 (s, 9H) ppm.

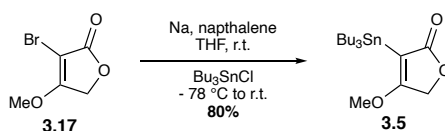
Vinyl bromide **3.17**



A solution of Br_2 (0.25 mL, 4.82 mmol) in CH_2Cl_2 (10.0 mL) was added slowly over five minutes to a solution 4-methoxy-2(5H)-furanone (**3.16**, 0.500 g, 4.83 mmol) in CH_2Cl_2 (30.0 mL) at $0\text{ }^{\circ}\text{C}$. The resulting solution was allowed to warm up to room temperature and stirred for 4.5 hours. The reaction was cooled back down to $0\text{ }^{\circ}\text{C}$ and NEt_3 (0.91 mL, 6.57 mmol) was added. The resulting mixture was allowed to warm up to room temperature and stirred 17 hours. The mixture was washed with aqueous HCl (25.0 mL, 1.0 M) and the layers were separated. The aqueous layer was extracted with CH_2Cl_2 (3 x 30.0 mL). The combined organic extracts were washed with brine (50.0 mL), dried over anhydrous Na_2SO_4 , filtered, and concentrated under reduced pressure. Purification by trituration with H_2O (60.0 mL) provided vinyl bromide **3.17** (0.517 g, 61%) as a light brown solid. $^1\text{H NMR}$ spectrum matches previously reported data.⁸

$^1\text{H NMR}$ (CDCl_3 , 400 MHz) δ 4.70 (s, 2H), 4.21 (s, 3H) ppm.

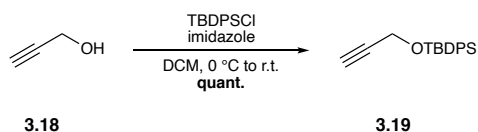
Vinyl stannane **3.5**



Sodium metal (0.357 g, 15.5 mmol) was rinsed with hexanes (60.0 mL) and added to a solution of naphthalene (2.00 g, 15.6 mmol) in THF (15.5 mL). The resulting mixture was sonicated for 4 hours to form a dark green solution. In a separate flask, a solution of bromide **3.17** (0.50 g, 2.51 mmol) in THF (13.0 mL) was cooled to -78 °C. Freshly prepared sodium naphthalenide (12.95 mL, 1.0 M in THF, 12.95 mmol) was transferred slowly over 5 minutes to the reaction flask and the resulting mixture was removed from the dry ice-acetone bath for 5 minutes. The dark greenish brown mixture was cooled back down to -78 °C, and Bu₃SnCl (3.51 mL, 12.95 mmol) was added. The reaction was warmed up to room temperature and stirred for 3 hours. The reaction was quenched with saturated aqueous NH₄Cl (50.0 mL). The layers were separated, and the aqueous layer was extracted with Et₂O (3 x 75.0 mL). The combined organic extracts were washed with brine (100.0 mL), dried over anhydrous Na₂SO₄, filtered, and concentrated under reduced pressure. The crude mixture was purified by silica chromatography (50% pentane, 45% Et₂O, 5% Et₃N) to provide vinyl stannane **21** (0.816 g, 80% yield) as a pale yellow oil. ¹H NMR spectrum matches previously reported data.⁹

¹H NMR (CDCl₃, 400 MHz) δ 4.75 (s, 2H), 3.84 (s, 3H), 1.56 – 1.46 (m, 7H), 1.41 – 1.23 (m, 6H), 1.13 – 1.03 (m, 5H), 0.89 (t, *J* = 7.3 Hz, 9H) ppm.

Propargyl silyl ether **3.19**

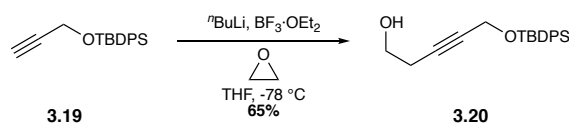


A solution of propargyl alcohol (**3.18**, 4.86 mL, 89.18 mmol) in DCM (50 mL) was cooled to 0 °C. Imidazole (13.38 g, 196.2 mmol) was added, followed by TBDPSCI (25.44 mL, 98.11 mmol). The reaction was allowed to warm up to room temperature over 16 hours. The reaction was quenched with DI H₂O (50 mL) and diluted with DCM (50 mL). The layers were separated, and the aqueous

layer was extracted with DCM (3 x 100 mL). The combined organic extracts were washed with brine (150 mL), dried over anhydrous Na₂SO₄, filtered, and concentrated under reduced pressure. Purification by flash chromatography on silica gel (95:5 Hexanes/EtOAc) provided propargyl silyl ether **3.19** (26.2 g, quantitative yield) as a yellow oily liquid. ¹H NMR spectrum matches previously reported data.⁴¹

¹H NMR (CDCl₃, 300 MHz) δ 7.82 – 7.59 (m, 4H), 7.51 – 7.33 (m, 6H), 4.31 (d, *J* = 2.4 Hz, 2H), 2.39 (t, *J* = 2.4 Hz, 1H), 1.06 (s, 9H) ppm.

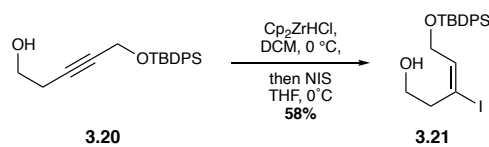
Homopropargyl alcohol **3.20**



A solution of propargyl silyl ether **3.19** (26.7 g, 90.67 mmol) in THF (300 mL) was cooled to -78 °C. ⁿBuLi (57.18 mL, 2.06 M in hexanes, 117.8 mmol) was added dropwise over 10 minutes to the reaction flask, and the resulting solution was allowed to stir at -78 °C for 1 hour. Freshly distilled BF₃·OEt₂ (15 mL, 117.8 mmol) was added dropwise over 5 minutes, and the resulting solution was stirred at -78 °C for 15 minutes. A solution of freshly condensed oxirane (5.43 mL, 108.8 mmol) in THF (10 mL) was added and the reaction was stirred at -78 °C for 2 hours. The reaction was quenched with saturated aqueous NH₄Cl (200 mL) and warmed to room temperature. The layers were separated, and the aqueous extracts were extracted with Et₂O (3 x 100 mL). The combined organic extracts were washed with brine (150 mL), dried over anhydrous Na₂SO₄, filtered, and concentrated under reduced pressure. Purification by flash chromatography on silica gel (9:1 to 4:1 Hex/EtOAc) provided homopropargyl alcohol **3.20** (9.91 g, 65%) as a yellow oil. ¹H NMR spectrum matches previously reported data.⁴²

¹H NMR (CDCl₃, 400 MHz) δ 7.85 – 7.63 (m, 4H), 7.49 – 7.30 (m, 6H), 4.33 (t, *J* = 2.1 Hz, 2H), 3.61 (q, *J* = 6.3 Hz, 2H), 2.40 (tt, *J* = 6.2, 2.2 Hz, 2H), 1.05 (s, 9H) ppm.

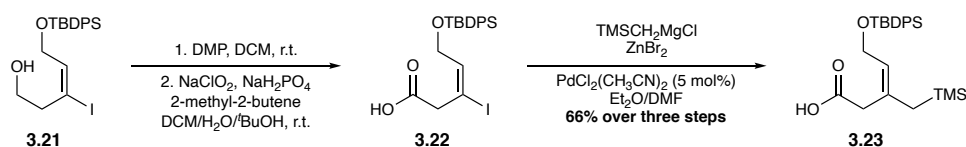
Alkenyl iodide **3.21**



In a nitrogen-filled glovebox, Schwartz's reagent (Cp_2ZrHCl , 6.091 g, 23.62 mmol) was added to a round-bottom flask, and the flask was sealed and removed from the glovebox. DCM (50 mL) was added and the resulting suspension was cooled to 0 °C. A solution of homopropargyl alcohol **3.20** (2.665 g, 7.87 mmol) in DCM (50 mL) was added over 5 minutes and the reaction was allowed to warm up to room temperature over 2 hours. The reaction was cooled back down to 0 °C and a solution of NIS (3.54 g, 15.75 mmol) in THF (100 mL) was added. The reaction was stirred at 0 °C for 3 hours. The reaction was quenched at 0 °C with a 1:1 mixture of saturated aqueous NaHCO_3 and saturated aqueous Na_2SO_3 (150 mL) and stirred at room temperature for 15 minutes. The resulting biphasic mixture was filtered through a plug of celite and rinsed with DCM (100 mL). The layers were separated, and the aqueous layer was extracted with DCM (3 x 100 mL). The combined organic extracts were dried over anhydrous Na_2SO_4 , filtered, and concentrated under reduced pressure. Purification by flash chromatography on silica gel provided alkenyl iodide **3.21** (2.13 g, 58%) as a pale yellow oil. ^1H NMR spectrum matched previously reported data.⁵

^1H NMR (CDCl_3 , 400 MHz) δ 7.73 – 7.62 (m, 4H), 7.48 – 7.35 (m, 6H), 6.55 (t, J = 6.7 Hz, 1H), 4.15 (d, J = 6.4 Hz, 2H), 3.64 (t, J = 5.9 Hz, 2H), 2.53 (t, J = 5.8 Hz, 2H), 1.57 (br s, 1H), 1.04 (s, 9H) ppm.

(*E*)-Allylsilane **3.23**



DMP (8.7 g, 21.2 mmol) was added to a solution of iodoalcohol **3.21** (6.6 g, 14.1 mmol) in DCM (100 mL) and resulting suspension was stirred at room temperature for 3 hours. The reaction was quenched with a 1:1 mixture of saturated aqueous NaHCO_3 and saturated aqueous Na_2SO_3 (100

mL) and the resulting biphasic mixture was stirred at room temperature for 10 minutes. The layers were separated, and the aqueous layer was extracted with Et₂O (3 x 50 mL). The combined organic extracts were washed with brine (150 mL), dried over anhydrous MgSO₄, filtered, and concentrated under reduced pressure.

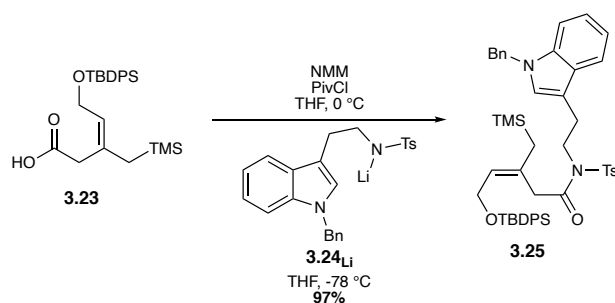
The crude iodoaldehyde product was dissolved in DCM (28 mL) and ^tBuOH (123 mL). 2-methyl-2-butene (64.23 mL, 60.63 mmol) was added, followed by an aqueous solution (100 mL) of NaH₂PO₄ (13.53 g, 112.8 mmol) and NaClO₂ (12.75 g, 141 mmol). The reaction was stirred at room temperature for 1 hour. The reaction was quenched with brine (100 mL) and diluted with DCM (100 mL). The layers were separated, and the aqueous layer was extracted with DCM (3 x 75 mL). The combined organic extracts were washed with brine (150 mL), dried over anhydrous Na₂SO₄, filtered, and concentrated under reduced pressure. Residual ^tBuOH was removed by azeotroping the crude residue with toluene (3 x 30 mL). Iodoacid **3.22** was carried forward crude without further purification.

Mg turnings (1.03 g, 42.3 mmol) were added to a separate two-necked round-bottom flask, and the flask was flame-dried under high vacuum. A single crystal of I₂ was added, the flask was equipped with a reflux condenser, and the flask was purged with nitrogen. Et₂O (50 mL) was added and the resulting mixture was allowed to stir for 30 minutes to activate the Mg. TMSCH₂Cl (5.9 mL, 42.3 mmol) was added and the reaction was allowed to stir for 4 hours. ZnBr₂ (10.17 g, 45.1 mmol) was added and the reaction mixture was allowed to stir at room temperature for 17 hours. The mixture was cooled to 0 °C and diluted with DMF (50 mL). A solution of crude iodoacid **3.22** in DMF (45 mL) was added, followed by a solution of Pd(MeCN)₂Cl₂ (0.181 g, 0.7 mmol) in DMF (5 mL). The reaction was allowed to warm up to room temperature over 16 hours. The reaction was quenched with saturated aqueous NH₄Cl (150 mL) and diluted with Et₂O (100 mL). The layers were separated, and the aqueous layer was extracted with Et₂O (3 x 50 mL). The combined organic extracts were washed with brine (100 mL) and 5% aqueous LiCl (100 mL), dried over anhydrous MgSO₄, filtered, and concentrated under reduced pressure. Purification by flash

chromatography on silica gel (9:1 to 4:1 Hex/EtOAc) provided (*E*)-allylsilane **3.23** (4.1 g, 66% over 3 steps) as a yellow oil. $^1\text{H NMR}$ spectrum matched previously reported data.⁵

$^1\text{H NMR}$ (CDCl_3 , 400 MHz) δ 7.88 – 7.63 (m, 4H), 7.52 – 7.34 (m, 6H), 5.48 (t, $J = 6.9$ Hz, 1H), 4.17 (d, $J = 6.9$ Hz, 2H), 3.00 (s, 2H), 1.63 (s, 2H), 1.03 (s, 9H), 0.02 (s, 9H) ppm.

Amide **3.25**



A solution of tryptamine **3.24** (2.68 g, 6.63 mmol) in THF (50.0 mL) and distilled DMPU (8.0 mL) was cooled to -78 °C. $n\text{BuLi}$ (3.85 mL, 2.06 M in hexanes, 7.94 mmol) was added dropwise over 5 minutes to the reaction flask, and the resulting solution was allowed to stir at -78 °C for 1 hour. In a separate flask, a solution of carboxylic acid **3.23** (4.1 g, 9.30 mmol) in THF (50.0 mL) was cooled to 0 °C. Distilled *N*-methylmorpholine (1.09 mL, 9.96 mmol), was added to the solution, followed by distilled pivaloyl chloride (1.14 mL, 9.30 mmol), and the mixture was allowed to stir at 0 °C for 1 hour. Stirring was stopped and the resulting suspension was allowed to settle for 1 hour. The supernatant was transferred *via* syringe to the solution of tryptamine **29**. The white precipitate was rinsed with THF (3 x 75 mL), the supernatant was transferred *via* syringe to the solution of tryptamine **3.24** and the mixture was allowed to stir at -78 °C for 18 hours. The reaction was quenched with saturated aqueous NH_4Cl (150 mL) and warmed to room temperature. The layers were separated, and the aqueous layer was extracted with Et_2O (3 x 100.0 mL). The combined organic extracts were washed with brine (150.0 mL), dried over anhydrous Na_2SO_4 , filtered, and concentrated under reduced pressure. Purification by flash column chromatography on silica gel (9:1 to 4:1 Hexanes/EtOAc) provided tosylamide **3.25** (5.33 g, 97%) as a sticky foam.

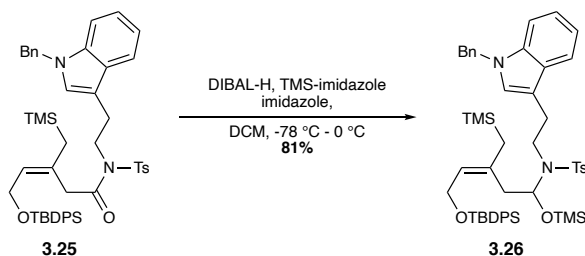
$^1\text{H NMR}$ (CDCl_3 , 400 MHz) δ 7.74 (d, $J = 7.9$ Hz, 1H), 7.67 (s, 1H), 7.67 - 7.63 (m, 4H), 7.41 - 7.34 (m, 4H), 7.31 - 7.21 (m, 4H), 7.18 - 7.12 (m, 3H), 7.11 - 7.08 (m, 3H), 6.92 (s, 1H), 5.42 (t, $J = 6.5$ Hz, 1H), 5.22 (s, 2H), 3.99 (d, $J = 6.5$ Hz, 2H), 3.99 - 3.93 (m, 2H), 3.18 (s, 2H), 3.14 - 3.08 (m, 2H), 2.33 (s, 3H), 1.40 (s, 2H), 1.00 (s, 9H), -0.04 (s, 9H) ppm.

$^{13}\text{C NMR}$ (CDCl_3 , 151 MHz) δ 170.5, 144.8, 137.6, 136.9, 136.7, 135.6, 134.0, 131.9, 129.9, 129.7, 128.8, 128.1, 127.8, 127.7, 127.5, 127.0, 126.7, 126.5, 122.0, 119.5, 119.4, 111.4, 109.8, 60.9, 50.0, 48.1, 40.2, 27.9, 26.9, 26.3, 21.6, 19.3, -1.3 ppm.

IR (thin film, cm^{-1}) 3069, 2954, 2856, 1699, 1495, 1428, 1353, 1247, 1158, 1110, 1089, 1046, 849.2, 738, 702.

HRMS (+ESI) calculated for $\text{C}_{49}\text{H}_{58}\text{N}_2\text{NaO}_4\text{SSi}_2$ $[\text{M}+\text{Na}]^+$ 849.3554, found 849.3532.

O-TMS hemiaminal **3.26**

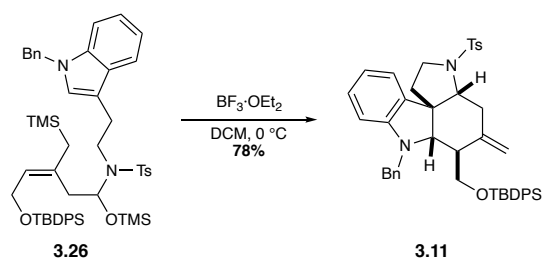


A solution of tosylamide **3.25** (3.00 g, 3.62 mmol) in CH_2Cl_2 (50.0 mL) was cooled to -78 °C. DIBAL-H (7.25 mL, 1.0 M in CH_2Cl_2 , 7.24 mmol) was added dropwise over 5 minutes to the reaction flask. The resulting solution was allowed to stir at -78 °C for 1 hour. 1-(Trimethylsilyl)imidazole (1.59 mL, 10.87 mmol) was added dropwise over 5 minutes to the reaction flask, followed by a solution of imidazole (0.246 g, 3.62 mmol) in CH_2Cl_2 (8 mL). The resulting mixture was stirred at -20 °C for 15 hours. The reaction was quenched by slow addition of saturated aqueous Rochelle's salt (50.0 mL) and the resulting biphasic mixture was stirred at room temperature until both layers were clear. The layers were separated, and the aqueous layer was extracted with CH_2Cl_2 (3 x 100.0 mL). The combined organic extracts were washed with brine (150.0 mL), dried over anhydrous Na_2SO_4 , filtered, and concentrated under reduced pressure. Purification by flash

column chromatography on silica gel (9:1 to 4:1 Hexanes/EtOAc) provided *O*-TMS hemiaminal **3.26** (2.64 g, 81%) as a colourless oil.

¹H NMR (CDCl₃, 500 MHz) δ 7.68 – 7.58 (m, 8H), 7.32 – 7.27 (m, 6H), 7.25 – 7.20 (m, 3H), 7.19 – 7.13 (m, 2H), 7.13 – 7.09 (m, 2H), 7.04 – 6.96 (m, 1H), 6.84 (s, 1H), 5.33 – 5.27 (m, 2H), 5.24 (s, 2H), 4.28 (dd, *J* = 12.7, 7.5 Hz, 1H), 4.17 (dd, *J* = 12.8, 5.7 Hz, 1H), 3.44 (ddd, *J* = 14.5, 11.8, 5.4 Hz, 1H), 3.26 (ddd, *J* = 14.5, 11.8, 4.9 Hz, 1H), 3.07 (tdd, *J* = 25.4, 13.5, 5.0 Hz, 2H), 2.34 (s, 3H), 2.27 (dd, *J* = 13.0, 9.4 Hz, 1H), 1.60 (dd, *J* = 13.1, 3.0 Hz, 1H), 1.53 – 1.49 (m, 1H), 1.01 (s, 9H), 0.03 (s, 9H), -0.05 (s, 9H) ppm.

Tetracyclic core **3.11**



A solution of *O*-TMS-hemiaminal **3.26** (3.69 g, 4.09 mmol) in CH₂Cl₂ (45.0 mL) was cooled to 0 °C. Freshly distilled BF₃·OEt₂ (2.6 mL, 20.46 mmol) was added drop-wise over 5 minutes, and the reaction was allowed to stir at 0 °C for 2 hours. The reaction was quenched with saturated aqueous NaHCO₃ (75.0 mL), and the resulting biphasic mixture was allowed to stir at room temperature for 15 minutes. The layers were separated, and the aqueous layer was extracted with CH₂Cl₂ (3 x 100.0 mL). The combined organic extracts were washed with brine (120.0 mL), dried over anhydrous Na₂SO₄, filtered, and concentrated under reduced pressure. Purification by flash column chromatography on silica gel (9:1 to 4:1 Hexanes/EtOAc) provided core structure **3.11** (2.25 g, 74%) as a white solid.

¹H NMR (CDCl₃, 600 MHz) δ 7.59 (d, *J* = 8.1 Hz, 2H), 7.56 (d, *J* = 6.8 Hz, 2H), 7.49 (d, *J* = 6.7 Hz, 2H), 7.48 – 7.42 (m, 1H), 7.42 – 7.34 (m, 3H), 7.29 – 7.21 (m, 6H), 7.18 (d, *J* = 7.8 Hz, 2H), 7.15 (d, *J* = 9.4 Hz, 2H), 6.99 (t, *J* = 7.2 Hz, 1H), 6.59 (t, *J* = 7.5 Hz, 1H), 6.18 (d, *J* = 7.8 Hz, 1H), 4.69 (s, 1H), 4.67 (s, 1H), 4.38 (d, *J* = 15.9 Hz, 1H), 4.26 (d, *J* = 16.0 Hz, 1H), 3.63 (td, *J* = 10.9,

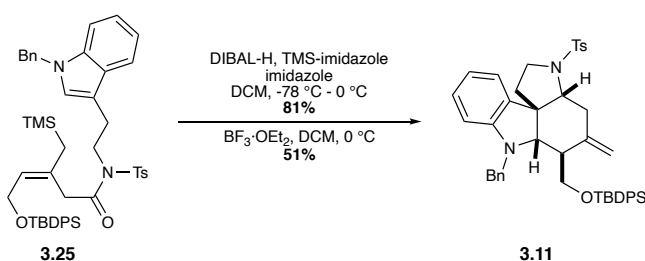
7.1 Hz, 1H), 3.51 (dd, $J = 10.1, 6.6$ Hz, 1H), 3.41 – 3.31 (m, 3H), 3.16 (dd, $J = 11.6, 7.0$ Hz, 1H), 2.97 (dd, $J = 16.8, 7.0$ Hz, 1H), 2.65 (dd, $J = 16.9, 11.6$ Hz, 1H), 2.55 (t, $J = 7.6$ Hz, 1H), 2.38 (s, 3H), 1.76 (dd, $J = 12.0, 6.9$ Hz, 1H), 1.08 (q, $J = 10.4$ Hz, 1H), 0.99 (s, 9H) ppm.

^{13}C NMR (CDCl_3 , 126 MHz) δ 150.60, 143.77, 141.43, 138.67, 135.71, 135.66, 133.64, 133.41, 132.59, 130.32, 130.01, 129.92, 129.82, 128.60, 128.55, 127.93, 127.86, 127.15, 127.10, 124.79, 116.93, 115.46, 105.48, 68.79, 67.33, 58.79, 54.86, 49.32, 48.20, 47.86, 36.65, 32.86, 27.01, 21.73, 19.34 ppm.

IR (thin film, cm^{-1}) 3069.3, 2928.9, 2856.8, 1600.7, 1484.2, 1351.4, 1164.5, 1109.0, 736.2, 702.3.

HRMS (+ESI) calculated for $\text{C}_{46}\text{H}_{51}\text{N}_2\text{O}_3\text{SSi}$ $[\text{M}+\text{H}]^+$ 739.3390, found 739.3381.

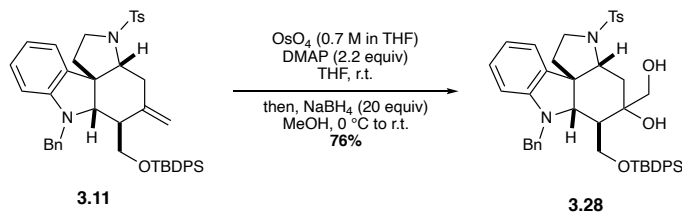
One-pot synthesis of tetracyclic core 3.11



A solution of tosylamide **3.25** (0.332 g, 0.402 mmol) in CH_2Cl_2 (5.0 mL) was cooled to -78 °C. DIBAL-H (0.804 mL, 1.0 M in CH_2Cl_2 , 0.804 mmol) was added dropwise over 5 minutes to the reaction flask. The resulting solution was allowed to stir at -78 °C for 1 hour. 1-(Trimethylsilyl)imidazole (0.177 mL, 1.208 mmol) was added dropwise over 5 minutes to the reaction flask, followed by a solution of imidazole (0.027 g, 3.62 mmol) in CH_2Cl_2 (1.5 mL). The resulting mixture was stirred at -20 °C for 15 hours, and at 0 °C for 1 hour. Freshly distilled $\text{BF}_3 \cdot \text{OEt}_2$ (0.254 mL, 2.01 mmol) was added dropwise over 5 minutes, and the reaction was allowed to stir at 0 °C for 1.5 hours. The reaction was quenched by slow addition of saturated aqueous Rochelle's salt (10.0 mL) and saturated aqueous NaHCO_3 (10.0 mL) and the resulting biphasic mixture was allowed to stir at room temperature for 15 minutes. The layers were separated, and the aqueous layer was extracted with Et_2O (3 x 20.0 mL). The combined organic extracts were washed with brine (40.0 mL), dried over anhydrous MgSO_4 , filtered, and concentrated under

reduced pressure. Purification by flash column chromatography on silica gel (9:1 to 4:1 Hexanes/EtOAc) provided tetracyclic amine **3.11** (0.152 g, 52%) as a white solid..

Diol **3.28**



THF (1.8 mL) was added to a flask containing core structure **3.11** (0.124 g, 0.167 mmol) and 4-(dimethylamino)pyridine (DMAP) (0.045 g, 0.369 mmol). OsO_4 (0.184 mL, 1.0 M in THF, 0.184 mmol) was added to the solution and it was allowed to stir at room temperature for 5 hours. MeOH (2.5 mL) was added to the reaction flask and it was cooled to 0 °C. NaBH_4 (0.127 g, 3.35 mmol) was added to the flask in portions, and the reaction was stirred at 0 °C for 15 minutes, and at room temperature for 17 hours. The reaction was diluted with EtOAc (5.0 mL) and quenched with DI H_2O (10.0 mL). The layers were separated, and the aqueous layer was extracted with EtOAc (3 x 20.0 mL). The combined organic extracts were washed with brine (50.0 mL), dried over anhydrous Na_2SO_4 , filtered, and concentrated under reduced pressure. Purification by flash column chromatography on silica gel (3:2 Hexanes/EtOAc) provided diol **3.28** (0.099 g, 76%) as a 1:1 mixture of diastereomers.

$^1\text{H NMR}$ (CDCl_3 , 500 MHz) (2:1 mixture of diastereomers) δ 7.85 (d, J = 8.1 Hz, 2H), 7.77 (d, J = 8.2 Hz, 4H), 7.67 – 7.62 (m, 8H), 7.59 (ddd, J = 9.3, 7.8, 1.4 Hz, 4H), 7.55 – 7.45 (m, 8H), 7.45 – 7.31 (m, 20H), 7.15 – 7.05 (m, 6H), 7.04 – 7.00 (m, 6H), 6.85 – 6.70 (m, 9H), 6.41 (t, J = 7.2 Hz, 2H), 4.00 (d, J = 14.8 Hz, 1H), 3.91 (dd, J = 28.8, 14.1 Hz, 4H), 3.88 – 3.82 (m, 6H), 3.76 (dd, J = 11.6, 3.1 Hz, 1H), 3.73 (d, J = 14.8 Hz, 1H), 3.69 (dd, J = 11.5, 4.1 Hz, 2H), 3.55 (td, J = 10.9, 7.2 Hz, 1H), 3.52 – 3.36 (m, 10H), 3.29 (t, J = 10.4 Hz, 1H), 3.16 (t, J = 10.2 Hz, 1H), 2.99 (d, J = 9.0 Hz, 1H), 2.95 (dd, J = 12.9, 3.3 Hz, 1H), 2.88 (dd, J = 13.0, 3.3 Hz, 1H), 2.82 (d, J = 8.3 Hz, 1H), 2.54 (dd, J = 12.9, 3.2 Hz, 1H), 2.45 (s, 6H), 2.44 (s, 3H), 2.28 (dd, J = 9.6, 3.5 Hz, 1H), 2.08 –

1.99 (m, 2H), 1.83 (t, $J = 12.9$ Hz, 1H), 1.80 (t, $J = 12.8$ Hz, 2H), 1.45 (ddd, $J = 9.2, 5.6, 3.8$ Hz, 2H), 1.31 – 1.08 (m, 10H), 1.02 (s, 18H), 1.00 (s, 9H) ppm.

^{13}C NMR (CDCl_3 , 126 MHz) (2:1 mixture of diastereomers) δ 149.20, 143.80, 143.70, 138.18, 135.80, 135.76, 135.70, 135.67, 133.36, 132.10, 130.43, 130.35, 130.32, 129.84, 129.77, 128.51, 128.46, 128.43, 128.40, 128.25, 128.24, 128.19, 128.15, 127.92, 127.36, 125.49, 125.34, 119.41, 119.37, 111.57, 110.36, 76.08, 74.08, 70.09, 66.79, 66.39, 65.93, 64.37, 63.56, 59.57, 58.79, 56.15, 53.77, 52.64, 49.80, 49.71, 46.68, 36.69, 36.49, 36.26, 26.85, 21.76, 19.17.

IR (thin film, cm^{-1}) 3466.0, 2930.4, 1599.5, 1471.2, 1332.9, 1215.9, 1160.6, 1044.3, 747.6, 700.0, 663.5.

HRMS (+ESI) calculated for $\text{C}_{46}\text{H}_{53}\text{N}_2\text{O}_5\text{SSi}$ $[\text{M}+\text{H}]^+$ 773.3444, found 773.3443.

Ketone 3.7



NaIO_4 (0.216 g, 1.01 mmol) was added to a solution of diol **3.28** (0.195 g, 0.253 mmol) in THF (3.0 mL) and DI H_2O (1.5 mL), and the resulting solution was allowed to stir at room temperature for 22 hours. The reaction was diluted with EtOAc (8.0 mL) and quenched with saturated aqueous NaHCO_3 (3.0 mL) and saturated aqueous Na_2SO_3 (3.0 mL). The resulting biphasic mixture was allowed to stir at room temperature for 15 minutes. The layers were separated and the aqueous layer was extracted with EtOAc (3 x 20.0 mL). The combined organic extracts were washed with brine (20.0 mL), dried over anhydrous Na_2SO_4 , filtered, and concentrated under reduced pressure. Purification by flash column chromatography on silica gel (9:1 to 4:1 Hexanes/EtOAc) provided ketone **3.7** (0.159 g, 85%) as an off-white solid.

^1H NMR (CDCl_3 , 600 MHz) δ 7.63 (d, $J = 8.1$ Hz, 2H), 7.54 – 7.48 (m, 4H), 7.47 – 7.41 (m, 2H), 7.39 – 7.32 (m, 4H), 7.28 (d, $J = 6.8$ Hz, 1H), 7.26 – 7.21 (m, 3H), 7.19 – 7.13 (m, 4H), 7.08 – 7.02 (m, 1H), 6.69 (t, $J = 7.5$ Hz, 1H), 6.33 (d, $J = 7.9$ Hz, 1H), 4.37 (d, $J = 15.3$ Hz, 1H), 4.03 (d, $J =$

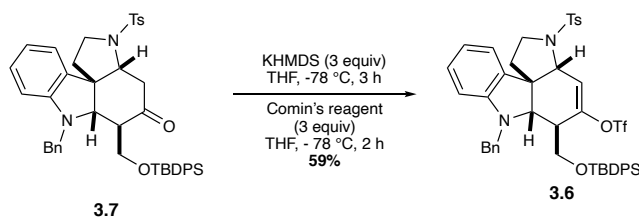
15.3 Hz, 1H), 3.72 – 3.61 (m, 3H), 3.57 (dd, $J = 10.0, 6.4$ Hz, 1H), 3.56 – 3.49 (m, 2H), 3.12 (dd, $J = 18.6, 6.2$ Hz, 1H), 2.85 (dd, $J = 18.6, 12.1$ Hz, 1H), 2.49 (t, $J = 6.0$ Hz, 1H), 2.38 (s, 3H), 1.95 (dd, $J = 12.0, 6.7$ Hz, 1H), 1.45 (q, $J = 10.8$ Hz, 1H), 0.94 (s, 9H) ppm.

^{13}C NMR (CDCl_3 , 151 MHz) δ 207.56, 149.99, 143.96, 137.58, 135.64, 135.63, 130.17, 130.12, 130.01, 129.43, 128.76, 128.02, 127.98, 127.77, 127.45, 125.57, 118.68, 107.72, 67.39, 65.12, 57.86, 54.91, 53.66, 48.19, 47.89, 42.71, 35.99, 26.96, 21.69, 19.36 ppm.

IR (thin film, cm^{-1}) 3050.0, 2929.4, 2856.8, 1705.7, 1599.5, 1478.5, 1350.9, 1162.1, 1092.0, 700.6, 732.7, 665.1

HRMS (+APCI) calculated for $\text{C}_{45}\text{H}_{49}\text{N}_2\text{O}_4\text{SSi}$ $[\text{M}+\text{H}]^+$ 741.3182, found 741.3184.

Vinyl triflate **3.6**



A solution of KHMDS (0.081 g, 0.342 mmol) in THF (0.5 mL) was cooled to -78°C . In a separate flask, a solution of ketone **3.7** (0.085 g, 0.114 mmol) in THF (0.5 mL) was cooled to -78°C . The solution of ketone **3.7** was added slowly over 10 minutes to the solution of KHMDS, and the resulting mixture was allowed to stir at -78°C for 3 hours. Comins' reagent (**3.14**, 0.134 g, 0.342 mmol) was added to the reaction flask, and the resulting mixture was allowed to stir at -78°C for 2 hours. The reaction was quenched with saturated aqueous NH_4Cl (3.0 mL), diluted with Et_2O (3.0 mL) and allowed to warm up to room temperature. The layers were separated, and the aqueous layer was extracted with Et_2O (3 x 10.0 mL). The combined organic extracts were washed with aqueous NaOH (3 N, 2 x 10.0 mL) and brine (15.0 mL), dried over anhydrous Na_2SO_4 , filtered, and concentrated under reduced pressure. Purification by flash column chromatography on silica gel (9:1 to 4:1 Hexanes/ EtOAc) provided kinetic enol triflate **3.6** (0.059 g, 59% yield).

^1H NMR (CDCl_3 , 600 MHz) δ 7.62 (d, $J = 8.3$ Hz, 2H), 7.50 (d, $J = 6.6$ Hz, 2H), 7.48 (d, $J = 6.6$ Hz, 2H), 7.46 – 7.42 (m, 2H), 7.38 – 7.29 (m, 4H), 7.29 – 7.21 (m, 6H), 7.13 (d, $J = 8.0$ Hz, 2H),

7.03 (td, $J = 7.7, 1.3$ Hz, 1H), 6.69 (td, $J = 7.5, 1.0$ Hz, 1H), 6.58 (d, $J = 2.2$ Hz, 1H), 6.30 (d, $J = 7.8$ Hz, 1H), 4.37 (d, $J = 15.5$ Hz, 1H), 4.09 (d, $J = 15.6$ Hz, 1H), 3.80 (d, $J = 1.8$ Hz, 1H), 3.76 (td, $J = 10.8, 7.0$ Hz, 1H), 3.62 (d, $J = 1.5$ Hz, 1H), 3.55 (dd, $J = 10.2, 5.1$ Hz, 1H), 3.47 (t, $J = 10.2$ Hz, 1H), 3.43 (dd, $J = 10.2, 6.3$ Hz, 1H), 2.70 (t, $J = 5.7$ Hz, 1H), 2.37 (s, 3H), 1.99 (dd, $J = 11.9, 6.9$ Hz, 1H), 1.51 – 1.42 (m, 1H), 0.93 (s, 9H) ppm.

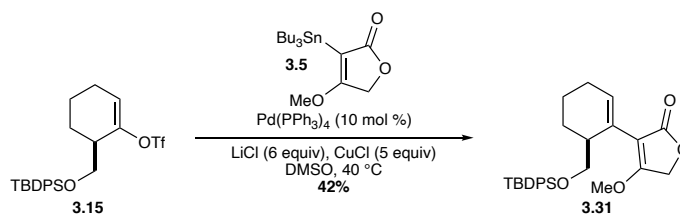
^{13}C NMR (CDCl_3 , 151 MHz,) δ 151.19, 150.01, 144.22, 137.78, 135.65, 135.58, 132.98, 132.64, 132.05, 130.90, 130.18, 130.16, 130.02, 128.76, 128.73, 128.24, 128.04, 128.00, 127.39, 127.29, 124.80, 120.98, 119.00, 118.45 (q, $J_{\text{CF}} = 321.6$ Hz), 107.54, 67.12, 63.58, 59.82, 57.87, 48.75, 48.05, 45.58, 34.83, 26.98, 21.71, 19.34 ppm.

^{19}F NMR (CDCl_3 , 376 MHz) δ -73.11 ppm.

IR (thin film, cm^{-1}) 2930.1, 2857.9, 1600.9, 1477.0, 1419.5, 1350.3, 1209.4, 1164.4, 1139.0, 1110.5, 733.8, 700.5, 608.2.

HRMS (+ESI) calculated for $\text{C}_{46}\text{H}_{47}\text{F}_3\text{KN}_2\text{O}_6\text{S}_2\text{Si}$ $[\text{M}+\text{K}]^+$ 911.2234, found 911.2236.

Stille coupling product **3.31**

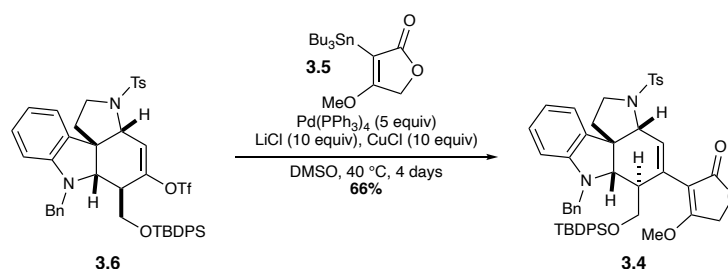


A Schlenk flask (10 mL) containing LiCl (0.037 g, 0.86 mmol), CuCl (0.071 g, 0.72 mmol), and $\text{Pd}(\text{PPh}_3)_4$ (0.017 g, 0.014 mmol) was degassed under high vacuum and backfilled with nitrogen (x 3). A solution of vinyl stannane **3.5** (0.070 g, 0.175 mmol) in DMSO (0.90 mL) was added to the flask, followed by a solution of enol triflate **3.15** (0.072 g, 0.143 mmol) in DMSO (0.90 mL). The resulting mixture was degassed by freeze-pump-thaw (-78 °C, over 4 cycles). The mixture was allowed to stir at room temperature for 40 minutes, and at 60 °C for 49 hours. The reaction mixture was cooled down to room temperature and quenched with aqueous NH_4OH (1.0 M, 3.0 mL) and diluted with Et_2O (4 mL). The layers were separated, and the aqueous layer was extracted

with Et₂O (3 x 5.0 mL). The combined organic extracts were washed with aqueous potassium fluoride (5.0 mL, 1.0 M) and brine (6.0 mL), dried over anhydrous Na₂SO₄, filtered, and concentrated under reduced pressure. Purification by flash column chromatography (1:1 pentane/Et₂O) provided coupling product **3.31** (0.026 g, 40%).

¹H NMR (CDCl₃, 400 MHz) δ 7.67 – 7.59 (m, 4H), 7.44 – 7.32 (m, 6H), 6.08 (td, *J* = 3.9, 1.3 Hz, 1H), 4.49 (s, 2H), 3.72 (s, 3H), 3.61 (dd, *J* = 10.1, 4.2 Hz, 1H), 3.54 (dd, *J* = 10.0, 7.9 Hz, 1H), 2.93 (s, 1H), 2.14 – 2.10 (m, 2H), 1.82 – 1.60 (m, 3H), 1.03 (s, 9H) ppm.

Stille coupling product **3.4**



A reaction tube (13 mL) containing LiCl (0.0019 g, 0.046 mmol), CuCl (0.0045 g, 0.046 mmol), and Pd(PPh₃)₄ (0.0266 g, 0.023 mmol) was degassed under high vacuum and purged with nitrogen. A solution of kinetic enol triflate **3.6** (0.004 g, 0.0046 mmol) in DMSO (0.08 mL) was added, followed by a solution of vinyl stannane **3.5** (0.00738 g, 0.0183 mmol) in DMSO (0.08 mL). The resulting mixture was degassed by freeze-pump-thaw (-78 °C, over 4 cycles). The mixture was allowed to stir at room temperature for 30 minutes, and 40 °C for 4 days. The reaction mixture was cooled down to room temperature, quenched with aqueous NH₄OH (1.0 M, 3.0 mL) and diluted with Et₂O (4 mL). The layers were separated, and the aqueous layer was extracted with Et₂O (3 x 5.0 mL). The combined organic extracts were washed with aqueous potassium fluoride (5.0 mL, 1.0 M) and brine (6.0 mL), dried over anhydrous Na₂SO₄, filtered, and concentrated under reduced pressure. Purification by preparatory TLC (1:1 Hexanes/EtOAc) provided coupling product **3.4** (0.0022 g, 66%).

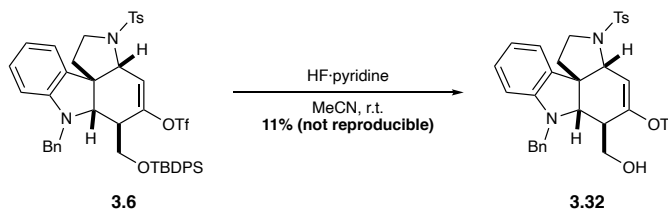
¹H NMR (CDCl₃, 600 MHz) δ 7.61 (d, *J* = 8.2 Hz, 2H), 7.50 (ddd, *J* = 10.5, 8.0, 1.3 Hz, 4H), 7.42 – 7.36 (m, 4H), 7.35 – 7.31 (m, 2H), 7.24 – 7.20 (m, 6H), 7.10 (d, *J* = 8.4 Hz, 2H), 6.92 (td, *J* =

7.7, 1.2 Hz, 1H), 6.82 (d, $J = 2.9$ Hz, 1H), 6.55 (td, $J = 7.4, 0.9$ Hz, 1H), 6.20 (d, $J = 8.2$ Hz, 1H), 4.57 (d, $J = 16.0$ Hz, 1H), 4.49 (d, $J = 16.0$ Hz, 1H), 4.44 (d, $J = 16.0$ Hz, 1H), 4.40 (d, $J = 15.9$ Hz, 1H), 3.81 – 3.73 (m, 1H), 3.69 – 3.66 (m, 4H), 3.62 – 3.59 (m, 2H), 3.57 (dd, $J = 9.7, 6.4$ Hz, 1H), 3.39 (t, $J = 10.3$ Hz, 1H), 3.20 – 3.14 (m, 1H), 2.35 (s, 3H), 1.93 (dd, $J = 11.9, 7.0$ Hz, 1H), 1.33 – 1.28 (m, 1H), 0.92 (s, 9H) ppm.

^{13}C NMR (CDCl₃, 151 MHz) δ 172.13, 172.02, 150.69, 138.48, 135.55, 133.38, 133.25, 131.88, 131.70, 131.66, 130.99, 129.70, 129.62, 128.40, 128.21, 127.69, 127.67, 127.17, 126.82, 124.53, 117.35, 106.04, 103.16, 67.39, 64.51, 64.45, 61.50, 57.95, 57.76, 48.19, 47.91, 42.93, 35.60, 26.76, 21.57, 19.14 ppm.

HRMS (+NSI) calculated for C₅₀H₅₃N₂O₆SSi [M+H]⁺ 837.3394, found 837.3409.

Alcohol **3.32**



HF-pyridine (0.03 mL) was added to a solution of silyl ether **3.6** (0.014 g, 0.016 mmol) in CH₃CN (0.2 mL) and the resulting mixture was allowed to stir at room temperature for 16 hours. The reaction was diluted with EtOAc (mL) and quenched with saturated aqueous NaHCO₃ (3 mL). The resulting mixture was allowed to stir at room temperature for 15 minutes. The layers were separated, and the aqueous layer was extracted with EtOAc (3 x 3 mL). The combined organic extracts were washed with brine, dried over anhydrous Na₂SO₄, filtered, and concentrated under reduced pressure. Purification by preparatory TLC (7:3 Hexanes/EtOAc x 2) provided alcohol **3.32** (0.0011 g, 11%).

^1H NMR (CDCl₃, 600 MHz) δ 7.71 (d, $J = 8.1$ Hz, 2H), 7.36 (d, 8.3 Hz, 1H), 7.32 – 7.28 (m, 6H), 7.06 (td, $J = 7.7, 1.2$ Hz, 1H), 6.73 (td, $J = 7.5, 1.0$ Hz, 1H), 6.62 (d, $J = 2.1$ Hz, 1H), 6.38 (d, $J = 7.8$ Hz, 1H), 4.48 (d, $J = 15.1$ Hz, 1H), 4.04 (d, $J = 15.1$ Hz, 1H), 3.95 (s, 1H), 3.79 (td, $J = 11.0, 7.0$ Hz, 1H), 3.71 (d, $J = 1.5$ Hz, 1H), 3.60 (dd, $J = 10.9, 4.9$ Hz, 1H), 3.53 (t, $J = 10.8$ Hz, 1H), 3.42 (d, $J =$

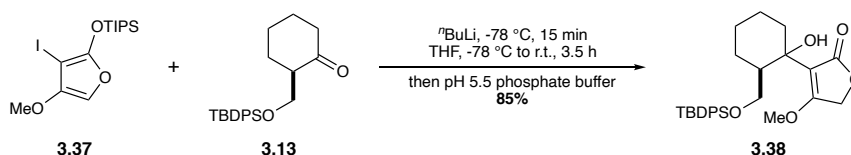
10.9 Hz, 1H), 2.61 – 2.55 (m, 1H), 2.45 (s, 3H), 2.01 (dd, $J = 11.9, 6.8$ Hz, 1H), 1.66 (q, $J = 10.6$ Hz, 1H) ppm.

^{13}C NMR (CDCl_3 , 151 MHz) δ 150.24, 149.91, 144.53, 137.48, 131.58, 131.11, 130.03, 128.89, 128.78, 128.35, 127.72, 127.70, 124.87, 122.22, 119.23, 118.42 (q, $J_{\text{CF}} = 320.9$ Hz), 107.63, 67.87, 62.72, 60.03, 57.71, 48.84, 48.26, 44.87, 34.70, 21.77 ppm.

IR (thin film, cm^{-1}) 3527.29, 2923.73, 2852.99, 2631.34, 2337.57, 1455.70, 1210.93, 1162.04, 1024.86, 781.00, 666.90, 610.11.

HRMS (+NSI) calculated for $\text{C}_{30}\text{H}_{30}\text{F}_3\text{N}_2\text{O}_6\text{S}_2$ $[\text{M}+\text{H}]^+$ 635.1497, found 635.1501.

Tertiary alcohol **3.38**



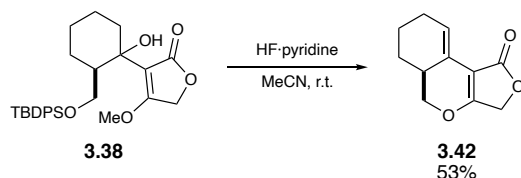
A solution of silyloxy furan **3.37** (0.817 g, 2.06 mmol) in THF (10.0 mL) was cooled to -78 °C. A solution of $n\text{BuLi}$ (1.26 mL, 1.63 M in hexanes, 2.06 mmol) was added drop-wise over 5 minutes to the reaction flask, and the resulting solution was allowed to stir at -78 °C for 15 minutes. A solution of ketone **3.13** (0.377 g, 1.03 mmol) in THF (5.0 mL) was added at -78 °C, and the resulting mixture was allowed to warm up to room temperature over 2 hours. The reaction was quenched with pH 5.5 aqueous phosphate buffer (20.0 mL) and the resulting biphasic mixture was allowed to stir at room temperature for 15 minutes. The layers were separated, and the aqueous layer was extracted with Et_2O (3 x 25.0 mL). The combined organic extracts were washed with brine (40.0 mL), dried over anhydrous MgSO_4 , filtered, and concentrated under reduced pressure. Purification by flash column chromatography on silica gel (2:1 to 1:1 Hexanes/ EtOAc) provided tertiary alcohol **3.38** (0.423 g, 85%).

^1H NMR (CDCl_3 , 600 MHz) δ 7.68 – 7.59 (m, 4H), 7.46 – 7.40 (m, 2H), 7.39 – 7.33 (m, 4H), 4.61 (s, 1H), 4.59 (s, 2H), 3.84 – 3.77 (m, 0H), 3.73 (s, 3H), 3.62 (dd, $J = 10.5, 3.0$ Hz, 1H), 2.14 (dq, $J = 11.5, 3.5$ Hz, 1H), 1.97 – 1.72 (m, 4H), 1.67 (d, $J = 12.7$ Hz, 1H), 1.60 (d, $J = 10.3$ Hz, 1H), 1.49 (dd, $J = 9.5, 4.2$ Hz, 1H), 1.35 (qt, $J = 11.0, 2.8$ Hz, 1H), 1.06 (s, 9H) ppm.

^{13}C NMR (CDCl_3 , 126 MHz) δ 173.28, 172.16, 135.72, 135.61, 129.82, 127.75, 127.74, 108.67, 67.21, 64.20, 57.17, 43.25, 37.08, 26.89, 25.68, 24.81, 20.83, 19.28 ppm.

HRMS (+NSI) calculated for $\text{C}_{28}\text{H}_{36}\text{NaO}_5\text{Si}$ $[\text{M}+\text{Na}]^+$ 503.2230, found 503.2219.

Diene 3.42

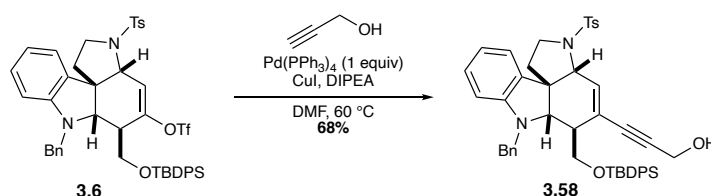


HF-pyridine (0.0165 mL) was added to a solution of tertiary alcohol **3.38** (0.070 g, 0.159 mmol) in CH_3CN (1.0 mL), and the resulting solution was allowed to stir at room temperature for 21 hours. The reaction was diluted with EtOAc (5.0 mL) and quenched with saturated aqueous NaHCO_3 (5.0 mL). The layers were separated and the aqueous layer was extracted with EtOAc (3 x 10.0 mL). The combined organic extracts were washed with brine (20.0 mL), dried over anhydrous Na_2SO_4 , filtered, and concentrated under reduced pressure. Purification by flash column chromatography on silica gel (7:3 Hexanes/EtOAc) provided endocyclic olefin **3.42** (0.015 mg, 53%).

^1H NMR (CDCl_3 , 600 MHz) δ 6.37 (dd, $J = 4.9, 2.5$ Hz, 1H), 4.66 (d, $J = 16.2$ Hz, 1H), 4.60 (d, $J = 16.3$ Hz, 1H), 4.47 (dd, $J = 10.6, 4.9$ Hz, 1H), 3.80 (dd, $J = 12.3, 10.6$ Hz, 1H), 2.64 – 2.54 (m, 1H), 2.31 – 2.10 (m, 2H), 1.99 – 1.89 (m, 1H), 1.88 – 1.78 (m, 1H), 1.72 – 1.60 (m, 1H), 1.15 – 1.11 (m, 1H) ppm.

HRMS (+APCI) calculated for $\text{C}_{11}\text{H}_{13}\text{O}_3$ $[\text{M}+\text{H}]^+$ 193.0865, found 193.0856.

Enyne 3.58



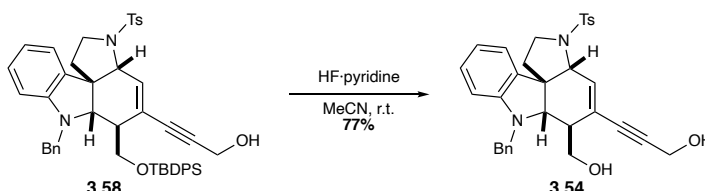
Propargyl alcohol (0.003 mL, 0.046 mmol) and DIPEA (0.05 mL) were added to a solution of vinyl triflate **3.6** (0.010 g, 0.0114 mmol), $\text{Pd}(\text{PPh}_3)_4$ (0.0132 g, 0.0114 mmol), and CuI (0.0026g, 0.0114 mmol) in DMF (0.1 mL). The resulting mixture was degassed by freeze-pump-thaw (-196

°C, over 3 cycles). The mixture was allowed to stir at room temperature for 15 minutes and at 60 °C for 20 hours. The reaction was diluted with EtOAc (3.0 mL) and quenched with saturated aqueous NH₄Cl (3.0 mL). The layers were separated, and the aqueous layer was extracted with EtOAc (2 x 4.0 mL). The combined organic extracts were washed with brine (10.0 mL), dried over anhydrous Na₂SO₄, filtered, and concentrated under reduced pressure. Purification by preparatory TLC (7:3 Hexanes/ EtOAc) provided propargyl alcohol **3.58** (0.0038 g, 43%).

¹H NMR (CDCl₃, 600 MHz) δ 7.61 (d, *J* = 8.2 Hz, 2H), 7.51 – 7.47 (m, 4H), 7.44 – 7.37 (m, 2H), 7.32 (t, *J* = 7.5 Hz, 2H), 7.30 – 7.21 (m, 6H), 7.19 (d, *J* = 6.8 Hz, 2H), 7.13 (d, *J* = 8.0 Hz, 2H), 6.98 (td, *J* = 7.7, 1.3 Hz, 1H), 6.87 (d, *J* = 2.7 Hz, 1H), 6.63 (t, *J* = 7.2 Hz, 1H), 6.22 (d, *J* = 7.8 Hz, 1H), 4.37 (d, *J* = 16.0 Hz, 1H), 4.29 (d, *J* = 16.2 Hz, 1H), 4.26 (d, *J* = 5.6 Hz, 2H), 3.72 (td, *J* = 10.7, 7.2 Hz, 1H), 3.68 (d, *J* = 1.4 Hz, 1H), 3.67 (d, *J* = 2.2 Hz, 1H), 3.62 (dd, *J* = 10.2, 4.6 Hz, 1H), 3.39 (t, *J* = 10.4 Hz, 1H), 3.37 (dd, *J* = 10.4, 7.9 Hz, 1H), 2.57 (dd, *J* = 7.8, 4.7 Hz, 1H), 2.37 (s, 3H), 1.91 (dd, *J* = 11.8, 7.1 Hz, 1H), 1.34 (q, *J* = 10.7 Hz, 1H), 0.93 (s, 9H) ppm.

HRMS (+APCI) calculated for C₄₈H₅₁O₄N₂SSi [M+H]⁺ 779.3339, found 779.3333.

Alkynediol **3.54**

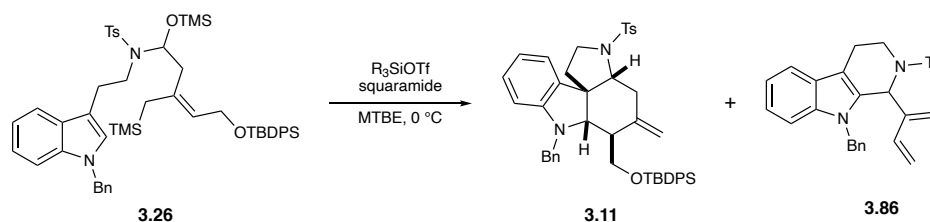


A solution of protected alcohol **3.58** (0.0033 g, 0.0042 mmol) in CH₃CN (0.2 mL) was prepared in a plastic centrifuge vial. HF·pyridine (0.05 mL) was added to the solution and the mixture was stirred at room temperature for 5.5 hours. The reaction was diluted with EtOAc (2.0 mL) and quenched with saturated aqueous NaHCO₃ (3.0 mL). The layers were separated, and the aqueous layer was extracted with EtOAc (3 x 3.0 mL). The combined organic extracts were washed with brine (7.0 mL), dried over anhydrous Na₂SO₄, filtered, and concentrated under reduced pressure. Purification by preparatory TLC (1:1 Hexanes/EtOAc) provided diol **3.54** (0.0017 g, 74%).

$^1\text{H NMR}$ (CDCl_3) δ 7.70 (d, $J = 8.3$ Hz, 2H), 7.34 (d, $J = 7.5$ Hz, 2H), 7.30 – 7.28 (m, 6H), 7.02 (td, $J = 7.7, 1.3$ Hz, 1H), 6.93 (d, $J = 2.6$ Hz, 1H), 6.68 (td, $J = 7.5, 1.0$ Hz, 1H), 6.32 (d, $J = 7.8$ Hz, 1H), 4.45 (d, $J = 15.3$ Hz, 1H), 4.32 (s, 2H), 4.15 (d, $J = 15.3$ Hz, 1H), 3.83 (d, $J = 1.6$ Hz, 1H), 3.76 (td, $J = 10.9, 7.0$ Hz, 1H), 3.67 (d, $J = 1.6$ Hz, 1H), 3.50 – 3.45 (m, 3H), 2.49 (t, $J = 5.4$ Hz, 1H), 2.44 (s, 3H), 1.98 (dd, $J = 11.9, 6.9$ Hz, 1H), 1.60 (q, $J = 10.2$ Hz, 3H) ppm.

HRMS (+NSI) calculated for $\text{C}_{32}\text{H}_{33}\text{O}_4\text{N}_2\text{S}$ $[\text{M}+\text{H}]^+$ 541.2161, found 541.2152.

General procedure for silyl triflate mediated annulation



A solution of hemiaminal **3.26** (1 equiv.) and squaramide catalyst (0.10 equiv.)¹⁰ in Et_2O (0.1 M) was cooled to $0\text{ }^\circ\text{C}$. Freshly distilled silyl triflate (1 equiv.) was added *via* microsyringe. The reaction was stirred at $0\text{ }^\circ\text{C}$ until TLC (7:3 Hex/EtOAc) indicated complete consumption of the starting material (~1 hour). 1,4-dinitrobenzene (0.25 equiv) in Et_2O (2 mL) was added and the reaction was quenched with saturated aqueous NaHCO_3 (2 mL). The mixture was allowed to stir at room temperature for 15 minutes. The layers were separated, and the aqueous layer was extracted with Et_2O (3 x 2 mL). The combined organic extracts were washed with brine (5 mL), dried over anhydrous MgSO_4 , filtered, and concentrated under reduced pressure. Integration against the 1,4-dinitrobenzene as an internal NMR standard indicated yields of tetracyclic core **3.11** and elimination product **3.86**. Purification by preparatory TLC (9:1 Hex/EtOAc, 2 sweeps) provided pure samples of **3.11** and **3.86**.

Data for **3.86**

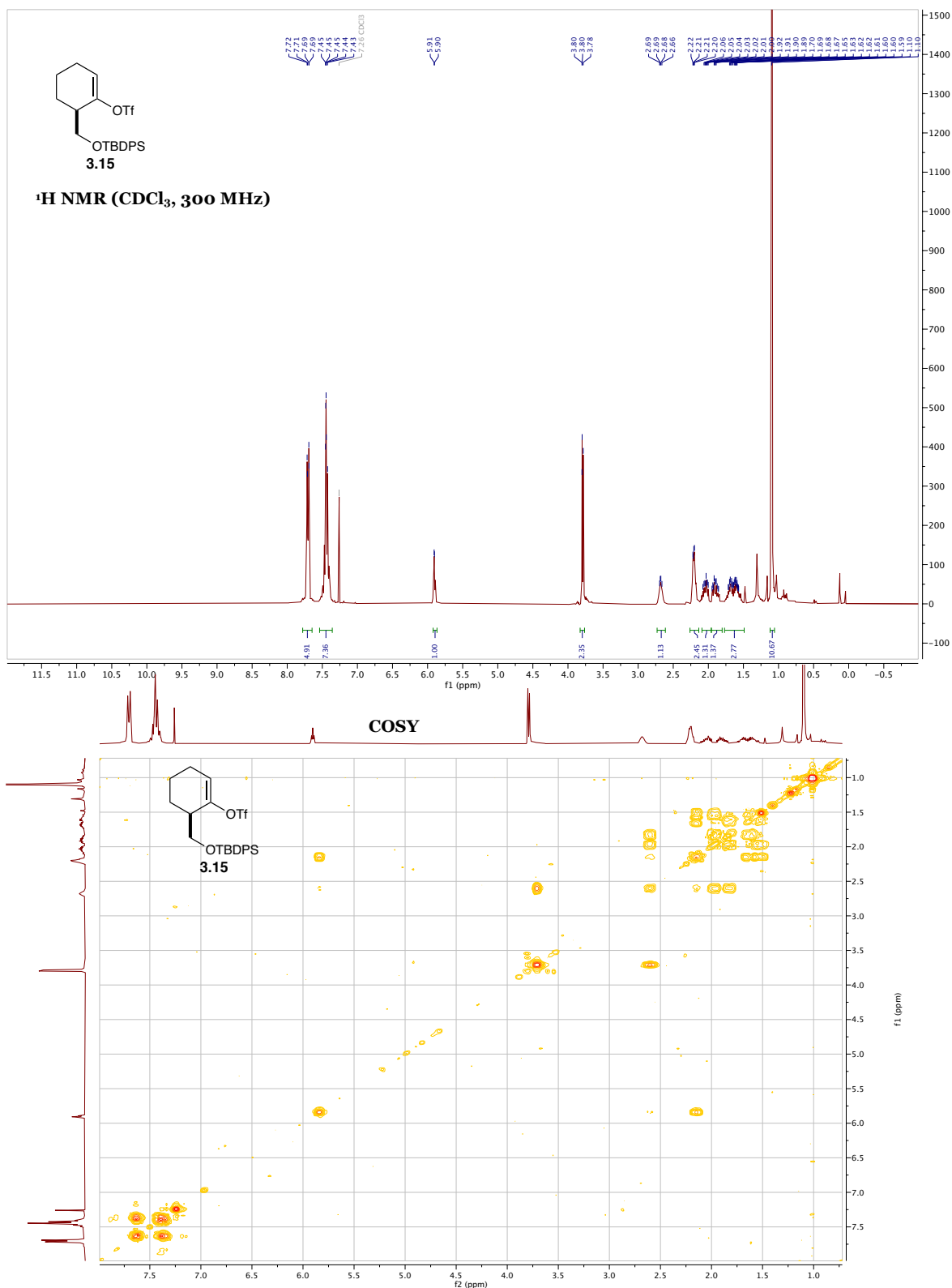
$^1\text{H NMR}$ (CDCl_3 , 600 MHz) δ 7.41 – 7.30 (m, 2H), 7.30 – 7.28 (m, 4H), 7.18 (d, $J = 7.3$ Hz, 1H), 7.13 (t, $J = 7.5$ Hz, 1H), 7.10 – 7.03 (m, 1H), 6.98 (d, $J = 8.9$ Hz, 2H), 6.96 – 6.92 (m, 2H), 6.38

¹⁰ No squaramide catalyst was added for racemic reactions with TMSOTf.

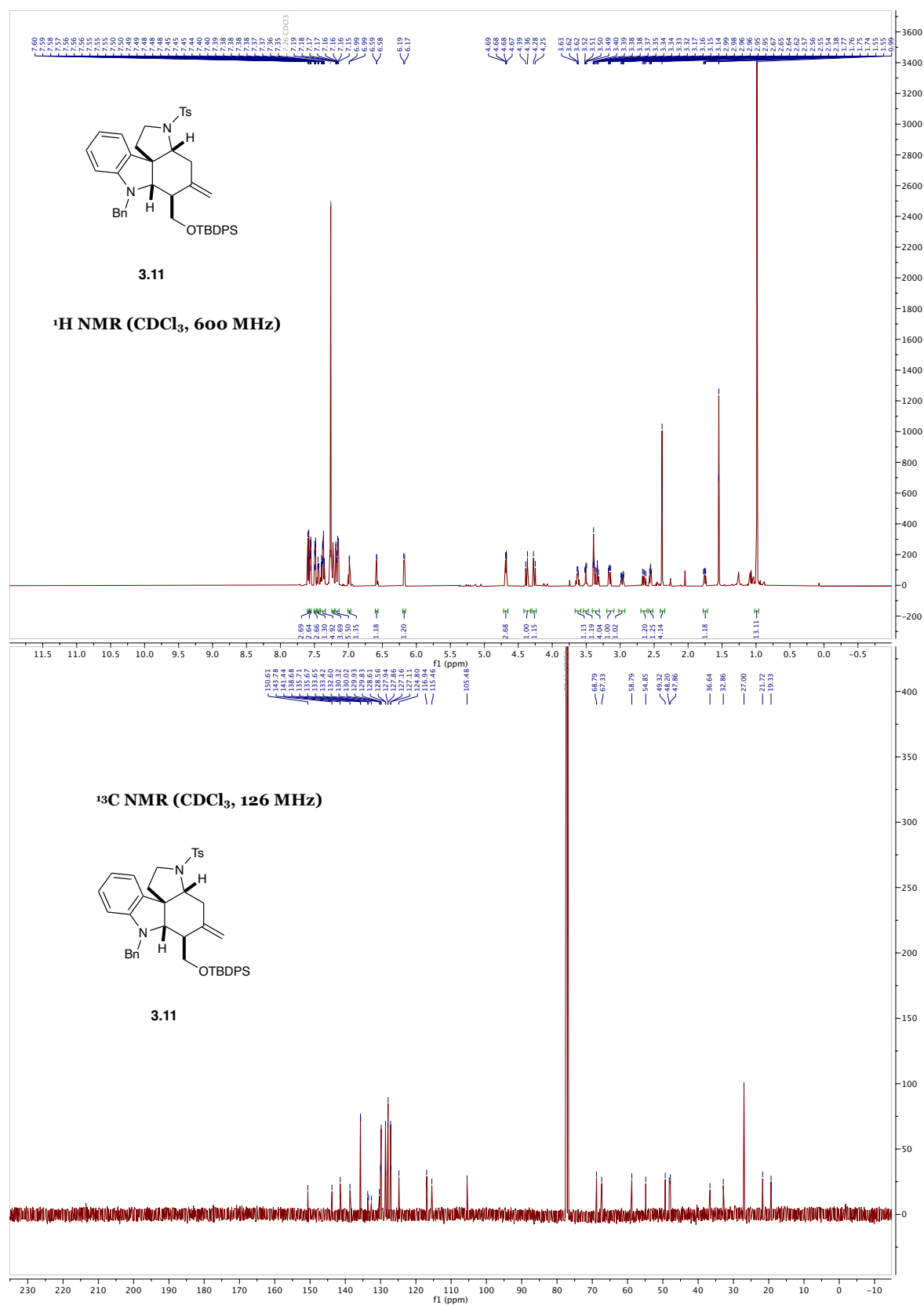
(dd, $J = 17.7, 10.8$ Hz, 1H), 5.37 (d, $J = 17.1$ Hz, 1H), 5.28 – 5.24 (m, 1H), 5.25 (d, $J = 17.2$ Hz, 1H), 5.22 (d, $J = 17.7$ Hz, 1H), 5.13 – 5.11 (m, 2H), 5.10 (d, $J = 10.9$ Hz, 1H), 5.05 (s, 1H), 4.11 (dd, $J = 14.8, 6.4$ Hz, 1H), 3.56 (ddd, $J = 14.9, 11.8, 5.3$ Hz, 1H), 2.72 – 2.63 (m, 2H), 2.61 (dd, $J = 15.6, 5.1$ Hz, 1H), 2.56 – 2.47 (m, 1H), 2.26 (s, 3H).

3.6 Spectral data

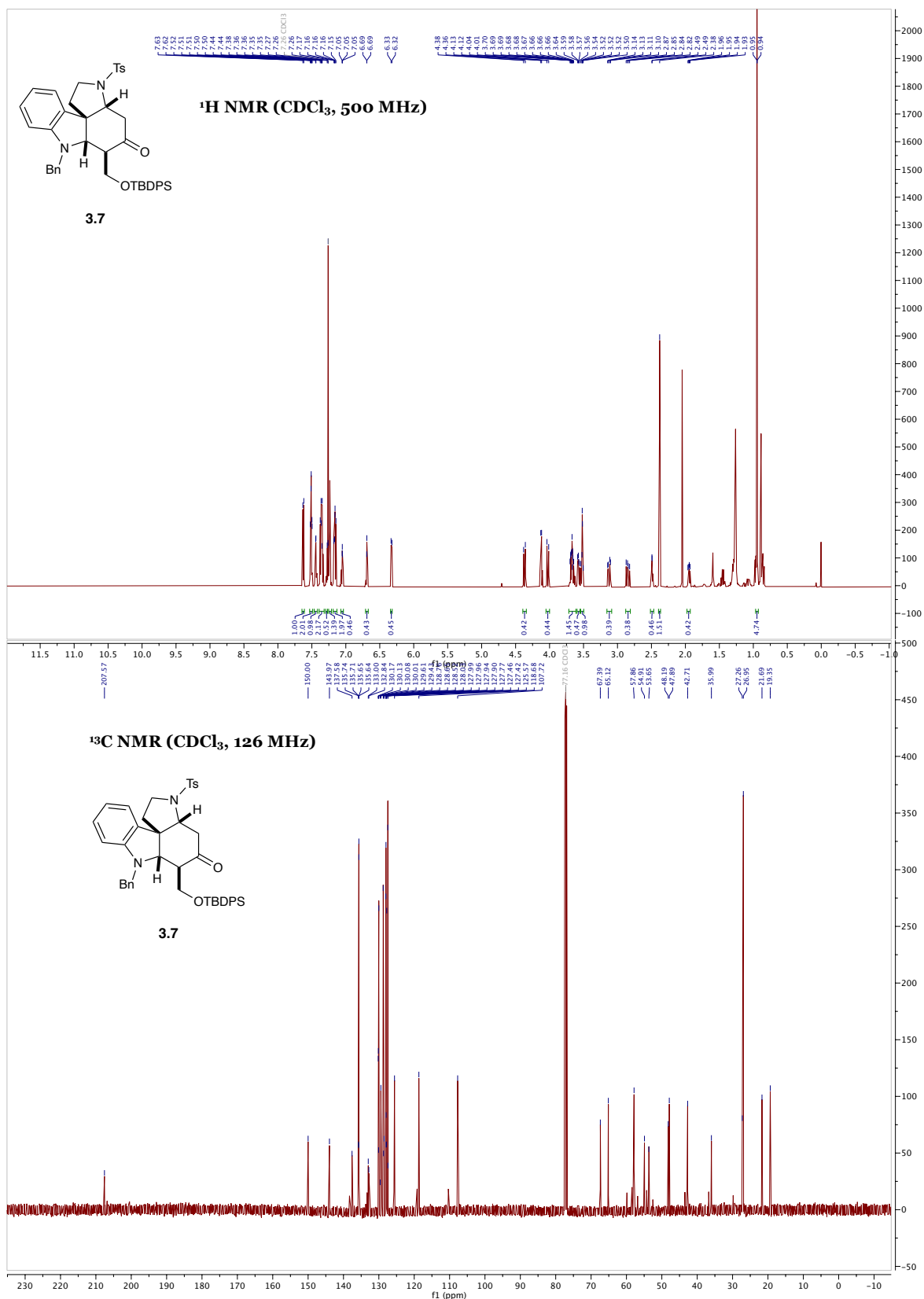
Vinyl triflate 3.15

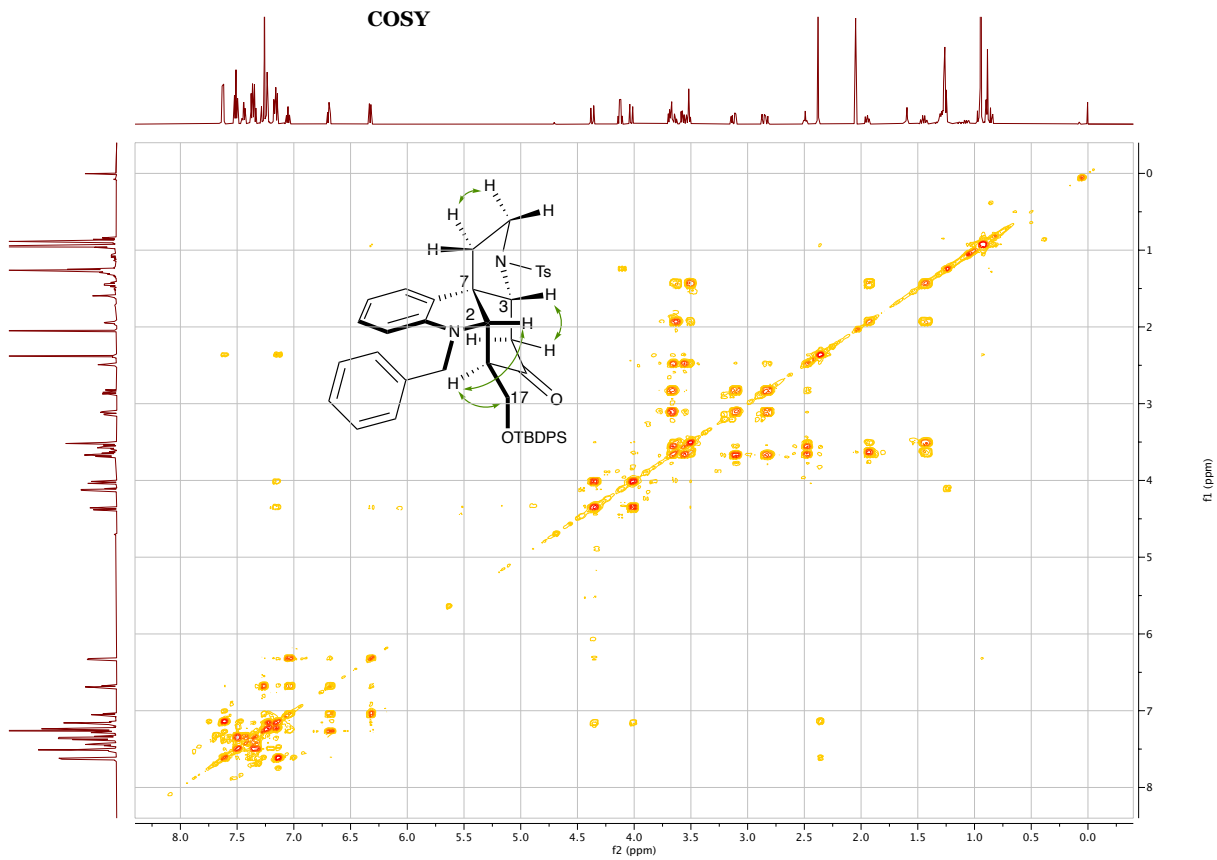


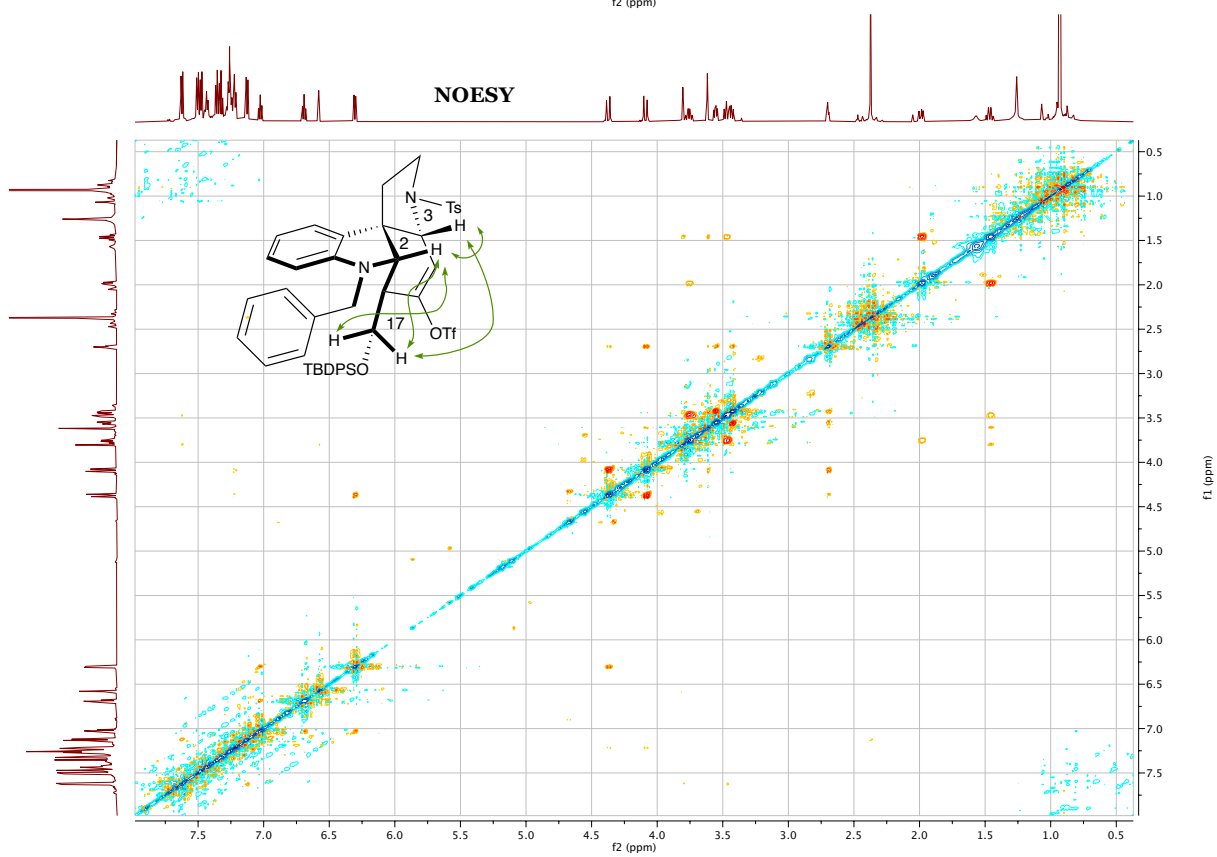
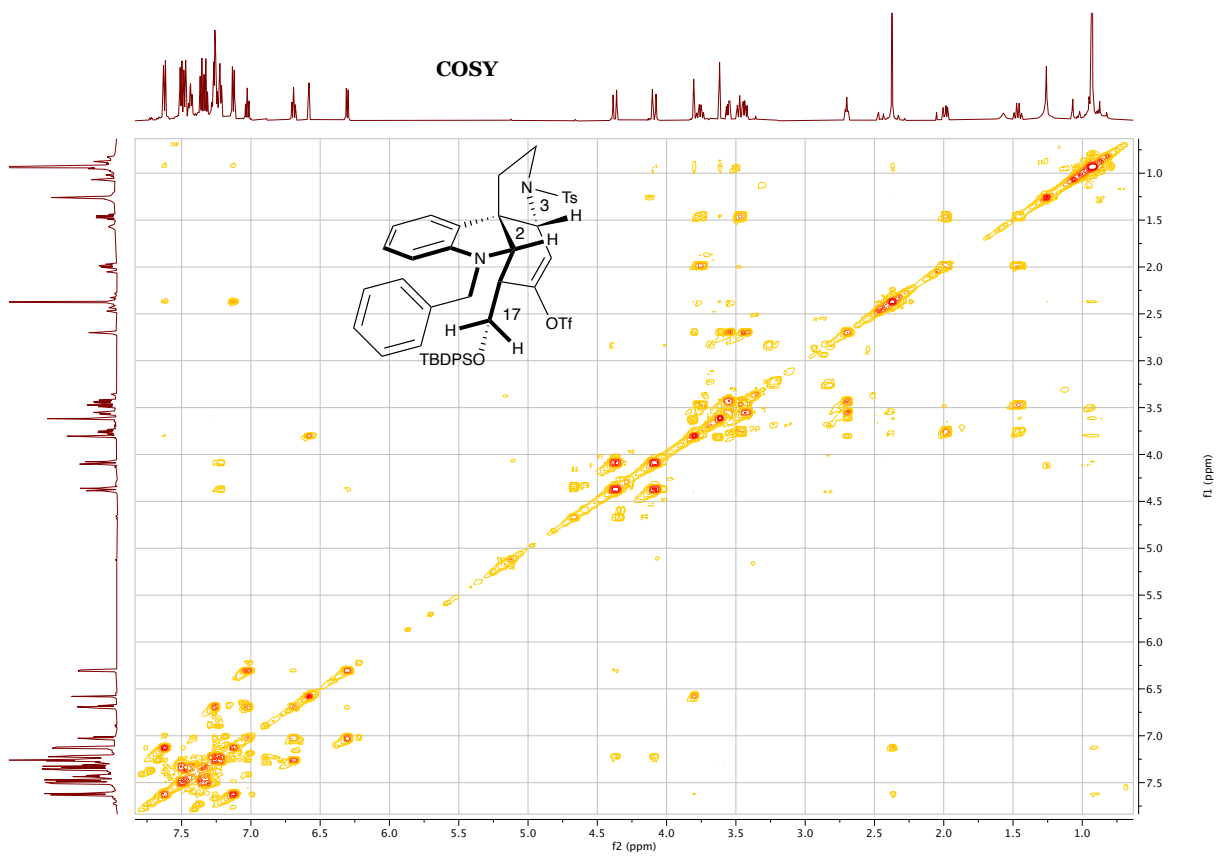
Tetracyclic core 3.11

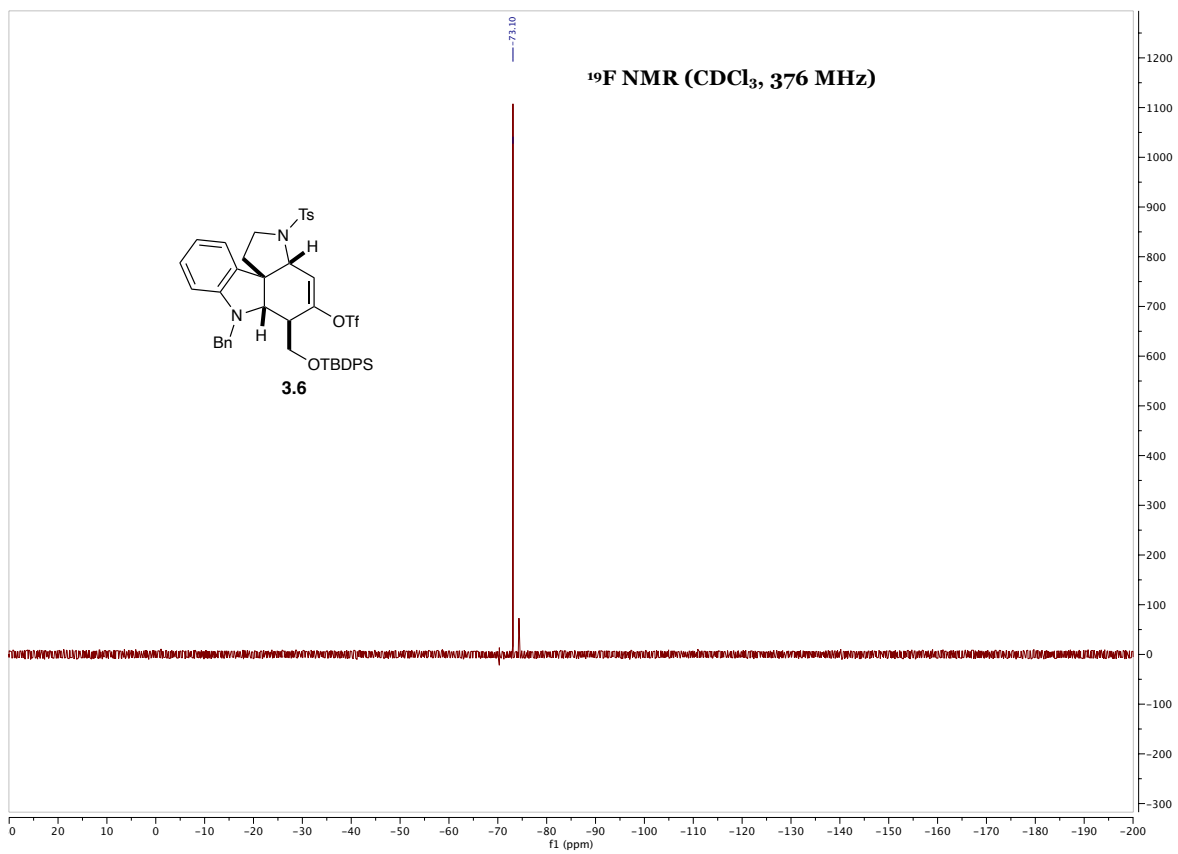


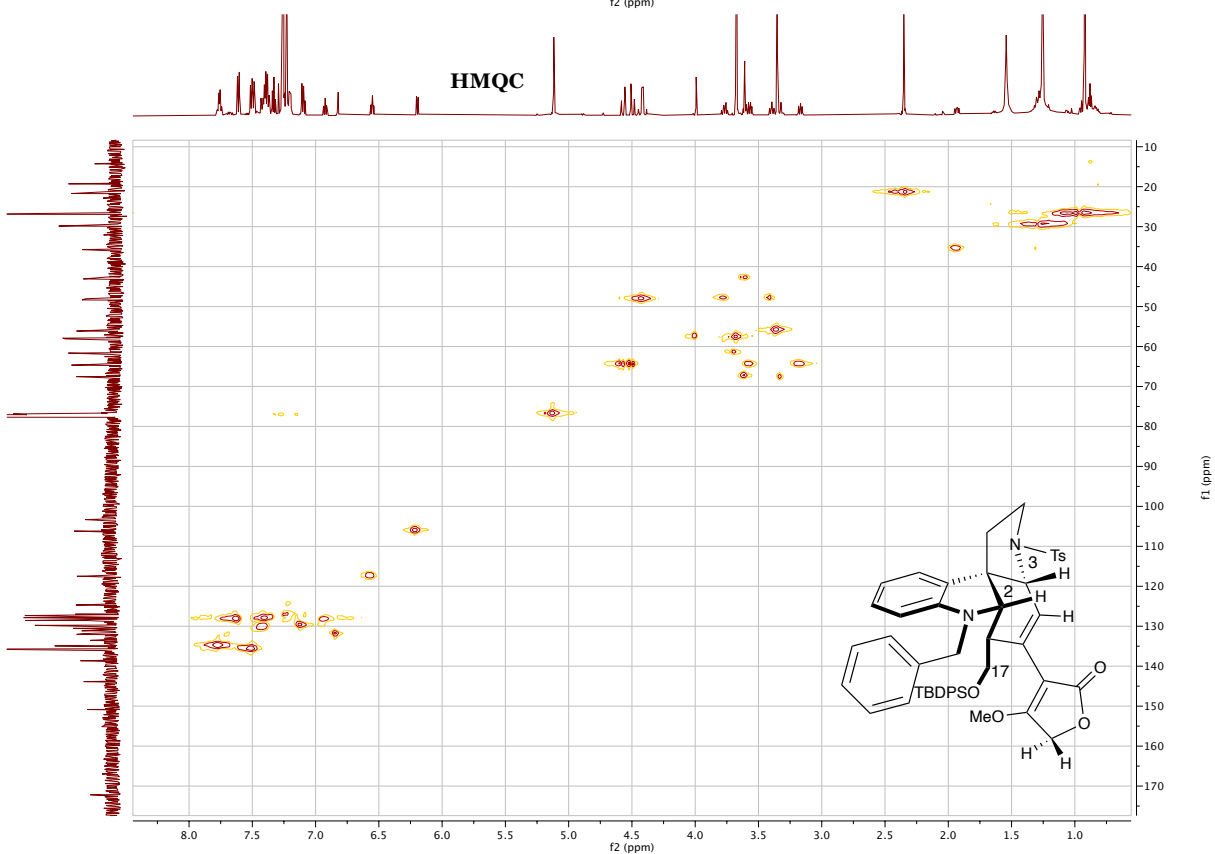
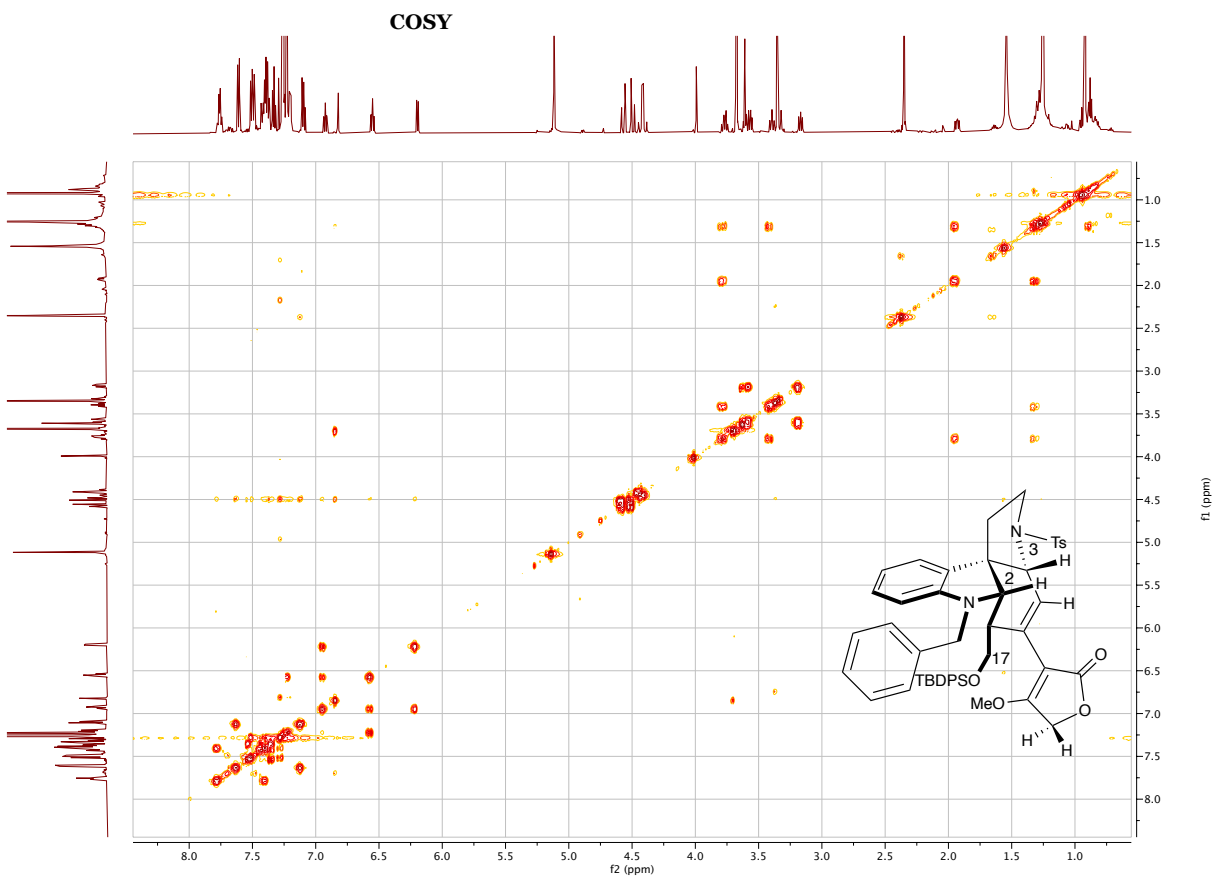
Ketone 3.7

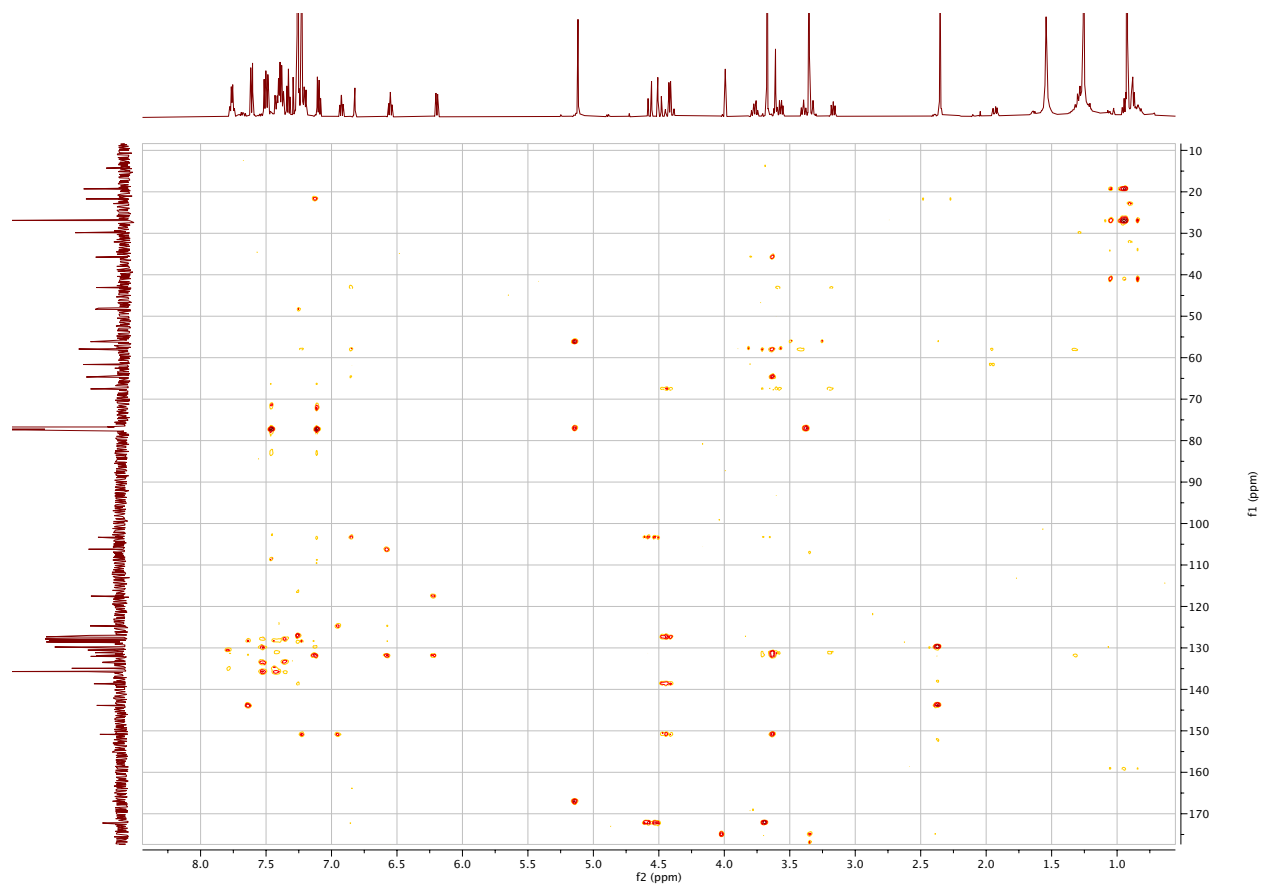




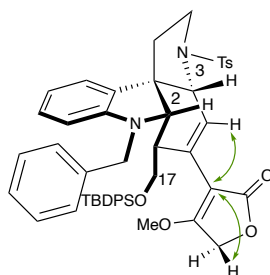


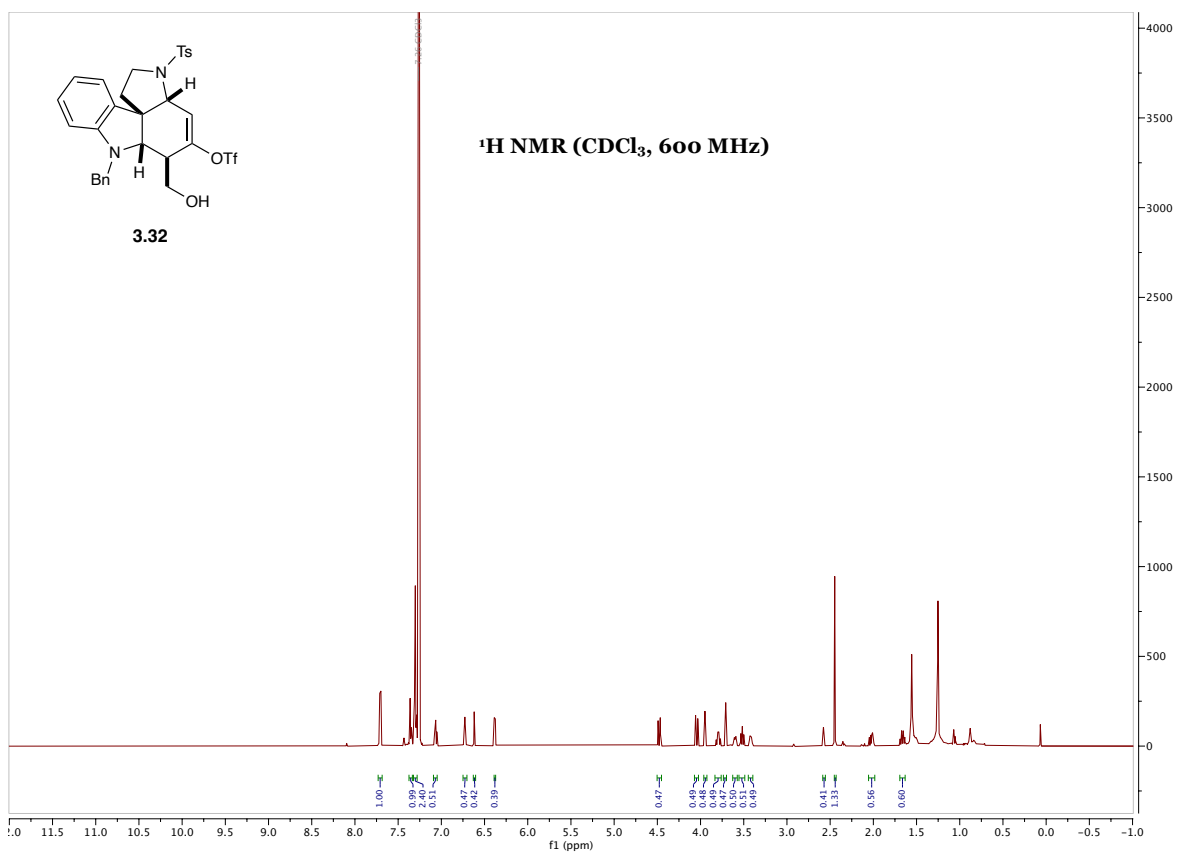


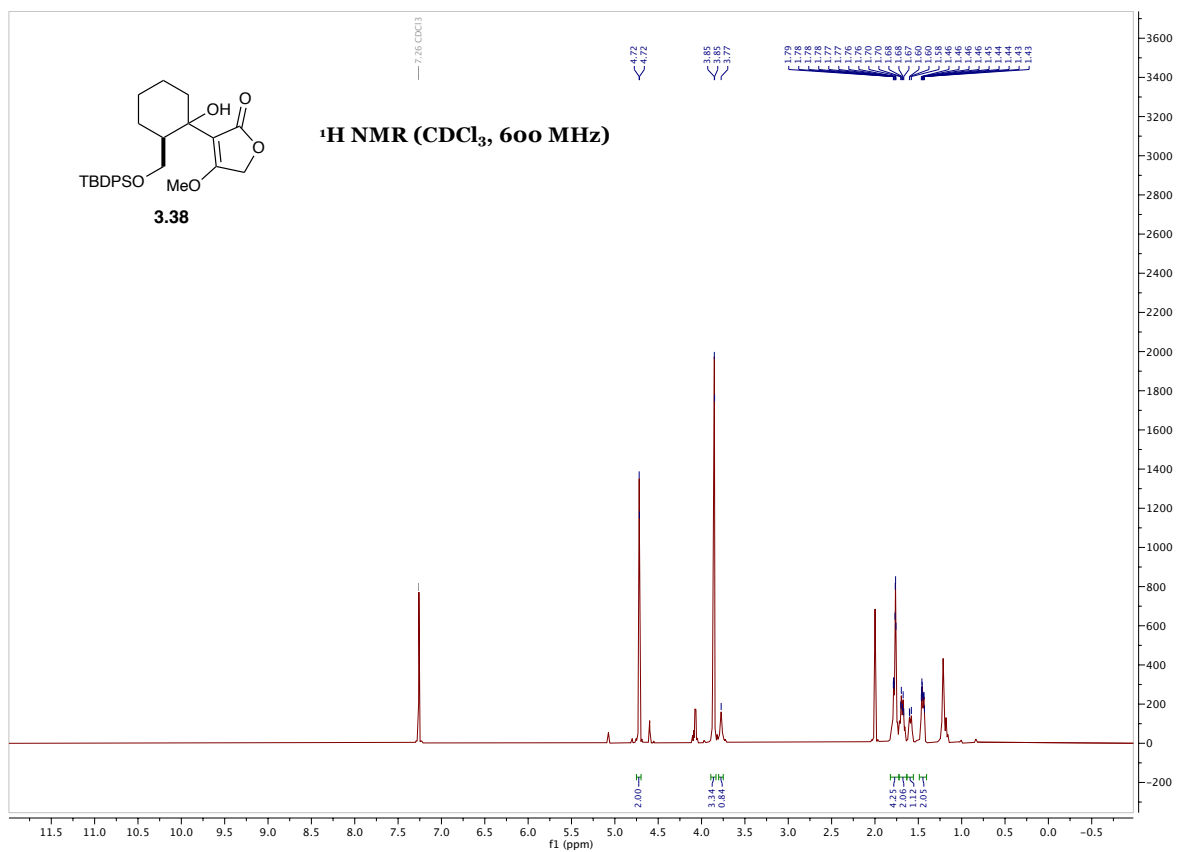




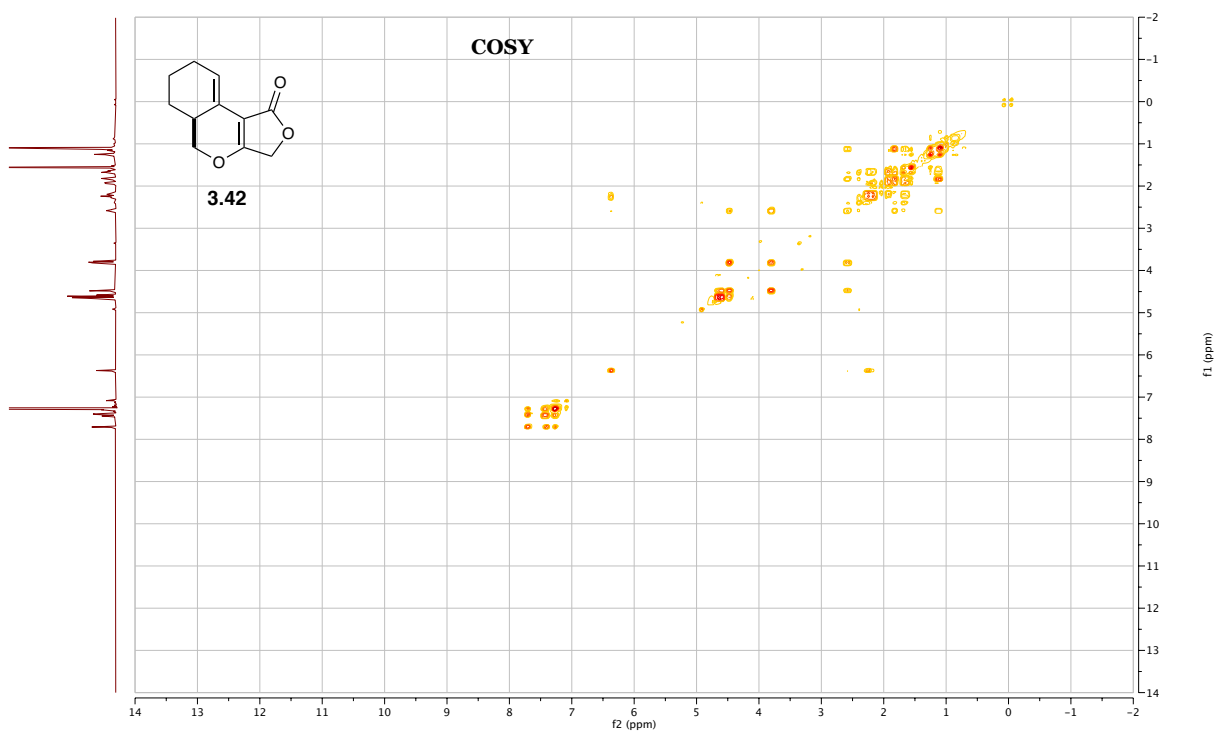
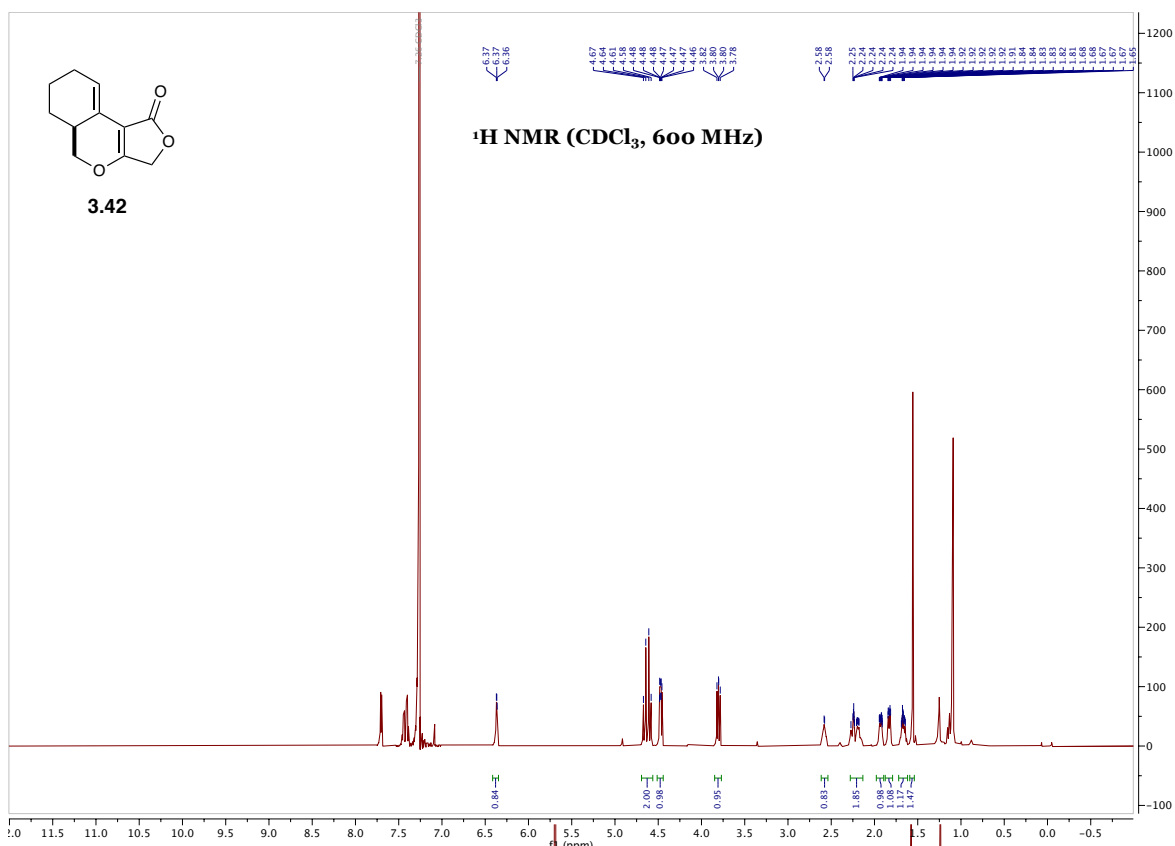
HMBC



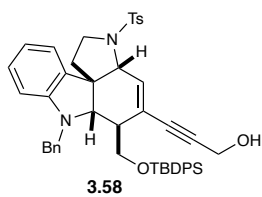
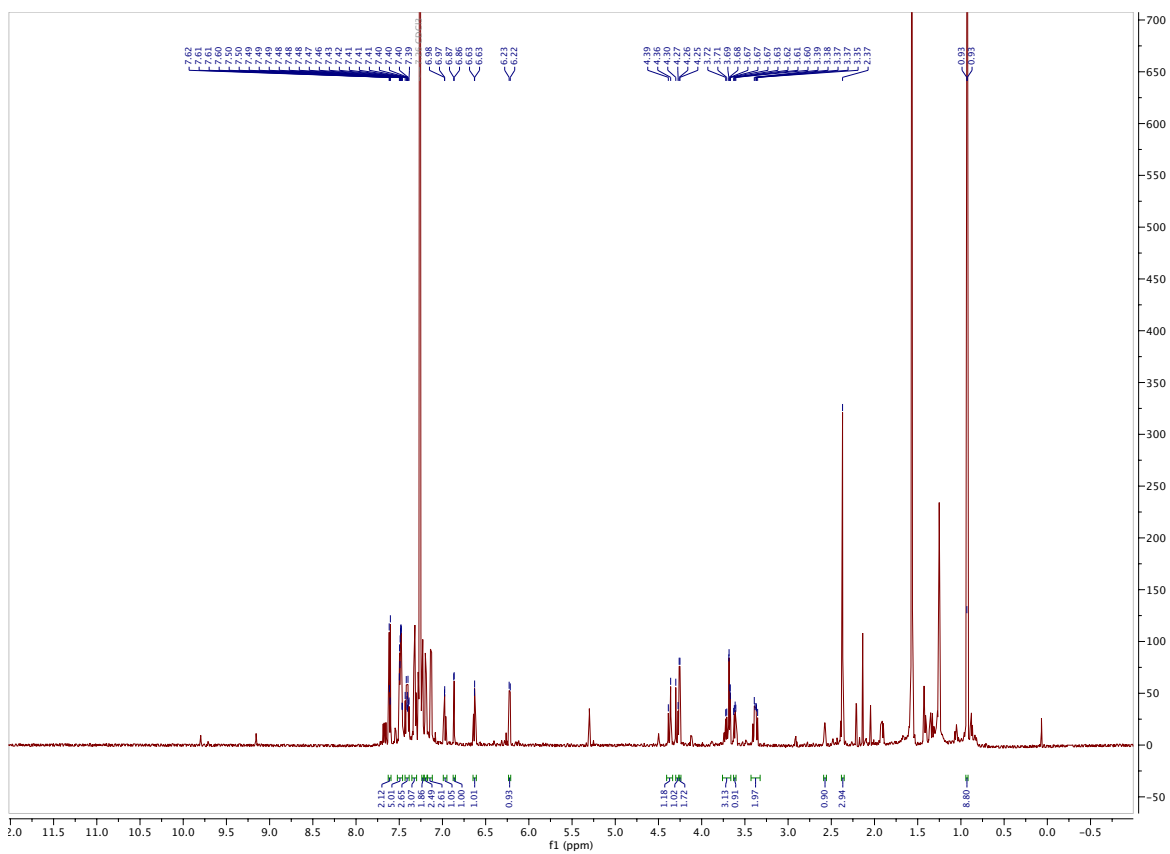
Primary alcohol **3.32**

Tertiary alcohol **3.38**

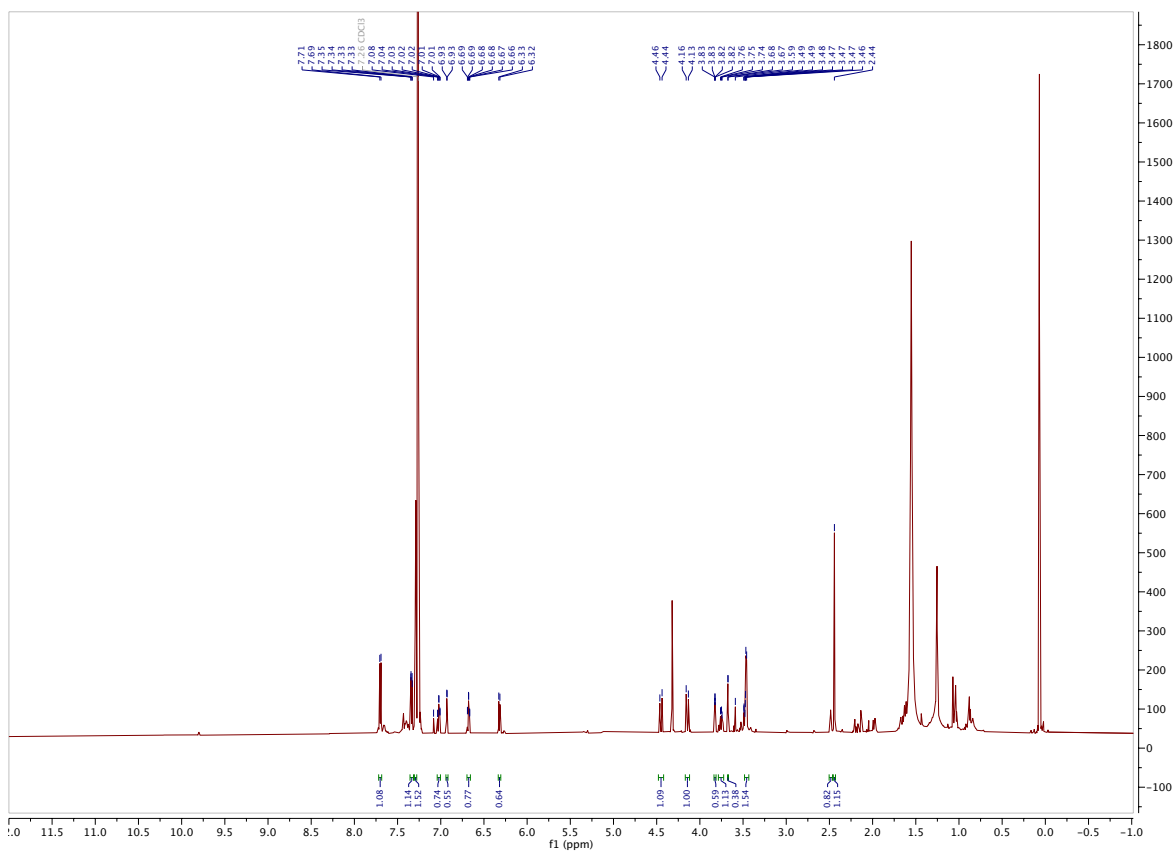
Tricyclic diene 3.42



Enyne 3.58

¹H NMR (CDCl₃, 600 MHz)

Alkynediol 3.54



3.7 References

- (1) Kazerouni, A. M.; Mancheno, D. E.; Blakey, S. B. Model Studies for the Total Synthesis of 11-Demethoxymyrtoidine and Myrtoidine. *Heterocycles* **2019**, *99*, 389.
- (2) Mancheno, D. E. Development of a Copper Catalyzed Aminoacetoxylation Reaction of Olefins, Development of an Intermolecular and Diastereoselective Iminium Cascade Reaction and Studies Towards the Synthesis of a Malagasy Alkaloid. Emory University, **2013**.
- (3) Delgado, R.; Blakey, S. B. Cascade Annulation Reactions To Access the Structural Cores of Stereochemically Unusual Strychnos Alkaloids. *European J. Org. Chem.* **2009**, *2009*, 1506–1510.
- (4) Kong, A.; Mancheno, D. E.; Boudet, N.; Delgado, R.; Andreansky, E. S.; Blakey, S. B. Total Synthesis of Malagashanine: A Chloroquine Potentiating Indole Alkaloid with Unusual Stereochemistry. *Chem. Sci.* **2017**, *8*, 697–700.
- (5) Andreansky, E. S.; Blakey, S. B. An Iminium Ion Cascade Annulation Strategy for the Synthesis of Akuammiline Alkaloid Pentacyclic Core Structures. *Org. Lett.* **2016**, *18*, 6492–6495.
- (6) Wipf, P.; Aslan, D. C. Synthesis of Bicyclic Ortho Esters by Epoxy Ester Rearrangements and Study of Their Ring-Opening Reactions. *J. Org. Chem.* **2001**, *66*, 337–343.
- (7) Comins, D. L.; Dehghani, A.; Foti, C. J.; Joseph, S. P. PYRIDINE-DERIVED TRIFLATING REAGENTS: N-(2-PYRIDYL)-TRIFLIMIDE AND N-(5-CHLORO-2-PYRIDYL)TRIFLIMIDE. *Org. Synth.* **1997**, *74*, 77.
- (8) Song, Y. S.; Lee, Y. J.; Kim, B. T.; Heo, J. N. An Efficient Procedure for the Synthesis of 3-Aryl-4-Methoxy-2(5H)-Furanones by Using the Microwave-Promoted Suzuki-Miyaura Coupling Reactions. *Tetrahedron Lett.* **2006**, *47*, 7427–7430.
- (9) Ley, S. V.; Wadsworth, D. J. Preparation of O-Methyl 3-Acyl Tetronic Acids by the Direct Acylation of Stannyl Tetronates. *Tetrahedron Lett.* **1989**, *30*, 1001–1004.

- (10) Zhang, D.; Ready, J. M. Directed Hydrozirconation of Propargylic Alcohols. *J. Am. Chem. Soc.* **2007**, *129*, 12088–12089.
- (11) Delgado, R. Development of a Novel Cascade Cyclisation Reaction and Its Application Towards the Total Synthesis of Malagashanine: A Chloroquine Efflux Inhibitor, Emory University, **2010**.
- (12) Han, X.; Stoltz, B. M.; Corey, E. J. Cuprous Chloride Accelerated Stille Reactions. A General and Effective Coupling System for Sterically Congested Substrates and for Enantioselective Synthesis. *J. Am. Chem. Soc.* **1999**, *121*, 7600–7605.
- (13) Espinet, P.; Echavarren, A. M. The Mechanisms of the Stille Reaction. *Angew. Chem. Int. Ed.* **2004**, *43*, 4704–4734.
- (14) Shenvi, R. A.; Guerrero, C. A.; Shi, J.; Li, C. C.; Baran, P. S. Synthesis of (+)-Cortistatin A. *J. Am. Chem. Soc.* **2008**, *130*, 7241–7243.
- (15) Franz F. Paintner Gerd Bauschke, L. A. A General Method for the Highly Regioselective Introduction of Substituents into the 3-Position of 5-Unsubstituted 4-O-Alkyl Tetronates. *Synlett* **2005**, *18*, 2735–2738.
- (16) Roslin, S.; Odell, L. R. Visible-Light Photocatalysis as an Enabling Tool for the Functionalisation of Unactivated C(sp³)-Substrates. *Eur. J. Org. Chem.* **2017**, *2017*, 1993–2007.
- (17) Crich, D.; Quintero, L. Radical Chemistry Associated with the Thiocarbonyl Group. *Chem. Rev.* **1989**, *89*, 1413–1432.
- (18) McCombie, S. W.; Motherwell, W. B.; Tozer, M. J. The Barton-McCombie Reaction. In *Organic Reactions* **2012**, *77*, 161–432.
- (19) Barton, D. H. R.; McCombie, S. W. A New Method for the Deoxygenation of Secondary Alcohols. *J. Chem. Soc. Perkin Trans. 1* **1975**, No. 16, 1574–1585.
- (20) Lackner, G. L.; Quasdorf, K. W.; Overman, L. E. Direct Construction of Quaternary Carbons from Tertiary Alcohols via Photoredox-Catalyzed Fragmentation of Tert-Alkyl N-

- Phthalimidoyl Oxalates. *J. Am. Chem. Soc.* **2013**, *135*, 15342–15345.
- (21) Chenneberg, L.; Baralle, A.; Daniel, M.; Fensterbank, L.; Goddard, J.-P.; Ollivier, C. Visible Light Photocatalytic Reduction of *O*-Thiocarbamates: Development of a Tin-Free Barton-McCombie Deoxygenation Reaction. *Adv. Synth. Catal.* **2014**, *356*, 2756–2762.
- (22) Zhang, X.; MacMillan, D. W. C. Alcohols as Latent Coupling Fragments for Metallaphotoredox Catalysis: Sp³-Sp² Cross-Coupling of Oxalates with Aryl Halides. *J. Am. Chem. Soc.* **2016**, *138*, 13862–13865.
- (23) Bürgi, H. B.; Dunitz, J. D.; Lehn, J. M.; Wipff, G. Stereochemistry of Reaction Paths at Carbonyl Centres. *Tetrahedron* **1974**, *30*, 1563–1572.
- (24) Li, R.; Bao, -Yuan; Zhao, R.; Shi, L. Progress and Developments in the Turbo Grignard Reagent I-PrMgClÁLiCl: A Ten-Year Journey. *Chem. Commun.* **2015**, *51*, 6884.
- (25) Bai, Y.; Davis, D. C.; Dai, M. Natural Product Synthesis via Palladium-Catalyzed Carbonylation. *J. Org. Chem* **2017**, *82*, 2319–2328.
- (26) Ma, K.; Martin, B. S.; Yin, X.; Dai, M. Natural Product Syntheses: Via Carbonylative Cyclisations. *Natural Product Reports.* **2019**, *36*, 174–219.
- (27) Carpenter, J.; Northrup, A. B.; Chung, deMichael; Wiener, J. J. M.; Kim, S.-G.; MacMillan, D. W. C. Total Synthesis and Structural Revision of Callipeltoside C. *Angew. Chem. Int. Ed.* **2008**, *47*, 3568–3572.
- (28) Hayes, P. Y.; Kitching, W. Total Synthesis and Absolute Stereochemistry of Plakortone D. *J. Am. Chem. Soc.* **2002**, *124*, 9718–9719.
- (29) Wilkerson-Hill, S. M.; Lavados, C. M.; Sarpong, R. The Diels–Alder Reactivity of 2-Vinylindenes: Synthesis of Functionalised Tetrahydrofluorenes. *Tetrahedron* **2016**, *72*, 3635–3640.
- (30) Kong, A.; Andreansky, E. S.; Blakey, S. B. Stereochemical Complexity in Oxocarbenium-Ion-Initiated Cascade Annulations for the Synthesis of the ABCD Core of Mattogrossine. *J. Org. Chem.* **2017**, *82*, 4477–4483.

- (31) Brak, K.; Jacobsen, E. N. Asymmetric Ion-Pairing Catalysis. *Angew. Chem. Int. Ed.* **2013**, *52*, 534–561.
- (32) Sewgobind, N. V.; Wanner, M. J.; Ingemann, S.; De Gelder, R.; Van Maarseveen, J. H.; Hiemstra, H. Enantioselective BINOL-Phosphoric Acid Catalyzed Pictet - Spengler Reactions of N-Benzyltryptamine. *J. Org. Chem.* **2008**, *73*, 6405–6408.
- (33) Kong, A. Synthetic Studies for Heterocycle Synthesis Part I: Intra/Intermolecular Olefin Diamination for the Stereoselective Synthesis of 3-Aminopiperidines Part II: Total Synthesis of Malagashanine and Synthetic Studies Toward Related Alkaloids, Emory University, **2014**.
- (34) Nakashima, D.; Yamamoto, H. Design of Chiral N-Triflyl Phosphoramidate as a Strong Chiral Brønsted Acid and Its Application to Asymmetric Diels-Alder Reaction. *J. Am. Chem. Soc.* **2006**, *128*, 9626–9627.
- (35) James, T.; Van Gemmeren, M.; List, B. Development and Applications of Disulfonimides in Enantioselective Organocatalysis. *Chem. Rev.* **2015**, *115*, 9388–9409.
- (36) Garcia-Garcia, P.; Lay, F.; Garcia-Garcia, P.; Rabalakos, C.; List, B. A Powerful Chiral Counteranion Motif for Asymmetric Catalysis. *Angew. Chem. Int. Ed.* **2009**, *48*, 4363–4366.
- (37) Xu, H.; Zuend, S. J.; Woll, M. G.; Tao, Y.; Jacobsen, E. N. Asymmetric Cooperative Catalysis of Strong Brønsted Acid-Promoted Reactions Using Chiral Ureas. *Science* **2010**, *327*, 986–990.
- (38) Raheem, I. T.; Thiara, P. S.; Peterson, E. A.; Jacobsen, E. N. Enantioselective Pictet-Spengler-Type Cyclisations of Hydroxylactams: H-Bond Donor Catalysis by Anion Binding. *J. Am. Chem. Soc.* **2007**, *129*, 13404–13405.
- (39) Banik, S. M.; Levina, A.; Hyde, A. M.; Jacobsen, E. N. Lewis Acid Enhancement by Hydrogen-Bond Donors for Asymmetric Catalysis. *Science* **2017**, *358*, 761–764.
- (40) Esposito, A.; Giovanni, C.; De Fenza, M.; Talarico, G.; Chino, M.; Palumbo, G.; Guaragna,

- A.; D'Alonzo, D. A Stereoconvergent Tsuji–Trost Reaction in the Synthesis of Cyclohexenyl Nucleosides. *Chem. Eur. J.* **2020**, *26*, 2597–2601.
- (41) Maleczka, R. E.; Gallagher, W. P. Stille Couplings Catalytic in Tin: A “Sn-F” Approach. *Org. Lett.* **2001**, *3*, 4173–4176.
- (42) Choo, H.; Beadle, J. R.; Chong, Y.; Trahan, J.; Hostetler, K. Y. Synthesis of the 5-Phosphono-Pent-2-En-1-Yl Nucleosides: A New Class of Antiviral Acyclic Nucleoside Phosphonates. *Bioorganic Med. Chem.* **2007**, *15*, 1771–1779.

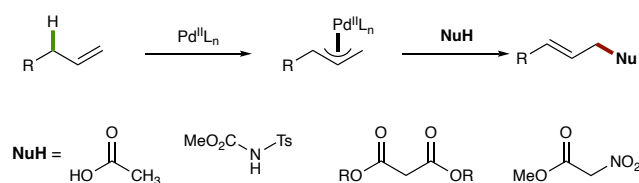
Part II: Development and Applications of Regio- and Enantioselective Group IX Metal-Catalysed Reactions

Chapter 4. Introduction to Rh- and Ir-Catalysed Allylic C–H Functionalisation¹

Allylic C–H functionalisation is an attractive alternative to allylic substitution. Dominated for a long time by palladium catalysis, significant recent contributions have revealed the potential of Rh(III)- and Ir(III)-catalysis in the advancement of this field. In this chapter, we will discuss the contributions of the Blakey lab in this arena and place them in context of recent advances in group IX metal-catalysed allylic C–H functionalisation. Part II of this dissertation will discuss the evolution of synthetic strategies towards RiPPs from our early work in this area of catalysis.

4.1 Allylic C–H functionalisation *via* π -allyl complexes

Transition metal-catalysed functionalisation of inert C–H bonds to form carbon-carbon (C–C) or carbon-heteroatom (C–X) bonds has evolved to become an essential part of the synthetic toolbox and has had a dramatic effect in the streamlining of complex molecule synthesis.^{2–9} In particular, allylic C–H functionalisation represents an attractive complement to allylic substitution reactions and Tsuji-Trost allylations,^{10–14} permitting the direct functionalisation of parent olefins without the need for any pre-functionalisation.



Scheme 4.1: Pd-catalysed allylic C–H functionalisation

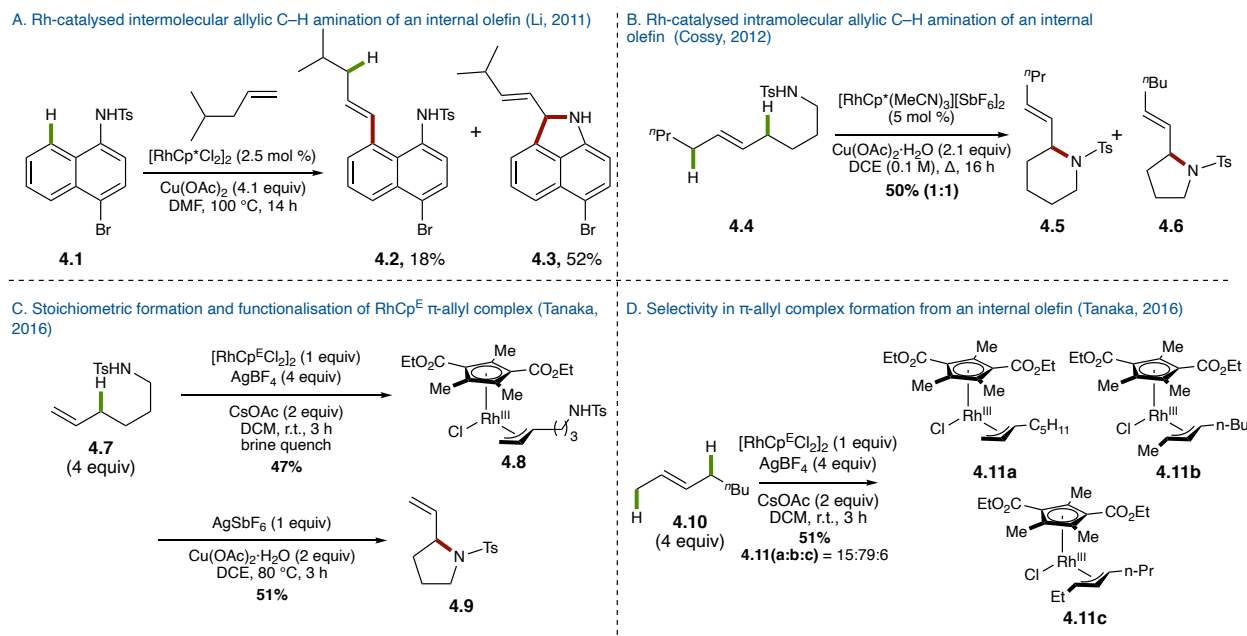
Until recently, the field of allylic C–H functionalisation *via* transition metal π -allyl complexes was dominated by palladium catalysis (Scheme 4.1).^{15,16} In an early contribution, White and co-workers reported a palladium catalyst system capable of catalytically generating a Pd(π -allyl)

complex which could be intercepted with a range of carbon, oxygen, and nitrogen nucleophiles.^{17–30} While these early advances have greatly expanded the field of allylic C–H functionalisation, the Pd-catalysed reactions are largely limited to the functionalisation of terminal olefins with stabilised nucleophiles. In most cases the formation of the linear functionalised product is observed.

Recent contributions, particularly from the Blakey lab, have expanded allylic C–H functionalisation to include Rh- and Ir-catalysis.^{31,32} These reports have expanded both the scope of compatible reaction partners as well as our mechanistic understanding of these reactions.

4.2 Early contributions to RhCp*-catalysed allylic C–H amination

In 2011, Li and co-workers demonstrated that, in the presence of excess Cu(OAc)₂, naphthalene **4.1** could undergo C–H olefination (to form product **4.2**), followed by formation allylic C–H functionalisation to form **4.3** as the major product (Scheme 4.2 A).³³ It is unclear whether this step takes place *via* a RhCp*(π -allyl) complex or through Wacker type amination followed by β -hydride elimination. The first systematic exploration of this area was disclosed in 2012, when Cossy and co-workers reported the RhCp*-catalysed intramolecular allylic C–H amination of alkenyl sulfonamides (Figure 4.2 B).³⁴ In one example, the internal olefin **4.4** could be functionalised to form piperidine **4.5** and pyrrolidine **4.6** (50% combined yield, 1:1 r.r.). The authors speculated that the reaction was proceeding through a RhCp*(π -allyl) complex produced by allylic C–H activation on either side of the internal olefin, and subsequent amination leading to products **4.5** and **4.6**.



Scheme 4.2: Early advances in RhCp^x-catalysed allylic C–H functionalisation

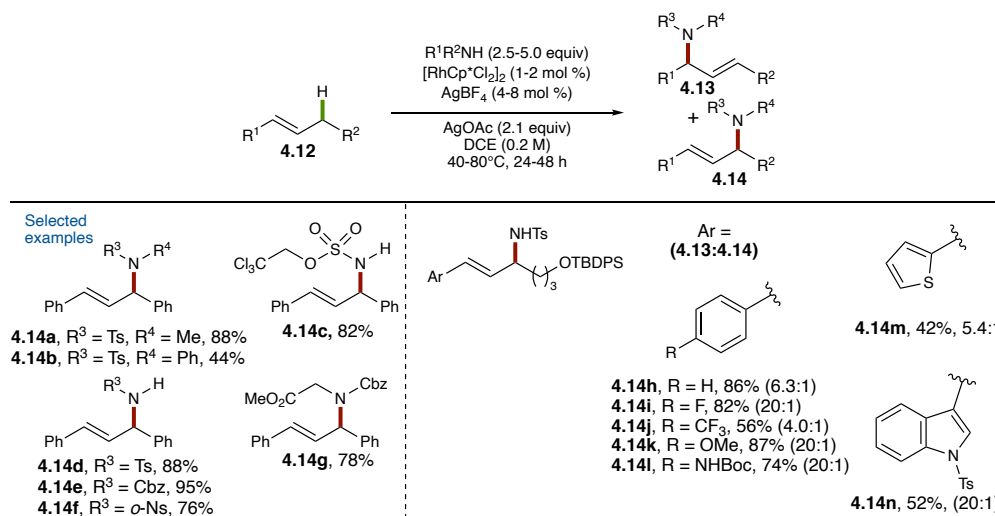
In 2016, Tanaka and co-workers reported the stoichiometric formation of RhCp^E(π-allyl) complex **4.8** and its conversion to vinylpyrrolidine **4.9** upon treatment with an external oxidant (Figure 4.2 C).³⁵ Complex **4.8** was also shown to catalyse the intramolecular allylic C–H amination of **4.7** to provide vinylpyrrolidine **4.9**, providing experimental support for Cossy's hypothesis of a RhCp*(π-allyl) catalytic intermediate. Additionally, the authors demonstrated that formation of the thermodynamically more stable internal RhCp^E(π-allyl) complexes **4.11b** and **4.11c** was favoured over the terminal complex **4.11a** (Figure 5.2 D), suggesting that RhCp complexes could potentially differentiate between similar allylic C–H bonds on unsymmetrical olefins.

4.3 RhCp*-catalysed intermolecular allylic C–H functionalisation using external oxidants

4.3.1 Allylic C–N bond formation

In 2017, Dr. Jacob Burman, a former graduate student in the Blakey lab, developed the RhCp*-catalysed intermolecular allylic C–H amination of internal olefins (Scheme 4.3).³⁶ The use of alkyl (**4.14a**) and aryl (**4.14b**) tosylamides, monoprotected amines (**4.14c–4.14f**), and *N*-Cbz-glycine

(**4.14g**) demonstrated the expanded scope of compatible nitrogen nucleophiles in this reaction. A wide array of electronically diverse β -alkylstyrenes (**4.14h–4.14l**), including substrates with oxidatively sensitive heteroaromatic rings (**4.14m** and **4.14n**), were aminated in high yields. Notably, in all cases, the reaction was selective for the conjugated allylic amine products **4.14**. Importantly, this was the first instance of allylic C–H functionalisation of an internal olefin with a nitrogen nucleophile that was activated with a single electron-withdrawing group. Dr. Burman demonstrated that the benzylic amine product, as well as minor amounts of the allylic acetate that was formed as a side product, equilibrated to form the thermodynamically favoured conjugated amine product. This observation indicated that C–N and C–O bond formation was reversible under the reaction conditions.

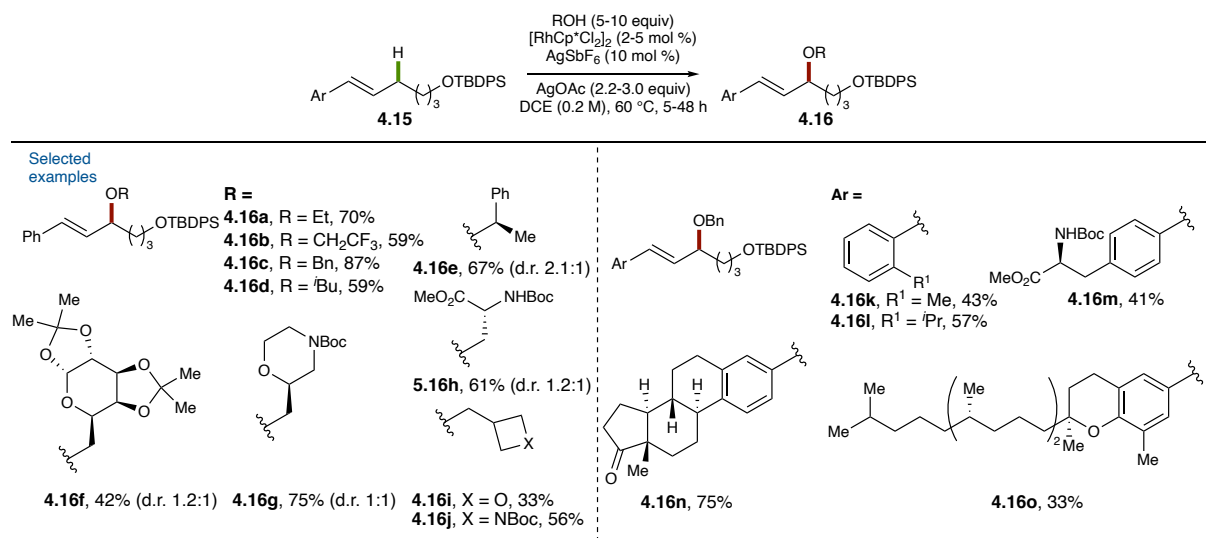


Scheme 4.3: $RhCp^*$ -catalysed intermolecular allylic C–H amination (Dr. Jacob Burman)

Jeganmohan and co-workers reported an $IrCp^*$ -catalysed variant of this reaction in 2019 and observed a similar trend in regioselectivity of styrenyl substrates for the conjugated products.³⁷ Furthermore, on substrates proceeding through unsymmetrical aryl-aryl $IrCp^*(\pi\text{-allyl})$ complexes, the product with the olefin in conjugation with the more electron-deficient ring was favoured.

4.3.2 Allylic C–O bond formation

In 2018, Taylor Nelson, a current graduate student in the Blakey lab expanded this reaction manifold to include alcohol nucleophiles to provide the allylic ether products (Scheme 4.4).³⁸ A wide range of primary (**4.16a–4.16c**) and secondary (**4.16d** and **4.16e**) alkyl alcohols were effective nucleophiles, as well as biologically relevant building blocks such as galactose (**4.16f**), morpholine (**4.16g**), and serine (**4.16h**) derivatives. Strained heterocycles like oxetanes (**4.16i**) or azetidines (**4.16j**) were also tolerated. Almost no diastereoselectivity was observed with stereogenic substrates (**4.16e**, **4.16f**, **4.16g**, or **4.16h**). β -Alkylstyrenes of increasing complexity, including phenylalanine- (**4.16m**), estrone- (**4.16n**), and tocopherol-derived (**4.16o**) substrates were converted to the allylic ether products in modest to good yields. The observed regioselectivity of this reaction was consistent with that observed in the amination reaction developed by Dr. Burman, delivering the allyl ether products with the olefin in conjugation with the olefin ring.

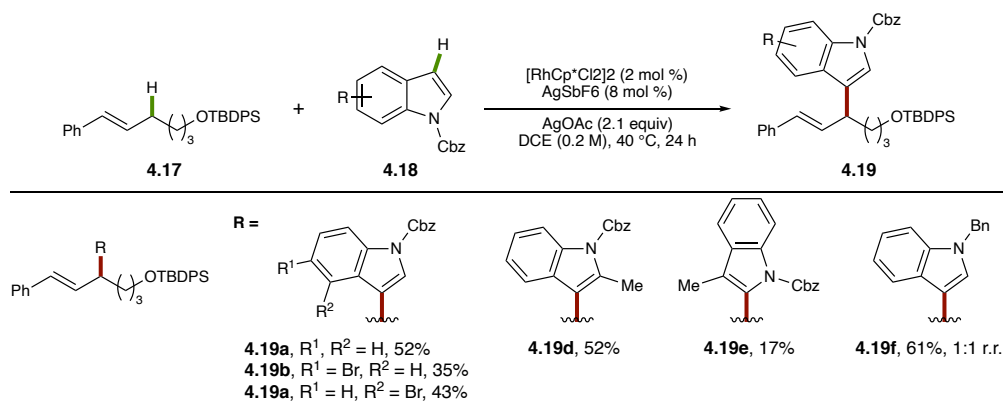


Scheme 4.4: RhCp*⁺-catalysed allylic C–H etherification using alcohols as nucleophiles (Taylor Nelson)

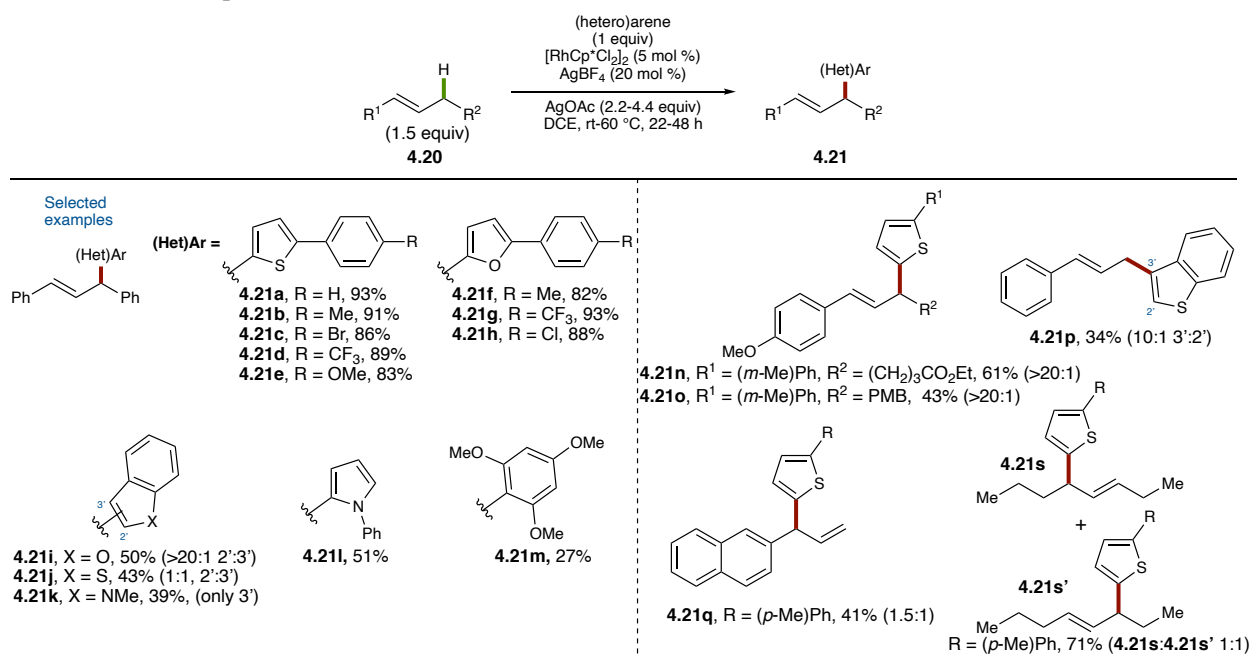
4.3.3 Allylic C–C bond formation

During the development of the allylic amination and etherification reactions, Dr. Caitlin Farr, a former graduate student in the Blakey lab, was concurrently working towards analogous C–C bond forming reactions using *N*-Cbz indoles as the arylating nucleophiles (Scheme 4.5). Under these conditions, β -alkylstyrene **4.19** could be arylated with an array of indoles. Brominated

indoles were well tolerated (**4.19b** and **4.19c**), as well as a methyl substituent situated at C2 (**4.19d**). Unsurprisingly, functionalisation occurred selectively at indole C3. However, when 3-methyl indole **4.18e** was used, allylation of the indole occurred selectively at C2. In all cases, the conjugated regioisomers were isolated selectively, consistent with the amination and etherification reactions discussed above. However, when the relatively electron-deficient *N*-Cbz indole was replaced with *N*-benzylindole (**4.18f**), conjugated arylation product **4.19f** and its benzylic regioisomer were isolated as a 1:1 mixture of isomers.

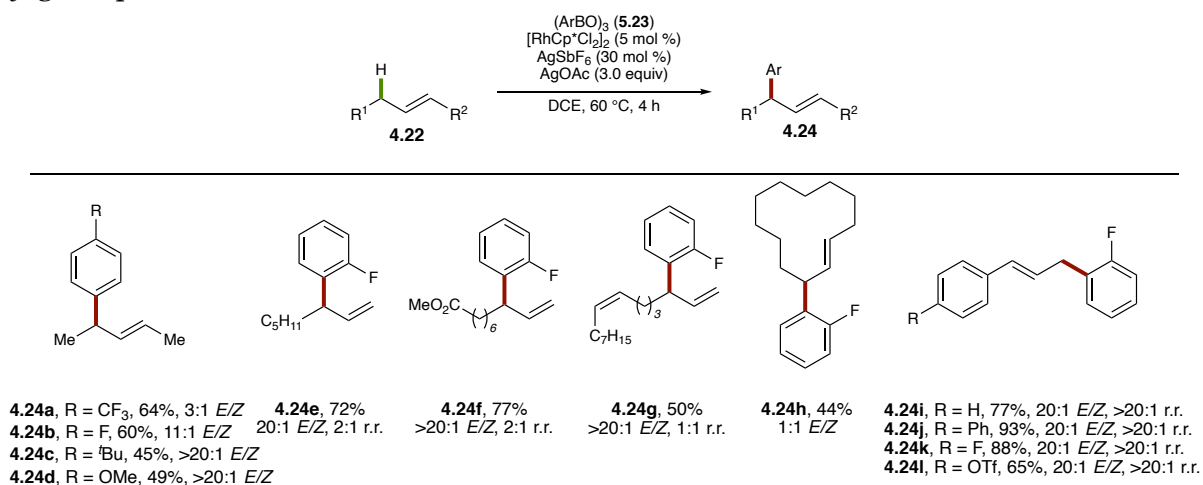


Scheme 4.5: RhCp^{*}-catalysed allylic C–H arylation using *N*-substituted indoles as nucleophiles (Dr. Caitlin Farr)



Scheme 4.6: RhCp^{*}-catalysed allylic C–H arylation using electron-rich (hetero)aromatics as nucleophiles (Glorius, 2018)

In 2018, Glorius and co-workers independently reported similar results concerning allylic C–H arylation with an expanded scope of heteroaromatic nucleophiles (Scheme 4.6).³⁹ 5-substituted thiophenes (**4.21a–4.21e**) and furans (**4.21f–4.21h**) were suitable nucleophiles, as well as benzofuran (**4.21i**), benzothiophene (**4.21j**), *N*-methylindole (**4.21k**), and pyrrole (**4.21l**). 1,3,5-trimethoxybenzene was also a suitably electron-rich nucleophile, providing the arylated product **4.21m**, albeit in lower yield. This reaction generally displayed good regioselectivity for the conjugated product.



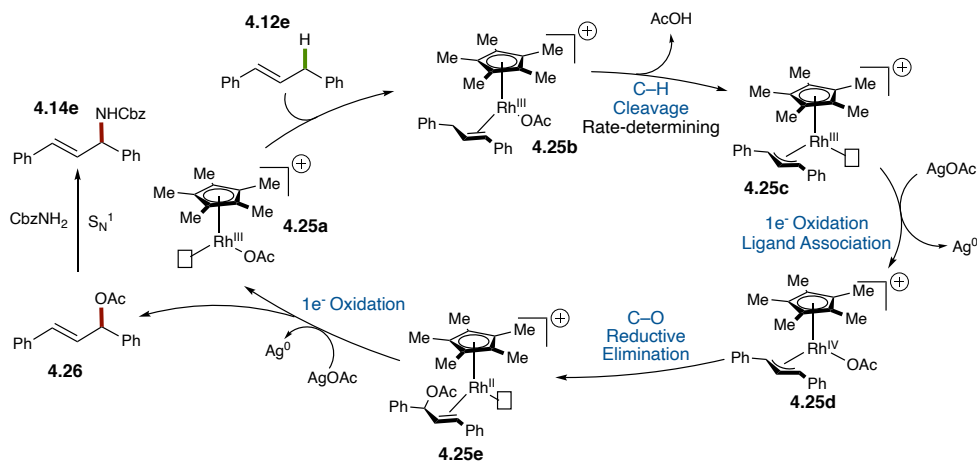
Scheme 4.7: RhCp*–catalysed allylic C–H arylation using triarylborexines as nucleophile (Glorius, 2019)

In 2019, Glorius and co-workers expanded the scope of RhCp*–catalysed allylic C–H arylation to include triarylborexines as the arylating reagents (Scheme 4.7).⁴⁰ The authors speculated that the reaction was proceeding by transmetalation of the triarylborexine with a RhCp*(π -allyl) complex and subsequent C–C reductive elimination to provide the allylic arylated products. A broad range of triarylborexines were tolerated; however, greater *E/Z* selectivity was observed with more electron-rich triarylborexines (**4.25c** and **4.25d**). The authors speculated that this was due to the greater rate of transmetalation, thereby preventing *syn-anti* isomerisation of the RhCp*(π -allyl) species leading to greater *E*-selectivity. Regioselectivity in these reactions suffered when performed on terminal olefins (**4.25e–4.25g**). However, a wide range of allylbenzene derivatives were arylated with excellent yields and selectivity (**4.25i–4.25l**).

Mechanistic studies conducted by the Glorius group indicated that C–H activation was occurring before the rate-determining step of the reaction. The authors also speculated that AgSbF_6 suppressed competitive homocoupling of the triarylboroxines, by decreasing the rate of transmetallation to the rhodium catalyst, or by accelerating the allylic C–H activation for productive C–H arylation.

4.3.4 Mechanistic investigations

Until recently, C–N reductive elimination from a $\text{Rh(III)Cp}^*(\pi\text{-allyl})$ complex was widely accepted to be the operative mechanism for allylic C–H amination.³⁴ Oxidation of the resulting Rh(I) species would then regenerate the Rh(III) active catalyst. However, Tanaka and co-workers demonstrated that $\text{RhCp}^E(\pi\text{-allyl})$ complex **4.8** was not converted to the allylic amine product until it was treated with $\text{Cu(OAc)}_2 \cdot \text{H}_2\text{O}$ (see Scheme 4.2 C).³⁵ Additionally, it was unclear whether C–N bond formation was occurring through inner-sphere reductive elimination or outer-sphere nucleophilic attack. Dr. Robert Harris, a former postdoctoral researcher in the Blakey lab, along with Taylor Nelson, and Daniel Salgueiro, a former undergraduate researcher in the Blakey lab, undertook an investigation into the mechanism of this reaction in collaboration with the MacBeth lab at Emory University and the Baik lab at KAIST.⁴¹



Scheme 4.8: Proposed catalytic cycle for RhCp^* -catalysed allylic C–H amination, supported by stoichiometric, kinetic, electrochemical, and computational studies (Dr. Robert Harris, Taylor Nelson, Daniel Salgueiro, et al.)

The established catalytic cycle is summarised in Scheme 5.8. Following activation of the dimeric pre-catalyst to form coordinatively unsaturated Rh(III)Cp* complex **4.25a**, olefin coordination and rate-determining C–H cleavage provides Rh(III)Cp*(π -allyl) complex **4.25c**. Oxidation of this complex provides the Rh(IV)Cp*(π -allyl)(OAc) complex **4.25d** which undergoes reductive elimination to form the allylic acetate complex **4.25e**. Dissociation of the allylic acetate **4.26** and subsequent S_N¹ type substitution with benzyl carbamate then provides the allylic amine product **4.14e**.

In addition to establishing a new mechanistic paradigm for RhCp*-catalysed reactions, this study also demonstrated that enantioselectivity in this 1st-generation manifold could not be induced by chiral ligands on the Rh-catalyst, since the key C–X bond formation occurs *via* an S_N¹ type allylic substitution. It is likely that the allylic etherification reaction developed by Taylor, and the heteroarylation reactions independently developed by Dr. Farr and the Glorius group operate under a similar mechanism. However, further mechanistic studies are required to establish a mechanism for the allylic arylation with triarylboroxine nucleophiles.

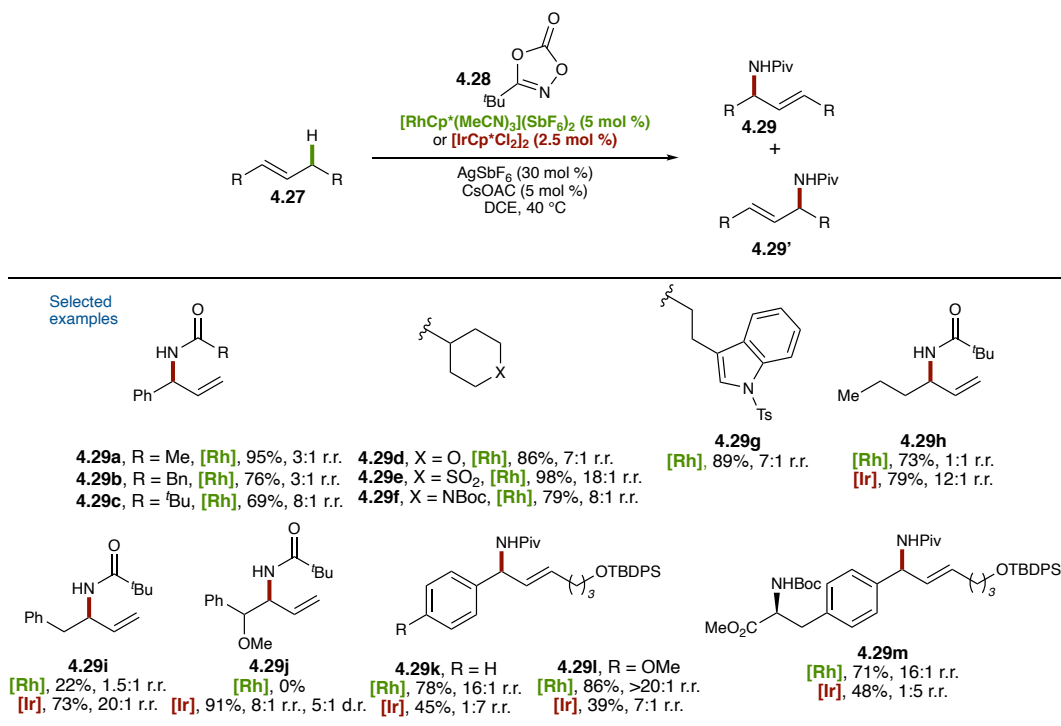
4.4 Allylic C–H amidation *via* direct C–N reductive elimination from M(V)-nitrenoid intermediates

4.4.1 RhCp*- and IrCp*-catalysed allylic C–H amidation

Dioxazolones were originally established as oxidative amidating reagents by Sukbok Chang and co-workers in the context of directed C(sp²)–H amidation.^{42–47} These reagents have recently been extended to C(sp³)–H amidation as well.^{48–51} Their proposed function is to oxidise Rh(III)Cp*- and Ir(III)Cp*-complexes to the corresponding M(V)Cp*-nitrenoid complexes.

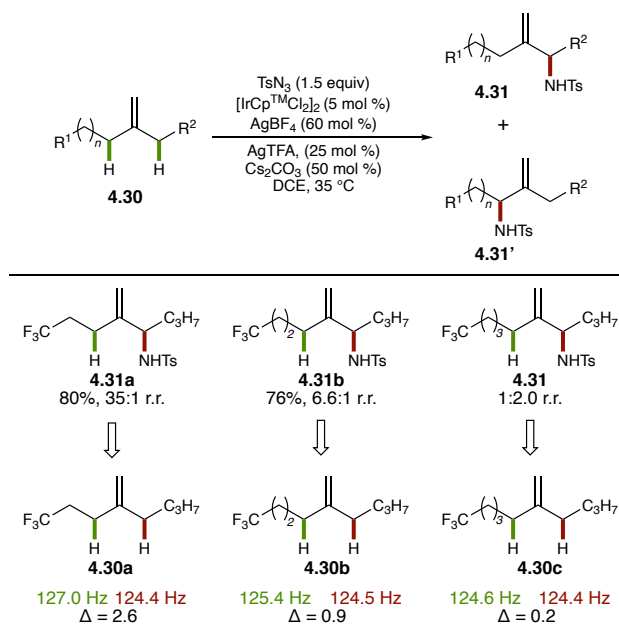
In 2019, along with Dr. Robert Harris and Dr. Caitlin Farr, Dr. Jacob Burman developed a new generation of allylic C–H functionalisation reactions in which the key C–N bonds are directly formed by reductive elimination, using dioxazolones as the nitrogen source (Scheme 4.9).⁵² Using [RhCp*(MeCN)₃](SbF₆)₂ as the catalyst, Dr. Burman was able to employ a wide range of

dioxazolones in the allylic C–H amidation of allylbenzene (**4.29a–4.29g**). In contrast to the allylic C–H amination discussed above, these reactions were generally selective for the branched amide products. The use of $[\text{IrCp}^*\text{Cl}_2]_2$ was critical to maintain high yields and regioselectivity for the branched product for terminal olefins that performed poorly under Rh-catalysis (**4.29h–4.29j**). This observation was consistent with reports of IrCp*-catalysed allylic C–H amidation that were independently reported by the groups of Rovis and Glorius around the same time.^{53,54}



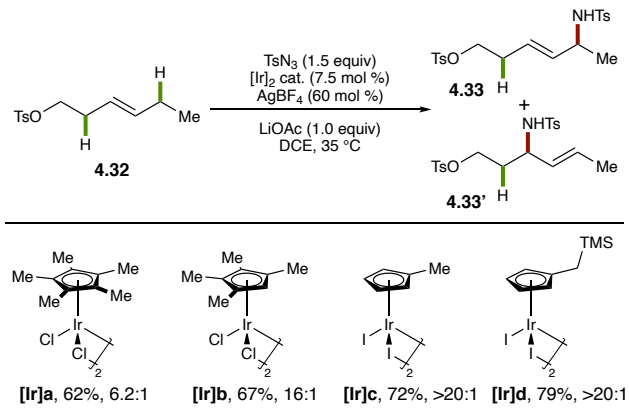
Scheme 4.9: RhCp*- and IrCp*-catalysed allylic C–H amidation using dioxazolones as oxidative amidating reagents (Dr. Jacob Burman)

When the reaction was performed on β -alkylstyrenes, Dr. Burman observed complementary reactivity between RhCp* and IrCp* catalysts (**4.29k–4.29m**). For example, the use of RhCp* as the catalyst provided pivalamide **4.29k** in 78% yield with 16:1 regioselectivity for the benzylic amide isomer. However, the yield was reduced and regioselectivity was overturned when IrCp* was used as the catalyst (45% yield, 1:7 r.r.). Similarly, **4.29l** was produced in high yield and selectivity (86%, >20:1 r.r.) with RhCp* as the catalyst, but both were reduced when IrCp* was used. The same regioselectivity profile was observed with phenylalanine-derived substrate **4.29m**.



Scheme 4.10: Regioselectivity of IrCpTM-catalysed allylic C–H activation is correlated with ¹J_{CH} coupling constants (Rovis, 2020)

In 2020, Rovis and co-workers expanded on this mechanistic paradigm, and reported new catalysts for C–H activation and sulfamidation of 1,1- and *trans*-1,2-disubstituted olefins that were able to differentiate between remarkably similar allylic C–H bonds (Scheme 4.10).⁵⁵¹¹ Using the slightly less bulky [IrCpTMCl₂]₂ (CpTM = tetramethylcyclopentadienyl) as the precatalyst and TsN₃ as the nitrogen source, a range of 1,1-disubstituted olefins were sulfamidated at the allylic position. The reaction was selective for the allylic position distal from an electron-withdrawing



Scheme 4.11: Development of a new Ir-catalyst for allylic C–H functionalisation (Rovis, 2020)

¹¹ This report from Rovis and co-workers was reported after the work detailed in the next chapter of this dissertation.

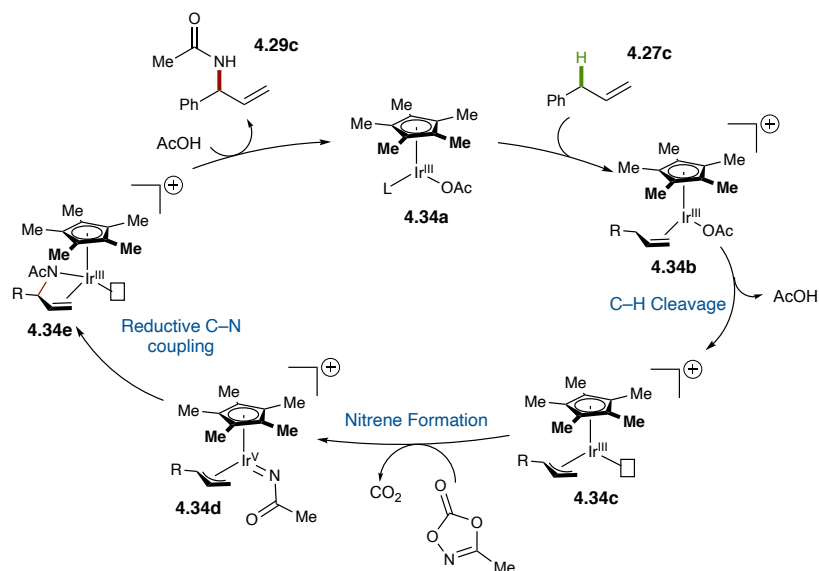
substituent, with the regioselectivity decreasing as the EWG was moved further away from the allylic position. The authors correlated this inductive influence of the EWG on regioselectivity with the $^1J_{\text{CH}}$ coupling constants of the allylic C–H bonds.

In the same report, a brief survey of IrCp-pre-catalysts showed that regioselectivity of the amidation improved as steric hindrance around the Cp ring was relieved (Scheme 4.11), with mono-methylated derivative **[Ir]c** providing the amide product in 72% yield and >20:1 r.r. A pendant silane was installed (**[Ir]d**) to increase electron-density through its hyperconjugative electron-donating effect while minimising the steric bulk around the catalyst.

4.4.2 Mechanistic investigation

The mechanism of allylic C–H amidation has been studied by our group and the Rovis group using kinetic and stoichiometric experiments. The isolation and characterisation of stoichiometric RhCp*- and IrCp*-complexes support the intermediacy of these complexes in the catalytic cycle. Regioconvergent allylic amidation of isomeric olefin substrates reported by Glorius and co-workers, as well as the regioisomeric product mixtures observed when the reaction is performed on 1,2-disubstituted olefins further support this notion. Intra- and intermolecular isotopic competition experiments reported by the Rovis group indicate that C–H activation is irreversible and may be involved in the rate-determining step of the reaction.

The following catalytic cycle has been proposed for this reaction (Scheme 4.12).^{52–54} Activation of the precatalyst provides the cationic complex **4.34a**. Olefin (**4.27c**) coordination, followed by allylic C–H activation provides the π -allyl complex **4.34c**. Dioxazolone coordination and decarboxylation provides the key M(V)-nitrenoid complex **4.34d** which can reductively eliminate to form the allylic C–N bond. Protodemetalation of complex **4.34e** then provides the allylic amide product **4.29c** and regenerates the active catalyst.



Scheme 4.12: Proposed catalytic cycle for 2nd-generation allylic C-H amidation

4.5 Conclusion

The Blakey lab has played an active and important role in developing Rh(III)- and Ir(III)-catalysed allylic C-H functionalisation, and has drastically expanded the scope of coupling partners that are compatible in these reactions. Following the development of C-N, C-O, and C-C bond forming reactions by Dr. Burman, Taylor Nelson, and Dr. Farr and the Glorius group, respectively, members of the Blakey lab established an operative catalytic cycle for this 1st-generation of allylic C-H functionalisation reactions. In this mechanism, the key C-X bonds are formed *via* an S_N¹ substitution of an allylic acetate intermediate, thus precluding the use of chiral ligands on the Rh(III)-catalyst to induce enantioselectivity. Following this, the next generation of allylic C-N bond forming reactions were developed, in which the key bond forming step was an inner-sphere reductive elimination, and this area has since seen intense interest from the chemical community. At this time, we began considering the synthetic applications of our lab's developing methodologies. In particular, we were interested in an emerging class of natural products called ribosomally-synthesised and post-translationally modified peptides (RiPPs), a broad series of macrocyclic peptide natural products containing unusual crosslinks between amino acid residues. However, the 2nd-generation of allylic C-H functionalisation was still in its

infancy, and it was clear that additional advancements were necessary before it could reach its true synthetic potential. Chapters 5 of this dissertation will focus on work done to expand the scope of nitrogen coupling partners in this reaction, and the development of a novel catalyst system for enantioselective variants of this reaction.

4.6 References

- (1) Kazerouni, A. M.; McKoy, Q. A.; Blakey, S. B. Recent Advances in Oxidative Allylic C–H Functionalization via Group IX-Metal Catalysis. *Chem. Commun.* **2020**, *56*, 13287–13300.
- (2) McMurray, L.; O’Hara, F.; Gaunt, M. J. Recent Developments in Natural Product Synthesis Using Metal-Catalysed C–H Bond Functionalisation. *Chem. Soc. Rev.* **2011**, *40*, 1885–1898.
- (3) Lafrance, M.; Blaquiere, N.; Fagnou, K. Aporphine Alkaloid Synthesis and Diversification via Direct Arylation. *Eur. J. Org. Chem.* **2007**, *2007*, 811–825.
- (4) Colby, D. A.; Bergman, R. G.; Ellman, J. A. Rhodium-Catalyzed C–C Bond Formation via Heteroatom-Directed C–H Bond Activation. *Chem. Rev.* **2010**, *110*, 624–655.
- (5) Davies, H. M. L.; Lian, Y. The Combined C–H Functionalization/Cope Rearrangement: Discovery and Applications in Organic Synthesis. *Acc. Chem. Res.* **2012**, *45*, 923–935.
- (6) Godula, K. C–H Bond Functionalization in Complex Organic Synthesis. *Science* **2006**, *312*, 67–72.
- (7) Ye, J.; Lautens, M. Palladium-Catalysed Norbornene-Mediated C–H Functionalization of Arenes. *Nat. Chem.* **2015**, *7*, 863–870.
- (8) Noisier, A. F. M.; Brimble, M. A. C-H Functionalization in the Synthesis of Amino Acids and Peptides. *Chem. Rev.* **2014**, *114*, 8775–8806.
- (9) Yamaguchi, J.; Yamaguchi, A. D.; Itami, K. C-H Bond Functionalization: Emerging Synthetic Tools for Natural Products and Pharmaceuticals. *Angew. Chem. Int. Ed.* **2012**, *51*, 8960–9009.
- (10) Cheng, Q.; Tu, H.-F.; Zheng, C.; Qu, J.-P.; Helmchen, G.; You, S.-L. Iridium-Catalyzed Asymmetric Allylic Substitution Reactions. *Chem. Rev.* **2019**, *119*, 1855–1969.
- (11) Butt, N. A.; Zhang, W. Transition Metal-Catalyzed Allylic Substitution Reactions with Unactivated Allylic Substrates. *Chem. Soc. Rev.* **2015**, *44*, 7929–7967.

- (12) Trost, B. M.; Crawley, M. L. Asymmetric Transition-Metal-Catalyzed Allylic Alkylations: Applications in Total Synthesis. *Chem. Rev.* **2003**, *103*, 2921–2944.
- (13) Qu, J.; Helmchen, G. Applications of Iridium-Catalyzed Asymmetric Allylic Substitution Reactions in Target-Oriented Synthesis. *Acc. Chem. Res.* **2017**, *50*, 2539–2555.
- (14) Turnbull, B. W. H.; Evans, P. A. Asymmetric Rhodium-Catalyzed Allylic Substitution Reactions: Discovery, Development and Applications to Target-Directed Synthesis. *J. Org. Chem.* **2018**, *83*, 11463–11479.
- (15) Fernandes, R. A.; Nallasivam, J. L. Catalytic Allylic Functionalization: Via π -Allyl Palladium Chemistry. *Org. Biomol. Chem.* **2019**, *17*, 8647–8672
- (16) Wang, R.; Luan, Y.; Ye, M. Transition Metal-Catalyzed Allylic C(sp³)-H Functionalization via η^3 -Allylmetal Intermediate. *Chin. J. Chem.* **2019**, *37*, 720–743.
- (17) Chen, M. S.; White, M. C. A Sulfoxide-Promoted, Catalytic Method for the Regioselective Synthesis of Allylic Acetates from Monosubstituted Olefins via C–H Oxidation. *J. Am. Chem. Soc.* **2004**, *126*, 1346–1347.
- (18) Chen, M. S.; Prabakaran, N.; Labenz, N. A.; White, M. C. Serial Ligand Catalysis: A Highly Selective Allylic C–H Oxidation. *J. Am. Chem. Soc.* **2005**, *127*, 6970–6971.
- (19) Vermeulen, N. A.; Delcamp, J. H.; White, M. C. Synthesis of Complex Allylic Esters via C–H Oxidation vs C–C Bond Formation. *J. Am. Chem. Soc.* **2010**, *132*, 11323–11328.
- (20) Strambeanu, I. I.; White, M. C. Catalyst-Controlled C–O versus C–N Allylic Functionalization of Terminal Olefins. *J. Am. Chem. Soc.* **2013**, *135*, 12032–12037.
- (21) Ammann, S. E.; Rice, G. T.; White, M. C. Terminal Olefins to Chromans, Isochromans, and Pyrans via Allylic C–H Oxidation. *J. Am. Chem. Soc.* **2014**, *136*, 10834–10837.
- (22) Diao, T.; Stahl, S. S. O₂-Promoted Allylic Acetoxylation of Alkenes: Assessment of “Push” versus “Pull” Mechanisms and Comparison between O₂ and Benzoquinone. *Polyhedron* **2014**, *84*, 96–102.
- (23) Osberger, T. J.; White, M. C. N -Boc Amines to Oxazolidinones via Pd(II)/Bis-

- Sulfoxide/Brønsted Acid Co-Catalyzed Allylic C–H Oxidation. *J. Am. Chem. Soc.* **2014**, *136*, 11176–11181.
- (24) Ammann, S. E.; Liu, W.; White, M. C. Enantioselective Allylic C–H Oxidation of Terminal Olefins to Isochromans by Palladium(II)/Chiral Sulfoxide Catalysis. *Angew. Chem. Int. Ed.* **2016**, *55*, 9571–9575.
- (25) Pattillo, C. C.; Strambeanu, I. I.; Calleja, P.; Vermeulen, N. A.; Mizuno, T.; White, M. C. Aerobic Linear Allylic C–H Amination: Overcoming Benzoquinone Inhibition. *J. Am. Chem. Soc.* **2016**, *138*, 1265–1272.
- (26) Fraunhoffer, K. J.; White, M. C. Syn -1,2-Amino Alcohols via Diastereoselective Allylic C–H Amination. *J. Am. Chem. Soc.* **2007**, *129*, 7274–7276.
- (27) Covell, D. J.; White, M. C. A Chiral Lewis Acid Strategy for Enantioselective Allylic C–H Oxidation. *Angew. Chem. Int. Ed.* **2008**, *47*, 6448–6451.
- (28) Reed, S. A.; White, M. C. Catalytic Intermolecular Linear Allylic C–H Amination via Heterobimetallic Catalysis. *J. Am. Chem. Soc.* **2008**, *130*, 3316–3318.
- (29) Young, A. J.; White, M. C. Catalytic Intermolecular Allylic C–H Alkylation. *J. Am. Chem. Soc.* **2008**, *130*, 14090–14091.
- (30) Reed, S. A.; Mazzotti, A. R.; White, M. C. A Catalytic, Brønsted Base Strategy for Intermolecular Allylic C–H Amination. *J. Am. Chem. Soc.* **2009**, *131*, 11701–11706.
- (31) Nelson, T. A. F.; Hollerbach, M. R.; Blakey, S. B. Allylic C–H Functionalization via Group 9 π -Allyl Intermediates. *Dalt. Trans.* **2020**, *49*, 13928–13935.
- (32) Manoharan, R.; Jeganmohan, M. Recent Advancements in Allylic C(sp³)–H Functionalization of Olefins Catalyzed by Rh(III) or Ir(III) Complexes. *Eur. J. Org. Chem., Early View*, <https://doi.org/10.1002/ejoc.202000936>.
- (33) Li, X.; Gong, X.; Zhao, M.; Song, G.; Deng, J.; Li, X. Rh(III)-Catalyzed Oxidative Olefination of N-(1-Naphthyl)Sulfonamides Using Activated and Unactivated Alkenes. *Org. Lett.* **2011**, *13*, 5808–5811.

- (34) Cochet, T.; Bellosta, V.; Roche, D.; Ortholand, J. Y.; Greiner, A.; Cossy, J. Rhodium(III)-Catalyzed Allylic C–H Bond Amination. Synthesis of Cyclic Amines from ω -Unsaturated N-Sulfonylamines. *Chem. Commun.* **2012**, *48*, 10745–10747.
- (35) Shibata, Y.; Kudo, E.; Sugiyama, H.; Uekusa, H.; Tanaka, K. Facile Generation and Isolation of π -Allyl Complexes from Aliphatic Alkenes and an Electron-Deficient Rh(III) Complex: Key Intermediates of Allylic C–H Functionalization. *Organometallics* **2016**, *35*, 1547–1552.
- (36) Burman, J. S.; Blakey, S. B. Regioselective Intermolecular Allylic C–H Amination of Disubstituted Olefins via Rhodium/ π -Allyl Intermediates. *Angew. Chem. Int. Ed.* **2017**, *56*, 13666–13669.
- (37) Sihag, P.; Jeganmohan, M. Iridium(III)-Catalyzed Intermolecular Allylic C–H Amidation of Internal Alkenes with Sulfonamides. *J. Org. Chem.* **2019**, *84*, 13053–13064.
- (38) Nelson, T. A. F.; Blakey, S. B. Intermolecular Allylic C–H Etherification of Internal Olefins. *Angew. Chem. Int. Ed.* **2018**, *57*, 14911–14915.
- (39) Lerchen, A.; Knecht, T.; Koy, M.; Ernst, J. B.; Bergander, K.; Daniliuc, C. G.; Glorius, F. Non-Directed Cross-Dehydrogenative (Hetero)Arylation of Allylic C(sp³)-H Bonds Enabled by C–H Activation. *Angew. Chem. Int. Ed.* **2018**, *57*, 15248–15252.
- (40) Knecht, T.; Pinkert, T.; Dalton, T.; Lerchen, A.; Glorius, F. Cp*⁺Rh(III)-Catalyzed Allyl–Aryl Coupling of Olefins and Arylboron Reagents Enabled by C(sp³)-H Activation. *ACS Catal.* **2019**, *9*, 1253–1257.
- (41) Harris, R. J.; Park, J.; Nelson, T. A. F.; Iqbal, N.; Salgueiro, D. C.; Bacsá, J.; Macbeth, C. E.; Baik, M. H.; Blakey, S. B. The Mechanism of Rhodium-Catalyzed Allylic C–H Amination. *J. Am. Chem. Soc.* **2020**, *142* (12), 5842–5851.
- (42) Park, J.; Lee, J.; Chang, S. Iterative C–H Functionalization Leading to Multiple Amidations of Anilides. *Angew. Chem. Int. Ed.* **2017**, *56*, 4256–4260.
- (43) Chen, Q. A.; Chen, Z.; Dong, V. M. Rhodium-Catalyzed Enantioselective Hydroamination

- of Alkynes with Indolines. *J. Am. Chem. Soc.* **2015**, *137*, 8392–8395.
- (44) Park, Y.; Heo, J.; Baik, M.-H.; Chang, S. Why Is the Ir(III)-Mediated Amido Transfer Much Faster Than the Rh(III)-Mediated Reaction? A Combined Experimental and Computational Study. *J. Am. Chem. Soc.* **2016**, *138*, 14020–14029.
- (45) Hwang, Y.; Park, Y.; Chang, S. Mechanism-Driven Approach To Develop a Mild and Versatile C–H Amidation through Ir III Catalysis. *Chem. Eur. J.* **2017**, *23*, 11147–11152.
- (46) Park, Y.; Jee, S.; Kim, J. G.; Chang, S. Study of Sustainability and Scalability in the Cp*Rh(III)-Catalyzed Direct C–H Amidation with 1,4,2-Dioxazol-5-Ones. *Org. Process Res. Dev.* **2015**, *19*, 1024–1029.
- (47) Park, J.; Chang, S. Comparative Catalytic Activity of Group 9 [CpMIII] Complexes: Cobalt-Catalyzed C-H Amidation of Arenes with Dioxazolones as Amidating Reagents. *Angew. Chem. Int. Ed.* **2015**, *54*, 14103–14107.
- (48) Tan, P. W.; Mak, A. M.; Sullivan, M. B.; Dixon, D. J.; Seayad, J. Thioamide-Directed Cobalt(III)-Catalyzed Selective Amidation of C(sp³)-H Bonds. *Angew. Chem. Int. Ed.* **2017**, *56*, 16550–16554.
- (49) Shi, H.; Dixon, D. J. Dithiane-Directed Rh(III)-Catalyzed Amidation of Unactivated C(sp³)-H Bonds. *Chem. Sci.* **2019**, *10*, 3733–3737.
- (50) Wang, H.; Park, Y.; Bai, Z.; Chang, S.; He, G.; Chen, G. Iridium-Catalyzed Enantioselective C(sp³)-H Amidation Controlled by Attractive Noncovalent Interactions. *J. Am. Chem. Soc.* **2019**, *141*, 7194–7201.
- (51) Hong, S. Y.; Park, Y.; Hwang, Y.; Kim, Y. B.; Baik, M.-H.; Chang, S. Selective Formation of γ -Lactams via C–H Amidation Enabled by Tailored Iridium Catalysts. *Science* **2018**, *35*, 1016–1021.
- (52) Burman, J. S.; Harris, R. J.; B. Farr, C. M.; Bacsá, J.; Blakey, S. B. Rh(III) and Ir(III)Cp* Complexes Provide Complementary Regioselectivity Profiles in Intermolecular Allylic C–H Amidation Reactions. *ACS Catal.* **2019**, *9* (6), 5474–5479.

- (53) Lei, H.; Rovis, T. Ir-Catalyzed Intermolecular Branch-Selective Allylic C–H Amidation of Unactivated Terminal Olefins. *J. Am. Chem. Soc.* **2019**, *141*, 2268–2273.
- (54) Knecht, T.; Mondal, S.; Ye, J.-H.; Das, M.; Glorius, F. Intermolecular, Branch-Selective, and Redox-Neutral Cp*Ir III -Catalyzed Allylic C–H Amidation. *Angew. Chemie Int. Ed.* **2019**, *58*, 7117–7121.
- (55) Lei, H.; Rovis, T. A Site-Selective Amination Catalyst Discriminates between Nearly Identical C–H Bonds of Unsymmetrical Disubstituted Alkenes. *Nat. Chem.* **2020**, *12*, 725–731.

Chapter 5. Development of 2nd-Generation Regio- and Enantioselective Allylic C–H Functionalisation

This chapter is focused on advancements made to the current 2nd-generation allylic C–H amidation literature developed by the Blakey, Rovis, and Glorius groups, in order to develop reactions for further synthetic applications. We will first begin with a discussion on the expansion of compatible nitrenoid precursors in this chemistry to include tosyl azide to provide allylic sulfonamides. We will move on to the development of a new planar chiral rhodium indenyl complex for enantioselective variants of these reactions.

5.1 Introduction

With a robust method for the synthesis of allylic amides in hand,^{1–3} we began considering the synthetic applications of the Blakey lab's allylic C–H functionalisation methodology. We were intrigued with the potential application of allylic C–H amidation to the synthesis of peptide natural products containing non-canonical amino acid residues, structural motifs that are present in a wide range of biologically relevant natural products (Figure 5.1).

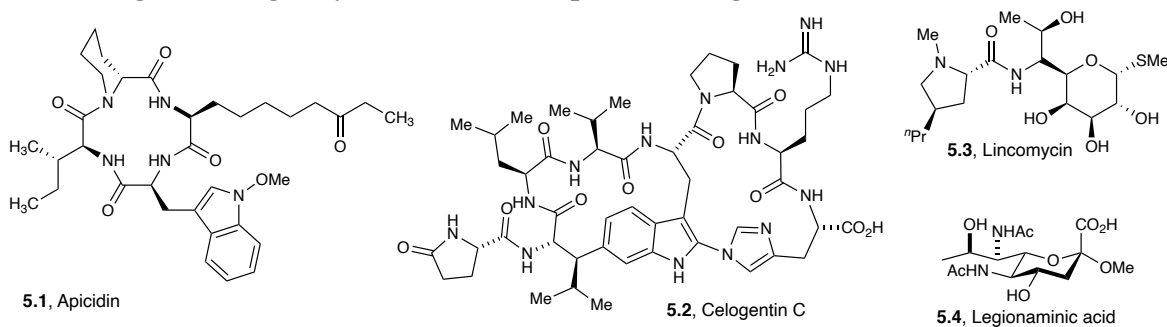
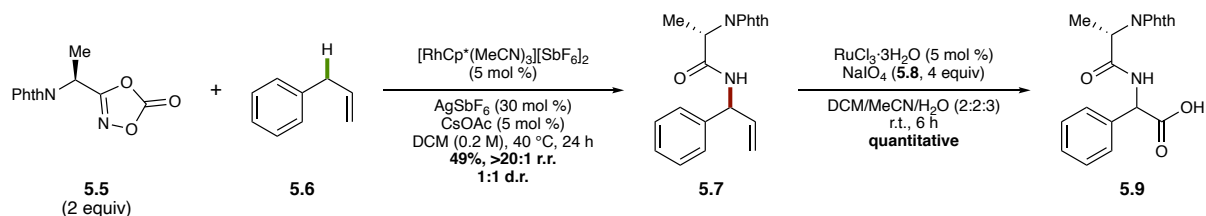


Figure 5.1: Unnatural amino acid residues are present in diverse classes of biologically relevant small molecules



Scheme 5.1: Allylic amidation/oxidative cleavage sequence to synthesise dipeptides containing non-canonical amino acid residues

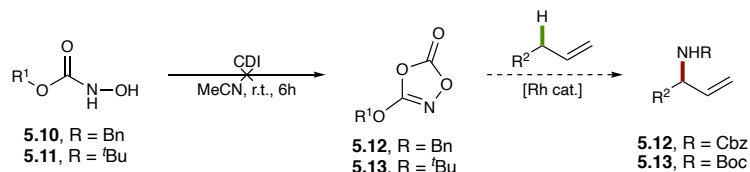
We hypothesised that the allylic amidation reaction could be used to synthesise and install unnatural amino acid fragments onto the structural frameworks of natural products like those depicted in Figure 5.1 *via* an allylic C–H amidation/oxidative cleavage sequence of steps. In an initial experiment (Scheme 5.1), we demonstrated that allylbenzene (**5.6**) could be amidated with alanine-derived dioxazolone **5.5** under the standard conditions developed by Dr. Burman (see chapter 4)⁴ to provide **5.7** (49% yield, 1:1 d.r.). Importantly, this was the first amino acid derived dioxazolone to be employed in the allylic C–H amidation, which was promising for our future synthetic studies. The terminal olefin in amide product **5.7** could then be oxidatively cleaved with $\text{RuCl}_3 \cdot \text{H}_2\text{O}$ (5 mol %) and NaIO_4 (4 equiv) to provide dipeptide **5.9** in quantitative yield.⁵ We envisioned that this two-step sequence could be strategically employed to assemble unnatural amino acid side chains by tuning the olefin coupling partner. However, it was clear that for broad applicability of this methodology, further development of this 2nd generation allylic C–H functionalisation was necessary.

Firstly, due to the innate decomposition pathway of dioxazolones, the current 2nd-generation allylic C–H functionalisation was limited to the synthesis of allylic amides. Despite the high value of these amide products, to improve the usability of these reactions in the synthesis of peptide natural products, we would need to develop a protocol for the synthesis of allylic amines with protecting groups that were more commonly employed in peptide synthesis. Secondly, with an allylic C–H amidation that proceeds through C–N reductive elimination, the stage was set for the development of an asymmetric variant of this reaction. Indeed, at this point, Dr. Farr had already laid the groundwork for a new class of chiral catalysts to achieve this goal. This chapter will focus on advancements made in these specific areas of allylic C–N bond formation.

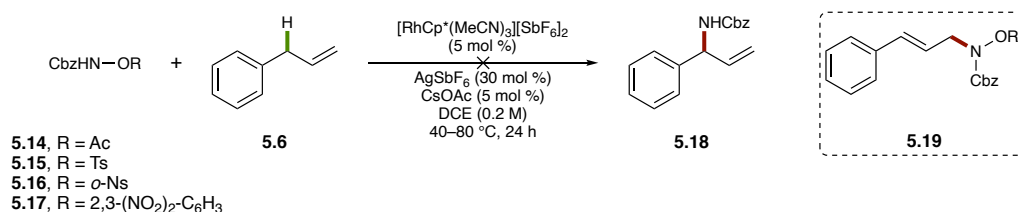
5.2 Development of alternate nitrenoid precursors for 2nd-generation allylic C–N bond formation

5.2.1 Survey of alternative electrophilic amines for allylic C–H amination

A. Attempts to synthesise oxy-dioxazolones for the synthesis of allylic carbamates



B. Activated hydroxylamines as nitrenoid precursors for the synthesis of allylic carbamates



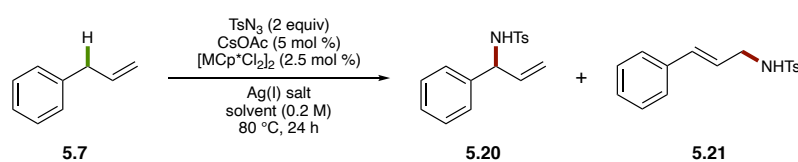
Scheme 5.2: Initial investigations of alternate nitrenoid precursors for allylic C–N bond formation

We first turned our attention to the development of alternate nitrenoid precursors for the synthesis of carbamate protected allylic amines. We initially attempted to synthesise benzyloxy- and *tert*-butyloxy dioxazolones **5.12** and **5.13**, respectively, from their hydroxycarbamate precursors (Scheme 5.2 A). Despite closely resembling the dioxazolones employed in the C(sp²)–H and C(sp³)–H amidation literature, these reagents have not been previously synthesised. Unfortunately, under the standard conditions for dioxazolone synthesis, we observed none of the desired dioxazolone products in either case. Instead, we observed complete consumption of the hydroxy carbamate starting materials and mixtures of unidentified products.

Next, we synthesised a series of electrophilic amines (**5.14–5.17**) by activating hydroxy benzylcarbamate with suitable leaving groups (Scheme 5.2 B).⁶ Similar reagents have been successfully employed in oxidative C–H amination reactions. However, when these reagents were subjected to the allylic C–H amination of allylbenzene, no trace of the desired allylic carbamate **5.18** was seen. All the reactions resulted in high recovery of unreacted starting hydroxylamines **5.14–5.17**. Interestingly, small quantities of the linear aminated products **5.19** were observed in the crude reaction mixtures. We hypothesise that in the presence of an external oxidant like

AgSbF₆ (30 mol %), none of which was utilised to activate the rhodium catalyst, product **5.19** could be formed *via* the 1st-generation allylic amination mechanism, i.e. oxidatively induced reductive elimination of an allylic acetate and Lewis acid-mediated S_N¹ substitution with the activated hydroxylamine. The regioselectivity of the observed side product is consistent with that observed in the 1st-generation reactions.

5.2.2 Development of allylic C–H sulfamidation using tosyl azide as a nitrenoid precursor⁷



entry	[MCp*Cl ₂] ₂	Ag(I) (mol%)	Solvent	% yield (5.20) ^a	% yield (5.21) ^a
1	[Cp*RhCl ₂] ₂	AgSbF ₆ (10)	DCE	13	4
2	[Cp*IrCl ₂] ₂	AgSbF ₆ (10)	DCE	17	8
3	[Cp*RhCl ₂] ₂	AgSbF ₆ (40)	DCE	trace	0
4	[Cp*IrCl ₂] ₂	AgSbF ₆ (40)	DCE	trace	0
5	[Cp*IrCl ₂] ₂	AgBF ₄ (10)	DCE	<5	trace
6	[Cp*IrCl ₂] ₂	AgOTs (10)	DCE	<5	trace
7	[Cp*IrCl ₂] ₂	AgNTf ₂ (10)	DCE	23	0
8	[Cp*IrCl ₂] ₂	AgNTf ₂ (10)	TFE	55	0
9	[Cp*IrCl ₂] ₂	AgNTf ₂ (10)	HFIP	60	0

Table 5.1: Optimisation of allylic C–H sulfamidation of allylbenzene with tosyl azide. ^aIsolated yields of amide products are reported

Tosyl azide has been previously used as a nitrenoid precursor in directed C(sp²)–H functionalisation reactions.⁸ While a tosyl group is far from an ideal nitrogen protecting group as compared to carbamate protecting groups, sulfonyl protecting groups can be easily cleaved under reductive conditions.⁹ We therefore explored the sulfamidation of allylbenzene with tosyl azide (Table 5.1).¹² We began our investigation with [RhCp*Cl₂]₂ (2.5 mol %) as the pre-catalyst, CsOAc (5 mol %) as the base, and AgSbF₆ (10 mol %) as the halide scavenger. Under these conditions, allylbenzene (**5.7**) was successfully sulfamidated at 80 °C in DCE (0.2 M) to provide **5.20** (13%

¹² During the course of this study, Rovis and co-workers reported isolated examples of allylic C–H sulfamidation with tosyl azide in their disclosure of allylic C–H amidation with dioxazolones. Additionally, their report of site-selective allylic C–H sulfamidation of 1,1-disubstituted olefins was reported after the completion of the work detailed in this chapter.

yield) and **5.21** (4% yield, entry 1). The yield of **5.20** was marginally improved when $[\text{IrCp}^*\text{Cl}_2]_2$ (2.5 mol %) was used as the pre-catalyst (entry 2). Based on observations made by Dr. Burman, we hypothesised that increased loading of Ag(I) would improve the yield of **5.20**. However, the use of AgSbF_6 (40 mol %) resulted in only trace quantities of the branched product **5.20** (entries 3 and 4). A brief survey of Ag(I) salts indicated that AgNTf_2 (10 mol %) was the best candidate (entries 5–7). While the yield of **5.20** was only slightly improved to 23%, the reaction displayed exclusive selectivity for the branched product, and no trace of **5.21** was observed. Lastly, the use of fluorinated solvents drastically improved the yield of this reaction (entries 8 and 9).¹³

5.2.3 Scope and limitations of allylic C–H sulfamidation

With conditions in hand for the allylic C–H amidation of allylbenzene, we explored the scope of this reaction on a range of olefins (Table 5.2). The reaction performed well on electron-rich (**5.23a**, 57% yield and **5.23b**, 61% yield) as well as electron-deficient (**5.23c**, 52% yield and **5.23e**, 46% yield). An aryl fluoride was also tolerated (**5.23d**, 67%). The sulfamidation of safrole had to be run for 48 hours to provide **5.23f** in 47% yield. Likewise, the sulfamidation of *o*-

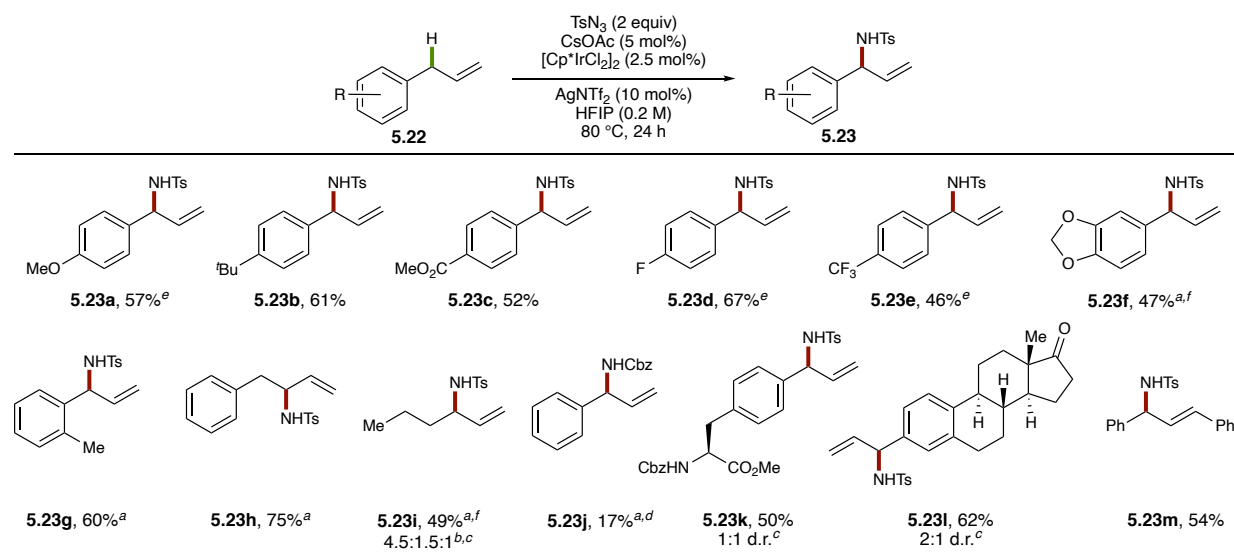


Table 5.2: Scope of olefin coupling partners. ^aReaction was run for 48 hours. ^bIsolated as a mixture of regioisomers at the 3-, 4-, and 2-positions, respectively (major isomer shown). ^cDetermined by integration of crude ¹H NMR spectrum. ^d CbzN_3 was used instead of TsN_3 . ^eReaction conducted by Steven Chen. ^fReaction conducted by Taylor Nelson.

¹³ Due to evaporation of the low-boiling HFIP at the elevated reaction temperature (entry 9), the reactions were conducted in sealed pressure tubes to ensure reproducibility.

allyltoluene required extended reaction times to provide sulfonamide **5.23g** in 60% yield., presumably due to the increased steric hindrance caused by the *o*-methyl substituent. 4-Phenylbutene (**5.22h**) and 1-hexene (**5.22i**), which proceed through non-conjugated π -allyl complexes also required extended reaction times (48 h) to provide tosylamides **5.23h** and **5.23i** (as a 4.5:1.5:1 mixture of regioisomers) in 75% and 49% yield, respectively. Since our initial goal was to synthesise allylic carbamates, we attempted this reaction with CbzN₃ as the nitrenoid precursor. However, after 48 hours, carbamate **5.23i** was only isolated in 17% yield. No starting azide was recovered from this reaction. The reaction was also effective on substrates derived from biologically relevant building blocks, providing phenylalanine derivative **5.23k** (50% yield) and estrone derivative **5.23l** (62% yield). The sulfamidation of 1,3-diphenylpropene to provide sulfonamide **5.23m** (54% yield) demonstrated that the reaction was effect on an internal olefin substrate. This investigation of the scope of compatible olefin coupling partners provided an ideal opportunity to mentor an undergraduate researcher, Steven Chen.

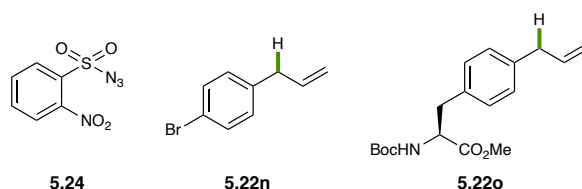
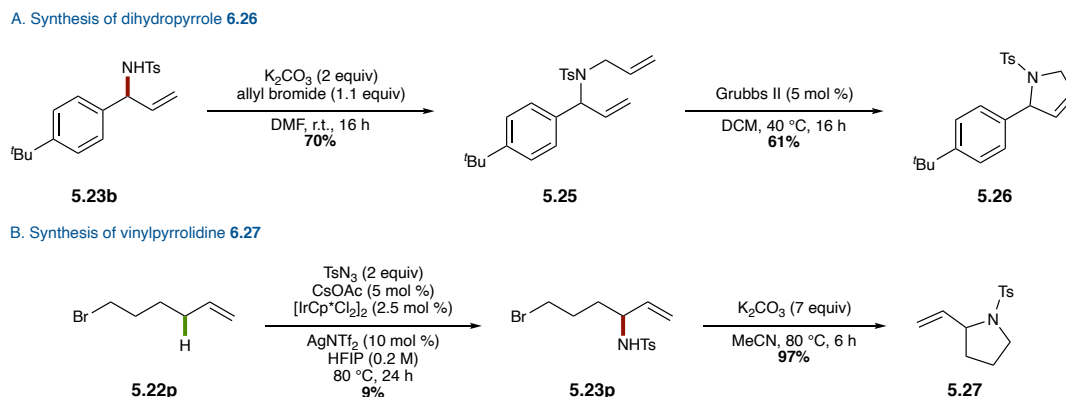


Figure 5.2: Unsuccessful substrates for allylic C–H sulfamidation

Substrates that were incompatible with the reaction conditions are shown in Figure 5.2. *o*-NsN₃ (**5.24**) was not a suitable nitrenoid precursor, largely due to its limited solubility in HFIP, even at the elevated reaction temperature. The reaction was also intolerant of aryl bromide (**5.22n**) and *tert*-butyl carbamate (**5.22o**) functionalities. In the latter case, switching out the Boc protecting group for a Cbz group allowed the reaction to proceed (**5.23k**, Table 5.2).

We further explored the synthetic utility of this reaction by derivatising the sulfonamide products obtained by allylic C–H functionalisation. Sulfonamide **5.23b** could be allylated (70% yield) and subjected to ring-closing metathesis (RCM) to provide dihydropyrrole **5.26** (Scheme 5.3 A). Taylor Nelson was able to sulfamidate bromohexene (**5.22p**) to provide sulfonamide

5.23p, albeit in a low yield of 9% (Scheme 5.3 B). Sulfonamide **5.23p** could then be subjected to base-promoted cyclisation to provide vinylpyrrolidine product **5.27** in excellent yields.



Scheme 5.3: Diversification of sulfonamide products

We have conducted a systematic study of the use of tosyl azide as a nitrenoid precursor in allylic C–N bond formation. While we did not achieve our initial goal of developing reagents for the synthesis of allylic carbamates *via* an inner-sphere reductive elimination mechanism, this work nevertheless expands the scope of nitrenoid sources compatible with this chemistry.

5.3 A new planar chiral catalyst for regio- and enantioselective allylic C–H amidation¹⁰

5.3.1 Overview of known chiral piano-stool cyclopentadienyl (Cp) complexes

Co-, Rh-, and Ir-cyclopentadienyl (Cp) and -pentamethylcyclopentadienyl (Cp^{*}) complexes have been established as excellent catalysts for directed C–H functionalisation reactions. As a result, several chiral variants of these “piano-stool” ligands have been developed and have had an enormous impact in the field of asymmetric C–H functionalisation (Figure 5.3).^{11–14} This renaissance in the development of chiral Cp ligands was largely inspired by the development of TADDOL-derived ligands (**5.28**) by Cramer group in 2012,¹⁵ as well as Rovis and Ward’s disclosure in the same year of an evolvable engineered streptavidin docked with biotinylated RhCp^{*} (**5.29**).¹⁶ However, both these ligand classes offer low opportunity for modularity, therefore limiting their use in catalysis.

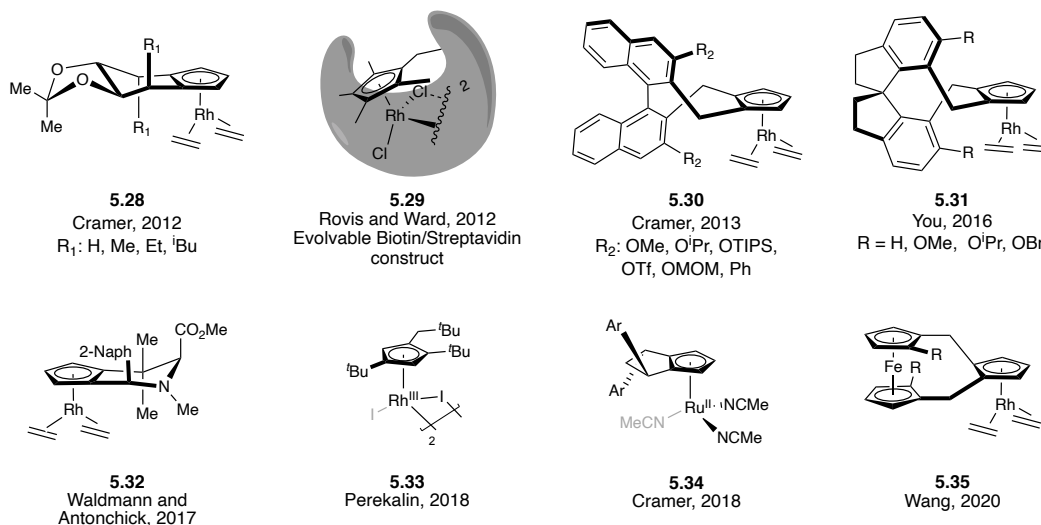


Figure 5.3: Known chiral “piano-stool” cyclopentadienyl (Cp) ligands

By far the most commonly employed chiral Cp ligands have been Cramer’s 2nd-generation BINOL-derived ligands (**5.30**) introduced in 2013,¹⁷ with over 25 derivatives reported to date. However, each member in this class of axially chiral ligands requires a multistep (9-12 steps) synthesis, thus hindering their widespread use.¹⁴ Despite this, the incredible capacity for enantioinduction displayed by these complexes in a wide range of mechanistically disparate reactions have resulted in repeated efforts to streamline the synthesis of these ligands. This was most recently exemplified by the modular route to this ligand framework reported by You and co-workers in 2020.¹⁸ The You group has also disclosed another axially chiral ligand family containing a spirocyclic backbone in 2016 (**5.31**).¹⁹

More recent examples of chiral Cp ligands include the piperidine-fused ligands reported by Waldmann and Antonchick in 2017 (**5.32**),²⁰ and the planar chiral complex developed by Perekalin and co-workers in 2018 (**5.33**).²¹ Additionally, Cramer and co-workers reported a 3rd-generation of cyclopentane-fused Cp ligands in 2018 (**5.34**),²² accessible by a convenient two-step enantioselective synthesis. More recently, in 2020, Wang and co-workers reported a Cp ligand equipped with a planar chiral ferrocene backbone (**5.35**).²³ While these very recently reported complexes from Waldmann and Antonchik, Perekalin, Cramer, and Wang et al. illustrate the chemical community’s burgeoning interest in the development of chiral Cp ligands of ever-

increasing efficiency, they have yet to see widespread application in asymmetric catalysis.

5.3.2 Introduction to the indenyl ligand

Due to the multistep syntheses required to access the most effective chiral Cp ligands discussed above, we turned our attention to a related but relatively underexplored ligand family. The indenyl ligand combines the Cp framework with a benzo-fused backbone which provides an innate electronic asymmetry to the ligand. Indeed, the indenyl ligand is known to be able to coordinate transition metals along a continuum between η^5 and η^3 binding modes, a phenomenon known as the indenyl effect (Figure 5.4).^{24–26} This ring slip can lead to pronounced differences in reactivity, most noticeably contributing to the acceleration of organometallic reactions and catalysis.²⁷ Additionally, it was our hypothesis that we could leverage the electronic asymmetry in the indenyl ligand to induce enantioselectivity in reactions proceeding through inner-sphere mechanisms.

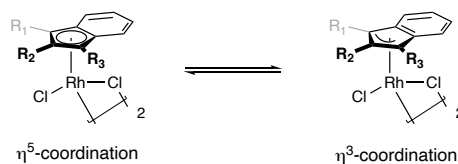
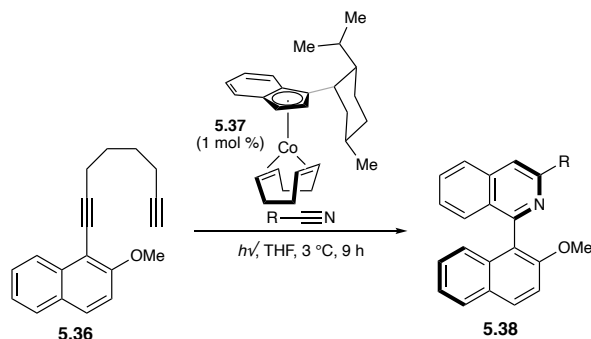


Figure 5.4: The indenyl effect – transition metal indenyl complexes are known to slip between η^5 and η^3 coordination modes

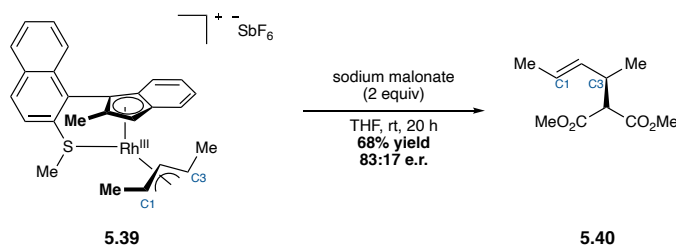
Planar chiral indenyl complexes of early transition metals have been well studied and documented; however, there are comparatively fewer examples of analogous late transition metal complexes.²⁷ In 1995, Heller and co-workers described the synthesis of a chiral pool-derived Co-indenyl complex **5.37** and its application to heterocyclotrimerisations of diyne **5.36** with alkylnitriles (Scheme 5.4 A).^{28–30} More recently, in 2018, Baker reported the synthesis of Rh-indenyl(π -allyl) complex **5.39** and its stoichiometric reaction with sodium malonate (Scheme 5.4 B).³¹ The allylic substitution product **5.40** was obtained in 68% yield and 83:17 e.r. Enantioinduction in this reaction was consistent with alkylation at the weaker Rh–C₃ bond, arising from the electronic asymmetry of the complex. Unfortunately, this complex was never shown to be catalytically competent, and required a long multistep synthesis involving several

difficult chiral resolutions. Additionally, the thioether functionality presented an oxidative liability and precludes its use in transformation proceeding through inner-sphere mechanisms due to a lack of available coordination sites on the metal center.

A. Chiral pool-derived Co-indenyl catalyst for atroposelective heterocyclotrimerisations (Heller, 1995)

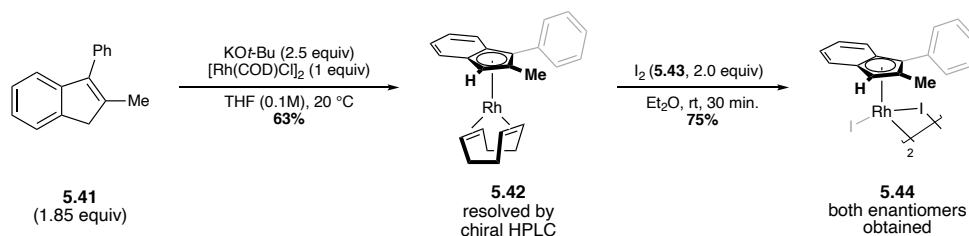


B. Allylic alkylation of a stoichiometric planar chiral Rh-indenyl(π -allyl) complex (Baker, 2018)



Scheme 5.4: Group IX metal planar chiral complexes

5.3.3 Catalyst preparation and development of enantioselective allylic C–H amidation (Dr. Caitlin Farr and Christopher Poff)



Scheme 5.5: Synthesis and chiral resolution of planar chiral Rh(III)-indenyl complex (Dr. Caitlin Farr and Christopher Poff)

We aimed to develop a modular and easily accessible planar chiral indenyl catalyst system that could be used for enantioselective allylic C–H amidation. To this end, Christopher Poff and Dr. Caitlin Farr began this investigation using 2-methyl-3-phenylindene (**5.41**) as the ligand, which was easily prepared in two steps from 2-methylindanone and phenylmagnesium bromide (Scheme 5.5).^{32,33} Complexation with $[\text{Rh}(\text{I})(\text{COD})\text{Cl}]_2$ provided complex **5.42** as a racemic mixture. Each enantiomer of this planar chiral complex was easily resolved by chiral HPLC and

oxidised to the corresponding Rh(III) diiodide dimer **5.44** (*R*-enantiomer shown).

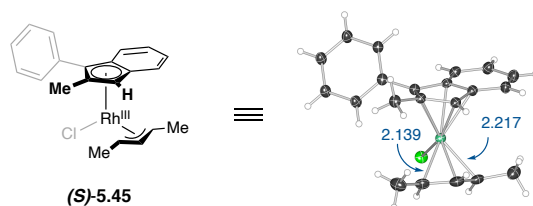
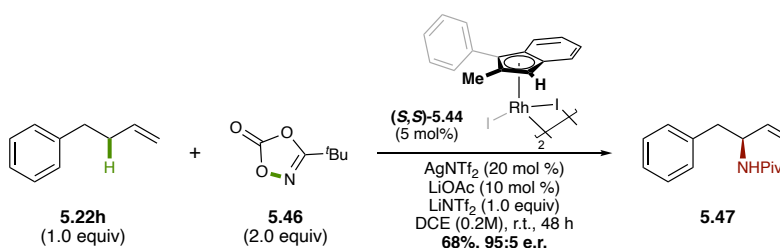


Figure 5.5: Assignment of absolute stereochemistry of the Rh-indenyl complex (Christopher Poff)

Christopher Poff was able to unambiguously assign the absolute stereochemistry of each enantiomer by synthesising and obtaining an X-ray crystal structure of the Rh(III)-indenyl(π -allyl) complex (*S*)-**5.45** (Figure 5.5).¹⁴ Analysis of the crystal structure shows that C1, C5, and C4 of the indenyl ligand have shorter Rh–C bonds (2.2105, 2.2225, 2.1285 Å, respectively) than C2 and C3 (2.3164 and 2.3106 Å). This observation is characteristic of the electronic asymmetry in the complex as a result of the slight slip from η^5 to η^3 . Furthermore, C20 of the π -allyl ligand – *trans* to the η^3 portion of the indenyl ligand – has a longer Rh–C bond (2.2196 Å) than C18 of the π -allyl ligand (2.1457 Å), which is consistent with different *trans* effects exerted by both sides of the indenyl ligand on the otherwise symmetrical π -allyl fragment. These observations indicate that the electronic asymmetry induced by the indenyl effect on the indenyl ligand is in fact translated to the π -allyl ligand.



Scheme 5.6: Optimised reaction conditions for enantioselective allylic C–H amidation (Dr. Caitlin Farr)

With a brief survey of reaction conditions, Dr. Farr was able to develop optimal conditions for the enantioselective allylic C–H amidation of 4-phenyl-1-butene (**5.22h**) with *tert*-butyldioxazolone (**5.46**, Scheme 5.6). Using the newly developed planar chiral Rh-indenyl

¹⁴ Stereochemical configuration was assigned using the rules of planar chirality laid out by Schlögl.⁵⁰

complex **(S,S)**-**5.44** (5 mol %) as the pre-catalyst, LiOAc (10 mol %) as the carboxylate base, and AgNTf₂ (20 mol %) as the halide scavenger, pivalamide **5.47** was obtained in 68% yield and 95:5 e.r.¹⁵ The reaction was performed at room temperature for 48 hours, because competitive dioxazolone decomposition was observed at elevated temperatures. Dr. Farr also observed that permethylation of the benzene backbone of the indenyl ligand resulted in higher yields but eroded enantioselectivity, while iridium complexes were ineffective at catalysing the allylic C–H amidation.

5.3.4 Scope and limitations of enantioselective allylic C–H amidation

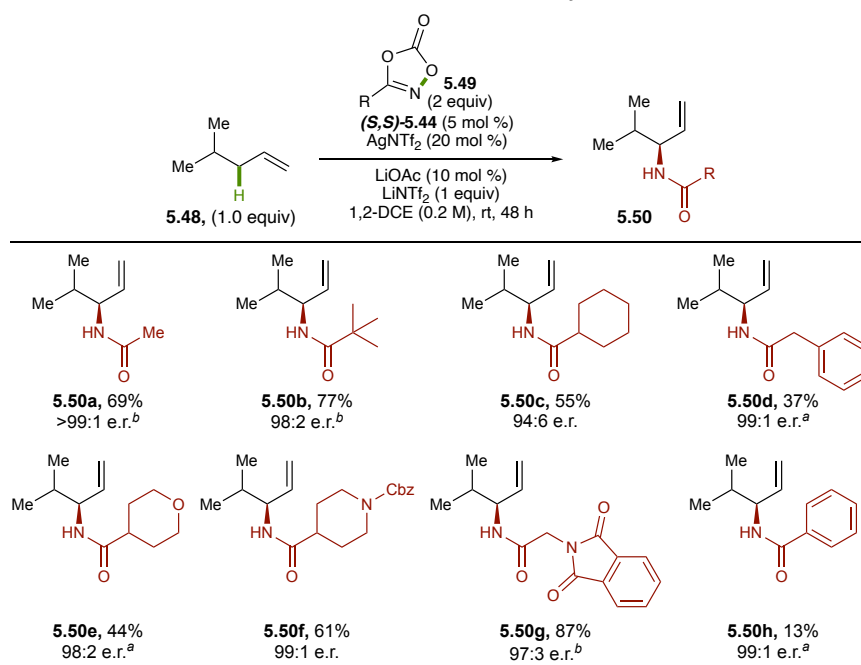


Table 5.3: Scope of dioxazolone coupling partners. ^aReaction conducted by Dr. Caitlin Farr. ^bReaction conducted by Christopher Poff

With a robust method for the enantioselective allylic C–H amidation of olefins in hand, we began investigating the scope of dioxazolone coupling partners compatible with these reaction conditions, along with Dr. Caitlin Farr and Christopher Poff (Table 5.3). Methyl-, *tert*-butyl, cyclohexyl, and benzyl-dioxazolone all provided the amide products (**5.50a–5.50d**, respectively) in moderate yields (37–77%) and excellent enantioselectivities (94:6–>99:1 e.r.). Ether and

¹⁵ The stereochemistry of amide products was assigned by conversion to their corresponding amino acids following the same allylic amidation/oxidative cleavage sequence outlined in Section 5.1 (Christopher Poff).

carbamate functionalities were also well tolerated, providing amides **5.50e** (44% yield, 98:2 e.r.) and **5.50f** (61% yield, 99:1 e.r.), respectively. Glycine-derived dioxazolone (**5.49g**) was also a suitable reaction partner, providing amide **5.50g** in 87% yield and 97:3 e.r. Phenyl dioxazolone (**5.49h**) only provided benzamide **5.50h** in 13%. This low reactivity is consistent with the low yields observed by Dr. Burman, the Rovis group, and the Glorius group when aryl dioxazolones were employed in the earlier reports of racemic allylic C–H amidation.^{1–3} The enantioselectivity of this reaction, however, remained excellent (99:1 e.r.).

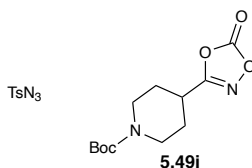


Figure 5.6: Unsuccessful nitrenoid precursors for enantioselective allylic C–H amidation

Unfortunately, tosyl azide was an incompatible nitrenoid precursor under these conditions, and the starting materials were recovered in high yields (Figure 5.6). The use of HFIP as the solvent, which was critical to the success of the racemic sulfamidation reaction discussed above, did not improve the reaction with (**S,S**)-**5.44** as the pre-catalyst. Similarly, no reaction was observed when *tert*-butyl carbamate protected piperidine dioxazolone **5.49i** was used, even though this substrate provided the amide product in good yields with IrCp* as the catalyst. However, switching the protecting group to a benzyl carbamate allowed the reaction to proceed (**5.50f**, Table 5.3).

We chose *tert*-butyl (**5.49b**) dioxazolone and Phth-glycine dioxazolone (**5.49g**) as amidating reagents with which to explore the compatibility of this reaction across a range of olefin coupling partners because 1) these reagents provided their corresponding amide products in the highest yields during our study of the dioxazolone scope of this reaction, and 2) they served as ideal representatives of electron-rich and electron-deficient dioxazolones, respectively.

With 1-hexene as the substrate, amide products **5.52a** and **5.52b** were isolated in good yields and enantioselectivities from *tert*-butyl dioxazolone (51% yield, 98:2 e.r.) and Phth-glycine dioxazolone (81% yield, 93:7 e.r.), respectively (Table 5.4). Olefin substrates containing protected

catalyst arrest.

5.3.5 Computational studies (Bohyun Park,¹⁶ Joonghee Won,¹⁶ Kimberly Sharp)

While the overall mechanism of this reaction is presumably similar to the racemic 2nd-generation amidation catalytic cycle discussed in Chapter 4,^{1-3,7} the origins of regio- and enantioselectivity with the newly developed rhodium indenyl catalyst were as yet unclear. Therefore, we collaborated with the Baik group at KAIST, who carried out density functional theory (DFT) calculations to shed some light on these questions of selectivity.³⁴

A complete energy profile diagram for the (**R,R**)-**5.44**-catalysed allylic C–H amidation of allylbenzene with *tert*-butyl dioxazolone is shown in Figure 5.7. Coordinatively unsaturated complex **A** can be reversibly coordinated by allylbenzene on both faces of the olefin to form complexes **B** and **B'**. The subsequent allylic C–H activation steps, traversing the transition-states **B-TS** and **B'-TS**, were calculated to be rate-limiting with barriers of 12.85 and 13.95 kcal/mol, respectively. The planar chiral indenyl ligand favours **B-TS**, in which the phenyl ring of the indenyl ligand and the phenyl ring of the π -allyl ligand are extended away from each other. Thus, the formation of π -allyl complex **C** was shown to be kinetically preferred by ~1.1 kcal/mol over its diastereomer **C'** during the C–H activation step. The stereochemical information set at this stage is preserved through the rest of the reaction, therefore establishing allylic C–H activation as rate- and enantiodetermining.

A $\Delta\Delta G^\ddagger$ of ~1.1 kcal/mol corresponds to about ~10:1 selectivity, while the experimentally observed selectivity for the *tert*-butyl amidation of allylbenzene was 93:7. Additionally, the calculations rightly indicate that the stereochemical outcome of the reaction is initially determined during the C–H activation step, before the dioxazolone coordinates the olefin. Experimentally, however, we observed that enantioselectivity of amidation with *tert*-butyl dioxazolone was different compared to Phth-glycine dioxazolone on an array of olefins. Based on

¹⁶ Baik group (KAIST)

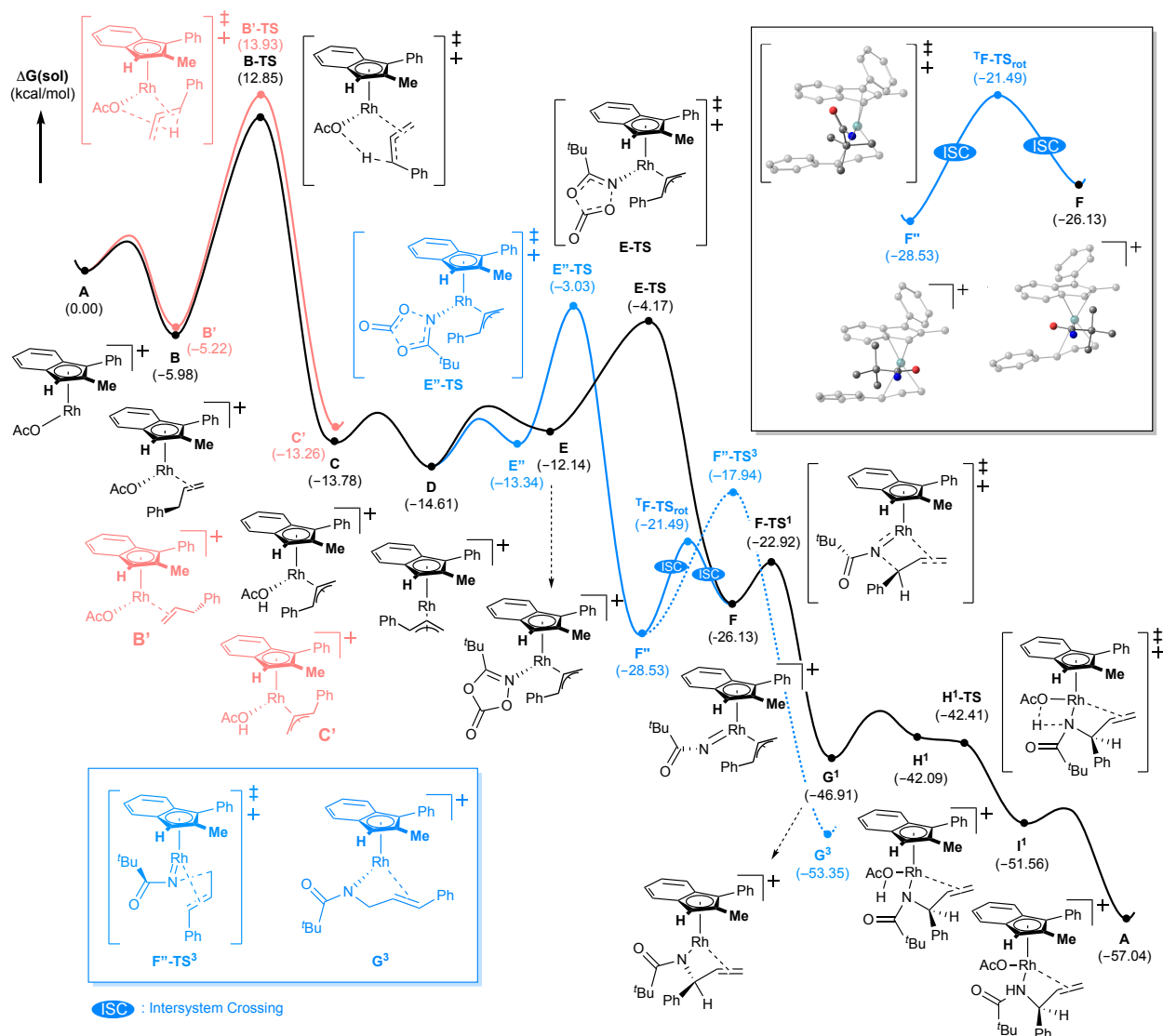


Figure 5.7: Energy coordinate diagram for the **(*R,R*)-5-44**-catalysed allylic C–H amidation of allylbenzene with *tert*-butyl dioxazolone (Bohyun Park, Joonghee Won, Kimberly Sharp)

these observations, it is clear that the dioxazolone plays a role in determining the enantioselectivity of the reaction.

Once the π -allyl complex **C** has been selectively formed, loss of acetic acid and coordination of dioxazolone can lead to complex **E**, in which the *tert*-butyl group is oriented *syn* to the terminus of the π -allyl ligand, or complex **E''**, in which the *tert*-butyl group is oriented *syn* to the phenyl group of the π -allyl ligand. Both isomers could traverse the transition states **E-TS** and **E''-TS**, to release CO_2 and irreversibly form the Rh(V)-nitrenoid complexes **F** and **F''**, respectively. Subsequently, **F''** can undergo reductive C–N bond formation to form the linear

allylic C–N bond (complex **G**³) *via* transition state **F**^{''}-**TS**³. Alternatively, **F** could reductively eliminate to form the allylic C–N bond at the branched position (complex **G**¹), traversing the transition state **F**-**TS**¹. Therefore, the initial calculations suggested that regioselectivity was determined by the orientation of the dioxazolone at the time of CO₂ extrusion to form the Rh(V)-nitrenoid intermediate. However, the energy difference between transition states for CO₂ expulsion (**E**-**TS** and **E**^{''}-**TS**) is only ~1.14 kcal/mol, which is inconsistent with the exclusive selectivity that was experimentally observed for the branched product in all cases.

The Baik group calculated that **F**^{''} and **F** can interconvert *via* the triplet transition state ¹**F**-**TS**_{rot},³⁵ thus allowing the nitrenoid intermediates to converge at complex **F**. The rather large energy difference between **F**-**TS**¹ and **F**^{''}-**TS**³ can be attributed to the asymmetry of the indenyl ligand. The Rh–C bond at the internal position of the π-allyl is weakened due to the different *trans* influence exerted by the indenyl ligand, making it more susceptible to attack by the imido nitrogen than the terminal carbon. This selectivity is sterically exacerbated by the phenyl substituent on the indenyl ligand, which hinders the bulky *tert*-butyl group on the nitrenoid from approaching the terminal carbon in **F**^{''}-**TS**³.

Thus, the allylic C–H cleavage step was determined to be rate- and enantiodetermining, although we hypothesise that the dioxazolone plays an as yet unclear role in enforcing this enantioselectivity. The regioselectivity of the reaction was calculated to be a direct result of the electronic asymmetry in indenyl ligand, leading to selective C–N bond formation at the carbon atom of the π-allyl ligand with the weaker Rh–C bond. Other members of the Blakey lab are currently working to develop a library of indenyl ligands for the catalysis of a broad array of reactions.

5.4 Conclusion

Having developed robust methods for the selective functionalisation of allylic C–H bonds, we turned our attention to the potential synthetic applications of this methodology. In an effort

to expand the 2nd-generation allylic C–N bond formation to provide allylic amines equipped with more commonly protecting groups, we attempted to develop alternate nitrenoid precursors to use in this reaction. Along with Taylor Nelson, we were able to optimise the allylic C–H sulfamidation reaction using tosyl azide as the nitrenoid source and worked to mentor undergraduate students Steven Chen and Kimberly Sharp to explore the functional group tolerance of this reaction. Further, alongside Dr. Caitlin Farr and Christopher Poff, we were able to develop a new planar chiral rhodium indenyl catalyst for the regio- and enantioselective allylic C–H amidation of unactivated mono- and disubstituted olefins. Computational studies, conducted by the Baik group at KAIST, indicate that allylic C–H cleavage is turnover-limiting and enantiodetermining, while reductive C–N bond formation from the Rh(V)-nitrenoid is regiodetermining. In the case of symmetrical π -allyl complexes, this step also serves as the enantiodetermining step of the reaction. Chapter 6 of this dissertation will focus on applying these newly developed methodologies towards the synthesis of an emerging class of biologically relevant natural products – ribosomally-synthesised and post-translationally modified peptides (RiPPs).

5.5 Experimental

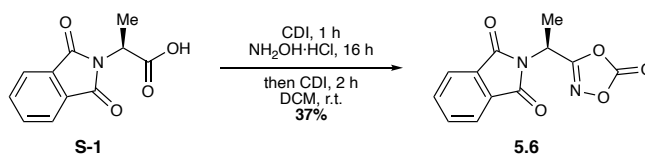
General Information

All reactions were carried out under a nitrogen atmosphere with anhydrous solvents in oven- or flame-dried glassware using the standard Schlenk technique, unless otherwise stated. Anhydrous dichloromethane (DCM), diethyl ether (Et₂O), tetrahydrofuran (THF), and toluene were obtained by passage through activated alumina using a *Glass Contours* solvent purification system. 1,2-Dichloroethane (DCE), 2,2,2-trifluoroethanol (TFE), and 1,1,1,3,3,3-hexafluoroisopropanol (HFIP) were distilled over calcium hydride (CaH₂) and stored over activated molecular sieves. Solvents for workup, extraction, and column chromatography were used as received from commercial suppliers without further purification. Pd(PPh₃)₄, LiCl, AgSbF₆, AgBF₄, AgOTf, AgNTf₂, CsOAc, LiNTf₂, LiOAc, [Cp*IrCl₂]₂, [Cp*RhCl₂]₂, 2-methyl-3-phenyl-1H-indene (2-Me-3-Ph-Ind), ((±)-[Rh(2-Me-3-Ph-Ind)(COD)]), (*S,S*)-[Rh(2-Me-3-Ph-Ind)₂], (*R,R*)-[Rh(2-Me-3-Ph-Ind)₂], and CDI were stored and weighed in a nitrogen-filled glovebox. All other chemicals were purchased from Sigma-Aldrich, Strem Chemicals, Oakwood Chemicals, Alfa Aesar, or Combi-Blocks, and used as received without further purification, unless otherwise stated. ¹H and ¹³C nuclear magnetic resonance (NMR) spectra were recorded on a Varian Inova 600 spectrometer (600 MHz ¹H, 151 MHz ¹³C), a Bruker 600 spectrometer (600 MHz ¹H, 151 MHz ¹³C), a Varian Inova 500 spectrometer (500 MHz ¹H, 126 MHz ¹³C), and a Varian Inova 400 spectrometer (400 MHz ¹H, 100 MHz ¹³C) at room temperature in CDCl₃ (neutralized and dried over anhydrous K₂CO₃) with internal CHCl₃ as the reference (7.26 ppm for ¹H, 77.16 ppm for ¹³C), unless otherwise stated. Chemical shifts (δ values) were reported in parts per million (ppm), and coupling constants (*J* values), in Hz. Multiplicity was indicated using the following abbreviations: s = singlet, d = doublet, t = triplet, q = quartet, qn = quintet, m = multiplet, br = broad. Infrared (IR) spectra were recorded using a Thermo Electron Corporation Nicolet 380 FT-IR spectrometer. High resolution mass spectra (HRMS) were obtained using a Thermo Electron Corporation Finigan LTQFTMS (at the Mass Spectrometry Facility, Emory University). Analytical thin layer

chromatography (TLC) was performed on precoated glass backed Silicycle SiliaPure 0.25 mm silica gel 60 plates and visualized with UV light, ethanolic p-anisaldehyde, or aqueous potassium permanganate (KMnO₄). Flash column chromatography was performed using Silicycle SiliaFlash F60 silica gel (40–63 μm) on a Biotage Isolera One system. Preparatory TLC was performed on pre-coated glass backed Silicycle SiliaPure 1.0 mm silica gel 60 plates.

Procedures and Characterisation

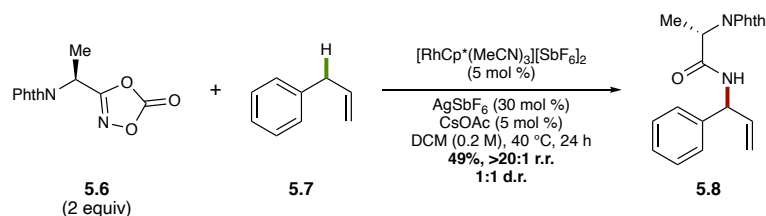
Phth-Ala-dioxazolone **5.6** (General Procedure A – dioxazolone synthesis)



CDI (1.11 g, 6.84 mmol) was added to a solution of phthalimide alanine **S-1** (1.00 g, 4.56 mmol) in MeCN (20 mL) and the reaction was stirred vigorously at room temperature for 3 hours. NH₂OH·HCl (0.476 g, 6.84 mmol) was added to the reaction flask and the reaction was stirred at room temperature for 17 hours. Additional CDI (1.11 g, 6.84 mmol) was added and the reaction was stirred at room temperature for 4 hours. The reaction was quenched with aqueous 1 N HCl (20 mL) and diluted with DCM (35 mL). The layers were separated, and the aqueous layer was extracted with DCM (3 x 20 mL). The combined organic extracts were washed with brine, dried over anhydrous Na₂SO₄, filtered, and concentrated under reduced pressure. Purification by chromatography on silica gel (3:1 – 1:1 Hexanes/EtOAc) provided Phth-alanine dioxazolone **5.6** (0.4343 g, 37%).

¹H NMR (CDCl₃, 500 MHz) δ 7.91 (dd, *J* = 5.5, 3.0 Hz, 2H), 7.80 (dd, *J* = 5.5, 3.0 Hz, 2H), 5.47 (q, *J* = 7.1 Hz, 1H), 1.84 (d, *J* = 7.2 Hz, 3H) ppm.

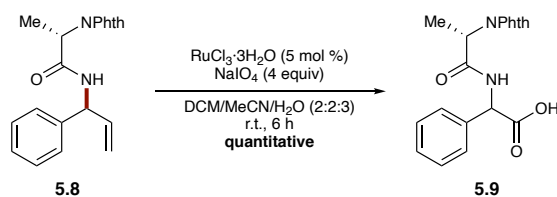
Allylic amide **5.8** (General Procedure B – racemic allylic amidation with nitrenoid precursors)



In a nitrogen-filled glovebox, CsOAc (0.0005 g, 0.0025 mmol), AgSbF_6 (0.0052 g, 0.015 mmol), and $[\text{RhCp}^*(\text{MeCN})_3](\text{SbF}_6)_2$ (0.0021 g, 0.0025 mmol) were added to an oven-dried 4-mL vial equipped with a magnetic stir bar and a Teflon-septum screw cap. The vial was sealed and brought out of the glovebox. Allylbenzene (**5.7**) (0.0059 g, 0.05 mmol) was added as a stock solution in DCE (0.125 mL), followed by a stock solution of Phth-alanine dioxazolone (**5.6**) (0.026 g, 0.10 mmol) in DCE (0.125 mL). The vial was sealed with Teflon and parafilm, and the reaction was stirred at 40 °C for 24 hours. The reaction was removed from heat and allowed to cool down to room temperature. The reaction was filtered through a pipette containing celite with EtOAc (10 mL) and the filtrate was concentrated under reduced pressure. Purification by preparatory TLC (2:1 Hexanes/EtOAc) provided allylic amide **5.8** (0.0082 g, 49%) as a 1:1 mixture of diastereomers.

$^1\text{H NMR}$ (CDCl_3 , 600 MHz) δ 7.85 (dd, $J = 5.5, 2.9$ Hz, 2H), 7.85 (dd, $J = 5.5, 2.9$ Hz, 2H), 7.73 (dd, $J = 5.6, 2.9$ Hz, 2H), 7.73 (dd, $J = 5.7, 2.8$ Hz, 2H), 7.36 – 7.30 (m, 4H), 7.30 – 7.23 (m, 6H), 6.42 (d, $J = 8.2$ Hz, 1H), 6.39 (d, $J = 7.8$ Hz, 1H), 5.99 (ddd, $J = 16.4, 10.6, 5.5$ Hz, 1H), 5.99 (ddd, $J = 16.4, 10.6, 5.5$ Hz, 1H), 5.93 – 5.56 (m, 2H), 5.33 – 5.19 (m, 4H), 4.97 (q, $J = 7.3$ Hz, 1H), 4.97 (q, $J = 7.3$ Hz, 1H), 1.73 (d, $J = 7.4$ Hz, 3H), 1.72 (d, $J = 7.3$ Hz, 3H) ppm.

Dipeptide **5.9**

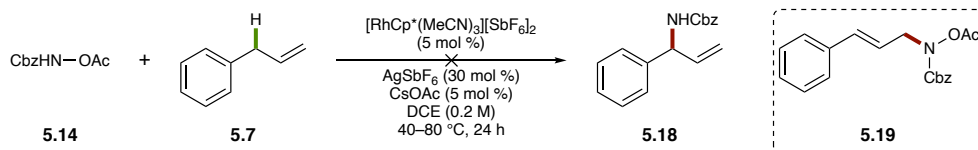


A solution of allylic amide **5.8** (1:1 d.r., 0.014 g, 0.042 mmol) in MeCN (0.23 mL), DCM (0.23 mL), and deionised H₂O (0.35 mL) was prepared. RuCl₃·H₂O (0.0004 g, 0.0021 mmol) and NaIO₄ (0.0358 g, 0.167 mmol) were added and the reaction was stirred at room temperature for 16 hours. The reaction was diluted with deionised H₂O (1 mL) and EtOAc (1 mL). The layers were separated, and the aqueous layer was extracted with EtOAc (2 x 0.5 mL). The combined organic extracts were washed with brine (2 mL), dried over anhydrous Na₂SO₄, filtered, and concentrated under reduced pressure to provide dipeptide **5.9** (0.0148 g, quantitative yield) as a 1:1 mixture of diastereomers. LC/MS showed the presence of the desired product and no additional impurities. No further purification was conducted.

¹H NMR (CDCl₃, 500 MHz) δ 7.89 – 7.81 (m, 4H), 7.78 – 7.68 (m, 4H), 7.43 – 7.30 (m, 10H), 7.12 (t, *J* = 8.0 Hz, 2H), 5.59 – 5.53 (m, 2H), 5.06 – 4.91 (m, 2H), 1.73 (d, *J* = 7.2 Hz, 3H), 1.72 (d, *J* = 7.6 Hz, 3H) ppm.

Oxy carbamates **5.14**–**5.17**⁶ were prepared according to previously reported procedures.

Allylic acetoxycarbamate **5.19**



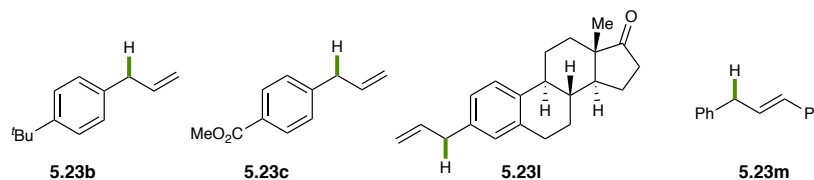
This reaction was performed according to General Procedure B using *N*-acetylbenzylcarbamate **5.14** as the nitrenoid precursor. Allylic acetoxycarbamate **5.19** was isolated as the major product, along with other unidentified impurities.

¹H NMR (CDCl₃, 600 MHz) δ 7.42 – 7.25 (m, 10H), 6.55 (d, *J* = 15.8 Hz, 1H), 6.20 (dt, *J* = 15.8, 6.6 Hz, 1H), 5.21 (s, 2H), 4.40 (d, *J* = 6.6 Hz, 2H), 2.12 (s, 3H) ppm.

HRMS (+NSI) calculated for C₁₉H₁₉NNaO₄ [M+Na]⁺ 348.1212, found 348.1206.

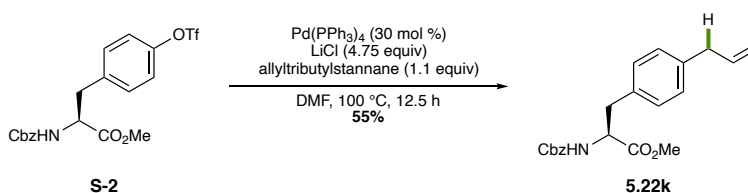
Experimental section – Section 5.2

Olefin substrates



Olefins **5.22b**,³⁶ **5.22c**,³⁷ **5.22l**,³⁸ and **5.22m**³⁹ were prepared according to previously reported procedures. Pd(PPh₃)₄ was used as the palladium pre-catalyst in all cases.

Phenylalanine-derived allylbenzene **5.22k**



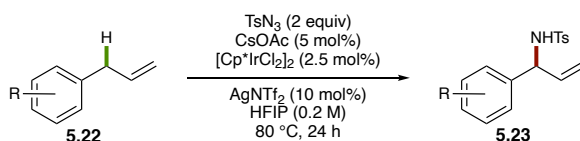
Reaction conducted by Taylor Nelson. In a nitrogen-filled glovebox, Pd(PPh₃)₄ (0.0553 g, 0.048 mmol) and LiCl (0.3022 g, 7.13 mmol) were added to an oven-dried 15 mL vial equipped with a magnetic stir bar and Teflon-septum screw cap. The vial was sealed and brought out of the glovebox. A solution of *N*-Cbz-(*p*-OTf)-Phe-OMe **S-2** (0.7003 g, 1.50 mmol) in DMF (6.30 mL) was added, followed by neat allyltributylstannane (0.600 mL, 1.67 mmol). The vial was placed in an aluminium heating block preheated to 100 °C and stirred for 12.5 h. The reaction was removed from heat, allowed to cool to room temperature, and quenched with aqueous NH₄OH (1 N, 7 mL). The layers were separated, and the aqueous layer was extracted with EtOAc (3 × 10 mL). The combined organic extracts were washed with brine (2 × 15 mL), dried over anhydrous Na₂SO₄, filtered, and concentrated under reduced pressure. Purification by flash chromatography on silica gel (0–100% EtOAc in Hexanes) provided **1k** (0.297 g, 55% yield).

¹H NMR (CDCl₃, 600 MHz) δ 7.43–7.31 (m, 5H), 7.14–7.08 (m, 2H), 7.06–7.00 (m, 2H), 5.95 (ddt, *J* = 17.5, 9.5, 6.7 Hz 1H), 5.21 (d, *J* = 8.3 Hz, 1H) 5.15–4.92 (m, 4H), 4.66 (dt, *J* = 8.3, 5.8 Hz, 1H), 3.73 (s, 3H), 3.36 (dd, *J* = 6.8, 1.6 Hz, 2H), 3.10 (dd, *J* = 14.9, 5.8 Hz, 2H) ppm.

^{13}C NMR (CDCl_3 , 151 MHz) 172.1, 155.7, 139.0, 137.4, 136.4, 133.4, 129.4, 129.0, 128.6, 128.6, 128.30, 128.2, 116.0, 67.1, 54.9, 52.4, 39.9, 37.9 ppm

HRMS (+NSI) calculated for $\text{C}_{21}\text{H}_{24}\text{O}_4\text{N}$ $[\text{M}+\text{H}]^+$ 354.1705, found 354.1706.

General Procedure C – allylic C–H sulfamidation

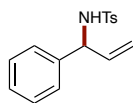


In a nitrogen-filled glovebox, CsOAc (0.0019 g, 0.010 mmol), AgNTf₂ (0.0078 g, 0.020 mmol), and [Cp*IrCl₂]₂ (0.0040 g, 0.005 mmol) were added to an oven-dried 7 mL pressure tube equipped with a magnetic stir bar and a screw cap. The tube was sealed and brought out of the glovebox. HFIP (0.5 mL) and TsN₃ (0.40 mmol, 2 equiv) were added through the side arm of the tube. For allylbenzene derivatives with known densities, a microsyringe was used for addition through the side arm of the pressure tube (0.20 mmol), followed by HFIP (0.5 mL) to wash the sides of the tube. All other allylbenzene derivatives (0.20 mmol) were added as stock solutions in HFIP (0.5 mL). The tube was sealed and placed in an aluminum heating block preheated to 80 °C, and stirred for 24–48 h, as indicated. The tube was removed from heat and allowed to cool to room temperature. The tube was opened to the side arm, and the septum was carefully removed to release pressure. The reaction was filtered through a pipet containing Celite with EtOAc (15 mL), and the filtrate was concentrated under reduced pressure. Purification by flash chromatography on silica gel (10–30% EtOAc in Hexanes) provided the tosylamide products.

Characterisation of allylic C–H sulfamidation products

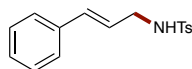
Prepared according to General Procedure C, using allylbenzene (5.7), (0.031 mL, 0.20 mmol), TsN₃ (0.061 mL, 0.40 mmol), [Cp*IrCl₂]₂ (0.0040 g, 0.005 mmol), AgSbF₆ (0.0078 g, 0.02 mmol), and CsOAc (0.0019 g, 0.01 mmol) in DCE (1.0 mL) at 80 °C for 24 h. Purification by flash

chromatography on silica gel (10–30% EtOAc in Hexanes) provided branched product **5.20** and linear product **5.21**. $^1\text{H NMR}$ spectra match previously reported data.^{39,40}



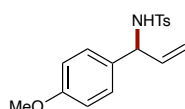
5.20

$^1\text{H NMR}$ (CDCl_3 , 500 MHz) δ 7.63 (d, $J = 8.3$ Hz, 2H), 7.24–7.18 (m, 5H), 7.12–7.07 (m, 2H), 5.86 (ddd, $J = 16.9, 10.5, 5.7$ Hz, 1H), 5.16–5.08 (m, 2H), 4.97–4.86 (m, 2H), 2.39 (s, 1H) ppm.



5.21

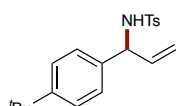
$^1\text{H NMR}$ (CDCl_3 , 400 MHz) δ 7.78 (d, $J = 8.3$ Hz, 2H), 7.42–7.10 (m, 7H), 6.44 (d, $J = 15.9$ Hz, 1H), 6.02 (dt, $J = 15.8, 6.4$ Hz, 1H), 4.46 (t, $J = 6.2$ Hz, 1H), 3.76 (td, $J = 6.3, 1.5$ Hz, 2H), 2.42 (s, 3H) ppm.



5.23a

Reaction conducted by Steven Chen. Prepared according to General Procedure C, using 4-allylanisole (**5.22a**) (0.031 mL, 0.20 mmol), TsN_3 (0.061 mL, 0.40 mmol), $[\text{Cp}^*\text{IrCl}_2]_2$ (0.0040 g, 0.005 mmol), AgNTf_2 (0.0078 g, 0.02 mmol), and CsOAc (0.0019 g, 0.01 mmol) in HFIP (1.0 mL) at 80 °C for 24 h. Purification by flash chromatography on silica gel (10–30% EtOAc in Hexanes) provided **5.23a** (0.0365 g, 57%). $^1\text{H NMR}$ spectrum matches previously reported data.⁴¹

$^1\text{H NMR}$ (CDCl_3 , 500 MHz) δ 7.63 (d, $J = 8.5$ Hz, 2H), 7.20 (d, $J = 8.6$ Hz, 2H), 7.01 (d, $J = 8.7$ Hz, 2H), 6.74 (d, $J = 8.9$ Hz, 2H), 5.85 (ddd, $J = 17.2, 10.1, 5.7$ Hz, 1H), 5.14–5.08 (m, 2H), 4.95 (d, $J = 7.5$ Hz, 1H), 4.90–4.85 (m, 1H), 3.75 (s, 3H), 2.39 (s, 3H) ppm.



5.23b

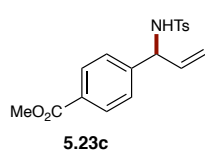
Prepared according to General Procedure C, using 1-allyl-4-(tertbutyl)benzene (**5.22b**) (0.0350 g, 0.20 mmol), TsN_3 (0.061 mL, 0.40 mmol), $[\text{Cp}^*\text{IrCl}_2]_2$ (0.0040 g, 0.005 mmol), AgNTf_2 (0.0078 g, 0.02 mmol), and CsOAc (0.0019 g,

0.01 mmol) in HFIP (1.0 mL) at 80 °C for 24 h. Purification by flash chromatography on silica gel (10–30% EtOAc in Hexanes) provided **5.23b** (0.0422 g, 61%).

¹H NMR (CDCl₃, 600 MHz) δ 7.61 (d, *J* = 8.3 Hz, 2H), 7.21 (d, *J* = 8.4 Hz, 2H), 7.16 (d, *J* = 7.8 Hz, 2H), 7.01 (d, *J* = 8.1 Hz, 2H), 5.87 (ddd, *J* = 17.1, 10.3, 5.9 Hz, 1H), 5.20–5.05 (m, 2H), 5.01 (d, *J* = 7.3 Hz, 1H), 4.95–4.91 (m, 1H), 2.37 (s, 3H), 1.27 (s, 9H) ppm.

¹³C NMR (CDCl₃, 151 MHz) δ 150.8, 143.1, 137.9, 137.4, 136.4, 129.4, 127.4, 126.9, 125.6, 116.7, 59.8, 34.6, 31.4, 21.6 ppm.

HRMS (+APCI) calculated for C₂₀H₂₉N₂O₂S [M+NH₄]⁺ 361.1950, found 361.1940.



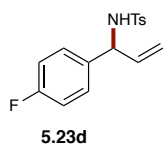
Prepared according to General Procedure C, using 4-methylallylbenzoate (**5.22c**) (0.0350 g, 0.20 mmol), TsN₃ (0.061 mL, 0.40 mmol), [Cp*IrCl₂]₂ (0.0040 g, 0.005 mmol), AgNTf₂ (0.0078 g, 0.02 mmol), and CsOAc (0.0019

g, 0.01 mmol) in HFIP (1.0 mL) at 80 °C for 24 h. Purification by flash chromatography on silica gel (10–30% EtOAc in Hexanes) provided **5.23c** (0.0361 g, 52%).

¹H NMR (CDCl₃, 600 MHz) δ 7.85 (d, *J* = 8.3 Hz, 2H), 7.61 (d, *J* = 8.3 Hz, 2H), 7.18 (d, *J* = 8.3 Hz, 2H), 7.16 (d, *J* = 8.0 Hz, 2H), 5.83 (ddd, *J* = 16.7, 10.3, 6.0 Hz, 1H), 5.37 (d, *J* = 7.7 Hz, 1H), 5.16–5.03 (m, 2H), 5.01–4.95 (m, 1H), 3.89 (s, 3H), 2.37 (s, 3H) ppm.

¹³C NMR (CDCl₃, 151 MHz) δ 166.8, 144.5, 143.6, 137.6, 136.5, 130.0, 129.8, 129.6, 127.3, 126.5, 117.7, 59.7, 52.3, 21.6 ppm.

HRMS (+APCI) calculated for C₁₈H₂₃N₂O₄S [M+NH₄]⁺ 363.1379, found 363.1376.



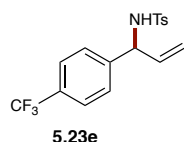
Reaction conducted by Steven Chen. Prepared according to General Procedure C, using 1-allyl-4-fluorobenzene (**5.22d**) (0.027 mL, 0.20 mmol), TsN₃ (0.061 mL, 0.40 mmol), [Cp*IrCl₂]₂ (0.0040 g, 0.005 mmol), AgNTf₂ (0.0078 g, 0.02 mmol), and CsOAc (0.0019 g, 0.01 mmol) in HFIP (1.0 mL) at 80 °C for 24 h. Purification by flash

chromatography on silica gel (10–30% EtOAc in Hexanes) provided **5.23d** (0.0422 g).

¹H NMR (CDCl₃, 600 MHz) δ 7.61 (d, *J* = 8.3 Hz, 2H), 7.19 (dd, *J* = 8.6, 0.8 Hz, 2H), 7.11–7.05 (m, 2H), 6.89 (t, *J* = 8.7 Hz, 2H), 5.83 (ddd, *J* = 17.0, 10.3, 5.8 Hz, 1H), 5.13 (d, *J* = 10.3 Hz, 1H), 5.10–5.06 (m, 2H), 4.96–4.90 (m, 1H), 2.39 (s, 3H) ppm.

¹³C NMR (CDCl₃, 151 MHz) δ 162.2 (d, *J*_{C-F} = 246.3 Hz), 143.5, 137.6, 136.9, 135.3 (d, *J*_{C-F} = 3.2 Hz), 129.5, 129.0 (d, *J*_{C-F} = 8.2 Hz), 127.3, 117.1, 115.5 (d, *J*_{C-F} = 21.5 Hz), 59.3, 21.6 ppm.

HRMS (+APCI) calculated for C₁₆H₁₇FNO₂S [M+H]⁺ 306.0964, found 306.0954.

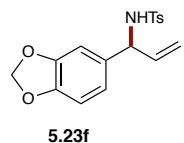


Reaction conducted by Steven Chen. Prepared according to General Procedure C, using 4-allyltrifluorotoluene (**5.22e**) (0.033 mL, 0.20 mmol), TsN₃ (0.061 mL, 0.40 mmol), [Cp*IrCl₂]₂ (0.0040 g, 0.005 mmol), AgNTf₂ (0.0078 g, 0.02 mmol), and CsOAc (0.0019 g, 0.01 mmol, 0.05 equiv) in HFIP (1.0 mL) at 80 °C for 24 h. Purification by flash chromatography on silica gel (10–30% EtOAc in Hexanes) provided **5.23e** (0.033 g). ¹H NMR spectrum matches previously reported data.¹

¹H NMR (CDCl₃, 500 MHz) δ 7.56 (d, *J* = 8.3 Hz, 2H), 7.41 (d, *J* = 8.4 Hz, 2H), 7.21 (d, *J* = 8.5 Hz, 2H), 7.13 (d, *J* = 8.0 Hz, 2H), 5.84 (ddd, *J* = 16.3, 10.3, 5.9 Hz, 1H), 5.37 (d, *J* = 7.4 Hz, 1H), 5.16 (d, *J* = 10.3 Hz, 1H), 5.11–4.97 (m, 2H), 2.36 (s, 3H) ppm;

¹³C NMR (CDCl₃, 126 MHz) δ 143.7, 143.27, 143.25, 137.4, 136.4, 130.1 (q, *J*_{C-F} = 32.5 Hz), 129.6, 129.5, 127.7, 127.3, 125.5 (q, *J*_{C-F} = 3.8 Hz), 117.9, 59.6, 21.5 ppm.

HRMS (+APCI) calculated for C₁₇H₂₀F₃N₂O₂S [M+NH₄]⁺ 373.1198, found 373.1192.

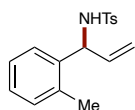


Reaction was performed by Taylor Nelson. Prepared according to General Procedure C, using safrole (**2.55f**) (0.029 mL, 0.20 mmol), TsN₃ (0.061 mL, 0.40 mmol), [Cp*IrCl₂]₂ (0.0040 g, 0.005 mmol), AgNTf₂ (0.0078 g, 0.02 mmol), and CsOAc (0.0019 g, 0.01 mmol) in HFIP (1.0 mL) at 80 °C for 48 h. Purified by flash chromatography on silica gel (10–30% EtOAc in Hexanes) to provide **5.23f** (0.0311 g, 47%).

¹H NMR (CDCl₃, 500 MHz) δ 7.63 (d, *J* = 8.3 Hz, 2H), 7.21 (d, *J* = 8.5 Hz, 1H), 6.64 (d, *J* = 8.0 Hz, 1H), 6.57 (dd, *J* = 8.0, 1.8 Hz, 1H), 6.53 (d, *J* = 1.8 Hz, 1H), 5.90 (d, *J* = 1.5 Hz, 1H), 5.89 (d, *J* = 1.4 Hz, 1H), 5.82 (ddd, *J* = 17.2, 10.1, 5.4 Hz, 1H), 5.16–5.08 (m, 2H), 4.88–4.81 (m, 2H), 2.40 (s, 3H) ppm.

¹³C NMR (CDCl₃, 151 MHz) δ 147.9, 147.3, 143.4, 137.8, 137.2, 133.4, 129.5, 127.4, 120.8, 116.9, 108.3, 107.7, 101.26, 77.2, 59.8, 21.6 ppm.

HRMS (+APCI) calculated for C₁₇H₁₈NO₄S [M+H]⁺ 332.0957, found 332.0943.



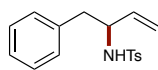
5.23g

Prepared according to General Procedure C using 1-allyl-2-methylbenzene (**5.22g**) (0.029 mL, 0.20 mmol), TsN₃ (0.061 mL, 0.40 mmol), [Cp*IrCl₂]₂ (0.0040 g, 0.005 mmol), AgNTf₂ (0.0078 g, 0.02 mmol), and CsOAc (0.0019 g, 0.01 mmol) in HFIP (1.0 mL) at 80 °C for 48 h. Purification by flash chromatography on silica gel (10–30% EtOAc in Hexanes) provided **5.23g** (0.0359 g, 60%).

¹H NMR (CDCl₃, 600 MHz) δ 7.60 (d, *J* = 8.2 Hz, 2H), 7.16 (d, *J* = 8.4 Hz, 2H), 7.07–7.01 (m, 3H), 5.85 (ddd, *J* = 17.1, 10.3, 5.5 Hz, 1H), 5.21–5.15 (m, 1H), 5.10 (dd, *J* = 10.3, 1.3 Hz, 1H), 5.06–4.96 (m, 1H), 4.85 (d, *J* = 7.2 Hz, 1H), 2.37 (s, 3H), 2.21 (s, 3H) ppm.

¹³C NMR (CDCl₃, 126 MHz) δ 143.3, 137.8, 137.4, 137.1, 135.6, 130.8, 129.5, 127.8, 127.2, 126.9, 126.4, 116.9, 56.5, 21.6, 19.3 ppm.

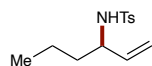
HRMS (+APCI) calculated for C₁₇H₂₀NO₂S [M+H]⁺ 302.1215, found 302.1204.



5.23h

Prepared according to General Procedure C using 4-phenylbutene (**5.22h**) (0.030 mL, 0.20 mmol), TsN₃ (0.061 mL, 0.40 mmol), [Cp*IrCl₂]₂ (0.0040 g, 0.005 mmol), AgNTf₂ (0.0078 g, 0.02 mmol), and CsOAc (0.0019 g, 0.01 mmol) in HFIP (1.0 mL) at 80 °C for 48 h. Purification by flash chromatography on silica gel (10–40% EtOAc in Hexanes) provided **5.23h** (0.045 g, 75%). ¹H NMR spectrum matches previously reported data.⁴²

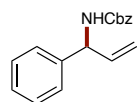
$^1\text{H NMR}$ (CDCl_3 , 400 MHz) δ 7.60 (d, $J = 8.3$ Hz, 2H), 7.27–7.16 (m, 5H), 7.05–7.00 (m, 2H), 5.68 (ddd, $J = 16.8, 10.4, 6.1$ Hz, 1H), 5.10–4.96 (m, 2H), 4.49 (d, $J = 7.3$ Hz, 1H), 4.07–3.95 (m, 1H), 3.08–2.61 (m, 2H), 2.41 (3H, s) ppm.



5.23i
4.5:1.5:1

Reaction conducted by Taylor Nelson. Prepared following General Procedure C using 1-hexene (**5.22i**) (0.025 mL, 0.20 mmol), TsN_3 (0.061 mL, 0.40 mmol), $[\text{Cp}^*\text{IrCl}_2]_2$ (0.0040 g, 0.005 mmol), AgNTf_2 (0.0078 g, 0.02 mmol), and CsOAc (0.0019 g, 0.01 mmol) in HFIP (1.0 mL) at 80 °C for 48 h. Purification by flash chromatography on silica gel (0–100% Et₂O in Hexanes) provided **5.23i** (0.025 g, 49%) as an inseparable mixture of regioisomers (4.5:1.5:1 r.r.). $^1\text{H NMR}$ spectra match previously reported data.^{43,44}

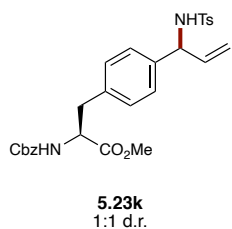
$^1\text{H NMR}$ (CDCl_3 , 399 MHz) δ 7.73 (m, 28H), 7.28 (m, 28H), 5.53 (ddd, $J = 17.0, 10.3, 6.6$ Hz, 9H), 5.45 (dt, $J = 15.4, 6.3$ Hz, 2H), 5.41–5.28 (m, 3H), 5.14 (dd, $J = 15.4, 6.6$ Hz, 2H), 5.05 (ddd, $J = 15.3, 7.4, 1.7$ Hz, 3H), 5.00–4.93 (m, 18 H), 4.58 (d, $J = 7.9$ Hz, 9H), 4.50 (d, $J = 7.6$ Hz, 5H), 3.97–3.82 (m, 2H), 3.76 (quint, $J = 6.8$ Hz, 9H), 3.61 (quint, $J = 7.2$ Hz, 3H), 2.42 (s, 42H), 1.95–1.80 (m, 5H), 1.56–1.16 (m, 33H), 0.83 (t, $J = 7.3$ Hz, 42H) ppm.



5.23j

Prepared according to General Procedure C using allylbenzene (**5.6**) (0.026 mL, 0.20 mmol), CbzN_3 (0.071 g, 0.40 mmol), $[\text{Cp}^*\text{IrCl}_2]_2$ (0.0040 g, 0.005 mmol), AgNTf_2 (0.0078 g, 0.02 mmol) and CsOAc (0.0019 g, 0.01 mmol) in HFIP (1.0 mL) at 80 °C for 48 h. Purification by flash chromatography on silica gel (10–30% EtOAc in Hexanes) provided **5.23j** (0.0091 g, 17%). $^1\text{H NMR}$ spectrum matches previously reported data.⁴⁵

$^1\text{H NMR}$ (CDCl_3 , 500 MHz) δ 7.40–7.27 (m, 10H), 6.01 (ddd, $J = 16.3, 10.6, 5.3$ Hz, 1H), 5.37 (br s, 1H), 5.26 (br s, 1H), 5.24–5.20 (m, 2H), 5.16–5.09 (m, 2H) ppm.

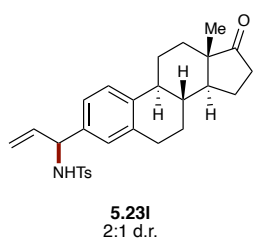


Prepared according to General Procedure C using Cbz-(p-allyl)-Phe-OMe (**5.22k**) (0.071 g, 0.20 mmol), TsN₃ (0.061 mL, 0.40 mmol), [Cp*IrCl₂]₂ (0.0040 g, 0.005 mmol), AgNTf₂ (0.0078 g, 0.02 mmol), and CsOAc (0.0019 g, 0.01 mmol) in HFIP (1.0 mL) at 80 °C for 24 h. Purification by flash chromatography on silica gel (30–50% EtOAc in Hexanes) provided **5.23k** with TsNH₂ impurities. Additional purification by preparatory TLC (30% EtOAc in Hexanes, 2 sweeps) provided **5.22k** (0.0495 g, 50%) as an inseparable mixture of diastereomers (1:1 d.r.).

¹H NMR (CDCl₃, 600 MHz) δ 7.64 (d, *J* = 8.4 Hz, 2H), 7.63 (d, *J* = 8.3 Hz, 2H), 7.40–7.30 (m, 10H), 7.21 (d, *J* = 8.3 Hz, 2H), 7.21 (d, *J* = 7.9 Hz, 2H), 7.03 (d, *J* = 8.1 Hz, 4H), 6.96 (d, *J* = 8.2 Hz, 2H), 6.95 (d, *J* = 8.1 Hz, 2H), 5.82 (ddd, *J* = 16.1, 10.3, 6.0 Hz, 1H), 5.82, (ddd, *J* = 17.0, 10.3, 6.0 Hz, 1H), 5.19–5.05 (m, 10H), 4.90 (q, *J* = 5.7 Hz, 2H), 4.73 (d, *J* = 7.3 Hz, 1H), 4.73 (d, *J* = 7.3 Hz, 1H), 4.62 (q, *J* = 6.0 Hz, 2H), 3.72 (s, 3H), 3.71 (s, 3H), 3.09 (dd, *J* = 13.9, 5.7 Hz, 1H), 3.08 (dd, *J* = 14.0, 5.7 Hz, 1H), 3.03 (dd, *J* = 14.2, 6.2 Hz, 2H), 2.39 (s, 3H), 2.39 (s, 3H) ppm.

¹³C NMR (CDCl₃, 151 MHz) δ 171.9, 155.7, 143.5, 138.5, 137.8, 137.07, 137.05, 136.3, 135.1, 129.73, 129.71, 129.6, 129.5, 128.7, 128.4, 128.3, 127.5, 127.4, 117.2, 117.1, 67.2, 59.6, 54.8, 52.5, 37.9, 37.9, 21.6 ppm.

HRMS (–APCI) calculated for C₂₈H₂₉N₂O₆S [M–H][–] 521.1746, found 521.1748.

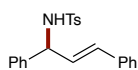


Prepared following General Procedure C using estrone allylbenzene (**5.22l**) (0.0503 g, 0.171 mmol), TsN₃ (0.061 mL, 0.40 mmol), [Cp*IrCl₂]₂ (0.0040 g, 0.005 mmol), AgNTf₂ (0.0078 g, 0.02 mmol), and CsOAc (0.0019 g, 0.01 mmol) in HFIP (1.0 mL) at 80 °C for 24 h. Purification by flash chromatography on silica gel (30–50% EtOAc in Hexanes) provided **5.23l** (0.0494 g, 62%) as an inseparable mixture of diastereomers (2:1 d.r.).

¹H NMR (CDCl₃, 500 MHz) 7.81 (d, *J* = 8.3 Hz, 2H), 7.63 (d, *J* = 8.4, 4H), 7.30 (d, *J* = 8.3 Hz, 2H), 7.19 (d, 8.6 Hz, 4H), 7.14 (dd, *J* = 8.0, 2.9 Hz, 3H), 6.89 (ddd, *J* = 7.9, 5.6, 2.0 Hz, 3H), 6.78 (dd, *J* = 3.5, 2.0 Hz, 3H), 5.84 (ddd, *J* = 15.4, 10.3, 6.0 Hz, 1H), 5.84 (ddd, *J* = 16.3, 10.3 Hz, 6.0 Hz, 2H), 5.17–5.08 (m, 3H), 4.99 (d, *J* = 7.0 Hz, 3H), 4.85 (q, *J* = 5.9 Hz, 3H), 2.85–2.69 (m, 5H), 2.50 (dd, *J* = 19.1, 8.8 Hz, 3H), 2.42 (s, 3H), 2.40 (s, 6H), 2.40–2.33 (m, 3H), 2.26–2.19 (m, 3H), 2.14 (dt, *J* = 19.0, 8.9 Hz, 3H), 2.08–2.02 (m, 3H), 2.01–1.91 (m, 6H), 1.69–1.56 (m, 4H), 1.56–1.44 (m, 12H), 1.44–1.32 (m, 3H), 0.90 (s, 3H), 0.90 (s, 6H) ppm.

¹³C NMR (CDCl₃, 126 MHz) δ 220.8, 143.6, 143.2, 139.53, 139.51, 139.4, 137.95, 137.92, 137.27, 137.26, 137.01, 136.98, 136.90, 129.8, 129.44, 129.42, 127.80, 127.78, 127.4, 126.6, 125.8, 124.6, 124.7, 116.71, 116.68, 59.80, 59.79, 50.6, 48.1, 44.4, 38.23, 38.22, 36.0, 31.7, 29.4, 26.5, 25.83, 25.82, 21.70, 21.66, 21.65, 21.63, 14.0 ppm.

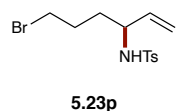
HRMS (+APCI) calculated for C₂₈H₃₄NO₃S [M+H]⁺ 464.2259, found 464.2264.



5.23m

Prepared following General Procedure C using 1,3-trans-diphenylpropene (**5.22m**) (0.038 mL, 0.20 mmol), TsN₃ (0.061 mL, 0.40 mmol), [Cp*IrCl₂]₂ (0.0040 g, 0.005 mmol), AgNTf₂ (0.0078 g, 0.02 mmol), and CsOAc (0.0019 g, 0.01 mmol) in HFIP (1.0 mL) at 80 °C for 24 h. Purification by flash chromatography on silica gel (10–30% EtOAc in Hexanes) provided **5.22m** (0.0393 g, 54%). ¹H NMR spectrum matches previously reported data.³⁹

¹H NMR (CDCl₃, 500 MHz) δ 7.65 (d, *J* = 8.3 Hz, 2H), 7.28–7.10 (m, 12H), 6.33 (dd, *J* = 15.8, 1.2 Hz, 1H), 6.07 (dd, *J* = 15.8, 6.8 Hz, 1H), 5.22 (d, *J* = 7.3 Hz, 1H), 5.11 (td, *J* = 7.1, 1.3 Hz, 1H), 2.31 (s, 3H) ppm.



5.23p

Reaction conducted by Taylor Nelson. Prepared according to General Procedure C, using 6-bromohexene (**5.22p**) (0.025 mL, 0.20 mmol), TsN₃ (0.061 mL, 0.40 mmol), [Cp*IrCl₂]₂ (0.0040 g, 0.005 mmol), AgNTf₂ (0.0078 g, 0.02 mmol), and CsOAc (0.0019

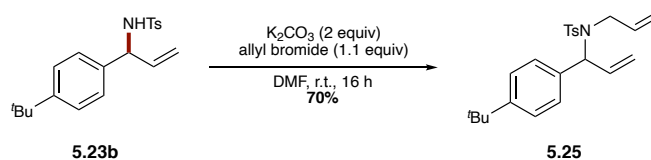
g, 0.01 mmol) in HFIP (1.0 mL) at 80 °C for 40 h. Purification by flash chromatography on silica gel (0–100% EtOAc in Hexanes) provided **5.23p** (0.0045 mg, 9%).

$^1\text{H NMR}$ (CDCl_3 , 400 MHz) δ 7.72 (d, $J = 8.1$ Hz, 2H), 7.31 (d, $J = 8.0$ Hz, 2H), 5.81 (ddd, $J = 16.8, 10.3, 6.0$ Hz, 1H), 5.28 (d, $J = 17.0$ Hz, 1H), 5.12 (d, $J = 10.2$ Hz, 1H), 4.13 (q, $J = 6.9, 6.3$ Hz, 1H), 3.45 (ddd, $J = 9.8, 7.2, 4.1$ Hz, 1H), 3.23 (dt, $J = 10.0, 7.5$ Hz, 1H), 2.43 (s, 3H), 2.08–1.57 (m, 4H) ppm.

$^{13}\text{C NMR}$ (CDCl_3 , 151 MHz) δ 143.4, 138.8, 135.4, 129.7, 127.7, 115.5, 62.1, 48.9, 32.4, 23.9, 21.7 ppm.

HRMS (+NSI) calculated for $\text{C}_{13}\text{H}_{18}\text{NO}_2\text{S}$ [$\text{M}-\text{Br}$] $^+$ 252.1058, found 252.1050.

Diallylsulfonamide **5.25**



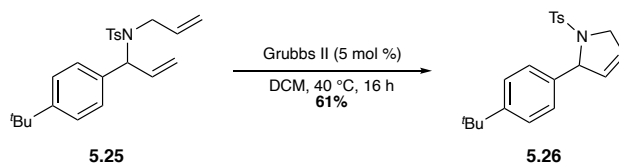
Allyl bromide (0.011 mL, 0.126 mmol) and K_2CO_3 (0.0316 g, 0.229 mmol) were added to a solution of *N*-(1-(4-(*tert*-butyl)phenyl)allyl)-4-methylbenzenesulfonamide (**5.23b**) (0.0393 g, 0.114 mmol) in DMF (0.50 mL), and the resulting mixture was stirred at room temperature. After 16 h, the reaction was diluted with water (5 mL) and EtOAc (5 mL). The layers were separated, and the aqueous layer was extracted with EtOAc (3 \times 5 mL). The combined organic extracts were washed with brine (2 \times 15 mL), dried over anhydrous Na_2SO_4 , filtered, and concentrated under reduced pressure. Purification by flash chromatography on silica gel (5–20% EtOAc in Hexanes) provided **5.25** (0.0305 g, 70%).

$^1\text{H NMR}$ (CDCl_3 , 500 MHz) δ 7.69 (d, $J = 8.3$ Hz, 2H), 7.29 (d, $J = 8.2$ Hz, 2H), 7.24 (d, $J = 8.6$ Hz, 2H), 7.14 (d, $J = 8.9$ Hz, 2H), 6.05 (ddd, $J = 17.2, 10.3, 7.0$ Hz, 1H), 5.62 (d, $J = 7.0$ Hz, 1H), 5.50 (ddt, $J = 16.2, 10.2, 6.3$ Hz, 1H), 5.26 (d, $J = 10.3$ Hz, 1H), 5.14 (d, $J = 17.1$ Hz, 1H), 4.97–4.84 (m, 2H), 3.83 (dd, $J = 16.3, 6.1$ Hz, 1H), 3.71 (dd, $J = 16.2, 6.6$ Hz, 1H), 2.42 (s, 3H), 1.30 (s, 9H) ppm.

^{13}C NMR (CDCl_3 , 126 MHz) δ 151.0, 143.0, 138.4, 135.5, 135.4, 135.1, 129.5, 128.2, 127.7, 125.4, 119.0, 117.2, 63.4, 48.1, 34.6, 31.5, 21.7 ppm.

HRMS (+APCI) calculated for $\text{C}_{23}\text{H}_{30}\text{NO}_2\text{S}$ $[\text{M}+\text{H}]^+$ 384.1997, found 384.1987.

Dihydropyrrole 5.26



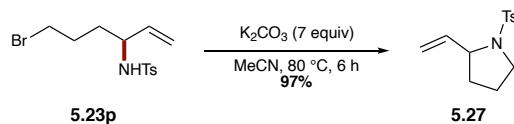
Grubbs II (0.0034 g, 0.00398 mmol) was added to a solution of *N*-allyl-*N*-(1-(4-(tert-butyl)phenyl)allyl)-4-methylbenzenesulfonamide **5.25** (0.0305 g, 0.0795 mmol) in DCM (1.50 mL), and the resulting mixture was stirred in an aluminium heating block preheated to 40 °C. After 16 h, the reaction was quenched with saturated aqueous NaHCO_3 (3 mL) and diluted with DCM (3 mL). The layers were separated, and the aqueous layer was extracted with DCM (3×3 mL). The combined organic extracts were washed with brine (8 mL), dried over anhydrous Na_2SO_4 , filtered, and concentrated under reduced pressure. Purification by flash chromatography (10–30% EtOAc in Hexanes) provided **5.26** (0.0171 g, 61%).

^1H NMR (CDCl_3 , 600 MHz) δ 7.46 (d, $J = 8.3$ Hz, 2H), 7.27 (d, $J = 8.4$ Hz, 2H), 7.14 (d, $J = 8.4$ Hz, 2H), 7.14 (d, $J = 8.5$ Hz, 2H), 5.79 (dq, $J = 6.1, 2.0$ Hz, 1H), 5.66 (dq, $J = 6.5, 2.2$ Hz, 1H), 5.51 (dq, $J = 6.3, 2.2$ Hz, 1H), 4.37 (dq, $J = 14.5, 2.3$ Hz, 1H), 4.25 (ddt, $J = 14.5, 5.7, 2.1$ Hz, 1H), 2.36 (s, 3H), 1.30 (s, 9H) ppm.

^{13}C NMR (CDCl_3 , 126 MHz) δ 150.9, 143.0, 137.3, 136.1, 130.8, 129.4, 127.3, 127.2, 125.4, 124.5, 70.0, 55.4, 34.6, 31.5, 21.6 ppm.

HRMS (+APCI) calculated for $\text{C}_{21}\text{H}_{26}\text{NO}_2\text{S}$ $[\text{M}+\text{H}]^+$ 356.1684, found 356.1670.

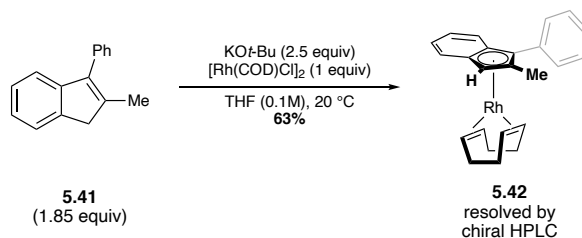
Vinylpyrrolidine 5.27



K_2CO_3 (0.0123 g, 0.0890 mmol) was added to a solution of tosylamide **5.23p** (0.0044 g, 0.013 mmol) in CH_3CN (0.4 mL). The vial was placed in a sand bath preheated to 80 °C and stirred for 6 h. The vial was removed from heat and allowed to cool to room temperature. The reaction was filtered through a Celite plug with EtOAc (10 mL), and the filtrate was concentrated under reduced pressure to provide **5.27** (0.0032 g, 96%). ^1H NMR spectrum matches previously reported data.⁴⁶ ^1H NMR (CDCl_3 , 400 MHz) δ 7.73 (d, $J = 8.0$ Hz, 2H), 7.34–7.29 (m, 2H), 5.81 (ddd, $J = 17.1$, 10.2, 6.0 Hz, 1H), 5.13 (dt, $J = 10.3$, 1.3 Hz, 1H), 3.46 (ddd, $J = 11.2$, 7.2, 4.1 Hz, 1H), 3.28– 3.09 (m, 1H), 2.43 (s, 3H), 1.86–1.57 (m, 4H) ppm.

Experimental – Section 5.3

(±)-[Rh(2-Me-3-Ph-Ind)(COD)] [(±)-5.42]



In a nitrogen-filled glovebox, 2-methyl-3-phenyl-1H-indene (**5.41**) (0.0580 g, 0.281 mmol), [Rh(COD)Cl₂] (0.0756 g, 0.153 mmol), and potassium tert-butoxide (0.0430 g, 0.383 mmol) were added to an oven-dried 4 mL vial equipped with a magnetic stir bar and a Teflon-septum screw cap. The vial was sealed and brought out of the glovebox. THF (2 mL) was added to the vial and the reaction was stirred at room temperature under a balloon of nitrogen for 16 hours. The reaction was filtered through a pipette containing celite with hexanes (6 mL) and the filtrate was concentrated under reduced pressure. Purification by flash chromatography on silica gel with hexanes provided (±)-[Rh(2-Me-3-Ph-Ind)(COD)] [(±)-**5.42**] (0.0960 g, 90%) as a yellow oil.

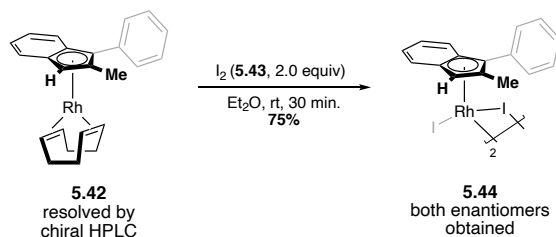
¹H NMR (CDCl₃, 600 MHz) δ 7.46 – 7.39 (m, 4H), 7.29 (tt, *J* = 6.0, 2.8 Hz, 1H), 7.27 – 7.24 (m, 2H), 7.07 – 7.01 (m, 2H), 5.01 (s, 1H), 3.86 (td, *J* = 7.4, 3.4 Hz, 2H), 3.62 (tt, *J* = 7.3, 3.0 Hz, 2H), 2.50 (d, *J* = 1.5 Hz, 3H), 1.97 – 1.83 (m, 4H), 1.79 – 1.67 (m, 4H) ppm.

¹³C NMR (CDCl₃, 151 MHz) δ 135.12, 129.28, 128.38, 126.15, 122.50, 121.80, 119.21, 117.32, 112.32 (d, *J*_{C-Rh} = 2.2 Hz), 111.60 (d, *J*_{C-Rh} = 2.7 Hz), 107.79 (d, *J*_{C-Rh} = 5.0 Hz), 95.47 (d, *J*_{C-Rh} = 3.6 Hz), 76.55 (d, *J*_{C-Rh} = 4.7 Hz), 71.98, 71.89, 69.11, 69.02, 31.43, 31.33, 14.80 ppm.

HRMS (+APCI) calculated for C₂₄H₂₅Rh [M]⁺ 416.10058, found 416.10045.

Chiral Resolution – Semi-prep HPLC (Chiracel OD-H column, 0% 2-Propanol in Hexanes, 2 mL/min) – (*S*)-[Rh(2-Me-3-PhInd)(COD)] *t* = 16.2 min. (*R*)-[Rh(2-Me-3-Ph-Ind)(COD)] *t* = 26.9 min. Utilizing a 10 x 250 mm column with stacked injections of variable sizes (10 mg/mL concentration) up to 307 mg of racemic monomer could be resolved over a 12 hour period.

(*S,S*)- and (*R,R*)-[Rh(2-Me-3-Ph-Ind)I₂]₂ [(*S,S*)-5.44] and [(*R,R*)-5.44]



To a 20 mL scintillation vial containing complex **(*S,S*)-5.42** (0.0515 g, 0.124 mmol) and a stir bar, iodine (0.0785 g, 0.309 mmol) was added and the vial was sealed with a rubber septum. Anhydrous Et₂O (5.0 mL) was added and the reaction stirred for 24 hours under a balloon of nitrogen. The reaction was filtered through a Büchner funnel and washed with Et₂O (50 mL, or until the filtrate is clear). The solid was collected and dried to afford **(*S,S*)-5.44** as a black solid (0.0593 g, 85%).

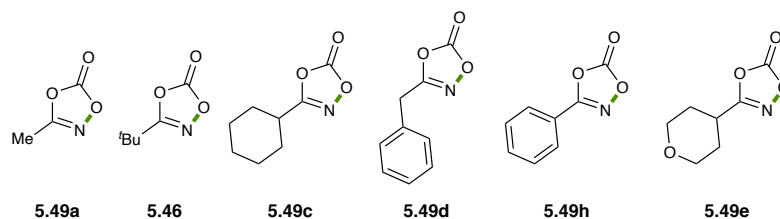
¹H NMR (DMSO-*d*₆, 600 MHz) δ 7.87 – 7.84 (m, 4H), 7.69 (dt, *J* = 8.5, 1.1 Hz, 2H), 7.63 – 7.56 (m, 2H), 7.51 – 7.48 (m, 6H), 7.44 – 7.41 (m, 2H), 6.46 (s, 2H), 2.25 (s, 6H) ppm.

¹³C NMR (DMSO-*d*₆, 151 MHz) δ 133.55, 132.42, 130.89, 129.20, 128.86, 128.41, 127.72, 125.49, 111.39 (d, *J*_{C-Rh} = 5.5 Hz), 107.32 (d, *J*_{C-Rh} = 3.6 Hz), 103.61 (d, *J*_{C-Rh} = 4.7 Hz), 94.84 (d, *J*_{C-Rh} = 6.0 Hz), 77.87 (d, *J*_{C-Rh} = 7.1 Hz), 13.61 ppm.

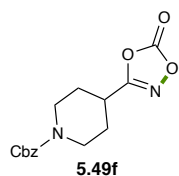
HRMS (+APCI) calculated for C₃₂H₂₆I₃Rh₂ [M-I]⁺ 996.72731, found 996.7258.

(*R,R*)-3 was prepared using the above procedure starting from **(*R*)-5.42**.

Dioxazolone substrates



Dioxazolones **5.49a**, **5.46**, **5.49c**, **5.49d**, **5.49h**, and **5.49e** were synthesised according to previously reported procedures.³

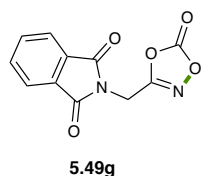


Prepared according General Procedure A using 1-((benzyloxy)carbonyl)piperidine-4-carboxylic acid. Purified by filtration through a plug of silica gel with DCM.

$^1\text{H NMR}$ (CDCl_3 , 500 MHz) δ 7.43 – 7.31 (m, 5H), 5.14 (s, 2H), 4.20 (s, 2H), 3.00 (s, 2H), 2.87 (tt, J = 11.1, 3.9 Hz, 1H), 2.06 – 1.97 (m, 2H), 1.83 – 1.66 (m, 2H) ppm.

$^{13}\text{C NMR}$ (CDCl_3 , 151 MHz) δ 167.92, 155.13, 153.96, 136.56, 128.69, 128.32, 128.13, 67.57, 42.83, 33.05, 27.20 ppm.

HRMS (+NSI) calculated for $\text{C}_{16}\text{H}_{20}\text{N}_2\text{NaO}_6$ $[\text{M}+\text{Na}+\text{MeOH}]^+$ 359.1219 and $\text{C}_{15}\text{H}_{16}\text{N}_2\text{NaO}_5$ $[\text{M}+\text{Na}]^+$ 327.0957, found 359.1214 and 327.0953.



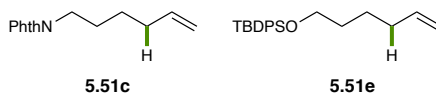
Reaction conducted by Christopher Poff. Prepared according to General Procedure A from *N*-phthaloylglycine. Purified by layered recrystallization from DCM and cold hexanes.

$^1\text{H NMR}$ (CDCl_3 , 600 MHz, Chloroform-*d*) δ 7.96 – 7.92 (m, 2H), 7.84 – 7.79 (m, 2H), 4.89 (s, 2H) ppm.

$^{13}\text{C NMR}$ (151 MHz, CDCl_3) δ 166.59, 161.47, 153.25, 135.02, 131.63, 124.28, 31.79 ppm.

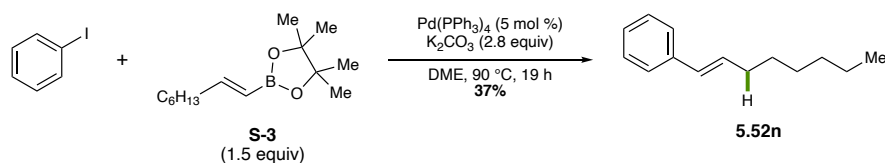
HRMS (+NSI) calculated for $\text{C}_{11}\text{H}_7\text{N}_2\text{O}_5$ $[\text{M} + \text{H}]^+$ calculated for 247.03495, found 247.0485.

Olefin substrates



Olefins **5.51c**⁴⁷ and **5.51e**⁴⁸ were synthesised according to previously reported procedures.

Octenyl styrene 5.52n



Reaction was conducted by Dr. Caitlin Farr. In a nitrogen-filled glovebox, $\text{Pd}(\text{PPh}_3)_4$ (0.142 g, 0.120 mmol) was added to an oven-dried 10-mL round bottom flask equipped with a magnetic

stir-bar and a septum. The round bottom flask was sealed and brought out of the glovebox. The flask was placed under N₂ atmosphere and DME (2.5 mL) was added. Boronic ester **S-3** (1.0 mL, 3.68 mmol), saturated aqueous K₂CO₃ (3 mL, 2M, 6.86 mmol), and iodobenzene (275 μL, 2.45 mmol) were added to the flask. The reaction was stirred at 90 °C under a balloon of nitrogen for 19 hours. The reaction was quenched with brine (5 mL). The layers were separated, and the aqueous layer was extracted with Et₂O (3 x 20 mL). The combined organic extracts were dried over anhydrous MgSO₄, filtered, and concentrated under reduced pressure. Purification by flash chromatography on silica gel (100% Hexanes) provided **5.52n** (0.1683 g, 37%) as a clear, colourless oil. ¹H NMR spectrum matches previously reported data.⁴⁹

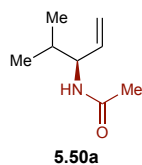
¹H NMR (CDCl₃, 600 MHz) δ 7.35 (d, *J* = 8.0 Hz, 2H), 7.30 (t, *J* = 7.4 Hz, 2H), 7.19 (td, *J* = 7.5, 1.2 Hz, 1H), 6.38 (dd, *J* = 15.8, 1.4 Hz, 1H), 6.24 (dtd, *J* = 15.4, 6.9, 1.1 Hz, 1H), 2.21 (tdd, *J* = 7.1, 5.8, 1.4 Hz, 2H), 1.47 (qnd, *J* = 8.0, 7.5, 1.2 Hz, 2H), 1.39 – 1.26 (m, 6H), 0.90 (td, *J* = 6.9, 1.4 Hz, 3H) ppm.

General Procedure D – enantioselective allylic C–H amidation

In a nitrogen-filled glovebox, LiOAc (0.0006 g, 0.010 mmol), AgNTf₂ (0.0078 g, 0.020 mmol), LiNTf₂ (0.0290 g, 0.10 mmol), and [Rh(2-Me-3-Ph-Ind)I₂]₂ (0.0056 g, 0.05 mmol, ((*R,R*) or (*S,S*), as indicated) were added to an oven-dried 4-mL vial equipped with a magnetic stir-bar and a Teflon-septum screw cap. The vial was capped and brought out of the glovebox. The olefin (0.10 mmol) was added as a stock solution in DCE (0.25 mL), followed by the dioxazolone (0.20 mmol) as a stock solution in DCE (0.25 mL). The reaction was stirred at room temperature (unless otherwise indicated) under a balloon of nitrogen for 48 hours. The reaction was filtered through a pipette containing celite with EtOAc (10 mL) and the filtrate was concentrated under reduced pressure. Purification by flash chromatography on silica gel provided the amide products.

Racemic amidation products were obtained by conducting the allylic C–H amidation under previously developed conditions.

Characterisation of enantioselective allylic C–H amidation products



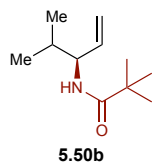
Reaction conducted by Christopher Poff. Prepared according to General Procedure D using 4-methylpentene (**5.48**) (0.0127 mL, 0.10 mmol, 1.0 equiv), 3-methyl-1,4,2-dioxazol-5-one (**5.49a**) (0.0202 g, 0.20 mmol, 2.0 equiv), LiOAc (0.0006 g, 0.010 mmol, 0.10 equiv), AgNTf₂ (0.0078 g, 0.020 mmol, 0.20 equiv), LiNTf₂ (0.0290 g, 0.10 mmol, 1.0 equiv), and (*S,S*)-[Rh(2-Me-3-Ph-Ind)I₂]₂ (0.0056 g, 0.005 mmol, 0.05 equiv) in DCE (0.5 mL) at room temperature for 48 hours. Purified by flash chromatography on silica gel (90–100% EtOAc in Hexanes) to provide **5.50a** (0.0098 g, 69%, >99:1 e.r.) as a yellow oil.

¹H NMR (CDCl₃, 600 MHz) δ 5.74 (ddd, *J* = 17.5, 10.2, 5.9 Hz, 1H), 5.41 (s, 1H), 5.17 – 5.11 (m, 2H), 4.34 (dtt, *J* = 9.1, 5.9, 1.6 Hz, 1H), 2.02 (s, 3H), 1.80 (qnd, *J* = 6.9, 5.7 Hz, 1H), 0.91 (d, *J* = 4.8 Hz, 3H), 0.90 (d, *J* = 4.9 Hz, 3H) ppm.

¹³C NMR (CDCl₃, 151 MHz) δ 169.43, 136.67, 115.62, 56.58, 32.01, 23.52, 18.64, 18.19 ppm.

HRMS (+APCI) calculated for C₈H₁₆NO [M+H]⁺ 142.12264, found 142.12267.

HPLC (AD-H column, 1% 2-propanol in Hexanes, 1 mL/min) *t*_M = 19.1 min, *t*_m = 22.8 min, >99:1 e.r.



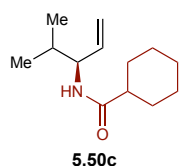
Reaction conducted by Christopher Poff. Prepared according to General Procedure D using 4-methylpentene (**5.48**) (0.0253 mL, 0.20 mmol, 1.0 equiv), 3-(*tert*-butyl)-1,4,2-dioxazol-5-one (**5.46**) (0.0573 g, 0.40 mmol, 2.0 equiv), LiOAc (0.0012 g, 0.020 mmol, 0.10 equiv), AgNTf₂ (0.0155 g, 0.040 mmol, 0.20 equiv), LiNTf₂ (0.0574 g, 0.20 mmol, 1.0 equiv), and (*S,S*)-[Rh(2-Me-3-Ph-Ind)I₂]₂ (0.0112 g, 0.01 mmol, 0.05 equiv) in DCE (0.5 mL) at room temperature for 48 hours. Purified by flash chromatography on silica gel (10–50% EtOAc in Hexanes) to provide **5.50b** (0.0285 g, 78% yield, 98:2 e.r.) as a white solid.

¹H NMR (CDCl₃, 600 MHz) δ 5.77 (ddd, *J* = 17.1, 10.6, 5.6 Hz, 1H), 5.54 (s, 1H), 5.13 – 5.07 (m, 2H), 4.38 – 4.32 (m, 1H), 1.82 (qnd, *J* = 6.9, 5.6 Hz, 1H), 1.22 (s, 9H), 0.90 (d, *J* = 6.8 Hz, 3H), 0.89 (d, *J* = 6.8 Hz, 3H) ppm.

$^{13}\text{C NMR}$ (CDCl_3 , 151 MHz) δ 177.66, 137.13, 115.15, 55.86, 38.92, 32.10, 27.71, 18.80, 17.98 ppm.

HRMS (+APCI) calculated for $\text{C}_{11}\text{H}_{22}\text{NO}$ $[\text{M}+\text{H}]^+$ 184.16926, found 184.16959.

HPLC (OJ-H column, 10% 2-propanol in Hexanes, 1 mL/min) $t_{\text{M}} = 5.6$ min, $t_{\text{m}} = 5.0$ min, 98:2 e.r.



Prepared according to General Procedure D using 4-methylpent-1-ene (**5.48**)

(0.0127 mL, 0.10 mmol, 1.0 equiv), 3-cyclohexyl-1,4,2-dioxazol-5-one (**5.49c**)

(0.0338 g, 0.20 mmol, 2.0 equiv), LiOAc (0.0006 g, 0.010 mmol, 0.10 equiv),

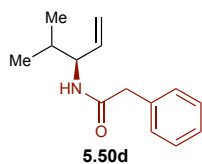
AgNTf₂ (0.0078 g, 0.020 mmol, 0.20 equiv), LiNTf₂ (0.0290 g, 0.10 mmol, 1.0 equiv), and (*S,S*)-[Rh(2-Me-3-Ph-Ind)₂]₂ (0.0056 g, 0.005 mmol, 0.05 equiv) in DCE (0.5 mL) at room temperature for 48 hours. Purified by flash chromatography on silica gel (10-30% EtOAc in Hexanes) to provide **5.50c** (0.0114 g, 55% yield, 94:6 e.r.) as a white solid.

$^1\text{H NMR}$ (CDCl_3 , 500 MHz) δ 5.75 (ddd, $J = 17.7, 10.0, 5.6$ Hz, 1H), 5.34 (d, $J = 9.2$ Hz, 1H), 5.14 – 5.08 (m, 2H), 4.36 (dtt, $J = 8.9, 5.6, 1.6$ Hz, 1H), 2.12 (tt, $J = 11.7, 3.5$ Hz, 1H), 1.88 (ddd, $J = 12.7, 3.6, 1.7$ Hz, 2H), 1.85 – 1.77 (m, 3H), 1.67 (dtd, $J = 9.5, 3.2, 1.6$ Hz, 1H), 1.46 (qd, $J = 12.1, 3.2$ Hz, 2H), 1.34 – 1.18 (m, 3H), 0.90 (d, $J = 8.3$ Hz, 3H), 0.88 (d, $J = 8.4$ Hz, 3H) ppm.

$^{13}\text{C NMR}$ (CDCl_3 , 126 MHz) δ 175.5, 137.2, 115.4, 55.9, 46.0, 32.2, 30.2, 30.0, 26.96, 25.93, 25.92, 18.9, 18.2 ppm.

HRMS (+APCI) calculated for $\text{C}_{13}\text{H}_{24}\text{NO}$ $[\text{M}+\text{H}]^+$ 210.1858, found 210.1848.

HPLC (AS-H column, 5% 2-propanol in Hexanes, 1 mL/min) $t_{\text{M}} = 13.8$ min, $t_{\text{m}} = 10.4$ min, 94:6 e.r.



Reaction conducted by Dr. Caitlin Farr. Prepared according to General

Procedure D using 4-methylpentene (**5.48**) (0.0127 mL, 0.10 mmol, 1.0 equiv),

3-benzyl-1,4,2-dioxazol-5-one (**5.49d**) (0.0354 g, 0.20 mmol, 2.0 equiv), LiOAc

(0.0006 g, 0.010 mmol, 0.10 equiv), AgNTf₂ (0.0078 g, 0.020 mmol, 0.20 equiv), LiNTf₂ (0.0290

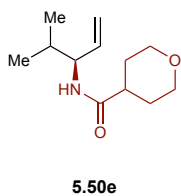
g, 0.10 mmol, 1.0 equiv) and (*S,S*)-[Rh(2-Me-3-Ph-Ind)₂I₂]₂ (0.0056 g, 0.005 mmol, 0.05 equiv) in DCE (0.5 mL) at room temperature for 48 hours. Purified by flash chromatography on silica gel (20-50% EtOAc in Hexanes) to provide **5.50d** (0.080 g, 37% yield, 99:1 e.r.) as a white solid.

¹H NMR (CDCl₃, 400 MHz) δ 7.41 – 7.35 (m, 2H), 7.34 – 7.27 (m, 3H), 5.66 (ddd, *J* = 17.2, 10.5, 5.5 Hz, 1H), 5.05 (dq, *J* = 10.5, 1.5 Hz, 1H), 4.95 (dq, *J* = 17.2, 1.5 Hz, 1H), 4.33 (dtd, *J* = 9.2, 5.5, 1.5 Hz, 1H), 1.70 (dt, *J* = 13.6, 6.8 Hz, 1H), 0.79 (d, *J* = 6.8 Hz, 3H), 0.73 (d, *J* = 6.9 Hz, 3H) ppm.

¹³C NMR (CDCl₃, 126 MHz) δ 170.41, 136.72, 135.20, 129.58, 129.24, 127.60, 115.39, 56.38, 44.25, 32.10, 18.74, 17.90 ppm.

HRMS (+APCI) calculated for C₁₄H₂₀NO [M+H]⁺ 218.15394, found 218.15361.

HPLC (AD-H column, 5% 2-propanol in Hexanes, 1 mL/min) *t*_M = 12.4 min, *t*_m = 10.1 min, 99:1 e.r.



Reaction conducted by Dr. Caitlin Farr. Prepared according to General Procedure

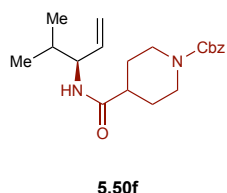
D using 4-methylpentene (**5.48**) (0.0127 mL, 0.10 mmol, 1.0 equiv), 3-(tetrahydro-2H-pyran-4-yl)-1,4,2-dioxazol-5-one (**5.49e**) (0.0342 g, 0.20 mmol, 2.0 equiv), LiOAc (0.0006 g, 0.010 mmol, 0.10 equiv), AgNTf₂ (0.0078 g, 0.020 mmol, 0.20 equiv), LiNTf₂ (0.0290 g, 0.10 mmol, 1.0 equiv) and (*S,S*)-[Rh(2-Me-3-Ph-Ind)₂I₂]₂ (0.0056 g, 0.005 mmol, 0.05 equiv) in DCE (0.5 mL) at room temperature for 48 hours. Purified by flash chromatography on silica gel (20-50% EtOAc in Hexanes) to provide **5.50e** (0.093 g, 44% yield, 98:2 e.r.) as a white solid.

¹H NMR (CDCl₃, 600 MHz) δ 5.76 (ddd, *J* = 17.1, 10.5, 5.8 Hz, 1H), 5.36 (d, *J* = 8.7 Hz, 1H), 5.16 – 5.10 (m, 2H), 4.37 (dtt, *J* = 9.0, 5.7, 1.6 Hz, 1H), 4.03 (ddd, *J* = 11.4, 4.0, 2.3 Hz, 2H), 3.43 (tt, *J* = 11.5, 2.4 Hz, 2H), 2.38 (tt, *J* = 11.3, 4.3 Hz, 1H), 1.90 – 1.73 (m, 5H), 0.91 (d, *J* = 6.8 Hz, 3H), 0.89 (d, *J* = 6.9 Hz, 3H) ppm.

¹³C NMR (CDCl₃, 151 MHz) δ 173.68, 136.91, 115.69, 67.44, 56.22, 42.72, 32.20, 29.53, 18.87, 18.22 ppm.

HRMS (+APCI) calculated for $C_{12}H_{22}NO_2$ $[M+H]^+$ 212.16451, found 212.16413 ppm.

HPLC (OD-H column, 5% 2-propanol in Hexanes, 1 mL/min) $t_M = 14.7$ min, $t_m = 10.4$ min, 98:2 e.r.



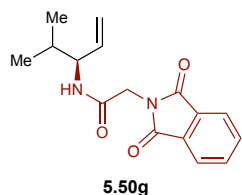
Prepared according to General Procedure D using 4-methylpent-1-ene (**5.48**) (0.0127 mL, 0.10 mmol, 1.0 equiv), benzyl 4-(5-oxo-1,4,2-dioxazol-3-yl)piperidine-1-carboxylate (**5.49f**) (0.0610 g, 0.20 mmol, 2.0 equiv), LiOAc (0.0006 g, 0.010 mmol, 0.10 equiv), AgNTf₂ (0.0078 g, 0.020 mmol, 0.20 equiv), LiNTf₂ (0.0290 g, 0.10 mmol, 1.0 equiv), and (*S,S*)-[Rh(2-Me-3-Ph-Ind)I₂]₂ (0.0056 g, 0.005 mmol, 0.05 equiv) in DCE (0.5 mL) at room temperature for 48 hours. Purified by flash chromatography on silica gel (30-50% EtOAc in Hexanes) to provide **5.50f** (0.0210 g, 61% yield, 99:1 e.r.) as a white solid.

¹H NMR (CDCl₃, 600MHz) δ 7.40 – 7.30 (m, 5H), 5.74 (ddd, $J = 16.8, 10.5, 5.8$ Hz, 1H), 5.41 (d, $J = 9.1$ Hz, 1H), 5.16 – 5.07 (m, 4H), 4.38 – 4.31 (m, 1H), 4.29 – 4.15 (m, 2H), 2.97 – 2.71 (m, 2H), 2.29 (ddt, $J = 11.6, 7.5, 3.7$ Hz, 1H), 1.88 – 1.78 (m, 2H) 1.80 (dq, $J = 13.6, 6.7$ Hz, 1H), 1.72 – 1.63 (s, 2H), 0.90 (d, $J = 6.7$ Hz, 3H), 0.88 (d, $J = 6.8$ Hz, 3H) ppm.

¹³C NMR (CDCl₃, 126 MHz) δ 173.63, 155.34, 136.85, 136.81, 128.63, 128.15, 128.02, 115.76, 67.31, 56.31, 43.61, 43.58, 32.18, 29.84, 28.98, 28.78, 18.86, 18.23 ppm.

HRMS (+APCI) calculated for $C_{20}H_{29}N_2O_3$ $[M+H]^+$ 345.2178, found 345.2165.

HPLC (AS-H column, 10% 2-propanol in hexanes, 1mL/min) $t_M = 20.1$ min, $t_m = 14.0$ min, 99:1 e.r.



Reaction conducted by Christopher Poff. Prepared according to General Procedure D using 4-methylpentene (**5.48**) (0.0127 mL, 0.10 mmol, 1.0 equiv), 2-((5-oxo-1,4,2-dioxazol-3-yl)methyl)isoindoline-1,3-dione (**5.49g**) (0.0492 g, 0.20 mmol, 2.0 equiv), LiOAc (0.0006 g, 0.010 mmol, 0.10 equiv), AgNTf₂ (0.0078 g, 0.020 mmol, 0.20 equiv), LiNTf₂ (0.0290 g, 0.10 mmol, 1.0 equiv), and (*S,S*)-

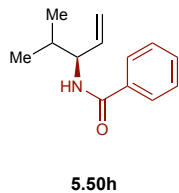
[Rh(2-Me-3-Ph-Ind)₂I₂]₂ (0.0056 g, 0.005 mmol, 0.05 equiv) in DCE (0.5 mL) at room temperature for 48 hours. Purified by flash chromatography on silica gel (20-50% EtOAc in Hexanes) to provide **5.50g** (0.0250 g, 87% yield, 97:3 e.r.) as a white solid.

¹H NMR (CDCl₃, 600 MHz) δ 7.89 (dd, *J* = 5.4, 3.1 Hz, 2H), 7.75 (dd, *J* = 5.5, 3.0 Hz, 2H), 5.74 (ddd, *J* = 17.2, 10.5, 5.9 Hz, 1H), 5.66 (d, *J* = 9.1 Hz, 1H), 5.20 – 5.13 (m, 2H), 4.37 (s, 2H), 4.35 (ddt, *J* = 9.0, 5.8, 1.6 Hz, 1H), 1.88 – 1.78 (m, 1H), 0.91 (d, *J* = 6.8 Hz, 3H), 0.90 (d, *J* = 6.9 Hz, 3H) ppm.

¹³C NMR (CDCl₃, 151 MHz, CDCl₃) δ 167.79, 165.45, 136.07, 134.28, 132.01, 123.68, 116.17, 57.04, 41.18, 32.03, 18.68, 18.08 ppm.

HRMS (+APCI) calculated for C₁₆H₁₉NO₃ [M+H]⁺ 287.13902, found 287.13889.

HPLC (OJ-H column, 10% 2-propanol in Hexanes, 1 mL/min) *t*_M = 20.2 min, *t*_m = 17.9 min, 97:3 e.r.



Reaction conducted by Dr. Caitlin Farr. Prepared according to General Procedure

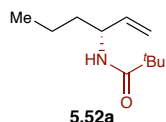
D using 4-methylpentene (**5.48**) (0.0127 mL, 0.10 mmol, 1.0 equiv), 3-phenyl-1,4,2-dioxazol-5-one (**5.49h**) (0.0326 g, 0.20 mmol, 2.0 equiv), LiOAc (0.0006 g, 0.010 mmol, 0.10 equiv), AgNTf₂ (0.0078 g, 0.020 mmol, 0.20 equiv), LiNTf₂ (0.0290 g, 0.10 mmol, 1.0 equiv) and (*S,S*)-[Rh(2-Me-3-Ph-Ind)₂I₂]₂ (0.0056 g, 0.005 mmol, 0.05 equiv) in DCE (0.5 mL) at room temperature for 48 hours. Purified by flash chromatography on silica gel (10-50% EtOAc in Hexanes) to provide **5.50h** (0.0026 g, 13% yield, 99:1 e.r.) as a white solid.

¹H NMR (CDCl₃, 600 MHz) δ 7.80 – 7.77 (m, 2H), 7.53 – 7.49 (m, 1H), 7.47 – 7.43 (m, 2H), 6.02 (d, *J* = 7.4 Hz, 1H), 5.85 (ddd, *J* = 17.1, 10.5, 5.8 Hz, 1H), 5.23 (dt, *J* = 17.2, 1.5 Hz, 1H), 5.19 (dt, *J* = 10.5, 1.4 Hz, 1H), 4.58 (dtt, *J* = 8.8, 5.7, 1.5 Hz, 1H), 1.94 (qnd, *J* = 6.9, 5.7 Hz, 1H), 0.99 (d, *J* = 3.9 Hz, 3H), 0.98 (d, *J* = 4.0 Hz, 3H) ppm.

¹³C NMR (CDCl₃, 151 MHz) δ 167.06, 136.81, 135.10, 131.58, 128.77, 126.97, 116.02, 57.02, 32.41, 18.95, 18.39 ppm.

HRMS (+APCI) calculated for $C_{13}H_{18}NO$ $[M+H]^+$ 204.13854, found 204.13854.

HPLC (AS-H column, 5% 2-propanol in Hexanes, 1 mL/min) $t_M = 21.5$ min, $t_m = 17.6$ min, 99:1 e.r.



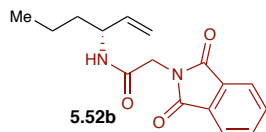
Reaction conducted by Christopher Poff. Prepared according to General Procedure D using hex-1-ene (**5.51a**) (0.0084 g, 0.10 mmol, 1.0 equiv), 3-(*tert*-butyl)-1,4,2-dioxazol-5-one (**5.46**) (0.0286 g, 0.20 mmol, 2.0 equiv), (*R,R*)-[Rh(2-Me-3-Ph-Ind) I_2] $_2$ (0.0056 g, 0.005 mmol, 0.05 equiv), LiOAc (0.0006 g, 0.010 mmol, 0.10 equiv), AgNTf $_2$ (0.0078 g, 0.020 mmol, 0.20 equiv), and LiNTf $_2$ (0.0290 g, 0.10 mmol, 1.0 equiv) in DCE (0.5 mL) at room temperature for 48 hours. Purified by flash chromatography on silica gel (10-30% EtOAc in Hexanes) to provide **5.52a** (0.0297 g, 90% yield, 98:2 e.r.) as a white solid.

1H NMR (CDCl $_3$, 500 MHz) δ 5.82 – 5.73 (m, 1H), 5.45 (s, 1H), 5.15 – 5.05 (m, 2H), 4.50 – 4.42 (m, 1H), 1.58 – 1.50 (m, 1H), 1.50 – 1.40 (m, 1H), 1.40 – 1.30 (m, 2H), 1.22 (s, 9H), 0.95 – 0.91 (m, 3H) ppm.

^{13}C NMR (CDCl $_3$, 126 MHz) δ 177.77, 139.00, 114.43, 50.78, 38.89, 37.24, 27.81, 19.14, 14.04 ppm.

HRMS (+APCI) calculated for $C_{11}H_{22}NO$ $[M+H]^+$ 184.16959, found 184.16954.

HPLC (WHELK column, 1% 2-propanol in Hexanes, 1 mL/min) $t_M = 18.4$ min, $t_m = 16.1$ min, 98:2 e.r.



Reaction conducted by Christopher Poff. Prepared according to General Procedure D using hex-1-ene (**5.51b**) (0.0084 g, 0.10 mmol, 1.0 equiv), 2-((5-oxo-1,4,2-dioxazol-3-yl)methyl)isoindoline-1,3-dione (**5.49g**) (0.0492 g, 0.20 mmol, 2.0 equiv), (*R,R*)-[Rh(2-Me-3-Ph-Ind) I_2] $_2$ (0.0056 g, 0.005 mmol, 0.05 equiv), LiOAc (0.0006 g, 0.010 mmol, 0.10 equiv), AgNTf $_2$ (0.0078 g, 0.020 mmol, 0.20 equiv), and LiNTf $_2$ (0.0290 g, 0.10 mmol, 1.0 equiv) in DCE (0.5 mL) at room temperature for 48 hours.

Purified by flash chromatography on silica gel (10-30% EtOAc in Hexanes) to provide **5.52b** (0.0297 g, 90% yield, 93:7 e.r.) as a white solid.

$^1\text{H NMR}$ (CDCl_3 , 600 MHz) δ 7.92 – 7.85 (m, 2H), 7.78 – 7.71 (m, 2H), 5.75 (ddd, $J = 17.2, 10.4, 5.7$ Hz, 1H), 5.59 (d, $J = 8.3$ Hz, 1H), 5.21 – 5.07 (m, 2H), 4.47 (dq, $J = 7.3, 5.9, 1.6$ Hz, 1H), 4.35 (s, 2H), 1.56 – 1.45 (m, 2H), 1.40 – 1.30 (m, 2H), 0.92 (t, $J = 7.3$ Hz, 3H) ppm.

$^{13}\text{C NMR}$ (CDCl_3 , 151 MHz) δ 167.93, 165.44, 137.96, 134.40, 134.34, 132.21, 132.18, 123.81, 115.43, 51.78, 41.18, 41.12, 37.03, 19.06, 13.95 ppm.

HRMS (+APCI) calculated for $\text{C}_{16}\text{H}_{19}\text{N}_2\text{O}_3$ $[\text{M}+\text{H}]^+$ 287.13902, found 287.13888.

HPLC (AD-H column, 5% 2-propanol in Hexanes, 1 mL/min) $t_{\text{M}} = 29.1$ min, $t_{\text{m}} = 31.6$ min, 93:7 e.r.



Prepared according to General Procedure D using 2-(hex-5-en-1-yl)isoindoline-1,3-dione (**5.51c**) (0.0230 g, 0.10 mmol, 1.0 equiv), 3-(*tert*-butyl)-1,4,2-dioxazol-5-one (**5.46**) (0.0286 g, 0.20 mmol, 2.0 equiv),

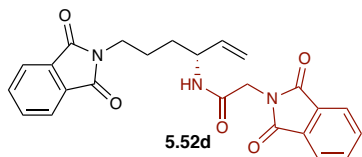
(*R,R*)-[Rh(2-Me-3-Ph-Ind) I_2] $_2$ (0.0056 g, 0.005 mmol, 0.05 equiv), LiOAc (0.0006 g, 0.010 mmol, 0.10 equiv), AgNTf $_2$ (0.0078 g, 0.020 mmol, 0.20 equiv), and LiNTf $_2$ (0.0290 g, 0.10 mmol, 1.0 equiv) in DCE (0.5 mL) at room temperature for 48 hours. Purified by flash chromatography on silica gel (10-30% EtOAc in Hexanes) to provide **5.52c** (0.0297 g, 90% yield, 98:2 e.r.) as a white solid.

$^1\text{H NMR}$ (CDCl_3 , 600 MHz) δ 7.83 (dd, $J = 5.4, 3.0$ Hz, 2H), 7.71 (dd, $J = 5.5, 2.9$ Hz, 2H), 5.74 (ddd, $J = 17.3, 10.4, 5.5$ Hz, 1H), 5.58 (d, $J = 8.6$ Hz, 1H), 5.16 – 5.05 (m, 2H), 4.55 – 4.46 (m, 1H), 3.70 (t, $J = 7.0$ Hz, 2H), 1.75 – 1.66 (m, 2H), 1.67 – 1.58 (m, 1H), 1.56 – 1.47 (m, 1H), 1.20 (s, 9H) ppm.

$^{13}\text{C NMR}$ (CDCl_3 , 126 MHz) δ 178.00, 168.55, 138.40, 134.09, 132.24, 123.37, 115.08, 50.68, 38.90, 37.84, 32.06, 27.75, 25.21 ppm.

HRMS (+APCI) calculated for $\text{C}_{19}\text{H}_{25}\text{N}_2\text{O}_3$ $[\text{M}+\text{H}]^+$ 329.1865, found 329.1859.

HPLC (AS-H column, 1% 2-propanol in Hexanes, 1 mL/min) $t_M = 13.1$ min, $t_m = 18.3$ min, 98:2 e.r.



Prepared according to General Procedure D using 2-(hex-5-en-1-yl)isoindoline-1,3-dione (**5.51d**) (0.0230 g, 0.10 mmol, 1.0 equiv), 2-((5-oxo-1,4,2-dioxazol-3-yl)methyl)isoindoline-1,3-dione

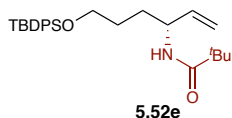
(**5.49g**) (0.0492 g, 0.20 mmol, 2.0 equiv), (*R,R*)-[Rh(2-Me-3-Ph-Ind) I_2] $_2$ (0.0056 g, 0.005 mmol, 0.05 equiv), LiOAc (0.0006 g, 0.010 mmol, 0.10 equiv), AgNTf $_2$ (0.0078 g, 0.020 mmol, 0.20 equiv), and LiNTf $_2$ (0.0290 g, 0.10 mmol, 1.0 equiv) in DCE (0.5 mL) at room temperature for 48 hours. Purified by flash chromatography on silica gel (50-66% EtOAc in Hexanes) to provide **5.52d** (0.0313 g, 73% yield, 92:8 e.r.) as a white solid.

$^1\text{H NMR}$ (CDCl $_3$, 600 MHz) δ 7.85 (dd, $J = 5.5, 3.1$ Hz, 2H), 7.78 (dd, $J = 5.4, 3.1$ Hz, 2H), 7.71 (dd, $J = 5.5, 3.0$ Hz, 2H), 7.70 (dd, $J = 5.5, 3.0$ Hz, 2H), 6.17 (d, $J = 8.5$ Hz, 1H), 5.72 (ddd, $J = 17.2, 10.4, 5.6$ Hz, 1H), 5.25 – 5.05 (m, 2H), 4.56 – 4.48 (m, 1H), 4.38 (s, 2H), 3.71 (t, $J = 7.0$ Hz, 2H), 1.75 (qn, $J = 7.3$ Hz, 2H), 1.67 – 1.58 (m, 1H), 1.57 – 1.48 (m, 1H) ppm.

$^{13}\text{C NMR}$ (CDCl $_3$, 151 MHz) δ 168.69, 167.99, 165.80, 137.53, 134.30, 134.13, 132.21, 132.14, 123.73, 123.40, 115.76, 51.93, 41.15, 37.71, 31.40, 25.46 ppm.

HRMS (+APCI) calculated for C $_{24}$ H $_{22}$ N $_3$ O $_5$ [M+H] $^+$ 432.1559, found 432.1552.

HPLC (AD-H column, 15% 2-propanol in Hexanes, 1.5 mL/min) $t_M = 25.2$ min, $t_m = 28.7$ min, 92:8 e.r.



Prepared according to General Procedure D using *tert*-butyl(hex-5-en-1-yl)oxydiphenylsilane (**5.51e**) (0.0339 g, 0.10 mmol, 1.0 equiv), 3-(*tert*-

butyl)-1,4,2-dioxazol-5-one (**5.46**) (0.0286 g, 0.20 mmol, 2.0 equiv), (*R,R*)-[Rh(2-Me-3-Ph-Ind) I_2] $_2$ (0.0056 g, 0.005 mmol, 0.05 equiv) LiOAc (0.0006 g, 0.010 mmol, 0.10 equiv), AgNTf $_2$ (0.0078 g, 0.020 mmol, 0.20 equiv), and LiNTf $_2$ (0.0290 g, 0.10 mmol, 1.0 equiv) in DCE (0.5

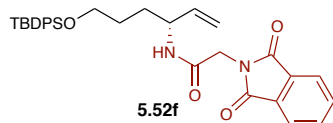
mL) at room temperature for 48 hours. Purified by flash chromatography on silica gel (10-30% EtOAc in Hexanes) to provide **5.52e** (0.0215 g, 49% yield, 90:10 e.r.) as a white solid.

¹H NMR (CDCl₃, 600 MHz) δ 7.65 (dt, *J* = 6.6, 1.5 Hz, 4H), 7.45 – 7.34 (m, 6H), 5.76 (ddd, *J* = 17.2, 10.4, 5.3 Hz, 1H), 5.46 (d, *J* = 7.8 Hz, 1H), 5.16 – 5.06 (m, 2H), 4.50 – 4.41 (m, 1H), 3.73 – 3.62 (m, 2H), 1.74 – 1.64 (m, 2H), 1.61 – 1.48 (m, 2H), 1.20 (s, 9H), 1.05 (s, 9H) ppm.

¹³C NMR (CDCl₃, 151 MHz) δ 177.66, 138.70, 135.55, 133.95, 133.91, 129.60, 127.64, 114.47, 63.51, 50.66, 38.74, 31.22, 28.89, 27.65, 26.89, 19.23 ppm.

HRMS (+APCI) calculated for C₂₇H₄₀NO₂Si [M+H]⁺ 438.2828, found 438.2820.

HPLC (AS-H column, 1% 2-propanol in Hexanes, 1 mL/min) *t*_M = 5.2 min, *t*_m = 4.5 min, 90:10 e.r.



Prepared according to General Procedure D using *tert*-butyl(hex-5-

en-1-yloxy)diphenylsilane (**5.51f**) (0.0339 g, 0.10 mmol, 1.0 equiv),

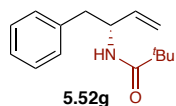
2-((5-oxo-1,4,2-dioxazol-3-yl)methyl)isindoline-1,3-dione (**5.49g**) (0.0492 g, 0.20 mmol, 2.0 equiv), (*R,R*)-[Rh(2-Me-3-Ph-Ind)I₂]₂ (0.0056 g, 0.005 mmol, 0.05 equiv), LiOAc (0.0006 g, 0.010 mmol, 0.10 equiv), AgNTf₂ (0.0078 g, 0.020 mmol, 0.20 equiv), and LiNTf₂ (0.0290 g, 0.10 mmol, 1.0 equiv) in DCE (0.5 mL) at 60 °C for 48 hours. Purified by flash chromatography on silica gel (10-50% EtOAc in Hexanes) to provide **5.52f** (0.0184 g, 34% yield, 97:3 e.r.) as an off-white solid.

¹H NMR (CDCl₃, 600 MHz) δ 7.87 (dd, *J* = 5.5, 3.0 Hz, 2H), 7.73 (dd, *J* = 5.5, 3.0 Hz, 2H), 7.68 – 7.63 (m, 4H), 7.47 – 7.35 (m, 6H), 5.74 (ddd, *J* = 17.2, 10.4, 5.6 Hz, 1H), 5.67 (d, *J* = 8.2 Hz, 1H), 5.20 – 5.10 (m, 2H), 4.49 – 4.41 (m, 1H), 4.29 (d, *J* = 2.1 Hz, 1H), 4.29 (d, *J* = 2.1 Hz, 1H), 3.68 (qd, *J* = 6.0, 3.0 Hz, 2H), 1.75 – 1.66 (m, 2H), 1.63 – 1.57 (m, 2H), 1.04 (s, 9H) ppm.

¹³C NMR (CDCl₃, 151 MHz) δ 167.89, 165.47, 137.83, 135.70, 134.36, 134.03, 132.19, 129.77, 127.82, 123.78, 115.57, 63.57, 51.85, 41.11, 31.15, 28.78, 27.05, 19.38 ppm.

HRMS (+APCI) calculated for C₃₂H₃₇N₂O₄Si [M+H]⁺ 541.2523, found 541.2509.

HPLC (AS-H column, 5% 2-propanol in Hexanes, 1 mL/min) $t_M = 56.2$ min, $t_m = 41.2$ min, 97:3 e.r.



Reaction conducted by Christopher Poff. Prepared according to General Procedure D using 4-phenylbutene (**5.51g**) (0.0127 mL, 0.10 mmol, 1.0 equiv), 3-

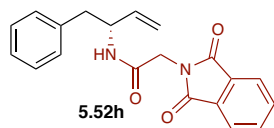
(*tert*-butyl)-1,4,2-dioxazol-5-one (**5.46**) (0.0338 g, 0.20 mmol, 2.0 equiv), (*R,R*)-[Rh(2-Me-3-Ph-Ind)₂]₂ (0.0056 g, 0.005 mmol, 0.05 equiv), LiOAc (0.0006 g, 0.010 mmol, 0.10 equiv), AgNTf₂ (0.0078 g, 0.020 mmol, 0.20 equiv), and LiNTf₂ (0.0290 g, 0.10 mmol, 1.0 equiv) in DCE (0.5 mL) at room temperature for 48 hours. Purified by flash chromatography on silica gel (10-25% EtOAc in Hexanes) to provide **5.52g** (0.0132 g, 57% yield, 98:2 e.r.) as a white solid.

¹H NMR (CDCl₃, 600 MHz) δ 7.30 – 7.27 (m, 2H), 7.24 – 7.20 (m, 1H), 7.19 – 7.15 (m, 2H), 5.85 (ddd, *J* = 17.2, 10.5, 5.2 Hz, 1H), 5.46 (d, *J* = 8.2 Hz, 1H), 5.12 – 5.05 (m, 2H), 4.78 (dtdt, *J* = 8.4, 6.8, 5.2, 1.7 Hz, 1H), 2.92 (dd, *J* = 13.7, 6.6 Hz, 1H), 2.83 (dd, *J* = 13.7, 6.8 Hz, 1H), 1.12 (s, 9H) ppm.

¹³C NMR (CDCl₃, 151 MHz) δ 177.71, 138.05, 137.35, 129.65, 128.50, 126.77, 114.91, 51.55, 41.03, 38.86, 27.65 ppm.

HRMS (+APCI) calculated for C₁₅H₂₂NO [M+H]⁺ 232.16959, found 232.16947.

HPLC (OD-H column, 5% 2-propanol in Hexanes, 1 mL/min) $t_M = 8.4$ min, $t_m = 7.6$ min, 98:2 e.r.



Reaction conducted by Dr. Caitlin Farr. Prepared according to General

Procedure D using 4-phenyl-1-butene (**5.51h**) (0.015 mL, 0.10 mmol, 1.0 equiv), 2-((5-oxo-1,4,2-dioxazol-3-yl)methyl)isoinidole-1,3-dione (**5.49g**) (0.0492 g, 0.20 mmol, 2.0 equiv), (*R,R*)-[Rh(2-Me-3-Ph-Ind)₂]₂ (0.0056 g, 0.005 mmol, 0.05 equiv), LiOAc (0.0006 g, 0.010 mmol, 0.10 equiv), AgNTf₂ (0.0078 g, 0.020 mmol, 0.20 equiv), and LiNTf₂ (0.0290 g, 0.10 mmol, 1.0 equiv) in DCE (0.5 mL) at 40 °C for 48 hours. Purified by flash

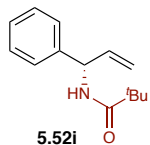
chromatography on silica gel (30-50% EtOAc in Hexanes) to provide **5.52h** (0.0151 g, 45% yield, 95:5 e.r.) as a white solid.

$^1\text{H NMR}$ (CDCl_3 , 600 MHz) δ 7.87 (dd, $J = 5.4, 3.0$ Hz, 2H), 7.75 (dd, $J = 5.4, 3.0$ Hz, 2H), 7.21 – 7.15 (m, 2H), 7.16 – 7.10 (m, 3H), 5.80 (ddd, $J = 17.3, 10.4, 5.4$ Hz, 1H), 5.71 (d, $J = 8.4$ Hz, 1H), 5.15 – 5.09 (m, 2H), 4.80 – 4.72 (m, 1H), 4.29 (s, 2H), 2.88 (dd, $J = 6.5, 1.7$ Hz, 2H) ppm.

$^{13}\text{C NMR}$ (CDCl_3 , 151 MHz) δ 167.79, 165.50, 136.90, 136.79, 134.40, 132.09, 129.62, 128.49, 126.77, 123.79, 115.87, 52.42, 41.17, 40.76 ppm.

HRMS (+APCI) calculated for $\text{C}_{20}\text{H}_{19}\text{N}_2\text{O}_3$ $[\text{M}+\text{H}]^+$ 335.13902, found 335.13887.

HPLC (AD-H column, 10% 2-propanol in Hexanes, 1 mL/min) $t_{\text{M}} = 18.4$ min, $t_{\text{m}} = 21.7$ min, 95:5 e.r.



Reaction conducted by Christopher Poff. Prepared according to General Procedure

D using allyl benzene (**5.6**) (0.0132 mL, 0.10 mmol, 1.0 equiv), 3-(*tert*-butyl)-1,4,2-dioxazol-5-one (**5.46**) (0.0286 g, 0.20 mmol, 2.0 equiv), LiOAc (0.0006 g, 0.010

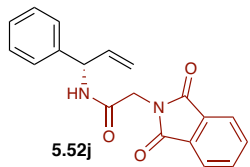
mmol, 0.10 equiv), AgNTf₂ (0.0078 g, 0.020 mmol, 0.20 equiv), LiNTf₂ (0.0290 g, 0.10 mmol, 1.0 equiv), and (*R,R*)-[Rh(2-Me-3-Ph-Ind)₂]₂ (0.0056 g, 0.200 mmol, 0.005 equiv) in DCE (0.5 mL) at room temperature for 48 hours. Purified by flash chromatography on silica gel (10-30% EtOAc in Hexanes) to provide **5.52i** (0.0150 g, 69% yield, 93:7 e.r.) as a colourless solid.

$^1\text{H NMR}$ (CDCl_3 , 600 MHz) δ 7.37 – 7.33 (m, 2H), 7.30 – 7.27 (m, 3H), 6.02 (ddd, $J = 17.1, 10.4, 5.3$ Hz, 1H), 5.85 (s, 1H), 5.62 (dd, $J = 7.9, 5.5$ Hz, 1H), 5.29 – 5.13 (m, 2H), 1.23 (s, 9H) ppm.

$^{13}\text{C NMR}$ (CDCl_3 , 151 MHz) δ 173.37, 140.84, 137.50, 128.78, 127.61, 127.11, 115.68, 54.78, 38.79, 27.61 ppm.

HRMS (+APCI) calculated for $\text{C}_{14}\text{H}_{20}\text{NO}$ $[\text{M}+\text{H}]^+$ 218.15339, found 218.15394.

HPLC (OJ-H column, 10% 2-propanol in Hexanes, 1 mL/min) $t_{\text{M}} = 9.1$ min, $t_{\text{m}} = 8.1$ min, 93:7 e.r.

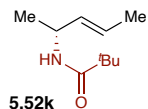


Prepared according to General Procedure D using allyl benzene (**5.6**) (0.0132 mL, 0.10 mmol, 1.0 equiv), 2-((5-oxo-1,4,2-dioxazol-3-yl)methyl)isoindoline-1,3-dione (**5.49g**) (0.0492 g, 0.20 mmol, 2.0 equiv), (*R,R*)-[Rh(2-Me-3-Ph-Ind)₂]₂ (0.0056 g, 0.005 mmol, 0.05 equiv), LiOAc (0.0006 g, 0.010 mmol, 0.10 equiv), AgNTf₂ (0.0078 g, 0.020 mmol, 0.20 equiv), and LiNTf₂ (0.0290 g, 0.10 mmol, 1.0 equiv) in DCE (0.5 mL) at 60 °C for 48 hours. Purified by flash chromatography on silica gel (10-50% EtOAc in Hexanes) to provide **5.52j** (0.0105 g, 33% yield, 93:7 e.r.) as a white solid.

¹H NMR (CDCl₃, 600 MHz) δ 7.88 (dd, *J* = 5.4, 3.0 Hz, 2H), 7.74 (dd, *J* = 5.5, 3.0 Hz, 2H), 7.38 – 7.33 (m, 2H), 7.31 – 7.27 (m, 3H), 6.04 (d, *J* = 8.2 Hz, 1H), 6.00 (ddd, *J* = 17.1, 10.4, 5.3 Hz, 1H), 5.66 – 5.59 (m, 1H), 5.30 – 5.23 (m, 2H), 4.40 (d, *J* = 16.0 Hz, 1H), 4.36 (d, *J* = 16.0 Hz, 1H) ppm.
¹³C NMR (CDCl₃, 151 MHz) δ 167.78, 165.15, 139.89, 136.54, 134.28, 132.01, 128.87, 127.90, 127.27, 123.68, 116.44, 55.59, 40.99 ppm.

HRMS (+APCI) calculated for C₁₉H₁₇N₂O₃ [M+H]⁺ 321.1239, found 321.1229.

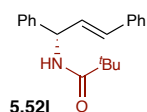
HPLC (OD-H column, 3% 2-propanol in Hexanes, 1 mL/min) *t*_M = 22.5 min, *t*_m = 19.0 min, 93:7 e.r.



Reaction conducted by Christopher Poff. Prepared according to General Procedure D using 2-pentene (**5.51k**) (0.0070 g, 0.10 mmol, 1.0 equiv), 3-(*tert*-butyl)-1,4,2-dioxazol-5-one (**5.46**) (0.0286 g, 0.20 mmol, 2.0 equiv), (*S,S*)-[Rh(2-Me-3-Ph-Ind)₂]₂ (0.0056 g, 0.005 mmol, 0.05 equiv), LiOAc (0.0006 g, 0.010 mmol, 0.10 equiv), AgNTf₂ (0.0078 g, 0.020 mmol, 0.20 equiv), and LiNTf₂ (0.0290 g, 0.10 mmol, 1.0 equiv) in DCE (0.5 mL) at 40 °C for 48 hours. Purified by flash chromatography on silica gel (5-25% EtOAc in Hexanes) to provide **5.52k** (0.0034 g, 21% yield determined by NMR integration, 91:9 d.r.) as an inseparable mixture of three regioisomers (0.0040 g overall, 24% total yield).

¹H NMR (CDCl₃, 500 MHz) δ 5.77 (ddd, *J* = 17.2, 10.4, 5.4 Hz, oH), 5.57 (dq, *J* = 15.4, 6.4, 1.5 Hz, 1H), 5.50 – 5.39 (m, 2H), 5.43 (ddq, *J* = 15.4, 5.5, 1.6 Hz, 1H), 5.25 (ddq, *J* = 10.5, 8.6, 1.8 Hz, oH), 4.77 (dt, *J* = 14.8, 7.4 Hz, oH), 4.48 (ddd, *J* = 8.1, 6.8, 5.5, 1.4 Hz, 1H), 4.39 (t, *J* = 6.9 Hz, oH), 3.80 (ddd, *J* = 6.4, 4.9, 1.3 Hz, oH), 2.07 – 1.99 (m, oH), 1.67 (dt, *J* = 6.4, 1.5 Hz, 3H), 1.65 – 1.58 (m, oH), 1.31 (s, oH), 1.23 (s, oH), 1.22 (s, oH), 1.20 (s, oH), 1.20 – 1.17 (m, 12H) ppm. ¹³C NMR (CDCl₃, 151 MHz) δ 177.50, 132.84, 132.41, 129.64, 126.64, 125.39, 114.65, 46.12, 42.54, 38.74, 32.08, 29.51, 27.75, 22.84, 21.68, 20.89, 17.87, 14.27, 13.38, 10.21 ppm.

HPLC (OJ-H column, 1% 2-propanol in Hexanes, 1 mL/min) *t*_M = 9.7 min, *t*_m = 11.0 min, 91:9 e.r. (e.r. determined by comparison to enantiopure D- and L-Piv-Ala-OMe after oxidative cleavage of olefin product to the carboxylic acid and subsequent methyl protection).



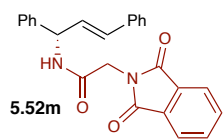
Reaction conducted by Dr. Caitlin Farr. Prepared according to General Procedure D using (*E*)-prop-1-ene-1,3-diyldibenzene (**5.511**) (0.0194 g, 0.10 mmol, 1.0 equiv), 3-(*tert*-butyl)-1,4,2-dioxazol-5-one (**5.46**) (0.0286 g, 0.20 mmol, 2.0 equiv), (*R,R*)-[Rh(2-Me-3-Ph-Ind)I₂]₂ (0.0056 g, 0.005 mmol, 0.05 equiv), LiOAc (0.0006 g, 0.010 mmol, 0.10 equiv), AgNTf₂ (0.0078 g, 0.020 mmol, 0.20 equiv), and LiNTf₂ (0.0290 g, 0.10 mmol, 1.0 equiv) in DCE (0.5 mL) at 40 °C for 48 hours. Purified by flash chromatography on silica gel (5-30% EtOAc in Hexanes) to provide **5.521** (0.0065 g, 22% yield, 98:2 e.r.) as a white solid.

¹H NMR (CDCl₃, 600 MHz) δ 7.37 (t, *J* = 7.2 Hz, 4H), 7.34 – 7.28 (m, 5H), 7.26 – 7.22 (m, 1H), 6.51 (dd, *J* = 16.0, 1.5 Hz, 1H), 6.35 (dd, *J* = 15.9, 6.1 Hz, 1H), 5.98 (d, *J* = 8.0 Hz, 1H), 5.80 (ddd, *J* = 8.0, 6.2, 1.3 Hz, 1H), 1.25 (s, 9H) ppm.

¹³C NMR (CDCl₃, 151 MHz) δ 177.49, 141.27, 136.62, 131.62, 129.23, 128.96, 128.71, 127.94, 127.75, 127.15, 126.69, 54.63, 38.98, 27.78 ppm.

HRMS (+APCI) calculated for C₂₀H₂₄NO [M+H]⁺ 294.18524, found 294.185123.

HPLC (AD-H column, 5% 2-propanol in Hexanes, 1 mL/min) *t*_M = 16.2 min, *t*_m = 13.8 min, 98:2 e.r.



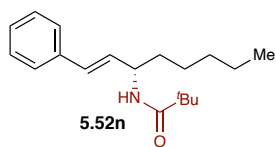
Reaction conducted by Dr. Caitlin Farr. Prepared according to General Procedure D using (*E*)-prop-1-ene-1,3-diylidibenzene (**5.51m**) (0.0194 mg, 0.10 mmol, 1.0 equiv), 2-((5-oxo-1,4,2-dioxazol-3-yl)methyl)isoindoline-1,3-dione (**5.49g**) (0.0492 g, 0.20 mmol, 2.0 equiv), (*R,R*)-[Rh(2-Me-3-Ph-Ind)₂I₂] (0.0056 g, 0.005 mmol, 0.05 equiv), LiOAc (0.0006 g, 0.010 mmol, 0.10 equiv), AgNTf₂ (0.0078 g, 0.020 mmol, 0.20 equiv), and LiNTf₂ (0.0290 g, 0.10 mmol, 1.0 equiv) in DCE (0.5 mL) at 60 °C for 48 hours. Purified by flash chromatography on silica gel (20-50% EtOAc in Hexanes) to provide **5.52m** (0.0175 g, 44% yield, 79:21 e.r.) as a white solid.

¹H NMR (CDCl₃, 600 MHz) δ 7.87 (dd, *J* = 5.4, 3.0 Hz, 2H), 7.73 (dd, *J* = 5.4, 3.0 Hz, 2H), 7.38 – 7.32 (m, 6H), 7.30 (t, *J* = 7.5 Hz, 3H), 7.23 (t, *J* = 7.3 Hz, 1H), 6.56 (dd, *J* = 15.9, 1.5 Hz, 1H), 6.32 (dd, *J* = 15.9, 6.0 Hz, 1H), 6.22 (d, *J* = 8.1 Hz, 1H), 5.80 (ddd, *J* = 7.8, 6.0, 1.5 Hz, 1H), 4.40 (s, 2H) ppm.

¹³C NMR (CDCl₃, 151 MHz) δ 167.92, 165.32, 140.35, 136.44, 134.39, 132.14, 132.05, 129.04, 128.70, 128.22, 128.00, 127.33, 126.76, 123.81, 55.42, 41.17 ppm.

HRMS (+APCI) calculated for C₂₅H₂₁N₂O₃ [M+H]⁺ 397.15467, found 397.15448.

HPLC (AD-H column, 8% 2-propanol in Hexanes, 1.5 mL/min) *t*_M = 40.0 min, *t*_m = 45.0 min, 79:21 e.r.



Reaction conducted by Dr. Caitlin Farr. Prepared according to General Procedure D using (*E*)-oct-1-en-1-ylbenzene (**5.51n**) (0.0188 g, 0.10 mmol, 1 equiv), 3-(*tert*-butyl)-1,4,2-dioxazol-5-one (**5.46**) (0.0286 g, 0.20 mmol, 2 equiv), (*R,R*)-[Rh(2-Me-3-Ph-Ind)₂I₂] (0.0056 g, 0.005 mmol, 0.05 equiv), LiOAc (0.0006 g, 0.010 mmol, 0.10 equiv), AgNTf₂ (0.0078 g, 0.020 mmol, 0.20 equiv), and LiNTf₂ (0.0290 g, 0.10 mmol, 1 equiv) in DCE (0.5 mL) at 40 °C for 48 hours. Purified by flash

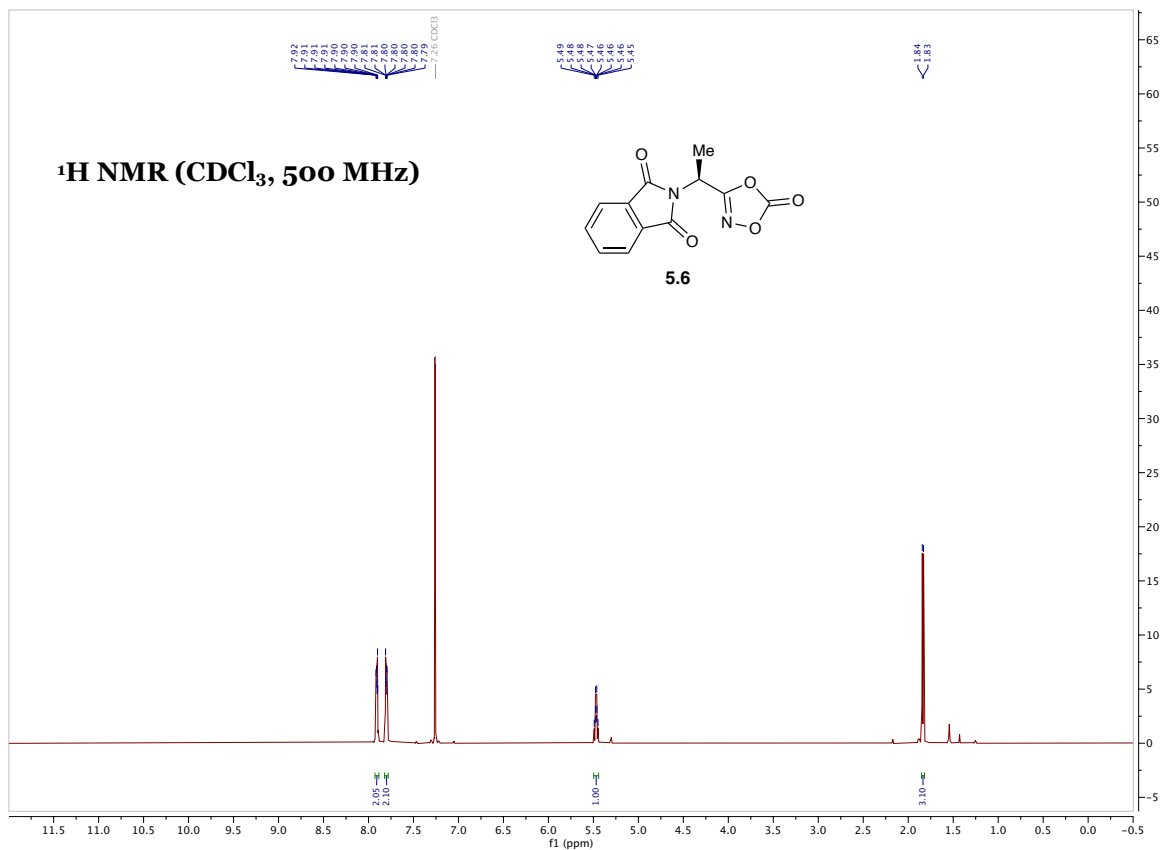
123.76, 55.28, 51.78, 41.22, 41.11, 35.24, 32.35, 31.67, 31.53, 28.84, 25.59, 22.64, 22.61, 14.18, 14.13 ppm.

HRMS (+APCI) calculated for $C_{24}H_{27}N_2O_3$ $[M+H]^+$ 391.20162, found 391.20136.

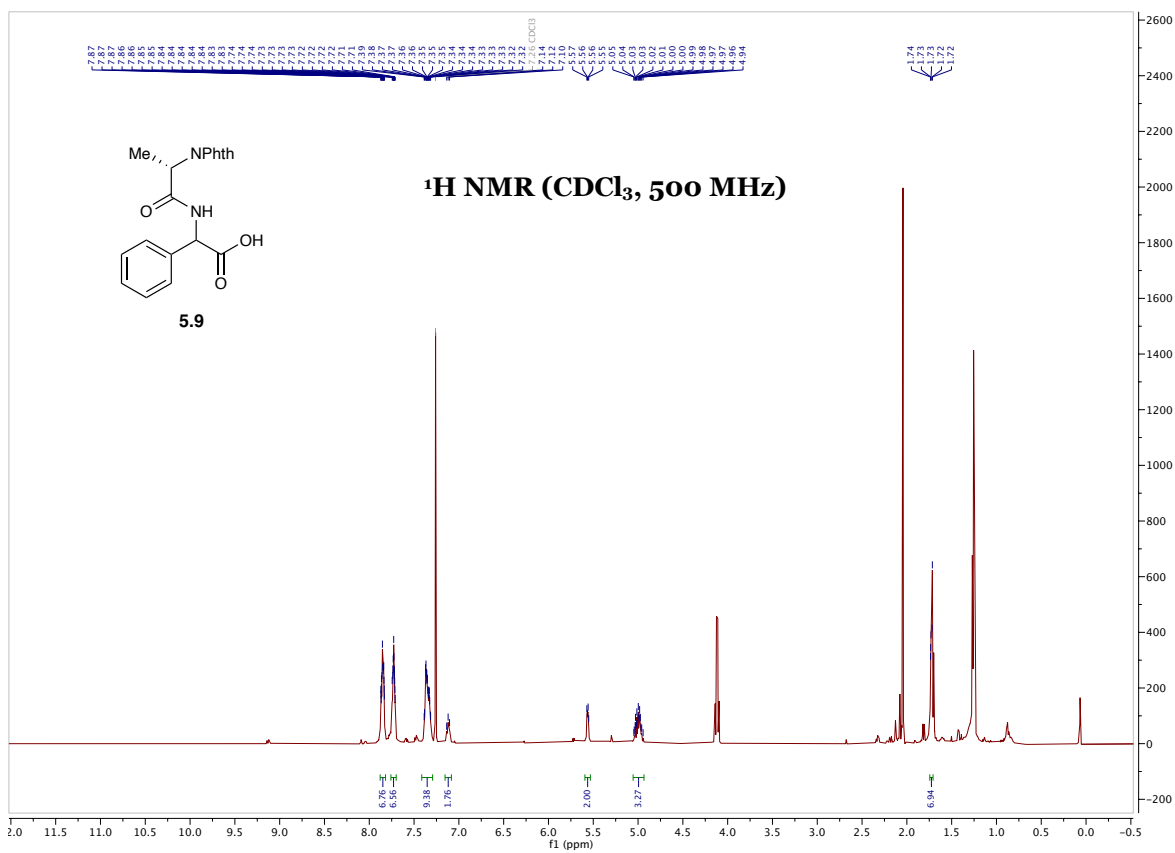
HPLC (AS-H column, 10% 2-propanol in Hexanes, 1 mL/min) $t_M = 28.0$ min, $t_m = 36.0$ min, 98:2 e.r.

5.6 Spectral data

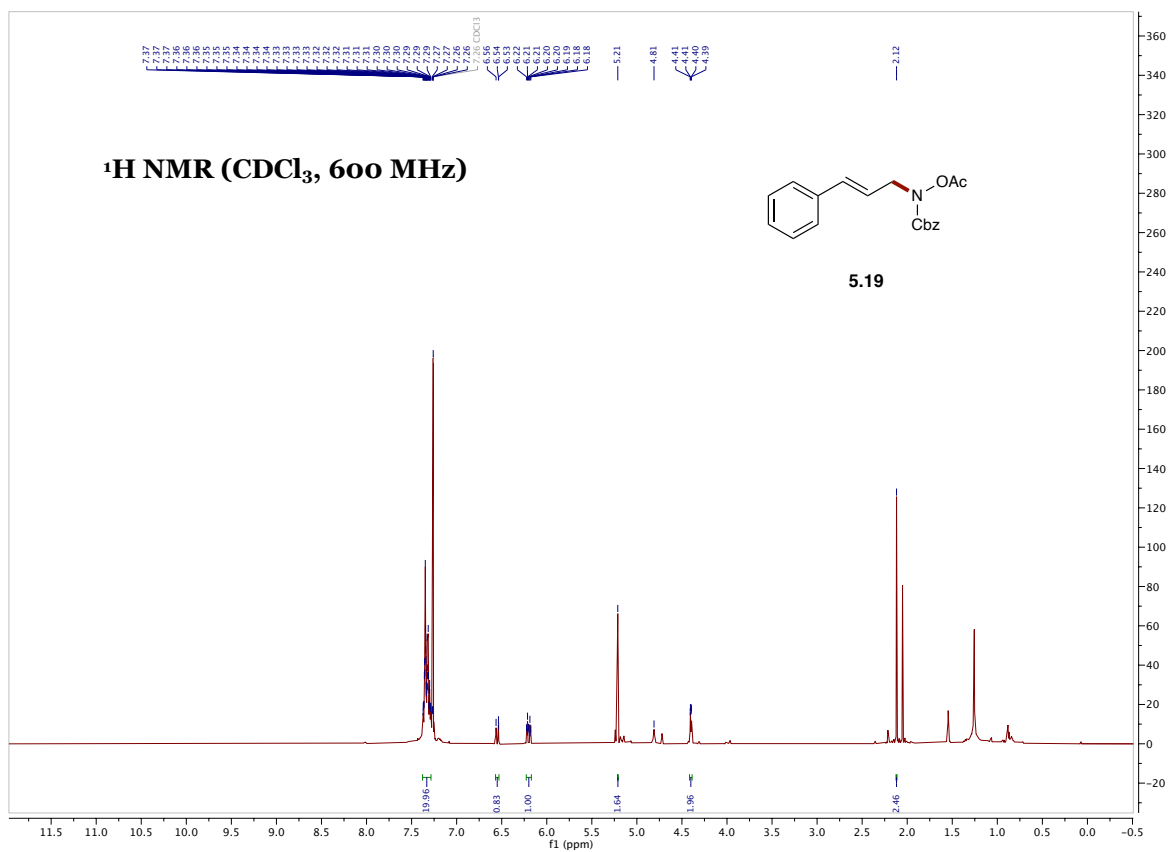
Phth-Ala-dioxazolone 5.6

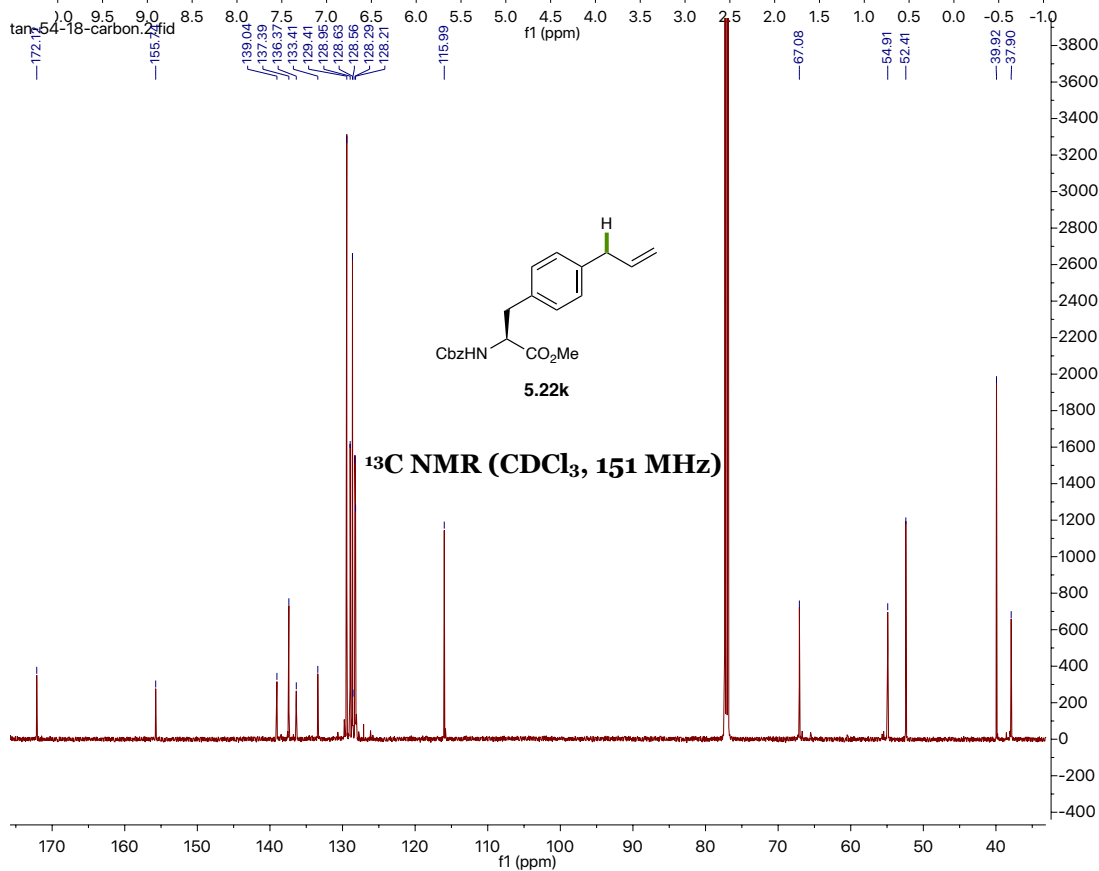
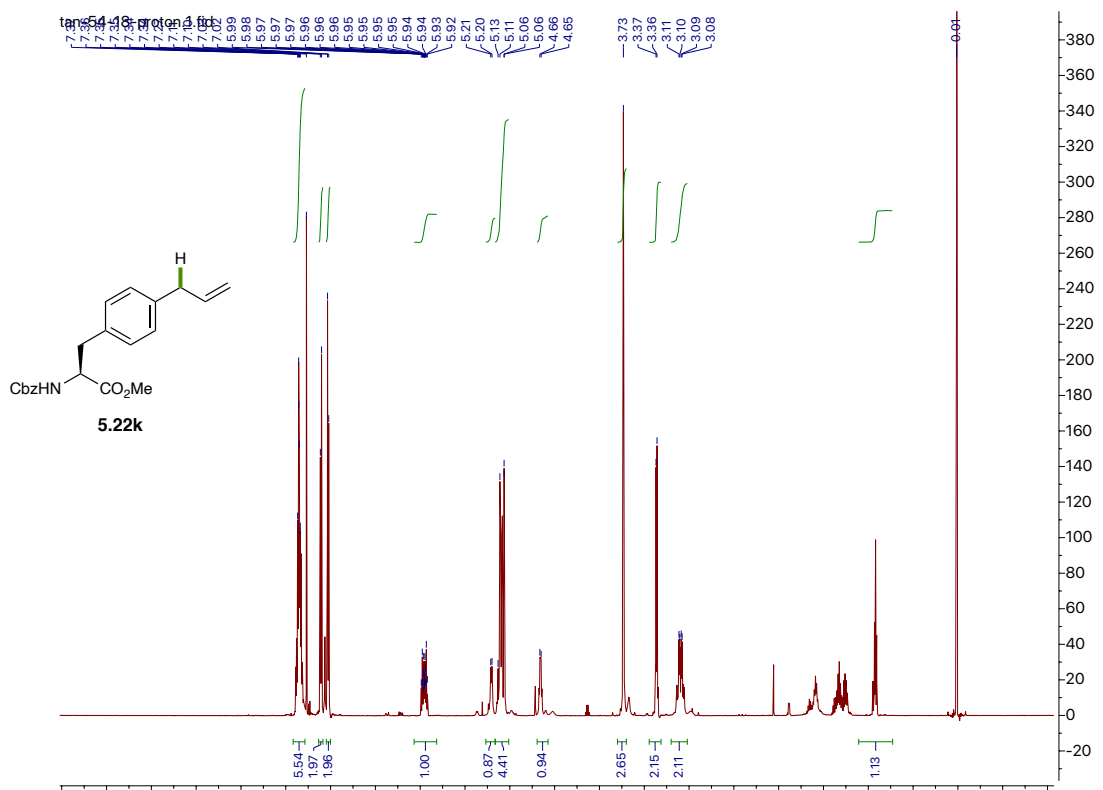


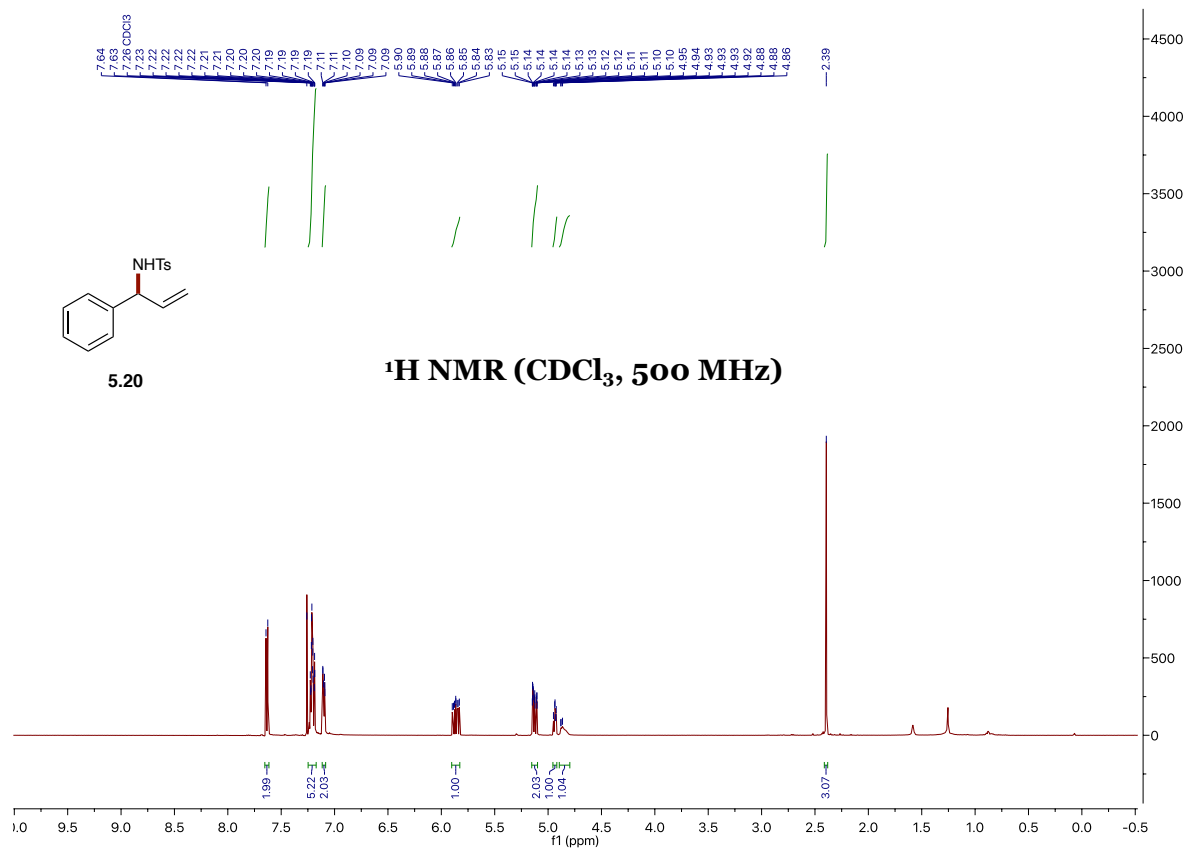
Dipeptide 5.9

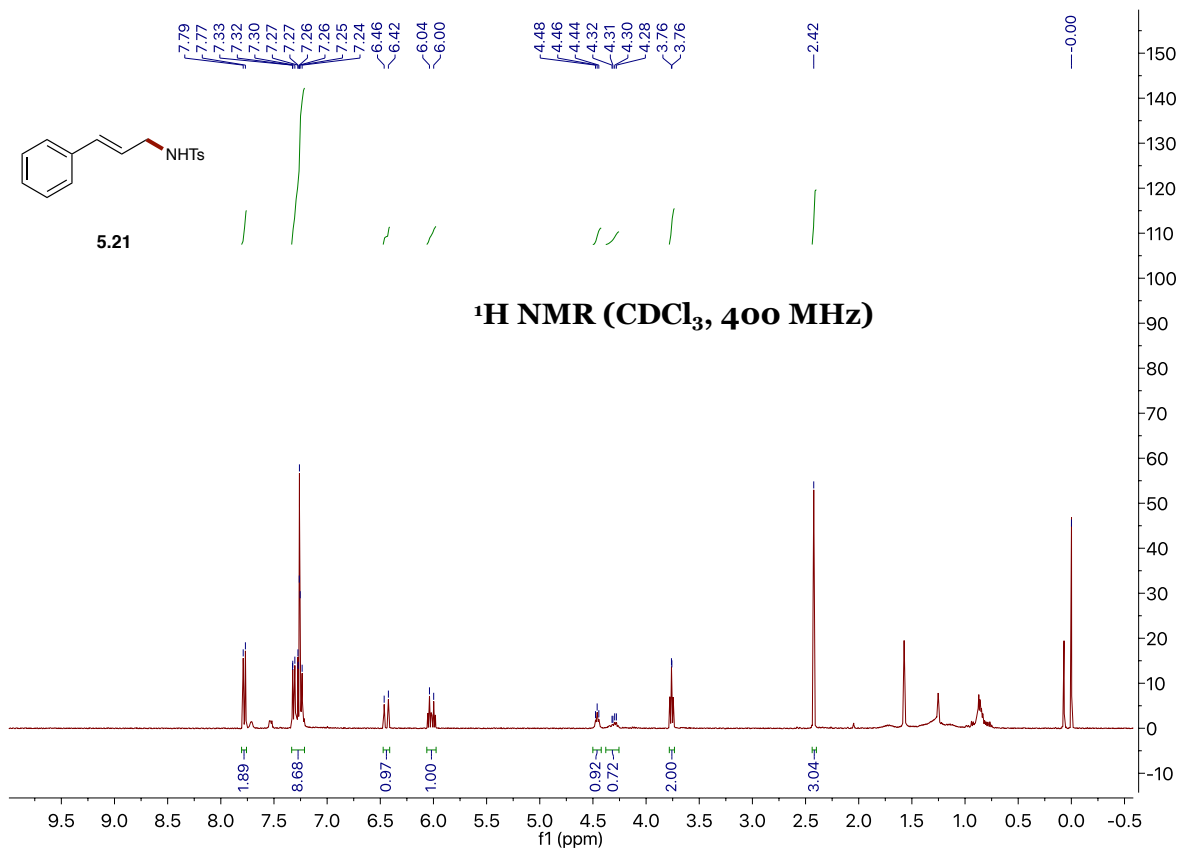


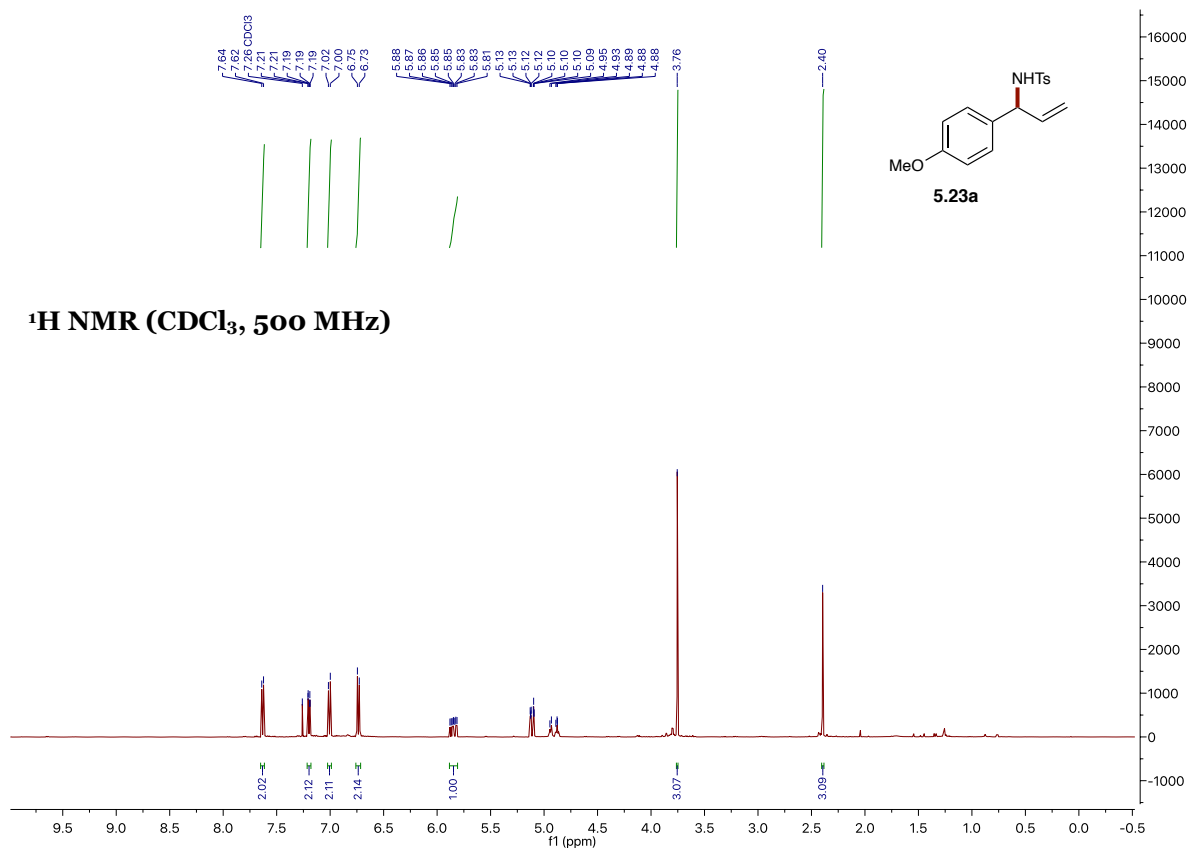
Allylic acetoxycarbamate 5.19 + unidentified impurities

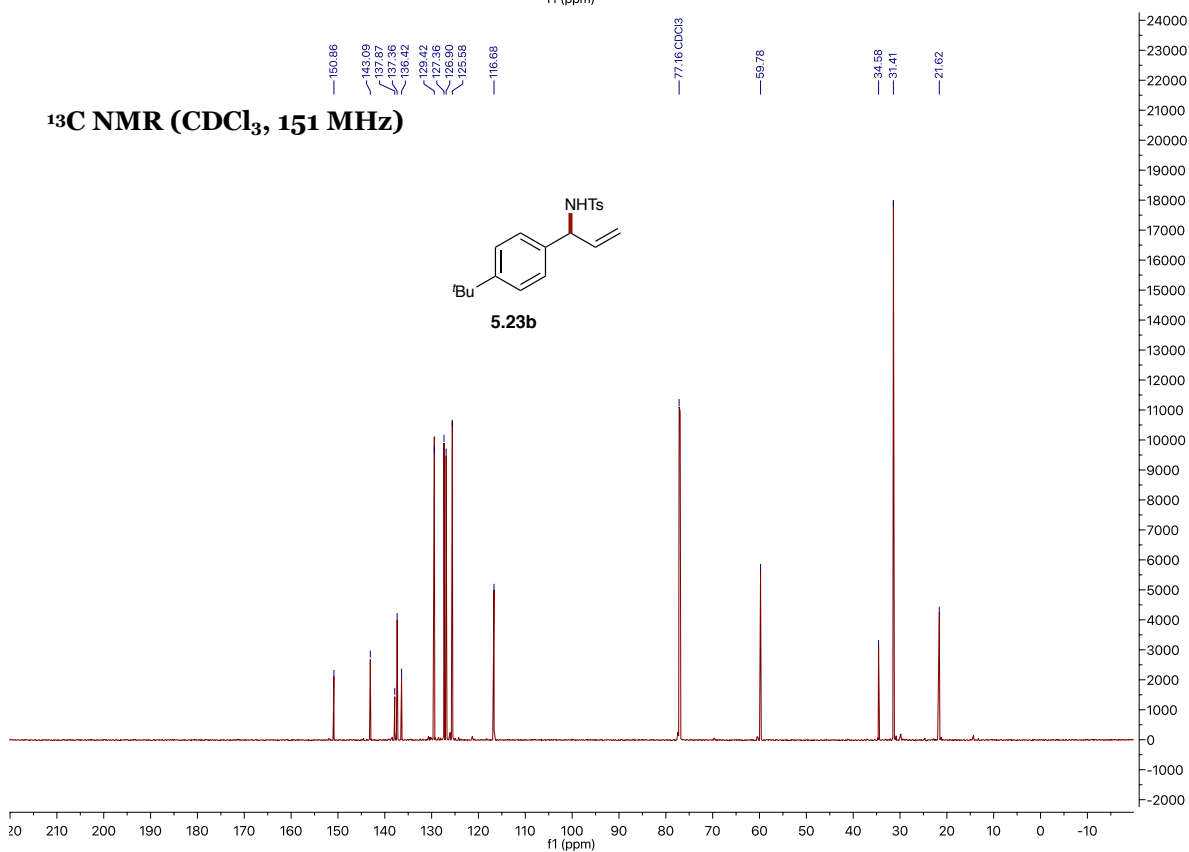
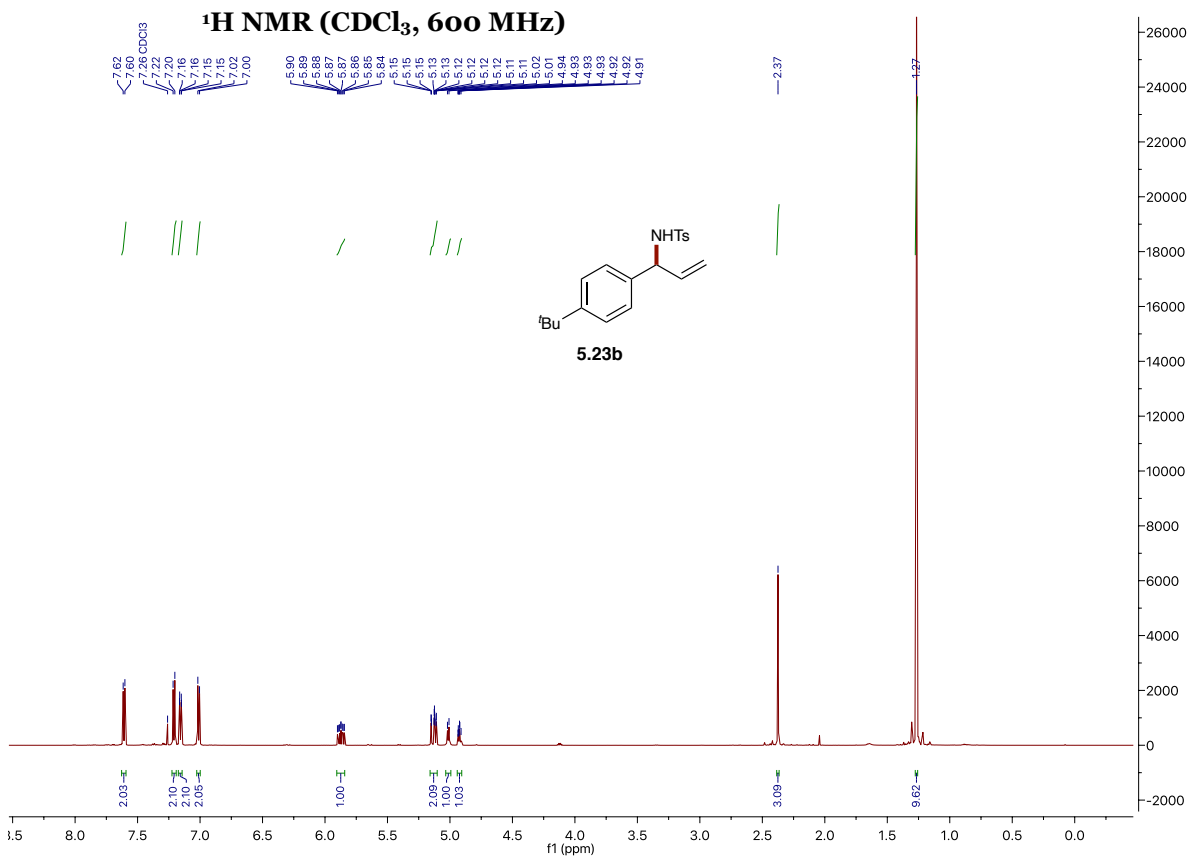


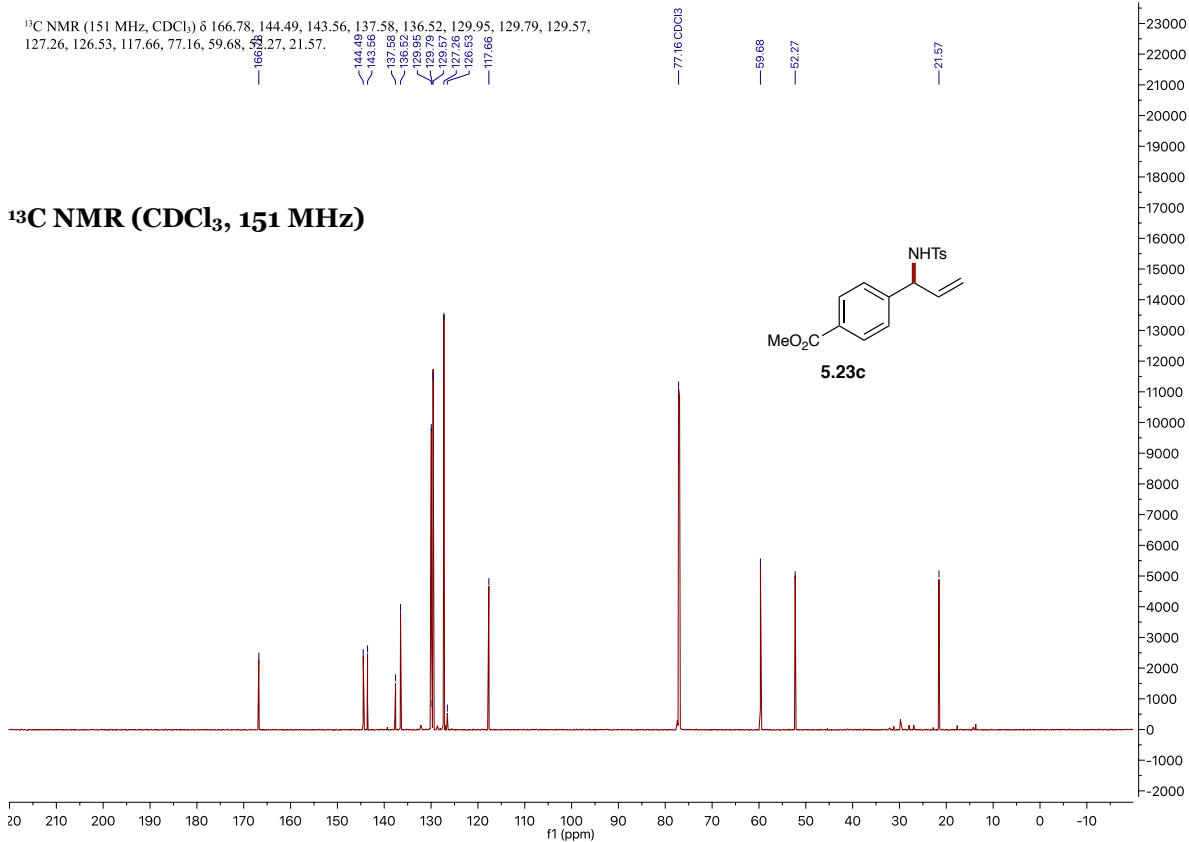
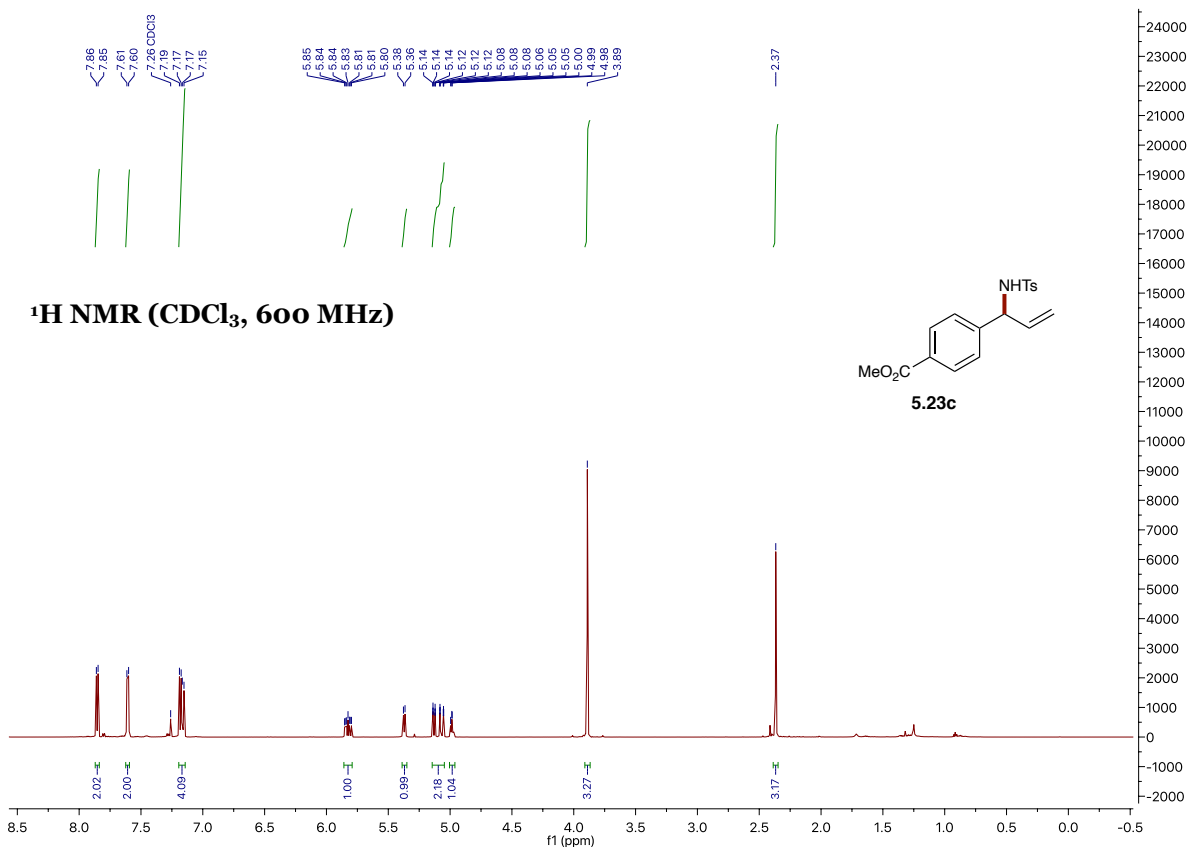
Phenylalanine-derived allylbenzene 5.22k $^1\text{H NMR}$ (CDCl_3 , 600 MHz)

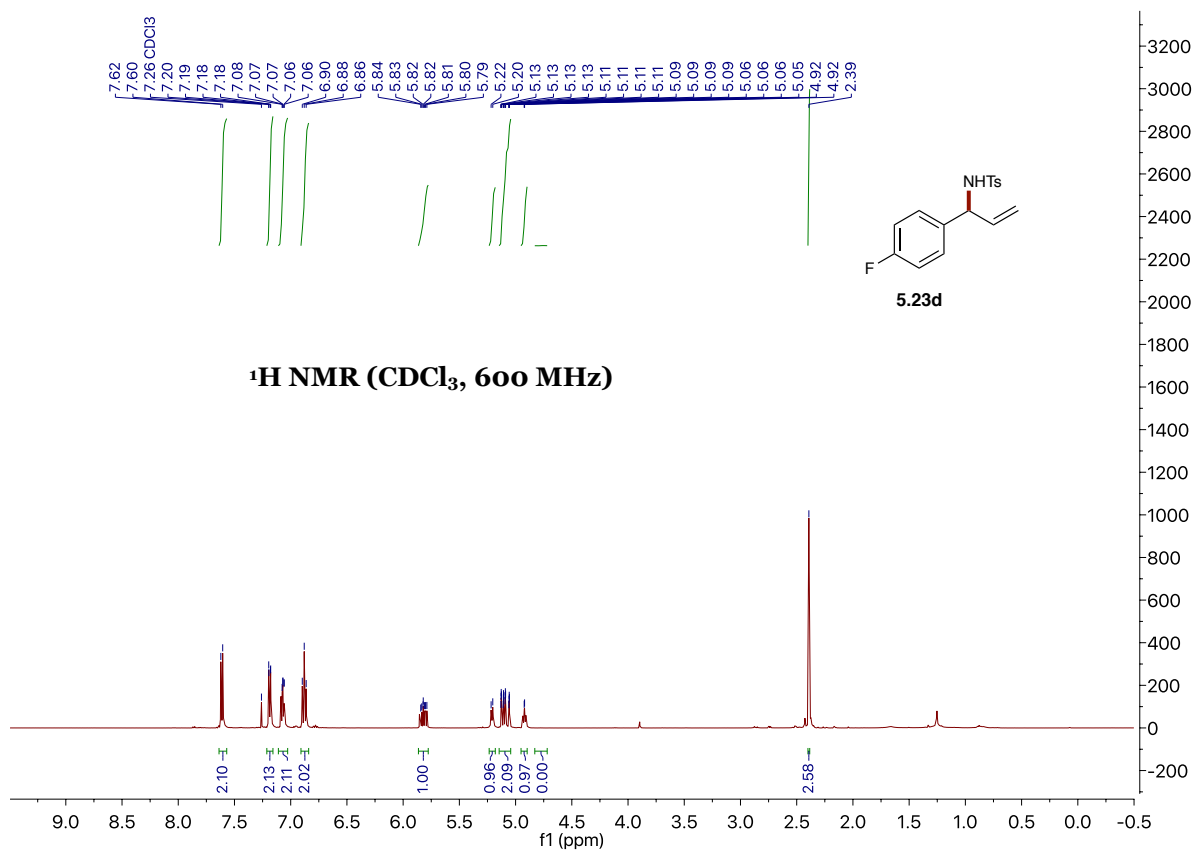




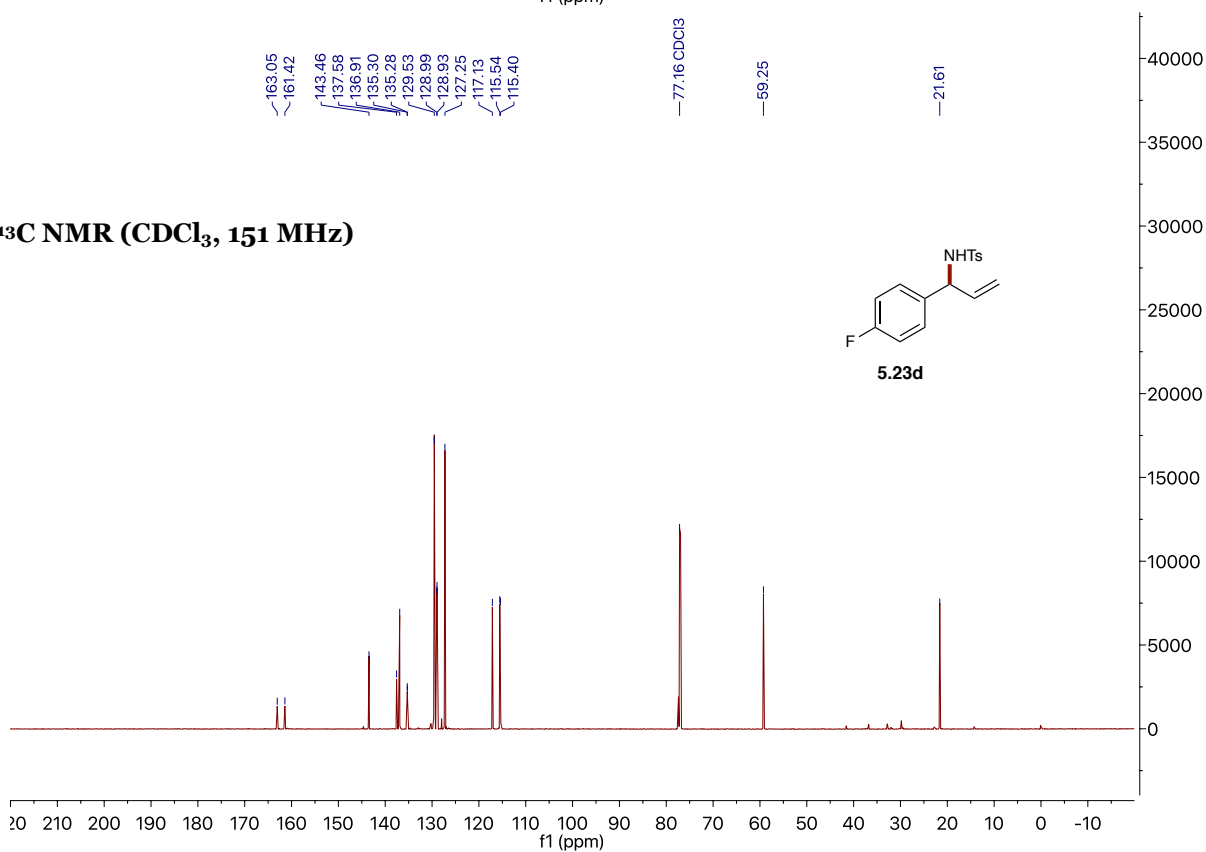


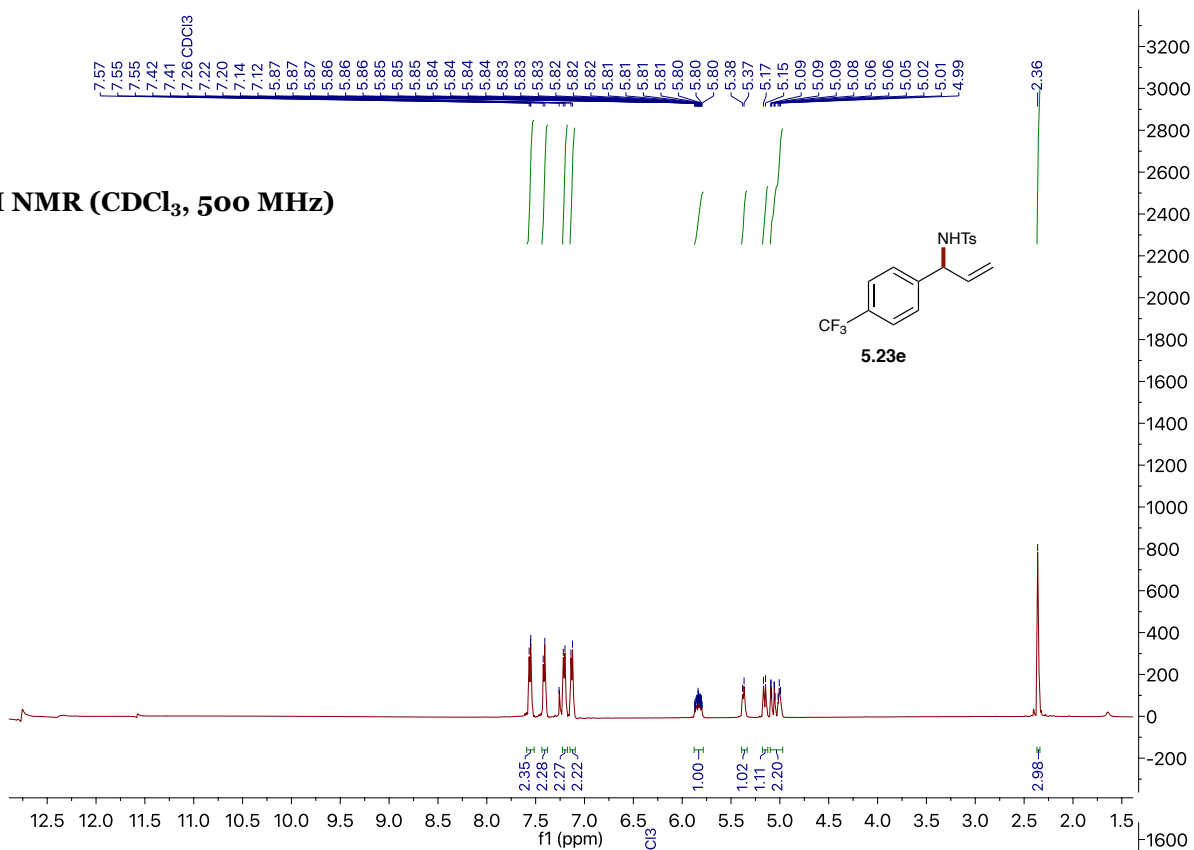
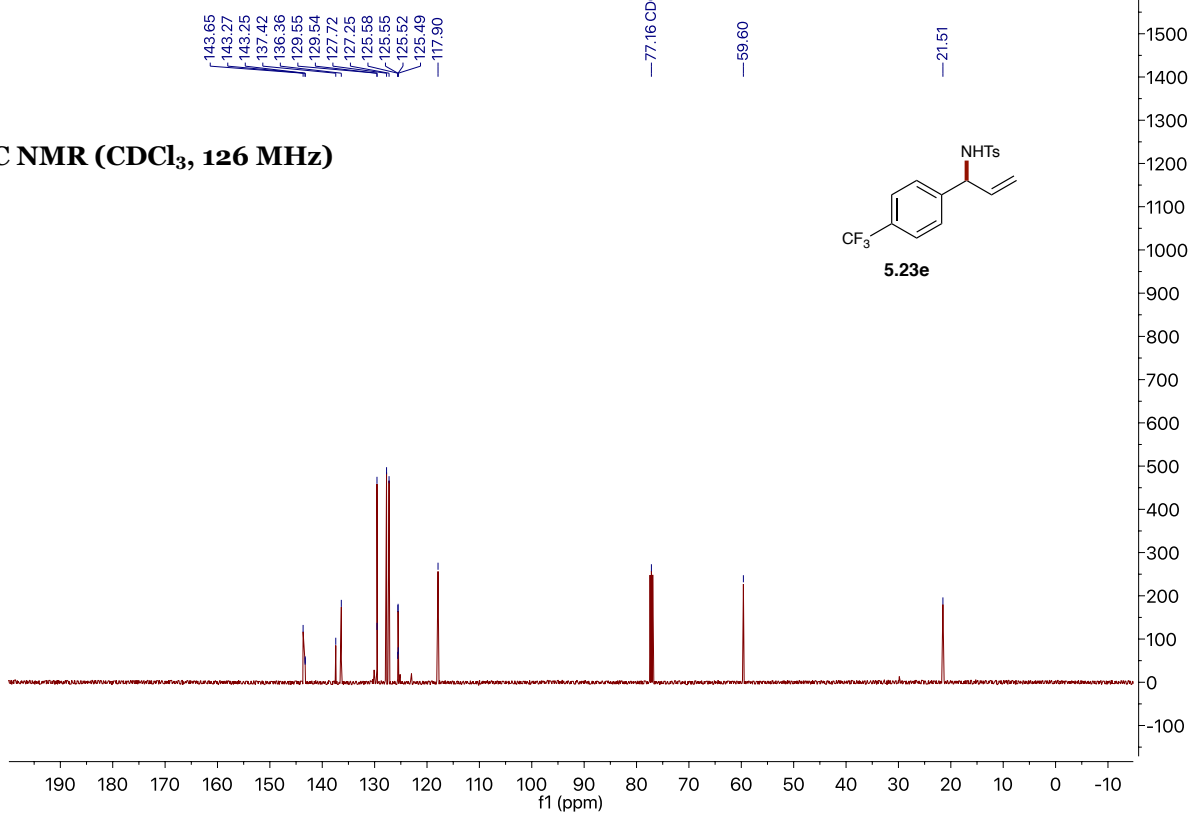


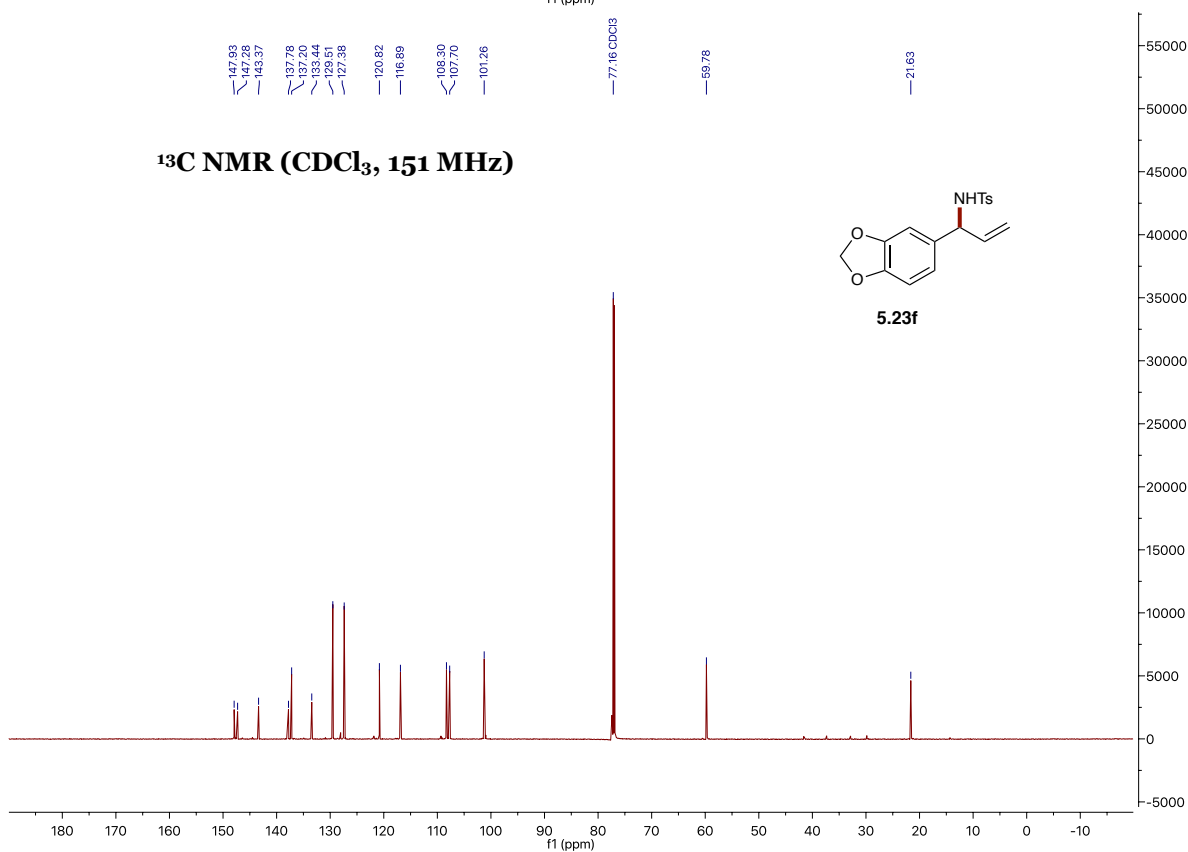
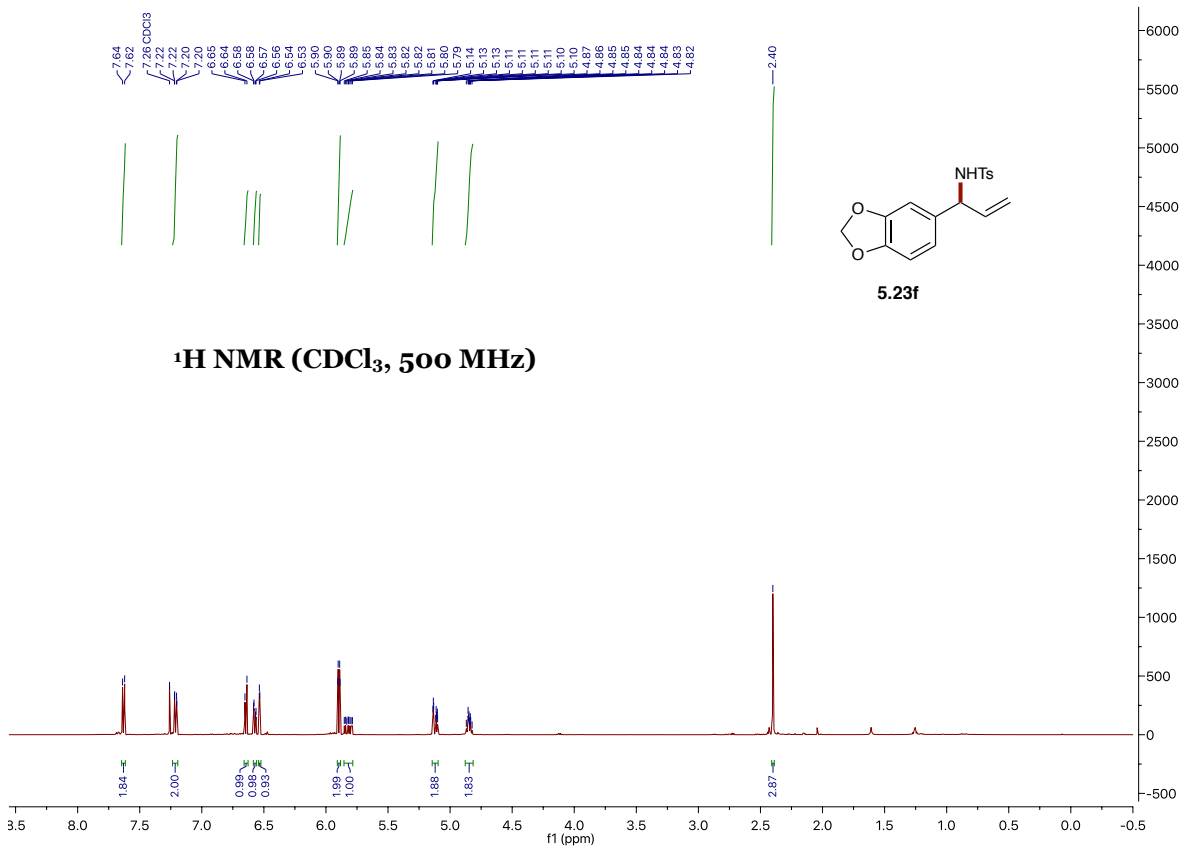


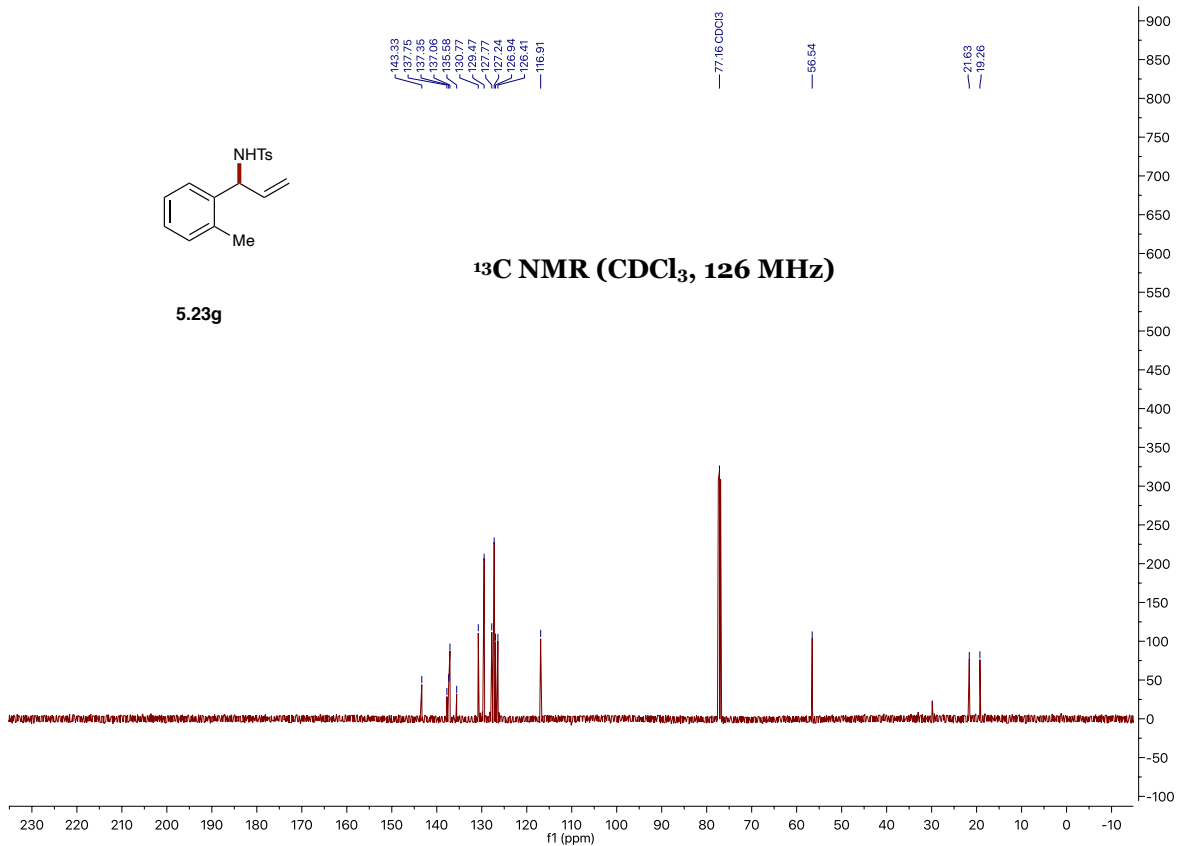
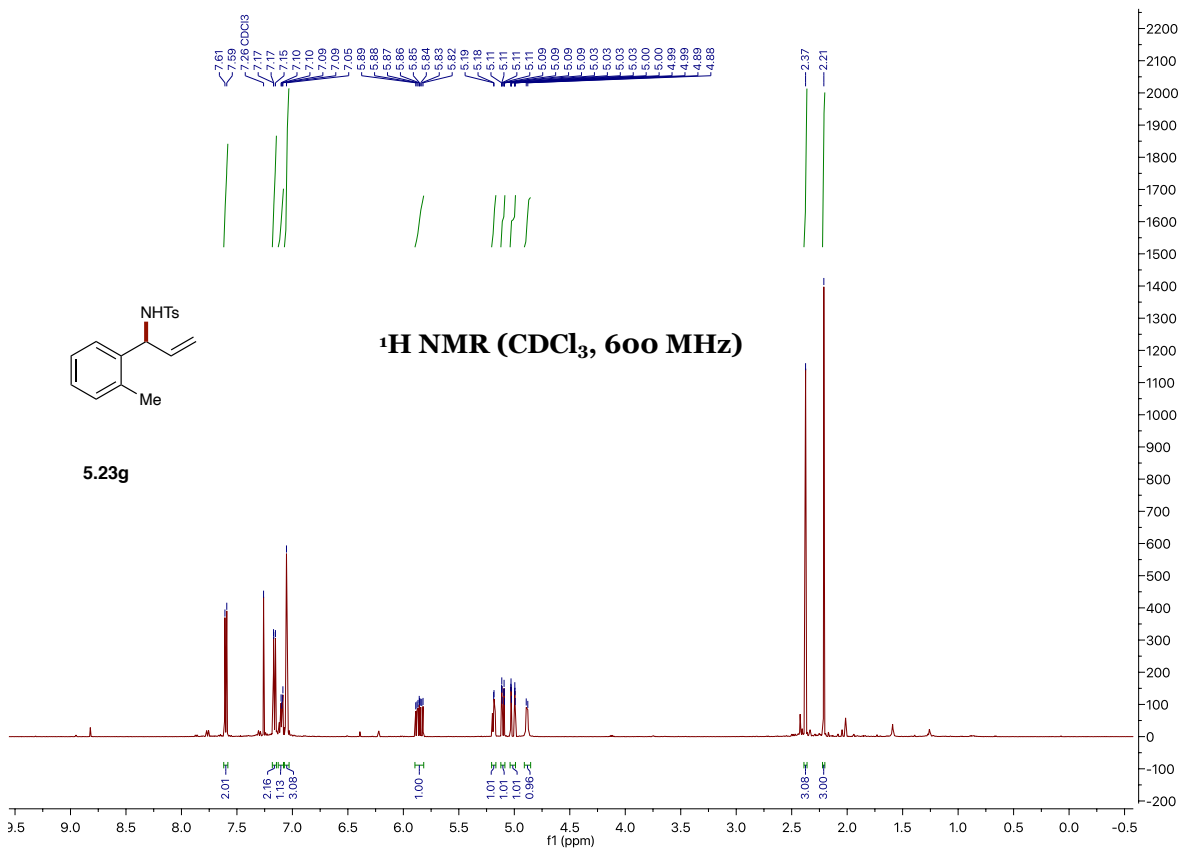


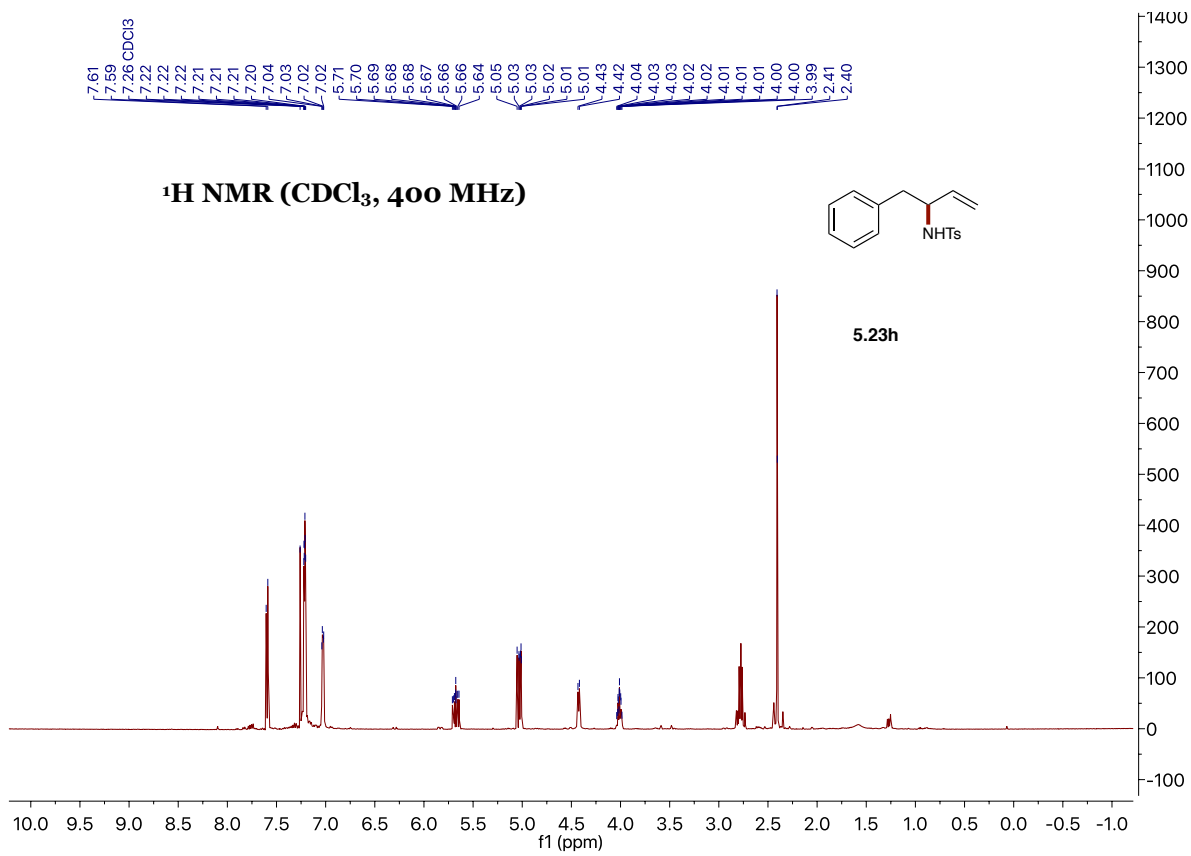
¹³C NMR (CDCl₃, 151 MHz)

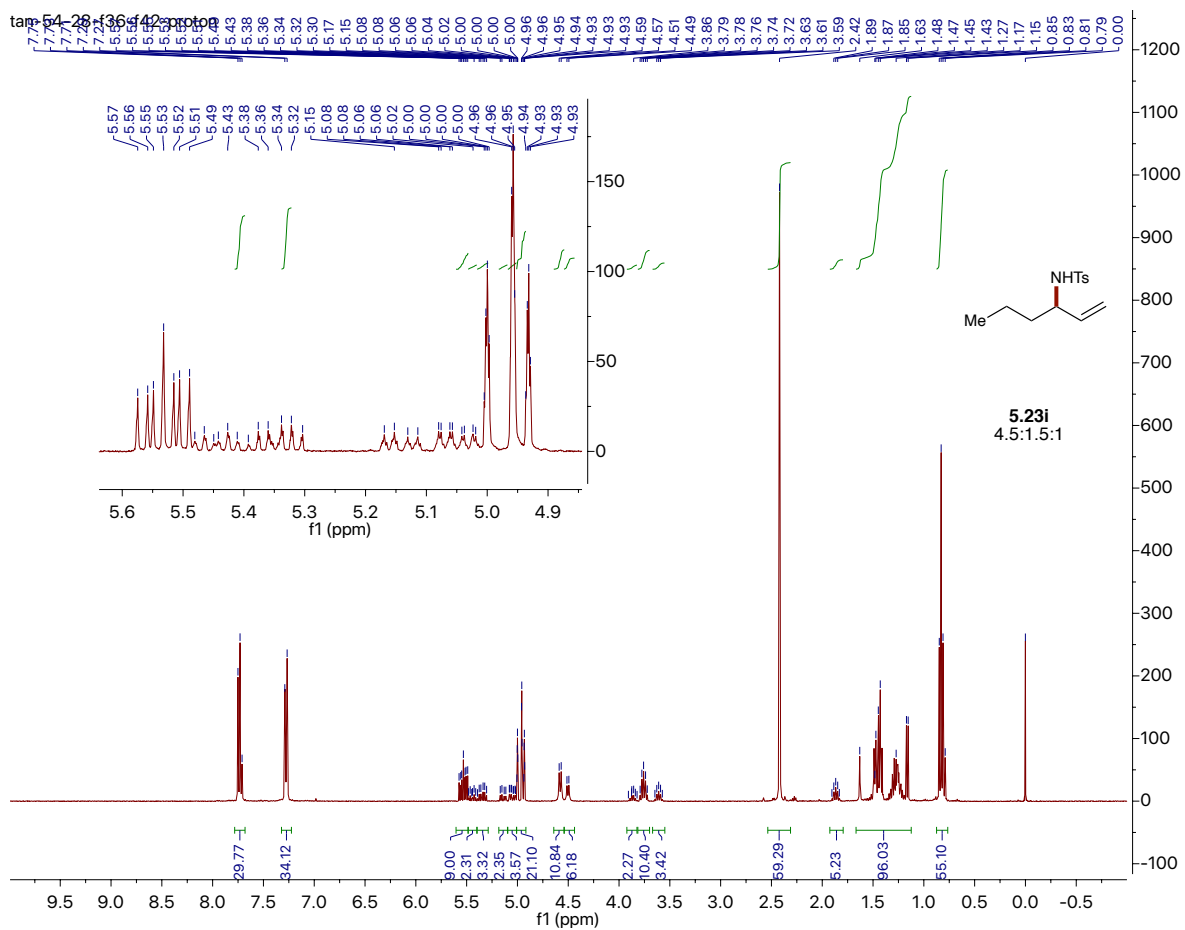


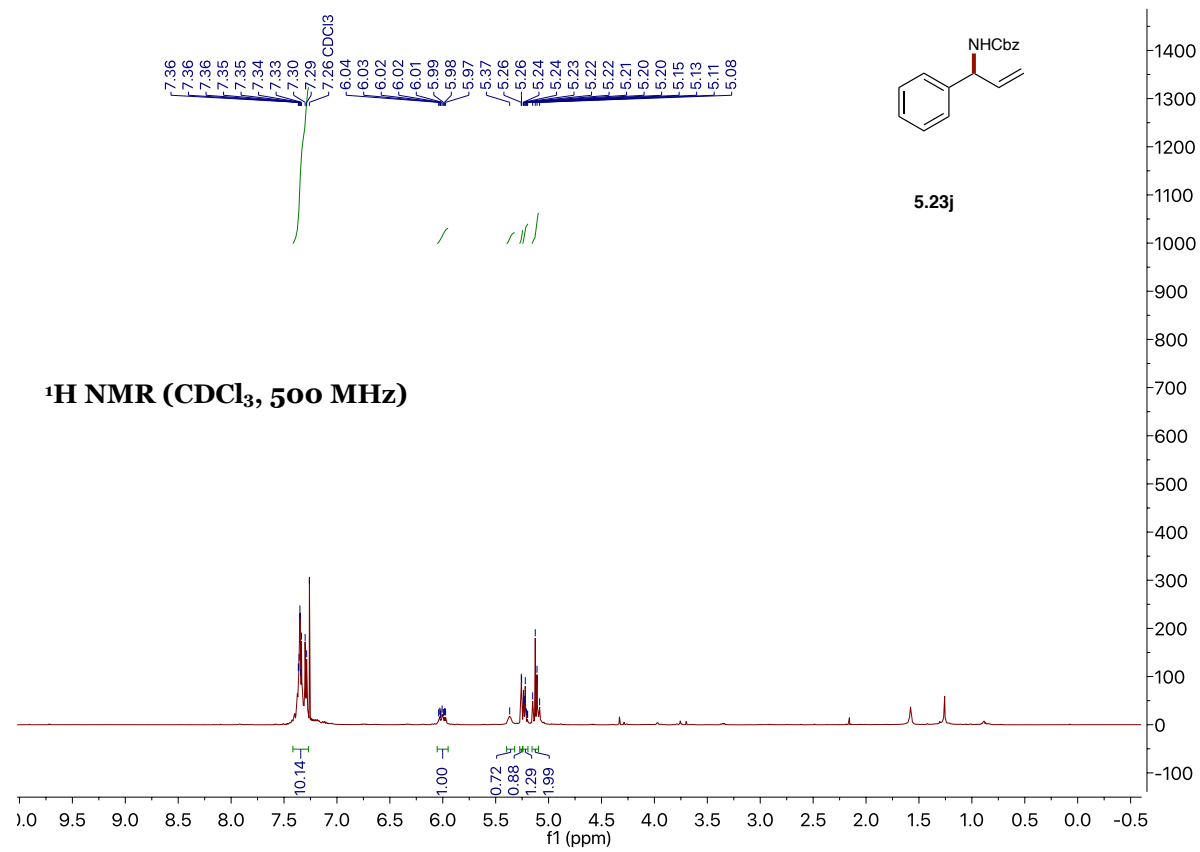
^1H NMR (CDCl_3 , 500 MHz) ^{13}C NMR (CDCl_3 , 126 MHz)

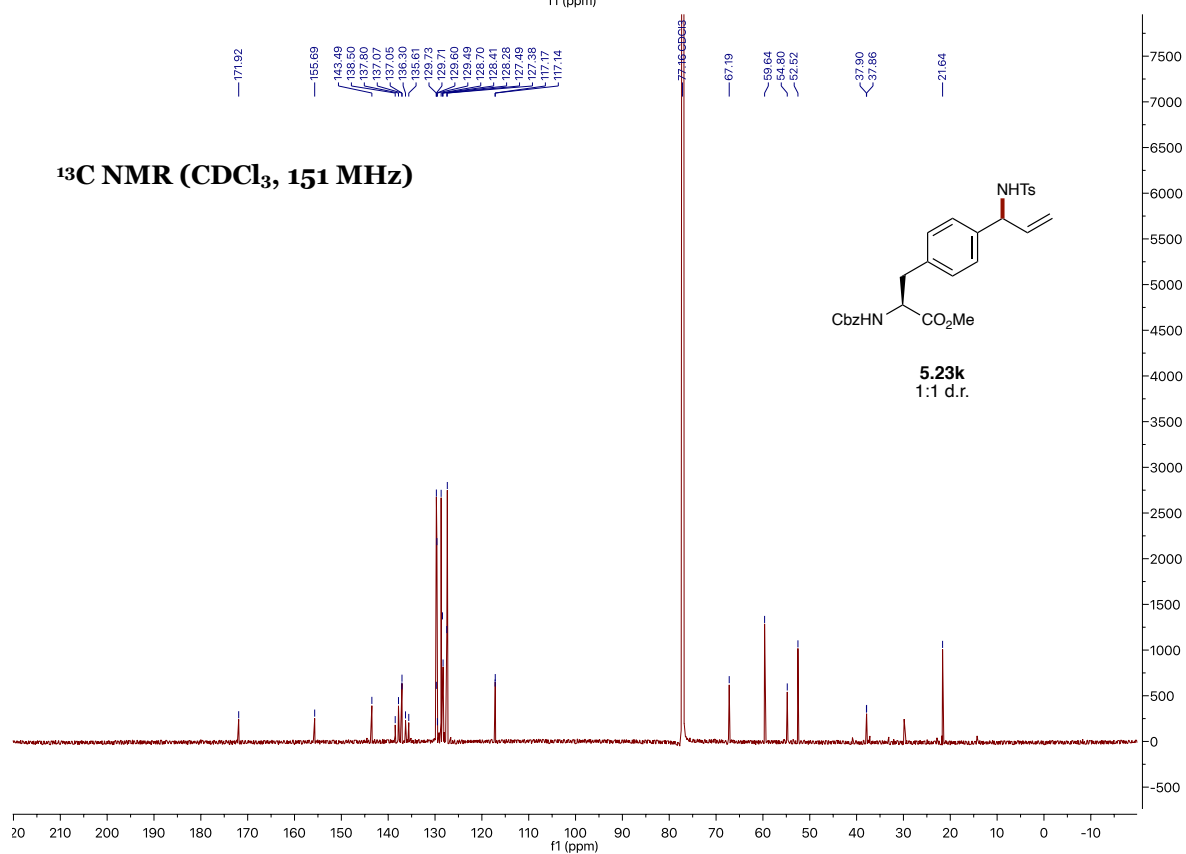
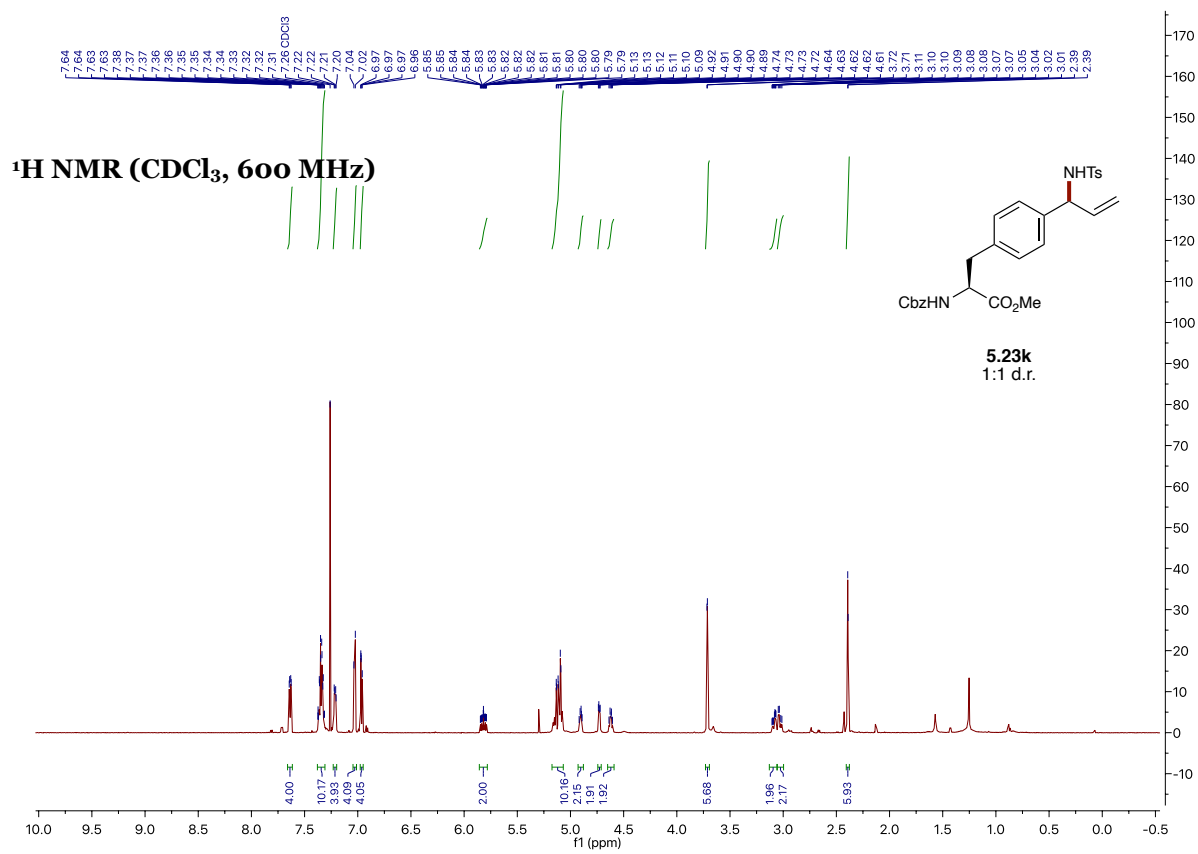


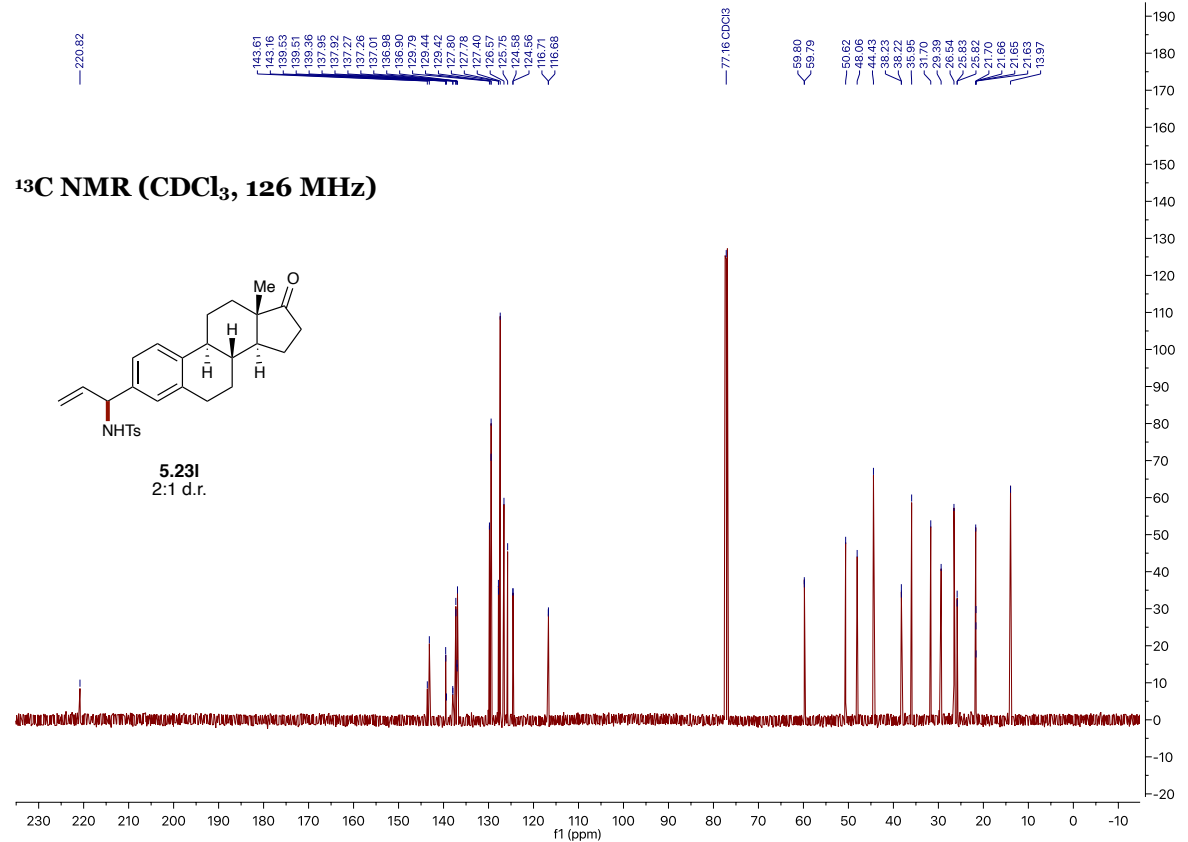
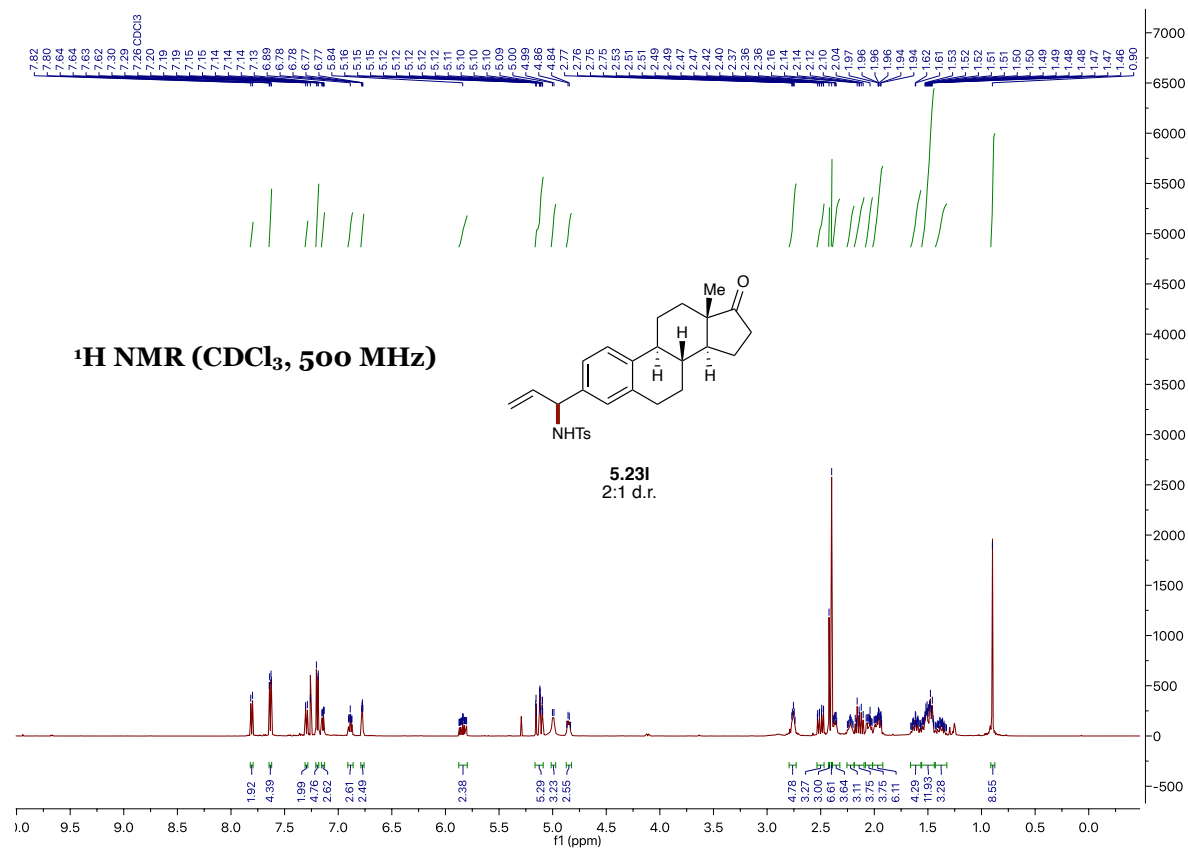


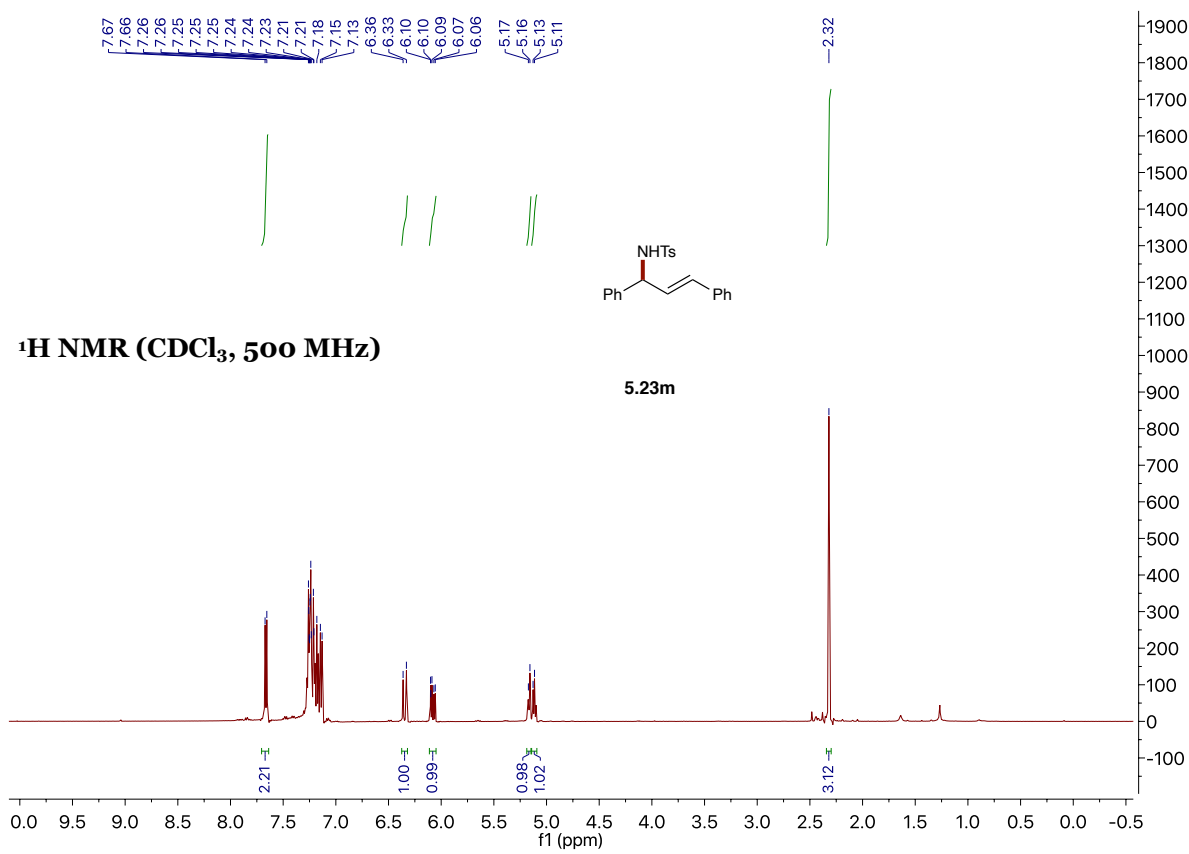


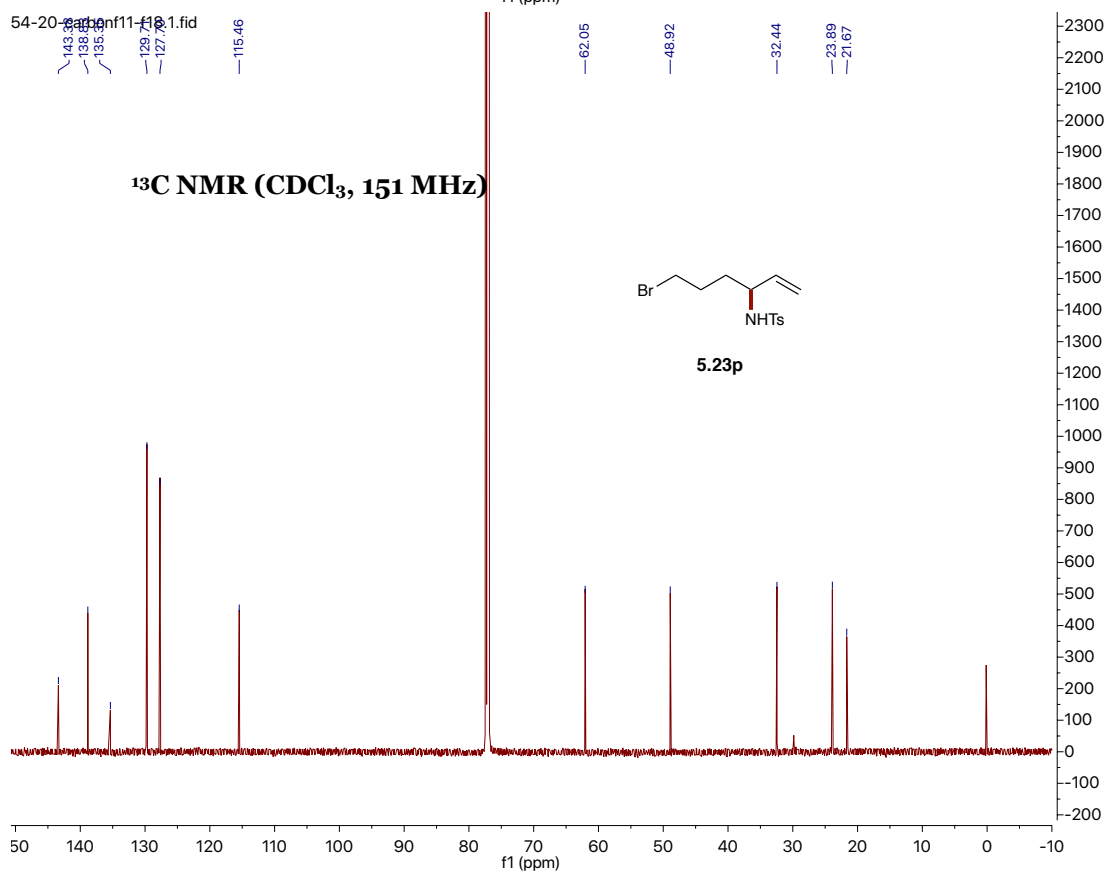
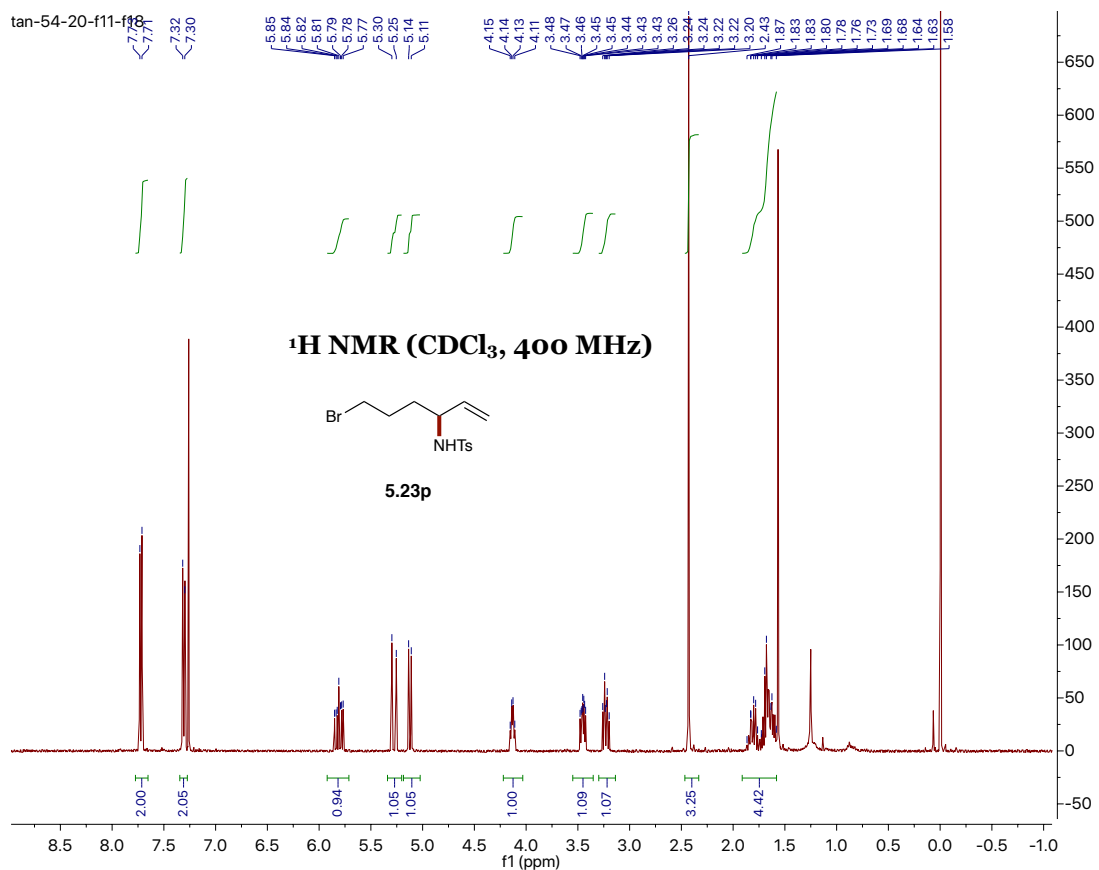
^1H NMR (CDCl_3 , 400 MHz)



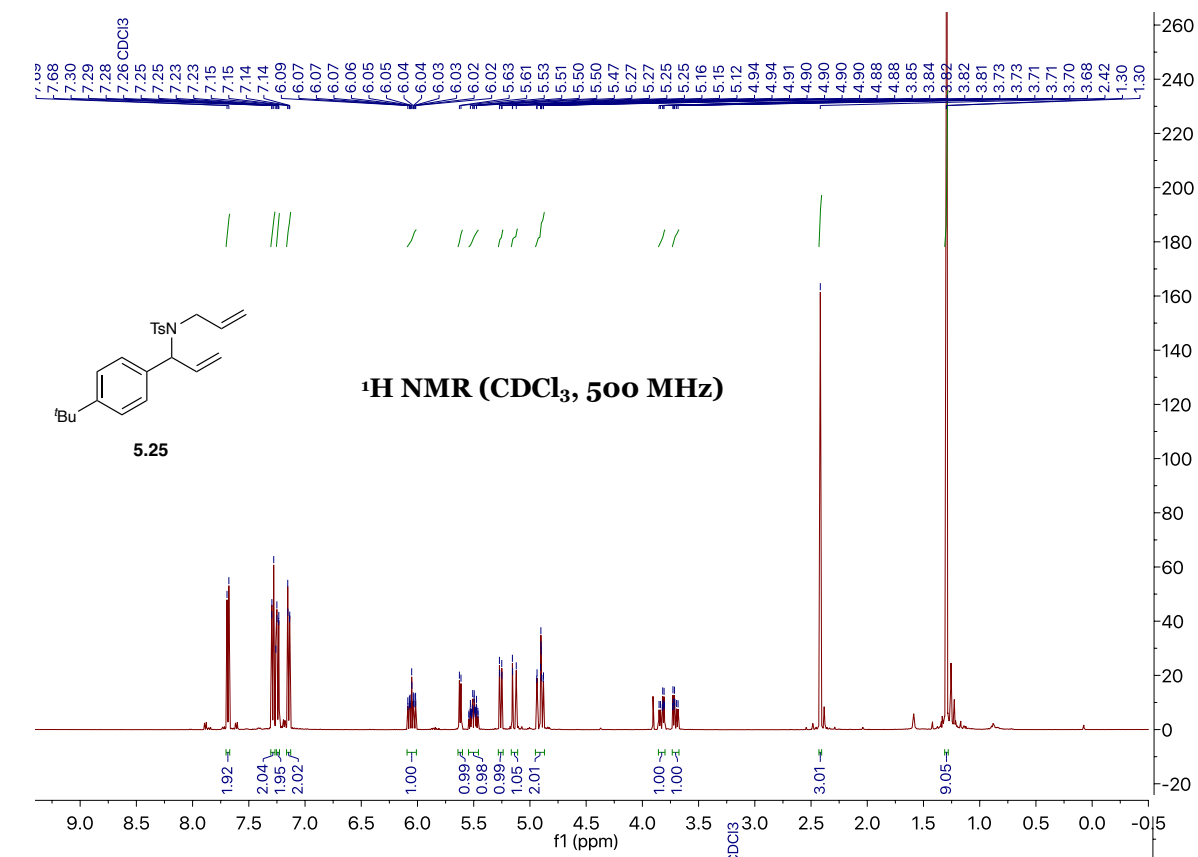
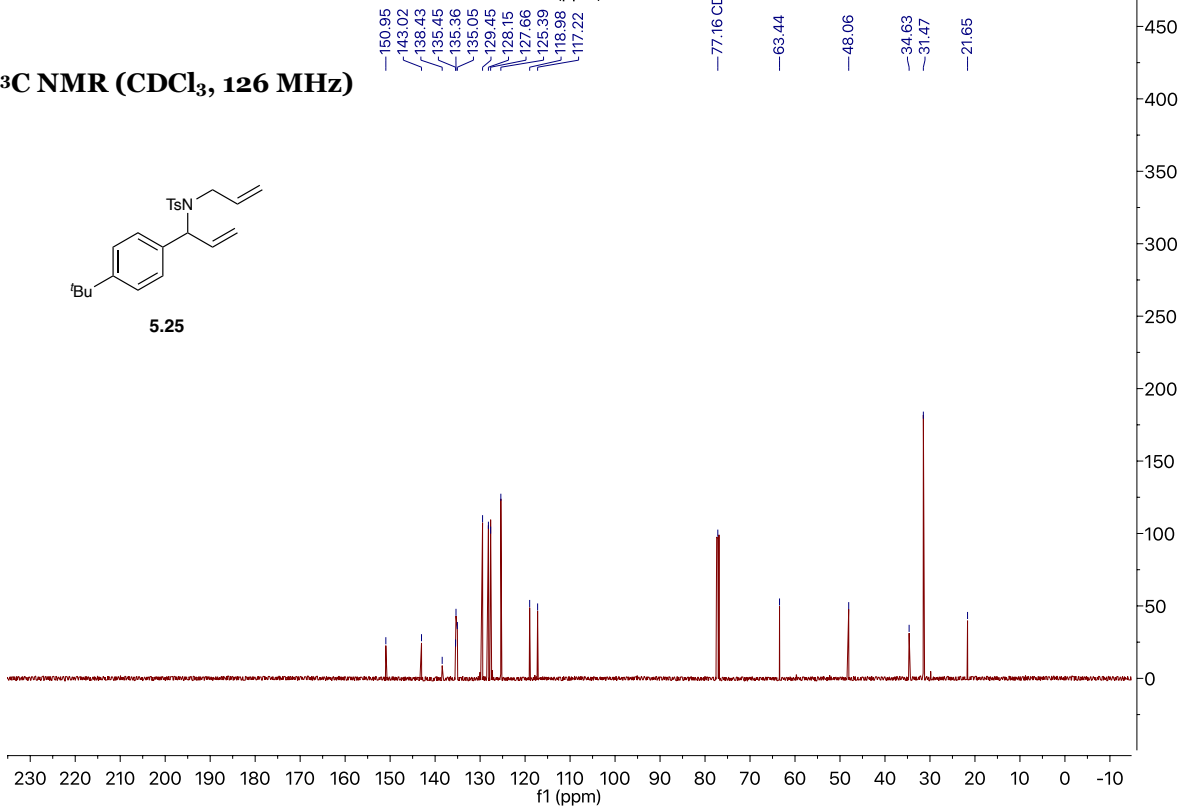




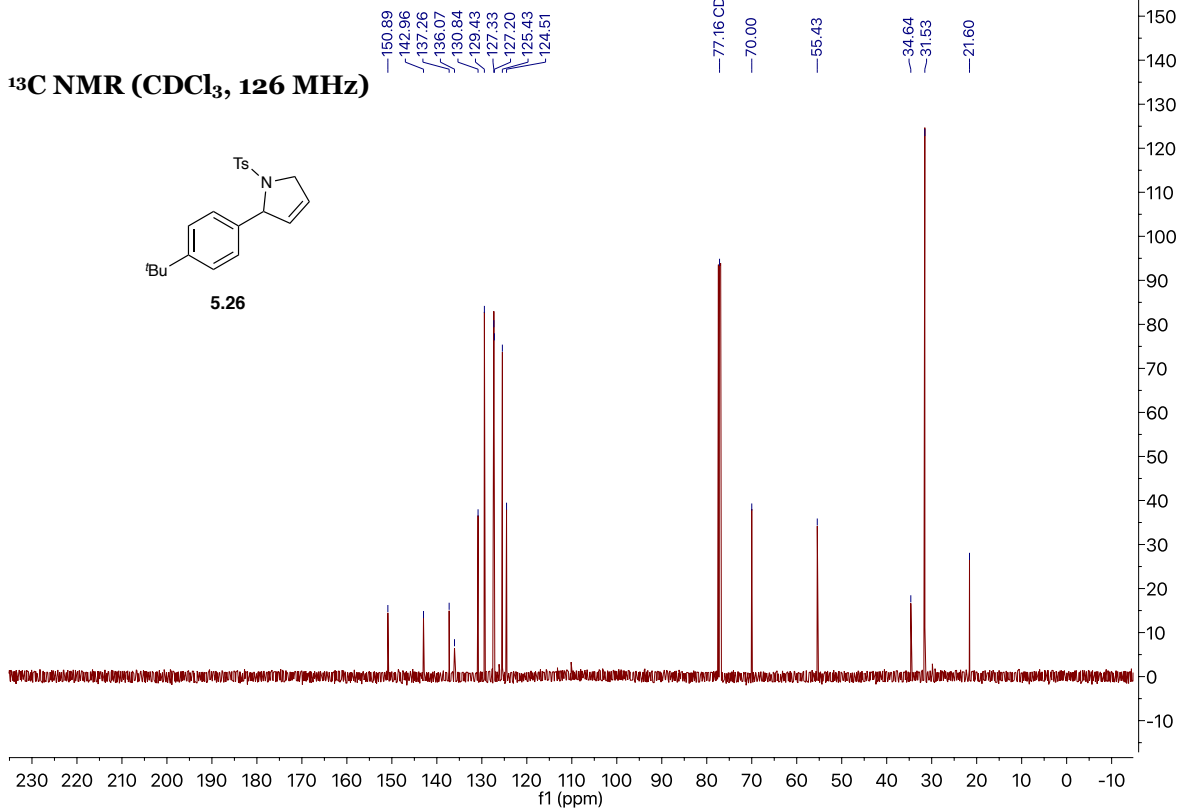
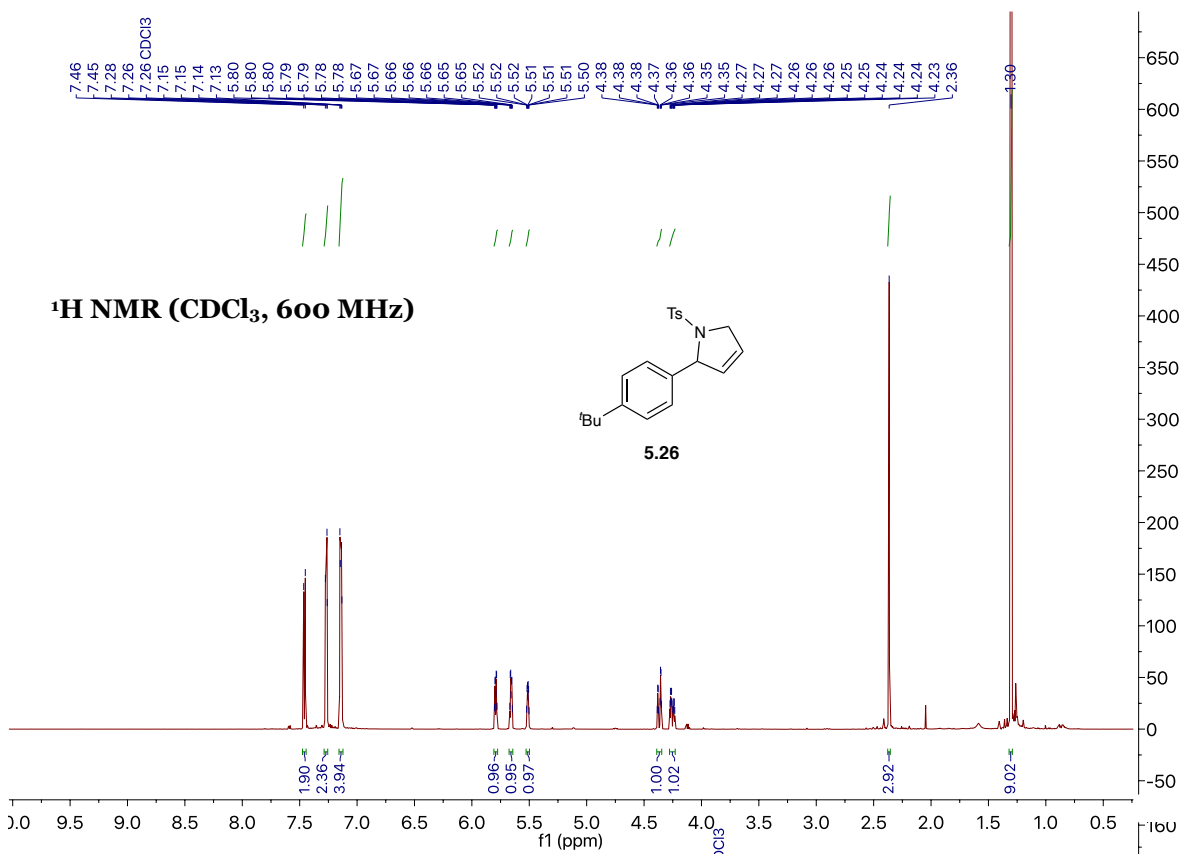




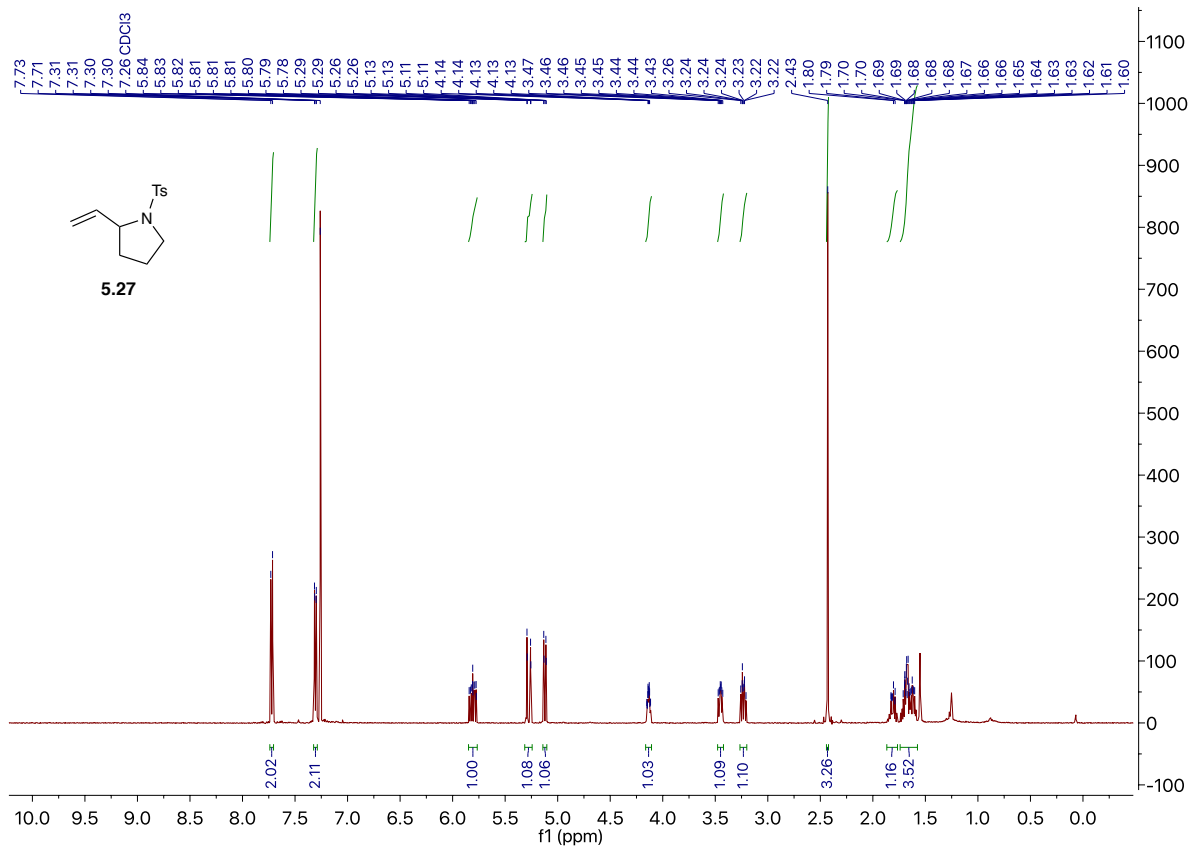
Diallylsulfonamide 5.25

**¹³C NMR (CDCl₃, 126 MHz)**

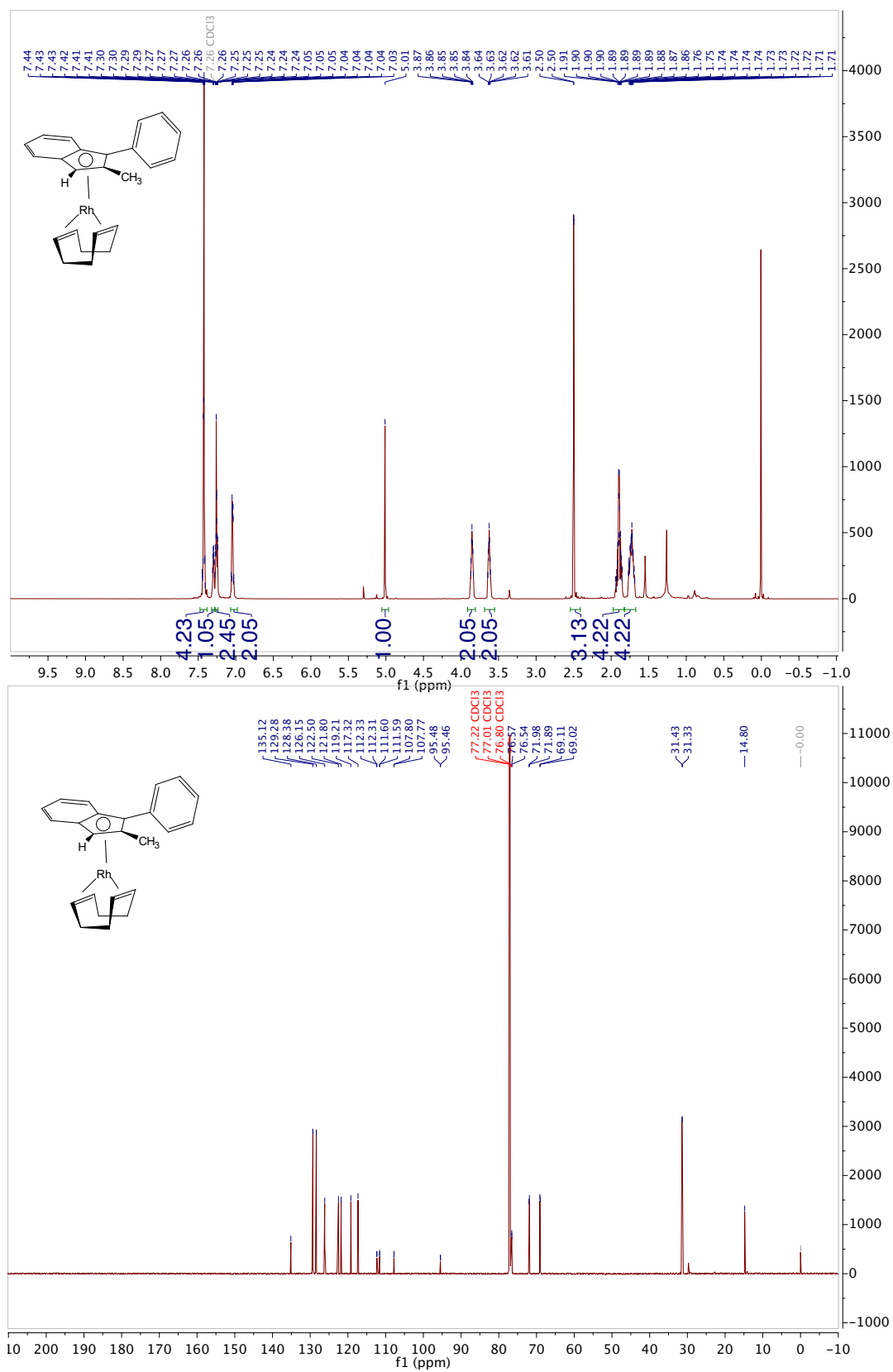
Dihydropyrrole 5.26

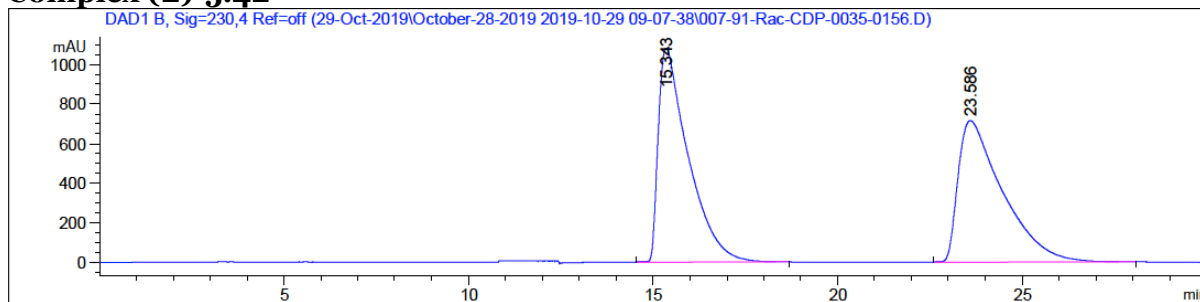


Vinylpyrrolidine 5.27

 ^1H NMR (CDCl_3 , 600 MHz)

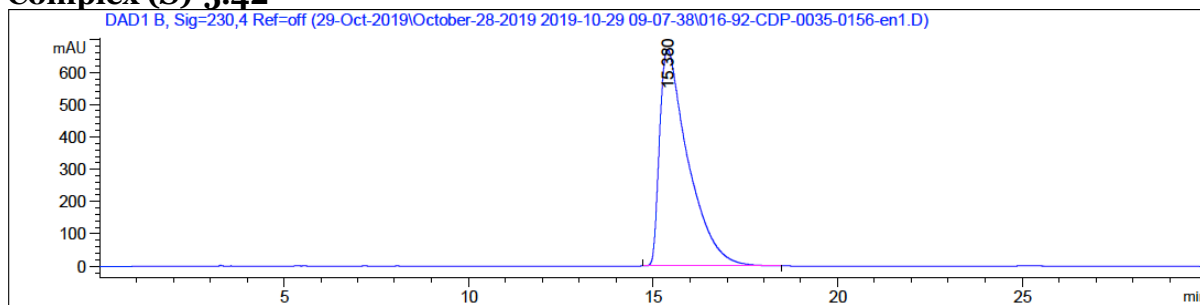
Complex (±)-5.42



Complex (\pm)-5.42

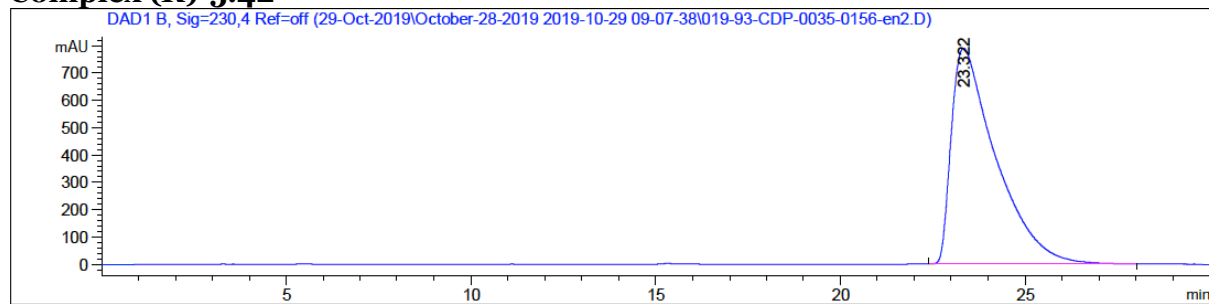
Peak #	RetTime [min]	Type	Width [min]	Area [mAU*s]	Height [mAU]	Area %
1	15.343	BB	0.6713	6.09575e4	1081.97058	50.4581
2	23.586	BB	0.9789	5.98507e4	715.51105	49.5419

Totals : 1.20808e5 1797.48163

Complex (S)-5.42

Peak #	RetTime [min]	Type	Width [min]	Area [mAU*s]	Height [mAU]	Area %
1	15.380	BB	0.6345	3.57966e4	669.86053	100.0000

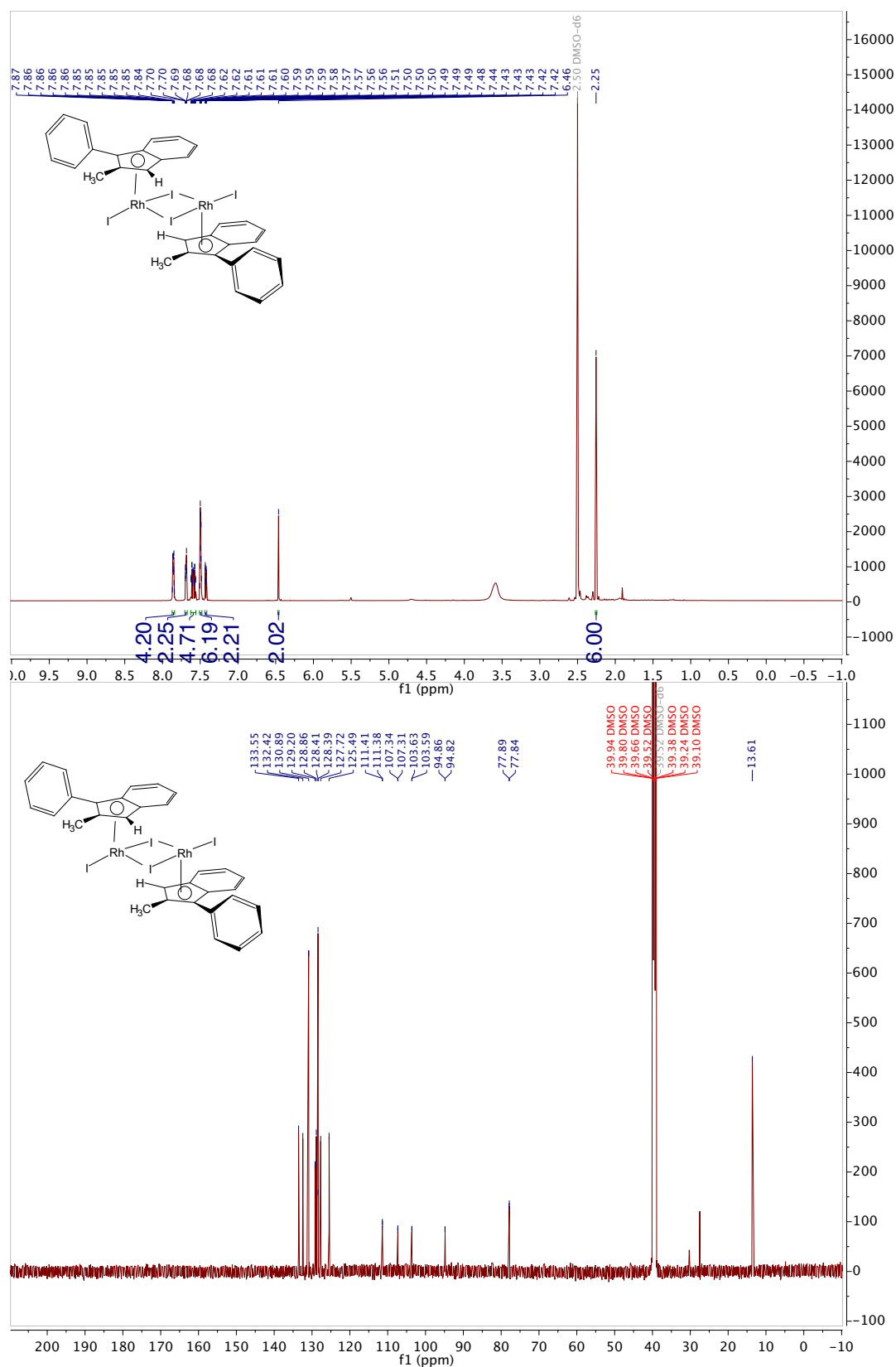
Totals : 3.57966e4 669.86053

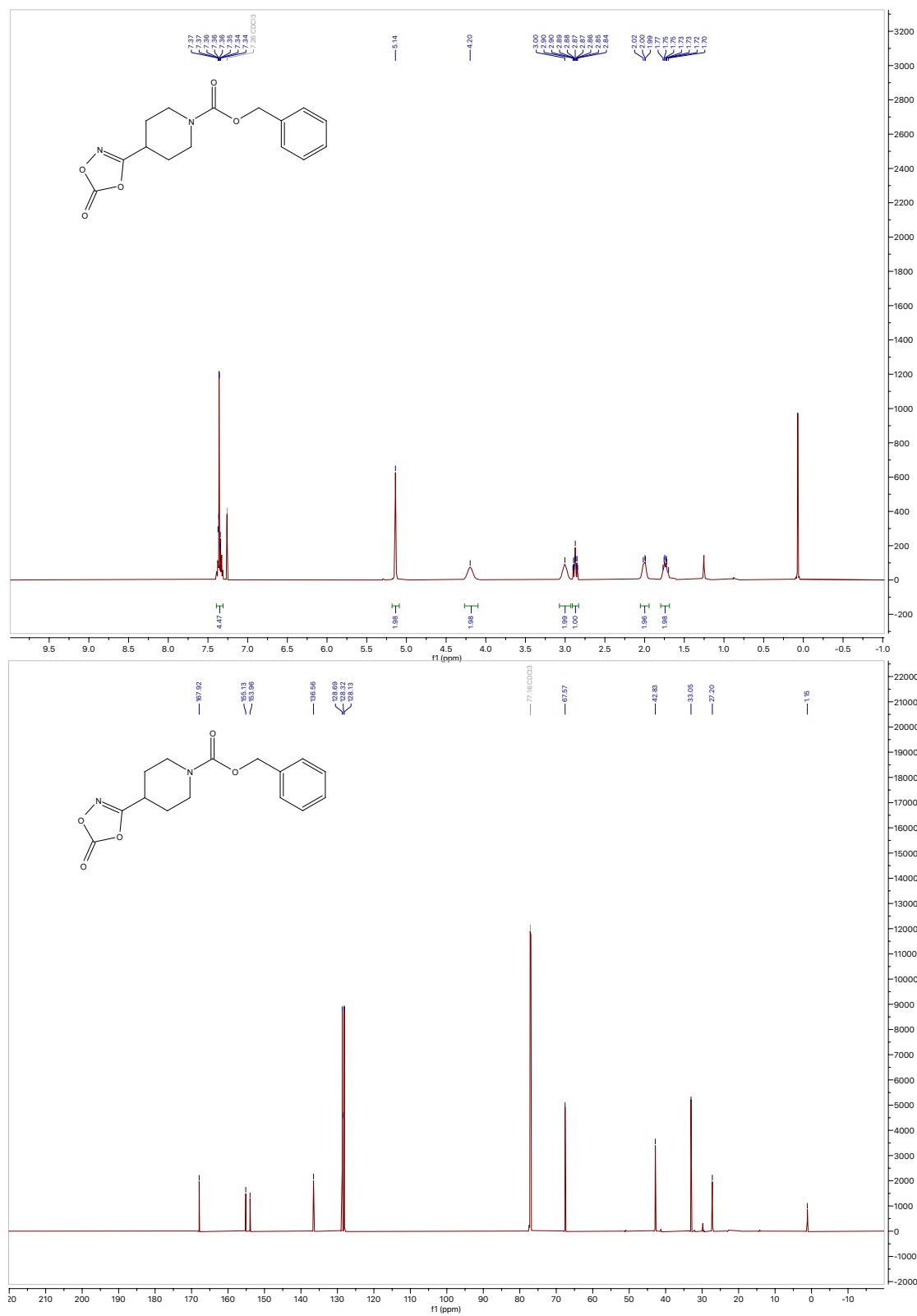
Complex (R)-5.42

Peak #	RetTime [min]	Type	Width [min]	Area [mAU*s]	Height [mAU]	Area %
1	23.322	BB	0.9844	6.60966e4	789.35767	100.0000

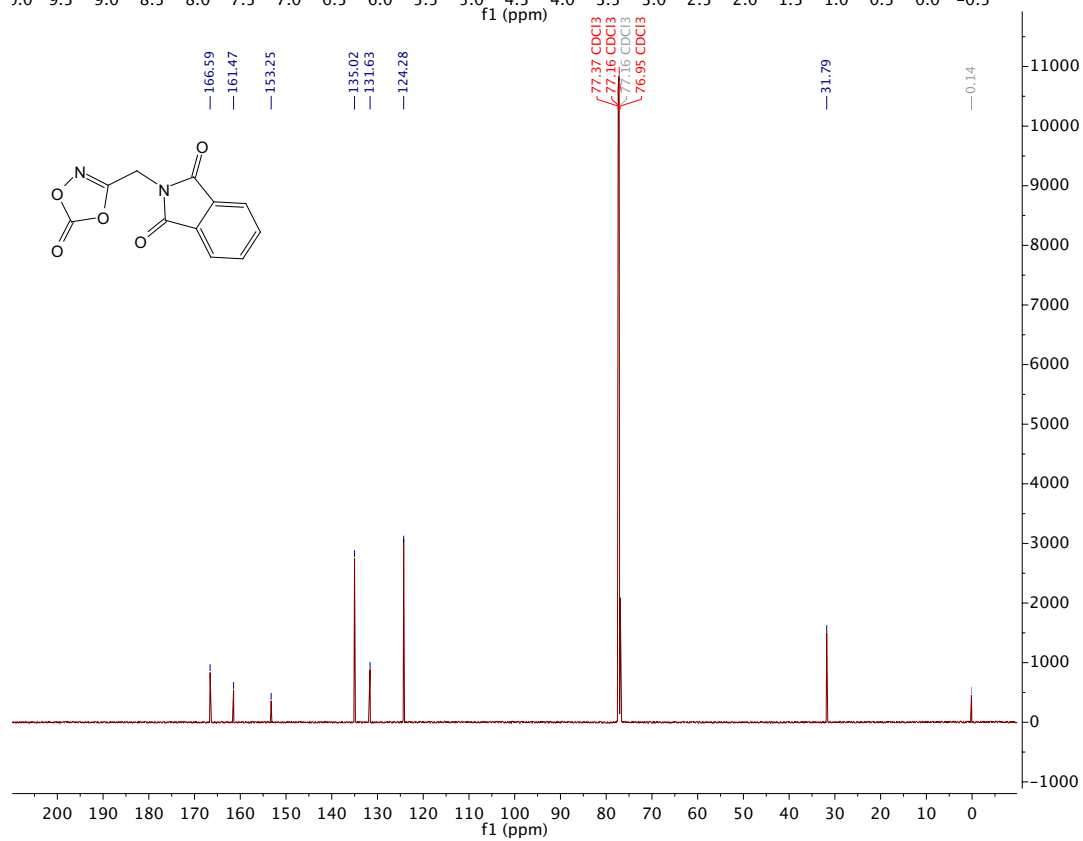
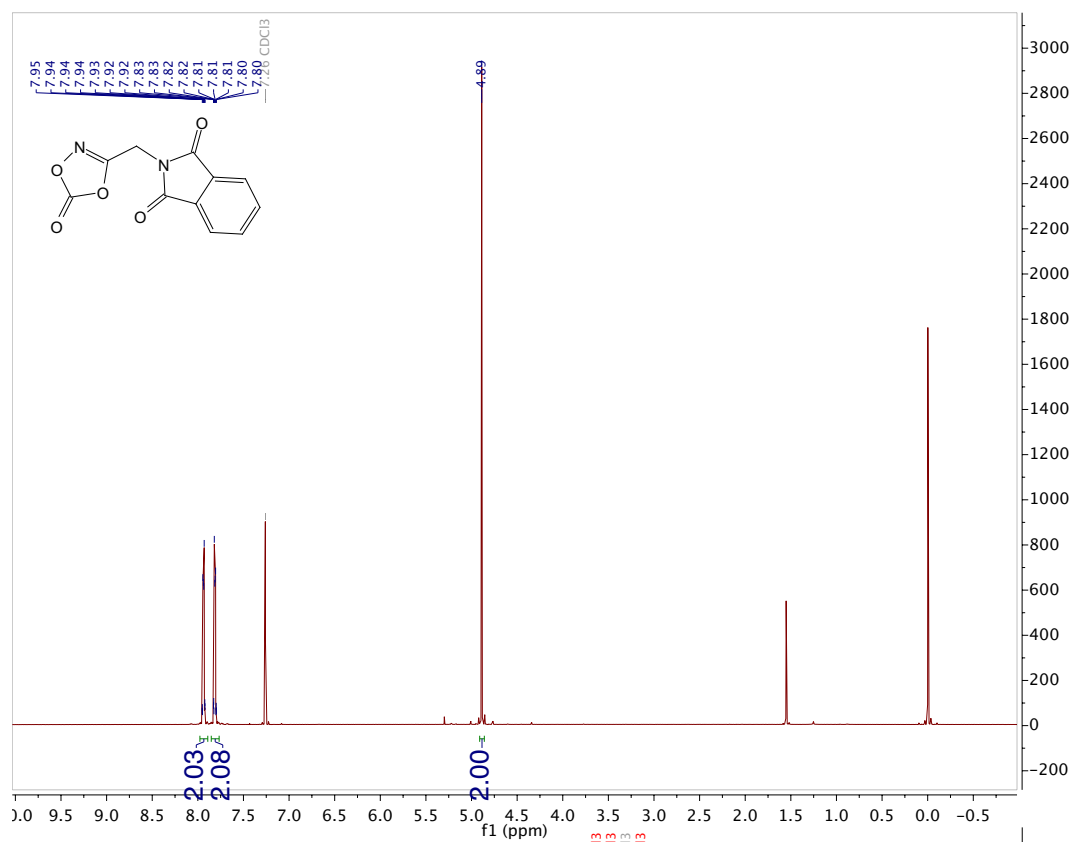
Totals : 6.60966e4 789.35767

Complex (S,S)-5.44

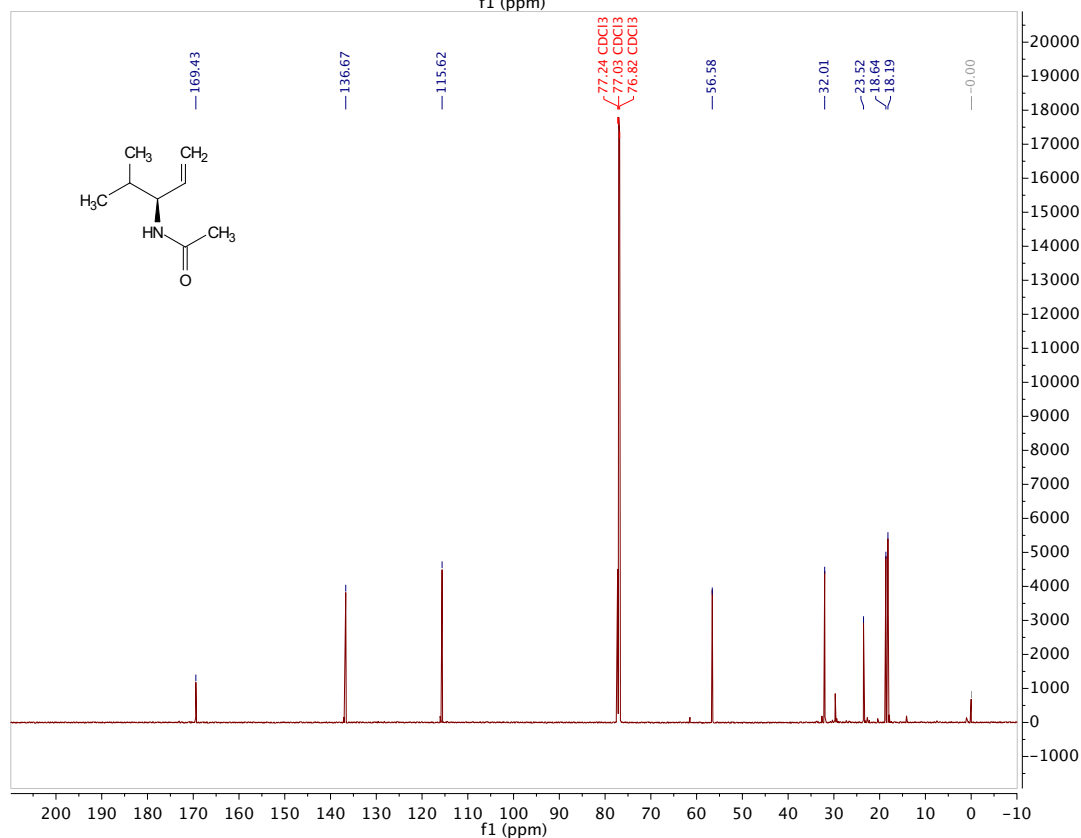
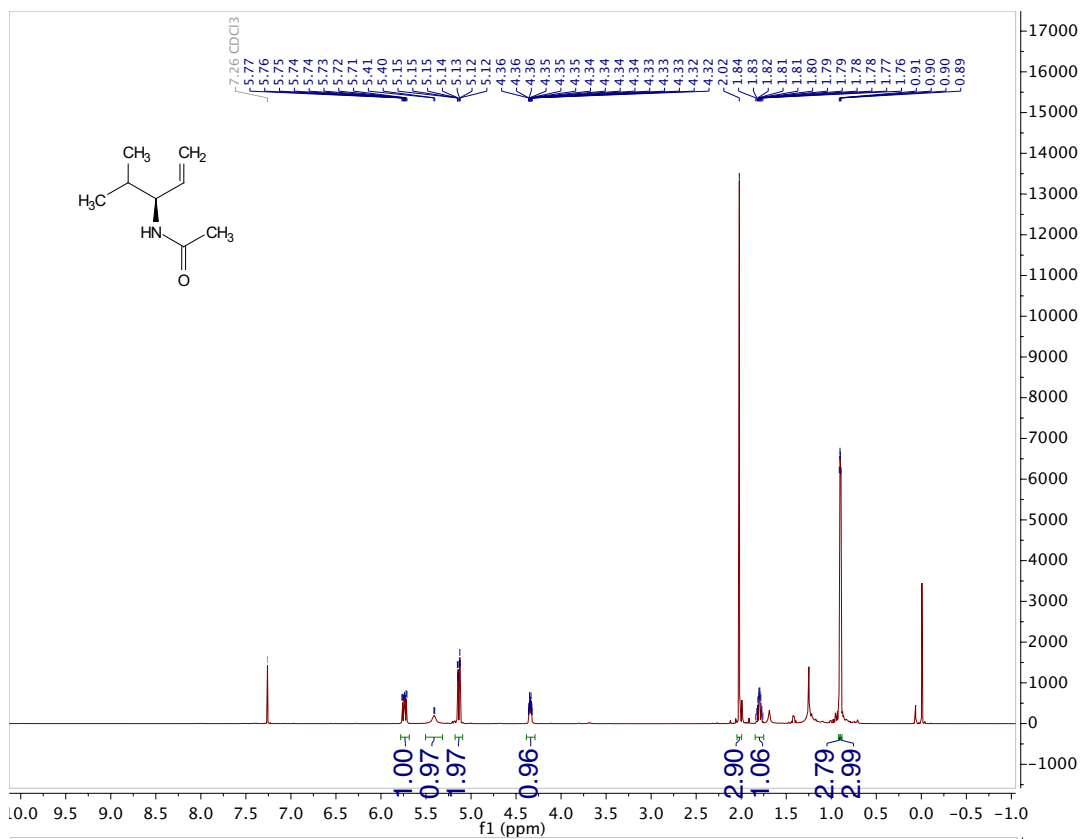


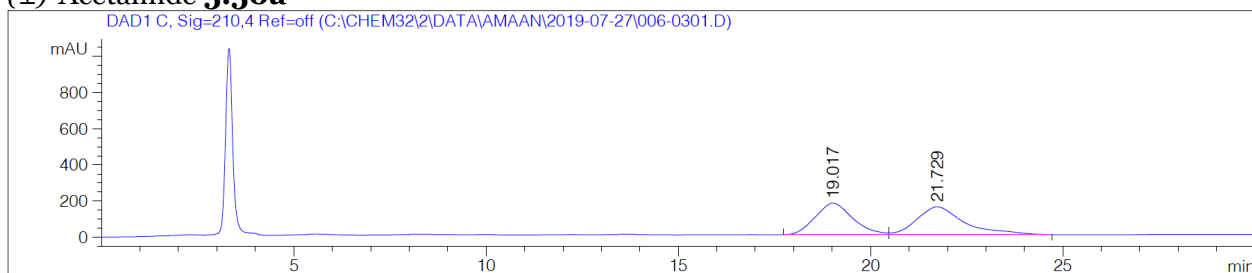
***N*-Cbz piperidine dioxazolone 5.49f**

Phth-glycine dioxazolone 5.49g



Acetamide 5.50a

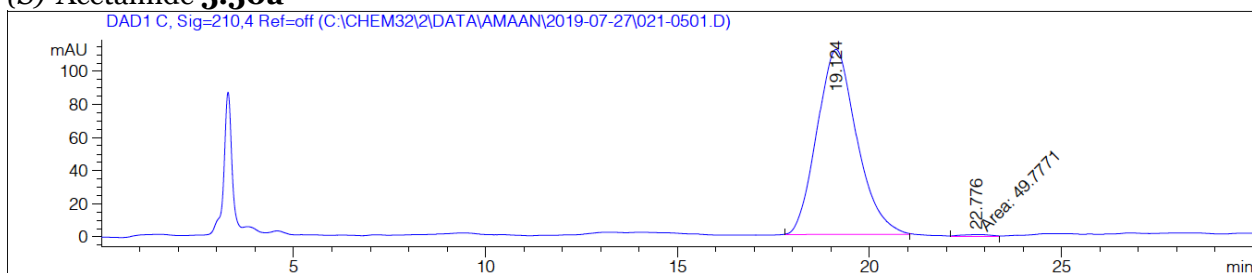


(±)-Acetamide 5.50a

Signal 1: DAD1 C, Sig=210,4 Ref=off

Peak #	RetTime [min]	Type	Width [min]	Area [mAU*s]	Height [mAU]	Area %
1	19.017	BV	0.9845	1.18197e4	174.45068	47.1135
2	21.729	VB	1.1997	1.32681e4	154.53239	52.8865

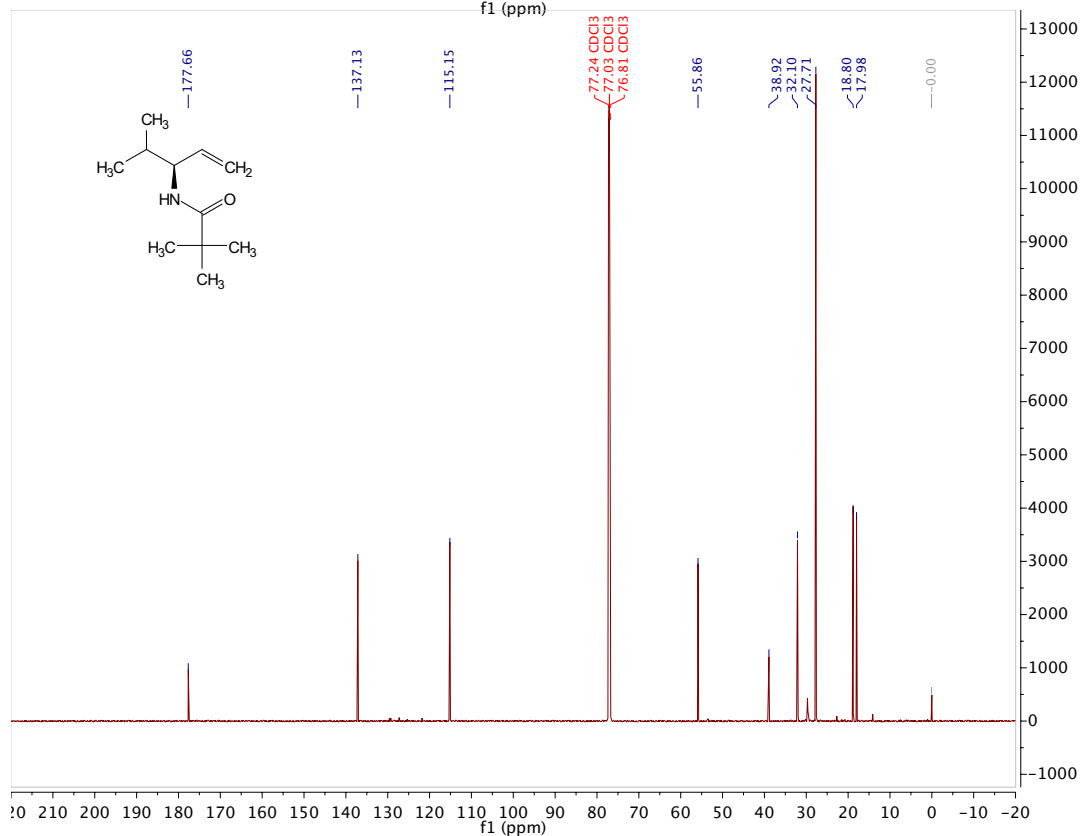
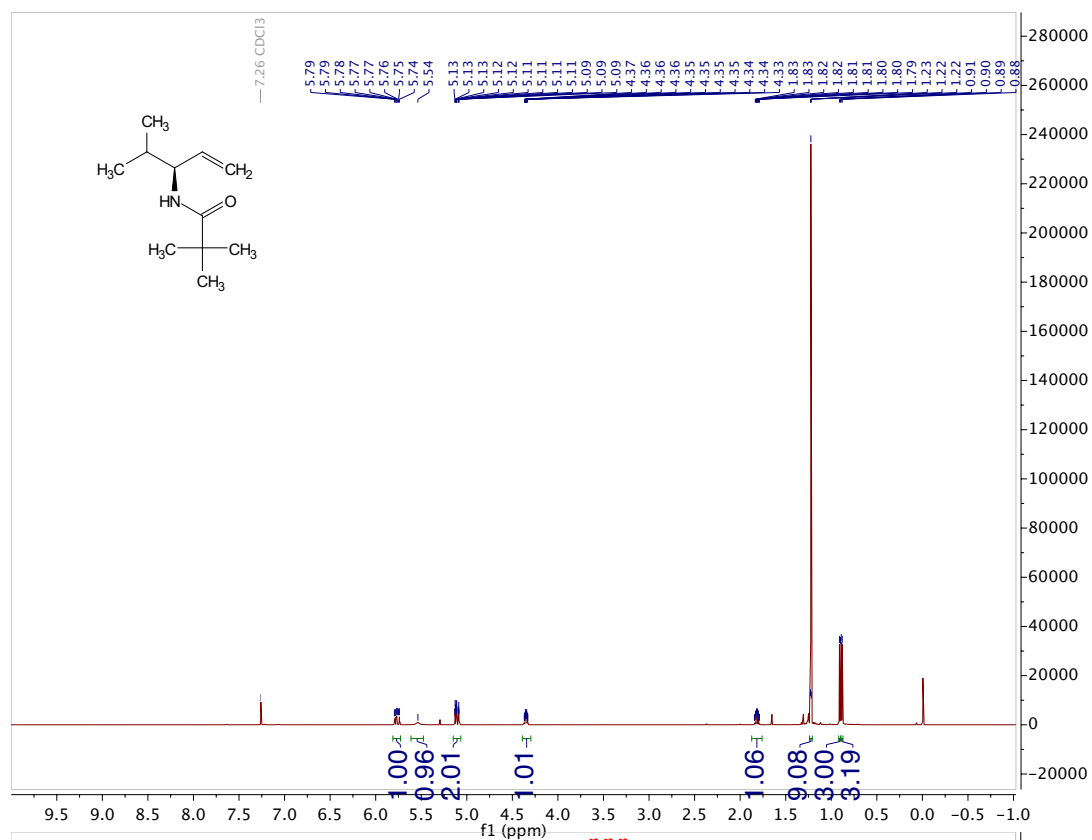
Totals : 2.50878e4 328.98308

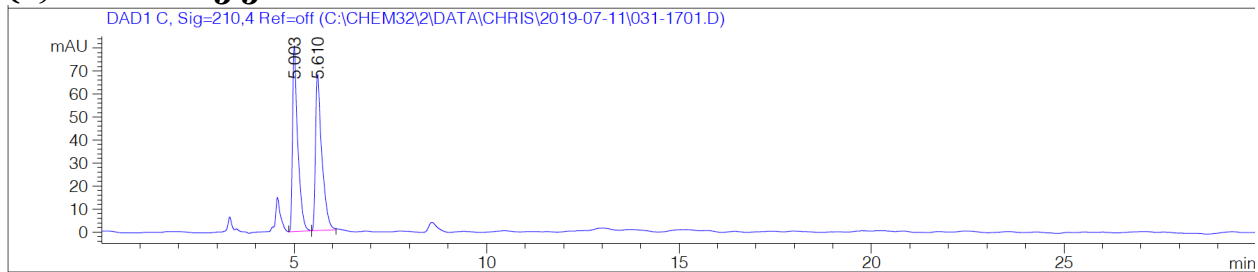
(S)-Acetamide 5.50a

Signal 1: DAD1 C, Sig=210,4 Ref=off

Peak #	RetTime [min]	Type	Width [min]	Area [mAU*s]	Height [mAU]	Area %
1	19.124	BB	1.0659	8066.80420	111.78791	99.3867
2	22.776	MM	0.8456	49.77714	9.81139e-1	0.6133

Totals : 8116.58134 112.76905

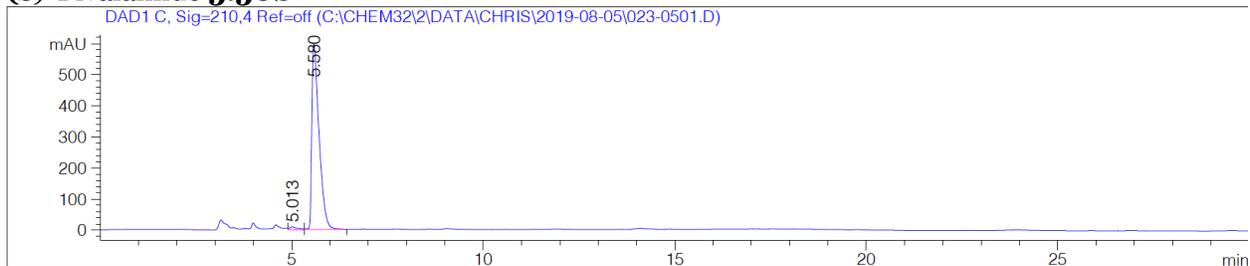
(S)-Pivalamide 5.50b

(±)-Pivalamide 5.50b

Signal 1: DAD1 C, Sig=210,4 Ref=off

Peak #	RetTime [min]	Type	Width [min]	Area [mAU*s]	Height [mAU]	Area %
1	5.003	VV	0.1348	767.14093	80.80962	50.2210
2	5.610	VB	0.1585	760.38782	67.99258	49.7790

Totals : 1527.52875 148.80220

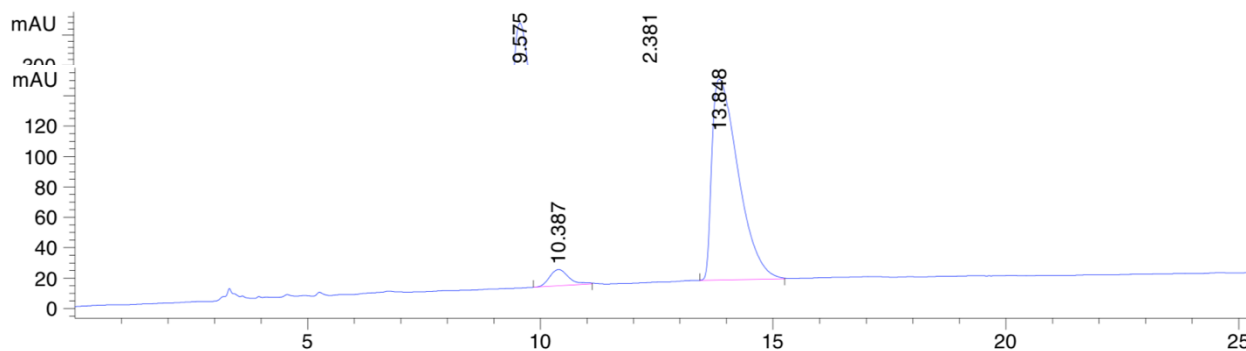
(S)-Pivalamide 5.50b

Signal 2: DAD1 C, Sig=210,4 Ref=off

Peak #	RetTime [min]	Type	Width [min]	Area [mAU*s]	Height [mAU]	Area %
1	5.013	VV	0.1808	126.23240	9.27309	1.6162
2	5.580	VB	0.1861	7684.32129	597.17950	98.3838

Totals : 7810.55369 606.45259

(±)-cyclohexanecarboxamide **5.50c**

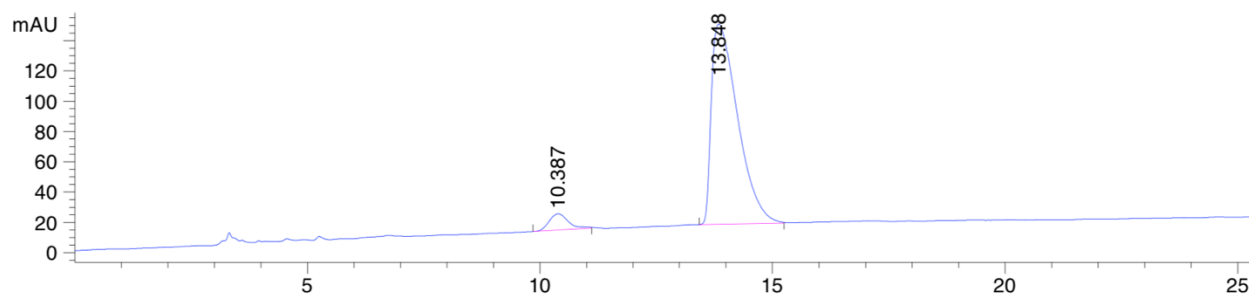


Signal 1: DAD1 C, Sig=210,4 Ref=off

Peak #	RetTime [min]	Type	Width [min]	Area [mAU*s]	Height [mAU]	Area %
1	10.387	BB	0.4364	308.14096	10.75106	5.6265
2	13.848	BB	0.6063	5168.50635	132.14665	94.3735

Totals : 5476.64731 142.89771

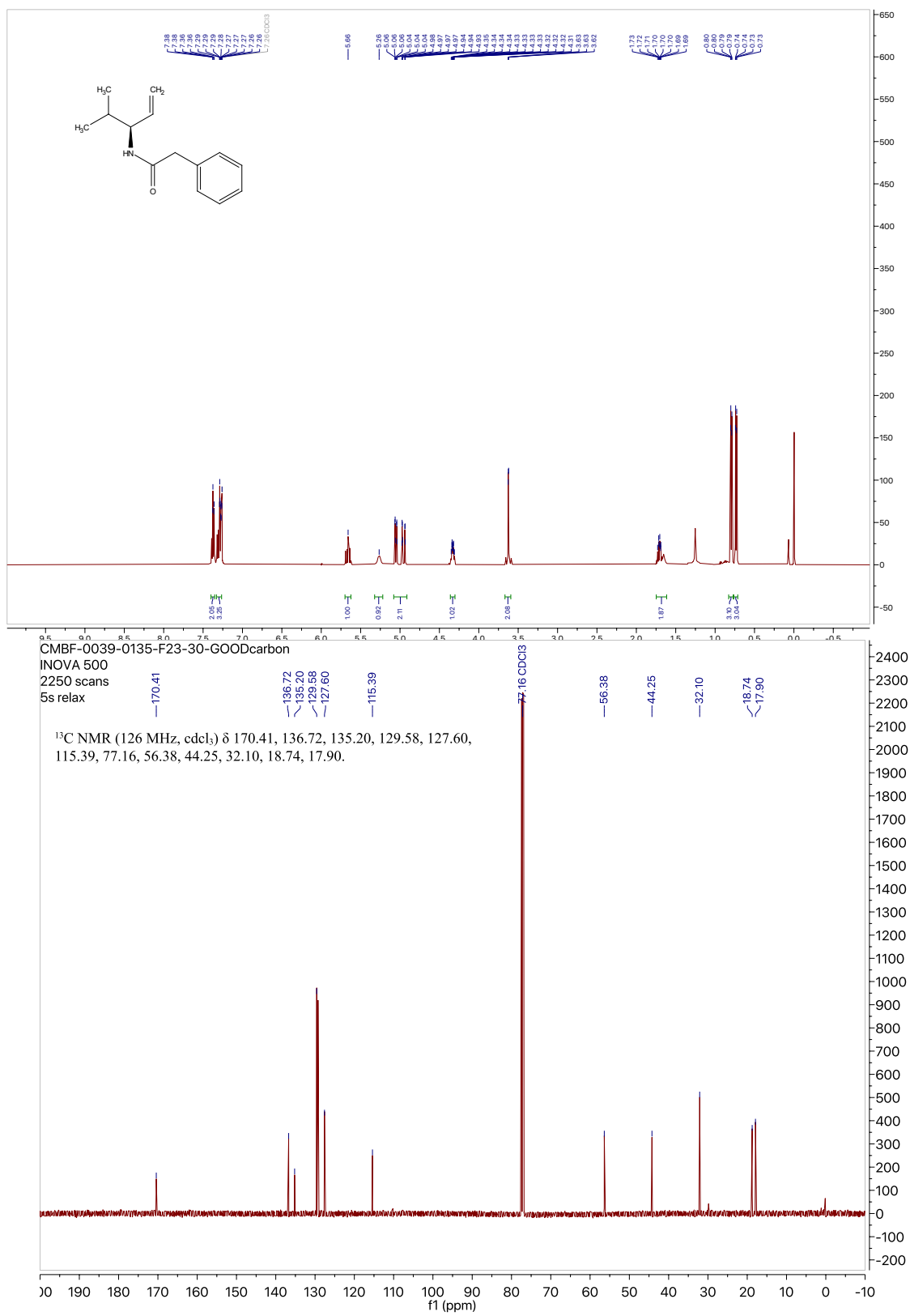
(S)- cyclohexanecarboxamide **5.50c**

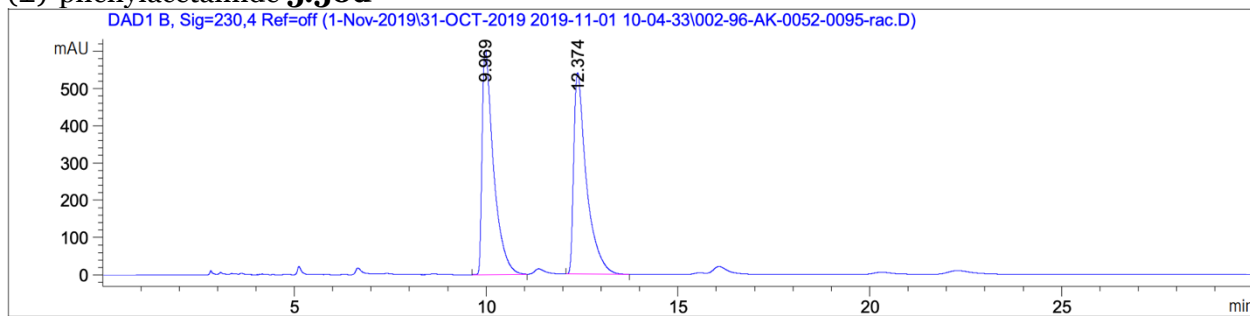


Signal 1: DAD1 C, Sig=210,4 Ref=off

Peak #	RetTime [min]	Type	Width [min]	Area [mAU*s]	Height [mAU]	Area %
1	10.387	BB	0.4364	308.14096	10.75106	5.6265
2	13.848	BB	0.6063	5168.50635	132.14665	94.3735

Totals : 5476.64731 142.89771

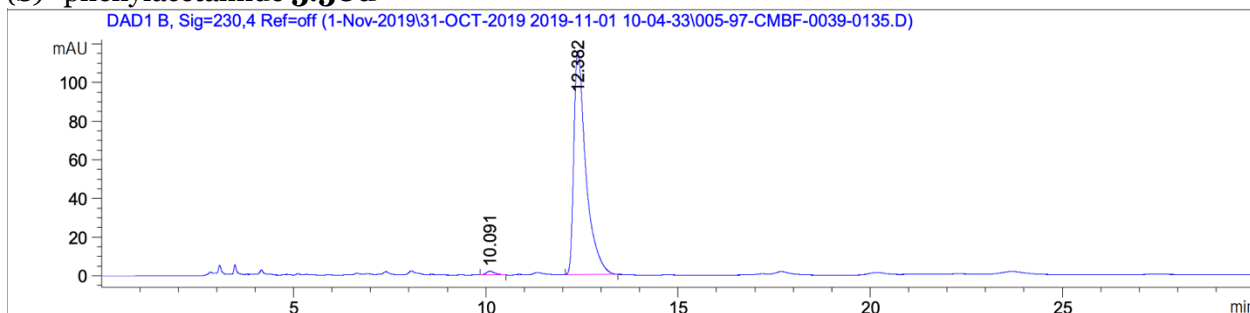
(S)-phenylacetamide **5.50d**

(±)-phenylacetamide 5.50d

Signal 2: DAD1 B, Sig=230,4 Ref=off

Peak #	RetTime [min]	Type	Width [min]	Area [mAU*s]	Height [mAU]	Area %
1	9.969	BB	0.2953	1.24203e4	601.79449	50.0175
2	12.374	BB	0.3257	1.24116e4	539.88324	49.9825

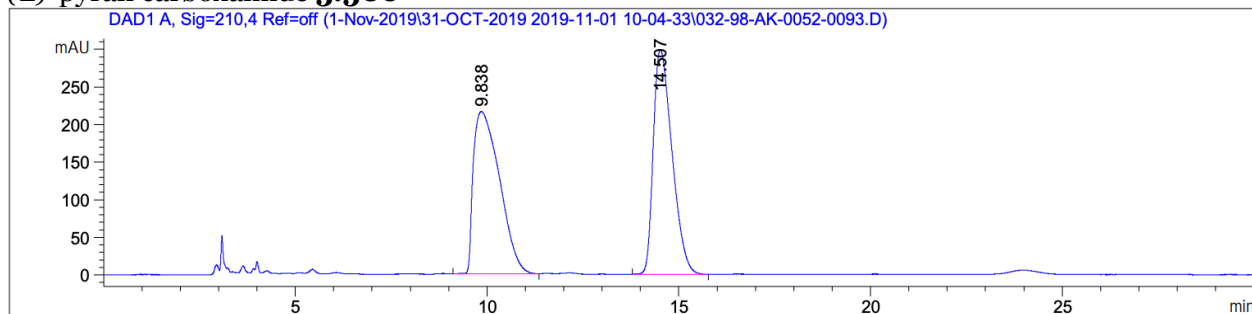
Totals : 2.48319e4 1141.67773

(S)- phenylacetamide 5.50d

Signal 2: DAD1 B, Sig=230,4 Ref=off

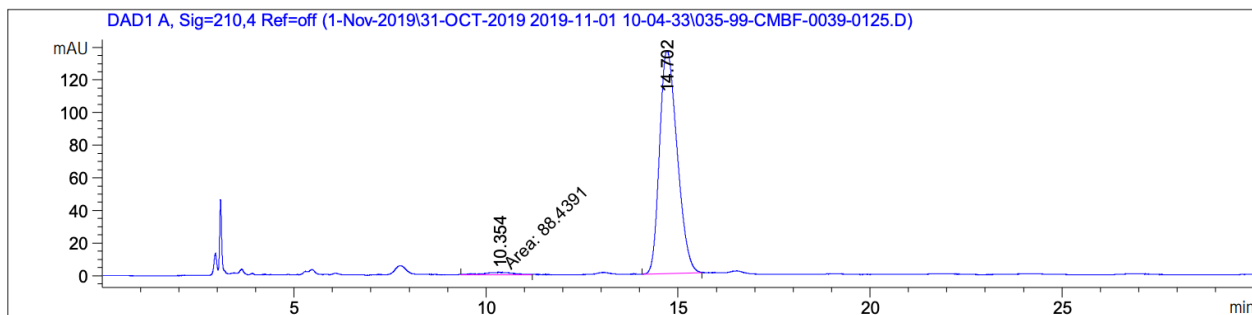
Peak #	RetTime [min]	Type	Width [min]	Area [mAU*s]	Height [mAU]	Area %
1	10.091	BB	0.1825	29.42900	1.91270	1.1574
2	12.382	BB	0.3081	2513.15894	115.86034	98.8426

Totals : 2542.58794 117.77304

(±)-pyran carboxamide 5.50e

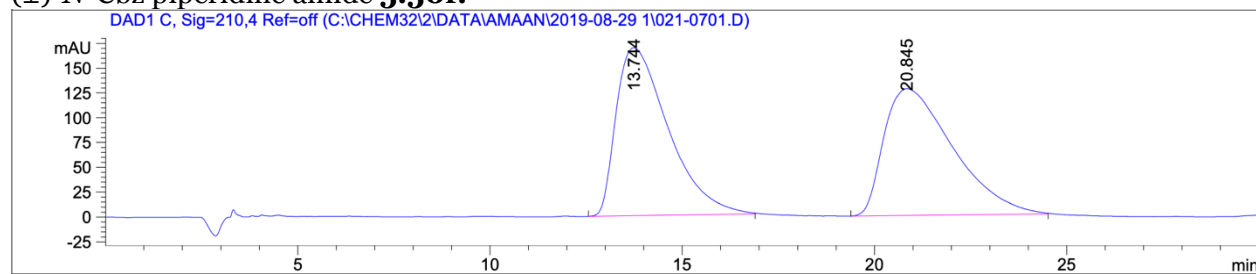
Peak #	RetTime [min]	Type	Width [min]	Area [mAU*s]	Height [mAU]	Area %
1	9.838	BB	0.5782	1.02362e4	216.05847	50.1859
2	14.507	BB	0.4867	1.01603e4	298.80368	49.8141

Totals : 2.03965e4 514.86215

(S)- pyran carboxamide 5.50e

Peak #	RetTime [min]	Type	Width [min]	Area [mAU*s]	Height [mAU]	Area %
1	10.354	MM	0.9799	88.43910	1.50416	1.9941
2	14.702	BB	0.3927	4346.60986	136.60260	98.0059

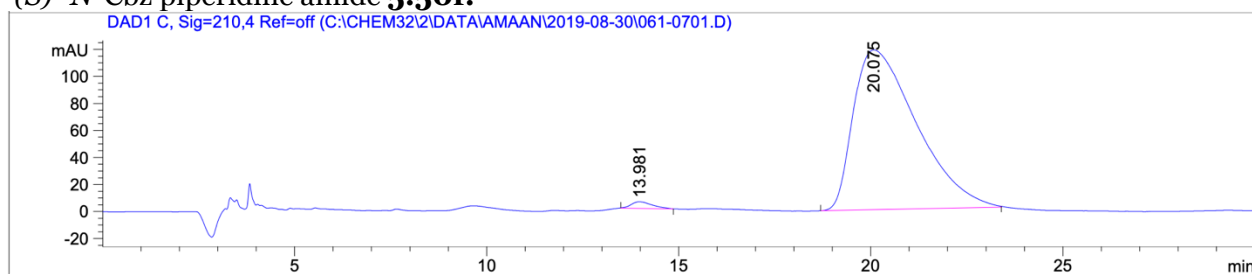
Totals : 4435.04897 138.10676

(±)-N-Cbz piperidine amide 5.5of:

Signal 1: DAD1 C, Sig=210,4 Ref=off

Peak #	RetTime [min]	Type	Width [min]	Area [mAU*s]	Height [mAU]	Area %
1	13.744	BB	1.4529	1.59141e4	169.26764	50.0525
2	20.845	BB	1.8050	1.58808e4	127.50879	49.9475

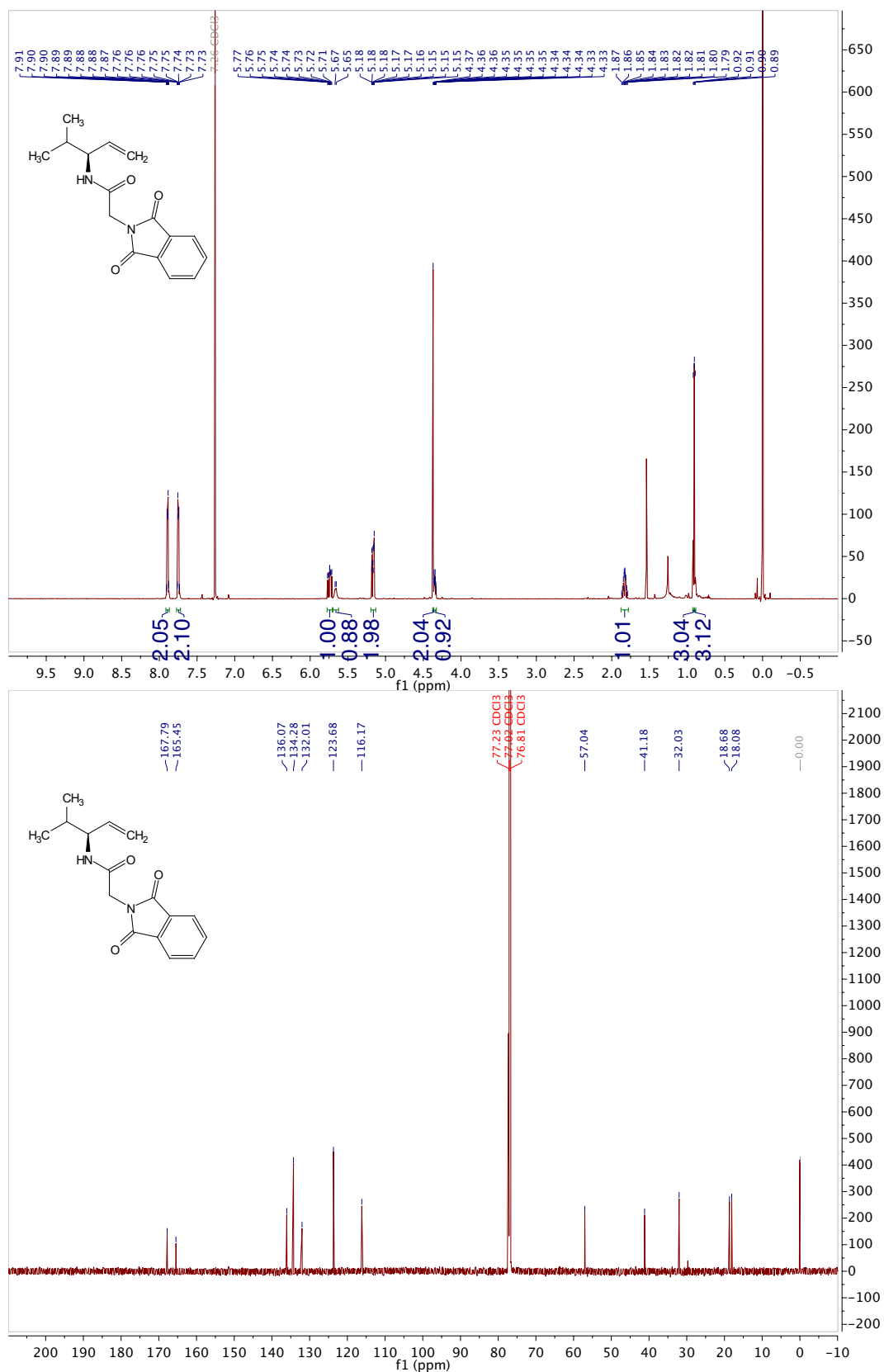
Totals : 3.17949e4 296.77643

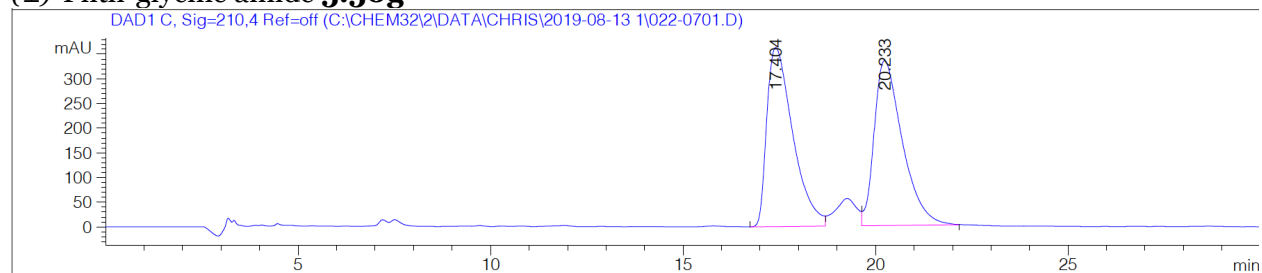
(S)-N-Cbz piperidine amide 5.5of:

Signal 1: DAD1 C, Sig=210,4 Ref=off

Peak #	RetTime [min]	Type	Width [min]	Area [mAU*s]	Height [mAU]	Area %
1	13.981	BB	0.5363	191.27362	4.95513	1.3938
2	20.075	BB	1.5830	1.35318e4	118.25837	98.6062

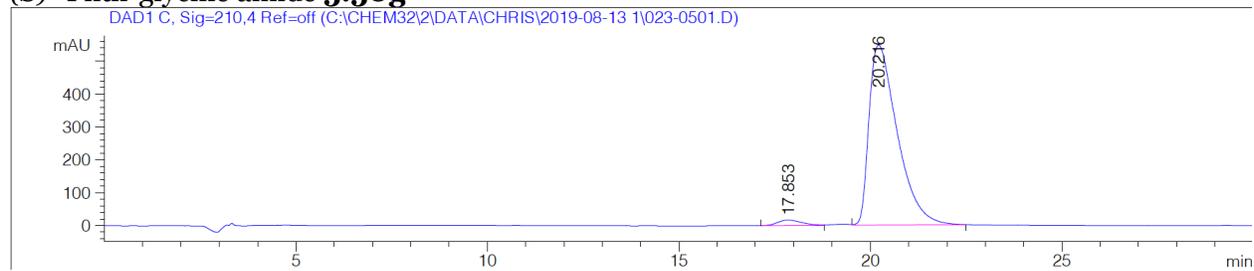
Totals : 1.37231e4 123.21350

(S)-Phth-glycine amide 5.50g

(±)-Phth-glycine amide 5.50g

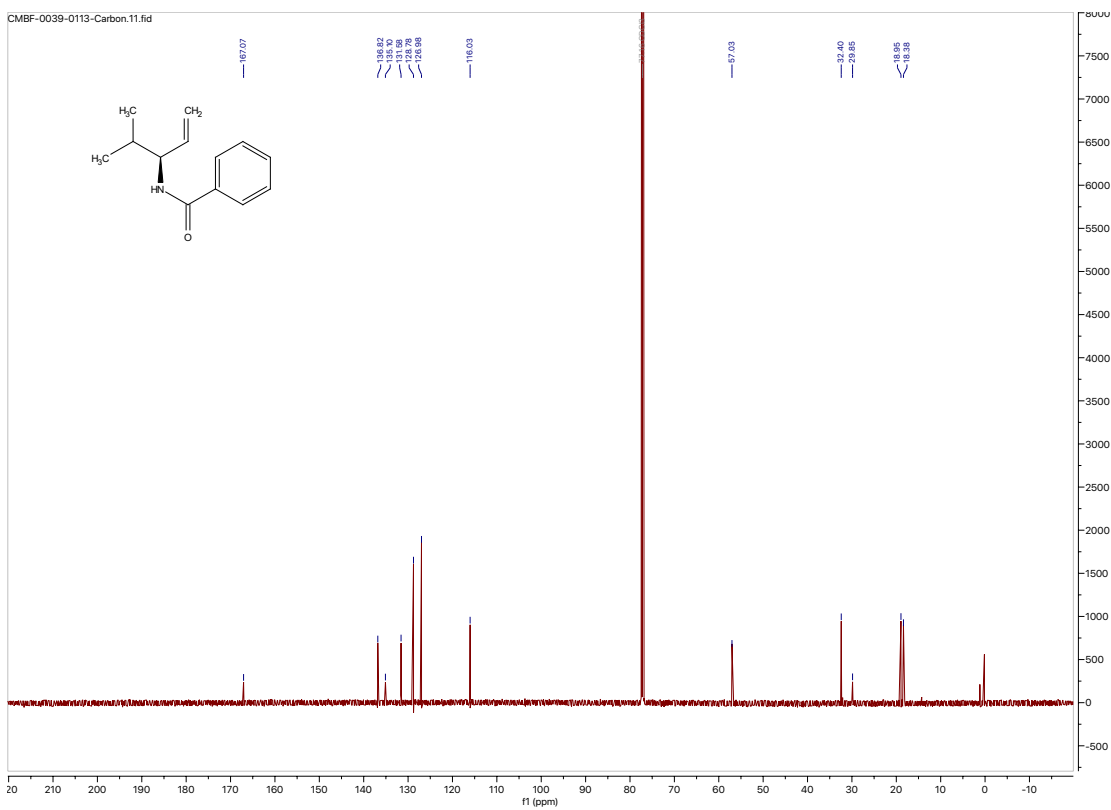
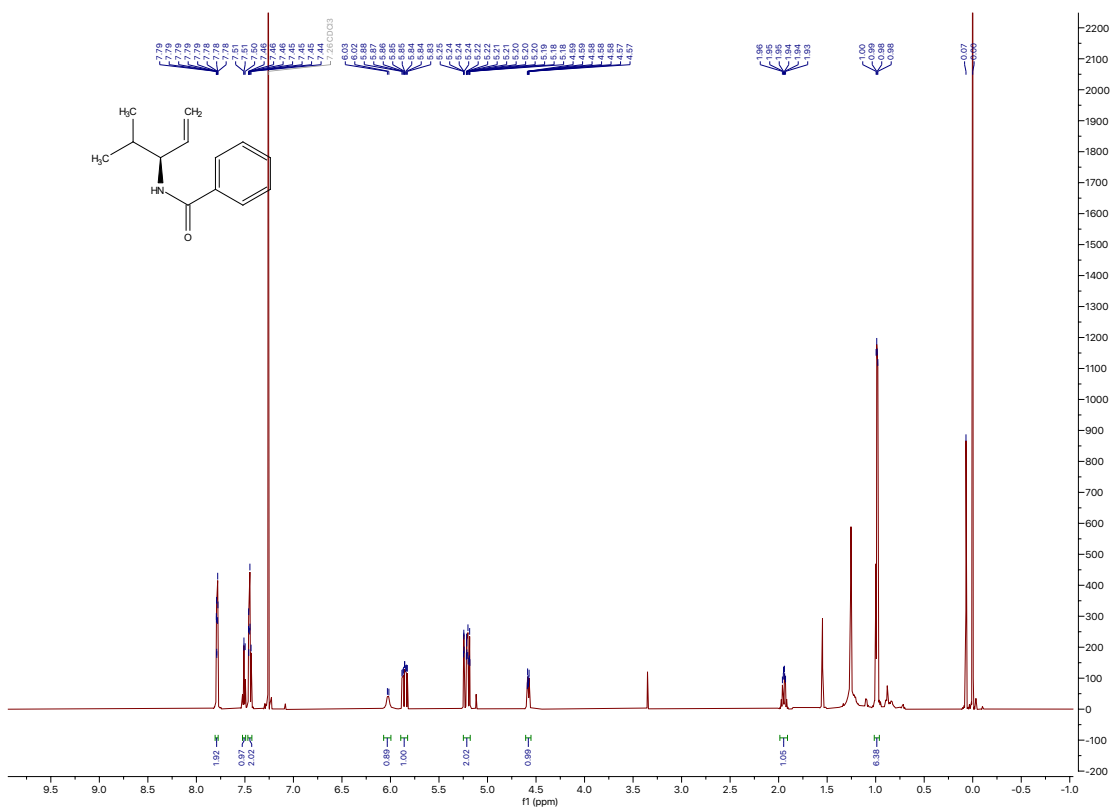
Peak #	RetTime [min]	Type	Width [min]	Area [mAU*s]	Height [mAU]	Area %
1	17.404	BV	0.7204	1.70021e4	362.99741	49.9559
2	20.233	VB	0.7666	1.70322e4	334.19327	50.0441

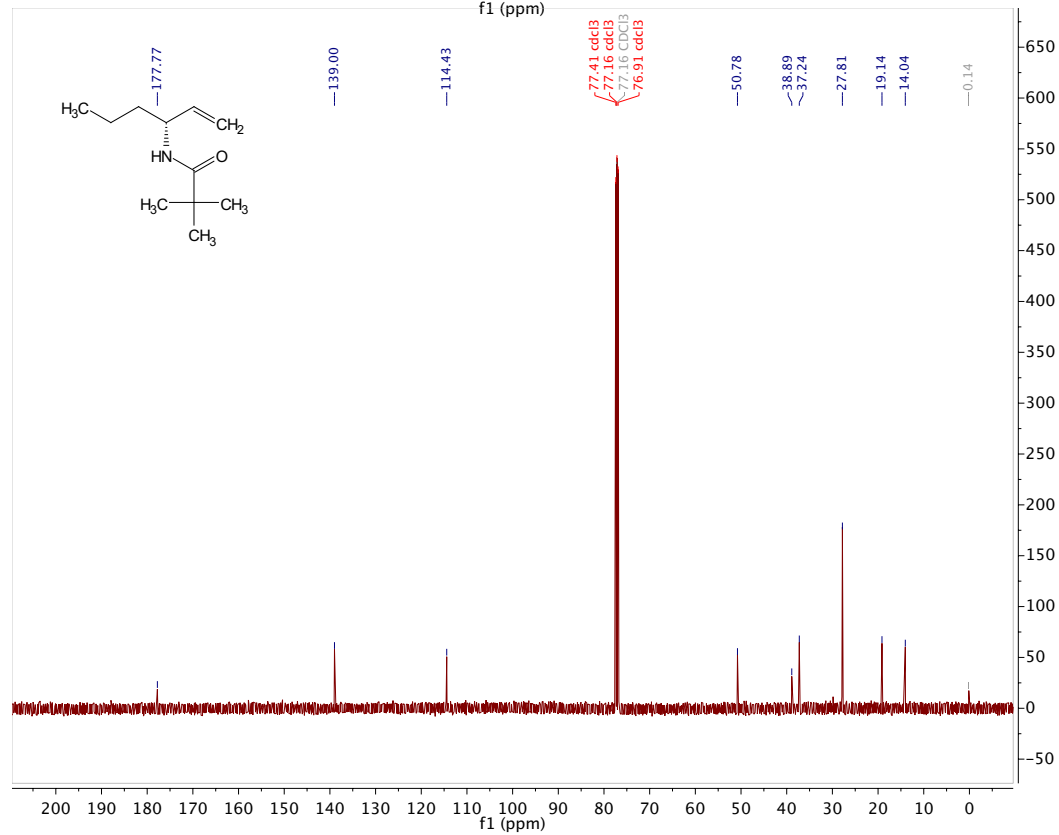
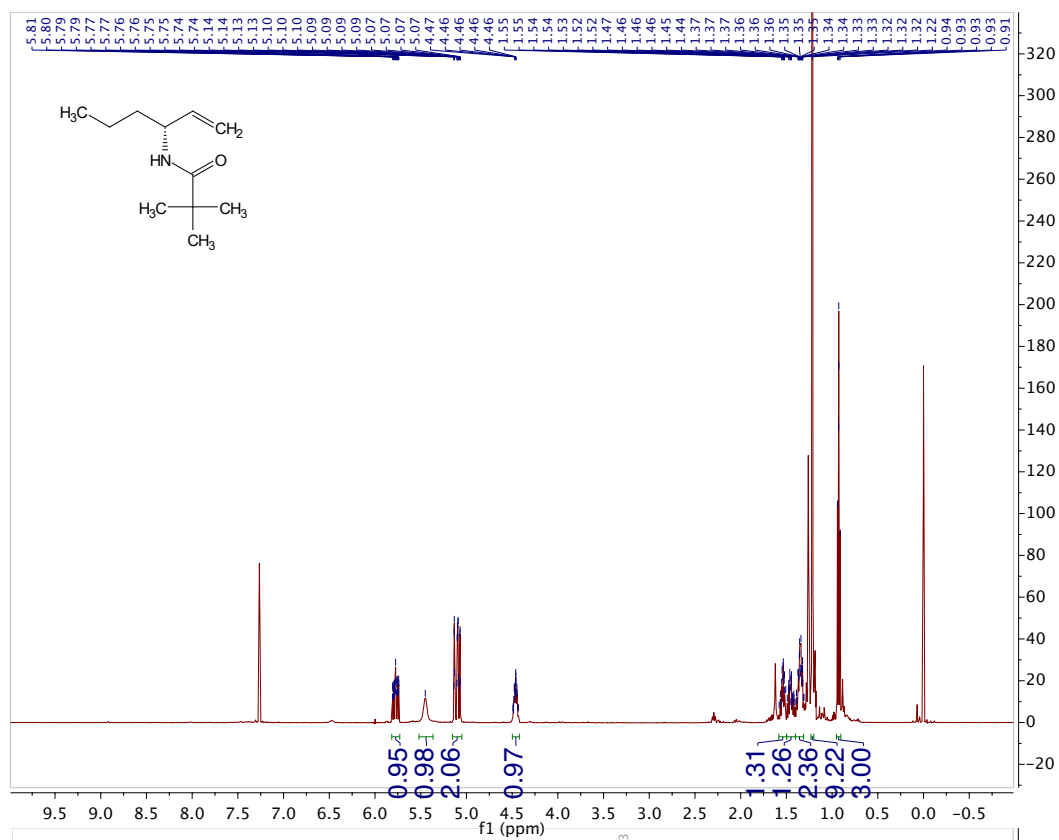
Totals : 3.40343e4 697.19067

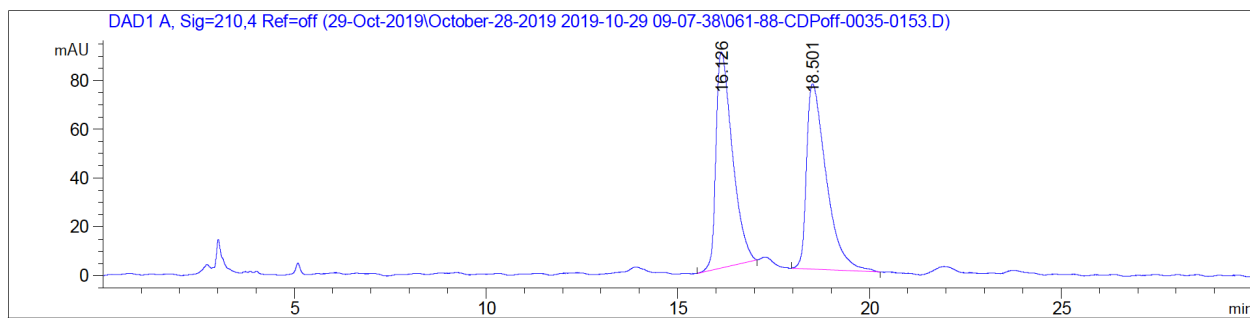
(S)- Phth-glycine amide 5.50g

Peak #	RetTime [min]	Type	Width [min]	Area [mAU*s]	Height [mAU]	Area %
1	17.853	BV	0.6325	740.67694	16.66547	2.5624
2	20.216	VB	0.7857	2.81644e4	547.89539	97.4376

Totals : 2.89050e4 564.56085

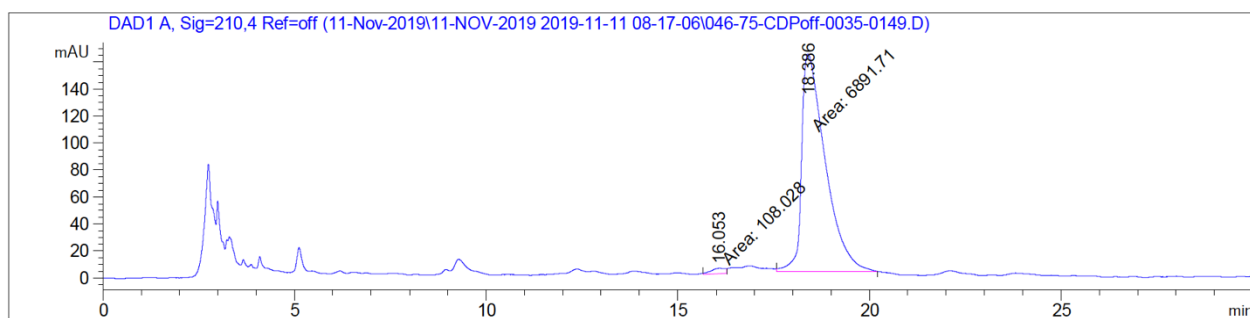
(S)-benzamide 5.50h

(R)-pivalamide 5.52a

(±)-pivalamide 5.52a

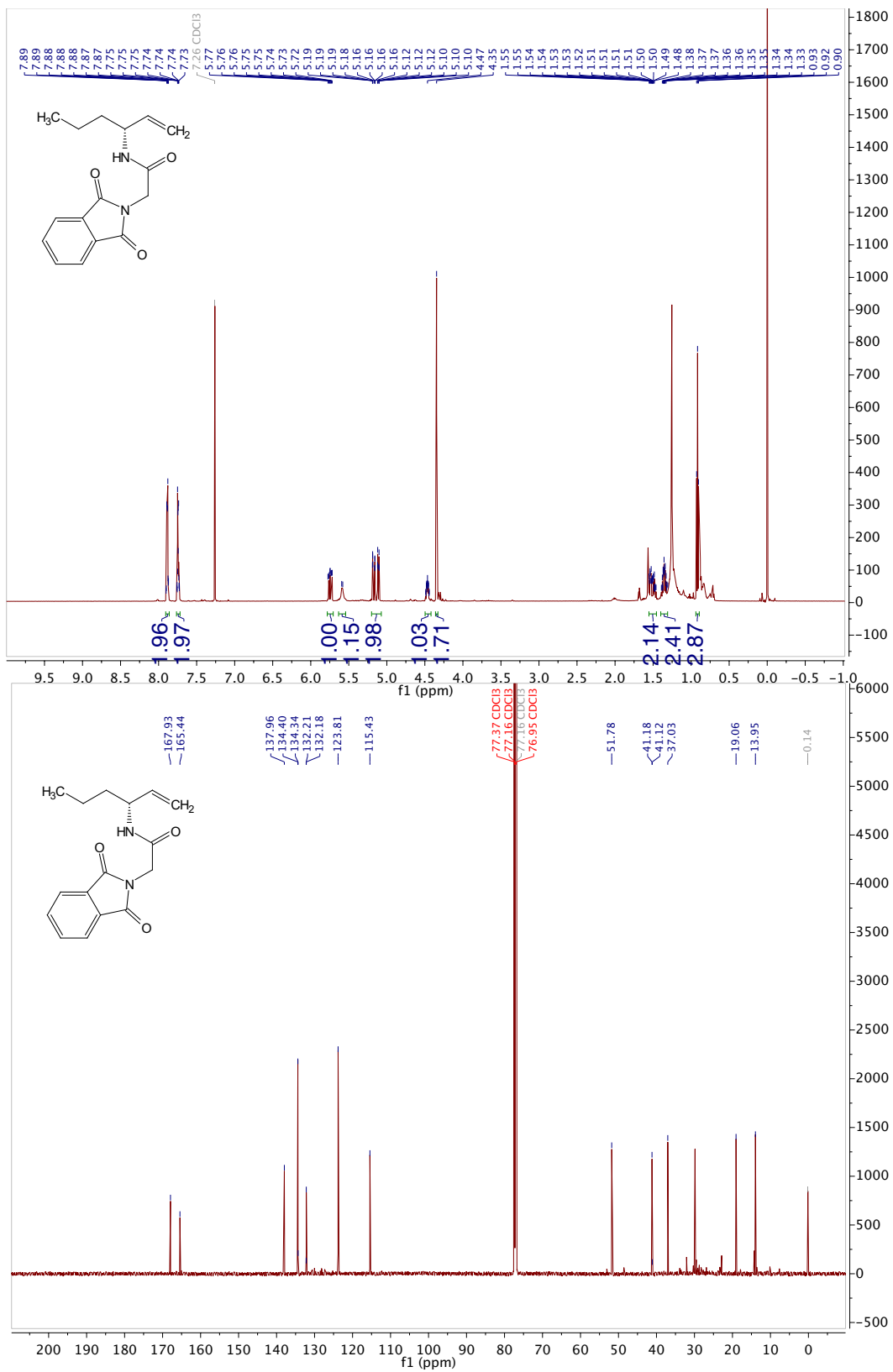
Peak #	RetTime [min]	Type	Width [min]	Area [mAU*s]	Height [mAU]	Area %
1	16.126	BB	0.3726	2631.26929	88.56808	49.1456
2	18.501	BB	0.4307	2722.75781	75.95327	50.8544

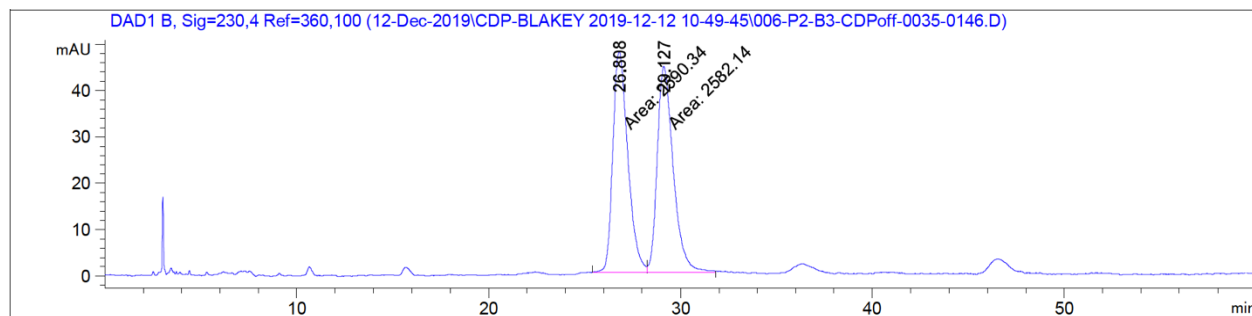
Totals : 5354.02710 164.52135

(R)- pivalamide 5.52a

Peak #	RetTime [min]	Type	Width [min]	Area [mAU*s]	Height [mAU]	Area %
1	16.053	MM	0.4373	108.02784	4.11707	1.5433
2	18.386	MM	0.7130	6891.71094	161.10773	98.4567

Totals : 6999.73878 165.22480

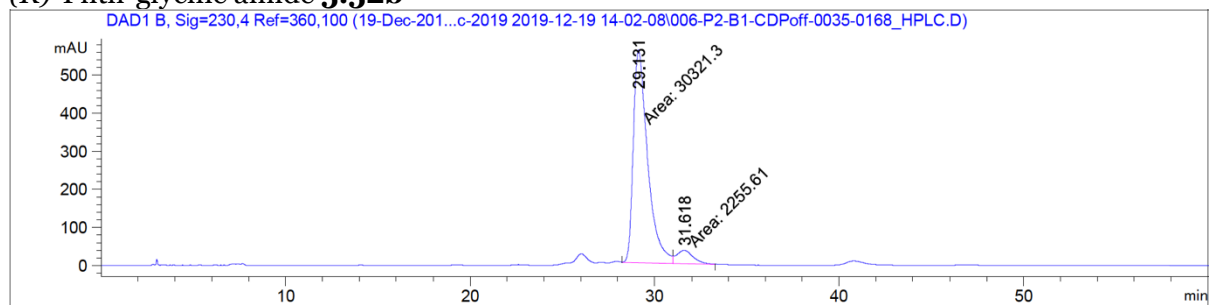
(R)-Phth-glycine amide 5.52b

(±)-Phth-glycine amide 5.52b

Signal 2: DAD1 B, Sig=230,4 Ref=360,100

Peak #	RetTime [min]	Type	Width [min]	Area [mAU*s]	Height [mAU]	Area %
1	26.808	MF	0.9051	2590.33911	47.69818	50.0793
2	29.127	FM	0.9676	2582.13672	44.47890	49.9207

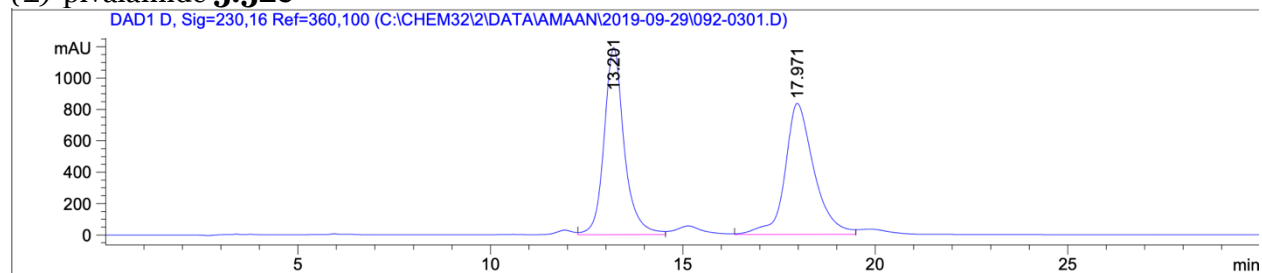
Totals : 5172.47583 92.17709

(R)-Phth-glycine amide 5.52b

Signal 2: DAD1 B, Sig=230,4 Ref=360,100

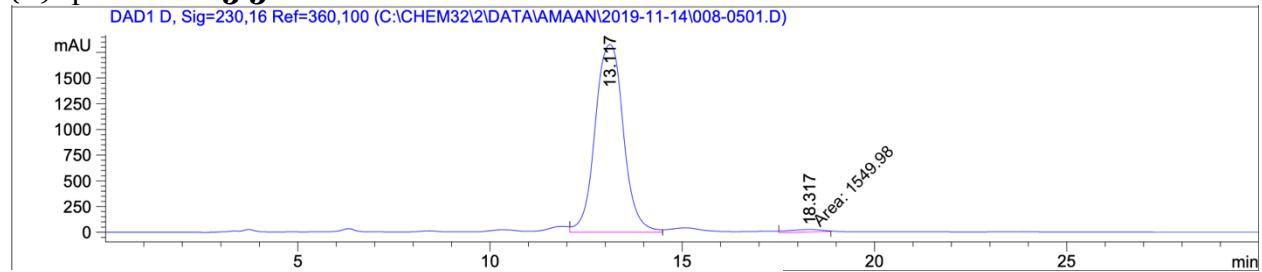
Peak #	RetTime [min]	Type	Width [min]	Area [mAU*s]	Height [mAU]	Area %
1	29.131	MF	0.9020	3.03213e4	560.25873	93.0761
2	31.618	FM	1.0542	2255.60840	35.66072	6.9239

Totals : 3.25769e4 595.91945

(±)-pivalamide 5.52c

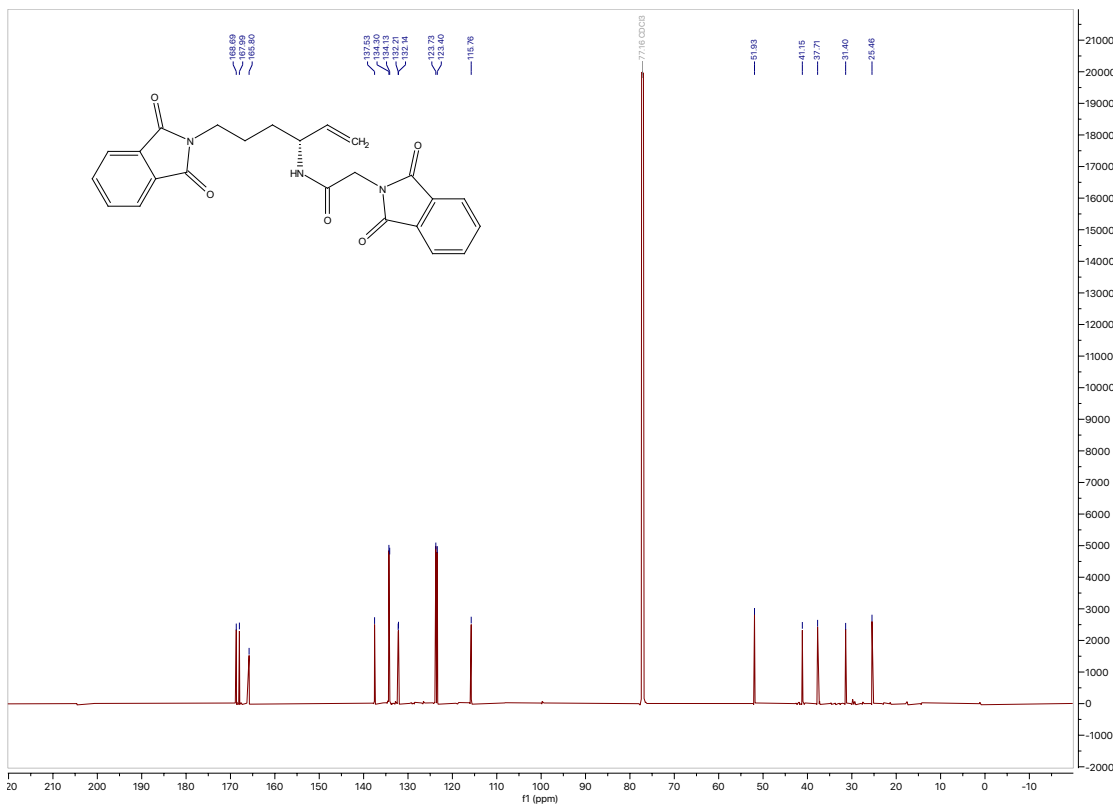
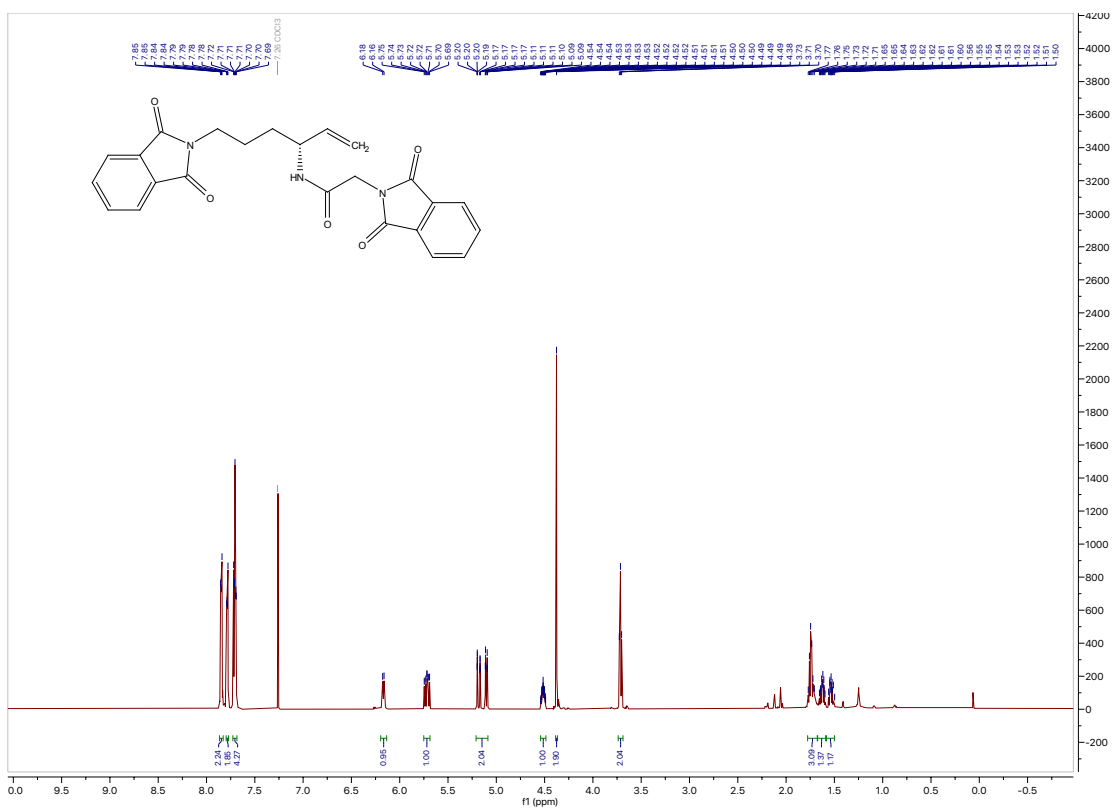
Peak #	RetTime [min]	Type	Width [min]	Area [mAU*s]	Height [mAU]	Area %
1	13.201	VV	0.5408	4.32601e4	1193.61682	49.6816
2	17.971	BV	0.7675	4.38145e4	835.98889	50.3184

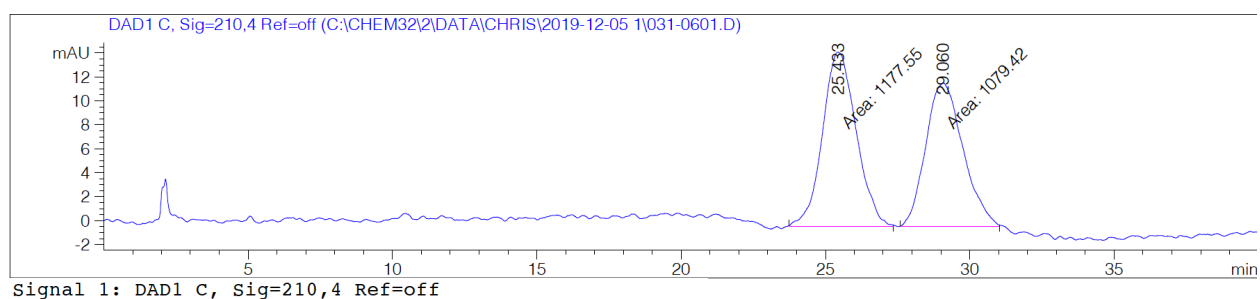
Totals : 8.70746e4 2029.60571

(R)- pivalamide 5.52c

Peak #	RetTime [min]	Type	Width [min]	Area [mAU*s]	Height [mAU]	Area %
1	13.117	VV	0.8071	9.34638e4	1826.09387	98.3687
2	18.317	MM	1.0358	1549.98071	24.93963	1.6313

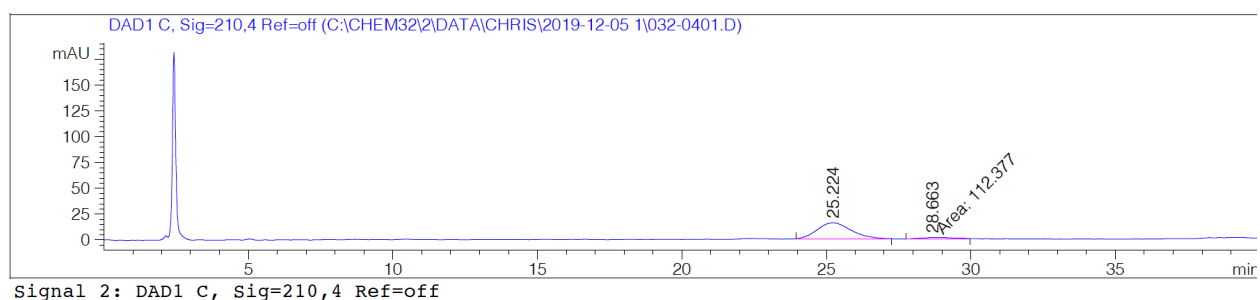
Totals : 9.50138e4 1851.03350

(R)-Phth-glycine amide 5.52d

(±)-Phth-glycine amide 5.52d

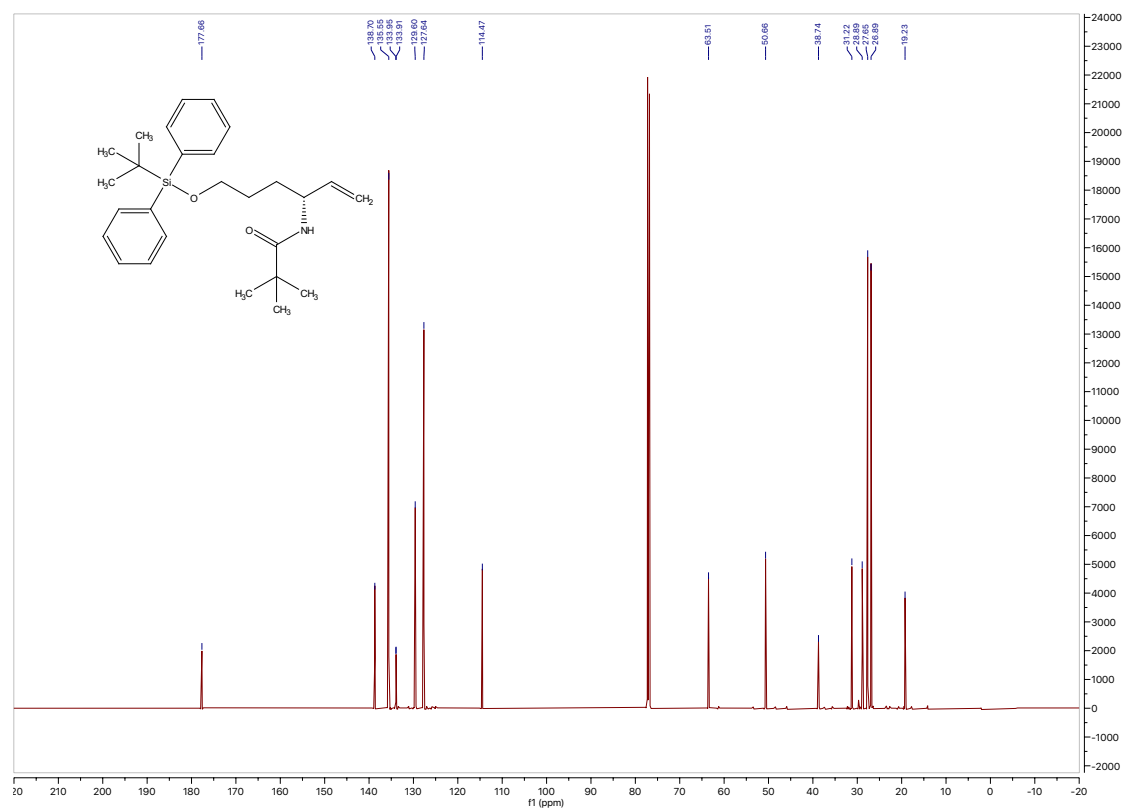
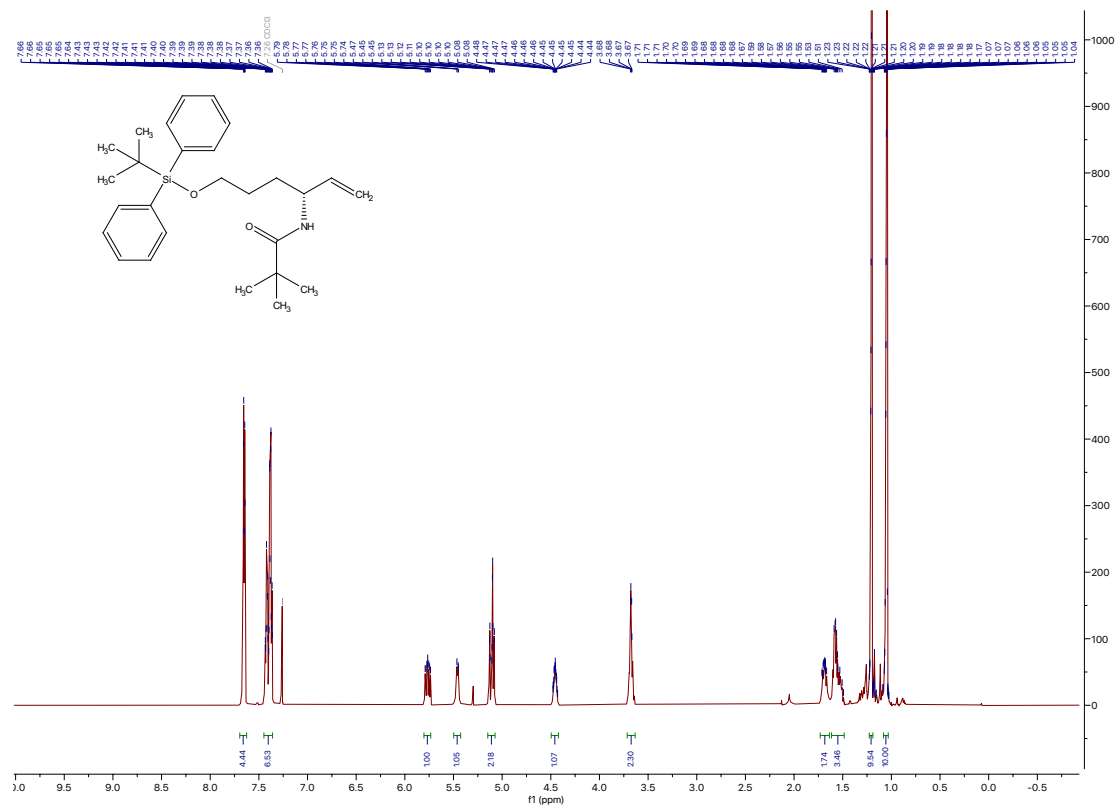
Peak #	RetTime [min]	Type	Width [min]	Area [mAU*s]	Height [mAU]	Area %
1	25.433	MM	1.3514	1177.55273	14.52247	52.1740
2	29.060	MM	1.4997	1079.41809	11.99581	47.8260

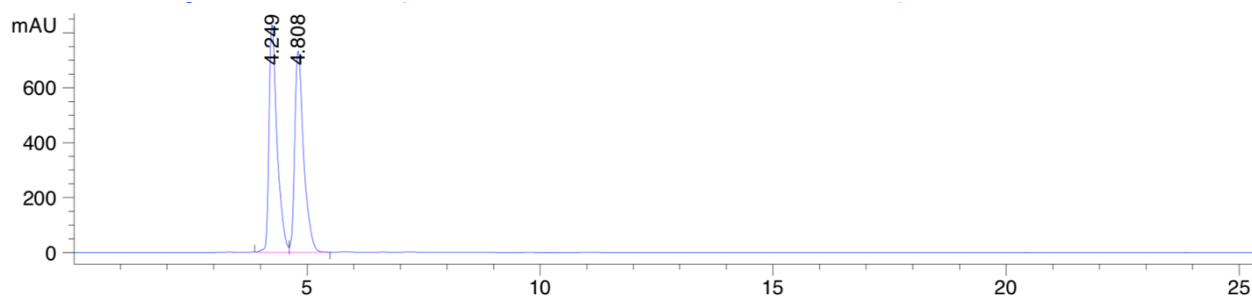
Totals : 2256.97083 26.51828

(R)- Phth-glycine amide 5.52d

Peak #	RetTime [min]	Type	Width [min]	Area [mAU*s]	Height [mAU]	Area %
1	25.224	BB	1.0140	1269.50793	15.49218	91.8678
2	28.663	MM	1.3726	112.37718	1.36449	8.1322

Totals : 1381.88512 16.85667

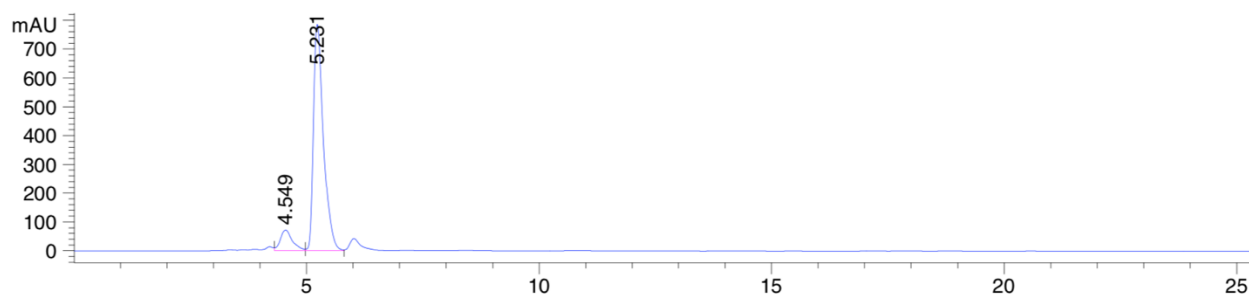
(R)-pivalamide 5.52e

(±)-pivalamide 5.52e

Signal 1: DAD1 D, Sig=230,16 Ref=360,100

Peak #	RetTime [min]	Type	Width [min]	Area [mAU*s]	Height [mAU]	Area %
1	4.249	BV	0.1793	1.00245e4	827.66113	50.5216
2	4.808	VB	0.2003	9817.56543	732.81635	49.4784

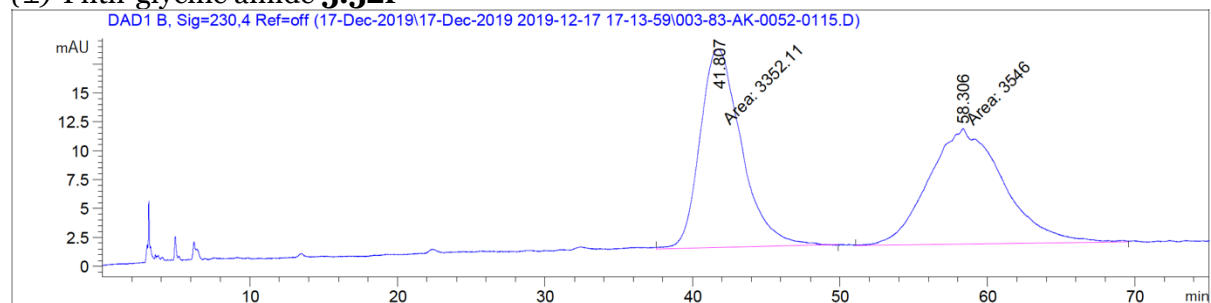
Totals : 1.98421e4 1560.47748

(R)- pivalamide 5.52e

Signal 1: DAD1 D, Sig=230,16 Ref=360,100

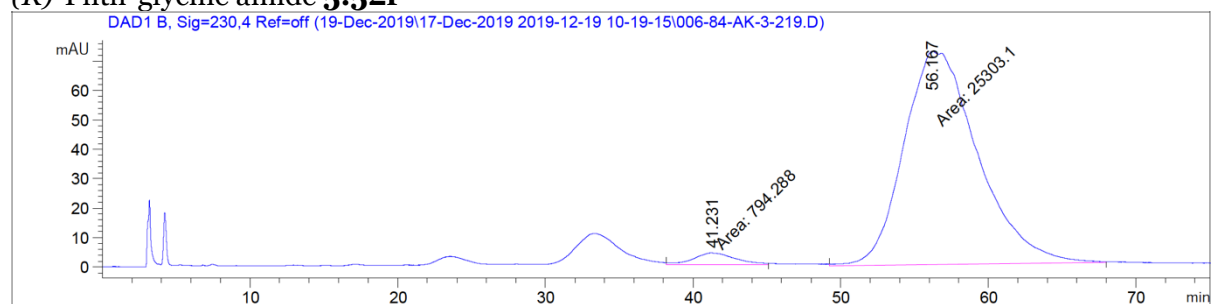
Peak #	RetTime [min]	Type	Width [min]	Area [mAU*s]	Height [mAU]	Area %
1	4.549	VV	0.2670	1279.76208	71.44872	9.8542
2	5.231	VV	0.2262	1.17072e4	784.25903	90.1458

Totals : 1.29870e4 855.70775

(±)-Phth-glycine amide 5.52f

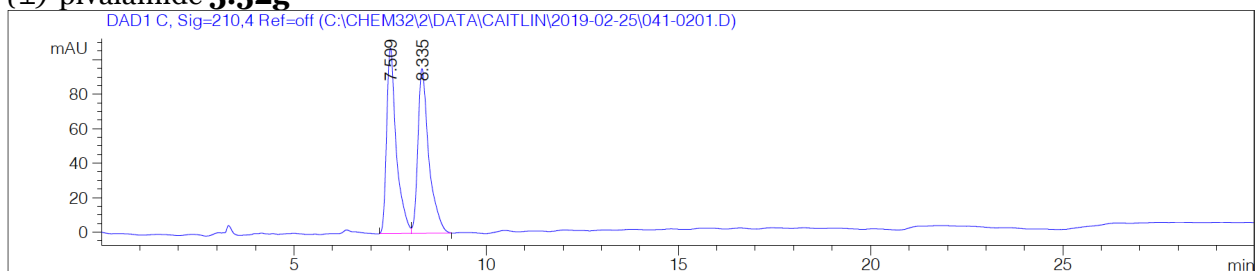
Peak #	RetTime [min]	Type	Width [min]	Area [mAU*s]	Height [mAU]	Area %
1	41.807	MM	3.2564	3352.10791	17.15645	48.5946
2	58.306	MM	5.9019	3545.99854	10.01379	51.4054

Totals : 6898.10645 27.17023

(R)-Phth-glycine amide 5.52f

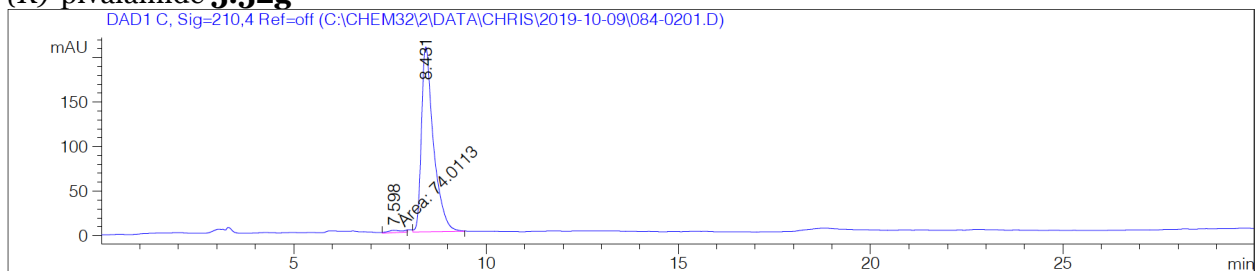
Peak #	RetTime [min]	Type	Width [min]	Area [mAU*s]	Height [mAU]	Area %
1	41.231	MM	3.2846	794.28815	4.03041	3.0436
2	56.167	MM	5.8123	2.53031e4	72.55560	96.9564

Totals : 2.60974e4 76.58601

(±)-pivalamide 5.52g

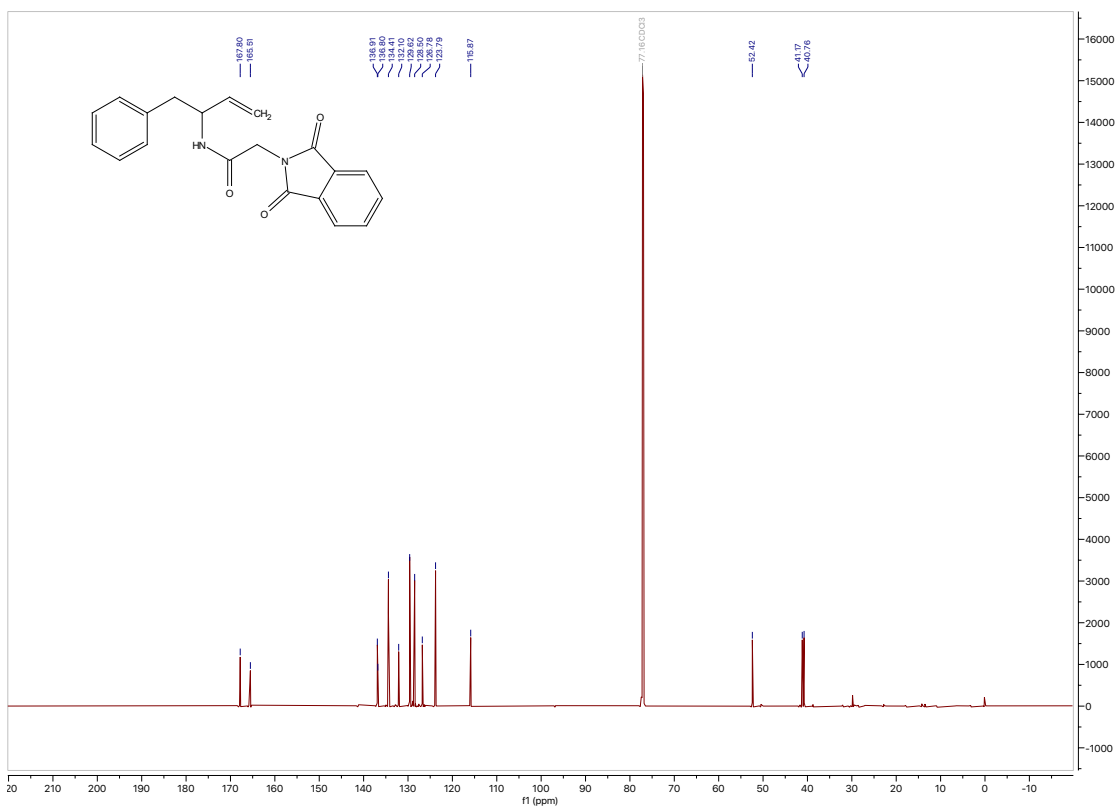
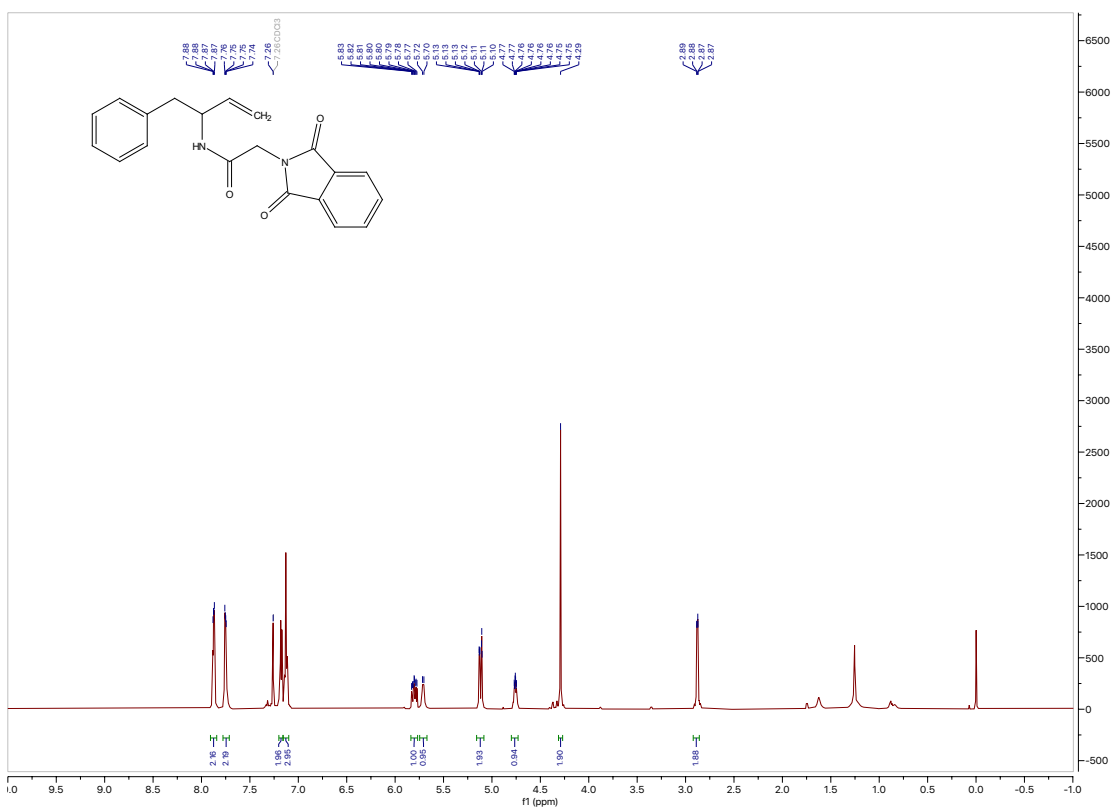
Peak #	RetTime [min]	Type	Width [min]	Area [mAU*s]	Height [mAU]	Area %
1	7.509	BV	0.2528	1852.07629	107.60557	49.7381
2	8.335	VB	0.2887	1871.58264	95.46971	50.2619

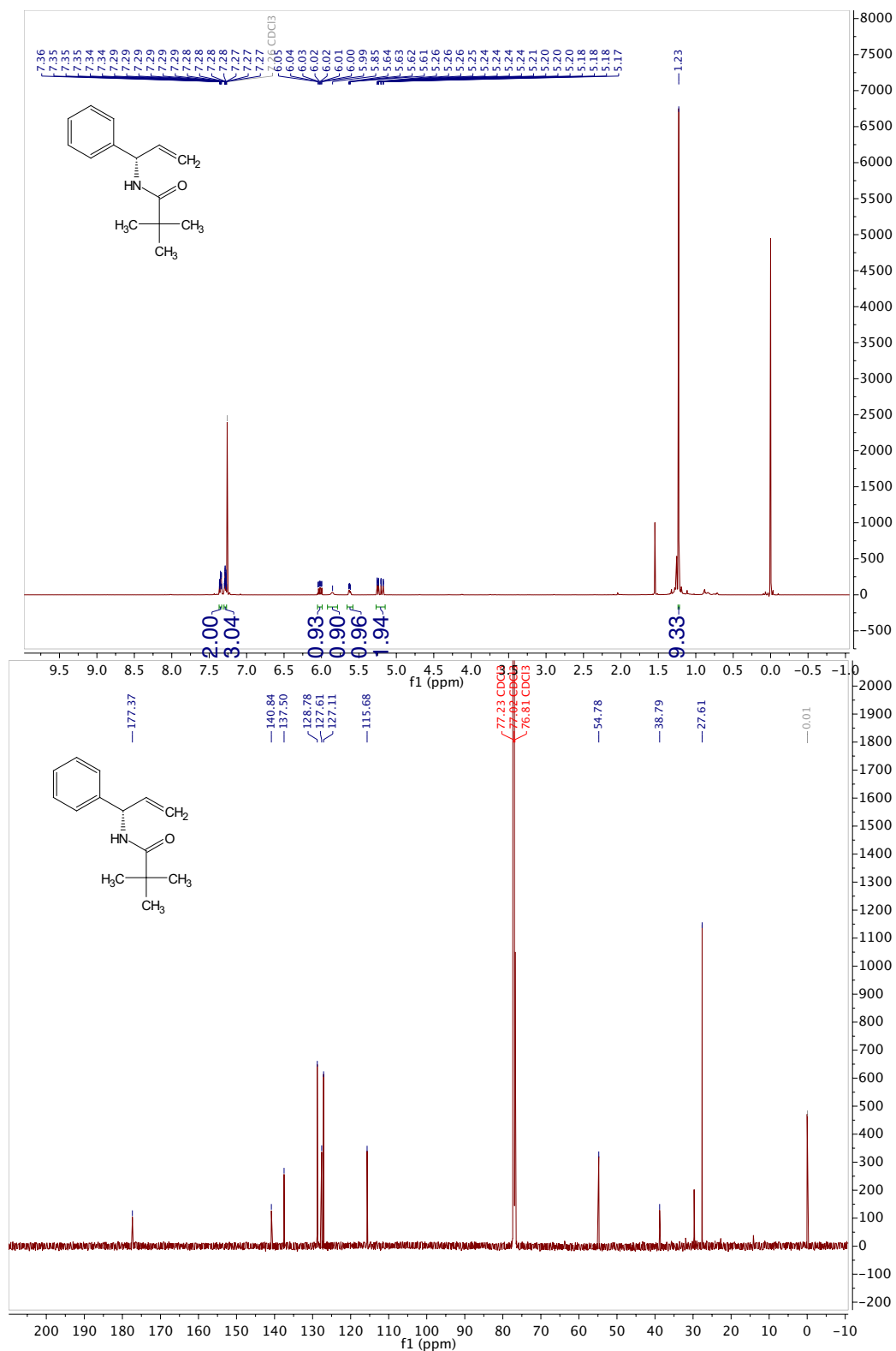
Totals : 3723.65894 203.07528

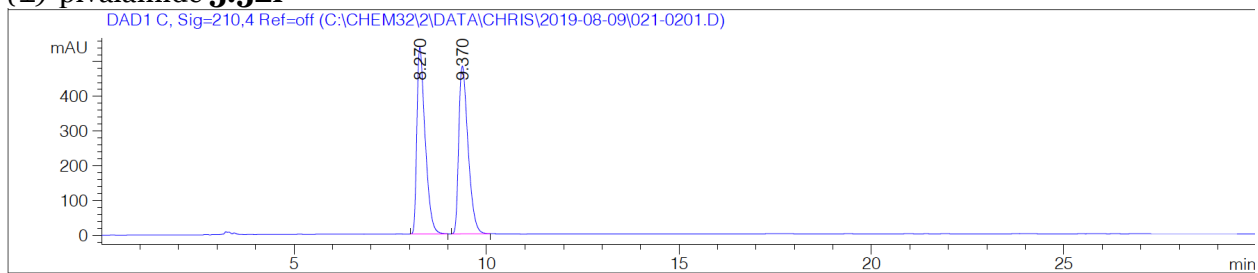
(R)-pivalamide 5.52g

Peak #	RetTime [min]	Type	Width [min]	Area [mAU*s]	Height [mAU]	Area %
1	7.598	MM	0.4611	74.01132	2.67536	1.6245
2	8.431	VB	0.3117	4481.90283	207.74052	98.3755

Totals : 4555.91415 210.41588

(R)-Phth-glycine amide 5.52h

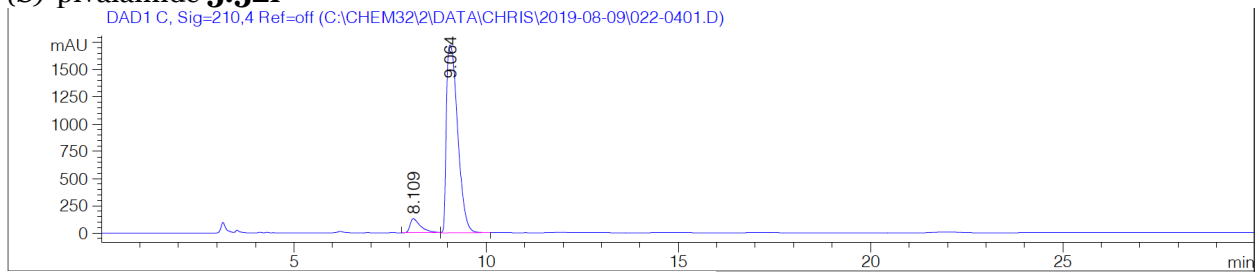
(S)-pivalamide 5.52i

(±)-pivalamide 5.52i

Signal 1: DAD1 C, Sig=210,4 Ref=off

Peak #	RetTime [min]	Type	Width [min]	Area [mAU*s]	Height [mAU]	Area %
1	8.270	BB	0.2251	7979.37158	537.64404	49.9904
2	9.370	BB	0.2526	7982.44971	483.54959	50.0096

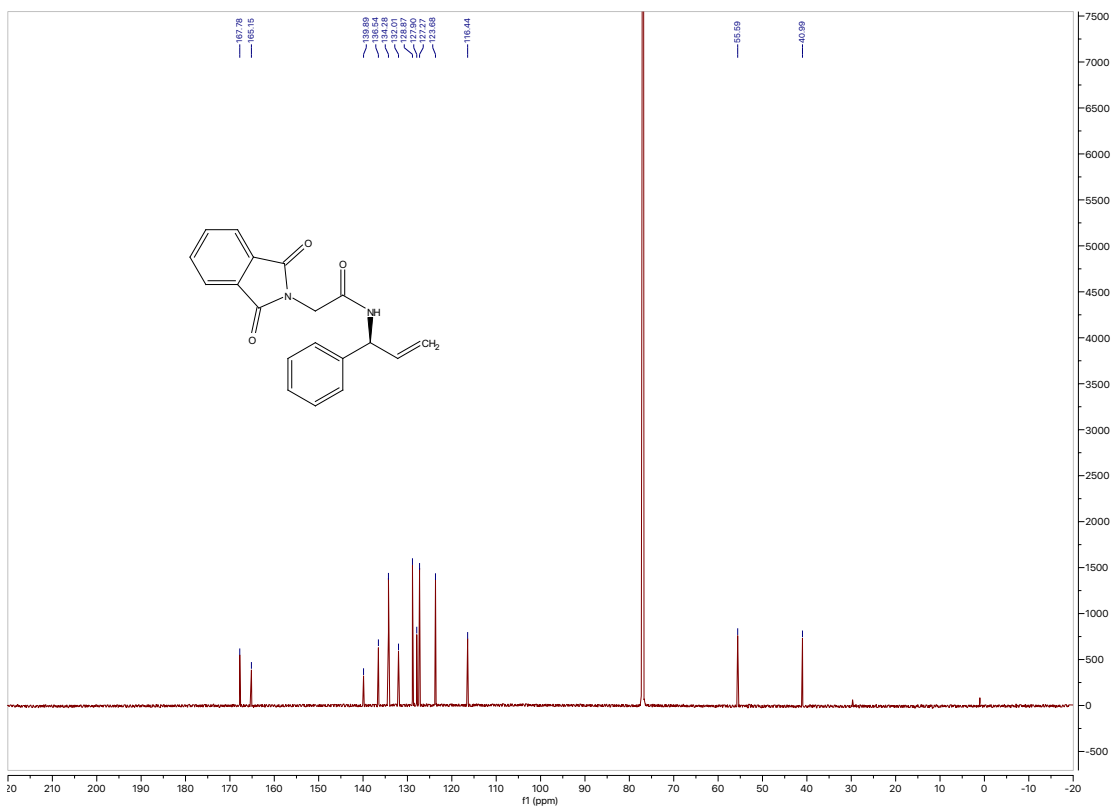
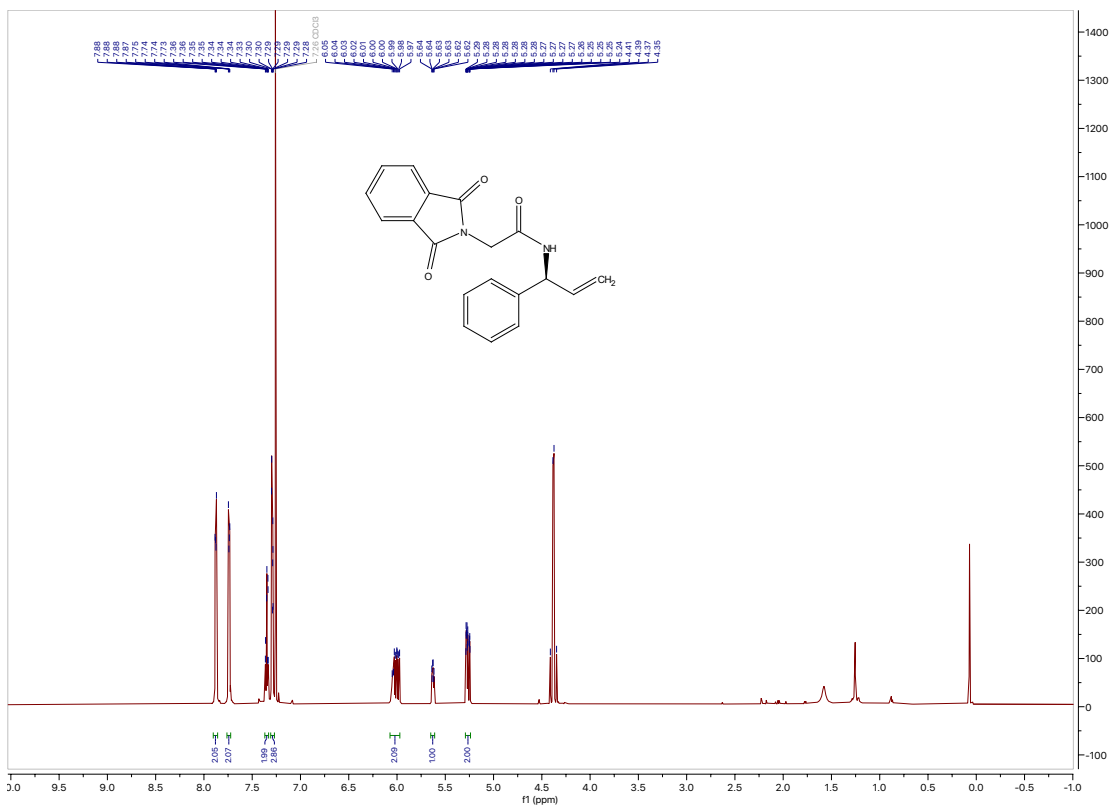
Totals : 1.59618e4 1021.19363

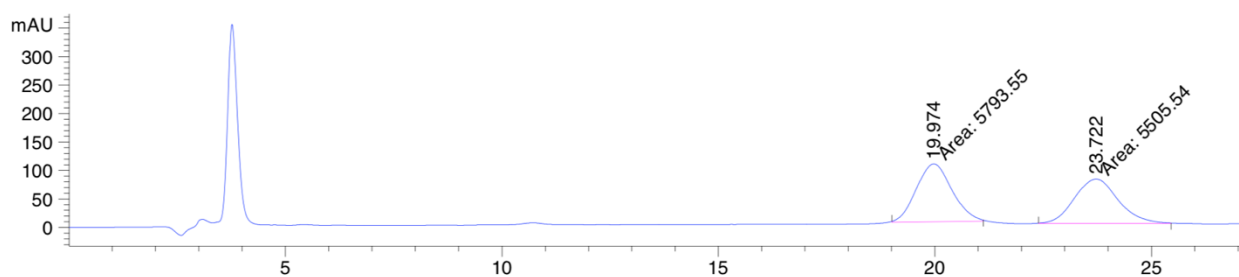
(S)-pivalamide 5.52i

Signal 2: DAD1 C, Sig=210,4 Ref=off

Peak #	RetTime [min]	Type	Width [min]	Area [mAU*s]	Height [mAU]	Area %
1	8.109	VV	0.2769	2515.46436	130.49010	6.6902
2	9.064	VB	0.3233	3.50839e4	1725.01147	93.3098

Totals : 3.75993e4 1855.50157

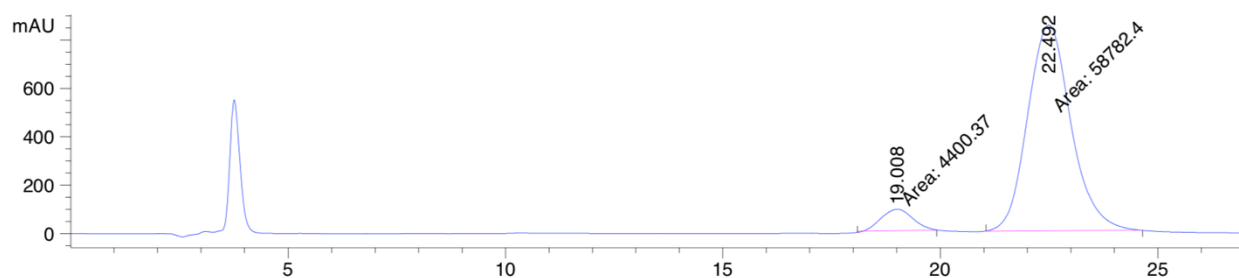
(S)-Phth-glycine amide 5.52j

(±)- Phth-glycine amide 5.52j

Signal 1: DAD1 C, Sig=210,4 Ref=off

Peak #	RetTime [min]	Type	Width [min]	Area [mAU*s]	Height [mAU]	Area %
1	19.974	MM	0.9513	5793.55469	101.50015	51.2745
2	23.722	MM	1.1756	5505.54199	78.05405	48.7255

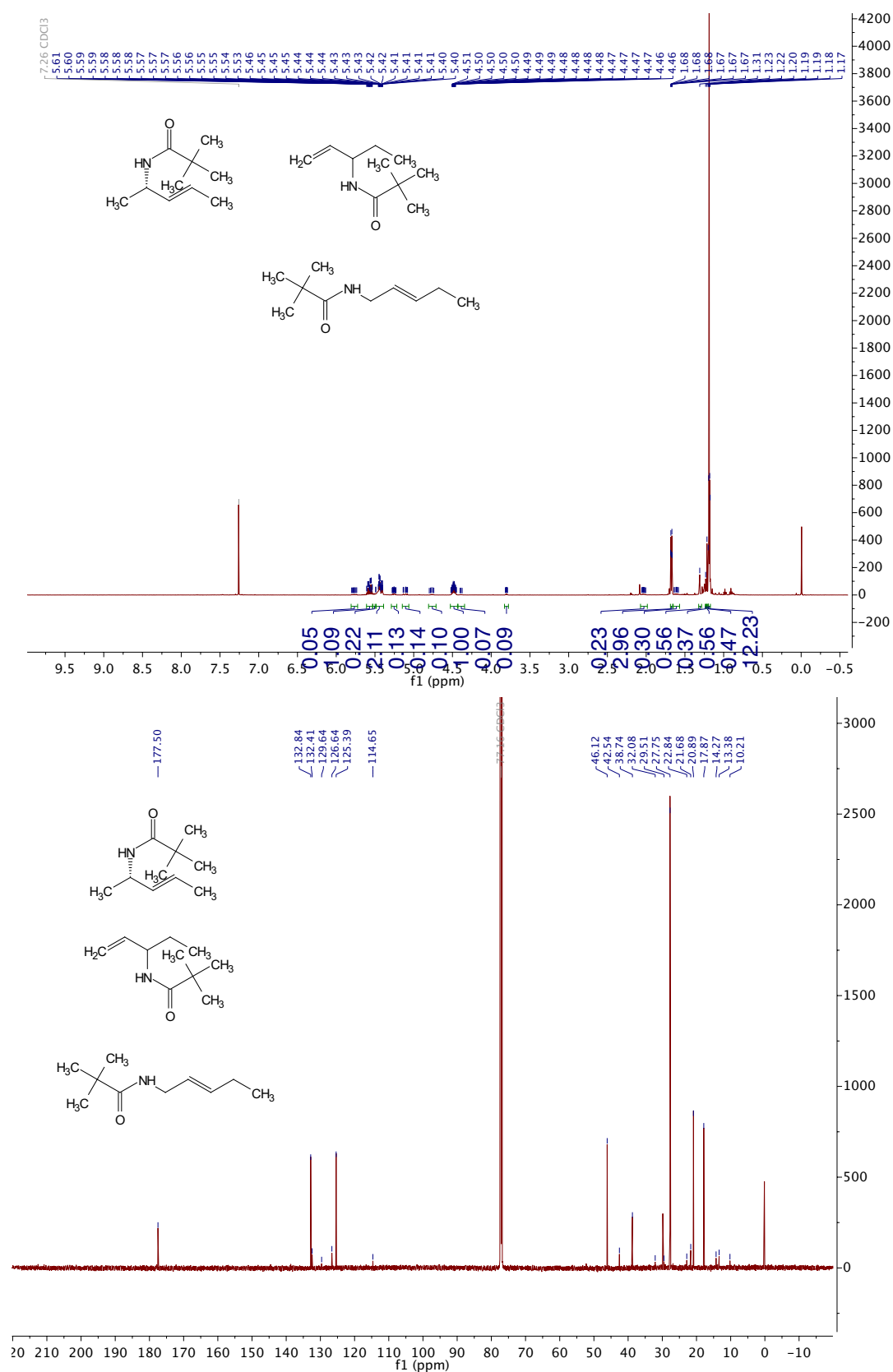
Totals : 1.12991e4 179.55421

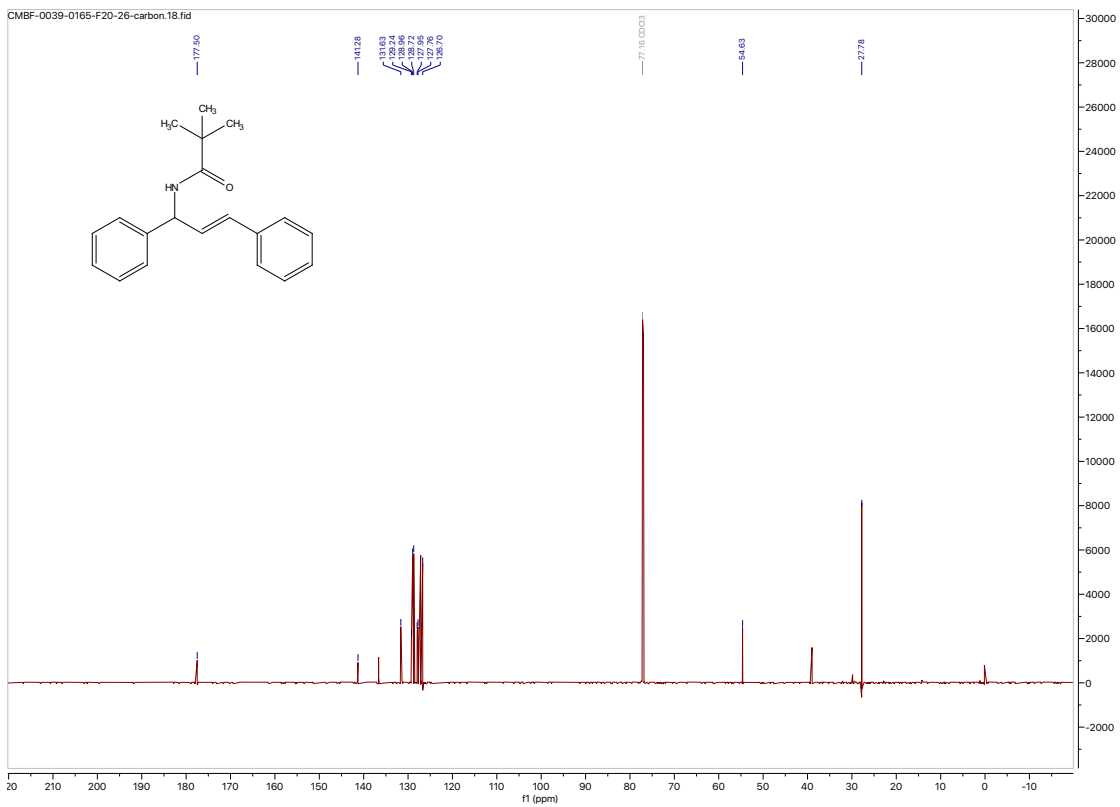
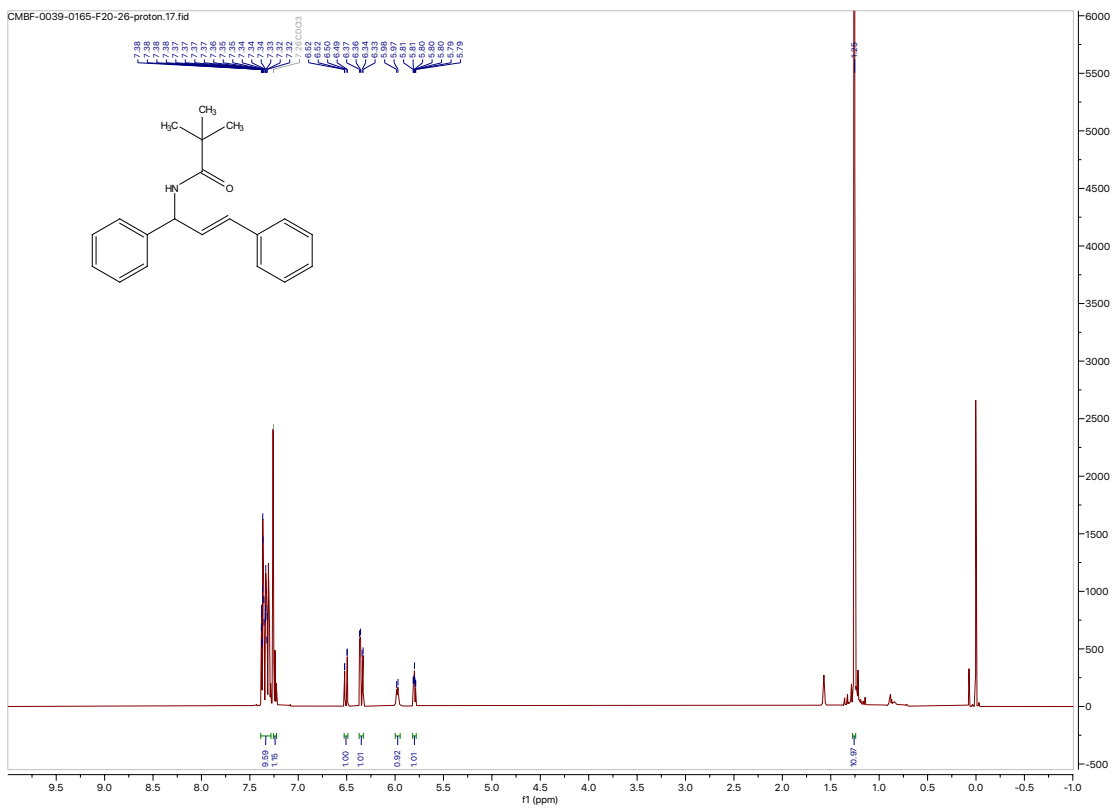
(S)- Phth-glycine amide 5.52j

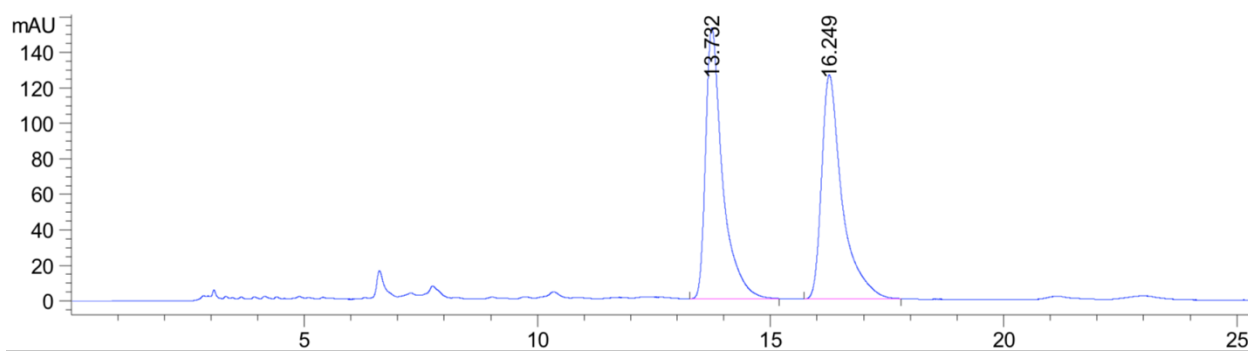
Signal 1: DAD1 C, Sig=210,4 Ref=off

Peak #	RetTime [min]	Type	Width [min]	Area [mAU*s]	Height [mAU]	Area %
1	19.008	MM	0.8312	4400.37354	88.22954	6.9645
2	22.492	MM	1.1531	5.87824e4	849.64386	93.0355

Totals : 6.31827e4 937.87340

(S)-pivalamide **5.52k** + regioisomers

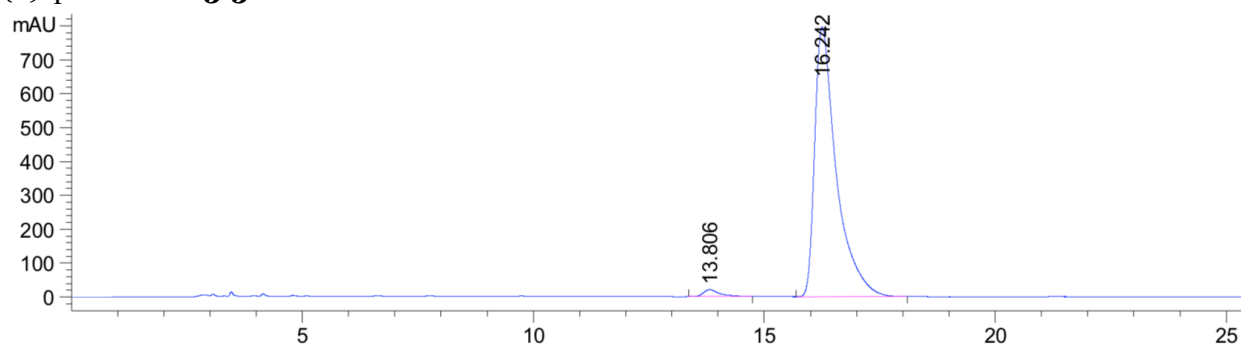
(S)-pivalamide 5.521

(±)-pivalamide 5.521

Signal 2: DAD1 B, Sig=230,4 Ref=off

Peak #	RetTime [min]	Type	Width [min]	Area [mAU*s]	Height [mAU]	Area %
1	13.732	BB	0.3546	3845.48267	152.53081	49.9790
2	16.249	BB	0.4231	3848.71924	126.26714	50.0210

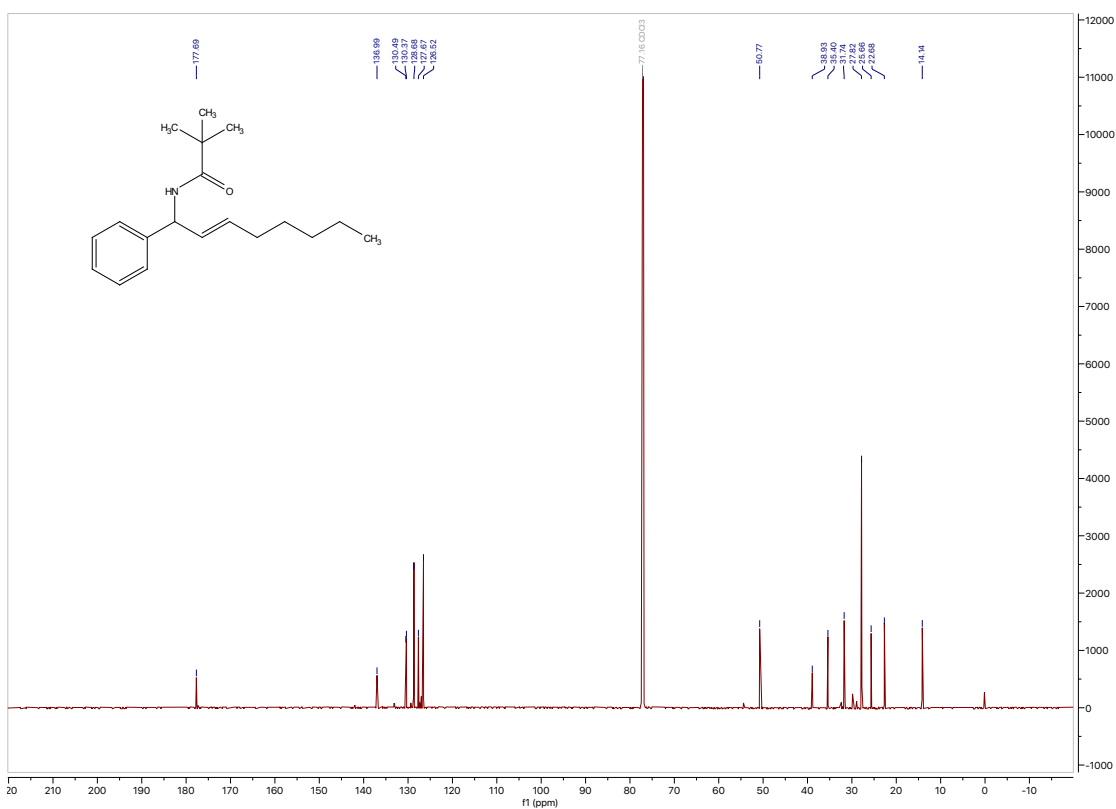
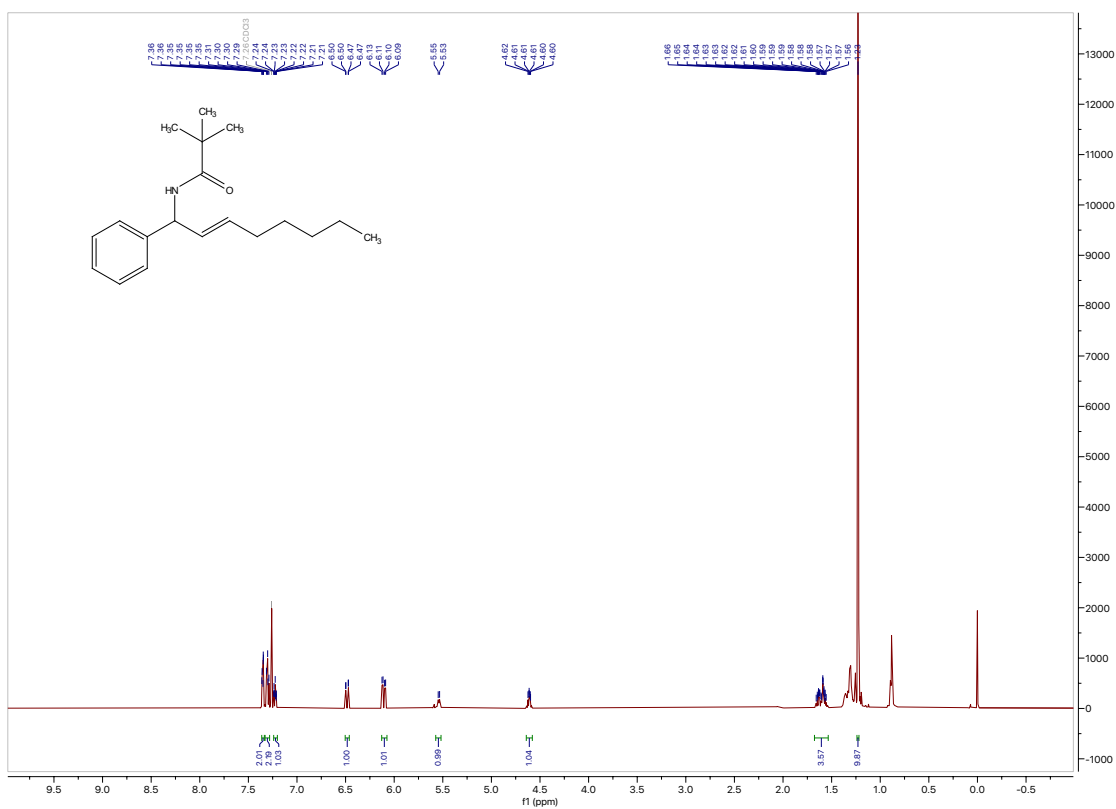
Totals : 7694.20190 278.79794

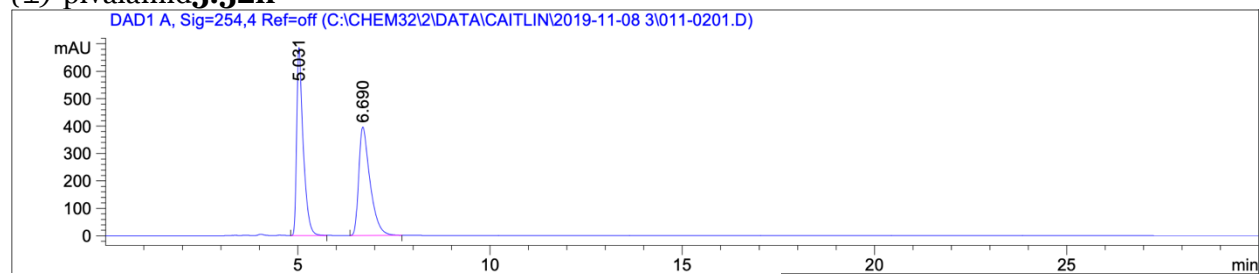
(S)-pivalamide 5.521

Signal 2: DAD1 B, Sig=230,4 Ref=off

Peak #	RetTime [min]	Type	Width [min]	Area [mAU*s]	Height [mAU]	Area %
1	13.806	BB	0.2922	508.97794	20.60517	1.9261
2	16.242	BB	0.4517	2.59169e4	795.23010	98.0739

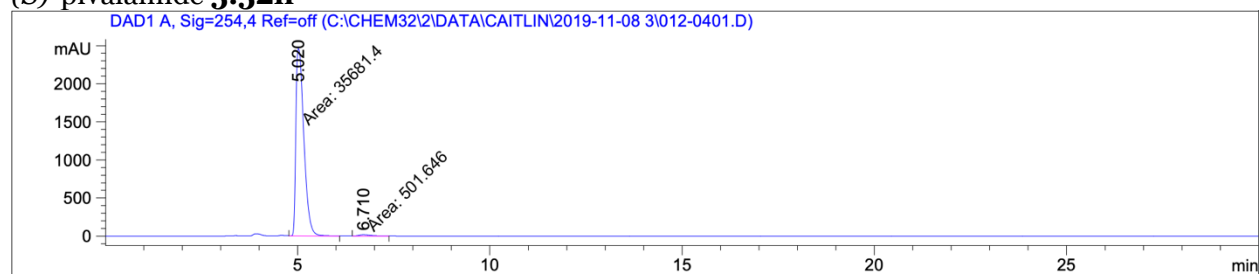
Totals : 2.64258e4 815.83527

(S)-pivalamide 5.52n

(±)-pivalamid 5.52n

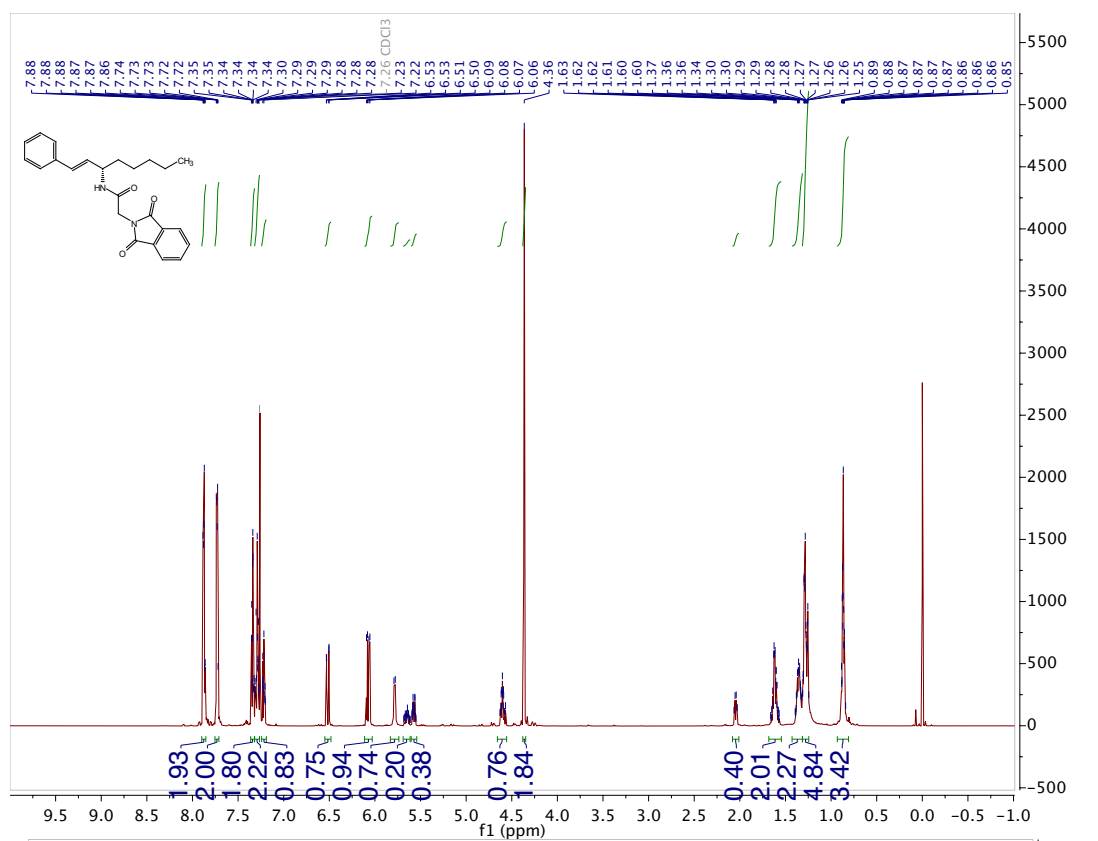
Peak #	RetTime [min]	Type	Width [min]	Area [mAU*s]	Height [mAU]	Area %
1	5.031	VB	0.1722	8128.28955	686.04407	50.1367
2	6.690	BB	0.3005	8083.97021	395.41028	49.8633

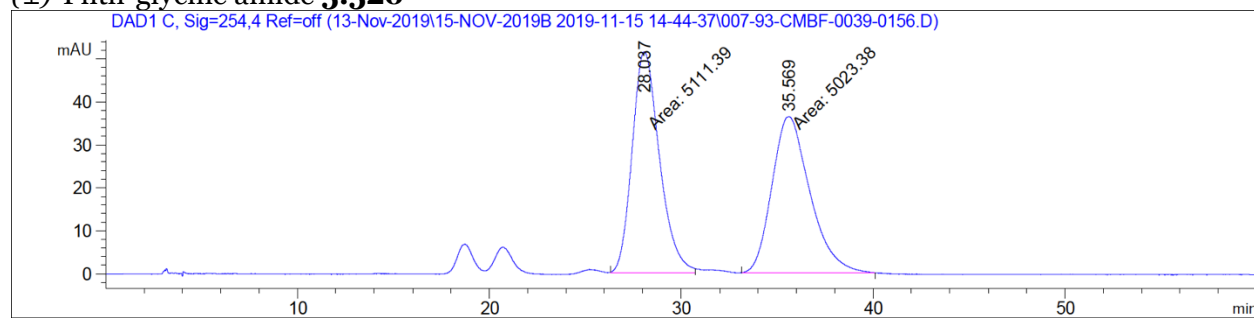
Totals : 1.62123e4 1081.45435

(S)-pivalamide 5.52n

Peak #	RetTime [min]	Type	Width [min]	Area [mAU*s]	Height [mAU]	Area %
1	5.020	MM	0.2419	3.56814e4	2458.60937	98.6136
2	6.710	MM	0.4265	501.64560	19.60351	1.3864

Totals : 3.61831e4 2478.21289

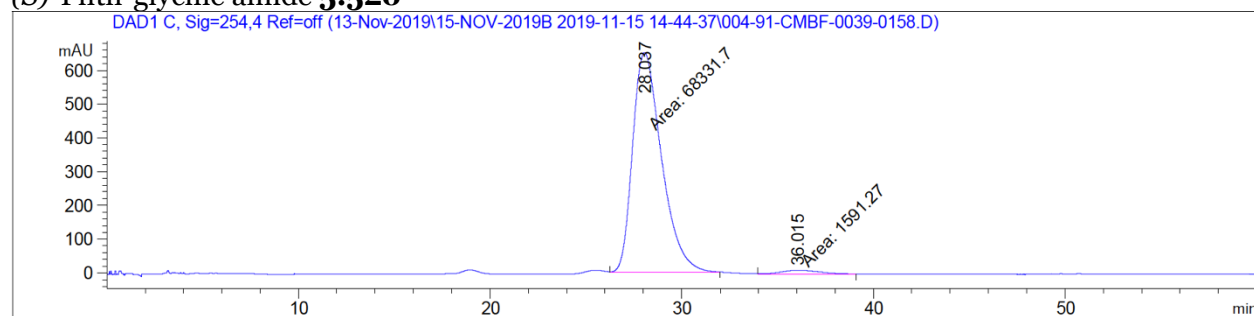
(S,E)-Phth-glycine amide 5.520

(±)-Phth-glycine amide 5.520

Signal 3: DAD1 C, Sig=254,4 Ref=off

Peak #	RetTime [min]	Type	Width [min]	Area [mAU*s]	Height [mAU]	Area %
1	28.037	MM	1.6556	5111.39160	51.45485	50.4342
2	35.569	MM	2.3009	5023.37891	36.38676	49.5658

Totals : 1.01348e4 87.84162

(S)-Phth-glycine amide 5.520

Signal 3: DAD1 C, Sig=254,4 Ref=off

Peak #	RetTime [min]	Type	Width [min]	Area [mAU*s]	Height [mAU]	Area %
1	28.037	MM	1.7505	6.83317e4	650.59467	97.7242
2	36.015	MM	2.3517	1591.27356	11.27731	2.2758

Totals : 6.99230e4 661.87197

5.7 References

- (1) Lei, H.; Rovis, T. Ir-Catalyzed Intermolecular Branch-Selective Allylic C-H Amidation of Unactivated Terminal Olefins. *J. Am. Chem. Soc.* **2019**, *141*, 2268–2273.
- (2) Knecht, T.; Mondal, S.; Ye, J.-H.; Das, M.; Glorius, F. Intermolecular, Branch-Selective, and Redox-Neutral Cp*Ir^{III}-Catalyzed Allylic C–H Amidation. *Angew. Chem. Int. Ed.* **2019**, *58*, 7117–7121.
- (3) Burman, J. S.; Harris, R. J.; B. Farr, C. M.; Bacsá, J.; Blakey, S. B. Rh(III) and Ir(III)Cp* Complexes Provide Complementary Regioselectivity Profiles in Intermolecular Allylic C–H Amidation Reactions. *ACS Catal.* **2019**, *9*, 5474–5479.
- (4) Burman, J. S.; Harris, R. J.; B. Farr, C. M.; Bacsá, J.; Blakey, S. B.; Farr, C. M. B.; Bacsá, J.; Blakey, S. B. Rh(III) and Ir(III)Cp* Complexes Provide Complementary Regioselectivity Profiles in Intermolecular Allylic C–H Amidation Reactions. *ACS Catal.* **2019**, 5474–5479.
- (5) Cooper, T. S.; Laurent, P.; Moody, C. J.; Takle, A. K. Asymmetric Synthesis of N-Protected Amino Acids by the Addition of Organolithium Carboxyl Synthons to ROPHy/SOPHy-Derived Aldoximes and Ketoximes. *Org. Biomol. Chem.* **2004**, *2*, 265–276.
- (6) Javorskis, T.; Sriubaite, S.; Bagdžiunas, G.; Orentas, E. N-Protected 1,2-Oxazetidines as a Source of Electrophilic Oxygen: Straightforward Access to Benzomorpholines and Related Heterocycles by Using a Reactive Tether. *Chem. A Eur. J.* **2015**, *21*, 9157–9164.
- (7) Kazerouni, A. M.; Nelson, T. A. F.; Chen, S. W.; Sharp, K. R.; Blakey, S. B. Regioselective Cp*Ir(III)-Catalyzed Allylic C–H Sulfamidation of Allylbenzene Derivatives. *J. Org. Chem.* **2019**, *84*, 13179–13185.
- (8) Scriven, E. F. V.; Turnbull, K. Azides: Their Preparation and Synthetic Uses. *Chem. Rev.* **1988**, *88*, 297–368.
- (9) Ji, S.; Gortler, L. B.; Waring, A.; Battisti, A.; Bank, S.; Closson, W. D.; Wriede, P. Cleavage of Sulfonamides with Sodium Naphthalene. *J. Am. Chem. Soc.* **1967**, *89*, 5311–5312.

- (10) Farr, C.; Kazerouni, A.; Park, B.; Poff, C.; Won, J.; Sharp, K.; Baik, M.-H.; Blakey, S. Designing a Planar Chiral Rhodium Indenyl Catalyst for Regio- and Enantioselective Allylic C–H Amidation. *J. Am. Chem. Soc.* **2020**, *142*, 13996–14004.
- (11) *Stereoselective Formation of Amines*; Li, W., Zhang, X., Eds.; Topics in Current Chemistry; Springer Berlin Heidelberg: Berlin, Heidelberg, **2014**, Vol. 343.
- (12) Wang, Y. M.; Buchwald, S. L. Enantioselective CuH-Catalyzed Hydroallylation of Vinylarenes. *J. Am. Chem. Soc.* **2016**, *138*, 5024–5027.
- (13) Newton, C. G.; Kossler, D.; Cramer, N. Asymmetric Catalysis Powered by Chiral Cyclopentadienyl Ligands. *J. Am. Chem. Soc.* **2016**, *138*, 3935–3941.
- (14) Cramer, N.; Mas-Roselló, J.; Herraiz, A. G.; Audic, B.; Laverny, A. Chiral Cyclopentadienyl Ligands: Design, Syntheses and Applications in Asymmetric Catalysis. *Angew. Chem.* **2020**, <https://doi.org/10.1002/anie.202008166>.
- (15) Ye, B.; Cramer, N. Chiral Cyclopentadienyl Ligands as Stereocontrolling Element in Asymmetric C-H Functionalization. *Science* **2012**, *338*, 504–506.
- (16) Hyster, T. K.; Knörr, L.; Ward, T. R.; Rovis, T. Biotinylated Rh(III) Complexes in Engineered Streptavidin for Accelerated Asymmetric C-H Activation. *Science* **2012**, *338*, 500–503.
- (17) Ye, B.; Cramer, N. A Tunable Class of Chiral Cp Ligands for Enantioselective Rhodium(III)-Catalyzed C-H Allylations of Benzamides. *J. Am. Chem. Soc.* **2013**, *135*, 636–639.
- (18) Cui, W. J.; Wu, Z. J.; Gu, Q.; You, S. L. Divergent Synthesis of Tunable Cyclopentadienyl Ligands and Their Application in Rh-Catalyzed Enantioselective Synthesis of Isoindolinone. *J. Am. Chem. Soc.* **2020**, *142*, 7379–7385.
- (19) Zheng, J.; Cui, W. J.; Zheng, C.; You, S. L. Synthesis and Application of Chiral Spiro Cp Ligands in Rhodium-Catalyzed Asymmetric Oxidative Coupling of Biaryl Compounds with Alkenes. *J. Am. Chem. Soc.* **2016**, *138*, 5242–5245.

- (20) Jia, Z.-J. J.; Merten, C.; Gontla, R.; Daniliuc, C. G.; Antonchick, A. P.; Waldmann, H. General Enantioselective C–H Activation with Efficiently Tunable Cyclopentadienyl Ligands. *Angew. Chem. Int. Ed.* **2017**, *56*, 2429–2434.
- (21) Trifonova, E. A.; Ankudinov, N. M.; Mikhaylov, A. A.; Chusov, D. A.; Nelyubina, Y. V.; Perekalin, D. S. A Planar-Chiral Rhodium(III) Catalyst with a Sterically Demanding Cyclopentadienyl Ligand and Its Application in the Enantioselective Synthesis of Dihydroisoquinolones. *Angew. Chem. Int. Ed.* **2018**, *57*, 7714–7718.
- (22) Wang, S.-G.; Park, S. H.; Cramer, N. A Readily Accessible Class of Chiral Cp Ligands and Their Application in Ru^{II}-Catalyzed Enantioselective Syntheses of Dihydrobenzoindoles. *Angew. Chem. Int. Ed.* **2018**, *57*, 5459–5462.
- (23) Liang, H.; Vasamsetty, L.; Li, T.; Jiang, J.; Pang, X.; Wang, J. A New Class of C₂-Symmetric Chiral Cp Ligand Derived from Ferrocene Scaffold: Design, Synthesis and Application. *Chem. A. Eur. J.* **2020**, <https://doi.org/10.1002/chem.202001814>.
- (24) Marder, T. B.; Calabrese, J. C.; Roe, D. C.; Tulip, T. H. The Slip-Fold Distortion of π -Bound Indenyl Ligands. Dynamic NMR and x-Ray Crystallographic Studies of $(\eta^5\text{-Indenyl})\text{RhL}_2$ Complexes. *Organometallics* **1987**, *6*, 2012–2014.
- (25) Hart-Davis, A. J.; Mawby, R. J. Reactions of π -Indenyl Complexes of Transition Metals. Part I. Kinetics and Mechanisms of Reactions of Tricarbonyl- π -Indenylmethylmolybdenum with Phosphorus(III) Ligands. *J. Chem. Soc. A Inorganic, Phys. Theor. Chem.* **1969**, 2403–2407.
- (26) Westcott, S. A.; Kakkar, A. K.; Stringer, G.; Taylor, N. J.; Marder, T. B. Flexible Coordination of Indenyl Ligands in Sandwich Complexes of Transition Metals. Molecular Structures of $[(\eta\text{-C}_9\text{R}_7)_2\text{M}]$ (M = Fe, R = H, Me; M = Co, Ni, R = H): Direct Measurement of the Degree of Slip-Fold Distortion as a Function of d-Electron Count. *J. Organomet. Chem.* **1990**, *394*, 777–794.
- (27) Trost, B. M.; Ryan, M. C. Indenylmetal Catalysis in Organic Synthesis. *Angew. Chem. Int.*

- Ed.* **2017**, *56*, 2862–2879.
- (28) Hapke, M.; Kral, K.; Fischer, C.; Spannenberg, A.; Gutnov, A.; Redkin, D.; Heller, B. Asymmetric Synthesis of Axially Chiral 1-Aryl-5,6,7,8-Tetrahydroquinolines by Cobalt-Catalyzed [2 + 2 + 2] Cycloaddition Reaction of 1-Aryl-1,7-Octadiynes and Nitriles. *J. Org. Chem.* **2010**, *75*, 3993–4003.
- (29) Heller, B.; Gutnov, A.; Fischer, C.; Drexler, H. J.; Spannenberg, A.; Redkin, D.; Sundermann, C.; Sundermann, B. Phosphorus-Bearing Axially Chiral Biaryls by Catalytic Asymmetric Cross-Cyclotrimerization and a First Application in Asymmetric Hydrosilylation. *Chem. Eur. J.* **2007**, *13*, 1117–1128.
- (30) Gutnov, A.; Heller, B.; Fischer, C.; Drexler, H. J.; Spannenberg, A.; Sundermann, B.; Sundermann, C. Cobalt(I)-Catalyzed Asymmetric [2+2+2] Cycloaddition of Alkynes and Nitriles: Synthesis of Enantiomerically Enriched Atropoisomers of 2-Arylpyridines. *Angew. Chem. Int. Ed.* **2004**, *43*, 3795–3797.
- (31) Baker, R. W. Asymmetric Induction via the Structural Indenyl Effect. *Organometallics* **2018**, *37*, 433–440.
- (32) Biosca, M.; Salomó, E.; de la Cruz-Sánchez, P.; Riera, A.; Verdaguer, X.; Pàmies, O.; Diéguez, M. Extending the Substrate Scope in the Hydrogenation of Unfunctionalized Tetrasubstituted Olefins with Ir-P Stereogenic Aminophosphine–Oxazoline Catalysts. *Org. Lett.* **2019**, *21*, 807–811.
- (33) Nalesnik, T. E.; Freudenberger, J. H.; Orchin, M. Hydrogenation Reactions with Hydridocobalt Tetracarbonyl. *J. Organomet. Chem.* **1981**, *221*, 193–197.
- (34) Geometry optimization, vibration, and solvation energy calculations were conducted with B3LYP-D3/LACVP** level of theory. Single point energies were re-evaluated with B3LYP-D3/Cc-PVTZ(-f) level of theory.
- (35) Kinauer, M.; Diefenbach, M.; Bamberger, H.; Demeshko, S.; Reijerse, E. J.; Volkmann, C.; Würtele, C.; Van Slageren, J.; De Bruin, B.; Holthausen, M. C.; et al. An

- Iridium(III/IV/V) Redox Series Featuring a Terminal Imido Complex with Triplet Ground State. *Chem. Sci.* **2018**, *9*, 4325–4332.
- (36) Ruppel, J. V.; Jones, J. E.; Huff, C. A.; Kamble, R. M.; Chen, Y.; Zhang, X. P. A Highly Effective Cobalt Catalyst for Olefin Aziridination with Azides: Hydrogen Bonding Guided Catalyst Design. *Org. Lett.* **2008**, *10* (10), 1995–1998.
- (37) Aguila, M. J. B.; Badiei, Y. M.; Warren, T. H. Mechanistic Insights into C-H Amination via Dicopper Nitrenes. *J. Am. Chem. Soc.* **2013**, *135*, 9399–9406.
- (38) Ma, R.; Christina White, M. C-H to C-N Cross-Coupling of Sulfonamides with Olefins. *J. Am. Chem. Soc.* **2018**, *140*, 3202–3205.
- (39) Burman, J. S.; Blakey, S. B. Regioselective Intermolecular Allylic C–H Amination of Disubstituted Olefins via Rhodium/ π -Allyl Intermediates. *Angew. Chem. Int. Ed.* **2017**, *56*, 13666–13669.
- (40) Prediger, P.; Barbosa, L. F.; Génisson, Y.; Correia, C. R. D. Substrate-Directable Heck Reactions with Arenediazonium Salts. The Regio- and Stereoselective Arylation of Allylamine Derivatives and Applications in the Synthesis of Naftifine and Abamines. *J. Org. Chem.* **2011**, *76*, 7737–7749.
- (41) Prasad, B. A. B.; Bisai, A.; Singh, V. K. 2-Aryl-N-Tosylazetidines as Formal 1,4-Dipoles for [4 + 2] Cycloaddition Reactions with Nitriles: An Easy Access to the Tetrahydropyrimidine Derivatives. *Org. Lett.* **2004**, *6*, 4829–4831.
- (42) Xing, D.; Yang, D. Gold(I)-Catalyzed Highly Regio- and Stereoselective Decarboxylative Amination of Allylic N-Tosylcarbamates via Base-Induced Aza-Claisen Rearrangement in Water. *Org. Lett.* **2010**, *12*, 1068–1071.
- (43) Fukumoto, Y.; Okazaki, N.; Chatani, N. A New Class of Redox Isomerization of *N*-Alkylpropargylamines into *N*-Alkylideneallylamines Catalyzed by a $\text{ReBr}(\text{CO})_5$ /Amine *N*-Oxide System. *Org. Lett.* **2019**, *21*, 1760–1765.
- (44) Mahy, J. P.; Bedi, G.; Battioni, P.; Mansuy, D. Allylic Amination of Alkenes by

- Tosyliminoiodobenzene: Manganese Porphyrins as Suitable Catalysts. *Tetrahedron Lett.* **1988**, *29*, 1927–1930.
- (45) Donohoe, T. J.; Race, N. J.; Bower, J. F.; Callens, C. K. A. Substituted Pyrroles via Olefin Cross-Metathesis. *Org. Lett.* **2010**, *12*, 4094–4097.
- (46) Cochet, T.; Bellosta, V.; Roche, D.; Ortholand, J. Y.; Greiner, A.; Cossy, J. Rhodium(III)-Catalyzed Allylic C-H Bond Amination. Synthesis of Cyclic Amines from ω -Unsaturated N-Sulfonylamines. *Chem. Commun.* **2012**, *48*, 10745–10747.
- (47) Wang, Y.; Wang, J.; Li, G. X.; He, G.; Chen, G. Halogen-Bond-Promoted Photoactivation of Perfluoroalkyl Iodides: A Photochemical Protocol for Perfluoroalkylation Reactions. *Org. Lett.* **2017**, *19*, 1442–1445.
- (48) Brooks, J. L.; Xu, L.; Wiest, O.; Tan, D. S. Diastereoselective Synthesis of Highly Substituted Tetrahydrofurans by Pd-Catalyzed Tandem Oxidative Cyclization-Redox Relay Reactions Controlled by Intramolecular Hydrogen Bonding. *J. Org. Chem.* **2017**, *82*, 57–75.
- (49) Fall, Y.; Berthiol, F.; Doucet, H.; Santelli, M. Palladium-Tetrakisphosphine Catalyzed Heck Reaction with Simple Alkenes: Influence of Reaction Conditions on the Migration of the Double Bond. *Synthesis* **2007**, *2007*, 1683–1696.
- (50) Schlögl, K. Stereochemistry of Metallocenes. 20 Years of Progress and Recent Advances. *J. Organomet. Chem.* **1986**, *300*, 219–248.

Chapter 6. Studies Towards the Total Synthesis of Darobactin A

In this chapter, we will discuss our efforts to develop a strategy for the synthesis of darobactin A, a ribosomally-synthesised post-translationally modified peptide (RiPP) natural product. We will begin with a brief introduction to RiPPs and their biosynthesis, followed by a discussion on the structure and biology of darobactin A, an antibiotic that has shown activity against Gram-negative bacteria. We will then discuss different synthetic strategies to assemble the right-hand Trp³-Lys⁵ cross-link present in the natural product.

6.1 Introduction

Ribosomally-synthesised and post-translationally modified peptides (RiPPs) are an emerging class of structurally diverse and biologically active natural products.^{1,2} A distinct characterising feature of these natural products is the presence of cross-linked peptide residues as a result of post-translational modifications (PTMs) by various cyclising enzymes. Biosynthetically, RiPPs originate from a precursor peptide made up of a central core peptide, a leader peptide, and in some cases, a follower peptide (Figure 6.1). PTMs take place on the core peptide to establish a modified core region. Removal of the leader and follower peptides then generates the mature RiPP product.^{3,4} Advances in genome sequencing and genome mining approaches have led to the rapid discovery of newer RiPP classes from novel biosynthetic gene clusters (BGCs). In particular, cyclophane macrocycles formed by post-translational cyclisation of a precursor peptide are increasingly common structural motifs in newer classes of RiPPs. These

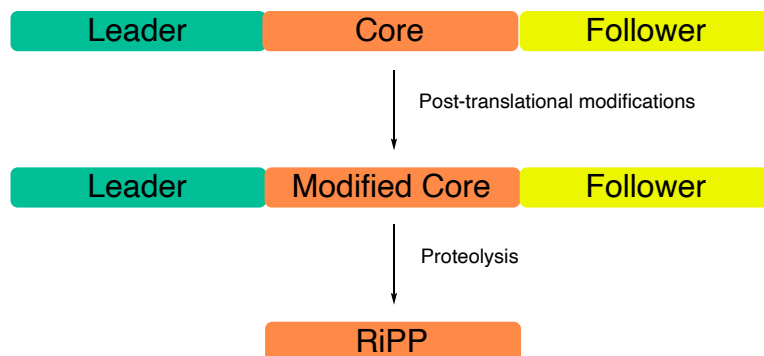


Figure 6.1: General representation of RiPP biosynthesis (Figure adapted from *Nat. Prod. Rep.* **2020**, DOI: 10.1039/d0np00027b)

PTMs typically manifest as C–C or C–O bonds between an aromatic side chain (such as Trp or Tyr) and another amino acid residue in the peptide.⁵

While modern bioinformatics tools have enabled the discovery of novel structural features, further characterisation and biological evaluation of these RiPPs is necessary. For example, the complete structure and relative stereochemistry of ryptides (**6.2**)⁶ and the orphan RiPP derived from the WGK gene cluster (**6.3**)⁷ have yet to be reported (Figure 6.2). Synthetic approaches to these natural products would allow complete stereochemical characterisation and provide valuable material for biological evaluation. Total synthesis also presents the opportunity to confirm the structures of fully characterised RiPPs, as exemplified by Boger's recent synthesis and stereochemical re-assignment of streptide (**6.4**),^{8,17} four years after its initial isolation and characterisation.⁹

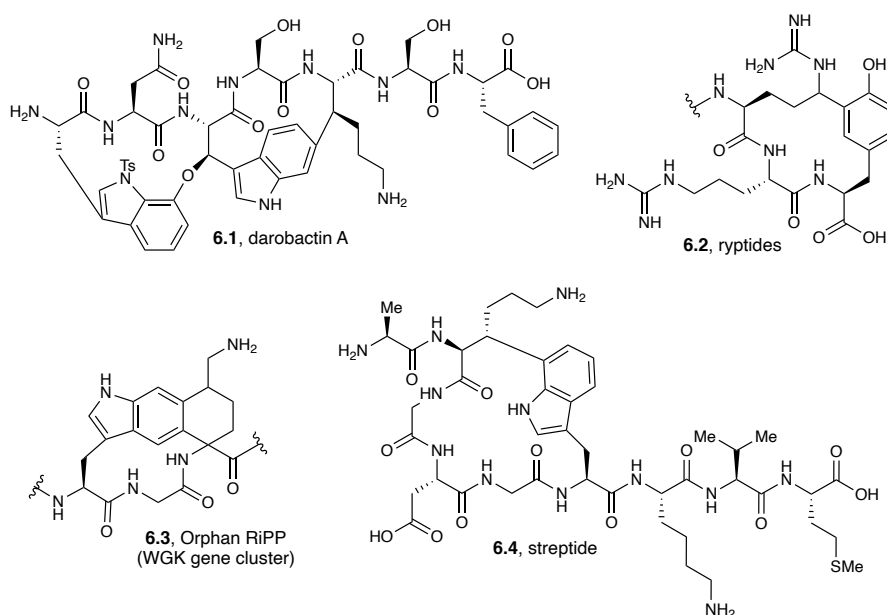


Figure 6.2: RiPPs containing cyclophane macrocycles

The synthesis of RiPPs presented an ideal and significant opportunity for us to demonstrate the synthetic applications of our recently reported synthetic methods and has developed into a major research thrust of the Blakey lab. In particular, along with David Laws, a graduate student in the Blakey lab, we are currently developing a synthetic route to darobactin A

¹⁷ Boger's synthesis of streptide will be discussed in further detail later in this chapter.

(6.1), a recently isolated RiPP that has shown preliminary biological activity against Gram-negative bacteria.¹⁰

6.2 Darobactin A – structure and biology

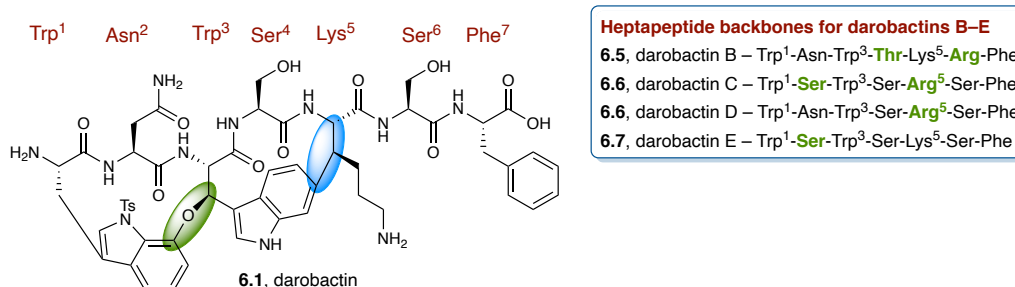


Figure 6.3: Darobactins A–E

Darobactin A is produced by a silent biosynthetic gene cluster (BGC) in several strains of *Photorhabdus khanii* and was first isolated and characterised in 2019 by Lewis and co-workers.¹⁰ Structurally, it is a modified heptapeptide with the amino acid sequence Trp¹-Asn²-Trp³-Ser⁴-Lys⁵-Ser⁶-Phe⁷ (Figure 6.3). The compound contains a post-translational modification in the form of a C–C bond between indole-C6 of Trp³ and the β -C of Lys⁵ (blue highlight), forming the right-hand macrocycle. Though this cross-link is uncommon in cyclophane-containing RiPPs, a similar macrocyclic Trp-Lys linkage is present in streptide (see Figure 6.2).⁹ Darobactin A also contains an additional cross-link at the indole-C7 of Trp¹ in the form of an ether linkage with the β -C of Trp³ (green highlight), which is unprecedented in known RiPP post-translational modifications. This cross-link forms the left-hand macrocycle of the natural product. The peptide precursor to darobactin A is encoded by *darA*, the structural gene of the larger *darABCDE* operon. The *darE* operon was found to encode a radical *S*-adenosyl methionine (SAM) enzyme, which are known to catalyse free-radical reactions¹¹ and were recently implicated in the formation of the Trp-Lys cross-link present in streptide.⁹ Lewis and co-workers suggest that this *darE* SAM enzyme is also responsible for the formation of Trp¹-Trp³ ether linkage. The authors' search also unearthed homologues of the *dar* operon that are proposed to encode four additional analogues of darobactin A, darobactins B–E, with modified heptapeptide backbones (Figure 6.3, blue inset).

All analogues of darobactin contain the Trp¹-Trp³ ether cross-link. The Trp³-Lys⁵ cross-link is also preserved in darobactins B and E, but is modified to a Trp³-Arg⁵ cross-link in darobactins C and D. Although the peptide precursor for darobactin A was most commonly observed, only 3 mg/L of the antibiotic was isolable from the strain of *P. khanii* in which it was most abundant.

Darobactin A exhibited activity against a range of Gram-negative pathogens like *Escherichia coli* and *Klebsiella pneumoniae*, but was largely inactive against Gram-positive bacteria. Lewis and co-workers observed *in vitro* inhibition of BamA, an outer membrane protein (OMP) – and a component of the larger BamABCDE (BAM) complex – which is responsible for folding and inserting additional outer membrane proteins from the periplasm into the outer membrane. Darobactin A also exhibited *in vivo* activity against *E. coli*, *K. pneumoniae*, and *Pseudomonas aeruginosa*.

The outer membrane is essential for the protection of Gram-negative bacteria, and its disruption can be lethal.^{12,13} To date, very few antibiotics can penetrate this barrier, highlighting the significance of darobactin A's anti-bacterial activity.^{14,15} Furthermore, the inhibition of BamA by darobactin A, a chaperone protein on the surface of the outer membrane, bypasses the longstanding problem of membrane permeability of Gram-negative bacteria. This, coupled with the low quantities of the antibiotic isolable from Nature, underscore the need for a synthetic route towards darobactin A.

6.3 Synthetic strategies towards related cyclophane macrocycle natural products

Before embarking on a synthetic campaign of darobactin A, a brief overview of successful synthetic strategies towards related cyclophane macrocycle natural products is appropriate. Specifically, in this section, we will discuss prior syntheses of celogentin C and streptide, a recently characterised RiPP natural product.

6.3.1 Synthesis of celogentin C

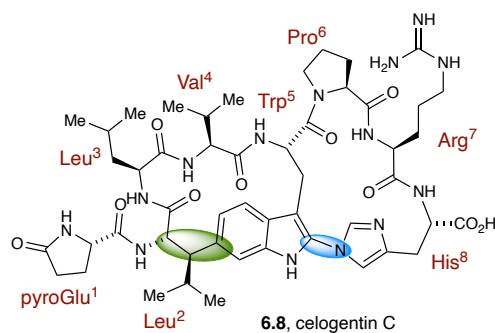
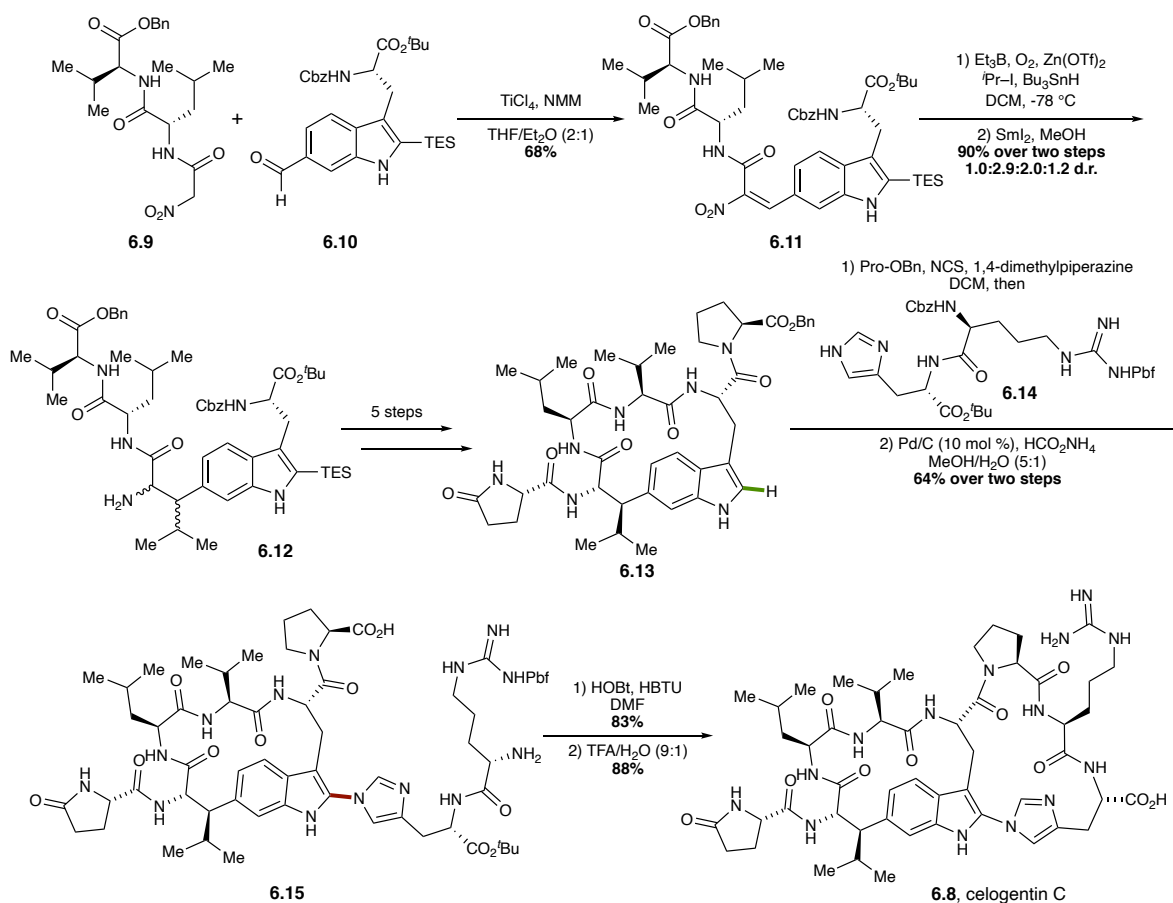


Figure 6.4: Celogentin C

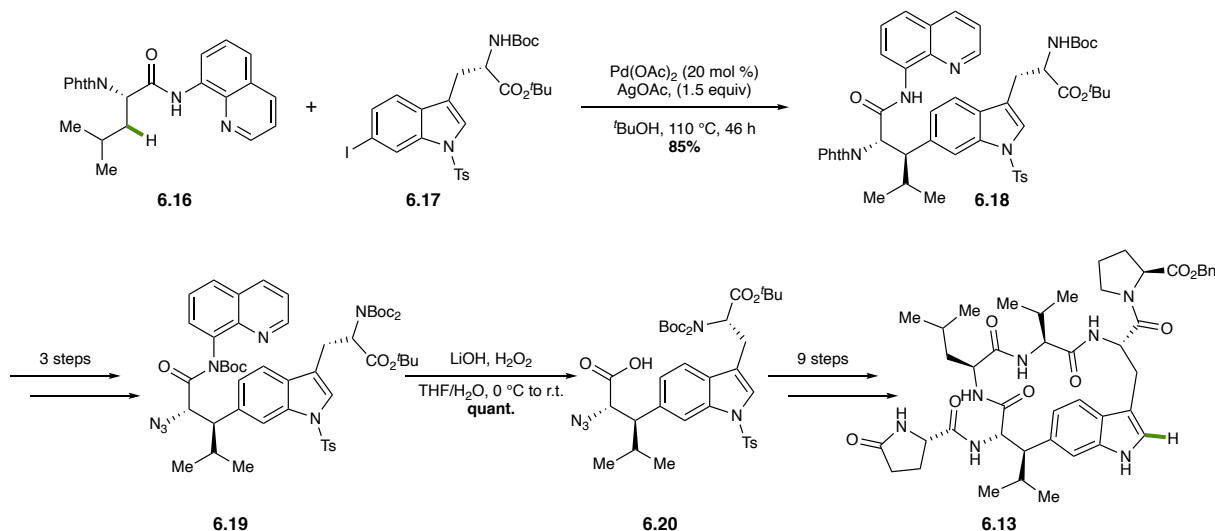


Scheme 6.1: Total synthesis of celogentin C *via* a Knoevenagel condensation/radical Michael addition sequence (Castle, 2009)

Celogentin C is a non-ribosomal peptide natural product that displays antimitotic activity by inhibiting tubulin polymerization (Figure 6.4).^{16–18} It is a modified octapeptide with the amino acid sequence pyroGlu¹-Leu²-Leu³-Val⁴-Trp⁵-Pro⁶-Arg⁷-His⁸. The compound contains a C–C cross-link between the β -C of Leu² and indole-C6 of Trp⁵ (highlighted in green), reminiscent of the Trp-Lys cross-link present in streptide and darobactin A, as well as a C–N cross-link between

indole-C2 of Trp⁵ and N1 of His⁷ (highlighted in blue).

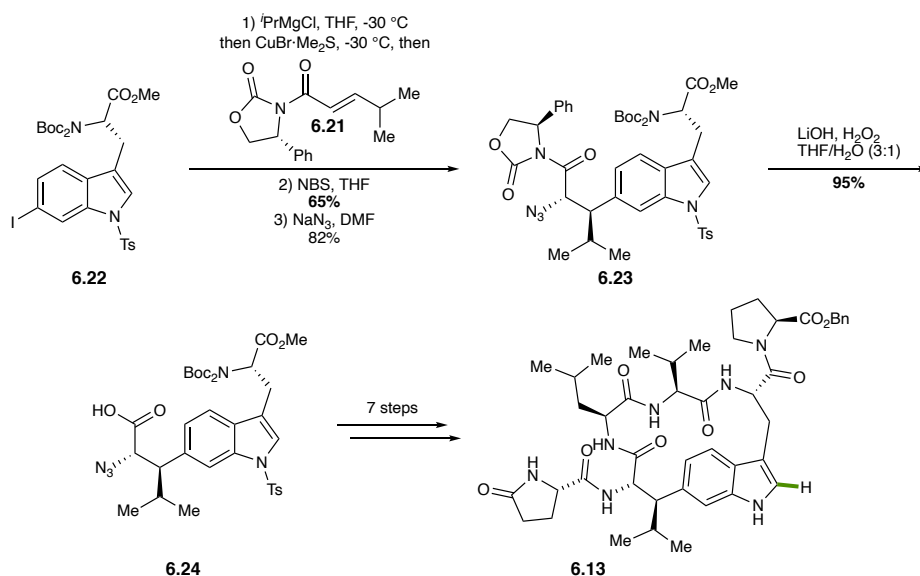
The first synthesis of this structurally daunting target was reported in 2009 by Castle and co-workers (Scheme 6.1).^{19,20} The Leu²-Trp⁵ cross-link was assembled by a Knoevenagel condensation of modified tripeptide **6.9** with tryptophan-derived aldehyde **6.10** to provide olefin **6.11** as a single stereoisomer, followed by a radical Michael addition to install the *iso*-propyl group in **6.12**. However, diastereoselectivity of this reaction was poor, delivering **6.12** as a mixture of diastereomers. A series of inter- and intramolecular peptide couplings delivered macrocycle **6.13**. The Trp⁵-His⁷ cross-link was cleverly established with a novel intermolecular oxidative coupling reaction between macrocycle **6.13** and Arg-His dipeptide **6.14**. The reaction was hypothesised to proceed through a dichlorinated intermediate which was converted to the required monochlorinated intermediate with Pro-OBn, and subsequent hydrogenolysis to provide **6.15**. Finally, macrocyclisation and deprotection completed the synthesis of celogentin C (**6.8**).



Scheme 6.2: Total synthesis of celogentin C *via* 8-aminoquinoline-directed β C–H arylation of Leu² (Chen, 2010)

In 2010, Chen and co-workers adopted a different strategy to address the Leu²-Trp⁵ cross-link (Scheme 6.2).²¹ They forged the C–C bond *via* an aminoquinoline-directed Pd-catalysed β C–H arylation of leucine **6.16** with indolyliodide **6.17** to provide **6.18** with excellent diastereoselectivity. Conversion of the phthalimide group into an azide and global Boc protection provided **6.19**, which could be treated with LiOH and H₂O₂ to remove the aminoquinoline

auxiliary to provide carboxylic acid **6.20**. Following a sequence of deprotection and peptide coupling steps, this intermediate was converted to macrocycle **6.13**, an intermediate in Castle's original route to celogentin C. Indeed, **6.13** was carried forward to the natural product following Castle's protocol for oxidative C–N coupling to form the Trp⁵-His⁷ cross-link and subsequently close the right-hand macrocycle.



Scheme 6.3: Formal synthesis of celogentin C *via* addition to a Michael acceptor equipped with a chiral auxiliary (Jia, 2010).

In the same year, Jia and co-workers completed a formal synthesis of celogentin C.²² Their approach involved the Michael addition of the Grignard reagent of aryl iodide **6.22** to an acceptor **6.21** equipped with a chiral auxiliary, and subsequent trapping with NBS. Substitution of the alkyl bromide with NaN_3 provided azide **6.23**. Following removal of the chiral auxiliary to provide **6.24**, a series of protecting group manipulations and peptide couplings provided Castle's macrocycle **6.13**, thus constituting a formal synthesis of celogentin C.

6.3.2 Synthesis of streptide

First isolated from *Streptococcus thermophilus*,^{23,24} streptide was fully characterised and established as a RiPP by Seyedsayamdost and co-workers in 2015 (Figure 6.5).⁹ The macrocyclic natural product is made up of a modified nonapeptide backbone with the amino acid sequence

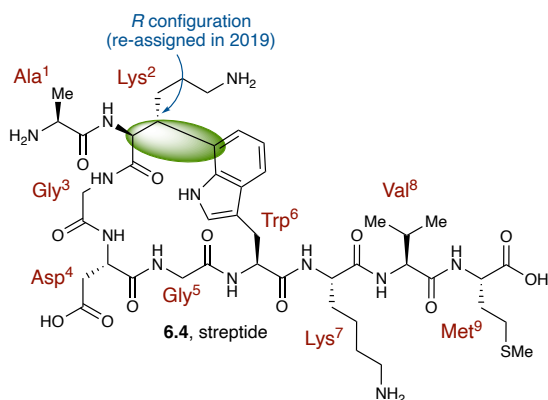


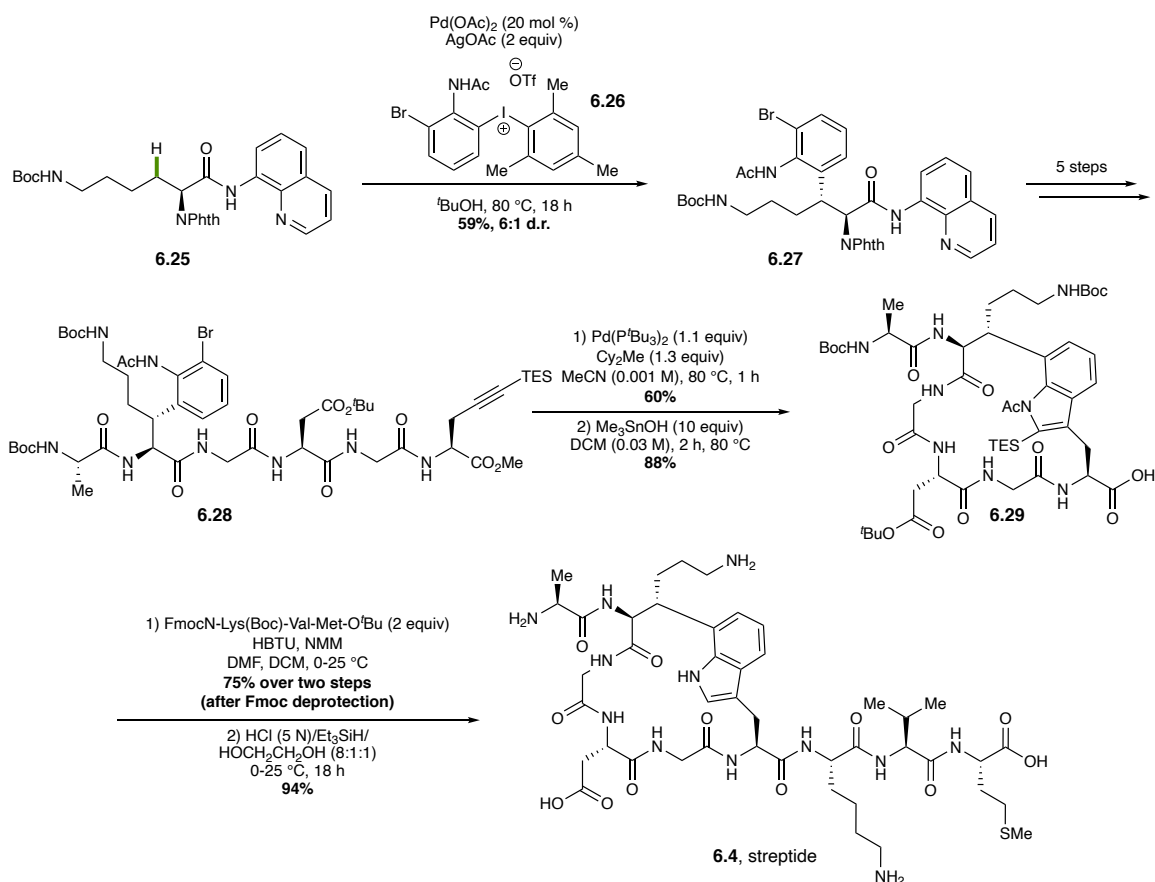
Figure 6.5: Streptide

Ala¹-Lys²-Gly³-Asp⁴-Gly⁵-Trp⁶-Lys⁷-Val⁸-Met⁹. Additionally, the compound contains one post-translational modification in the form of a C–C bond between the β -C of Lys² and indole-C7 of Trp⁶ (highlighted in green), formed by a radical SAM metalloenzyme. Although initially assigned with *S* configuration, the stereochemistry of the PTM stereocenter was reassigned in 2019 with the disclosure of the first total synthesis of streptide by Boger and co-workers in collaboration with Seyedsayamdost.⁸

In this approach to streptide (Scheme 6.4), the Lys²-Trp⁶ cross-link was established by 8-aminoquinoline-directed β C–H arylation of lysine **6.25** with diaryliodonium salt **6.26** to provide **6.27** in 59% yield with 6:1 d.r.¹⁸ Use of an iodoaniline instead of the diaryliodonium salt only resulted in modest yields of the arylated product. Intermediate **6.27** was converted to the hexapeptide **6.28** through a sequence of protecting group manipulations and peptide coupling steps. This hexapeptide was subjected to a previously developed macrocyclising heteroannulation reaction with Pd(P^{*t*}Bu₃)₂ (1.1 equiv) to provide the cyclic core of streptide **6.29** after hydrolysis of the C-terminal methyl ester with excess Me₃SnOH; the use of LiOH resulted in epimerisation and partial indole deacetylation. Attachment of the Lys⁷-Val⁸-Met⁹ tripeptide chain, followed by global deprotection of the *tert*-butyl esters and carbamates and the triethylsilyl ether, completed the

¹⁸ The major diastereomer had the correct relative stereochemistry and was carried forward to the completed natural product, and the minor diastereomer was also converted to the epimer of streptide.

synthesis of streptide.



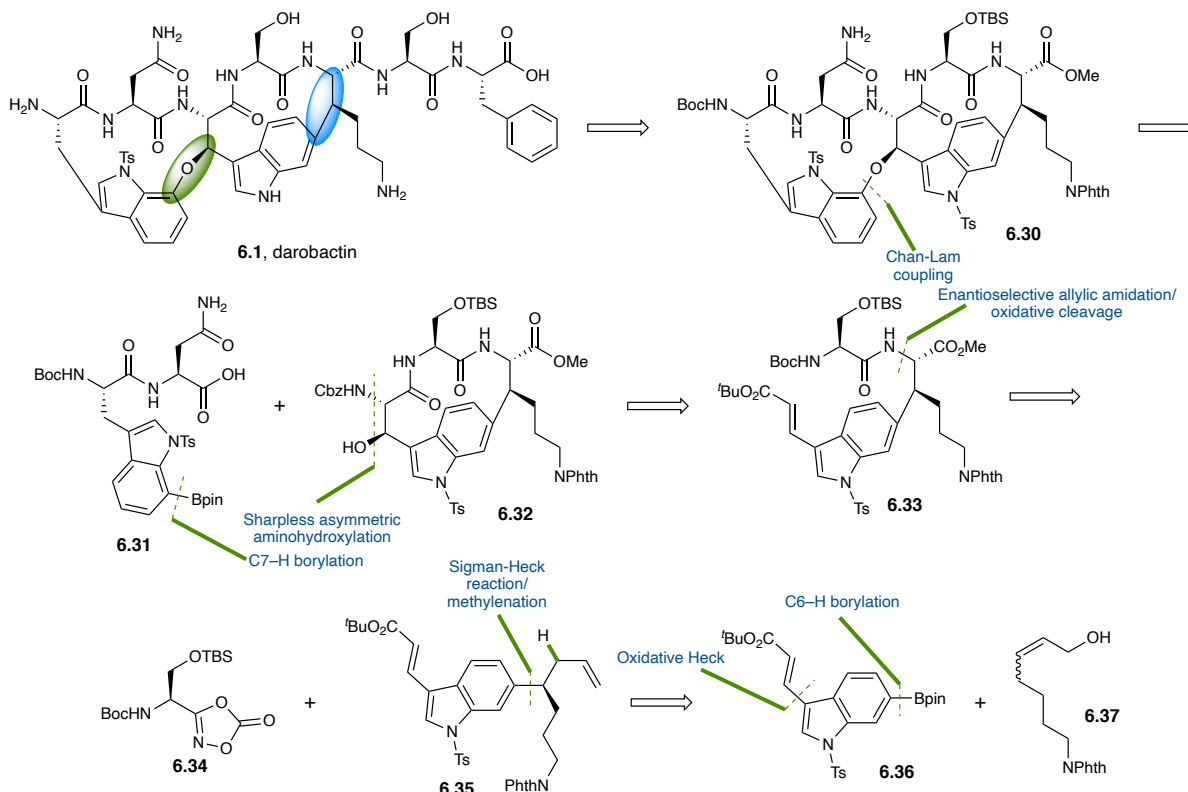
Scheme 6.4: Total synthesis and stereochemical re-assignment of streptide (Boger, Seyedsayamdost, 2019)

6.4 Evolution of a synthetic strategy towards darobactin A

6.4.1 Initial approach – enantioselective allylic amidation/oxidative cleavage sequence

Our retrosynthetic plan for the synthesis of darobactin A is outlined in Scheme 6.5. The natural product would be obtained by late stage installation of the Ser⁶-Phe⁷ dipeptide chain and global deprotection of bicyclic intermediate **6.30**. The C–O cross-link between Trp¹ and Trp³ would be established by inter- or intramolecular Chan-Lam coupling between secondary alcohol **6.32** and boronic ester **6.31**,²⁵ which would in turn be accessed by C7–H borylation as reported by Movassaghi and co-workers.²⁶ The aminoalcohol motif in **6.32** would be assembled by Sharpless asymmetric aminohydroxylation of acrylate **6.33**.²⁷ In this approach, Trp³-Lys⁵ cross-linked motif would be set up by enantioselective allylic amidation of olefin **6.35** with serine-

derived dioxazolone **6.34**,²⁸ followed by oxidative cleavage of the terminal olefin. Stereogenic substrate **6.35** would be generated by a redox-relay Sigman-Heck reaction of arylboronic ester **6.36** with allylic alcohol **6.37**²⁹ and Wittig olefination of the resulting aldehyde.

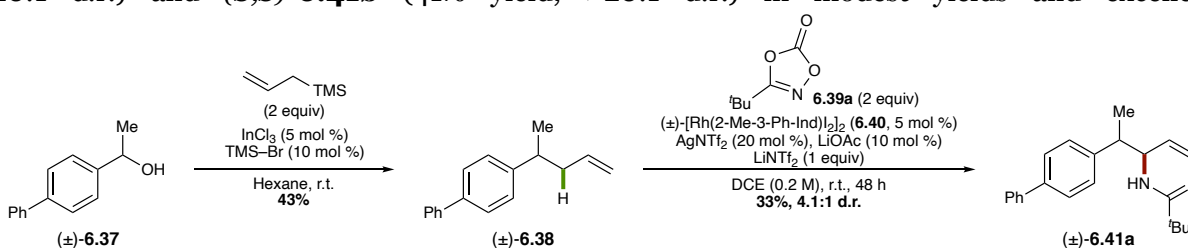


Scheme 6.5: Initial retrosynthetic plan to access darobactin A via an allylic amidation/oxidative cleavage sequence to assemble the Trp³-Lys⁵ cross-link.

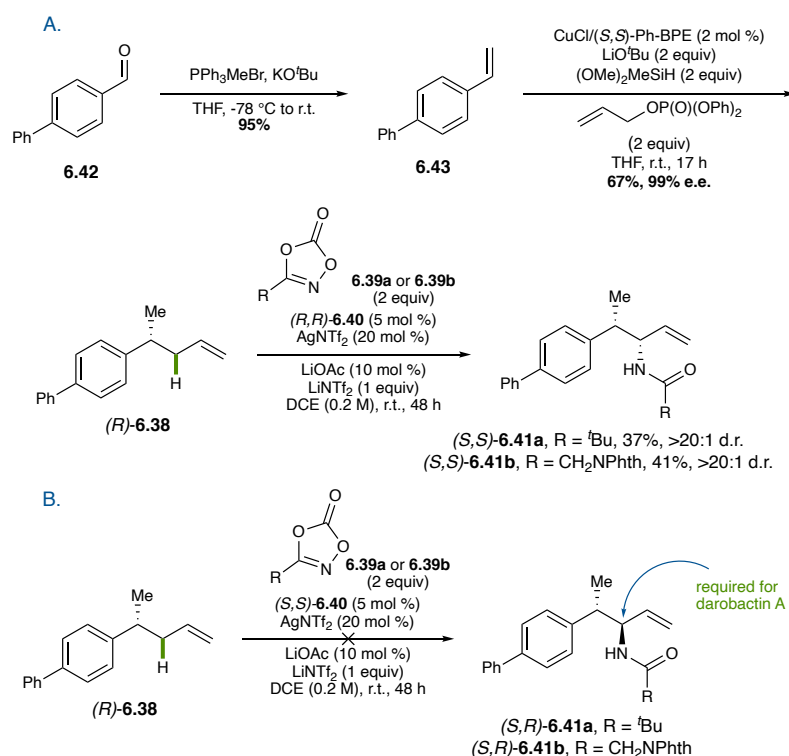
We have already established conditions for the oxidative cleavage of enantioenriched amide products derived from allylic amidation (see Chapter 5). However, in the context of darobactin A, we had to ensure that stereogenic olefin and dioxazolone substrates were amenable to our enantioselective allylic C–H amidation reaction without compromising their stereochemical integrity. To this end, we prepared the racemic olefin substrate **6.38** with a homoallylic stereocenter by In-catalysed allylation of commercially available alcohol **6.37** (Scheme 6.6).³⁰ This substrate was then subjected to allylic C–H amidation with *tert*-butyl dioxazolone **6.39a**, catalysed by a racemic mixture of our recently developed planar chiral rhodium indenyl catalyst **6.40**. Under these conditions, pivalamide **6.41a** was obtained in a modest yield of 33% with 4.1:1 d.r, indicating that the homoallylic methyl substituent imparted

very little stereoselection to the reaction. We were therefore excited at the prospect of efficiently selectively accessing both diastereomers of **6.41a** using both enantiomers of **6.40**.

To test this hypothesis, we prepared enantioenriched **6.38** following the sequence of steps in Scheme 6.7. Wittig methylenation of biphenyl aldehyde **6.42** provided vinyl biphenyl **6.43**.³¹ Enantioselective hydroallylation of this substrate, as developed by Buchwald and co-workers, provided (*R*)-**6.38** in 67% yield with excellent enantioselectivity.³² (*R,R*)-**6.40**-catalysed enantioselective allylic C–H amidation of (*R*)-**6.38** with *tert*-butyl dioxazolone **6.39a** or Phth-glycine dioxazolone **6.39b** provided the corresponding amide products (*S,S*)-**6.41a** (37% yield, >20:1 d.r.) and (*S,S*)-**6.41b** (41% yield, >20:1 d.r.) in modest yields and excellent



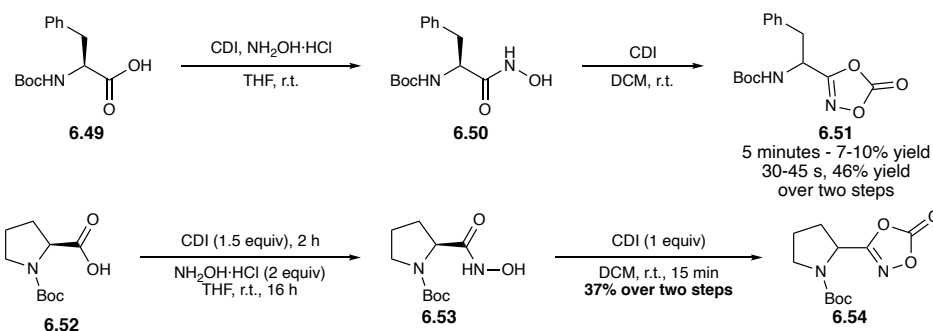
Scheme 6.6: Preparation and racemic allylic C–H amidation of racemic homoallylic stereogenic olefin



Scheme 6.7: Preparation and enantioselective allylic C–H amidation of (*R*)-**6.38**

To probe this issue, Quincy McKoy, a graduate student in the Blakey lab, converted *L*-Phth-alanine (**6.47**) to its corresponding hydroxamic acid **6.48**. HPLC analysis confirmed that no epimerisation had taken place at this stage. Treatment with CDI then converted hydroxamic acid **6.48** to dioxazolone **6.45**. HPLC analysis at this stage indicated that complete racemisation of the alanine stereocenters had occurred during conversion to the dioxazolone, which explains the low diastereoselectivity observed in Scheme 6.8.

We hypothesise that the key to suppressing racemisation during dioxazolone synthesis would be to use a carbonyl source other than CDI, which generates basic imidazole during the reaction. Additionally, it is possible that the use of the electron-withdrawing phthalimide protecting group at the *N*-terminus exacerbates the acidity of the α -proton of the dioxazolone. Therefore, we first turned our attention towards the synthesis of amino acid-derived dioxazolones with carbamate protecting groups.



Scheme 6.10: Synthesis of stereogenic amino acid-derived dioxazolones

We targeted Boc-protected phenylalanine and Boc-protected proline derivatives as suitable representatives of secondary and tertiary protected amines, respectively (Scheme 6.10). Conversion of Boc-Phe-OH (**6.49**) to its corresponding hydroxamic acid **6.50** occurred smoothly and the crude residue was carried forward. Surprisingly, we observed that carbonylative cyclisation of this intermediate occurred almost instantaneously when treated with CDI at room temperature. TLC analysis of the reaction mixture 3-5 minutes after addition of CDI showed complete consumption of the hydroxamic acid and appearance of a new spot, which was determined to be the desired dioxazolone **6.51** by ^1H and ^{13}C NMR. However, very low quantities of dioxazolone **6.51** were isolable in yields ranging from 7–10% over two steps. Upon addition of

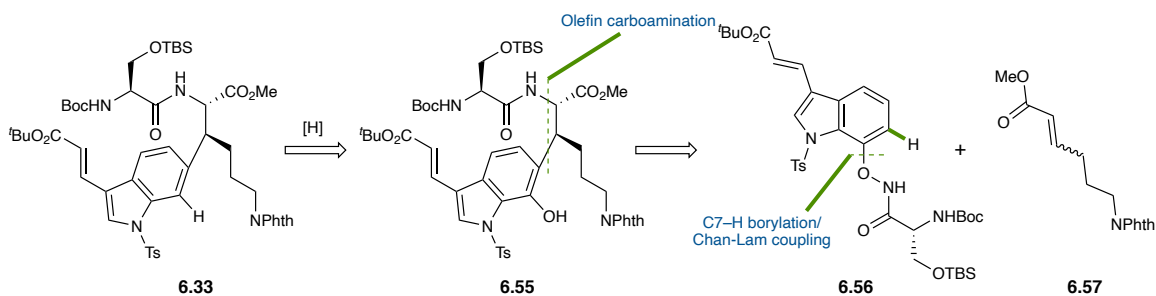
CDI to the flask, the reaction mixture rapidly changed from a cloudy white suspension to a clear, colourless solution (within 30 seconds). By quenching the reaction with saturated aqueous NaHCO₃ as soon as its appearance changed, we were able to isolate **6.51** in 46% yield over two steps. Similarly, Boc-Pro-OH (**6.52**) was converted to hydroxamic acid **6.53** and the crude product was treated with CDI to provide dioxazolone **6.54** in 37% yield over two steps.

Unfortunately, solubility issues prevented Quincy from immediately establishing whether any racemisation of these dioxazolones had occurred or not. In the meantime, we subjected dioxazolones **6.51** and **6.54** to RhCp*- and IrCp*-catalysed allylic C–H amidation conditions (not shown). However, no desired allylic amide products were observed in either case, even at elevated temperatures. Instead, unidentified side products, presumably arising from dioxazolone decomposition, were observed in the crude ¹H NMR spectra.

Our original plan for establishing the Trp³-Lys⁵ cross-link present in darobactin A centred around an allylic C–H amidation/oxidative cleavage sequence of reactions, and we conducted preliminary reactions to test the feasibility of stereogenic olefin- and dioxazolone-coupling partners. The enantioselective allylic C–H amidation of a homoallylic stereogenic olefin showed that the mismatched diastereomer was required for the synthesis of darobactin A, and that our catalyst system was as yet unable to access this diastereomer. Secondly, Quincy McKoy determined that chiral amino acid-derived dioxazolones racemised during their preparation, severely hampering their utility in the synthesis of darobactin A. Furthermore, the allylic amidation sequence does not deliver the product at the required oxidation state, requiring an additional oxidative cleavage step to continue the synthesis. For these reasons, we decided to abandon this approach, and develop an alternate strategy to assemble the Trp³-Lys⁵ cross-link of darobactin A.¹⁹

¹⁹ At this time, David Laws began working on this project alongside us, with the primary goal of establishing conditions for the Chan-Lam coupling to forge the C–O–C linkage between Trp¹ and Trp³.

6.4.2 Revised approach – olefin carboamination

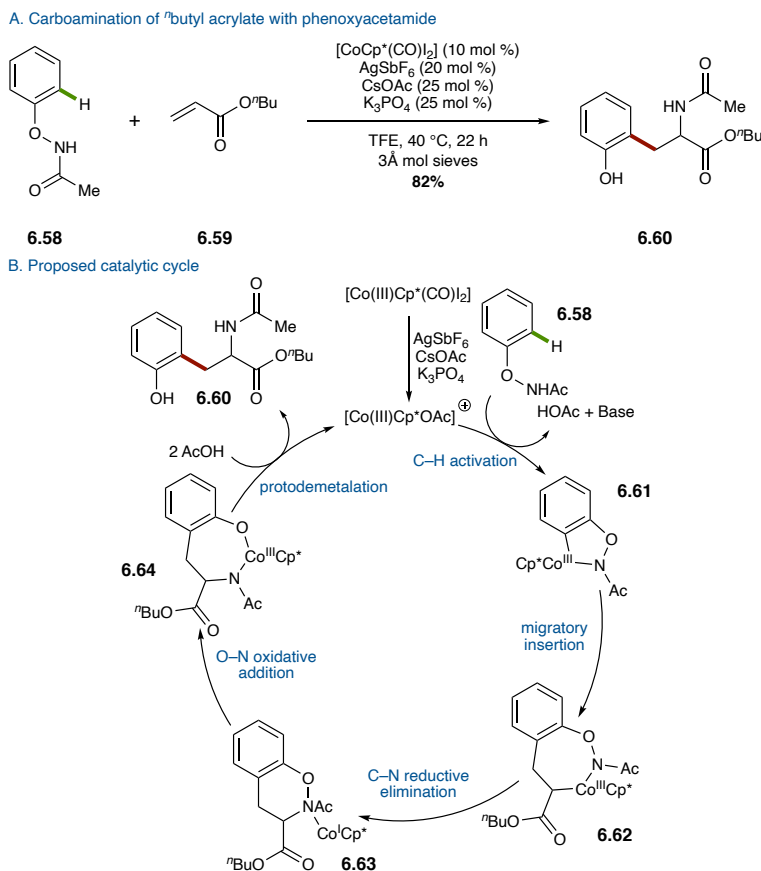


Scheme 6.11: Revised plan to establish the Trp³-Lys⁵ cross-link – stereoselective carboamination of acrylate **6.57**

Our revised strategy to establish the Trp³-Lys⁵ cross-link is shown in Scheme 6.11. Intermediate **6.33** would be accessed by triflation and reduction of 7-hydroxyindole **6.55**. The C–C cross-linkage and the adjacent C–N bond would be formed stereoselectively *via* an *ortho* C–H functionalisation/carboamination reaction between indole **6.56** and olefin **6.57**. C7-H borylation²⁶ and Cu-mediated coupling would forge the aryl C–O present in **6.56**.³³ Glorius and co-workers have previously shown that treatment of phenoxyacetamide (**6.58**) and *n*butyl acrylate (**6.59**) with [CoCp*(CO)I₂] (10 mol %) in the presence of AgSbF₆ (20 mol %), CsOAc (25 mol %), and K₃PO₄ (25 mol %) provides hydroxylated phenylalanine **6.60** in 82% yield (Scheme 6.12 A).³⁴

The proposed mechanism for the CoCp*-catalysed carboamination reaction is depicted in Scheme 6.12 B. Directed C(sp²)–H activation at the *ortho* position of phenoxyacetamide (**6.58**) provides metallocycle **6.61**. Migratory insertion with *n*butyl acrylate then forms the C–C bond to provide alkyl Co(III)Cp*-complex **6.62**. The authors propose that C–N reductive elimination at this stage forms the C–N bond and provide Co(I)Cp*-complex **6.63**. Oxidative addition and protodemetalation then provides amino acid product **6.60** and regenerates the Co(III)Cp* active catalyst. However, a mechanism in which oxidative addition to access a Co(V)-intermediate precedes C–N reductive elimination cannot be ruled out. RhCp*-complexes were shown to be

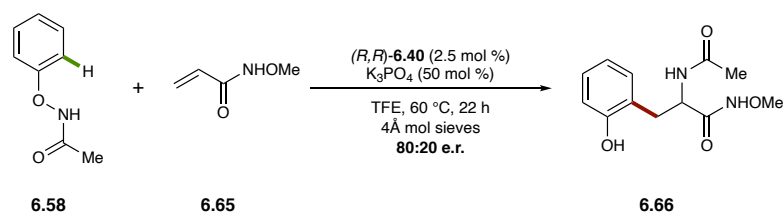
ineffective catalysts for the carboamination of acrylates, instead predominantly providing the oxidative Heck products arising from β -hydride elimination of the alkyl Rh(III)Cp*-complex.



Scheme 6.12: CoCp*-catalysed intermolecular carboamination of acrylates *via* directed C(sp²)-H activation of phenoxyacetamide (Glorius, 2016)

An independent and simultaneous report from Liu and co-workers demonstrated that to achieve the same reaction under RhCp*-catalysis, *N*-methoxyacrylamide was required as the olefin acceptor (not shown).³⁵ In Liu's work, competitive β -hydride elimination of the putative alkyl RhCp*-complex was suppressed by coordinatively saturating the metal centre with the *N*-methoxyamide motif, while the oxidative Heck products were formed in the absence of a bidentate coupling partner (as observed by Glorius and co-workers). A similar tactic was employed by Rovis and co-workers in 2015.³⁶ However, the use of CoCp*-catalysts obviated the need for such limitations, due to the slower rate of β -hydride elimination of Co-complexes.

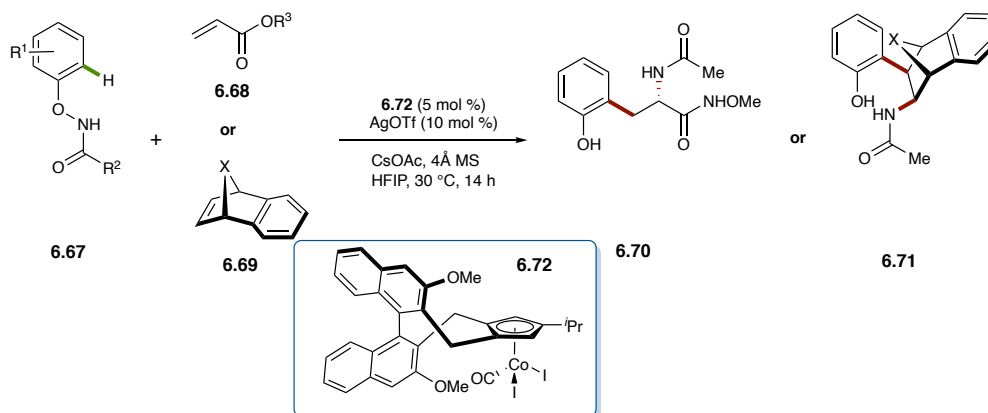
For this strategy to be feasible in the context of darobactin A, certain advances had to be made to the reactions reported by Rovis, Glorius, and Liu. Despite three iterations of intermolecular carboamination triggered by C(sp²)-H activation, no asymmetric variants of this reaction had been reported at this stage. We considered this an ideal opportunity to apply our recently developed planar chiral indenyl complexes, which were originally developed for enantioselective allylic C-H functionalisation, as catalysts for a mechanistically distinct reaction. Secondly, both examples of carboamination with phenoxyacetamide, reported by Glorius and Liu, involved terminal acrylates or acrylamides as the olefin reaction partner, respectively; we would need to extend the scope of this reaction to include disubstituted olefins. Furthermore, by appending an amino acid residue to the phenoxyamide, we could directly install the required amino acid chain present in darobactin A. Lastly, Glorius's work demonstrated that Co-catalysis was essential for the successful carboamination of acrylates, which are more synthetically tractable than *N*-methoxyacrylamides. We would need to expand our planar chiral indenyl catalyst catalogue to include cobalt complexes.



Scheme 6.13: Preliminary experiment – enantioselective carboamination of *N*-methoxyacrylamide with phenoxyacetamide

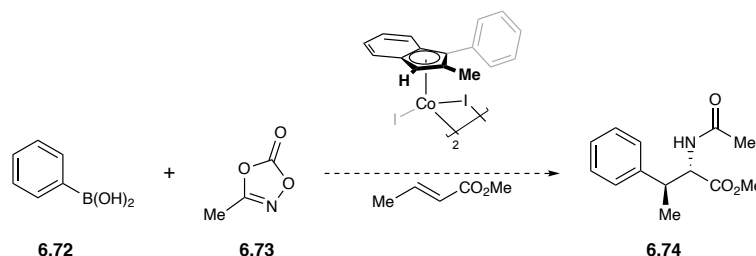
As a preliminary experiment, we performed the enantioselective carboamination of *N*-methoxyacrylamide (**6.65**) with phenoxyacetamide (**6.58**) under Liu's conditions using (*R,R*)-**6.40** as the catalyst at 60 °C. The reaction proceeded very sluggishly and showed minor amounts of the desired amino acid **6.60** and large quantities of unreacted phenoxyacetamide in the crude ¹H NMR spectrum. In order to avoid losing the small quantity of product that was observed, a filtered sample of the crude reaction mixture was prepared and run down the chiral HPLC,

showing a modest e.r. of 80:20 for this reaction.²⁰ Unfortunately, we were unable to isolate pure samples of **6.66** by chromatography on silica gel. Nevertheless, this experiment established that we could apply our planar chiral rhodium indenyl catalysts to intermolecular carboamination reactions.



Scheme 6.14: Co-catalysed enantioselective intermolecular carboamination of monosubstituted acrylates and strained bicyclic olefins with aryloxyamides (Cramer, 2020).

For the reasons discussed earlier, and based on our preliminary experiments, we expected that a chiral Co-catalyst would be necessary for this reaction to proceed efficiently. At this stage, however, Cramer and co-workers reported the enantioselective intermolecular carboamination of olefins with aryloxyamides using BINOL-derived Co-complex **6.72** (5 mol %) as the catalyst, AgOTf (10 mol %) as the halide scavenger, and CsOAc as the base (Scheme 6.14).³⁷ Under these conditions, a range of substituted aryloxyamides could be applied to the carboamination of various monosubstituted acrylates (**6.68**) and strained bicyclic olefins (**6.69**) to provide products **6.70** or **6.71**, respectively. Consistent with previous findings from Glorius and Liu, Cramer and



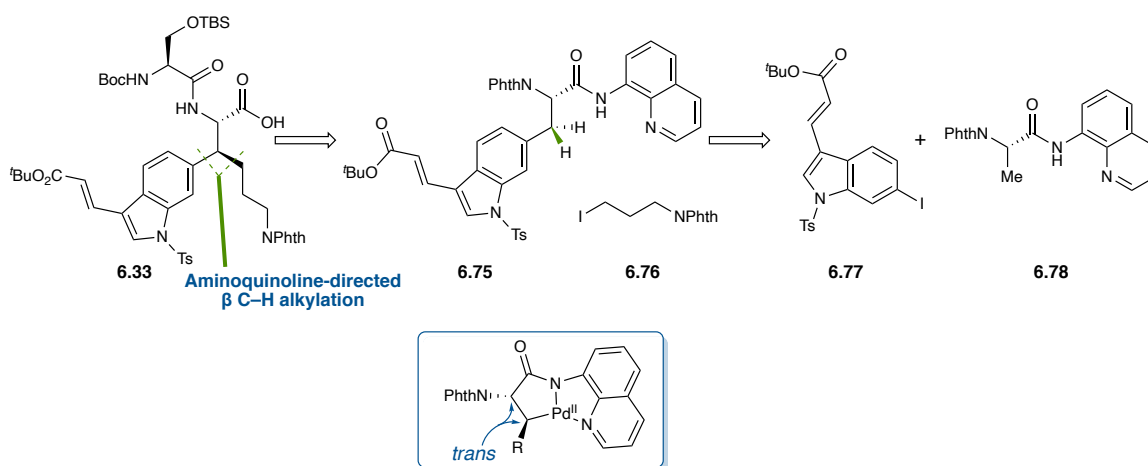
Scheme 6.15: Proposed Co-catalysed enantioselective three-component carboamination with an internal acrylate, an aryl boronic acid, and a dioxazolone (Christopher Poff)

²⁰ The peaks for (+)- and (-)-**6.66** were identified by repeating the racemic reaction developed by Liu and co-workers.

co-workers report that this reaction is specific to Co-catalysis; Rh-complexes were shown to be ineffective catalysts for this reaction.

We therefore turned our attention towards further developing this reaction for the enantioselective carboamination of 1,2-disubstituted acrylates as olefin acceptors that are more representative of darobactin A. Furthermore, this reaction leaves behind a phenol moiety which is absent on Trp³ of darobactin A and would have to be reductively removed. In the context of RiPPs synthesis, future work will also be directed towards the development of a three-component carboamination reaction with an internal acrylate, an aryl boronic acid, and a dioxazolone as the amidating reagent (Scheme 6.15). This project was taken over by Christopher Poff, a graduate student in the Blakey lab. In the meantime, we turned our attention towards an alternate strategy to install the Trp³-Lys⁵ cross-link present in darobactin A.

6.4.3 Current approach – iterative aminoquinoline-directed β C–H functionalisation of alanine

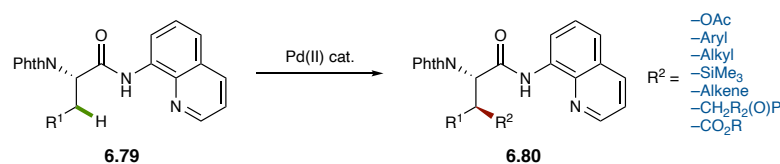


Scheme 6.16: Current plan to establish the Trp³-Lys⁵ cross-link – iterative β C–H arylation/alkylation sequence of alanine **6.78** equipped with an 8-aminoquinoline directing auxiliary

As our current strategy to assemble the Trp³-Lys⁵ darobactin A cross-link, we are investigating the iterative aminoquinoline-directed β C–H functionalisation of phthalimidoyl alanine **6.78** equipped with an 8-aminoquinoline directing auxiliary (Scheme 6.16). Inspired by Chen's synthesis of celogentin C (see Scheme 6.2)²¹ and Boger's synthesis of streptide (see Scheme 6.4),⁸ this approach would allow us to diastereoselectively form the C–C bond between the two

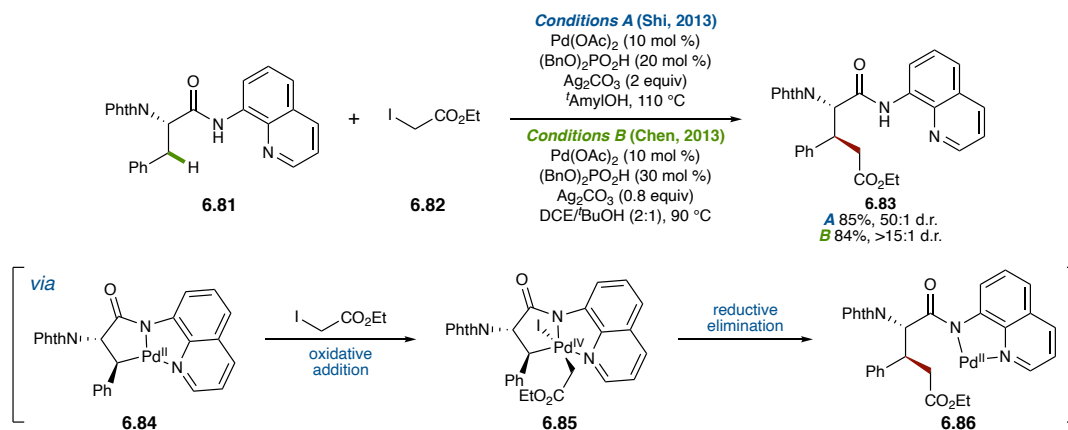
amino acid residues. In both of these prior syntheses, β C–H arylation of a canonical amino acid residue (Leu or Lys, respectively) stereoselectively formed the C–C cross-links present in the natural products. The observed diastereoselectivity is a result of the putative *trans* metalacyclic intermediate that is favoured during these reactions (Scheme 6.16, blue inset). However, the relative stereochemistry of the Trp³-Lys⁵ cross-link in darobactin A is opposite to those present in celogentin C and streptide, thus ruling out direct β C–H arylation of lysine as a viable path forward. Thus, this approach involves the sequential C–H arylation of alanine **6.78** with aryl iodide **6.77**, followed by diastereoselective C–H alkylation of **6.75** with alkyl iodide **6.76** proceeding through a *trans* metalacyclic intermediate.

6.4.3.1 Aminoquinoline-directed β C–H alkylation of amino acids



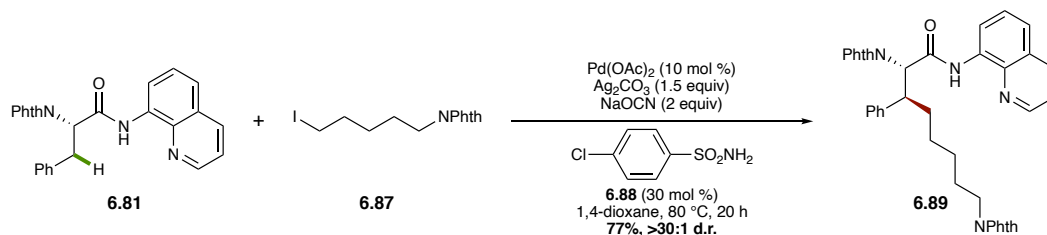
Scheme 6.17: 8-Aminoquinoline-directed β C–H functionalisation of amino acids

The 8-aminoquinoline motif was first reported as a directing auxiliary for catalytic reactions by Corey and co-workers for Pd-catalysed β C–H acetoxylation.³⁸ β C–H arylation reactions, the first examples of C–C bond formation, were also independently reported by Corey and Daugulis.³⁹ In the intervening years since Corey's seminal report, 8-aminoquinoline-directed β C–H functionalisation of amino acids has been expanded to include alkylation, alkenylation, silylation, and carboxylation, among other reactions (Scheme 6.17).^{40–42} While C–H arylation has seen the most widespread use in the synthesis of complex molecules, as exemplified by the syntheses of celogentin C and streptide, C–H alkylation reactions are comparatively much less studied.



Scheme 6.18: β C–H alkylation of phenylalanine with alkyl iodides lacking β hydrogen atoms (Shi, Chen, 2013)

In 2013, Shi⁴³ and Chen⁴⁴ independently reported the β alkylation secondary C–H bonds of amino acids (Scheme 6.18). Under their very similar conditions, phenylalanine **6.81** could be alkylated with α -iodoacetate **6.82** to provide modified peptide **6.83** in good yields. However, these early reports were limited to alkyl electrophiles without β -hydrogen atoms. The authors propose a catalytic mechanism in which oxidative addition of α -iodoacetate **6.82** with *trans* Pd(II)-metalacyclic **6.84** intermediate leads to Pd(IV)-complex **6.85**. Rapid C–C reductive elimination of this complex and protodemetalation of **6.86** then provides the desired product. Alkyl electrophiles with β -hydrogen atoms were reportedly incompatible with this reaction due to competing β -hydride elimination of the putative Pd(IV)-intermediate **6.85**.



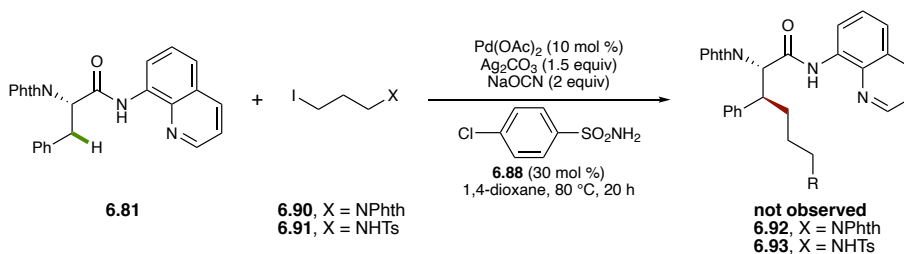
Scheme 6.19: Modified conditions for β C–H alkylation of phenylalanine with alkyl iodides containing β -hydrogen atoms (Shi, 2014)

In 2014, Shi and co-workers addressed this challenge and reported conditions for the β functionalisation of secondary C(sp³)–H bonds of amino acids with alkyl electrophiles containing β -hydrogen atoms (Scheme 6.19).⁴⁵ Key to the success of this reaction was the use of *p*-Cl-benzenesulfonamide (**6.88**, 30 mol %) as a reversibly coordinating ligand to suppress β -hydride elimination of the Pd(IV) intermediate. NaOCN (2 equiv) was also added as an additional halide

scavenger. Under these conditions, alkyl iodide **6.87** could be employed as an alkylating reagent to provide modified peptide **6.89** in 77% yield and >30:1 d.r.

6.4.3.2 Model studies with phenylalanine

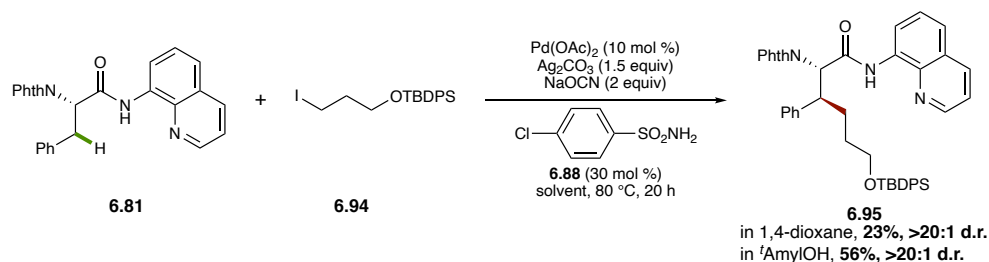
To test the feasibility of this strategy, we first decided to conduct the β C–H alkylation of phenylalanine **6.81** with known differentially protected iodo-propylamine electrophiles **6.90**^{46,47} and **6.91**^{48,49} (Scheme 6.20). Interestingly, under the reaction conditions, only trace amounts of alkylation product **6.92** (identified by the presence of an indicative doublet α C–H peak) were observed with low reproducibility when iodide **6.90** was used as the electrophile. When iodosulfonamide **6.91** was used, no trace of alkylation product **6.93** was observed. In both cases, complete consumption of the alkyl iodide electrophile and large amounts of unreacted **6.81** were observed by TLC analysis and in the crude ¹H NMR spectra. Additionally, the crude ¹H NMR spectra indicated the presence of unidentified side products, presumably resulting from decomposition of the iodide electrophiles. The presence of olefinic peaks suggests β -hydride elimination as a possible side reaction pathway.



Scheme 6.20: Model β C–H alkylation of phenylalanine **6.81** with protected iodopropylamines

This result was especially curious because Shi and co-workers have previously demonstrated the use of iodide **6.87**, which differs from iodide **6.90** only by a chain length of two methylenes, as a feasible electrophile in this reaction (see Scheme 6.19). We hypothesise that alkyl iodide electrophiles containing Lewis basic functionality (such as phthalimides or sulfonamides) could coordinate the Pd center, thus preventing Pd(IV)-Pd(II) C–C reductive elimination. This could explain the unproductive consumption of the aminoiodide electrophiles **6.90** and **6.91** under the reaction conditions, whereas aminoiodide **6.87**, in which the Lewis basic functionality

is two carbons further, leads to productive C–C coupling. We successfully repeated the β C–H alkylation of phenylalanine **6.81** with 1-iodohexane, as reported by Shi and co-workers (not shown), which suggested that the poor reactivity observed with iodides **6.90** and **6.91** was indeed due to the Lewis basic functional groups present on these electrophiles.



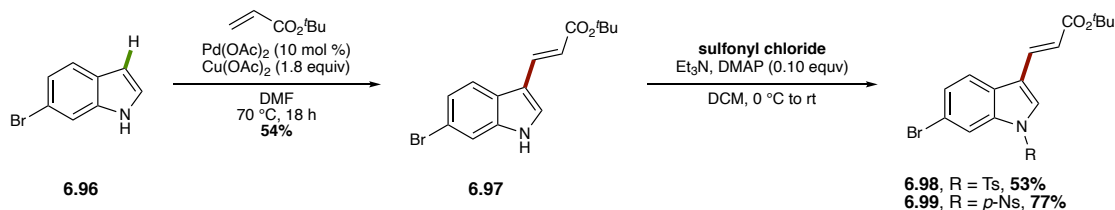
Scheme 6.21: β C–H alkylation of phenylalanine **6.81** with alkyl iodide **6.94**

We hypothesised that an electrophile containing a less Lewis basic amine-surrogate would allow the reaction to proceed. With this in mind, we conducted the β C–H arylation of phenylalanine **6.81** with iodo-silyl ether **6.94**^{47,50} under Shi’s modified conditions. Indeed, this electrophile had been previously used by Shi and co-workers in the functionalisation of β -methylalanine. When we performed the reaction in 1,4-dioxane at 80 °C, we isolated modified phenylalanine **6.95** in 23% yield as a single diastereomer (as determined by crude ¹H NMR). Importantly, no side products arising from decomposition of iodide **6.94** were observed in this reaction. We were able to increase the yield of **6.95** to 56% by switching the solvent to ^tAmylOH, which is very well-precedented in reactions of this type. With a feasible electrophile for the β C–H alkylation in hand, we decided to move on to the synthesis of the C–H arylation coupling partner. We envisioned that the TBDPS-protected alcohol could eventually be displaced with a sulfonyl-protected amine after β C–H functionalisation.

6.4.3.3 β C–H arylation with aryl iodide **6.77**

We began our synthesis of aryl iodide **6.77** (see Scheme 6.16) with the oxidative C₃ olefination of 6-bromoindole (**6.96**), adapting the procedure laid out by Gaunt and co-workers.⁵¹ Thus, treatment of 6-bromoindole with ^tbutyl acrylate in the presence of Pd(OAc)₂ (10 mol %) and CuOAc (1.8 equiv) as an external stoichiometric oxidant in DMF at 70 °C for 18 h regioselectively

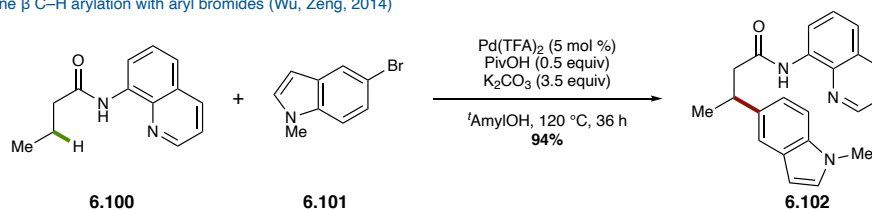
provided the C3 alkenylated product **6.97** in 54% yield (Scheme 6.22). The indole nitrogen was then protected with a Ts and *p*-Ns group to provide **6.98** (53%) and **6.99** (77%), respectively. We expected to employ the same protecting group on the Trp¹ and Trp³ indoles as well as on the Lys⁵ amine, which could be simultaneously removed at a later stage in the synthesis.



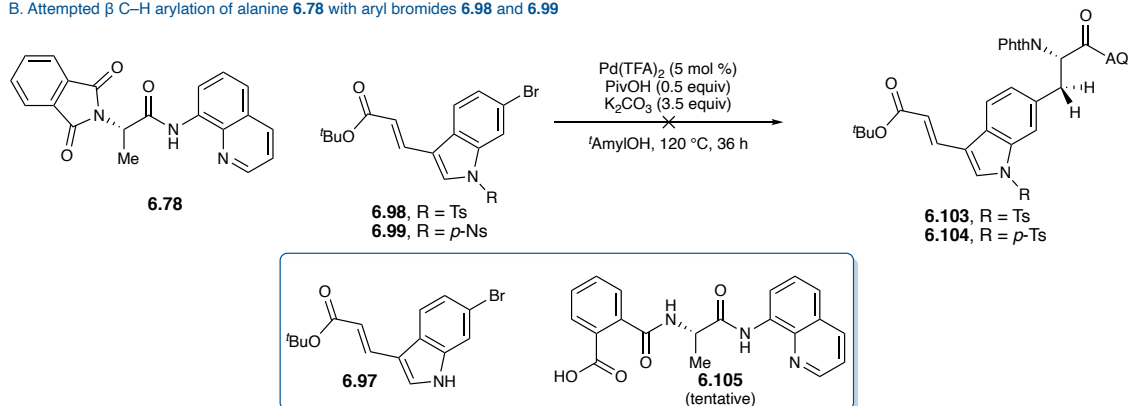
Scheme 6.22: Synthesis of C3-alkenylated indoles **6.98** and **6.99**

Before converting **6.98** and **6.99** to their respective aryl iodides, we first attempted the β C–H arylation of alanine **6.78** with the aryl bromides themselves. In 2014, Wu and Zeng reported the β C–H arylation of aminoquinoline-containing carboxamides with aryl bromides (Scheme 6.23 A). Pd(TFA)₂ was found to be a superior catalyst compared to Pd(OAc)₂. However, no amino acid derivatives were reported in the substrate scope of this reaction.

A. Aminoquinoline β C–H arylation with aryl bromides (Wu, Zeng, 2014)



B. Attempted β C–H arylation of alanine **6.78** with aryl bromides **6.98** and **6.99**



Scheme 6.23: Aminoquinoline-directed β C–H arylation with aryl bromides

Unfortunately, when we attempted this reaction with aryl bromides **6.98** and **6.99** under the reported conditions, we did not observe any arylated products **6.100** or **6.101** (Scheme 6.23 B). Instead we observed deprotected indole **6.97** as a major side product, as well as another

compound that we have tentatively assigned as carboxylic acid **6.105**, arising from ring-opening of the phthalimide functional group.

6.5 Conclusion and Future Work

We have explored different strategies to assemble the Trp³-Lys⁵ cross-link present in darobactin A. In our initial approach, we envisioned establishing the C–C bond with *via* a Sigman-Heck reaction and converting the resulting aldehyde to a corresponding terminal olefin. Our newly developed enantioselective allylic C–H amidation would then install the amino acid fragment. However, further investigation by Quincy McKoy showed that amino acid-derived dioxazolones racemised during their synthesis, rendering this strategy infeasible. We next envisioned a stereoselective carboamination reaction across an internal olefin to form a C–C and C–N bond in a single step. While an enantioselective variant of this reaction was recently reported by Cramer and co-workers, further work is necessary for this reaction to be feasible in the context of darobactin A. Christopher Poff is currently working on further development of this reaction. Our current strategy was inspired by Chen's synthesis of celogentin C and Boger's synthesis of streptide, and involves the iterative β C–H arylation and alkylation of alanine equipped with an aminoquinoline directing group. Model studies indicated that we would require a protected alcohol as a precursor to the amine. Current work is directed towards accessing the aryl iodide coupling partner required for the reaction, which we will access *via* aromatic Finkelstein iodination of the aryl bromide.⁵² This chapter concludes Part II of this dissertation.

6.6 Experimental

General Information

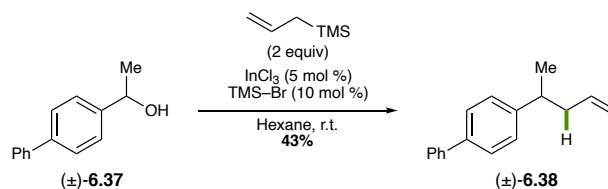
All reactions were carried out under a nitrogen atmosphere with anhydrous solvents in oven- or flame-dried glassware using the standard Schlenk technique, unless otherwise stated.

Anhydrous dichloromethane (DCM), diethyl ether (Et₂O), tetrahydrofuran (THF), and toluene were obtained by passage through activated alumina using a *Glass Contours* solvent purification system. 1,2-Dichloroethane (DCE), 2,2,2-trifluoroethanol (TFE), and *tert*-Amyl alcohol were distilled over calcium hydride (CaH₂) and stored over activated molecular sieves. Solvents for workup, extraction, and column chromatography were used as received from commercial suppliers without further purification. InCl₃, AgSbF₆, CsOAc, LiNTf₂, LiOAc, [Cp*IrCl₂]₂, [Cp*RhCl₂]₂, (*S,S*)-[Rh(2-Me-3-Ph-Ind)I₂]₂, (*R,R*)-[Rh(2-Me-3-Ph-Ind)I₂]₂, and CDI were stored and weighed in a nitrogen-filled glovebox. All other chemicals were purchased from Sigma-Aldrich, Strem Chemicals, Oakwood Chemicals, Alfa Aesar, or Combi-Blocks, and used as received without further purification, unless otherwise stated. ¹H and ¹³C nuclear magnetic resonance (NMR) spectra were recorded on a Varian Inova 600 spectrometer (600 MHz ¹H, 151 MHz ¹³C), a Bruker 600 spectrometer (600 MHz ¹H, 151 MHz ¹³C), a Varian Inova 500 spectrometer (500 MHz ¹H, 126 MHz ¹³C), and a Varian Inova 400 spectrometer (400 MHz ¹H, 100 MHz ¹³C) at room temperature in CDCl₃ (neutralized and dried over anhydrous K₂CO₃) with internal CHCl₃ as the reference (7.26 ppm for ¹H, 77.16 ppm for ¹³C), unless otherwise stated. Chemical shifts (δ values) were reported in parts per million (ppm), and coupling constants (*J* values), in Hz. Multiplicity was indicated using the following abbreviations: s = singlet, d = doublet, t = triplet, q = quartet, qn = quintet, m = multiplet, br = broad. Infrared (IR) spectra were recorded using a Thermo Electron Corporation Nicolet 380 FT-IR spectrometer. High resolution mass spectra (HRMS) were obtained using a Thermo Electron Corporation Finigan LTQFTMS (at the Mass Spectrometry Facility, Emory University). Analytical thin layer chromatography (TLC) was performed on precoated glass backed Silicycle SiliaPure 0.25 mm

silica gel 60 plates and visualized with UV light, ethanolic p-anisaldehyde, or aqueous potassium permanganate (KMnO₄). Flash column chromatography was performed using Silicycle SiliaFlash F60 silica gel (40–63 μm) on a Biotage Isolera One system. Preparatory TLC was performed on pre-coated glass backed Silicycle SiliaPure 1.0 mm silica gel 60 plates.

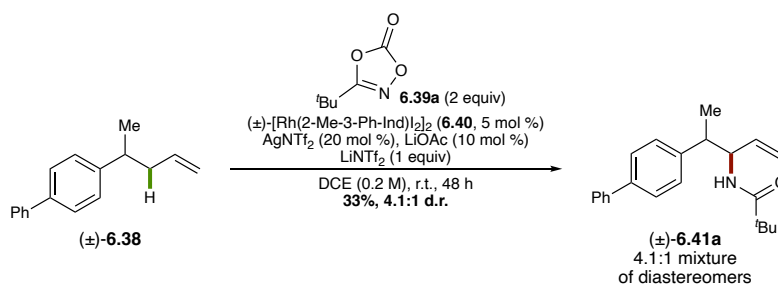
Procedures and Characterisation

Olefin (±)-6.38



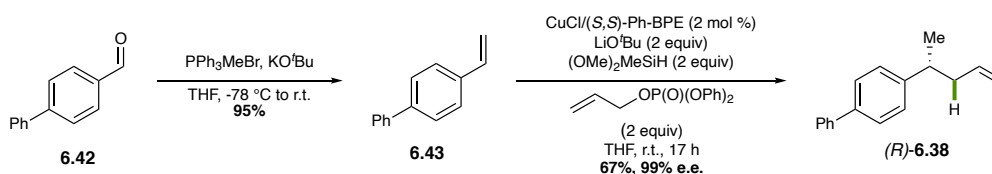
This procedure was adapted from Baba and co-workers.³⁰ In a nitrogen-filled glovebox, InCl₃ (0.056 g, 0.25 mmol) was weighed into a round-bottom flask equipped with a magnetic stir bar. The flask was capped with a septum and brought out of the glovebox. Hexane (3 mL), allyltrimethylsilane (1.6 mL, 10.0 mmol), and TMS-Br (0.065 mL, 0.50 mmol) were added to the reaction flask. A solution of alcohol (±)-6.37 in hexane (3 mL) was added slowly over 5 minutes and the reaction was stirred at room temperature for 24 hours. The reaction was quenched with saturated aqueous NaHCO₃ (10 mL) and diluted with Et₂O (10 mL). The layers were separated, and the aqueous layer was washed with Et₂O (2 x 10 mL). The combined organic extracts were washed with brine (30 mL), dried over anhydrous MgSO₄, filtered, and concentrated under reduced pressure. Purification by flash chromatography on silica gel (0–2% Et₂O in Hexanes) provided (±)-6.38 (0.484 g, 43%). ¹H NMR spectrum matches previously reported data.³⁰

¹H NMR (CDCl₃, 500 MHz) δ 7.62 – 7.59 (m, 2H), 7.57 – 7.52 (m, 2H), 7.44 (dd, *J* = 8.5, 7.0 Hz, 2H), 7.38 – 7.32 (m, 1H), 7.29 (d, *J* = 8.2 Hz, 2H), 5.77 (ddt, *J* = 17.4, 10.2, 7.1 Hz, 1H), 5.04 (ddtd, *J* = 17.1, 2.1, 1.4, 0.6 Hz, 1H), 5.00 (ddq, *J* = 10.2, 2.0, 1.0 Hz, 1H), 2.86 (h, *J* = 7.0 Hz, 1H), 2.45 (dt, *J* = 13.7, 6.7 Hz, 1H), 2.34 (dt, *J* = 13.8, 7.5 Hz, 1H), 1.31 (d, *J* = 6.9 Hz, 3H) ppm.

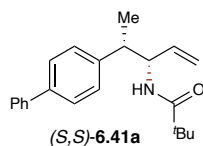
Pivalamide (\pm)-**6.41a**

Prepared according to the general procedure for allylic C–H amidation (see Chapter 5 experimental, General Procedure D) using (\pm)-**6.40** (0.0056 g, 0.005 mmol), AgNTf₂ (0.0078 g, 0.020 mmol), LiOAc (0.00066 g, 0.010 mmol), LiNTf₂ (0.029 g, 0.10 mmol), *tert*-butyl dioxazolone **6.39a** (0.029 g, 0.20 mmol), and (\pm)-**6.38** (0.022 g, 0.10 mmol) in DCE (0.25 mL) at room temperature for 48 hours. The reaction was filtered through a celite plug with EtOAc (8 mL) and the filtrate was concentrated under reduced pressure. Purification by flash chromatography on silica gel provided (\pm)-**6.41a** as a ~4:1 mixture of diastereomers (0.0107 g, 33%).

¹H NMR (CDCl₃, 600 MHz) δ 7.61 – 7.58 (m, 10H), 7.58 – 7.53 (m, 10H), 7.44 (td, J = 7.9, 2.2 Hz, 10H), 7.34 (td, J = 7.3, 1.3 Hz, 5H), 7.27 (d, J = 8.2 Hz, 2H), 7.24 (d, J = 8.2 Hz, 8H), 5.83 (ddd, J = 16.7, 10.4, 5.9 Hz, 1H), 5.71 (ddd, J = 16.9, 10.5, 6.1 Hz, 4H), 5.51 (d, J = 8.9 Hz, 4H), 5.40 (d, J = 8.7 Hz, 1H), 5.15 – 5.11 (m, 5H), 5.12 – 5.06 (m, 5H), 4.71 (dtt, J = 9.3, 6.3, 1.6 Hz, 4H), 4.66 (dtt, J = 8.7, 5.9, 1.5 Hz, 1H), 3.03 (p, J = 7.0 Hz, 4H), 2.99 (p, J = 7.1 Hz, 1H), 1.35 (d, J = 7.4 Hz, 15H), 1.19 (s, 36H), 1.05 (s, 9H) ppm.



(*R*)-**6.38** was prepared in two steps from biphenyl aldehyde **6.42** according to previously reported procedures.^{31,32}

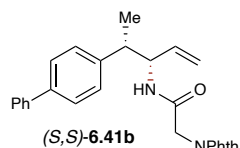


Pivalamide (S,S)-6.41a: Prepared according to the general procedure for enantioselective allylic amidation (see Chapter 5 experimental, General Procedure D) using (*R*)-4-(pent'4-en-2-yl)-1,1'-biphenyl [(*R*)-6.38] (0.0220 g, 0.10 mmol, 1.0 equiv), 3-(*tert*-butyl)-1,4,2-dioxazol-5-one (**6.39a**) (0.0286 g, 0.20 mmol, 2.0 equiv), (*R,R*)-[Rh(2-Me-3-Ph-Ind)₂]₂ [(*R,R*)-6.40] (0.0056 g, 0.005 mmol, 0.05 equiv), LiOAc (0.0006 g, 0.010 mmol, 0.10 equiv), AgNTf₂ (0.0078 g, 0.020 mmol, 0.20 equiv), and LiNTf₂ (0.0290 g, 0.10 mmol, 1.0 equiv) in DCE (0.5 mL) at 40 °C for 48 hours. Purified by flash chromatography on silica gel (5-30% EtOAc in Hexanes) to provide (**S,S**)-6.41a (0.0120 g, 37% yield, >20:1 d.r.) as a white solid.

¹H NMR (CDCl₃, 600 MHz) δ 7.59 (d, *J* = 8.0 Hz, 1H), 7.55 (d, *J* = 8.3 Hz, 1H), 7.44 (t, *J* = 7.8 Hz, 1H), 7.37 – 7.32 (m, 1H), 7.24 (dd, *J* = 8.2, 2.4 Hz, 2H), 5.70 (ddd, *J* = 16.8, 10.4, 6.1 Hz, 1H), 5.50 (d, *J* = 8.8 Hz, 1H), 5.15 – 5.04 (m, 1H), 4.75 – 4.66 (m, 1H), 3.03 (q, *J* = 6.9 Hz, 1H), 1.35 (d, *J* = 7.2 Hz, 2H), 1.19 (s, 2H) ppm.

¹³C NMR (CDCl₃, 126 MHz) δ 177.53, 141.48, 140.90, 139.83, 135.58, 128.92, 128.87, 127.38, 127.13, 127.10, 116.42, 55.82, 43.57, 39.00, 27.77, 18.00 ppm.

HRMS (+APCI) calculated for C₂₂H₂₈NO [M + H]⁺ 322.2171, found 322.2167.



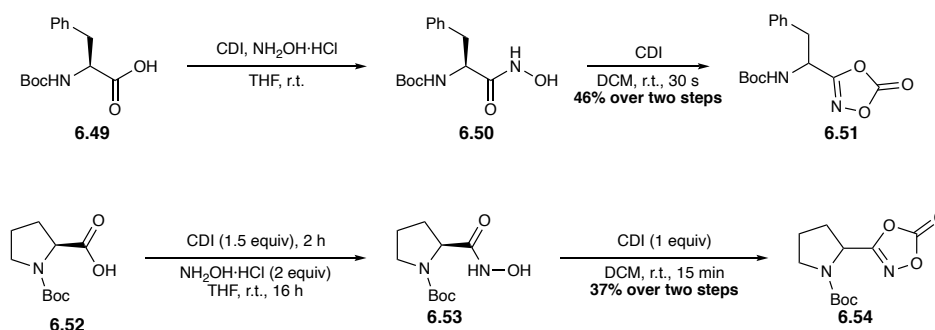
N-Phth-glycine amide (S,S)-6.41b: Prepared according to the general procedure for enantioselective allylic amidation (see Chapter 5, General Procedure D) using (*R*)-4-(pent'4-en-2-yl)-1,1'-biphenyl [(*R*)-6.38]

(0.0220 g, 0.10 mmol, 1.0 equiv), 2-((5-oxo-1,4,2-dioxazol-3-yl)methyl)isoindoline-1,3-dione (**6.39b**) (0.0492 g, 0.20 mmol, 2.0 equiv), (*R,R*)-[Rh(2-Me-3-Ph-Ind)₂]₂ [(*R,R*)-6.40] (0.0056 g, 0.005 mmol, 0.05 equiv), LiOAc (0.0006 g, 0.010 mmol, 0.10 equiv), AgNTf₂ (0.0078 g, 0.020 mmol, 0.20 equiv), and LiNTf₂ (0.0290 g, 0.10 mmol, 1.0 equiv) in DCE (0.5 mL) at 60 °C for 48 hours. Purified by flash chromatography on silica gel (20-50% EtOAc in Hexanes) to provide (**S,S**)-6.41b (0.0290 g, 41% yield, >20:1 d.r.) as a white solid.

$^1\text{H NMR}$ (CDCl_3 , 600 MHz) δ 7.85 (dd, $J = 5.4, 3.0$ Hz, 2H), 7.67 (dd, $J = 5.4, 3.0$ Hz, 2H), 7.50 – 7.47 (m, 2H), 7.44 – 7.37 (m, 4H), 7.36 – 7.32 (m, 1H), 7.19 (d, $J = 8.2$ Hz, 2H), 5.68 (ddd, $J = 17.0, 10.5, 6.3$ Hz, 1H), 5.59 (d, $J = 9.0$ Hz, 1H), 5.20 – 5.09 (m, 2H), 4.76 – 4.65 (m, 1H), 4.37 (d, $J = 16.1$ Hz, 1H), 4.31 (d, $J = 16.0$ Hz, 1H), 3.05 (q, $J = 7.1$ Hz, 1H), 1.34 (d, $J = 7.2$ Hz, 3H) ppm.

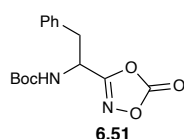
$^{13}\text{C NMR}$ (CDCl_3 , 151 MHz) δ 167.82, 165.37, 140.77, 140.71, 139.85, 134.42, 134.29, 132.04, 128.89, 128.85, 127.37, 127.12, 127.11, 123.79, 117.48, 56.48, 43.24, 41.30, 17.89 ppm.

HRMS (+APCI) calculated for $\text{C}_{27}\text{H}_{25}\text{N}_2\text{O}_3$ $[\text{M} + \text{H}]^+$ 425.1865, found 425.1869.



Amino acid-derived hydroxamic acids 6.50 and 6.53 were synthesised according to previously reported procedures for hydroxamic acids and were carried forward crude without further purification.^{53,54}

General Procedure A: Synthesis of amino acid-derived dioxazolones from hydroxamic acids: CDI (1 equiv) was added to a solution of hydroxamic acid (1 equiv) in DCM and the resulting mixture was stirred for the indicated time. The reaction mixture was filtered through a plug of silica and washed with DCM (~50 mL). The filtrate was concentrated under reduced pressure to provide the amino acid-derived dioxazolones.



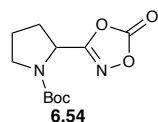
Boc-Phe-dioxazolone 6.51: Prepared according to General Procedure A using Boc-Phe-NHOH **6.50** (0.7245 g, 2.585 mmol) and CDI (0.4191 g, 2.585 mmol) in DCM (20 mL) at room temperature for 30 seconds to provide Boc-Phe-dioxazolone **6.51** (0.3642 g, 46% over two steps). Used without further purification.

$^1\text{H NMR}$ (CDCl_3 , 500 MHz) δ 7.39 – 7.28 (m, 3H), 7.20 – 7.12 (m, 2H), 5.05 (app s, 1H), 4.81

(app s, 1H), 3.22 – 3.08 (m, 2H), 1.41 (s, 9H) ppm.

^{13}C NMR (CDCl₃, 151 MHz) δ 165.76, 154.58, 153.71, 134.08, 129.27, 128.98, 128.02, 48.07, 37.85, 28.31 ppm.

HRMS (-APCI) calculated for C₁₅H₁₇N₂O₅ [M – H]⁻ 305.1173, found 305.1146.



Boc-Pro-dioxazolone 6.54: Prepared according to General Procedure A using

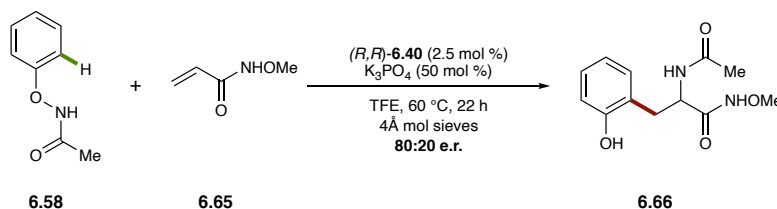
Boc-Pro-NHOH **6.53** (0.322 g, 1.40 mmol) and CDI (0.227 g, 1.40 mmol) in DCM

(10 mL) at room temperature for 15 minutes to provide Boc-Pro-dioxazolone **6.54** (0.1327 g, 37% over two steps) as a 1:1 mixture of rotamers. Used without further purification.

^1H NMR (CDCl₃, 600 MHz, CDCl₃) δ 4.84 – 4.78 (m, 1H), 4.73 – 4.63 (m, 1H), 3.56 – 3.35 (m, 4H), 2.40 – 2.23 (m, 2H), 2.18 – 1.97 (m, 6H), 1.45 (s, 9H), 1.42 (s, 9H) ppm.

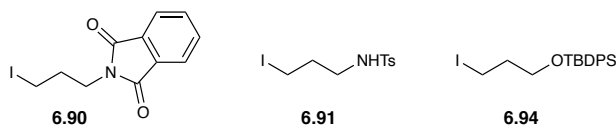
^{13}C NMR (CDCl₃, 151 MHz) δ 166.89, 166.69, 154.17, 154.05, 153.88, 153.18, 124.93, 81.45, 81.15, 52.23, 46.62, 46.40, 30.78, 29.88, 28.41, 28.36, 24.28, 23.58 ppm.

HRMS (+NSI) calculated for C₁₁H₁₇N₂O₅ [M + H]⁺ 257.1137, found 257.1132.



In a nitrogen-filled glovebox, *N*-phenoxyacetamide (**6.58**) (0.012 g, 0.079 mmol), K₃PO₄ (0.007 g, 0.033 mmol), 4Å MS (~50 mg), and (*R,R*)-**6.40** (0.0019 g, 0.0017 mmol) were added to a 4-mL vial equipped with a magnetic stir bar and a Teflon-septum cap. The vial was sealed and brought out of the glovebox. A solution of *N*-methoxyacrylamide (**6.65**) (0.0067 g, 0.066 mmol) in TFE (0.4 mL) was added and the vial was sealed with Teflon and parafilm. The reaction was stirred at 60 °C for 24 hours. The reaction was removed from heat and allowed to cool to room temperature. The reaction was filtered through a plug of celite with EtOAc (8 mL) and the filtrate was concentrated under reduced pressure. Minimal quantities of the desired product **6.66** was detected in the crude ^1H NMR spectrum by comparison to previously reported ^1H NMR data.³⁵ Enantioselectivity was determined by HPLC analysis of the crude reaction mixture.

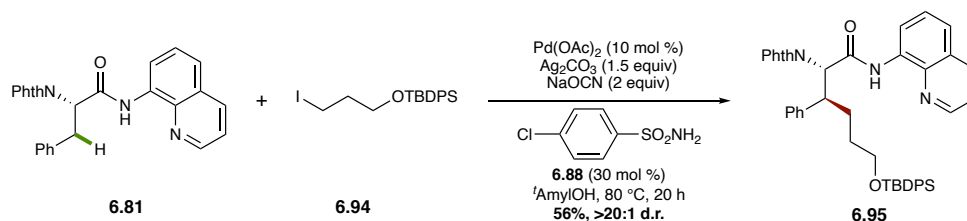
HPLC (AD-H column, 10% 2-propanol in Hexanes, 1 mL/min) $t_M = 17.5$ min, $t_m = 25.6$ min,



80:20 e.r.

Alkyl iodides **6.90**,^{46,47} **6.91**,^{48,49} and **6.94**^{47,50} were prepared according to previously reported procedures.

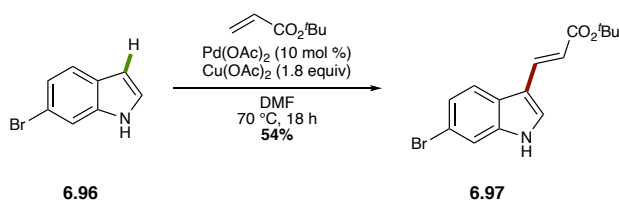
This procedure was adapted from previously reported work by Shi and co-workers.⁴⁵



Phenylalanine **6.81** (0.021 g, 0.050 mmol), Pd(OAc)₂ (0.0011 g, 0.005 mmol), NaOCN (0.0065 g, 0.10 mmol), Ag₂CO₃ (0.021 g, 0.075 mmol), and 4-chlorobenzenesulfonamide (**6.88**) (0.0029 g, 0.015 mmol) were added to a 4-mL vial equipped with a magnetic stir bar and Teflon-septum cap. The vial was sealed, and evacuated and backfilled with nitrogen three times. A solution of alkyl iodide **6.94** (0.042 g, 0.10 mmol) in *t*Amyl alcohol (0.5 mL) was added and the vial was sealed with Teflon and parafilm. The reaction was stirred at 80 °C for 36 h. The reaction was removed from heat and allowed to cool to room temperature. The reaction mixture was filtered through a plug of celite with DCM (8 mL) and the filtrate was concentrated under reduced pressure. Purification by flash chromatography on silica gel (10-30% EtOAc in Hexanes) provided modified amino acid **6.95** (0.0201 g, 56%) as a single detectable diastereomer.

¹H NMR (CDCl₃, 400 MHz) δ 10.72 (br s, 1H), 8.85 (dd, $J = 4.3, 1.7$ Hz, 1H), 8.81 (dd, $J = 5.3, 3.7$ Hz, 1H), 8.14 (dd, $J = 8.3, 1.7$ Hz, 1H), 7.69 (dd, $J = 5.5, 3.0$ Hz, 2H), 7.59 (dd, $J = 5.5, 3.0$ Hz, 2H), 7.57 – 7.47 (m, 6H), 7.43 (dd, $J = 8.3, 4.2$ Hz, 1H), 7.33 (dd, $J = 7.3, 1.7$ Hz, 2H), 7.30 – 7.27 (m, 3H), 7.25 – 7.20 (m, 3H), 7.15 (t, $J = 7.6$ Hz, 2H), 7.05 (t, $J = 7.3$ Hz, 1H), 5.23 (d, $J = 11.8$ Hz, 1H), 4.20 (td, $J = 11.6, 3.2$ Hz, 1H), 3.54 (t, $J = 6.2$ Hz, 2H), 1.92 – 1.77 (m, 2H), 1.41 –

1.29 (m, 2H), 0.86 (s, 9H) ppm.

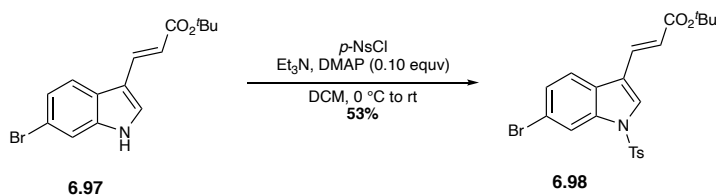


Adapted from previously reported procedures.⁵¹ 6-bromoindole (**6.96**) (0.0392 g, 0.20 mmol) and Cu(OAc)₂ (0.0654 g, 0.360 mmol) were weighed into a 4-mL vial equipped with a magnetic stir bar and Teflon-septum cap. *Tert*-butyl acrylate (0.0581 mL, 0.40 mmol) was added *via* microsyringe. Pd(OAc)₂ (0.0045 g, 0.020 mmol) was added as a solution in DMF (0.40 mL). DMSO (0.044 mL) was added and the reaction was stirred at 70 °C for 24 hours. The reaction was removed from heat and allowed to cool to room temperature. The mixture was diluted with H₂O (1 mL) and EtOAc (1 mL) and the resulting biphasic mixture was filtered through a plug of celite. The layers were separated, and the aqueous layer was washed with EtOAc (3 x 5 mL). The combined organic extracts were washed with brine, dried over anhydrous Na₂SO₄, filtered, and concentrated under reduced pressure. Purification by flash chromatography on silica gel (10–40% EtOAc in Hexanes) provided cinnamate **6.97** (0.035 g, 54%).

¹H NMR (CDCl₃, 600 MHz) δ 8.63 (br s, 1H), 7.77 (d, *J* = 14.4 Hz, 1H), 7.75 (d, *J* = 6.9 Hz, 1H), 7.56 (d, *J* = 1.7, 1H), 7.42 (d, *J* = 2.7 Hz, 1H), 7.33 (dd, *J* = 8.5, 1.7 Hz, 1H), 6.35 (d, *J* = 16.0 Hz, 1H), 1.56 (s, 9H) ppm.

¹³C NMR (CDCl₃, 151 MHz) δ 167.76, 137.99, 136.68, 128.83, 124.69, 124.40, 121.74, 116.80, 116.24, 114.87, 113.80, 80.36, 28.46 ppm.

HRMS (+APCI) calculated for C₁₅H₁₇BrNO₂ [M + H]⁺ 322.0443, found 322.0275.

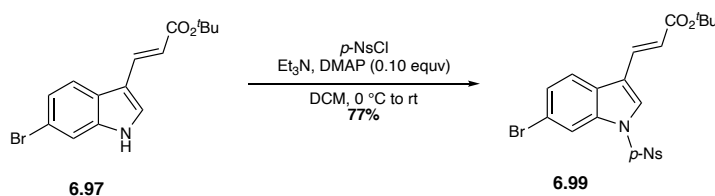


Adapted from previously reported procedures.⁵⁵ TsCl (0.108 g, 0.564 mmol), DMAP (0.0069 g, 0.0564 mmol), and Et₃N (0.0857 g, 0.846 mmol) were added to a solution of cinnamate **6.97** (0.200 g, 0.621 mmol) in DCM (7 mL) and the reaction was stirred at room temperature for 16

hours. The reaction was diluted with H₂O (10 mL). The layers were separated, and the aqueous layer was washed with DCM (3 x 10 mL). The combined organic extracts were washed with brine, dried over anhydrous Na₂SO₄, filtered, and concentrated under reduced pressure.

Purification by flash chromatography on silica gel (10-40% EtOAc in Hexanes) provided **6.98** (0.151 g, 56%).

¹H NMR (CDCl₃, 400 MHz) δ 8.18 (d, *J* = 1.8, Hz, 1H), 7.82 – 7.74 (m, 3H), 7.64 (d, *J* = 8.5 Hz, 1H), 7.62 (d, *J* = 16.1, Hz, 1H), 7.43 (dd, *J* = 8.5, 1.8 Hz, 1H), 7.28 (d, *J* = 8.7, Hz, 1H), 6.39 (d, *J* = 16.1 Hz, 1H), 2.38 (s, 3H), 1.53 (s, 9H) ppm.

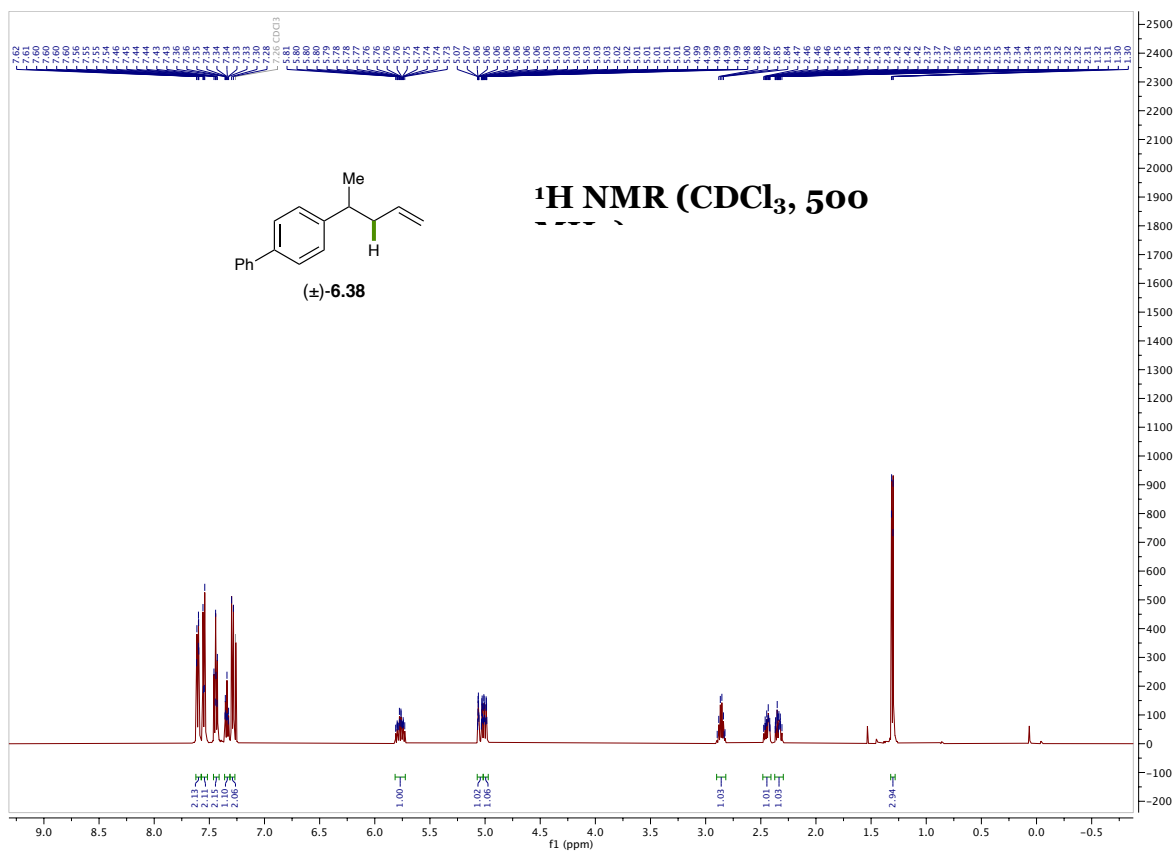


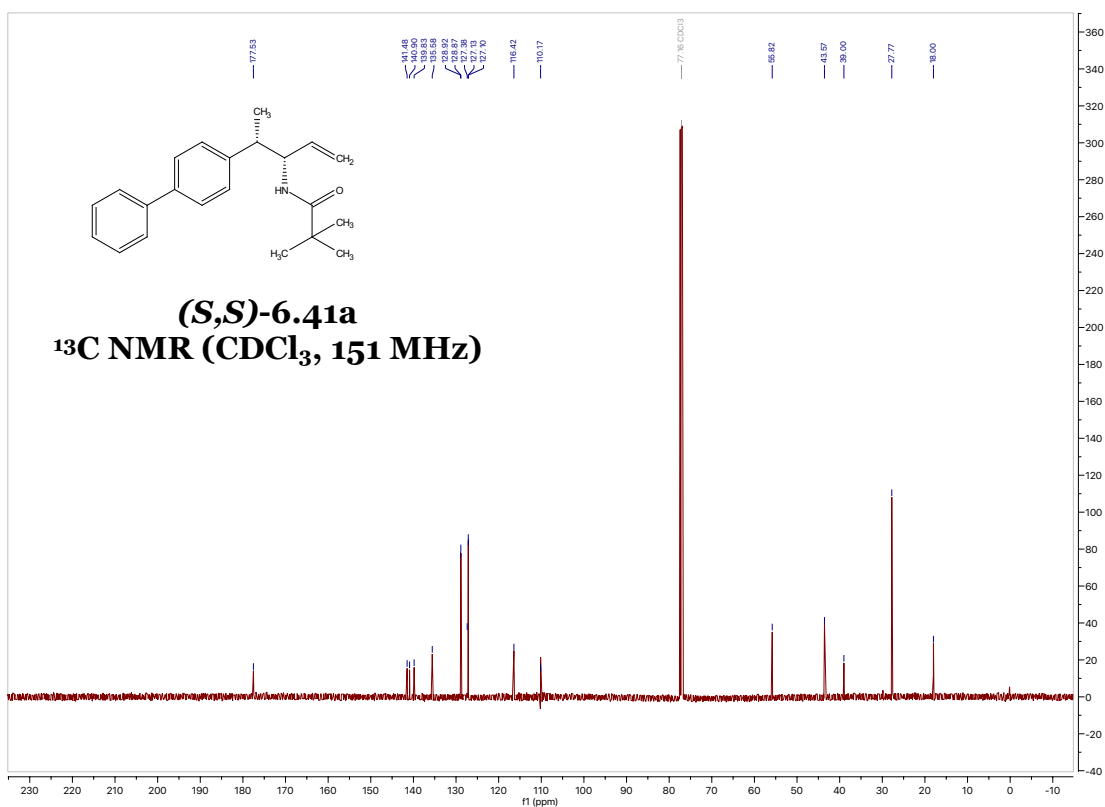
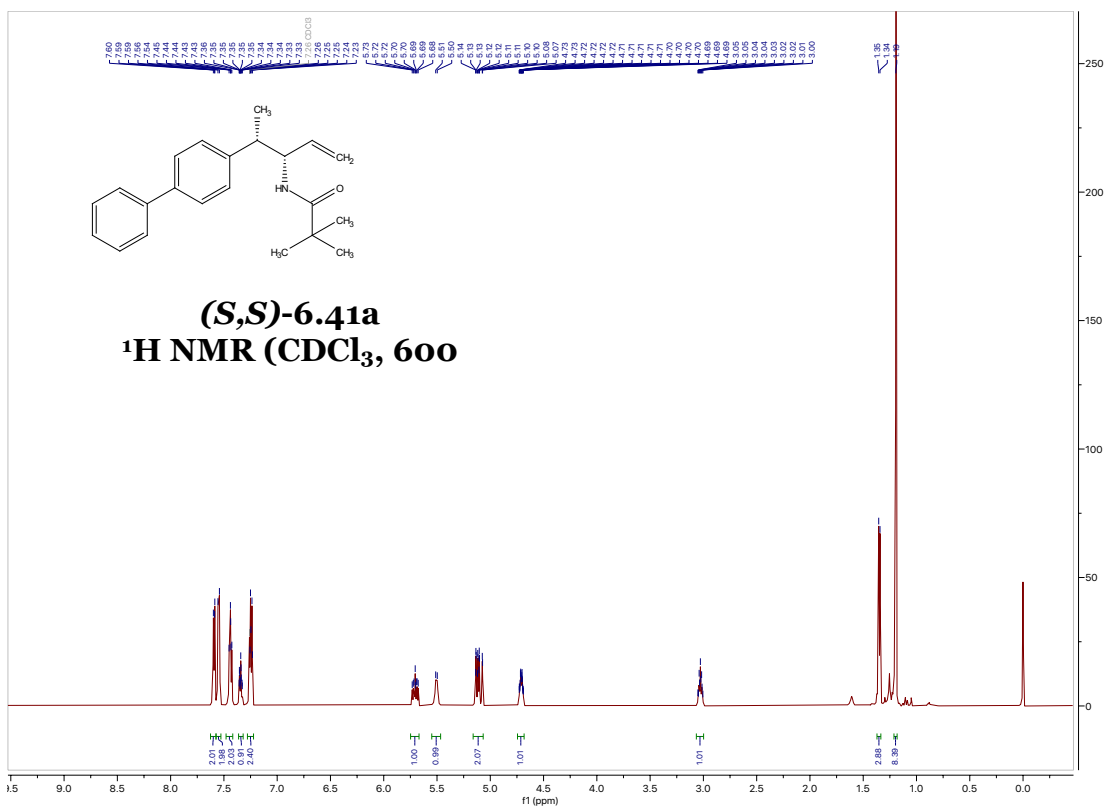
Adapted from previously reported procedures.⁵⁵ The reaction was conducted as described above for compound **6.98** with *p*-NsCl (0.1483 g, 0.669 mmol), DMAP (0.0082 g, 0.0669 mmol), Et₃N (0.140 mL, 1.00 mmol), and **6.97** (0.2372 g, 0.736 mmol) in DCM (7 mL). Purification by flash chromatography on silica gel (20-50% EtOAc in Hexanes) provided **6.99** (0.2623 g, 77%).

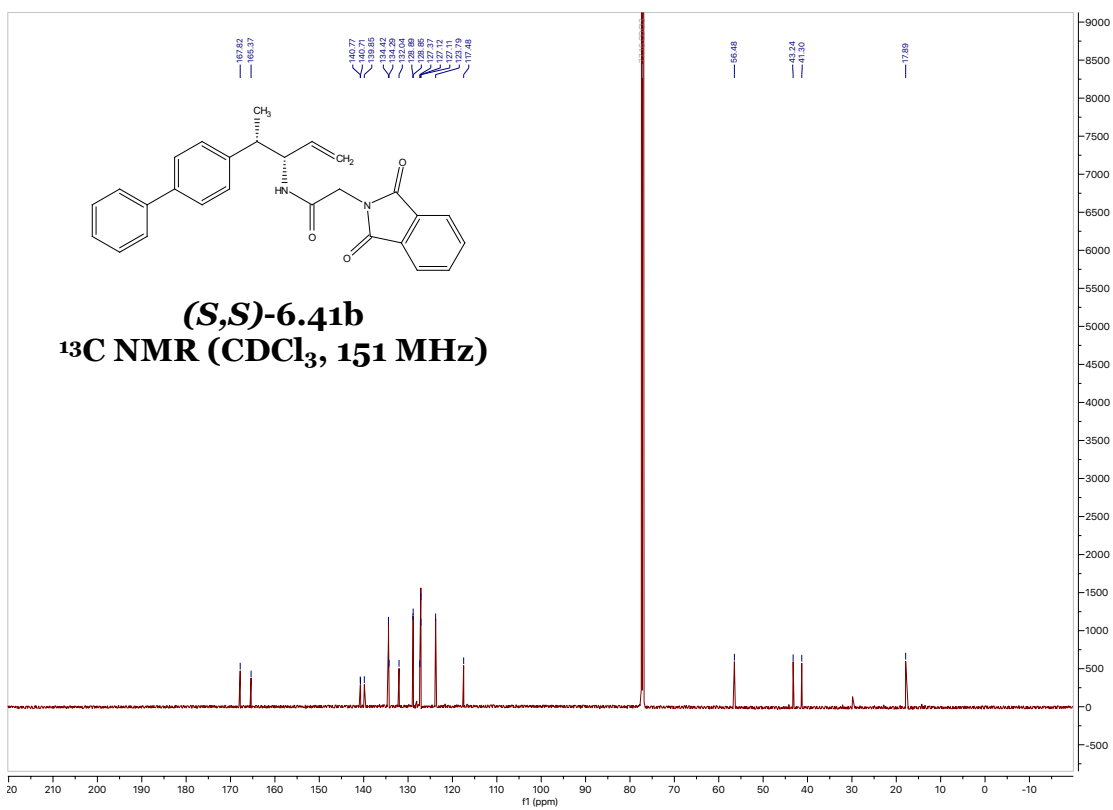
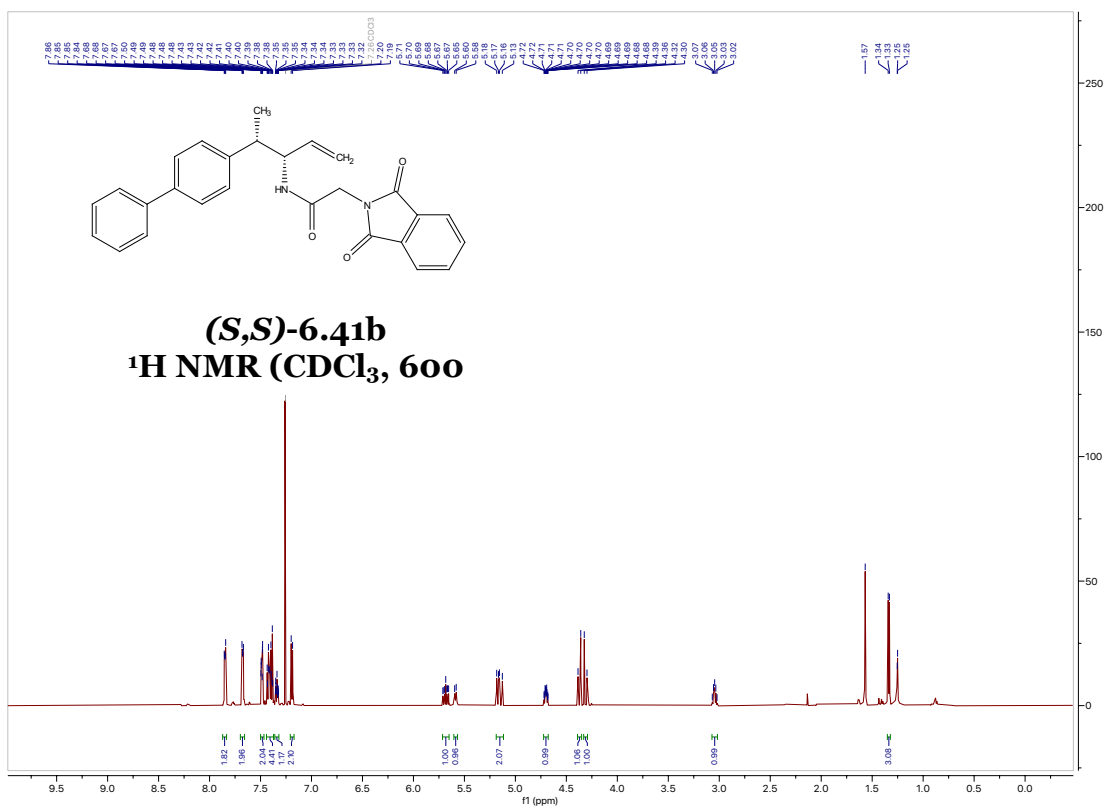
¹H NMR (CDCl₃, 600 MHz) δ 8.33 (d, *J* = 8.8 Hz, 2H), 8.18 (d, *J* = 1.7 Hz, 1H), 8.08 (d, *J* = 8.8 Hz, 2H), 7.73 (s, 1H), 7.66 (d, *J* = 8.5 Hz, 1H), 7.61 (d, *J* = 16.2 Hz, 1H), 7.48 (dd, *J* = 8.5, 1.7 Hz, 1H), 6.42 (d, *J* = 16.2 Hz, 1H), 1.53 (s, 9H) ppm.

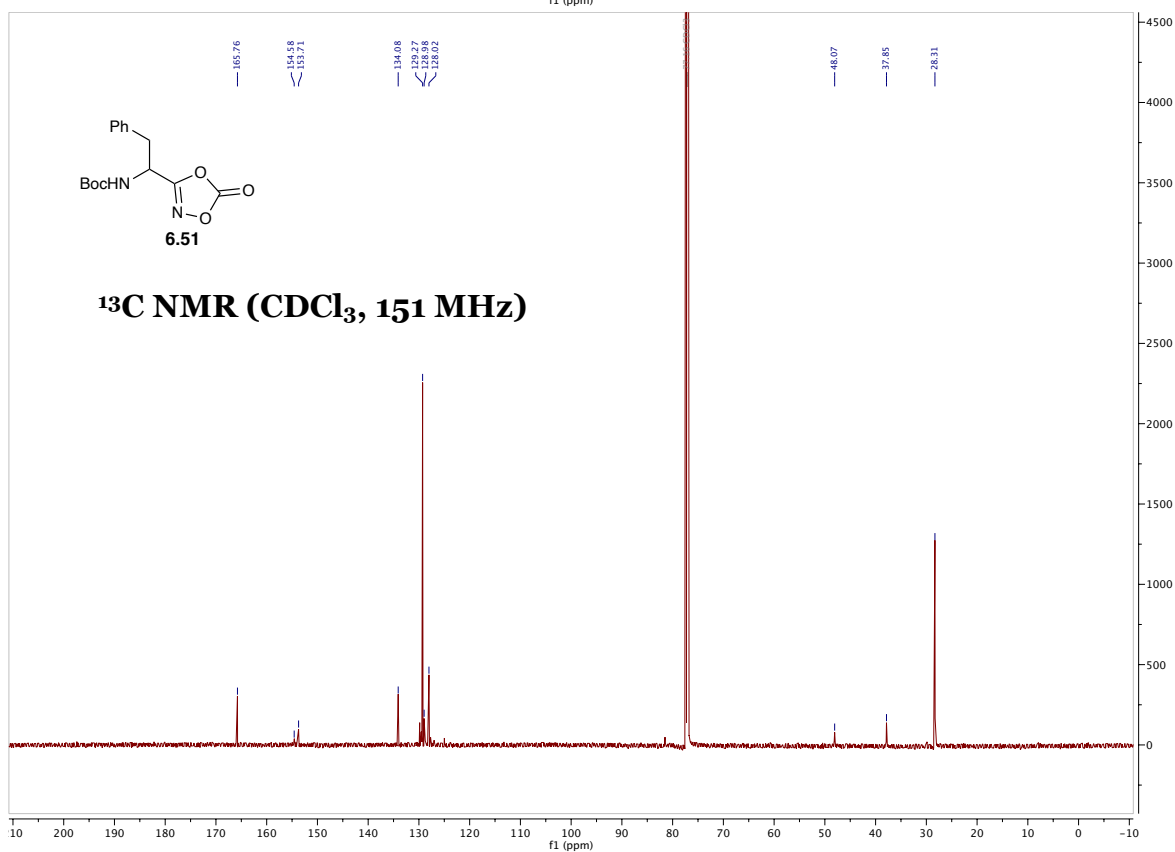
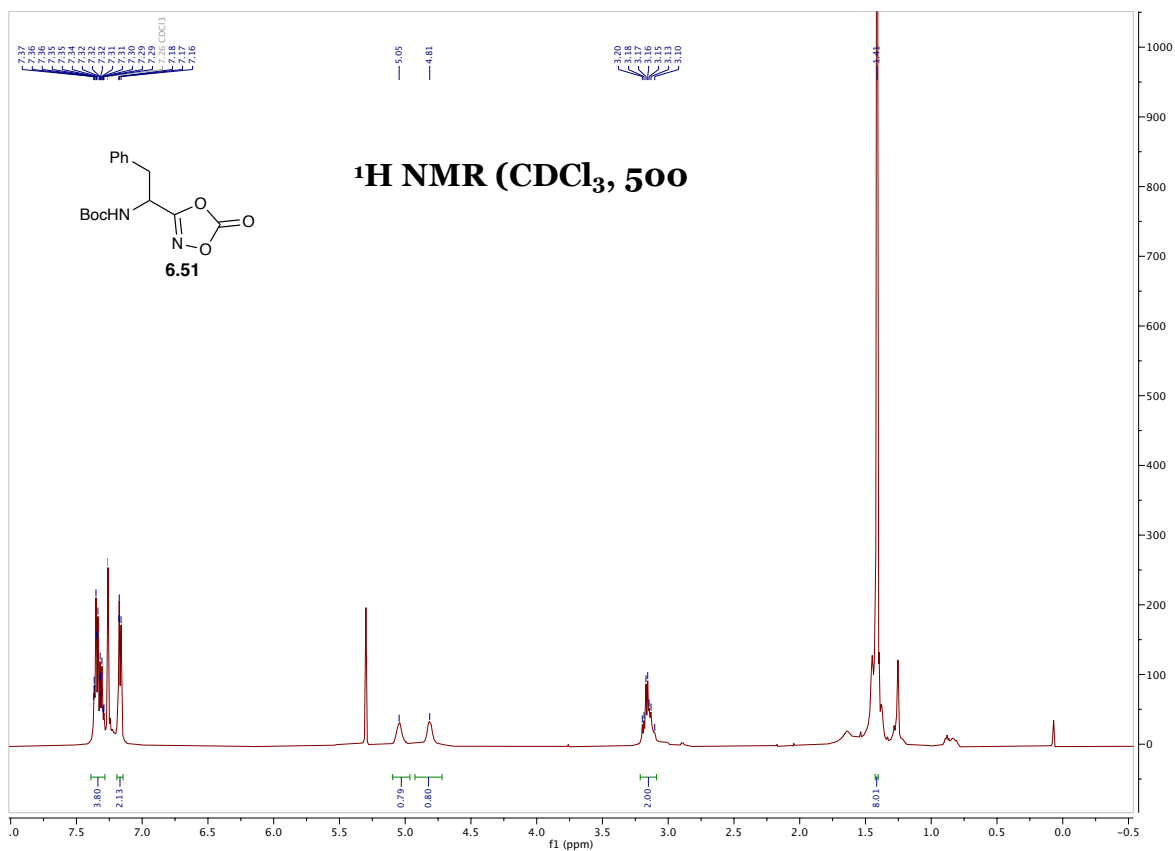
¹³C NMR (CDCl₃, 151 MHz) δ 165.84, 151.00, 142.71, 136.13, 133.02, 128.24, 128.18, 127.37, 127.15, 124.91, 122.12, 122.08, 119.87, 119.70, 116.79, 81.01, 28.19 ppm.

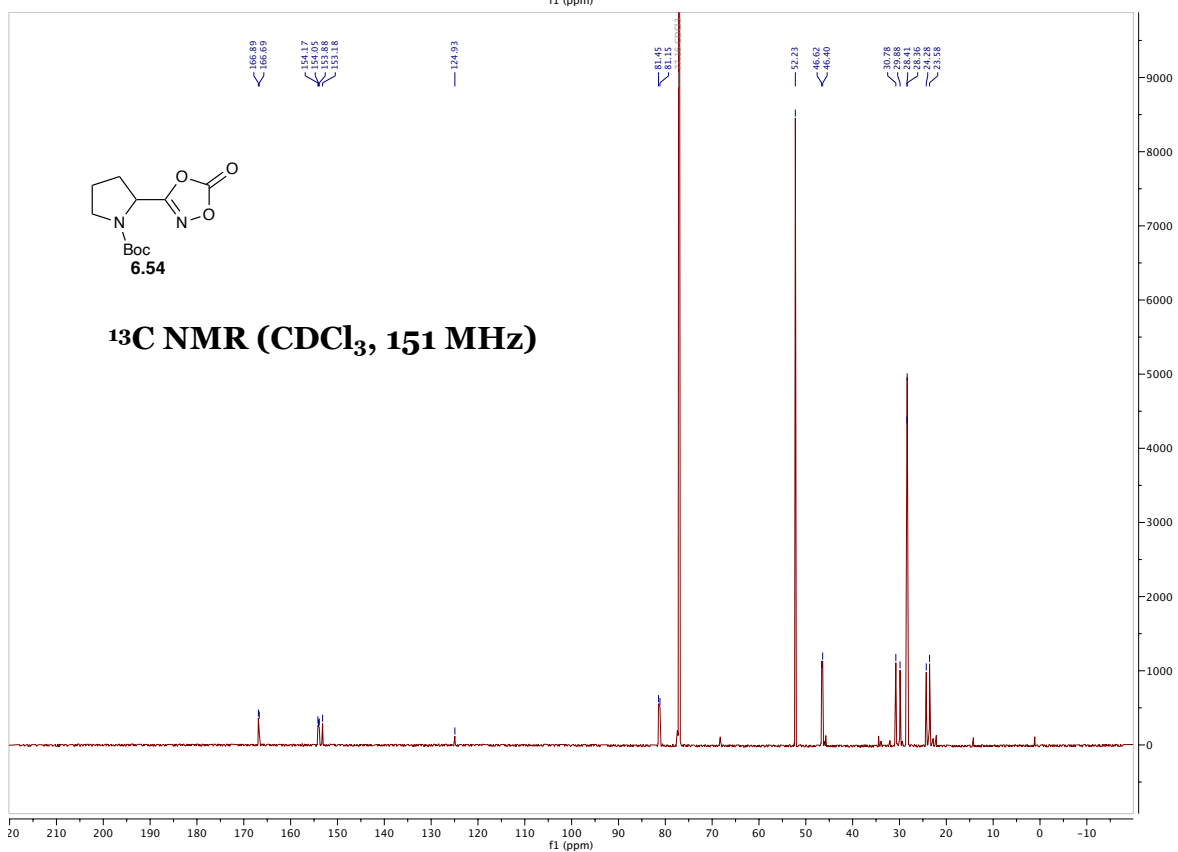
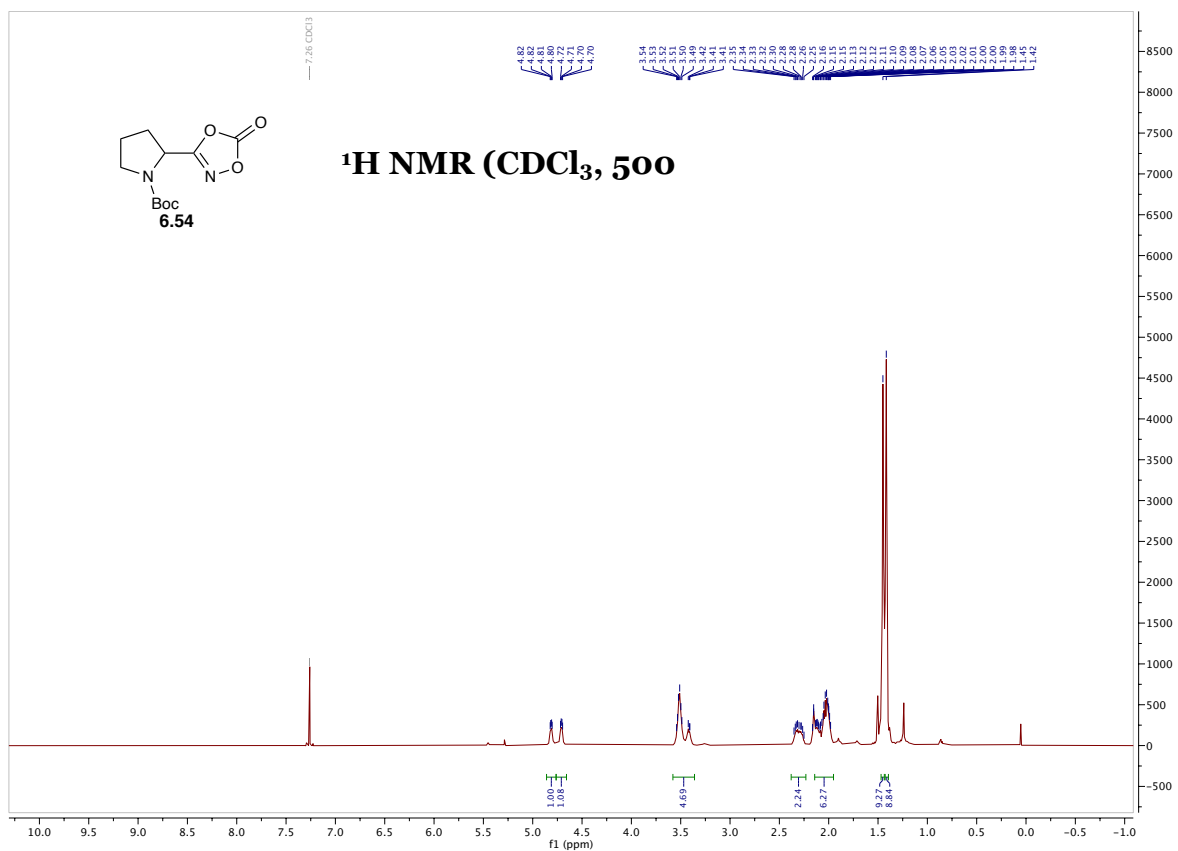
6.7 Spectral data



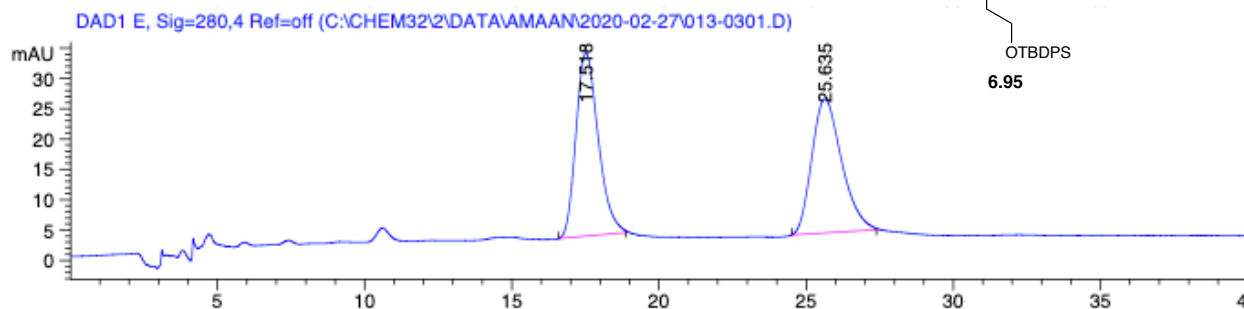
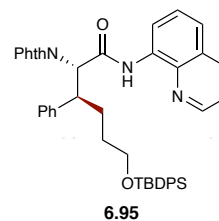








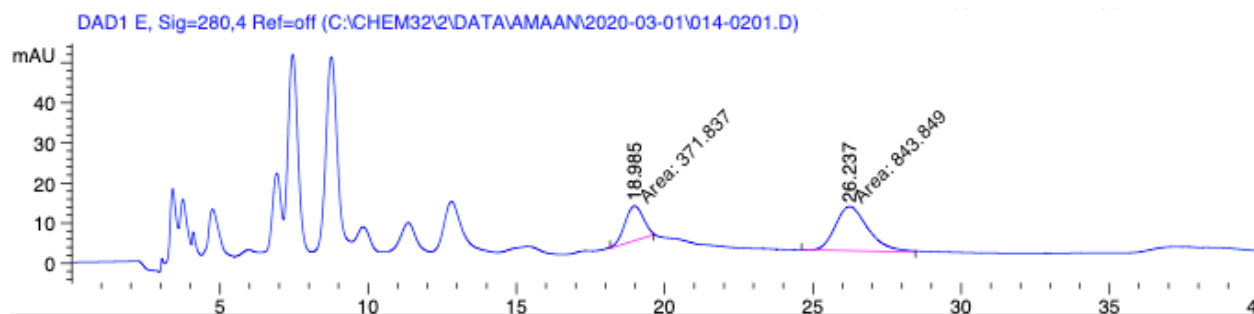
Modified amino acid 6.95



Signal 4: DAD1 E, Sig=280,4 Ref=off

Peak #	RetTime [min]	Type	Width [min]	Area [mAU*s]	Height [mAU]	Area %
1	17.518	BB	0.7990	1587.54187	30.21640	50.4838
2	25.635	BB	1.0184	1557.11292	22.08911	49.5162

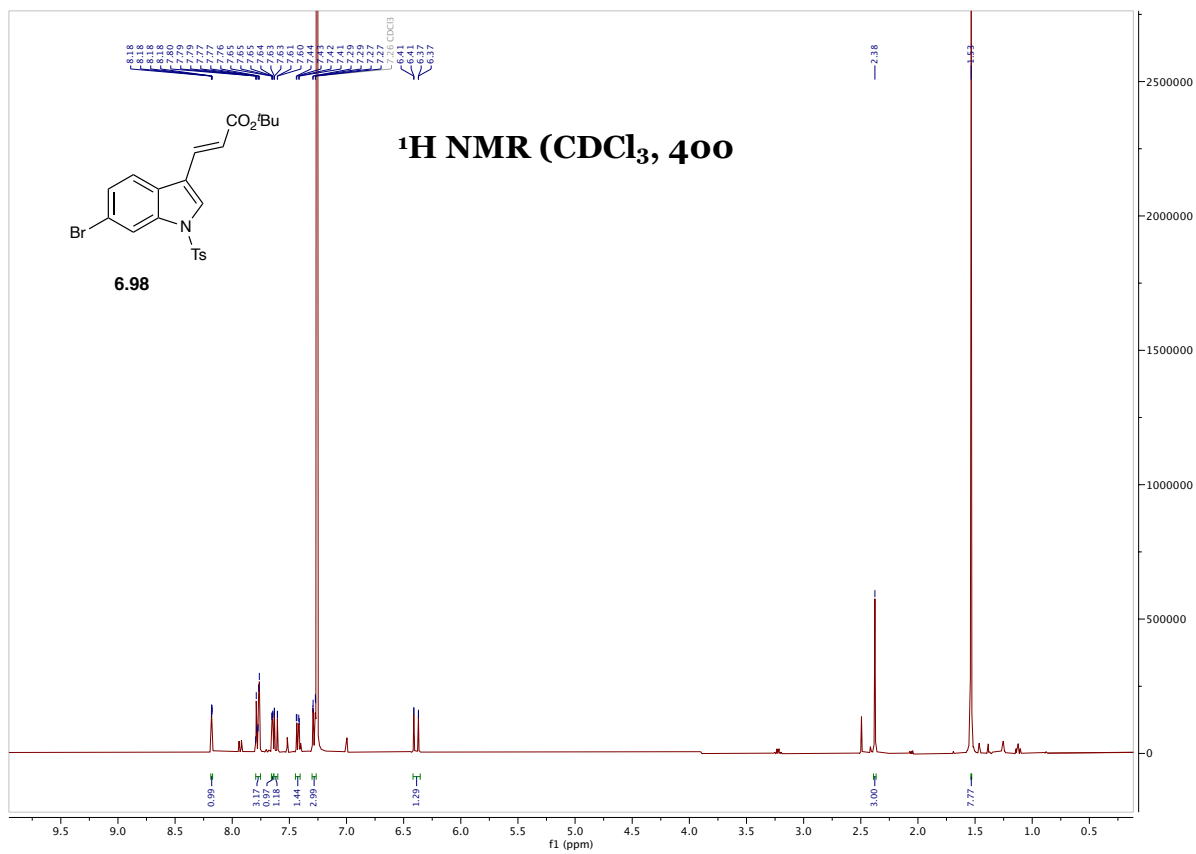
Totals : 3144.65479 52.30551



Signal 4: DAD1 E, Sig=280,4 Ref=off

Peak #	RetTime [min]	Type	Width [min]	Area [mAU*s]	Height [mAU]	Area %
1	17.518	BB	0.7990	1587.54187	30.21640	50.4838
2	25.635	BB	1.0184	1557.11292	22.08911	49.5162

Totals : 3144.65479 52.30551



6.8 References

- (1) Montalbán-López, M.; Scott, T. A.; Ramesh, S.; Rahman, I. R.; van Heel, A. J.; Viel, J. H.; Bandarian, V.; Dittmann, E.; Genilloud, O.; Goto, Y.; et al. New Developments in RiPP Discovery, Enzymology and Engineering. *Nat. Prod. Rep.* **2020**.
<https://doi.org/10.1039/donp00027b>.
- (2) Arnison, P. G.; Bibb, M. J.; Bierbaum, G.; Bowers, A. A.; Bugni, T. S.; Bulaj, G.; Camarero, J. A.; Campopiano, D. J.; Challis, G. L.; Clardy, J.; et al. Ribosomally Synthesized and Post-Translationally Modified Peptide Natural Products: Overview and Recommendations for a Universal Nomenclature. *Nat. Prod. Rep.* **2013**, *30*, 108–160.
- (3) Plat, A.; Kuipers, A.; Rink, R.; N. Moll, G. Mechanistic Aspects of Lanthipeptide Leaders. *Curr. Protein Pept. Sci.* **2013**, *14*, 85–96.
- (4) Yang, X.; Van Der Donk, W. A. Ribosomally Synthesized and Post-Translationally Modified Peptide Natural Products: New Insights into the Role of Leader and Core Peptides during Biosynthesis. *Chem. Eur. J.* **2013**, *19*, 7662–7677.
- (5) Nguyen, T. Q. N.; Tooh, Y. W.; Sugiyama, R.; Nguyen, T. P. D.; Purushothaman, M.; Leow, L. C.; Hanif, K.; Yong, R. H. S.; Agatha, I.; Winnerdy, F. R.; et al. Post-Translational Formation of Strained Cyclophanes in Bacteria. *Nat. Chem.* **2020**, *12*, 1042–1053.
- (6) Caruso, A.; Martinie, R. J.; Bushin, L. B.; Seyedsayamdost, M. R. Macrocyclization via an Arginine-Tyrosine Crosslink Broadens the Reaction Scope of Radical S-Adenosylmethionine Enzymes. *J. Am. Chem. Soc.* **2019**, *141*, 16610–16614.
- (7) Bushin, L. B.; Clark, K. A.; István, I.; Seyedsayamdost, M. R. Charting an Unexplored Streptococcal Biosynthetic Landscape Reveals a Unique Peptide Cyclization Motif. *J. Am. Chem. Soc.* **2018**, *140*, 17674–17684.
- (8) Isley, N. A.; Endo, Y.; Wu, Z. C.; Covington, B. C.; Bushin, L. B.; Seyedsayamdost, M. R.; Boger, D. L. Total Synthesis and Stereochemical Assignment of Streptide. *J. Am. Chem.*

- Soc.* **2019**, *141*, 17361–17369.
- (9) Schramma, K. R.; Bushin, L. B.; Seyedsayamdost, M. R. Structure and Biosynthesis of a Macrocyclic Peptide Containing an Unprecedented Lysine-to-Tryptophan Crosslink. *Nat. Chem.* **2015**, *7*, 431–437.
- (10) Imai, Y.; Meyer, K. J.; Iinishi, A.; Favre-Godal, Q.; Green, R.; Manuse, S.; Caboni, M.; Mori, M.; Niles, S.; Ghiglieri, M.; et al. A New Antibiotic Selectively Kills Gram-Negative Pathogens. *Nature* **2019**, *576*, 459–464.
- (11) Yokoyama, K.; Lilla, E. A. C-C Bond Forming Radical SAM Enzymes Involved in the Construction of Carbon Skeletons of Cofactors and Natural Products. *Nat.l Prod. Rep* **2018**, *35*, 660–694.
- (12) Lomovskaya, O.; Lewis, K. Emr, an Escherichia Coli Locus for Multidrug Resistance. *Proc. Natl. Acad. Sci. U. S. A.* **1992**, *89*, 8938–8942.
- (13) Li, X. Z.; Nikaido, H. Efflux-Mediated Drug Resistance in Bacteria. *Drugs* **2004**, *64*, 159–204.
- (14) Payne, D. J.; Gwynn, M. N.; Holmes, D. J.; Pompliano, D. L. Drugs for Bad Bugs: Confronting the Challenges of Antibacterial Discovery. *Nat. Rev. Drug Discov.* **2007**, *6*, 29–40.
- (15) Lewis, K. Platforms for Antibiotic Discovery. *Nat. Rev. Drug Discov.* **2013**, *12*, 371–387.
- (16) Morita, H.; Shimbo, K.; Shigemori, H.; Kobayashi, J. Antimitotic Activity of Moroidin, a Bicyclic Peptide from the Seeds of *Celosia Argentea*. *Bioorg. Med. Chem. Lett.* **2000**, *10*, 469–471.
- (17) Suzuki, H.; Morita, H.; Iwasaki, S.; Kobayashi, J. New Antimitotic Bicyclic Peptides, Celogentins D-H, and J, from the Seeds of *Celosia Argentea*. *Tetrahedron* **2003**, *59*, 5307–5315.
- (18) Kobayashi, J.; Suzuki, H.; Shimbo, K.; Takeya, K.; Morita, H. Celogentins A-C, New Antimitotic Bicyclic Peptides from the Seeds of *Celosia Argentea*. *J. Org. Chem.* **2001**, *66*,

- 6626–6633.
- (19) Ma, B.; Litvinov, D. N.; He, L.; Banerjee, B.; Castle, S. L. Total Synthesis of Celogentin C. *Angew. Chem. Int. Ed.* **2009**, *48*, 6104–6107.
- (20) Ma, B.; Banerjee, B.; Litvinov, D. N.; He, L.; Castle, S. L. Total Synthesis of the Antimitotic Bicyclic Peptide Celogentin C. *J. Am. Chem. Soc.* **2010**, *132*, 1159–1171.
- (21) Feng, Y. Q.; Chen, G. Total Synthesis of Celogentin C by Stereoselective C-H Activation. *Angew. Chem. Int. Ed.* **2010**, *49*, 958–961.
- (22) Hu, W. M.; Zhang, F. Y.; Xu, Z. R.; Liu, Q.; Cui, Y. X.; Jia, Y. X. Stereocontrolled and Efficient Total Synthesis of (-)-Stephanotic Acid Methyl Ester and (-)-Celogentin C. *Org. Lett.* **2010**, *12*, 956–959.
- (23) Fleuchot, B.; Gitton, C.; Guillot, A.; Vidic, J.; Nicolas, P.; Besset, C.; Fontaine, L.; Hols, P.; Leblond-Bourget, N.; Monnet, V.; et al. Rgg Proteins Associated with Internalized Small Hydrophobic Peptides: A New Quorum-Sensing Mechanism in Streptococci. *Mol. Microbiol.* **2011**, *80*, 1102–1119.
- (24) Ibrahim, M.; Guillot, A.; Wessner, F.; Algaron, F.; Besset, C.; Courtin, P.; Gardan, R.; Monnet, V. Control of the Transcription of a Short Gene Encoding a Cyclic Peptide in *Streptococcus Thermophilus*: A New Quorum-Sensing System? *J. Bacteriol.* **2007**, *189*, 8845–8854.
- (25) El Khatib, M.; Molander, G. A. Copper(II)-Mediated O-Arylation of Protected Serines and Threonines. *Org. Lett.* **2014**, *16*, 4944–4947.
- (26) Loach, R. P.; Fenton, O. S.; Amaike, K.; Siegel, D. S.; Ozkal, E.; Movassaghi, M. C7-Derivatization of C3-Alkylindoles Including Tryptophans and Tryptamines. *J. Org. Chem.* **2014**, *79*, 11254–11263.
- (27) Feldman, K. S.; Fodor, M. D. Extending Pummerer Reaction Chemistry. Application to the Total Synthesis of (±)-Dibromoagelaspongins. *J. Am. Chem. Soc.* **2008**, *130* (45), 14964–14965.

- (28) Farr, C. M. B.; Kazerouni, A. M.; Park, B.; Poff, C. D.; Won, J.; Sharp, K. R.; Baik, M. H.; Blakey, S. B. Designing a Planar Chiral Rhodium Indenyl Catalyst for Regio- And Enantioselective Allylic C-H Amidation. *J. Am. Chem. Soc.* **2020**, *142*, 13996–14004.
- (29) Mei, T. S.; Werner, E. W.; Burckle, A. J.; Sigman, M. S. Enantioselective Redox-Relay Oxidative Heck Arylations of Acyclic Alkenyl Alcohols Using Boronic Acids. *J. Am. Chem. Soc.* **2013**, *135*, 6830–6833.
- (30) Saito, T.; Nishimoto, Y.; Yasuda, M.; Baba, A. Direct Coupling Reaction between Alcohols and Silyl Compounds: Enhancement of Lewis Acidity of Me₃SiBr Using InCl₃. *J. Org. Chem.* **2006**, *71*, 8516–8522.
- (31) Kee, C. H.; Ariffin, A.; Awang, K.; Takeya, K.; Morita, H.; Hussain, S. I.; Chan, K. M.; Wood, P. J.; Threadgill, M. D.; Lim, C. G.; et al. Challenges Associated with the Synthesis of Unusual O-Carboxamido Stilbenes by the Heck Protocol: Intriguing Substituent Effects, Their Toxicological and Chemopreventive Implications. *Org. Biomol. Chem.* **2010**, *8*, 5646–5660.
- (32) Wang, Y. M.; Buchwald, S. L. Enantioselective CuH-Catalyzed Hydroallylation of Vinylarenes. *J. Am. Chem. Soc.* **2016**, *138*, 5024–5027.
- (33) Petrassi, H. M.; Sharpless, K. B.; Kelly, J. W. The Copper-Mediated Cross-Coupling of Phenylboronic Acids and N-Hydroxyphthalimide at Room Temperature: Synthesis of Aryloxyamines. *Org. Lett.* **2001**, *3*, 139–141.
- (34) Lerchen, A.; Knecht, T.; Daniliuc, C. G.; Glorius, F. Unnatural Amino Acid Synthesis Enabled by the Regioselective Cobalt(III)-Catalyzed Intermolecular Carboamination of Alkenes. *Angew. Chem. Int. Ed.* **2016**, *5*, 15166–15170.
- (35) Hu, Z.; Tong, X.; Liu, G. Rhodium(III) Catalyzed Carboamination of Alkenes Triggered by C-H Activation of N-Phenoxyacetamides under Redox-Neutral Conditions. *Org. Lett.* **2016**, *18*, 1702–1705.
- (36) Piou, T.; Rovis, T. Rhodium-Catalysed Syn-Carboamination of Alkenes via a Transient

- Directing Group. *Nature* **2015**, *527*, 86–90.
- (37) Cramer, N.; Ozols, K.; Onodera, S.; Woźniak, Ł. Cobalt(III)-Catalyzed Enantioselective Intermolecular Carboaminations via C–H Functionalizations. *Angew. Chemie Int. Ed.* **2020**, anie.202011140. <https://doi.org/10.1002/anie.202011140>.
- (38) Subba Reddy, B. V; Rajender Reddy, L.; Corey, E. J. Novel Acetoxylation and C–C Coupling Reactions at Unactivated Positions in R-Amino Acid Derivatives. *J. Am. Chem. Soc.* **2006**, *8*, 3391–3394.
- (39) Tran, L. D.; Daugulis, O. Nonnatural Amino Acid Synthesis by Using Carbon-Hydrogen Bond Functionalization Methodology. *Angew. Chem. Int. Ed.* **2012**, *51*, 5188–5191.
- (40) Brandhofer, T.; García Mancheño, O. Site-Selective C–H Bond Activation/Functionalization of Alpha-Amino Acids and Peptide-Like Derivatives. *Eur. J. Org. Chem.* **2018**, *2018*, 6050–6067.
- (41) Noisier, A. F. M.; Brimble, M. A. C-H Functionalization in the Synthesis of Amino Acids and Peptides. *Chem. Rev.* **2014**, *114*, 8775–8806.
- (42) Chen, Z.; Rong, M. Y.; Nie, J.; Zhu, X. F.; Shi, B. F.; Ma, J. A. Catalytic Alkylation of Unactivated C(sp³)-H Bonds for C(sp³)-C(sp³) Bond Formation. *Chem. Soc. Rev.* **2019**, *48*, 4921–4942.
- (43) Chen, K.; Hu, F.; Zhang, S. Q.; Shi, B. F. Pd(II)-Catalyzed Alkylation of Unactivated C(sp³)-H Bonds: Efficient Synthesis of Optically Active Unnatural α -Amino Acids. *Chem. Sci.* **2013**, *4*, 3906–3911.
- (44) Zhang, S. Y.; Li, Q.; He, G.; Nack, W. A.; Chen, G. Stereoselective Synthesis of β -Alkylated α -Amino Acids via Palladium-Catalyzed Alkylation of Unactivated Methylene C(sp³)-H Bonds with Primary Alkyl Halides. *J. Am. Chem. Soc.* **2013**, *135*, 12135–12141.
- (45) Chen, K.; Shi, B. F. Sulfonamide-Promoted Palladium(II)-Catalyzed Alkylation of Unactivated Methylene C(sp³)-H Bonds with Alkyl Iodides. *Angew. Chem. Int. Ed.* **2014**, *53*, 11950–11954.

- (46) Ratel, M.; Provencher-Girard, A.; Zhao, S. S.; Breault-Turcot, J.; Labrecque-Carbonneau, J.; Branca, M.; Pelletier, J. N.; Schmitzer, A. R.; Masson, J. F. Imidazolium-Based Ionic Liquid Surfaces for Biosensing. *Anal. Chem.* **2013**, *85*, 5770–5777.
- (47) Nappi, M.; He, C.; Whitehurst, W. G.; Chappell, B. G. N.; Gaunt, M. J. Selective Reductive Elimination at Alkyl Palladium(IV) by Dissociative Ligand Ionization: Catalytic C(sp³)-H Amination to Azetidines. *Angew. Chem. Int. Ed.* **2018**, *57*, 3178–3182.
- (48) Nugent, J.; Arroniz, C.; Shire, B. R.; Sterling, A. J.; Pickford, H. D.; Wong, M. L. J.; Mansfield, S. J.; Caputo, D. F. J.; Owen, B.; Mousseau, J. J.; et al. A General Route to Bicyclo[1.1.1]Pentanes through Photoredox Catalysis. *ACS Catal.* **2019**, *9*, 9568–9574.
- (49) Beltran, F.; Fabre, I.; Ciofini, I.; Miesch, L. Direct Spirocyclization from Keto-Sulfonamides: An Approach to Azaspiro Compounds. *Org. Lett.* **2017**, *19*, 5042–5045.
- (50) El Fangour, S.; Balas, L.; Rossi, J. C.; Fedenyuk, A.; Gretskeya, N.; Bobrov, M.; Bezuglov, V.; Hillard, C. J.; Durand, T. Hemisynthesis and Preliminary Evaluation of Novel Endocannabinoid Analogues. *Bioorg. Med. Chem. Lett.* **2003**, *13*, 1977–1980.
- (51) Grimster, N. P.; Gauntlett, C.; Godfrey, C. R. A.; Gaunt, M. J. Palladium-Catalyzed Intermolecular Alkenylation of Indoles by Solvent-Controlled Regioselective C-H Functionalization. *Angew. Chem. Int. Ed.* **2005**, *44*, 3125–3129.
- (52) Klapars, A.; Buchwald, S. L. Copper-Catalyzed Halogen Exchange in Aryl Halides: An Aromatic Finkelstein Reaction. *J. Am. Chem. Soc.* **2002**, *124*, 14844–14845.
- (53) Usachova, N.; Leitis, G.; Jirgensons, A.; Kalvinsh, I. Synthesis of Hydroxamic Acids by Activation of Carboxylic Acids with *N, N'*-Carbonyldiimidazole: Exploring the Efficiency of the Method. *Synth. Commun.* **2010**, *40*, 927–935.
- (54) Giacomelli, G.; Porcheddu, A.; Salaris, M. Simple One-Flask Method for the Preparation of Hydroxamic Acids. *Org. Lett.* **2003**, *5*, 2715–2717.
- (55) Guo, J.; Hao, Y.; Ji, X.; Wang, Z.; Liu, Y.; Ma, D.; Li, Y.; Pang, H.; Ni, J.; Wang, Q. Optimization, Structure-Activity Relationship, and Mode of Action of Nortopsentin

Analogues Containing Thiazole and Oxazole Moieties. *J. Agric. Food Chem.* **2019**, *67* (36), 10018–10031.